PERIVASCULAR ADIPOSE TISSUE (PVAT) IN HEALTH AND DISEASE

EDITED BY: Stephanie W. Watts and Maik Gollasch
PUBLISHED IN: Frontiers in Physiology

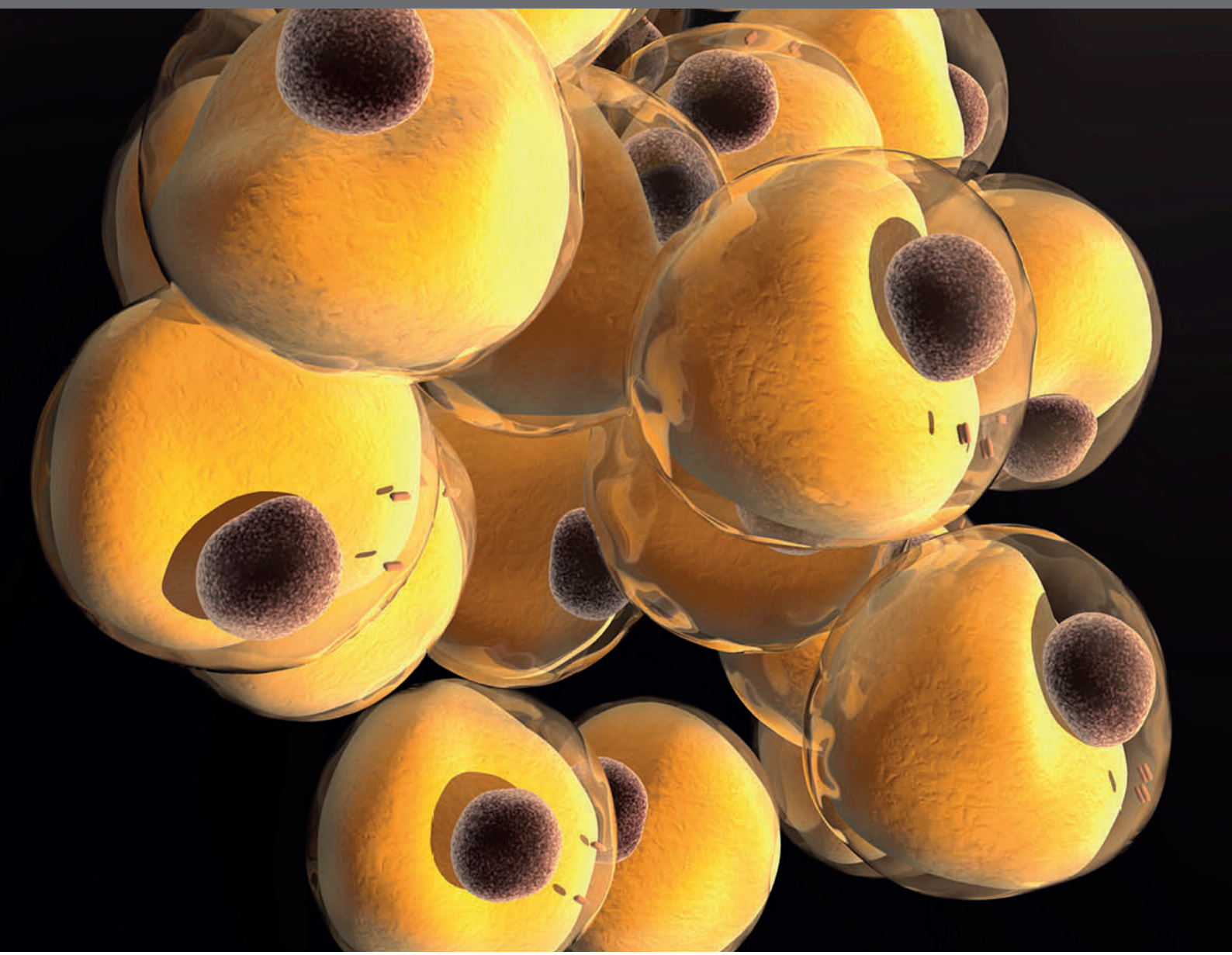

frontiers Research Topics

frontiers

ISSN 1664-8714
ISBN 978-2-88945-603-1
DOI 10.3389/978-2-88945-603-1

About Frontiers

Frontiers is more than just an open-access publisher of scholarly articles: it is a pioneering approach to the world of academia, radically improving the way scholarly research is managed. The grand vision of Frontiers is a world where all people have an equal opportunity to seek, share and generate knowledge. Frontiers provides immediate and permanent online open access to all its publications, but this alone is not enough to realize our grand goals.

Frontiers Journal Series

The Frontiers Journal Series is a multi-tier and interdisciplinary set of open-access, online journals, promising a paradigm shift from the current review, selection and dissemination processes in academic publishing. All Frontiers journals are driven by researchers for researchers; therefore, they constitute a service to the scholarly community. At the same time, the Frontiers Journal Series operates on a revolutionary invention, the tiered publishing system, initially addressing specific communities of scholars, and gradually climbing up to broader public understanding, thus serving the interests of the lay society, too.

Dedication to Quality

Each Frontiers article is a landmark of the highest quality, thanks to genuinely collaborative interactions between authors and review editors, who include some of the world's best academicians. Research must be certified by peers before entering a stream of knowledge that may eventually reach the public - and shape society; therefore, Frontiers only applies the most rigorous and unbiased reviews.
Frontiers revolutionizes research publishing by freely delivering the most outstanding research, evaluated with no bias from both the academic and social point of view. By applying the most advanced information technologies, Frontiers is catapulting scholarly publishing into a new generation.

What are Frontiers Research Topics?

Frontiers Research Topics are very popular trademarks of the Frontiers Journals Series: they are collections of at least ten articles, all centered on a particular subject. With their unique mix of varied contributions from Original Research to Review Articles, Frontiers Research Topics unify the most influential researchers, the latest key findings and historical advances in a hot research area! Find out more on how to host your own Frontiers Research Topic or contribute to one as an author by contacting the Frontiers Editorial Office: researchtopics@frontiersin.org

PERIVASCULAR ADIPOSE TISSUE (PVAT) IN HEALTH AND DISEASE

Topic Editors:
Stephanie W. Watts, Michigan State University, United States
Maik Gollasch, Max Delbruck Center for Molecular Medicine, Germany

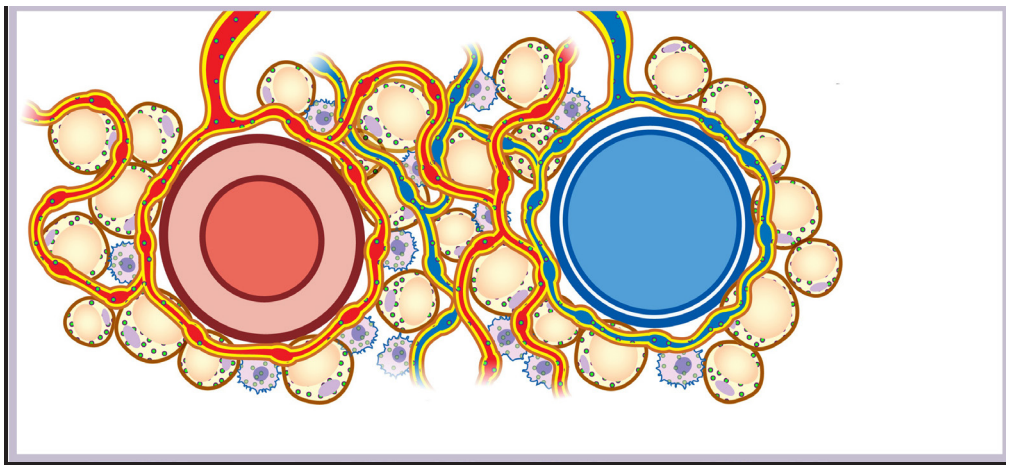

Rendering of PVAT around an artery (red) and vein (blue). Round yellow cells = adipocytes, purple cells = immune cells, red and blue lines are potential nerves. Illustrated by Chris McKee (http://www.cmedart.com/).

Cover image: Design_Cells/Shutterstock.com

Citation: Watts, S. W., Gollasch, M., eds. (2018). Perivascular Adipose Tissue (PVAT) in Health and Disease. Lausanne: Frontiers Media. doi: 10.3389/978-2-88945-603-1

Table of Contents

frontiers in Physiology

EDITORIAL
published: 30 July 2018
doi: 10.3389/fphys.2018.01004

Editorial: Perivascular Adipose Tissue (PVAT) in Health and Disease

Stephanie W. Watts[1]* *and Maik Gollasch*[2]

[1] *Pharmacology and Toxicology, Michigan State University, East Lansing, MI, United States,* [2] *Experiment and Clinical Research Center, Medical Clinic of Nephrology and Internal Intensive Care, Charité Universitätsmedizin Berlin, Berlin, Germany*

Keywords: perivascular adipose tissue, cardiovacsular Disease(s), vascular dysfunction, immune system, adipose tissue

Editorial on the Research Topic

Perivascular Adipose Tissue (PVAT) in Health and Disease

The field of perivascular adipose tissue (PVAT) research began with a simple and elegant study published in 1991, and the year 2018 finds us with substantially greater knowledge that this adipose tissue around a blood vessel possesses profound abilities to modify vascular tone. Soltis and Cassis (1991) performed the original studies on the isolated rat thoracic aorta, demonstrating that removal of the PVAT around the aorta shifted the contraction to NE to the left in a way that was functionally dependent on NE uptake. These studies were the first to suggest the PVAT was more than structural support, and were followed by an important study in 2002 demonstrating that PVAT from healthy subjects contains factors that directly relaxed contracted arteries (Lohn et al., 2002). Since then these and other findings resulted in the phrase of PVAT being "anti-contractile" in health. PubMed lists over 700 publications on perivascular adipose tissue (search June 17, 2018). The contributions made in this Frontiers Research Topic are significant because they add to each of the considerations that have been given to PVAT relative to its role in vascular function.

The cell types that constitute PVAT appear to be different in different sites of the body, with the adipocyte type in PVAT including brown, beige and white adipocytes (Pfeifer et al.). This was elegantly discussed by Pond with a historical perspective on accuracy and artistry in Western Europe (Pond). Adipocyte type appears not be static with the finding that the browning of PVAT is associated with aging (Kong et al.). The adipocyte is but one cell type that could contribute to PVAT being supportive of vessel health, or contributing to vascular dysfunction in disease.

The ability of PVAT to be beneficial to a vessel in health is further supported by the observations that PVAT produces other relaxant substances such as palmitic acid methyl ester (Wang et al.), harbors atheroprotective B cells (Srikakulapu et al.), and provides mitochondrial function that blunts atherosclerosis (Xiong et al.). In the human, preservation of PVAT improves saphenous vein graft function with the "no-touch" technique (Vestergaard et al.), a finding that encourages keeping the PVAT layer intact in isolated veins before grafting. PVAT works in concert with the vessel it surrounds; this relationship is biologically important given the importance of the molecule insulin receptor substrate 2 (IRS2) to modify insulin-induced changes in vasomotor tone in a PVAT dependent manner (Turaihi et al.). The mechanisms by which PVAT achieve an anti-contractile effect (e.g., mediators, signal transduction pathways) may not be the same in the human and rodent. Thus, the fields continued push to study human vessels remains important.

A significant reason for investigating PVAT is the loss of the anticontractile effect of PVAT in cardiovascular diseases, as reviewed by da Costa et al and demonstrated specifically in the condition of a high fat diet (Almabrouk et al.), in atherosclerosis (Tanaka and Sata), in metabolic syndrome (da Costa et al.), and other non-atherosclerotic vascular diseases

OPEN ACCESS

Edited and reviewed by:
Gerald A. Meininger, University of Missouri, United States

***Correspondence:**
Stephanie W. Watts
wattss@msu.edu

Specialty section:
This article was submitted to Vascular Physiology, a section of the journal Frontiers in Physiology

Received: *19 June 2018*
Accepted: *09 July 2018*
Published: *30 July 2018*

Citation:
Watts SW and Gollasch M (2018) Editorial: Perivascular Adipose Tissue (PVAT) in Health and Disease. Front. Physiol. 9:1004. doi: 10.3389/fphys.2018.01004

(Horimatsu et al.). By contrast to these findings that suggests PVAT may play a role in the pathology of cardiovascular diseases, work by Baltieri suggests that PVAT may be protective of endothelial function and insulin-induced vasodilation of the hypercholesterolemic mouse (Baltieri et al.). There remains the question of when, temporally, changes in PVAT occur relative to the disease proper, such that interventions at the level of PVAT could influence disease outcome.

This Frontiers Research Topic in PVAT is a view into the rich places of research that have yet to be tapped relative to understanding the role PVAT plays both in health and disease. We are grateful to our contributors for sharing their important work.

AUTHOR CONTRIBUTIONS

SW drafted the editorial, and MG read and modified editorial.

FUNDING

SW supported by HL117847.

REFERENCES

Lohn, M., Dubrovska, G., Lauterbach, B., Luft, F. C., Gollasch, M., and Sharma, A. M. (2002). Periadvential fat releases a vascular relaxing factor. *FASEB J.* 16, 1057–1063. doi: 10.1096/fj.02-0024com

Soltis, E. E., and Cassis, L. A. (1991). Influence of perivascular adipose tissue on rat aortic smooth muscle responsiveness. *Clin. Exp. Hypertension A* 13, 277–296.

Conflict of Interest Statement: The authors declare that the research was conducted in the absence of any commercial or financial relationships that could be construed as a potential conflict of interest.

frontiers in Physiology

ORIGINAL RESEARCH
published: 23 May 2018
doi: 10.3389/fphys.2018.00583

Palmitic Acid Methyl Ester and Its Relation to Control of Tone of Human Visceral Arteries and Rat Aortas by Perivascular Adipose Tissue

Ning Wang[1]*, *Artur Kuczmanski*[1,2], *Galyna Dubrovska*[1] and *Maik Gollasch*[1,3]*

[1] Experimental and Clinical Research Center, Charité – Universitätsmedizin Berlin and Max-Delbrück Center for Molecular Medicine in the Helmholtz Association (MDC), Berlin, Germany, [2] HELIOS Klinikum Berlin-Buch, Berlin, Germany, [3] Medical Clinic of Nephrology and Internal Intensive Care, Charité – Universitätsmedizin Berlin, Berlin, Germany

OPEN ACCESS

Edited by:
Michael A. Hill,
University of Missouri, United States

Reviewed by:
Vladimir V. Matchkov,
Aarhus University, Denmark
Tim Murphy,
University of New South Wales, Australia

***Correspondence:**
Ning Wang
ning.wang@charite.de
Maik Gollasch
maik.gollasch@charite.de

Specialty section:
This article was submitted to Vascular Physiology, a section of the journal Frontiers in Physiology

Received: 04 October 2017
Accepted: 01 May 2018
Published: 23 May 2018

Citation:
Wang N, Kuczmanski A, Dubrovska G and Gollasch M (2018) Palmitic Acid Methyl Ester and Its Relation to Control of Tone of Human Visceral Arteries and Rat Aortas by Perivascular Adipose Tissue. Front. Physiol. 9:583. doi: 10.3389/fphys.2018.00583

Background: Perivascular adipose tissue (PVAT) exerts anti-contractile effects on visceral arteries by release of various perivascular relaxing factors (PVRFs) and opening voltage-gated K^+ (K_V) channels in vascular smooth muscle cells (VSMCs). Palmitic acid methyl ester (PAME) has been proposed as transferable PVRF in rat aorta. Here, we studied PVAT regulation of arterial tone of human mesenteric arteries and clarified the contribution of K_V channels and PAME in the effects.

Methods: Wire myography was used to measure vasocontractions of mesenteric artery rings from patients undergoing abdominal surgery. Isolated aortic rings from Sprague-Dawley rats were studied for comparison. PVAT was either left intact or removed from the arterial rings. Vasocontractions were induced by external high K^+ (60 mM), serotonin (5-HT) or phenylephrine. PAME (10 nM–3 μM) was used as vasodilator. K_V channels were blocked by XE991, a K_V7 (KCNQ) channel inhibitor, or by 4-aminopyridine, a non-specific K_V channel inhibitor. PAME was measured in bathing solutions incubated with rat peri-aortic or human visceral adipose tissue.

Results: We found that PVAT displayed anti-contractile effects in both human mesenteric arteries and rat aortas. The anti-contractile effects were inhibited by XE991 (30 μM). PAME (EC_{50} ~1.4 μM) was capable to produce relaxations of PVAT-removed rat aortas. These effects were abolished by XE991 (30 μM), but not 4-aminopyridine (2 mM) or NDGA (10 μM), a lipoxygenases inhibitor. The cytochrome P450 epoxygenase inhibitor 17-octadecynoic acid (ODYA 10 μM) and the soluble epoxide hydrolase inhibitor 12-(3-adamantan-1-ylureido)-dodecanoic acid (AUDA 10 μM) slightly decreased PAME relaxations. PAME up to 10 μM failed to induce relaxations of PVAT-removed human mesenteric arteries. 5-HT induced endogenous PAME release from rat peri-aortic adipose tissue, but not from human visceral adipose tissue.

Conclusions: Our data also suggest that K_v7 channels are involved in the anti-contractile effects of PVAT on arterial tone in both rat aorta and human mesenteric arteries. PAME could contribute to PVAT relaxations by activating K_v7 channels in rat aorta, but not in human mesenteric arteries.

Keywords: XE991, adipocyte-derived relaxing factor (ADRF), perivascular adipose tissue (PVAT), KCNQ channels, K_v channels

INTRODUCTION

Perivascular adipose tissue (PVAT), which surrounds the aorta, its vascular branches and many other arteries, is now recognized as dynamic paracrine organ and important metabolic sensor (Szasz et al., 2013; Gil-Ortega et al., 2015; Gollasch, 2017). PVAT does not only provide mechanical protection to vessels but also regulates vascular function by releasing perivascular adipose relaxing factors (PVRFs), particularly a transferable adipocyte-derived relaxing factor (ADRF), which diminishes the contractile actions of vasoconstrictors such as phenylephrine (PE), serotonin (5-HT), angiotensin II and U46619 (Löhn et al., 2002; Yiannikouris et al., 2010). The anti-contractile effect of PVAT has been observed in both large and small arteries of rats, mice, pigs and humans (Bunker and Laughlin, 1985; Szasz and Webb, 2012; Gollasch, 2017). The anti-contractile effects of PVAT rely on the opening of K^+ channels in vascular smooth muscle cells (VSMCs) (Tano et al., 2014). This action occurs without involvement of NO, prostaglandin I_2 (prostacyclin) or endothelium-derived hyperpolarizing factor (EDHF) (Löhn et al., 2002; Li et al., 2013).

VSMC K_v7 channels are considered to play a key role for vasodilation by ADRF released from PVAT (Gollasch, 2017). Consistently, the anti-contractile effects of PVAT are abolished by the K_v7 channel blocker XE991 in rat and mouse visceral arteries (Löhn et al., 2002; Schleifenbaum et al., 2010; Tsvetkov et al., 2016b). Although, the exact nature of ADRF is unknown, adiponectin, Ang 1–7, H_2S and palmitic acid methyl ester (PAME) have been proposed as ADRF candidates (Fang et al., 2009; Lee et al., 2011; Gu and Xu, 2013; Lynch et al., 2013). The effects of adiponectin on vascular tone are mediated by activation of calcium-activated K^+ (BK_{Ca}) channels on VSMCs and adipocytes and by endothelial mechanisms (Lynch et al., 2013; Baylie et al., 2017), or K_v channel-dependent mechanisms (Fésüs et al., 2007). PAME is one of the most abundant fatty acids in mammalian cells (Lau et al., 2017), and represents an endogenous naturally occurring fatty acid methyl ester (Fukuda et al., 1967). This compound has been reported to have the ability to inhibit Kupffer cells which are resident macrophages in the liver regulating inflammatory processes by secretion of TNF-alpha and NO (Cai et al., 2005). PAME is also known to exhibit anti-fibrotic effects (Fukunishi et al., 2011) and to act as potent vasodilator released in retina and myometrium (Lee et al., 2010, 2011; Crankshaw et al., 2014). A recent report identified PAME as novel, potent vasodilator released from PVAT in rat aorta, which exhibits vascular relaxation by opening K_v channels in smooth muscle cells (Lee et al., 2011). Although these findings suggest that PAME could represent a potential mediator in control of vasotonus and blood pressure in rats, the role of K_v7 channels in PVAT regulation of human arterial tone and vasodilatory PAME effects remains to be established. Therefore, we tested the hypothesis that XE991-sensitive K_v (K_v7) channels are involved in the anti-contractile effects of PVAT on human mesenteric arteries. Furthermore, we investigated the contribution of endogenous PAME to PVAT regulation of arterial tone in human mesenteric arteries and the role of K_v7 channels in vasodilatory PAME effects. Isolated aortic rings from Sprague-Dawley rats were studied for comparison. Finally, we tested whether PAME might contribute to PVAT regulation of arterial tone by involving metabolism of endogenous lipid epoxides.

MATERIALS AND METHODS

Isometric Contractions of Rat Vessels

The local animal review board of Berlin (LAGESO) approved all studies, according to American Physiological Society criteria. Male Sprague-Dawley rats (200–300 g, 8–10 weeks; Charles River, Sulzfeld/Berlin Germany) were killed, and the thoracic aortas were removed, and quickly transferred to cold (4°C) oxygenated (95% O_2/5% CO_2) physiological salt solution (PSS), and dissected into 2 mm rings, respectively. Perivascular fat and connective tissue were either removed [(−) fat] or left [(+) fat] intact as previously described. The rings were placed under force of 20 mN. The bath solution volume was 20 mL of a vessel myograph (Schuler tissue bath system, Hugo Sachs Elektronik, Freiburg, Germany). After 1 h equilibration, contractile force was measured isometrically using standard bath procedures and solutions as described (Dubrovska et al., 2004; Kohn et al., 2012; Brennan et al., 2016).

Cumulative concentration response curves were obtained for PAME (Löhn et al., 2002) in the presence and absence of the K^+ channel or enzyme inhibitors, 10,10-bis(4-pyridinylmethyl)-9(10H)-anthracenone dihydrochloride (XE991); 4-aminopyridine (4-AP); nordihydroguaiaretic acid (NDGA); 17-octadecadiynoic acid (ODYA); or 12-(3-adamantan-1-ylureido)-dodecanoic acid (AUDA). Tension was expressed as a percentage of the steady-state tension (100%) obtained with isotonic external 60 mM KCl. To test for the presence of functional endothelium, rings were contracted with 1 μM PE and once the vessels reached a stable maximum tension, the vessels were stimulated with 10 μM acetylcholine (ACh) and relaxation was confirmed (>80%) (Löhn et al., 2002). In some rings, the endothelium was removed by gently abrading the luminal surface of the vessel with a stainless steel

pin to determine the contribution of the endothelium to PAME relaxation. Functional endothelium was considered absent if 10 μM ACh did not produce relaxation (Löhn et al., 2002).

In bioassay experiments, we transferred aliquots of bath solution from aorta with PVAT incubated in a donor bath chamber to vessel preparations without PVAT in an acceptor bath chamber of the Schuler tissue bath system (Hugo Sachs Elektronik, Freiburg, Germany). Cumulative response curves were obtained in the presence and absence of 5-HT (total incubation time, 5 min). The volume of the solutions in the bath was 20 mL. In most experiments, transfer interval of aliquots was 15–20 min; the volume of the aliquots was 3 or 5 mL. Transfer of bath solution aliquots from aortic vessels without PVAT or fresh PSS did not affect contraction of vessel preparations without PVAT in the acceptor bath chamber (Löhn et al., 2002).

Isometric Contractions of Human Vessels

Procedures were performed in accordance with the ethics guidelines of the National Health and Medical Research Council of Germany. All patients provided informed consent for participation in this study. Mesenteric tissue was taken from 12 patients (1 female, 11 males) undergoing surgical treatment of bowel carcinoma or inflammatory bowel disorders [colon cancer ($n = 3$), sigma cancer ($n = 4$), rectal cancer ($n = 1$), colon adenoma ($n = 1$), Crohn's disease ($n = 1$), and sigmoid diverticulitis ($n = 1$)]. The mean age of the patients was 69 years (range: 46–80), the mean BMI of the patients was 25 kg/m^2 (range: 20–30 kg/m^2), which is expected for the general population, since adopting the WHO classification is that ∼50% or more of the general adult population will always be in the overweight range (now pre-obese, BMI 25–30 kg/m^2), at least in the US and Western Europe (Nuttall, 2015). Few patients were taking drugs, including β-blockers ($n = 4$), angiotensin-converting-enzyme inhibitors ($n = 2$), metformin ($n = 2$), calcium channel blocker ($n = 1$), diuretic ($n = 1$), or fibrates ($n = 1$). Immediately after lower intestinal surgery, mesenteric arteries were excised from resected mesenteric tissue, and quickly transferred to cold (4°C) oxygenated (95% O_2/5% CO_2) PSS, and dissected into 1 mm rings. PVAT was either removed [(−) fat] or left [(+) fat] intact as previously described (Schleifenbaum et al., 2014). Each ring was positioned between two stainless steel wires in a 5-mL organ bath of a Small Vessel Myograph (DMT 610M; Danish Myo Technology, Denmark) (Tsvetkov et al., 2016a). The organ bath was filled with PSS. The bath solution was continuously oxygenated with a gas mixture of 95% O_2 and 5% CO_2, and kept at 37°C (pH 7.4). The rings were placed under force of 3 mN. The software Chart5 (AD Instruments Ltd. Spechbach, Germany) was used for data acquisition and display. The rings were pre-contracted with 60 mM KCl and equilibrated until a stable resting tension was acquired. Chemicals were added to the bath solution if not indicated otherwise. Vessels were pre-contracted with either 5-HT or phenylephrine. All chemicals were added to the bath solution (PSS).

Gas Chromatography/Mass Spectrometry (GC/MS) Analysis

PAME measurements were performed by Shanghai Ingeer Certification Assessment Co, Ltd (ICAS, Shanghai, China). GC/MS analysis was performed using an Agilent ChemStation. For determination of endogenous PAME concentrations in bath solutions, rat peri-aortic and human visceral adipose tissue (3 g each) were incubated in 15 mL-Eppendorf tubes with 10 mL PSS solutions, with or without 5-HT 5 μM (30 min, in 37°C water bath). PSS was oxygenated (95% O_2/5% CO_2) for 30 min before use. After removal of adipose tissue, the PSS solution were dissolved in hexane (1:3 volume ratio), extracted and vortexed. Next, 1 mL water was added to the solution. In order to ensure that the concentration of PAME between the aqueous and the lipophilic phase was in equilibrium the samples were shaken by hand for 4 min. Thereafter, the phases were separated by centrifugation and the lipophilic hexane phase containing fatty acid methyl esters was removed and dried under nitrogen. The fatty acid methyl ester residues were re-dissolved in 50 μL hexane and transferred into an autosampler vial. Samples were analyzed by using a fully automated Agilent 7890A-5977B system equipped with a flame ionization detector. Peaks of re-dissolved PAME were identified by comparison with PAME standard and their nominal concentrations were determined (Yi et al., 2014; Siegert et al., 2017). (+) Fat masses were measured in rat aortic (2 mm) and human mesenteric artery (1 mm) rings ($n = 6$ each) to calculate magnitudes of effective [PAME] in the 20 or 5 mL myograph bath chambers, respectively.

Materials and Statistics

The composition of PSS (in mM) was 119 NaCl, 4.7 KCl, 1.2 KH_2PO4, 25 $NaHCO_3$, 1.2 $MgSO_4$, 11.1 glucose, and 1.6 $CaCl_2$. The composition of 60 mM KCl solution (in mM) was 59 NaCl, 60 KCl, 1.2 KH_2PO4, 25 $NaHCO_3$, 1.2 $MgSO_4$, 11.1 glucose, and 1.6 $CaCl_2$. All salts were purchased from Sigma Aldrich (Schnelldorf, Germany). XE991 was purchased from Tocris (Bristol, UK). 5-HT, phenylephrine (PE), 4-aminopyridine (4-AP), nordihydroguaiaretic acid (NDGA), 17-octadecynoic acid (ODYA), 12-(3-adamantan-1-ylureido)-dodecanoic acid (AUDA) were purchased from Sigma Aldrich (Schnelldorf, Germany). PAME were purchased from Cayman Chemical (Ann Arbor, Michigan, USA).

Data were analyzed by Prism version 5.0 (GraphPad Software, La Jolla, California, USA) and were shown as mean ± SD or mean ± SEM. Paired, unpaired Student's *t*-tests or one-way ANOVA were used as appropriate. In **Figures 1C**, **2C**, statistical significance was determined by two-way ANOVA or repeated-measures two-way ANOVA, followed by Bonferroni *post-hoc* test, and using Prism 6 software. A value of $P < 0.05$ was considered statistically significant; n represents the number of arteries tested.

RESULTS

Contraction of Rat Aortas and Human Mesenteric Arteries With and Without PVAT Under K_v7 Channel Inhibition

We first investigated the role of K_v7 channels in the anti-contractile effects of PVAT in rat aortas. Rat aortic rings without PVAT [(−) fat] showed stronger contractions to 5-HT (relative increase, 60–100% between 2 and 10 μM 5-HT) than vessels

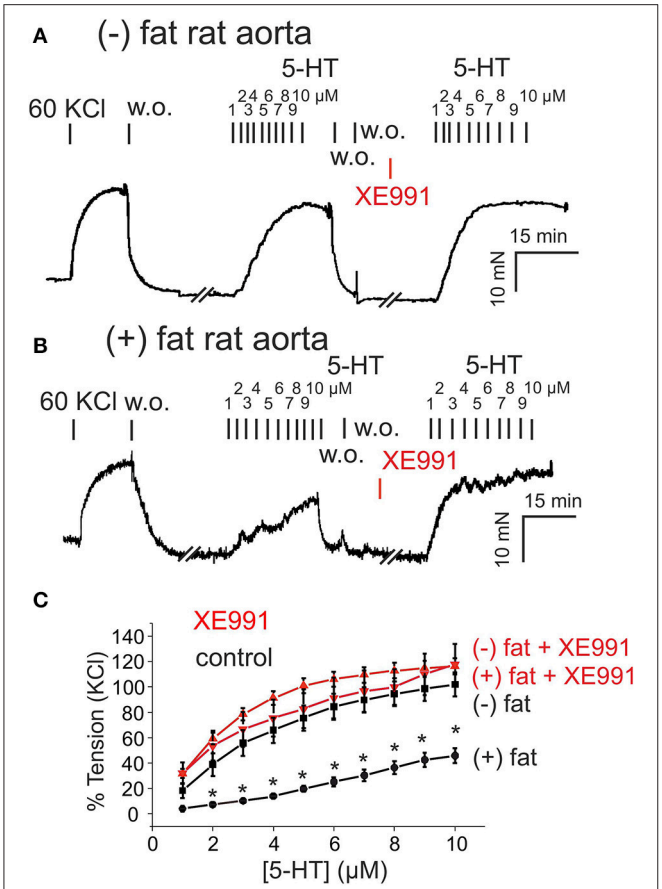

FIGURE 1 | Presence of anti-contractile effects of perivascular adipose tissue (PVAT) in rat aorta and their inhibition by XE991. **(A,B)** Original recordings showing inhibition of the anti-contractile effects of PVAT by XE991. Incubation of (–) fat aortic rings with 30 μM XE-991 **(A)** had no effect on the contractile response. Incubation of (+) fat aortic rings with 30 μM XE991 **(B)** increased the contractile response to 5-HT. **(C)** Concentration-response curves for 5-HT (1–10 μM) in (+) fat vessels in the presence ($n = 6$) and absence of XE991 ($n = 6$) and in (–) fat vessels in the presence ($n = 12$) and absence of XE991 ($n = 6$). *$p < 0.05$ for (+) fat control vessels compared to all other groups each, 60 KCl, 60 mM KCl.

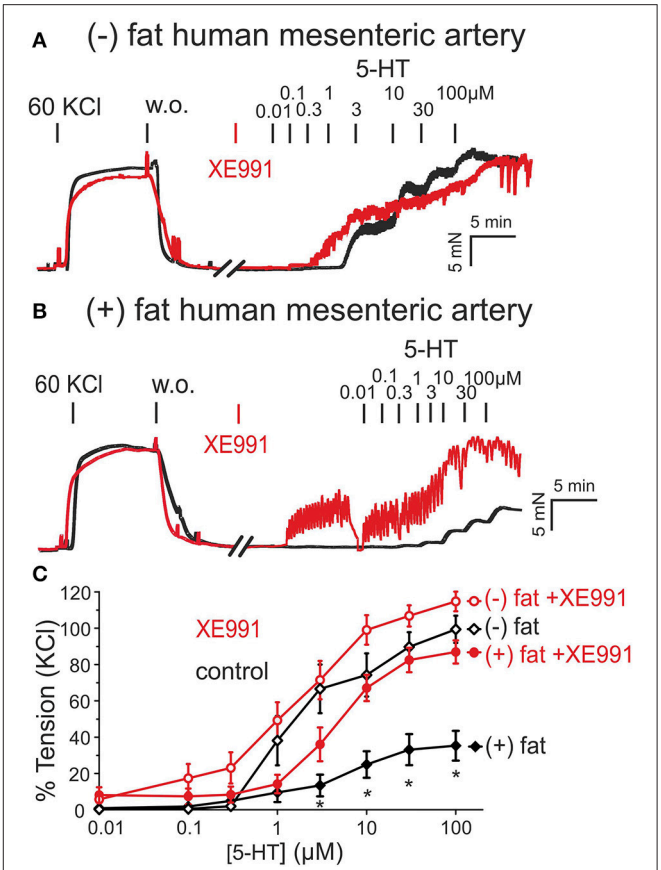

FIGURE 2 | Presence of anti-contractile effects of PVAT in human mesenteric arteries and their inhibition by XE991. **(A,B)** Original recordings showing inhibition of the anti-contractile effects of PVAT by XE991 (30 μM). Recordings are shown in the presence (red curves) and absence (black curves) of XE991. XE991 had no effects on 5-HT contractions in (–) fat rings **(A)**, but increased 5-HT contractions in (+) fat rings **(B)**. **(C)** Concentration-response curves for 5-HT (0.01–100 μM) in (+) fat vessels in the presence ($n = 13$) and absence of XE991 ($n = 15$) and in (–) fat vessels in the presence ($n = 10$) and absence of XE991 ($n = 10$). *$p < 0.05$, $p < 0.05$ for (+) fat control vessels compared to all other groups each.

with PVAT [(+) fat] (**Figure 1**). Incubation of the vessels with the K_v7 channel inhibitor XE991 (30 μM, 30 min) inhibited the anti-contractile effects of PVAT mediated by transferable ADRF in rat aortic rings (**Figures 1B,C**, **Supplementary Figures 1**). XE991 slightly (<20%) increased contractions of (–) fat rat aortic rings in response to 5-HT, but there was no difference between contractions of (–) fat and (+) fat rings in response to 5-HT (**Figures 1A,C**). Contraction of (–) fat and (+) fat aortic rings obtained by 60 mM KCl containing PSS were not different (13.07 ± 1.29 mN, $n = 16$ vs. 10.81 ± 1.19 mN, $n = 14$, $P > 0.05$, respectively).

Similar results were observed in human visceral arteries. Human mesenteric arteries without PVAT [(−) fat] showed significantly stronger contractions in response to 5-HT than vessels with PVAT [(+) fat] (**Figure 2**). Incubation of the vessel rings with XE991 (30 μM, 30 min) inhibited the anti-contractile effects of PVAT (**Figures 2B,C**). XE991 did not affect 5-HT-induced contractions in (–) fat human mesenteric artery rings (**Figures 2A,C**).

Similar data were obtained when vessels were contracted with phenylephrine (**Supplementary Figures 2**). These data suggest that PVAT displays anti-contractile effects in both rat aortas and human mesenteric arteries mediated by XE991-sensitive K_v7 channels, and occur independently of the vasoconstrictor agonists used, i.e., serotoninergic or alpha-adrenergic agonists. Contraction of (–) fat and (+) fat human mesenteric arterial rings obtained by 60 mM KCl containing PSS were not different (19.46 ± 3.60 mN, $n = 10$ vs. 21.00 ± 2.15 mN, $n = 12$, $P > 0.05$, respectively).

PAME Relaxations and Effects of NDGA, ODYA, and AUDA

Exogenous PAME (EC_{50} ~1.4 μM; maximal relaxation E_{max} ~25%) was capable of producing relaxations of (–) fat rat aortas (**Figure 3**). PAME relaxations were not affected by removal

of the endothelium (**Figure 3C**). Pre-treatment of aortic rings with XE991 (30 μM, 30 min) prevented the relaxant effects of PAME (**Figures 3B,F**). PAME effects were not abolished by the K_v channel blocker 4-aminopyridine (4-AP 2 mM, 10 min) (**Figure 3D**) or NDGA (10 μM, 30 min), a lipoxygenases inhibitor (**Figure 3G**). The cytochrome P450 epoxygenase inhibitor 17-octadecynoic acid (ODYA 10 μM, 30 min) slightly inhibited PAME relaxations in rat aorta (**Figure 3E**). However, the soluble epoxide hydrolase inhibitor 12-(3-adamantan-1-ylureido)-dodecanoic acid (AUDA 10 μM, 30 min) did not increase PAME relaxations (**Figure 3H**), which is expected for involvement of P450 expoygenase mediators. Instead, it inhibited PAME relaxations implicating non-specific effects of ODYA in inhibiting PAME effects. PAME up to 10 μM failed to induce relaxations of (–) fat human mesenteric arteries (**Figure 4**). Pre-treatment of the vessels with XE991 (30 μM, 30 min) did not affect the lack of PAME effects (**Figures 4B,C**). Taken together, the results indicate that exogenous PAME at relatively high concentrations (EC_{50} >1 μM) can induce slight (E_{max} ~25%) relaxations in pre-contracted rat aortic rings, which are mediated by opening of K_v7 channels. In contrast, PAME is not a potent vasodilator (up to 10 μM) of human mesenteric arteries.

Role of PAME in ADRF-Containing Bath Solutions of Rat Aortas and Contribution of K_v7 Channels

To demonstrate that the intact aortic preparation releases ADRF which can abrogate vascular contraction by opening VSMC K_v7 channels (Tano et al., 2014; Gollasch, 2017), we performed bioassay experiments where we transferred aliquots of the bath solution from an intact donor preparation incubated in 2 μM 5-HT-containing solution to vessel preparations without PVAT, pre-contracted with 5-HT. This maneuver transferred the factor (Tano et al., 2014; Gollasch, 2017) released by either intact preparations or isolated perivascular adipose tissue (PVAT) (**Figure 5B**) to arteries without adipose tissue (Tano et al., 2014). Bath solutions from (+) fat rings incubated with 5-HT produced stronger relaxations than bath solutions from (+) fat rings incubated in PSS without 5-HT (**Figures 5A** right, **B**), indicating that ADRF release is increased by 5-HT. According to the proposed K_v7 channel mechanism (Tano et al., 2014; Gollasch, 2017), ADRF produced relaxations, which were inhibited by XE991 (30 μM) (**Supplementary Figures 1**). Next, we were interested in [PAME] in ADRF-containing bath solutions and whether PAME release from PVAT can be stimulated by 5 μM 5-HT. We found that 5-HT is capable to release endogenous

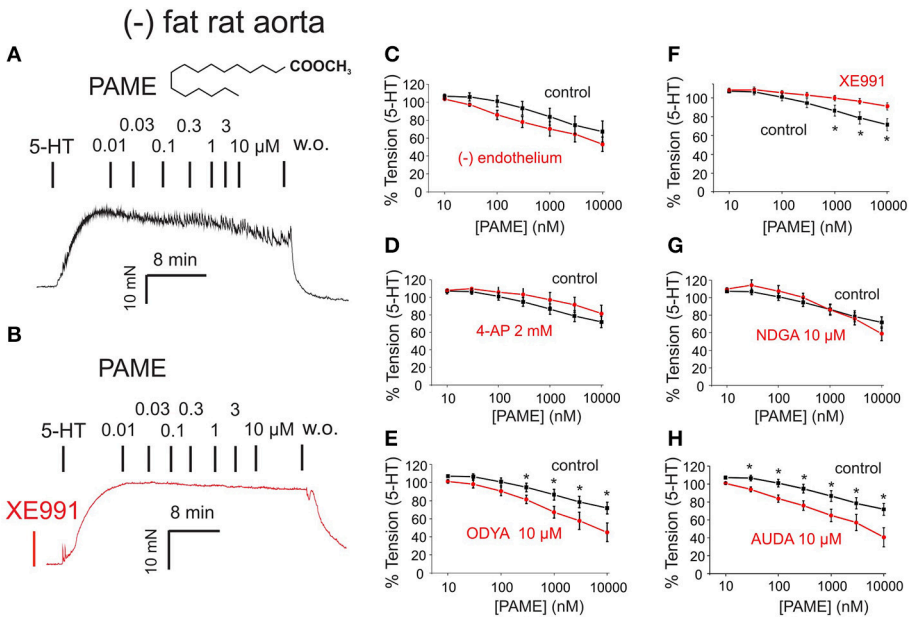

FIGURE 3 | Effects of palmitic acid methyl ester (PAME, 0.01–10 μM) on rat aorta. The effects are shown in the absence (control, black curves) and presence (red curves) of inhibitors of K_v channels [4-aminopiridine (4-AP) 2 mM] or XE991 30 μM, lipoxygenase (LOX 15,12,5) (nordihydroguaiaretic acid (NDGA) 10 μM), cytochrome P450 (CYP) [17-octadecynoic acid (17-ODYA) 10 μM], and soluble epoxide hydrolase (sEH) [12-(3-adamantan-1-yl-ureido)dodecanoic acid (AUDA) 10 μM]. The effects were studied in the presence (+) and absence (–) of endothelium in 2 μM 5-HT precontracted (–) fat aortic rings. **(A,B)** Original recordings demonstrating the relaxant effect of PAME (0.01–10 μM) and inhibition of this effect **(B)** by pre-treatment of the vessels with 30 μM XE991. **(C)** Concentration-response curves for PAME in (–) fat aortic rings in the presence (Control) ($n = 8$) and absence (–) of the endothelium ($n = 6$). **(D)** Concentration-response curves for PAME in the absence ($n = 13$) and presence ($n = 7$) of 2 mM 4-AP in (–) fat aortic rings. **(E)** Concentration-response curves for PAME in non-treated ($n = 13$) and 10 μM 17-ODYA treated ($n = 6$) (–) fat aortic rings. *$p < 0.05$. **(F)** Concentration-response curves for PAME in the absence ($n = 6$) and presence ($n = 6$) of 30 μM XE991 in (–) fat aortic rings. *$p < 0.05$. **(G)** Concentration-response curves for PAME in non-treated ($n = 13$) and 10 μM NDGA ($n = 6$) treated (–) fat aortic rings. **(H)** Concentration-response curves for PAME in non-treated ($n = 13$) and 10 μM AUDA treated ($n = 6$) (–) fat aortic rings. Data are expressed as mean ± SEM. *$p < 0.05$.

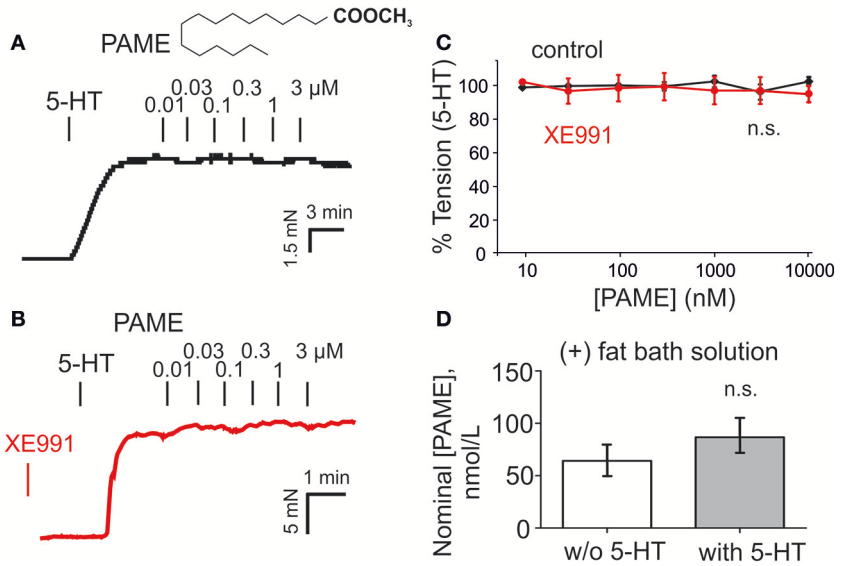

FIGURE 4 | Lack of palmitic acid methyl ester (PAME, 0.01–10 μM) to induce relaxation in human mesenteric artery rings and measurements of PAME in bath solutions from human (+) fat mesenteric artery rings. **(A,B)** Original recordings demonstrating lack of vasorelaxant effects of PAME (0.01–3 μM) in (–) fat rings. Effects of PAME are shown in the absence (control, black curves) and presence (red curves) of XE991. The effects were studied on 2 μM 5-HT pre-contracted (–) fat mesenteric artery rings. **(C)** Concentration-response curves for PAME in (–) fat rings in the presence (Control) (PAME 0.01–3 μM, $n = 12$; PAME 10 μM, $n = 8$) and absence (PAME 0.01–3 μM, $n = 12$; PAME 10 μM, $n = 8$) of XE991. **(D)** Production of PAME shows no difference between bath solutions from human visceral adipose tissue incubated in the presence ($n = 8$) and absence of 5-HT ($n = 8$). w/o, without; n.s., not significant.

PAME from rat aortic PVAT samples (**Figure 5C**). However, the PAME concentrations in 10 mL PSS solutions containing 3 g rat aortic PVAT samples were lower than 300 nM, indicating that effective PAME concentrations in myograph bath chambers are in the range of <1 nM (i.e., 500 times lower). **Figures 5C, 3A–H** show that [PAME] lower than 1 nM are unable to affect wall tension to produce relaxations of (–) rat aortas. These data indicate that PAME cannot be the transferable ADRF we seek.

Endogenously Released PAME Levels in Bath Solutions of Human Visceral Adipose Tissue Are Low and Not Controlled by 5-HT

Endogenously released nominal PAME levels were also detected in aliquots of bath-solutions containing 3 g human visceral adipose tissue in 10 mL PSS (**Figure 4D**). However, in contrast to the rat aorta (**Figure 5C**), PAME levels were even lower and 5-HT (5 μM) was unable to induce endogenous PAME release in the adipose tissue samples. These data indicate that 5-HT can induce PAME release from rat peri-aortic adipose tissue, but not from human visceral adipose tissue, where spontaneous PAME release is even lower and not controlled by 5-HT.

DISCUSSION

In the present study, we investigated the roles of K_V7 channels and PAME in PVAT regulation of arterial tone in human visceral mesenteric arteries. The major findings are that XE991-sensitive K_V (K_V7) channels are involved in the anti-contractile effects of PVAT on human mesenteric arteries, similarly to rat aortas. Furthermore, exogenous PAME displays properties of a PVRF in rat aorta, where it may contribute to paracrine PVAT regulation of arterial tone, but not in human mesenteric arteries. Our data indicate that PAME is not ADRF. Nevertheless, the data support previous findings (Lee et al., 2011) suggesting that fatty acids, particularly perivascular adipose tissue-derived methyl palmitate (PAME), can play a role in paracrine regulation of vascular tone and possibly in the pathogenesis of hypertension in rats, where deficiency or malfunction of K_V channels (Gálvez et al., 2006; Galvez-Prieto et al., 2008), particularly K_V7 channels (Jepps et al., 2011; Li et al., 2013; Zavaritskaya et al., 2013), have been suggested to be involved. Our results suggest that these effects could involve malfunctional K_V7 channels, independently of metabolism of endogenous lipid epoxides. Since the [PAME] released into bath media were exceptionally low, we conclude that PAME released from PVAT only in close proximity to VSMCs can regulate arterial tone in rat aorta.

PVAT Effects and K_V7 Channels

We demonstrated earlier that PVAT markedly attenuates the contractile response to 5-HT, phenylephrine and angiotensin II in aortic and mesenteric ring preparations of rats (Löhn et al., 2002; Verlohren et al., 2004). The data suggest a major role of the K_V7 family of K^+ channels as putative downstream targets of ADRF, which is a major PVRF released from PVAT to reduce arterial

tone (Zavaritskaya et al., 2013; Gollasch, 2017). This suggestion is supported by findings showing that XE991 (K_v7 blocker) inhibited the anti-contractile effects of PVAT in visceral arteries of rats and mice (Schleifenbaum et al., 2010; Tano et al., 2014) (this study). Data were obtained by two different vasoconstrictor agonists, namely 5-HT and phenylephrine, indicating that K_v7 channel targeting could be common mechanism for PVAT regulation of arterial tone. We employed XE991 at 30 μmol/L to ensure effective block of the K_v7 channels because native VSMC $K_v7.4$ and $K_v7.5$ channels are inhibited by this compound with IC_{50} of 5.5 and 65 μmol/L, respectively (Tykocki et al., 2017). The XE991 effects are unlikely mediated by inhibition of BK_{Ca} or $K_v7.1$ channels (Tsvetkov et al., 2016b, 2017). Our present results show that PVAT displayed anti-contractile effects in human mesenteric arteries. The anti-contractile effects were inhibited by XE991, supporting the idea that K_v7 channels are involved in PVAT regulation of arterial tone in humans. Data obtained on *Kcnq1*$^{-/-}$ mice (Tsvetkov et al., 2016b) suggest that these effects are mediated by K_v7 channels distinct from $K_v7.1$, i.e., most likely $K_v7.3$, $K_v7.4$ and/or $K_v7.5$, which are all expressed in mesenteric artery VSMCs from rats (Mackie et al., 2008; Jepps et al., 2011; Zavaritskaya et al., 2013), mice (Yeung et al., 2007; Tsvetkov et al., 2016b, 2017), and humans (Ng et al., 2011).

PAME Effects and K_v7 Channels

We found that PAME was capable to produce relaxations of rat aortas. These effects were inhibited by XE991. The effects were not inhibited 2 mM 4-AP, but see (Lee et al., 2011). In contrast, PAME at similar concentrations did not relax human mesenteric arteries. Together, these data suggest that PAME could contribute to PVAT relaxations by activating K_v7 channels in rat aorta, but not in human mesenteric arteries. The results are in line with the idea that 4-AP is not inhibiting K_v7 channels in rat aorta. We next explored the role of PAME and K_v7 channels in the anti-contractile effects of PVAT in rat aorta using a bioassay approach (Gálvez et al., 2006; Galvez-Prieto et al., 2008). In these experiments, we confirmed earlier findings indicating that 5-HT induces vessel relaxation by releasing a transferable vasoactive substance (ADRF) from PVAT into the bath solution (Maenhaut and Van de Voorde, 2011; Gollasch, 2012). As a negative control, we transferred aliquots of periadventitial fat solution in a similar fashion without 5-HT. We found that these aliquots produced less potent relaxations in rat aortas without PVAT suggesting that 5-HT is capable to stimulate the release of ADRF from PVAT. Moreover, inhibition of K_v7 channels in (–) fat aortic rings by XE991 disrupted these effects in our bioassay experiment. We previously demonstrated that ADRF effects occur without involvement of the endothelium (Gollasch, 2012). Thus, the present data indicate that 5-HT induces ADRF release from PVAT, which displays anti-contractile properties though activation of XE991-sensitive (K_v7) K_v channels in VSMCs. We next focused on PAME bioactivity and release under these conditions. This part of our study is important for understanding the role of PAME as putative ADRF and/or paracrine PVRF. We found that PAME (EC_{50} ~1.4 μM) only slightly relaxed rat aortas (E_{max}, about 25%), whereas similar concentrations of PAME had no effects on human mesenteric arteries.

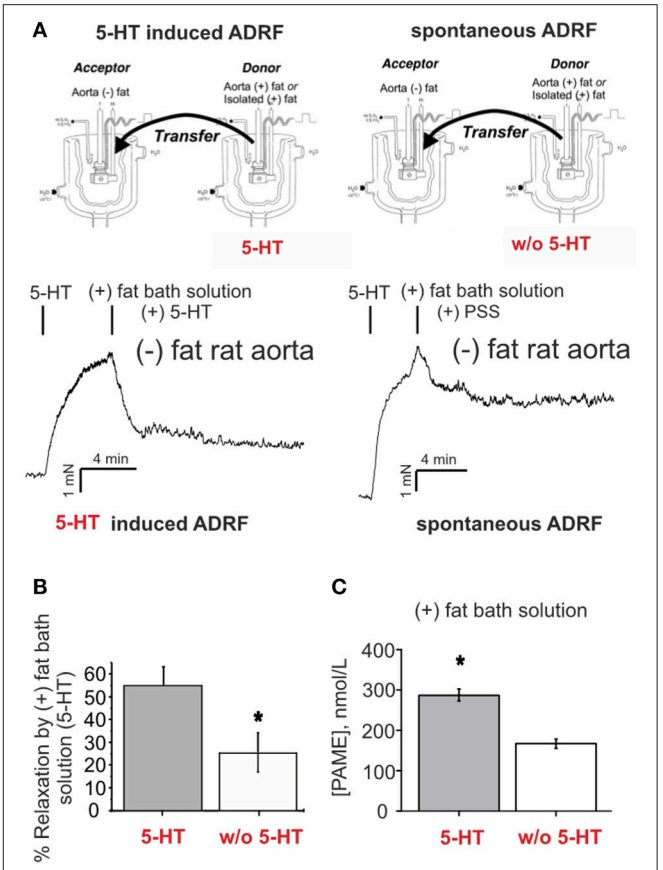

FIGURE 5 | Relaxation of (–) fat aortic rings induced by transfer of bath solutions from (+) fat rat aortic rings. **(A)** Original recordings demonstrating stronger relaxations of ADRF-containing bath solutions from (+) fat rings incubated with 5-HT than from (+) fat rings incubated in PSS without 5-HT. **(B)** Bath solutions from (+) fat rings incubated with 5-HT produced stronger relaxations than bath solutions from (+) fat rings incubated in PSS without 5-HT. Relaxation is expressed as a percentage of the steady-state tension (100%) obtained with 2 μM 5-HT. Data are expressed as mean ± SEM of 6 (left bar) and 5 rings (right bar) prepared from 6 and 5 animals, respectively. **(C)** Bath solutions from rat peri-aortic adipose tissue incubated in the presence 5-HT ($n = 8$) produced more PAME than bath solutions from rat peri-aortic adipose tissue incubated in the absence of 5-HT ($n = 8$). *$p < 0.05$.

PAME Source and Metabolism

Palmitic acid, or hexadecanoic acid in IUPAC nomenclature, is the most common saturated fatty acid found in plants, animals and humans. Together with stearic acid and oleic acid, palmitate acid belongs to the free fatty acids (FFAs), which play an important role as a source of energy for the body (Ibarguren et al., 2014). Endogenous PAME appears to play a role in modulation of the autonomic ganglionic transmission and vasodilatory effects of nitric oxide (NO) (Lin et al., 2008). In plants, palmitate acid can be metabolized through the lipoxygenase pathway (Osipova et al., 2010). However, there is no evidence that palmitate acid is metabolized through the lipoxygenase pathway in animals or humans. Although palmitate acid seems to have some effects on lipoxygenase and cyclooxygenase in platelets (Sakai et al., 1976), there

are no reports that this occurs in other mammalian cells. Consistently, it is not surprising that NDGA, a non-selective lipoxygenase inhibitor, failed to inhibit exogenous PAME relaxation in rat aorta in our study, suggesting no involvement of lipoxygenases metabolites in the PAME effects in the vasculature.

Dietary triacylglycerols with palmitic acid can reduce plasma phospholipid arachidonic and docosahexaenoic acids *in vivo* (Innis and Dyer, 1997). To rule out involvement of cytochrome P450 (CYP) metabolites in PAME relaxation in rat aorta, we tested the effects of a CYP epoxygenases and FFA ω-hydrolases inhibitor (ODYA), and a soluble epoxide hydrolase inhibitor (AUDA), which blocks breakdown and inactivation of CYP–derived active vasodilatory metabolites from arachidonic acid, linoleic acid, eicosapentaenoic acid and docosahexaenoic acid (Hercule et al., 2007, 2009). Since ODYA (10 μM) and AUDA (10 μM) did not produce reciprocal effects on PAME relaxations, we conclude that PAME is a vasodilator in rat aorta independently of metabolism of endogenous lipid epoxides.

PAME Released by PVAT

Most vessels possess some amount and type of PVAT, varying from mostly brown fat (thoracic aorta) to mixed brown and white fat (mesenteric vessels) (Watts et al., 2013). We were able to detect endogenously released PAME in bathing solutions of both rat peri-aortic and human visceral adipose tissues. Furthermore, 5-HT was capable to induce PAME release from rat peri-aortic adipose tissue, indicating a humoral active release process. However, the measured nominal concentrations of PAME were too low to explain transferable ADRF properties in both vascular preparations under study. Together, we suggest that PAME is actively released from PVAT and displays properties of relaxing factor in rat aorta, but not in human mesenteric arteries, where it may contribute as paracrine PVRF to PVAT regulation of arterial tone, independently of metabolism of endogenous lipid epoxides. It will be interesting to determine human mesenteric PVAT is unresponsive to PAME release and action because it is mostly white adipose tissue.

In conclusion, our studies implicate important roles of K_v7 channels in PVAT control of arterial tone in both rat aorta and human mesenteric arteries, which supports previous findings obtained on other, non-human arteries (Gollasch, 2017). Furthermore, our study highlights the potential role of PAME to contribute as paracrine PVRF to regulation of vascular contraction by opening K_v7 channels, at least in rats. Our study has translational implications since malfunction of PVAT/K_v7 channels has been proposed to contribute and to serve as therapeutic targets to improve vascular dysfunction in experimental obesity and hypertension (Rahmouni, 2014), but data on existence of this prototype of vasoregulation in human vessels were missing. Further studies are warranted to investigate PVRFs, K_v7 and other vascular potassium channels to develop new prevention and treatment strategies for cardiovascular disorders associated with obesity and hypertension.

AUTHOR CONTRIBUTIONS

All authors planned and designed the experimental studies. NW, AK, and GD performed the wire myography experiments. NW and MG drafted the article, and all authors, contributed to its completion.

FUNDING

This work was supported by the Deutsche Forschungsgemeinschaft (DFG) and the Deutsche Akademische Austauschdienst (DAAD) to MG and NW was supported by Xiamen University Hospital Nr. 2 and China Council Scholarship. We acknowledge support from the Deutsche Forschungsgemeinschaft (DFG) and the Open Access Publication Fund of Charité - Universitätsmedizin Berlin.

ACKNOWLEDGMENTS

We thank Dmitry Tsvetkov and Xiaoming Lian for discussions and critical reading the manuscript. We also thank Prof. Jochen Strauß (Klinik für Anästhesie, perioperative Medizin und Schmerztherapie, Helios Klinikum Berlin), Prof. Martin Strik and his team (Klinik für Allgemein-, Viszeral- und Onkologische Chirurgie, Helios Klinikum Berlin) for support.

SUPPLEMENTARY MATERIAL

The Supplementary Material for this article can be found online at: https://www.frontiersin.org/articles/10.3389/fphys.2018.00583/full#supplementary-material

Supplementary Figure S1 | Original recordings demonstrating relaxation of (–) fat rat aortic rings by transfer of ADRF-containing bath solutions from (+) fat rat aortic rings **(A)**, and pre-treatment of (–) fat vessels with 30 μM XE991 can inhibit relaxation of transfer ADRF-containing bath solutions in (–) fat rat aortic rings **(B)**.

Supplementary Figure S2 | Presence of anti-contractile effects of perivascular fat in human mesenteric arteries and their inhibition by XE991. **(A,B)** Original recordings showing inhibition of the anti-contractile effects of perivascular fat by XE991 (30 μM). Recordings are shown in the presence (red curves) and absence (black curves) of XE991. XE991 had no effects on phenylephrine contractions in (–) fat rings **(A)**, but increased phenylephrine contractions in (+) fat rings **(B)**. **(C)** Concentration-response curves for phenylephrine in (+) fat vessels in the presence ($n = 23$) and absence of XE991 ($n = 18$) and in (–) fat vessels in the presence (closed circle, $n = 25$) and absence of XE991 ($n = 17$). $^*p < 0.05$ for (+) fat control vessels compared to all other groups each.

REFERENCES

Baylie, R., Ahmed, M., Bonev, A. D., Hill-Eubanks, D. C., Heppner, T. J., Nelson, M. T., et al. (2017). Lack of direct effect of adiponectin on vascular smooth muscle cell BKCa channels or $Ca^{(2+)}$ signaling in the regulation of small artery pressure-induced constriction. *Physiol. Rep.* 5:e13337. doi: 10.14814/phy2.13337

Brennan, L., Morton, J. S., Quon, A., and Davidge, S. T. (2016). Postpartum vascular dysfunction in the reduced uteroplacental perfusion model of preeclampsia. *PLoS ONE* 11:e0162487. doi: 10.1371/journal.pone.0162487

Bunker, A. K., and Laughlin, M. H. (1985). Influence of exercise and perivascular adipose tissue on coronary artery vasomotor function in a familial hypercholesterolemic porcine atherosclerosis model. *J. Appl. Physiol.* 108, 490–497.

Cai, P., Kaphalia, B. S., and Ansari, G. A. (2005). Methyl palmitate: inhibitor of phagocytosis in primary rat Kupffer cells. *Toxicology* 210, 197–204. doi: 10.1016/j.tox.2005.02.001

Crankshaw, D. J., Walsh, J. M., and Morrison, J. J. (2014). The effects of methyl palmitate, a putative regulator from perivascular fat, on the contractility of pregnant human myometrium. *Life Sci.* 116, 25–30. doi: 10.1016/j.lfs.2014.08.018

Dubrovska, G., Verlohren, S., Luft, F. C., and Gollasch, M. (2004). Mechanisms of ADRF release from rat aortic adventitial adipose tissue. *Am. J. Physiol. Heart Circ. Physiol.* 286, H1107–H1113. doi: 10.1152/ajpheart.00656.2003

Fang, L., Zhao, J., Chen, Y., Ma, T., Xu, G., Tang, C., et al. (2009). Hydrogen sulfide derived from periadventitial adipose tissue is a vasodilator. *J. Hypertens.* 27, 2174–2185. doi: 10.1097/HJH.0b013e328330a900

Fésüs, G., Dubrovska, G., Gorzelniak, K., Kluge, R., Huang, Y., Luft, F. C., et al. (2007). Adiponectin is a novel humoral vasodilator. *Cardiovasc. Res.* 75, 719–727. doi: 10.1016/j.cardiores.2007.05.025

Fukuda, J., Mizukami, E., and Imaichi, K. (1967). Production of methyl esters of fatty acids as artifacts during the concentration of methanolic extracts of serum or plasma lipids. *J. Biochem.* 61, 657–658. doi: 10.1093/oxfordjournals.jbchem.a128597

Fukunishi, H., Yagi, H., Kamijo, K., and Shimada, J. (2011). Role of a mutated residue at the entrance of the substrate access channel in cytochrome p450 engineered for vitamin D(3) hydroxylation activity. *Biochemistry* 50, 8302–8310. doi: 10.1021/bi2006493

Gálvez, B., de Castro, J., Herold, D., Dubrovska, G., Arribas, S., Gonzalez, M. C., et al. (2006). Perivascular adipose tissue and mesenteric vascular function in spontaneously hypertensive rats. *Arterioscler. Thromb. Vasc. Biol.* 26, 1297–1302. doi: 10.1161/01.ATV.0000220381.40739.dd

Galvez-Prieto, B., Dubrovska, G., Cano, M. V., Delgado, M., Aranguez, I., Gonzalez, M. C., et al. (2008). A reduction in the amount and anti-contractile effect of periadventitial mesenteric adipose tissue precedes hypertension development in spontaneously hypertensive rats. *Hypertens. Res.* 31, 1415–1423. doi: 10.1291/hypres.31.1415

Gil-Ortega, M., Somoza, B., Huang, Y., Gollasch, M., and Fernandez-Alfonso, M. S. (2015). Regional differences in perivascular adipose tissue impacting vascular homeostasis. *Trends Endocrinol. Metab.* 26, 367–375. doi: 10.1016/j.tem.2015.04.003

Gollasch, M. (2012). Vasodilator signals from perivascular adipose tissue. *Br. J. Pharmacol.* 165, 633–642. doi: 10.1111/j.1476-5381.2011.01430.x

Gollasch, M. (2017). Adipose-vascular coupling and potential therapeutics. *Annu. Rev. Pharmacol. Toxicol.* 57, 417–436. doi: 10.1146/annurev-pharmtox-010716-104542

Gu, P., and Xu, A. (2013). Interplay between adipose tissue and blood vessels in obesity and vascular dysfunction. *Rev. Endocr. Metab. Disord.* 14, 49–58. doi: 10.1007/s11154-012-9230-8

Hercule, H. C., Salanova, B., Essin, K., Honeck, H., Falck, J. R., Sausbier, M., et al. (2007). The vasodilator 17,18-epoxyeicosatetraenoic acid targets the pore-forming BK alpha channel subunit in rodents. *Exp. Physiol.* 92, 1067–1076. doi: 10.1113/expphysiol.2007.038166

Hercule, H. C., Schunck, W. H., Gross, V., Seringer, J., Leung, F. P., Weldon, S. M., et al. (2009). Interaction between P450 eicosanoids and nitric oxide in the control of arterial tone in mice. *Arterioscler. Thromb. Vasc. Biol.* 29, 54–60. doi: 10.1161/ATVBAHA.108.171298

Ibarguren, M., Lopez, D. J., and Escriba, P. V. (2014). The effect of natural and synthetic fatty acids on membrane structure, microdomain organization, cellular functions and human health. *Biochim. Biophys. Acta* 1838, 1518–1528. doi: 10.1016/j.bbamem.2013.12.021

Innis, S. M., and Dyer, R. (1997). Dietary triacylglycerols with palmitic acid (16:0) in the 2-position increase 16:0 in the 2-position of plasma and chylomicron triacylglycerols, but reduce phospholipid arachidonic and docosahexaenoic acids, and alter cholesteryl ester metabolism in formula-Fed piglets. *J. Nutr.* 127, 1311–1319. doi: 10.1093/jn/127.7.1311

Jepps, T. A., Chadha, P. S., Davis, A. J., Harhun, M. I., Cockerill, G. W., Olesen, S. P., et al. (2011). Downregulation of Kv7.4 channel activity in primary and secondary hypertension. *Circulation* 124, 602–611. doi: 10.1161/CIRCULATIONAHA.111.032136

Kohn, C., Schleifenbaum, J., Szijarto, I. A., Marko, L., Dubrovska, G., Huang, Y., et al. (2012). Differential effects of cystathionine-γ-lyase-dependent vasodilatory H2S in periadventitial vasoregulation of rat and mouse aortas. *PLoS ONE* 7:e41951. doi: 10.1371/journal.pone.0041951

Lau, C. E., Tredwell, G. D., Ellis, J. K., Lam, E. W., and Keun, H. C. (2017). Metabolomic characterisation of the effects of oncogenic PIK3CA transformation in a breast epithelial cell line. *Sci. Rep.* 7:46079. doi: 10.1038/srep46079

Lee, Y. C., Chang, H. H., Chiang, C. L., Liu, C. H., Yeh, J. I., Chen, M. F., et al. (2011). Role of perivascular adipose tissue-derived methyl palmitate in vascular tone regulation and pathogenesis of hypertension. *Circulation* 124, 1160–1171. doi: 10.1161/CIRCULATIONAHA.111.027375

Lee, Y. C., Chang, H. H., Liu, C. H., Chen, M. F., Chen, P. Y., Kuo, J. S., et al. (2010). Methyl palmitate: a potent vasodilator released in the retina. *Invest. Ophthalmol. Vis. Sci.* 51, 4746–4753. doi: 10.1167/iovs.09-5132

Li, R., Andersen, I., Aleke, J., Golubinskaya, V., Gustafsson, H., and Nilsson, H. (2013). Reduced anti-contractile effect of perivascular adipose tissue on mesenteric small arteries from spontaneously hypertensive rats: role of Kv7 channels. *Eur. J. Pharmacol.* 698, 310–315. doi: 10.1016/j.ejphar.2012.09.026

Lin, H. W., Liu, C. Z., Cao, D., Chen, P. Y., Chen, M. F., Lin, S. Z., et al. (2008). Endogenous methyl palmitate modulates nicotinic receptor-mediated transmission in the superior cervical ganglion. *Proc. Natl. Acad. Sci. U.S.A.* 105, 19526–19531. doi: 10.1073/pnas.0810262105

Löhn, M., Dubrovska, G., Lauterbach, B., Luft, F. C., Gollasch, M., and Sharma, A. M. (2002). Periadventitial fat releases a vascular relaxing factor. *FASEB J.* 16, 1057–1063. doi: 10.1096/fj.02-0024com

Lynch, F. M., Withers, S. B., Yao, Z., Werner, M. E., Edwards, G., Weston, A. H., et al. (2013). Perivascular adipose tissue-derived adiponectin activates BK(Ca) channels to induce anticontractile responses. *Am. J. Physiol. Heart Circ. Physiol.* 304, H786–H795. doi: 10.1152/ajpheart.00697.2012

Mackie, A. R., Brueggemann, L. I., Henderson, K. K., Shiels, A. J., Cribbs, L. L., Scrogin, K. E., et al. (2008). Vascular KCNQ potassium channels as novel targets for the control of mesenteric artery constriction by vasopressin, based on studies in single cells, pressurized arteries, and *in vivo* measurements of mesenteric vascular resistance. *J. Pharmacol. Exp. Ther.* 325, 475–483. doi: 10.1124/jpet.107.135764

Maenhaut, N., and Van de Voorde, J. (2011). Regulation of vascular tone by adipocytes. *BMC Med.* 9:25. doi: 10.1186/1741-7015-9-25

Ng, F. L., Davis, A. J., Jepps, T. A., Harhun, M. I., Yeung, S. Y., Wan, A., et al. (2011). Expression and function of the K+ channel KCNQ genes in human arteries. *Br. J. Pharmacol.* 162, 42–53. doi: 10.1111/j.1476-5381.2010.01027.x

Nuttall, F. Q. (2015). Body mass index: obesity, BMI, and health: a critical review. *Nutr. Today* 50, 117–128. doi: 10.1097/NT.0000000000000092

Osipova, E. V., Lantsova, N. V., Chechetkin, I. R., Mukhitova, F. K., Hamberg, M., and Grechkin, A. N. (2010). Hexadecanoid pathway in plants: lipoxygenase dioxygenation of (7Z,10Z,13Z)-hexadecatrienoic acid. *Biochem. Mosc.* 75, 708–716. doi: 10.1134/S0006297910060052

Rahmouni, K. (2014). Obesity-associated hypertension: recent progress in deciphering the pathogenesis. *Hypertension* 64, 215–221. doi: 10.1161/HYPERTENSIONAHA.114.00920

Sakai, S., Ryoyama, K., Koshimura, S., and Migita, S. (1976). Studies on the properties of a streptococcal preparation OK-432 (NSC-B116209) as an immunopotentiator. I. Activation of serum complement components and peritoneal exudate cells by group A streptococcus. *Jpn. J. Exp. Med.* 46, 123–133.

Schleifenbaum, J., Kassmann, M., Szijarto, I. A., Hercule, H. C., Tano, J. Y., Weinert, S., et al. (2014). Stretch-activation of angiotensin II type 1a receptors contributes to the myogenic response of mouse mesenteric and renal arteries. *Circ. Res.* 115, 263–272. doi: 10.1161/CIRCRESAHA.115.302882

Schleifenbaum, J., Kohn, C., Voblova, N., Dubrovska, G., Zavarirskaya, O., Gloe, T., et al. (2010). Systemic peripheral artery relaxation by KCNQ channel openers and hydrogen sulfide. *J. Hypertens.* 28, 1875–1882. doi: 10.1097/HJH.0b013e32833c20d5

Siegert, E., Paul, F., Rothe, M., and Weylandt, K. H. (2017). The effect of omega-3 fatty acids on central nervous system remyelination in fat-1 mice. *BMC Neurosci.* 18:19. doi: 10.1186/s12868-016-0312-5

Szasz, T., Bomfim, G. F., and Webb, R. C. (2013). The influence of perivascular adipose tissue on vascular homeostasis. *Vasc. Health Risk Manag.* 9, 105–116. doi: 10.2147/VHRM.S33760

Szasz, T., and Webb, R. C. (2012). Perivascular adipose tissue: more than just structural support. *Clin. Sci.* 122, 1–12. doi: 10.1042/CS20110151

Tano, J. Y., Schleifenbaum, J., and Gollasch, M. (2014). Perivascular adipose tissue, potassium channels, and vascular dysfunction. *Arterioscler. Thromb. Vasc. Biol.* 34, 1827–1830. doi: 10.1161/ATVBAHA.114.303032

Tsvetkov, D., Kassmann, M., Tano, J. Y., Chen, L., Schleifenbaum, J., Voelkl, J., et al. (2017). Do KV 7.1 channels contribute to control of arterial vascular tone? *Br. J. Pharmacol.* 174, 150–162. doi: 10.1111/bph.13665

Tsvetkov, D., Shymanets, A., Huang, Y., Bucher, K., Piekorz, R., Hirsch, E., et al. (2016a). Better understanding of Phosphoinositide 3-Kinase (PI3K) pathways in vasculature: towards precision therapy targeting angiogenesis and tumor blood supply. *Biochem. Mosc.* 81, 691–699. doi: 10.1134/S0006297916070051

Tsvetkov, D., Tano, J. Y., Kassmann, M., Wang, N., Schubert, R., and Gollasch, M. (2016b). The role of DPO-1 and XE991-sensitive potassium channels in perivascular adipose tissue-mediated regulation of vascular tone. *Front. Physiol.* 7:335. doi: 10.3389/fphys.2016.00335

Tykocki, N. R., Boerman, E. M., and Jackson, W. F. (2017). Smooth muscle ion channels and regulation of vascular tone in resistance arteries and arterioles. *Compr. Physiol.* 7, 485–581. doi: 10.1002/cphy.c160011

Verlohren, S., Dubrovska, G., Tsang, S. Y., Essin, K., Luft, F. C., Huang, Y., et al. (2004). Visceral periadventitial adipose tissue regulates arterial tone of mesenteric arteries. *Hypertension* 44, 271–276. doi: 10.1161/01.HYP.0000140058.28994.ec

Watts, S. W., Dorrance, A. M., Penfold, M. E., Rourke, J. L., Sinal, C. J., Seitz, B., et al. (2013). Chemerin connects fat to arterial contraction. *Arterioscler. Thromb. Vasc. Biol.* 33, 1320–1328. doi: 10.1161/ATVBAHA.113.301476

Yeung, S. Y., Pucovsky, V., Moffatt, J. D., Saldanha, L., Schwake, M., Ohya, S., et al. (2007). Molecular expression and pharmacological identification of a role for K(v)7 channels in murine vascular reactivity. *Br. J. Pharmacol.* 151, 758–770. doi: 10.1038/sj.bjp.0707284

Yi, T., Li, S. M., Fan, J. Y., Fan, L. L., Zhang, Z. F., Luo, P., et al. (2014). Comparative analysis of EPA and DHA in fish oil nutritional capsules by GC-MS. *Lipids Health Dis.* 13:190. doi: 10.1186/1476-511X-13-190

Yiannikouris, F., Gupte, M., Putnam, K., and Cassis, L. (2010). Adipokines and blood pressure control. *Curr. Opin. Nephrol. Hypertens.* 19, 195–200. doi: 10.1097/MNH.0b013e3283366cd0

Zavaritskaya, O., Zhuravleva, N., Schleifenbaum, J., Gloe, T., Devermann, L., Kluge, R., et al. (2013). Role of KCNQ channels in skeletal muscle arteries and periadventitial vascular dysfunction. *Hypertension* 61, 151–159. doi: 10.1161/HYPERTENSIONAHA.112.197566

Conflict of Interest Statement: The authors declare that the research was conducted in the absence of any commercial or financial relationships that could be construed as a potential conflict of interest.

frontiers in Physiology

ORIGINAL RESEARCH
published: 18 April 2018
doi: 10.3389/fphys.2018.00400

Decrease of Perivascular Adipose Tissue Browning Is Associated With Vascular Dysfunction in Spontaneous Hypertensive Rats During Aging

Ling-Ran Kong[1], Yan-Ping Zhou[1], Dong-Rui Chen[1], Cheng-Chao Ruan[1,2] and Ping-Jin Gao[1,2]*

[1] State Key Laboratory of Medical Genomics, Shanghai Key Laboratory of Hypertension, Department of Hypertension at Ruijin Hospital and Shanghai Institute of Hypertension, Shanghai Jiao Tong University School of Medicine, Shanghai, China, [2] Key Laboratory of Stem Cell Biology, Institute of Health Sciences, Shanghai Jiao Tong University School of Medicine and Shanghai Institutes for Biological Sciences, Chinese Academy of Sciences, Shanghai, China

OPEN ACCESS

Edited by:
Maik Gollasch,
Charité – Universitätsmedizin Berlin, Germany

Reviewed by:
Hamidah Abu Bakar,
University of Selangor, Malaysia
Bradley S. Fleenor,
Ball State University, United States

***Correspondence:**
Cheng-Chao Ruan
ccruan@sibs.ac.cn

Specialty section:
This article was submitted to Vascular Physiology, a section of the journal Frontiers in Physiology

Received: 08 January 2018
Accepted: 04 April 2018
Published: 18 April 2018

Citation:
Kong L-R, Zhou Y-P, Chen D-R, Ruan C-C and Gao P-J (2018) Decrease of Perivascular Adipose Tissue Browning Is Associated With Vascular Dysfunction in Spontaneous Hypertensive Rats During Aging. Front. Physiol. 9:400. doi: 10.3389/fphys.2018.00400

Functional perivascular adipose tissue (PVAT) is necessary to maintain vascular physiology through both mechanical support and endocrine or paracrine ways. PVAT shows a brown adipose tissue (BAT)-like feature and the browning level of PVAT is dependent on the anatomic location and species. However, it is not clear whether PVAT browning is involved in the vascular tone regulation in spontaneously hypertensive rats (SHRs). In the present study, we aimed to illustrate the effect of aging on PVAT browning and subsequent vasomotor reaction in SHRs. Herein we utilized histological staining and western blot to detect the characteristics of thoracic PVAT (tPVAT) in 8-week-old and 16-week-old SHR and Wistar-Kyoto (WKY) rats. We also detected vascular reactivity analysis to determine the effect of tPVAT on vasomotor reaction during aging. The results showed that tPVAT had a similar phenotype to BAT, including smaller adipocyte size and positive uncoupling protein-1 (UCP1) staining. Interestingly, the tPVAT of 8-week-old SHR showed increased BAT phenotypic marker expression compared to WKY, whereas the browning level of tPVAT had a more dramatic decrease from 8 to 16 weeks of age in SHR than age-matched WKY rats. The vasodilation effect of tPVAT on aortas had no significant difference in 8-week-old WKY and SHR, whereas this effect is obviously decreased in 16-week-old SHR compared to WKY. In contrast, tPVAT showed a similar vasoconstriction effect in 8- or 16-week-old WKY and SHR rats. Moreover, we identified an important vasodilator adenosine, which regulates adipocyte browning and may be a potential PVAT-derived relaxing factor. Adenosine is dramatically decreased from 8 to 16 weeks of age in the tPVAT of SHR. In summary, aging is associated with a decrease of tPVAT browning and adenosine production in SHR rats. These may result in attenuated vasodilation effect of the tPVAT in SHR during aging.

Keywords: PVAT, browning, adenosine, vasodilation, SHR

INTRODUCTION

Perivascular adipose tissue (PVAT) is a structure surrounding most of the blood vessels, which plays vital roles in vascular physiopathology (Brown et al., 2014). As an essential part of the vasculature, PVAT is involved in various vascular diseases, including atherosclerosis, aneurysm, and hypertension (Takemori et al., 2007; Verhagen and Visseren, 2011; Sakaue et al., 2017). It is well established that adipose tissue includes brown adipose tissue (BAT) and white adipose tissue (WAT). WAT predominately serves to store energy. In contrast, BAT dissipates energy through uncoupled respiration and thermogenesis, and protects against metabolic disorders (Kozak, 2010). PVAT shows a BAT-like feature and the browning level of PVAT is dependent on the anatomic location and species (Britton and Fox, 2011). Thoracic PVAT (tPVAT) shares structural, genetic, and proteomics features with BAT (Chang et al., 2012), including several small multilocular lipid droplets and abundant mitochondria. Previous studies showed that the tPVAT of spontaneously hypertensive rats (SHRs) has structural and functional changes compared with Wistar-Kyoto (WKY) rats (Galvez et al., 2006). Hypertension is a highly prevalent disease with advancing age. Aging is also associated with whole-body adipose tissue redistribution, with a relative loss of BAT in interscapular area and an accumulation of WAT in the trunk and visceral areas (Schosserer et al., 2017). Several reports suggest that aging induces superoxide production and inhibits adiponectin expression in PVAT, leading to arterial stiffening (Fleenor et al., 2014; Agabiti-Rosei et al., 2017). However, little is known about the changes in browning level in the tPVAT of SHR rats during aging.

As an active endocrine organ, PVAT not only releases abundant adipokines to regulate vascular functions, it can also produce small molecular active substances such as nitric oxide and reactive oxygen species, which could directly regulate vascular contraction and relaxation (Victorio et al., 2016). For example, compared to WKY, the PVAT of SHR releases significantly less methyl palmitate, these contribute to vascular tone regulation and pathogenesis of hypertension (Lee et al., 2011). However, there are many other PVAT derivatives which may play important roles under both physiological and pathological conditions. Adenosine, a vasorelaxant substance, is an endogenous purine nucleoside comprised of adenine and ribose joined by a glycosidic bond (Borea et al., 2016). The terminal synthesis of extracellular adenosine is mediated by CD73 (ecto-5-nucleotidase), following activity of CD39 (nucleoside triphosphate dephosphorylase). It is well known that adenosine formed by CD73 plays a key role in the regulation of cardiac inflammation and fibrosis (Quast et al., 2017). Adenosine could be produced by adipocytes through activating CD73 (Burghoff et al., 2013). It is a novel activator of brown and beige fat, and abundantly exists in BAT (Gnad et al., 2014).Therefore, we speculated that adenosine might be a PVAT-derived relaxing factor (PVRF) and we hypothesized that the aging-reduced browning level of PVAT is associated with decrease of adenosine production, which is associated with the regulation of vasomotor reaction in SHR rats.

MATERIALS AND METHODS

Animals

Experiments were conducted in 8-week-old and 16-week-old male WKY and SHR. The rats were provided by Shanghai SLAC Laboratory Animal Company. Body weight was measured in conscious animals, then the rats were anesthetized with intraperitoneal injection of pentobarbital (5 mg/100 g) and sacrificed. The tPVAT, subcutaneous WAT (sWAT), and interscapular BAT (iBAT) were dissected out and immersed in liquid nitrogen immediately for subsequent analysis. Animals were housed under standard laboratory conditions and had a free access to drinking water and food. All animal procedures were approved in accordance with institutional guidelines established by the Committee of Ethics on Animal Experiments at the Shanghai Jiao Tong University School of Medicine.

Blood Pressure and Body Weight Measurement

Blood pressures were measured as described previously (Jin et al., 2017). Briefly, systolic and diastolic blood pressure (SBP and DBP) was measured in conscious rats by the tail-cuff method (BP-2000, Visitech Systems, United States) and the average of at least 20 readings was calculated. Blood pressure and body weight were measured with 10 rats in each group.

Histological Analysis

For hematoxylin/eosin (HE) staining, thoracic aortas with intact surrounding tPVAT were fixed in 10% formaldehyde at 4°C for 48 h, washed in water, and embedded in paraffin. Cross-sections (5 μm) were deparaffinized in xylene, rehydrated, and washed in physiological basic salt solution (PBS). PVAT cross-sectional area was measured by HE staining as previously described (Ma et al., 2010). Images were captured using a Carl Zeiss Axio Imager M2 microscope (Carl Zeiss Corporation, Germany). Morphometric analysis was performed with software Image-Pro Plus (Media Cybernetics, United States) by counting the number of adipocytes in the same area (×200 magnification image) of four animals in each group as previously described (Sheng et al., 2016).

To identify brown adipocytes from white adipocytes in the tPVAT, we performed UCP1 immunohistochemical staining in PVAT of SHR and WKY rats. Endogenous peroxidase activity was quenched in hydrogen peroxide for 10–15 min and then the sections were washed three times in PBS buffer. Sections were then incubated with the primary antibody, anti-rabbit UCP1 antibody (1:100 dilution) (Abcam, ab23841) at 4°C overnight, and then washed in PBS and incubated with the secondary antibody (1:200 dilution) (Proteintech, SA00001-2). Tissue sections were counterstained with Mayer's hematoxylin solution, rinsed in running tap water, dehydrated, and mounted with permanent mounting medium. Control sections were incubated with PBS in place of the primary antibody. Sections with primary antibody omitted in staining were used as controls. UCP1-positive adipocyte area was counted under microscope with the software Image-Pro Plus (Media Cybernetics, United States).

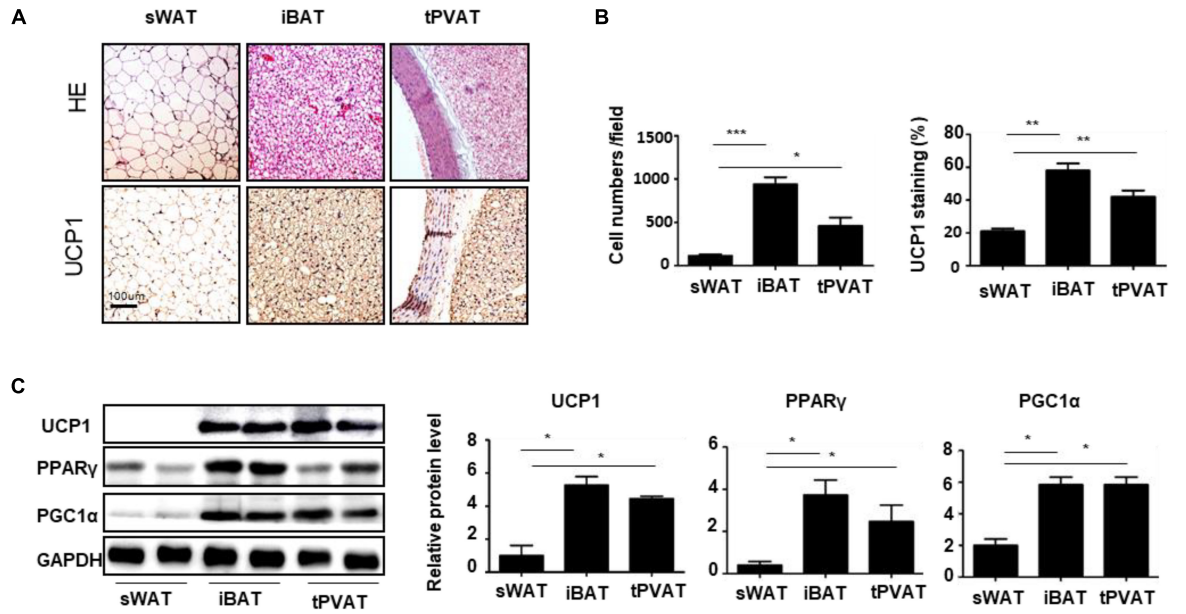

FIGURE 1 | Characteristic differences among sWAT, iBAT, and tPVAT. **(A)** Representative HE and UCP1 staining images of sWAT, iBAT, and tPVAT from 8-week-old WKY rats. Magnification bar = 100 μm. **(B)** Quantitative analysis of cell numbers and UCP1 signals in sWAT, iBAT, and tPVAT from WKY rats ($n = 4$). **(C)** Western blot analysis of UCP1, PGC1α, and PPARγ protein levels in sWAT, iBAT, and tPVAT. GAPDH serves as internal control. Quantitative results are shown on the right ($n = 4$). $^{*}p < 0.05$; $^{**}p < 0.01$; $^{***}p < 0.001$.

Western Blot Analysis

The frozen tPVAT, sWAT, and iBAT tissues were lysed in RIPA buffer (Merck Millipore, 20-188) containing 1% protease inhibitor cocktail (Biotool, B14002). The protein extractions were collected for western blot as previously described (Harms et al., 2014). The primary antibodies were as follows: anti-UCP1 (1:1000 dilution) (Abcam, ab23841), anti-peroxisome proliferator-activated receptor-γ (PPARγ, 1:1000 dilution) (Santa Cruz, sc-7273), anti-PPARγ-coactivator 1-α (PGC1α, 1:1000 dilution) (Santa Cruz, sc-13067), anti-CD73 (1:1000 dilution) (Abcam, ab108248), and GAPDH monoclonal antibody (1:4000 dilution) (Proteintech, HRP-6004). Immunoreactive bands were highlighted by electrochemiluminescence (ECL) technology and quantified using imaging software Quantity One (Bio-Rad Laboratory, Spain).

Vascular Reactivity in Thoracic Arteries

Thoracic aorta from 8-week-old WKY was isolated and the PVAT was carefully removed. The aorta was cut into 2–3 mm rings and put in cell culture plate. tPVAT (0.3 g) was obtained from 8-week-old or 16-week-old donor WKY and SHR under anesthesia and snipped into small pieces. The rings were incubated with tPVAT in Dulbecco's Modified Eagle's Medium (DMEM) for 12 h in 37°C. Then each aorta was fixed on the isometric force transducer (Danish Myo Technology Model 610 M, Denmark) in a 5 ml organ bath, aerating with 95% O_2 and 5% CO_2 under an initial resting tension of 2.5 mN (Zhou et al., 2014). Lumen diameter was recorded in a Power Lab/8sp data acquisition system (A.D. Instruments, Castle Hill, Australia). Aorta was incubated in oxygenated Krebs' medium (containing: KCl 4.7 mM, NaCl 118 mM, $CaCl_2$ 2.5 mM, KH_2PO_4 1.2 mM, $MgSO_4$ 1.2 mM, glucose 11 mM, and $NaHCO_3$, 25 mM) for 60 min at pH 7.4 and 37°C. The contractility was tested three times by high K^+ mediums (60 mM KCl) to stabilize the contraction. A dose–response curve of phenylephrine (PHE, 0.01–100 μM) was performed to assess the vasoconstriction response and cumulative concentration–response curves of acetylcholine (ACH, 0.01–100 μM) were constructed with a PHE pre-contraction (3 μM). For testing vascular reactivity, we isolated the tPVAT from 8-week-old WKY, 16-week-old WKY, 8-week-old SHR, and 16-weeke-old SHRs, respectively.

Adenosine Measurement

Adenosine level in the conditioned medium was determined using mouse/rat adenosine ELISA kit (zc-54044, ZCI BIO). Briefly, the tPVAT was incubated in DMEM for 12 h and the medium was centrifuged at 3000 rpm for 10 min. Then the medium was immediately stored at −80°C until assaying. ELISA was performed according to the manufacturer's instructions. A monoclonal antibody specific for mouse/rat adenosine was pre-coated onto a microplate. Standards and samples were pipetted into the wells and any adenosine present was bound by the immobilized antibody. After washing away any unbound substances, an enzyme-linked polyclonal antibody specific for mouse/rat adenosine was added to the wells. Following a wash to remove any unbound antibody–enzyme reagents, a substrate solution was added to the wells. The enzyme reaction yielded a blue product that turned yellow when the stop solution was added. The intensity of the color measured is in proportion to the amount of adenosine bound in the initial step. The sample values

were then read off the standard curve. The reactions were read using an ELISA reader RT-6000 (Rayto, United States) at 450 nm. Data are expressed in pictogram per milliliter.

Statistical Analysis

All values are given as means ± SEM. Statistical analysis was performed using one-tailed or two-tailed Student's *t*-test. For experiments in which more than two groups were compared, two-way analysis of variant (ANOVA) was used and followed by the *post hoc* Dunnett's test for data with more than two groups (Levene's tests for equal variance). Dunnett's T3 test was used for *post hoc* test comparison for the analysis of unequal variances (Welch's and Brown–Forsythe's test). *P*-value of 0.05 or less was deemed statistically significant in all of these statistical tests.

RESULTS

Characteristics of tPVAT

To explore the characteristics of tPVAT, we detected the sWAT, iBAT, and tPVAT from WKY rats. HE staining revealed that tPVAT showed a similar phenotype to iBAT, including smaller adipocyte size and increased UCP1 staining compared to sWAT (**Figures 1A,B**). Moreover, tPVAT and iBAT shared a similar thermogenic marker protein expression pattern including UCP1, PPARγ, and PGC1α (**Figure 1C**). These demonstrate that tPVAT has similar features to iBAT, whereas it is clearly different from sWAT.

Characteristics of tPVAT Browning in SHR During Aging

Next, we determined the changes in the tPVAT in WKY and SHRs during aging. The body weight of WKY rats at 8 and 16 weeks of age was higher than those of SHR (227.2 ± 4.6 g in 8-week-old WKY, 203.6 ± 2.1 g in 8-week-old SHR, 256.3 ± 6.6 g in 16-week-old WKY, and 227.2 ± 4.6 g in 16-week-old SHR) (**Figure 2A**). The SBP and DBP showed a much greater increase in SHR compared with WKY at 16 weeks of age (SBP 125.3 ± 2.6 mmHg and DBP 93.1 ± 2.7 mmHg in 16-week-old WKY, SBP 177.3 ± 2.8 mmHg and 132.1 ± 3.5 mmHg in 16-week-old SHR), whereas the SBP and DBP had a slight increase in 8-week-old SHR (SBP 114.2 ± 2.4 mmHg and DBP

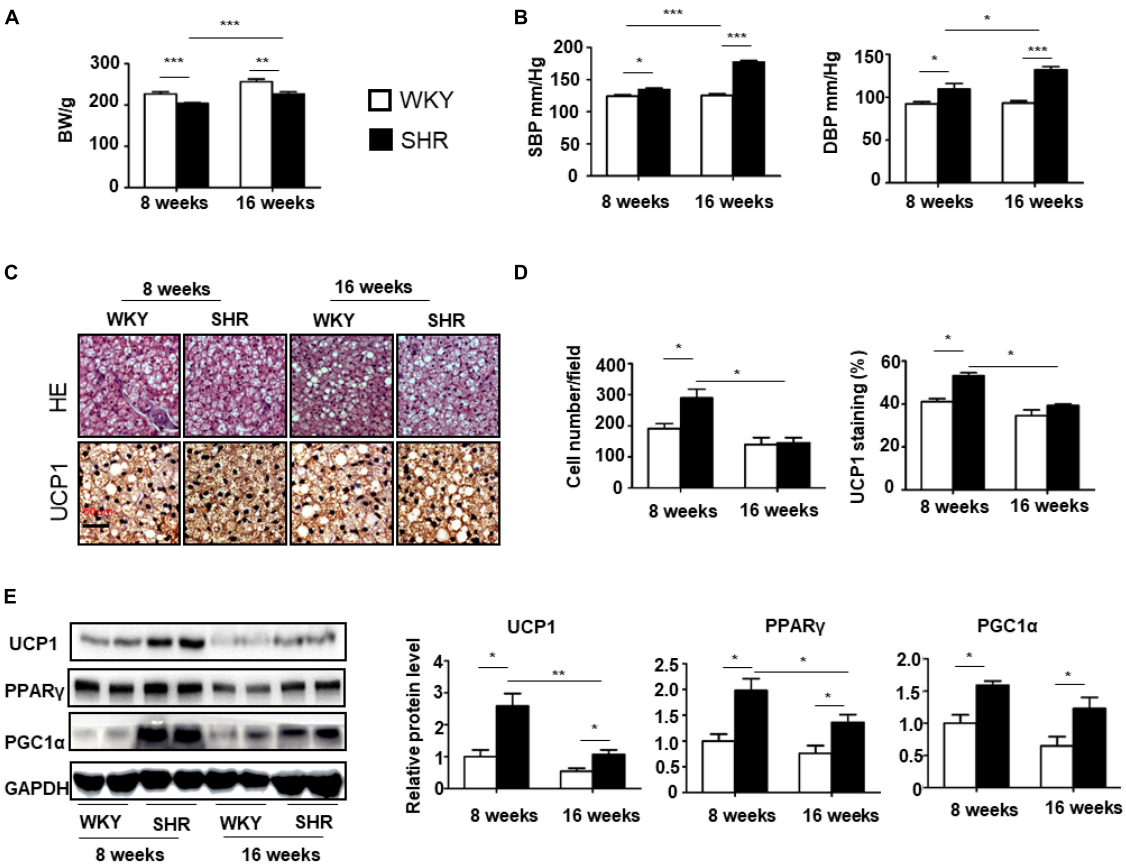

FIGURE 2 | Browning level of tPVAT increases in SHR during aging. **(A)** The body weight of 8-week-old and 16-week-old WKY and SHR (n = 10). **(B)** The SBP and DBP of 8-week-old and 16-week-old WKY and SHR (n = 10). **(C)** Representative HE and UCP1 staining images of the tPVAT of 8-week-old and 16-week-old WKY and SHR. Magnification bar = 50 μm. **(D)** Quantitative analysis of cell numbers and UCP1 signals in tPVAT from 8-week-old and 16-week-old WKY and SHR rats (n = 4). **(E)** Western blot analysis of UCP1, PGC1a, and PPARγ expression levels in the tPVAT of 8-week-old and 16-week-old WKY and SHR. Quantitative results are shown on the right (n = 4). *$p < 0.05$; **$p < 0.01$; ***$p < 0.001$.

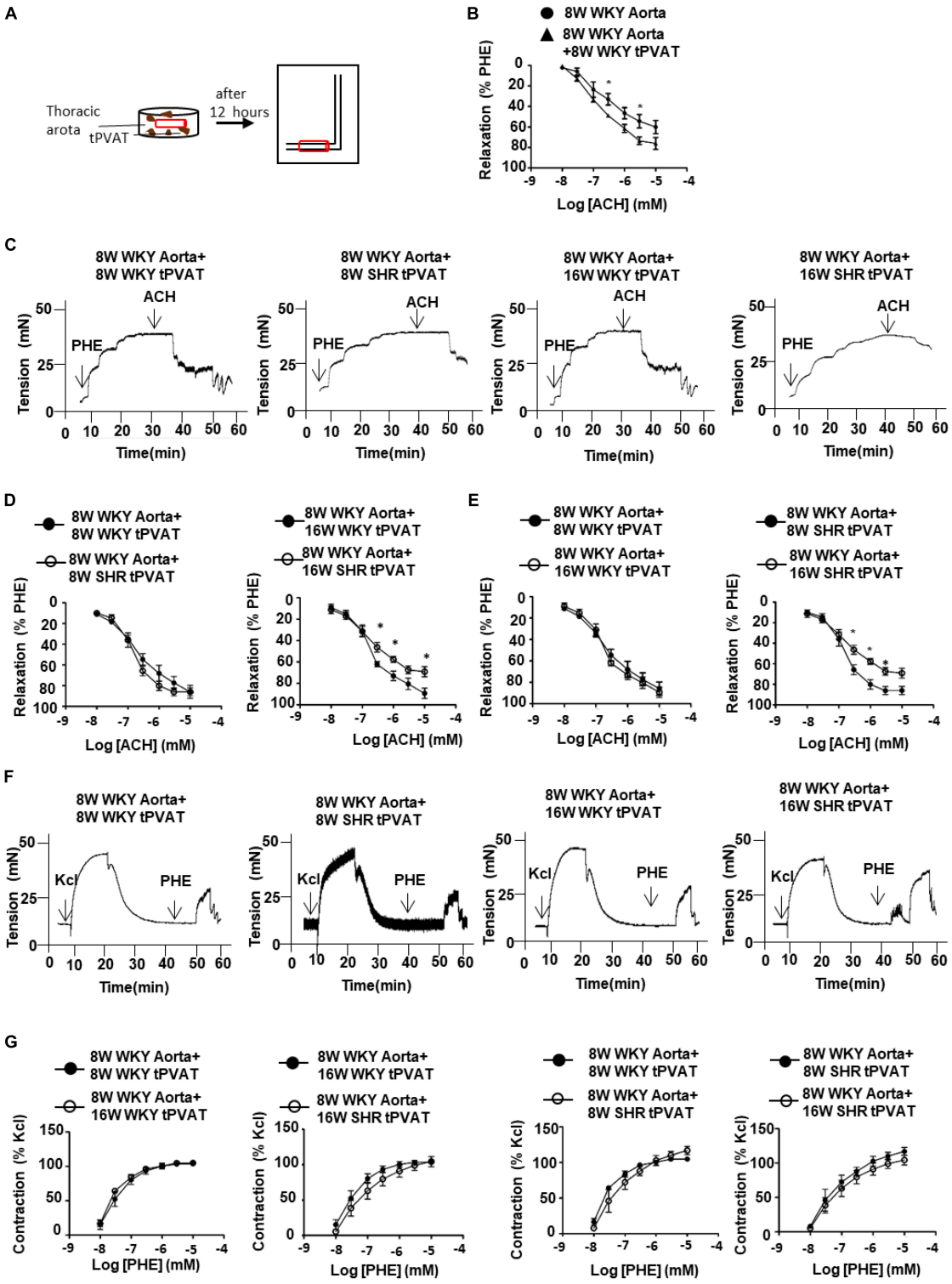

FIGURE 3 | Thoracic aorta reactivity incubated with tPVAT from WKY or SHR. **(A)** Illustration of bioassay protocol. **(B)** Average percent relaxation of thoracic aorta to ACH with or without 12 h tPVAT treated ($n = 6$). **(C)** Representative raw tracing of diastolic response to ACH after PHE (3 μM) pre-contraction. The thoracic aorta rings were collected from 8-week-old WKY rats and the PVAT adjacent to the rings was cleaned. The donor tPVAT were collected from 8-week-old and 16-week-old WKY or SHR. The rings were incubated with tPVAT in DMEM for 12 h at 37°C. **(D)** Average percent relaxation to ACH of thoracic aorta treated with 8-week-old or 16-week-old WKY or SHR tPVAT ($n = 6$). **(E)** Average percent relaxation to ACH of thoracic aorta treated with 8-week-old or 16-week-old WKY or SHR tPVAT ($n = 6$). **(F)** Representative raw traces showing dose-dependent aortic ring constriction in response to PHE after KCl (60 mM) pre-contraction. **(G)** Average percent contraction to PHE of thoracic aorta treated with 8-week-old or 16-week-old WKY or SHR tPVAT ($n = 6$). $^{*}p < 0.05$; $^{**}p < 0.01$; $^{***}p < 0.001$.

92.3 ± 2.6 mmHg in 8-week-old WKY, SBP 134.5 ± 2.5 mmHg and 109.4 ± 6.4 mmHg in 8-week-old SHR) (**Figure 2B**). To delineate the changes of tPVAT browning during aging in SHR, we detected expression of brown adipocyte markers in the tPVAT of 8-week-old and 16-week-old SHR and WKY rats. Compared with WKY rats, tPVAT browning activity including smaller-size adipocytes and UCP1 staining were elevated in 8-week-old SHR, but these phenotypic changes were blunted in 16-week-old SHR (**Figures 2C,D**). In accordance with these histological changes, the UCP1 and PPARγ expression showed a dramatic decrease in 16-week-old SHR compared to 8-week-old SHR, whereas UCP1, PPARγ, and PGC1α levels had no statistical difference between 8-week-old and 16-week-old WKY rats (**Figure 2E**).

The Effects of tPVAT on Vasomotor Reaction

Next, to determine whether tPVAT is involved in the regulation of vascular contraction and relaxation in WKY and SHR, we utilized tPVAT to incubate thoracic aorta and analyzed the aortic vasomotor reactions (**Figure 3A**). Thoracic aortas without tPVAT from 8-week-old WKY were incubated with or without 0.3 g tPVAT from WKY or SHRs for 12 h. In aortas incubated with tPVAT, vasodilation to ACH was increased compared to those without tPVAT incubation (**Figure 3B**). Then we collected tPVAT from 8- or 16-week-old WKY and SHR to incubate thoracic aortas from 8-week-old WKY. Interestingly, the vasodilative effect had no significant difference between groups incubated with tPVAT from 8-week-old WKY and SHR. In contrast, 16-week-old WKY showed an enhanced vascular relaxation effect compared to age-matched SHR (**Figures 3C,D**). More importantly, the vasodilative effect of the tPVAT from 16-week-old SHR was significantly attenuated compared to 8-week-old SHR, whereas this effect of tPVAT had no significant difference between 16-week-old and 8-week-old WKY (**Figures 3C,E**). In addition, vasocontraction of thoracic aortas incubated with WKY and SHR tPVAT showed no significant differences at 8 or 16 weeks of age (**Figures 3F,G**). These suggest a decreased PVRF production in the tPVAT of SHRs during aging.

The tPVAT-Derived Adenosine in SHRs

A previous study showed a significant increase of adenosine in the process of BAT activation (Biswas, 2017). To determine whether tPVAT produces and releases adenosine, we firstly detected CD73 expression, which is necessary for adenosine production (Quast et al., 2017). CD73 level in the tPVAT had no significant difference between 8-week-old WKY and SHR. Interestingly, CD73 level dramatically decreased in 16-week-old SHR compared with 8-week-old SHR, whereas CD73 level had no significant changes in WKY during aging (**Figure 4A**). Consistently, adenosine concentration showed no significant difference in the tPVAT-conditioned medium of 8-week-old SHR (116.2 ± 8.0 pg/ml) and WKY (139.4 ± 8.4 pg/ml). In contrast, adenosine significantly decreased in the PVAT-conditioned medium of 16-week-old SHR (87.6 ± 6.1 pg/ml) compared with 16-week-old WKY (138.3 ± 11.3 pg/ml) or 8-week-old SHR (**Figure 4B**). These data suggest that the changes of PVAT-derived adenosine in SHR might contribute to vascular tone dysfunction.

DISCUSSION

This is the first study providing evidence that tPVAT browning level and related relaxing factor adenosine are decreased in SHR rats during aging. A comparison of the expression of BAT phenotypic makers in the tPVAT of 8- or 16-week-old WKY and SHRs allowed us to conclude that the browning level in SHR tPVAT is much higher than WKY, but declines quickly in SHR during aging. Accordingly, tPVAT-derived adenosine decreased from 8 to 16 weeks of age in SHR. Thoracic aorta incubated with 16-week-old SHR tPVAT showed decreased diastolic activity compared to 8-week-old SHR or 16-week-old WKY rats.

PVAT can resemble either WAT or BAT depending on the anatomical localization. Abdominal and mesenteric PVAT

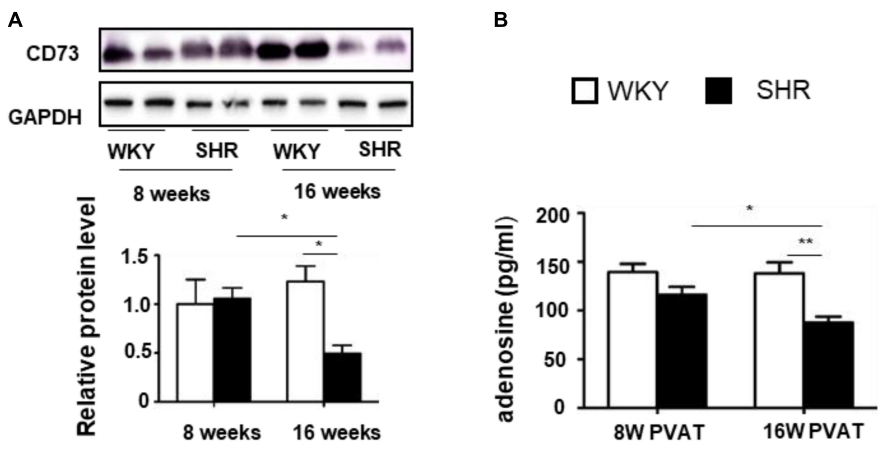

FIGURE 4 | CD73 expression and adenosine production in the tPVAT of SHR decrease during aging. **(A)** Western blot analysis of CD73 protein level in the tPVAT of 8-week-old and 16-week-old WKY and SHR. Quantitative results are shown on the lower panel ($n = 4$). **(B)** Adenosine concentration (ELISA) in the tPVAT-conditional media from 8-week-old and 16-week-old WKY and SHR ($n = 4$). *$p < 0.05$; **$p < 0.01$; ***$p < 0.001$.

appears to be similar to WAT with large lipid droplets and low expression of UCP1. In contrast, tPVAT is morphologically and functionally similar to BAT (Fitzgibbons et al., 2011). These contribute to maintaining intravascular temperature during cold exposure via initiating thermogenesis. Activation of PVAT by β3-adrenergic receptor increases lipid uptake and protects against atherosclerosis (Berbee et al., 2015). Compared to WKY, the PVAT of SHR shows a smaller adipocyte size, a lower total lipid, and a decline of leptin. These may together contribute to vascular resistance and dysfunction in SHR (Li et al., 2013). Herein we provided direct evidence that the tPVAT of SHR has a higher level of BAT markers than WKY, including UCP1, PPARγ and PGC1α. Aging is associated with a ubiquitous decline of BAT activity throughout the life (Lecoultre and Ravussin, 2011). We herein first provide evidence that the browning level of SHR tPVAT shows a greater decline than WKY rats during aging from 8 to 16 weeks of age. It is well known that the blood pressure elevates quickly from 8 to 16 weeks of age in SHR rats. Our results provide a potential possibility that the earlier loss of browning in the PVAT might contribute to the blood pressure elevation in SHR rats.

Perivascular adipose tissue significantly modulates vascular contraction and relaxation via releasing PVRF and PVAT-derived contracting factor (PVCF) (Gao et al., 2006). The exact constituents of PVRF and PVCF are not yet fully understood. However, several bioactive substances have been suggested to regulate vasomotor reactions. Among these, adiponectin is the most studied PVRF. Adiponectin knockout mice or neutralizing antibody against adiponectin blocks the vasodilator response of PVAT. Obesity-induced decline of adiponectin attenuates the anti-contractile effect of PVAT (Almabrouk et al., 2018). Besides adipokines, eNOS has also been demonstrated to be expressed in PVAT. NO synthesized from eNOS is responsible for the vasodilating properties of PVAT. It is worth noting that tPVAT exhibits an increase in eNOS expression and NO production compared to abdominal PVAT (Victorio et al., 2016). On the other hand, few PVCF has been documented to regulate vascular contraction. A recent report showed that brown adipocytes in the tPVAT produce and release angiotensinogen, which contributes to the regulation of PVAT contractile property and blood pressure elevation (Chang et al., 2018). Herein, we provide the first evidence that adenosine may be a potential PVRF, which is decreased in the tPVAT of SHRs during aging. Adenosine, as a small molecular metabolite, has been demonstrated to be produced by browning adipocytes (Ammar et al., 2004). We further provide evidence of adenosine production in the tPVAT in the present study. The tPVAT has a similar vasomotor reaction and adenosine release in 8-week-old WKY and SHR rats. In accordance with loss of brown adipocytes, the tPVAT of 16-week-old SHR produces less adenosine compared with 8-week-old SHR. Consistently, the tPVAT shows attenuated diastolic effect in SHR during aging, whereas the contractive effect has no significant change. Taken together with a previous study, which showed a decreased relaxing factor methyl palmitate in the PVAT of SHR (Lee et al., 2011), these provide evidence that PVAT of SHR dysfunction might be due to the lower PVRF production. The present study provides novel evidence that the browning level of tPVAT is closely associated with vasorelaxation in hypertension.

Since rodent PVAT has been demonstrated to be histologically and functionally different compared to most types of human PVAT (Chatterjee et al., 2009), more human studies are needed to determine the accurate mechanisms by which PVAT-derived substances modulate vascular homeostasis in hypertension during aging. Although CD73-regulated adenosine release from the tPVAT affects vascular function in hypertension, the detailed mechanism and signaling pathways of this adenosine-dependent response remain to be further investigated in the future. The influence of aging on PVAT browning progress and tPVAT-derived adenosine production also needs to be documented in the future preclinical studies.

In summary, we demonstrate that aging induces a dramatic decrease of tPVAT browning in SHRs, which is associated with reduced adenosine production in tPVAT and attenuated vasorelaxing effect on the aorta. Notwithstanding the complexity of human hypertension compared to rodent models, our unique observation indicates an attractive possibility that the PVAT could serve as a therapeutic tool for preventing hypertensive vascular dysfunction during aging.

AUTHOR CONTRIBUTIONS

P-JG, C-CR, and L-RK designed the experiments and wrote the paper. L-RK and D-RC performed the animal experiments and analytical methods. L-RK and Y-PZ performed *in vivo* imaging. L-RK, C-CR, and P-JG analyzed the data.

FUNDING

This work was support by grants from the National Natural Science Foundation of China (91539202, 81570221, 81770495, and 91739303) and Shanghai Municipal Commission of Health and Family Planning (2017YQ076 and 201540222).

REFERENCES

Agabiti-Rosei, C., Favero, G., De Ciuceis, C., Rossini, C., Porteri, E., Rodella, L. F., et al. (2017). Effect of long-term treatment with melatonin on vascular markers of oxidative stress/inflammation and on the anticontractile activity of perivascular fat in aging mice. *Hypertens. Res.* 40, 41–50. doi: 10.1038/hr.2016.103

Almabrouk, T. A. M., White, A. D., Ugusman, A. B., Skiba, D. S., Katwan, O. J., Alganga, H., et al. (2018). High fat diet attenuates the anticontractile activity of aortic PVAT via a mechanism involving AMPK and reduced adiponectin secretion. *Front. Physiol.* 9:51. doi: 10.3389/fphys.2018.00051

Ammar, E. M., Said, S. A., and Hassan, M. S. (2004). Enhanced vasoconstriction and reduced vasorelaxation induced by testosterone and nandrolone in

hypercholesterolemic rabbits. *Pharmacol. Res.* 50, 253–259. doi: 10.1016/j.phrs.2004.03.010

Berbee, J. F., Boon, M. R., Khedoe, P. P., Bartelt, A., Schlein, C., Worthmann, A., et al. (2015). Brown fat activation reduces hypercholesterolaemia and protects from atherosclerosis development. *Nat. Commun.* 6:6356. doi: 10.1038/ncomms7356

Biswas, H. M. (2017). Effect of adrenocorticotropic hormone on *UCP1* gene expression in brown adipocytes. *J. Basic Clin. Physiol. Pharmacol.* 28, 267–274. doi: 10.1515/jbcpp-2016-0017

Borea, P. A., Gessi, S., Merighi, S., and Varani, K. (2016). Adenosine as a multi-signalling guardian angel in human diseases: when, where and how does it exert its protective effects. *Trends Pharmacol. Sci.* 37, 419–434. doi: 10.1016/j.tips.2016.02.006

Britton, K. A., and Fox, C. S. (2011). Perivascular adipose tissue and vascular disease. *Clin. Lipidol.* 6, 79–91. doi: 10.2217/clp.10.89

Brown, N. K., Zhou, Z., Zhang, J., Zeng, R., Wu, J., Eitzman, D. T., et al. (2014). Perivascular adipose tissue in vascular function and disease: a review of current research and animal models. *Arterioscler. Thromb. Vasc. Biol.* 34, 1621–1630. doi: 10.1161/atvbaha.114.303029

Burghoff, S., Flogel, U., Bongardt, S., Burkart, V., Sell, H., Tucci, S., et al. (2013). Deletion of CD73 promotes dyslipidemia and intramyocellular lipid accumulation in muscle of mice. *Arch. Physiol. Biochem.* 119, 39–51. doi: 10.3109/13813455.2012.755547

Chang, L., Villacorta, L., Li, R., Hamblin, M., Xu, W., Dou, C., et al. (2012). Loss of perivascular adipose tissue on peroxisome proliferator-activated receptor-gamma deletion in smooth muscle cells impairs intravascular thermoregulation and enhances atherosclerosis. *Circulation* 126, 1067–1078. doi: 10.1161/circulationaha.112.104489

Chang, L., Xiong, W., Zhao, X., Fan, Y., Guo, Y., Garcia-Barrio, M., et al. (2018). Bmal1 in perivascular adipose tissue regulates resting phase blood pressure through transcriptional regulation of angiotensinogen. *Circulation* doi: 10.1161/circulationaha.117.029972 [Epub ahead of print].

Chatterjee, T. K., Stoll, L. L., Denning, G. M., Harrelson, A., Blomkalns, A. L., Idelman, G., et al. (2009). Proinflammatory phenotype of perivascular adipocytes: influence of high-fat feeding. *Circ. Res.* 104, 541–549. doi: 10.1161/CIRCRESAHA.108.182998

Fitzgibbons, T. P., Kogan, S., Aouadi, M., Hendricks, G. M., Straubhaar, J., and Czech, M. P. (2011). Similarity of mouse perivascular and brown adipose tissues and their resistance to diet-induced inflammation. *Am. J. Physiol. Heart Circ. Physiol.* 301, H1425–H1437. doi: 10.1152/ajpheart.00376.2011

Fleenor, B. S., Eng, J. S., Sindler, A. L., Pham, B. T., Kloor, J. D., and Seals, D. R. (2014). Superoxide signaling in perivascular adipose tissue promotes age-related artery stiffness. *Aging Cell* 13, 576–578. doi: 10.1111/acel.12196

Galvez, B., de Castro, J., Herold, D., Dubrovska, G., Arribas, S., Gonzalez, M. C., et al. (2006). Perivascular adipose tissue and mesenteric vascular function in spontaneously hypertensive rats. *Arterioscler. Thromb. Vasc. Biol.* 26, 1297–1302. doi: 10.1161/01.ATV.0000220381.40739.dd

Gao, Y. J., Takemori, K., Su, L. Y., An, W. S., Lu, C., Sharma, A. M., et al. (2006). Perivascular adipose tissue promotes vasoconstriction: the role of superoxide anion. *Cardiovasc. Res.* 71, 363–373. doi: 10.1016/j.cardiores.2006.03.013

Gnad, T., Scheibler, S., von Kugelgen, I., Scheele, C., Kilic, A., Glode, A., et al. (2014). Adenosine activates brown adipose tissue and recruits beige adipocytes via A2A receptors. *Nature* 516, 395–399. doi: 10.1038/nature13816

Harms, M. J., Ishibashi, J., Wang, W., Lim, H. W., Goyama, S., Sato, T., et al. (2014). Prdm16 is required for the maintenance of brown adipocyte identity and function in adult mice. *Cell Metab.* 19, 593–604. doi: 10.1016/j.cmet.2014.03.007

Jin, L., Piao, Z. H., Sun, S., Liu, B., Kim, G. R., Seok, Y. M., et al. (2017). Gallic acid reduces blood pressure and attenuates oxidative stress and cardiac hypertrophy in spontaneously hypertensive rats. *Sci. Rep.* 7:15607. doi: 10.1038/s41598-017-15925-1

Kozak, L. P. (2010). Brown fat and the myth of diet-induced thermogenesis. *Cell Metab.* 11, 263–267. doi: 10.1016/j.cmet.2010.03.009

Lecoultre, V., and Ravussin, E. (2011). Brown adipose tissue and aging. *Curr. Opin. Clin. Nutr. Metab. Care* 14, 1–6. doi: 10.1097/MCO.0b013e328341221e

Lee, Y. C., Chang, H. H., Chiang, C. L., Liu, C. H., Yeh, J. I., Chen, M. F., et al. (2011). Role of perivascular adipose tissue-derived methyl palmitate in vascular tone regulation and pathogenesis of hypertension. *Circulation* 124, 1160–1171. doi: 10.1161/circulationaha.111.027375

Li, R., Andersen, I., Aleke, J., Golubinskaya, V., Gustafsson, H., and Nilsson, H. (2013). Reduced anti-contractile effect of perivascular adipose tissue on mesenteric small arteries from spontaneously hypertensive rats: role of Kv7 channels. *Eur. J. Pharmacol.* 698, 310–315. doi: 10.1016/j.ejphar.2012.09.026

Ma, L., Ma, S., He, H., Yang, D., Chen, X., Luo, Z., et al. (2010). Perivascular fat-mediated vascular dysfunction and remodeling through the AMPK/mTOR pathway in high-fat diet-induced obese rats. *Hypertens. Res.* 33, 446–453. doi: 10.1038/hr.2010.11

Quast, C., Alter, C., Ding, Z., Borg, N., and Schrader, J. (2017). Adenosine formed by CD73 on T cells inhibits cardiac inflammation and fibrosis and preserves contractile function in transverse aortic constriction-induced heart failure. *Circ. Heart Fail.* 10:e003346. doi: 10.1161/CIRCHEARTFAILURE.116.003346

Sakaue, T., Suzuki, J., Hamaguchi, M., Suehiro, C., Tanino, A., Nagao, T., et al. (2017). Perivascular adipose tissue angiotensin II Type 1 receptor promotes vascular inflammation and aneurysm formation. *Hypertension* 70, 780–789. doi: 10.1161/hypertensionaha.117.09512

Schosserer, M., Grillari, J., Wolfrum, C., and Scheideler, M. (2017). Age-induced changes in white, brite, and brown adipose depots: a mini-review. *Gerontology* 64, 229–236. doi: 10.1159/000485183

Sheng, L. J., Ruan, C. C., Ma, Y., Chen, D. R., Kong, L. R., Zhu, D. L., et al. (2016). Beta3 adrenergic receptor is involved in vascular injury in deoxycorticosterone acetate-salt hypertensive mice. *FEBS Lett.* 590, 769–778. doi: 10.1002/1873-3468.12107

Takemori, K., Gao, Y. J., Ding, L., Lu, C., Su, L. Y., An, W. S., et al. (2007). Elevated blood pressure in transgenic lipoatrophic mice and altered vascular function. *Hypertension* 49, 365–372. doi: 10.1161/01.HYP.0000255576.16089.b9

Verhagen, S. N., and Visseren, F. L. (2011). Perivascular adipose tissue as a cause of atherosclerosis. *Atherosclerosis* 214, 3–10. doi: 10.1016/j.atherosclerosis.2010.05.034

Victorio, J. A., Fontes, M. T., Rossoni, L. V., and Davel, A. P. (2016). Different anti-contractile function and nitric oxide production of thoracic and abdominal perivascular adipose tissues. *Front. Physiol.* 7:295. doi: 10.3389/fphys.2016.00295

Zhou, W., Hong, M., Zhang, K., Chen, D., Han, W., Shen, W., et al. (2014). Mechanisms of improved aortic stiffness by arotinolol in spontaneously hypertensive rats. *PLoS One* 9:e88722. doi: 10.1371/journal.pone.0088722

Conflict of Interest Statement: The authors declare that the research was conducted in the absence of any commercial or financial relationships that could be construed as a potential conflict of interest.

frontiers in Physiology

ORIGINAL RESEARCH
published: 06 April 2018
doi: 10.3389/fphys.2018.00341

Increased *O*-GlcNAcylation of Endothelial Nitric Oxide Synthase Compromises the Anti-contractile Properties of Perivascular Adipose Tissue in Metabolic Syndrome

Rafael M. da Costa[1], Josiane F. da Silva[1], Juliano V. Alves[1], Thiago B. Dias[1], Diane M. Rassi[1], Luis V. Garcia[2], Núbia de Souza Lobato[3] and Rita C. Tostes[1]*

[1] Department of Pharmacology, Ribeirao Preto Medical School, University of Sao Paulo, Ribeirao Preto, Brazil, [2] Department of Biomechanics, Medicine and Locomotive Apparatus Rehabilitation, Ribeirao Preto Medical School, University of Sao Paulo, Ribeirao Preto, Brazil, [3] Department of Physiology, Institute of Health Sciences, Federal University of Goias, Jatai, Brazil

OPEN ACCESS

Edited by:
Stephanie W. Watts, Michigan State University, United States

Reviewed by:
Brett M. Mitchell, Texas A&M Health Science Center, United States
Rudolf Schubert, Universität Heidelberg, Germany

***Correspondence:**
Rafael M. da Costa
rafael.menezess@yahoo.com.br

Specialty section:
This article was submitted to Vascular Physiology, a section of the journal Frontiers in Physiology

Received: *07 December 2017*
Accepted: *20 March 2018*
Published: *06 April 2018*

Citation:
da Costa RM, Silva JFd, Alves JV, Dias TB, Rassi DM, Garcia LV, Lobato NdS and Tostes RC (2018) Increased O-GlcNAcylation of Endothelial Nitric Oxide Synthase Compromises the Anti-contractile Properties of Perivascular Adipose Tissue in Metabolic Syndrome. Front. Physiol. 9:341. doi: 10.3389/fphys.2018.00341

Under physiological conditions, the perivascular adipose tissue (PVAT) negatively modulates vascular contractility. This property is lost in experimental and human obesity and in the metabolic syndrome, indicating that changes in PVAT function may contribute to vascular dysfunction associated with increased body weight and hyperglycemia. The *O*-linked β-N-acetylglucosamine (*O*-GlcNAc) modification of proteins (*O*-GlcNAcylation) is a unique posttranslational process that integrates glucose metabolism with intracellular protein activity. Increased flux of glucose through the hexosamine biosynthetic pathway and the consequent increase in tissue-specific *O*-GlcNAc modification of proteins have been linked to multiple facets of vascular dysfunction in diabetes and other pathological conditions. We hypothesized that chronic consumption of glucose, a condition that progresses to metabolic syndrome, leads to increased *O*-GlcNAc modification of proteins in the PVAT, decreasing its anti-contractile effects. Therefore, the current study was devised to determine whether a high-sugar diet increases *O*-GlcNAcylation in the PVAT and how increased *O*-GlcNAc interferes with PVAT vasorelaxant function. To assess molecular mechanisms by which *O*-GlcNAc contributes to PVAT dysfunction, thoracic aortas surrounded by PVAT were isolated from Wistar rats fed either a control or high sugar diet, for 10 and 12 weeks. Rats chronically fed a high sugar diet exhibited metabolic syndrome features, increased *O*-GlcNAcylated-proteins in the PVAT and loss of PVAT anti-contractile effect. PVAT from high sugar diet-fed rats for 12 weeks exhibited decreased NO formation, reduced expression of endothelial nitric oxide synthase (eNOS) and increased *O*-GlcNAcylation of eNOS. High sugar diet also decreased OGA activity and increased superoxide anion generation in the PVAT. Visceral adipose tissue samples from hyperglycemic patients showed increased levels of *O*-GlcNAc-modified proteins, increased ROS generation and decreased OGA activity. These data indicate that *O*-GlcNAcylation contributes to metabolic syndrome-induced PVAT dysfunction and that *O*-GlcNAcylation of eNOS may be targeted in the development of novel therapies for vascular dysfunction in conditions associated with hyperglycemia.

Keywords: PVAT, *O*-GlcNAc, high-sugar diet, eNOS, vascular function

INTRODUCTION

The perivascular adipose tissue (PVAT) is a highly active endocrine organ that releases a wide variety of adipokines that control vascular smooth muscle tone in veins, conductance arteries, and vessels of smaller caliber (Szasz and Webb, 2012). The vasoactive factors released by the PVAT (Adventitium-Derived Relaxing Factors—ADRF) under physiological conditions include adiponectin, angiotensin- (1-7), hydrogen peroxide, leptin, nitric oxide (NO), and other agents that negatively modulate vascular contraction, that is, the PVAT exerts an anti-contractile effect and is essential for the maintenance of vascular function (Fernandez-Alfonso et al., 2013; Xia and Li, 2017).

In obesity and metabolic syndrome, there is an increase in the amount of PVAT accompanied by changes in the PVAT pattern of adipokines expression, infiltration, and activation of circulating inflammatory cells (Lumeng et al., 2007), hypoxia, and oxidative stress (Gao, 2007). The net effect of these changes is a profound impairment of the vasoactive properties of PVAT, leading to an imbalance in favor of PVAT-derived vasoconstrictor substances, as well as changes in their signaling pathways in the vasculature (da Costa et al., 2017). The predominant mechanisms leading to a dysfunctional PVAT in obesity and metabolic syndrome have not been identified so far.

Post-translational modifications of intrinsic components of PVAT seem to contribute to the loss of its anti-contractile effect in metabolic and cardiovascular diseases. As an example, reduced NO synthase phosphorylation in the serine activation residue (Ser^{1177}) and decreased phosphorylation of adenosine monophosphate-activated protein kinases, which positively regulate NO synthase activity, have been reported in the PVAT of animals fed a high fat diet for 6 months (Ma et al., 2010).

Among the many types of post-translational modifications, a great deal of interest has been directed to *O*-GlcNAcylation, i.e., glycosylation with *N*-acetyl-glucosamine (*O*-GlcNAc), which occurs by the addition of *N*-acetyl-glucosamine to the oxygen of the hydroxyl group of serine and threonine residues. Various cytoplasmic and nuclear proteins, including kinases, phosphatases, transcription factors, and cytoskeletal proteins are targets of *O*-GlcNAcylation (Hart et al., 2007). The activity of the enzymes *O*-GlcNAc transferase (OGT) and *O*-GlcNAcase (OGA) directly control the *O*-GlcNAc process. Whereas, OGT catalyzes the addition of *N*-acetyl-glucosamine in the target proteins, the enzyme OGA catalyzes the hydrolytic removal of *O*-GlcNAc (Lima et al., 2009). It is noteworthy that both enzymes are themselves targeted for *O*-GlcNAcylation and other post-translational modifications (Laczy et al., 2009).

O-GlcNAcylation integrates glucose metabolism with the activity of innumerable intracellular proteins. Increased glucose flow through the hexosamine biosynthesis pathway and increased *O*-GlcNAc modification of proteins are associated with the multiple facets of vascular dysfunction in diabetes mellitus and obesity, including endothelial function impairment, inflammation, fibrosis, and metabolic dysfunction (Lima et al., 2009). However, the contribution of *O*-GlcNAcylation to PVAT dysfunction in metabolic syndrome has not been determined. Thus, we hypothesized that increased *O*-GlcNAcylation of endothelial NO synthase (eNOS) in the PVAT produces loss of its anti-contractile effect leading to PVAT and vascular dysfunctions in metabolic syndrome. In the present study, we sought to determine whether chronic high sugar diet and the subsequent metabolic syndrome increase *O*-GlcNAcylation in the PVAT and how increased *O*-GlcNAc interferes with PVAT vasorelaxant function.

MATERIALS AND METHODS

In Vivo Studies

All experimental protocols were performed in accordance with the National Council for Animal Experimentation Control (CONCEA) and were approved by the Ethics Committee on Animal Use (CEUA) of the University of Sao Paulo, Ribeirao Preto, Brazil (Protocol n° 206/2016).

Six week-old male Wistar rats were obtained from the University of Sao Paulo, Ribeirao Preto, Brazil and maintained in the Animal Facility of the Pharmacology Department, Ribeirao Preto Medical School, on 12-h light/dark cycles under controlled temperature (22 ± 1°C) with *ad libitum* access to food and water. After a 1-week acclimatization period, rats were randomly divided into two groups: (1) rats maintained on a control diet; (2) rats receiving a high sugar diet for 10 or 12 weeks. The high sugar diet consisted of 33% control diet (Nuvilab® CR1, Nuvital, Brazil), 33% condensed milk, and 7% sucrose by weight, the remaining being water (Silva et al., 2016). The energy density was 12.26 kJ/g for the control diet and 13.35 kJ/g for the high sugar diet. After the treatment period, rats were killed by carbon dioxide (CO_2) inhalation.

Humans Samples

This study was approved by the Research Ethics Committee of the University of Sao Paulo (Protocol n° 14189/2012) and all the stated rules for human research were followed. Visceral adipose tissue was taken from portions of the omentum from patients with bowel cancer submitted to surgical procedures at the Clinics Hospital of the Ribeirao Preto Medical School at the University of Sao Paulo (8 male patients, 42–75 years-old). All patients provided signed informed and written consent prior to participation in this study. The specimens were taken from macroscopically normal tissue, and care was taken to exclude adipose tissue supplying the area of the tumor. Patients were divided into the following groups: normoglycemic patients (blood glucose lower than 100 mg/dL) and chronic hyperglycemic patients (blood glucose over 150 mg/dL). Visceral adipose tissue is directly associated with the function of resistance arteries (Farb et al., 2012) and allows the investigation of the involvement of these deposits on vascular function. The use of human adipose tissue surrounding the aorta, which would better correlate with the animal studies, was not possible.

Biochemical Profile of Rats Fed the Control and High Sugar Diets

Glucose levels were determined using a glucose analyzer (Accu-Check, Roche Diagnostics, Brazil). In addition, total cholesterol

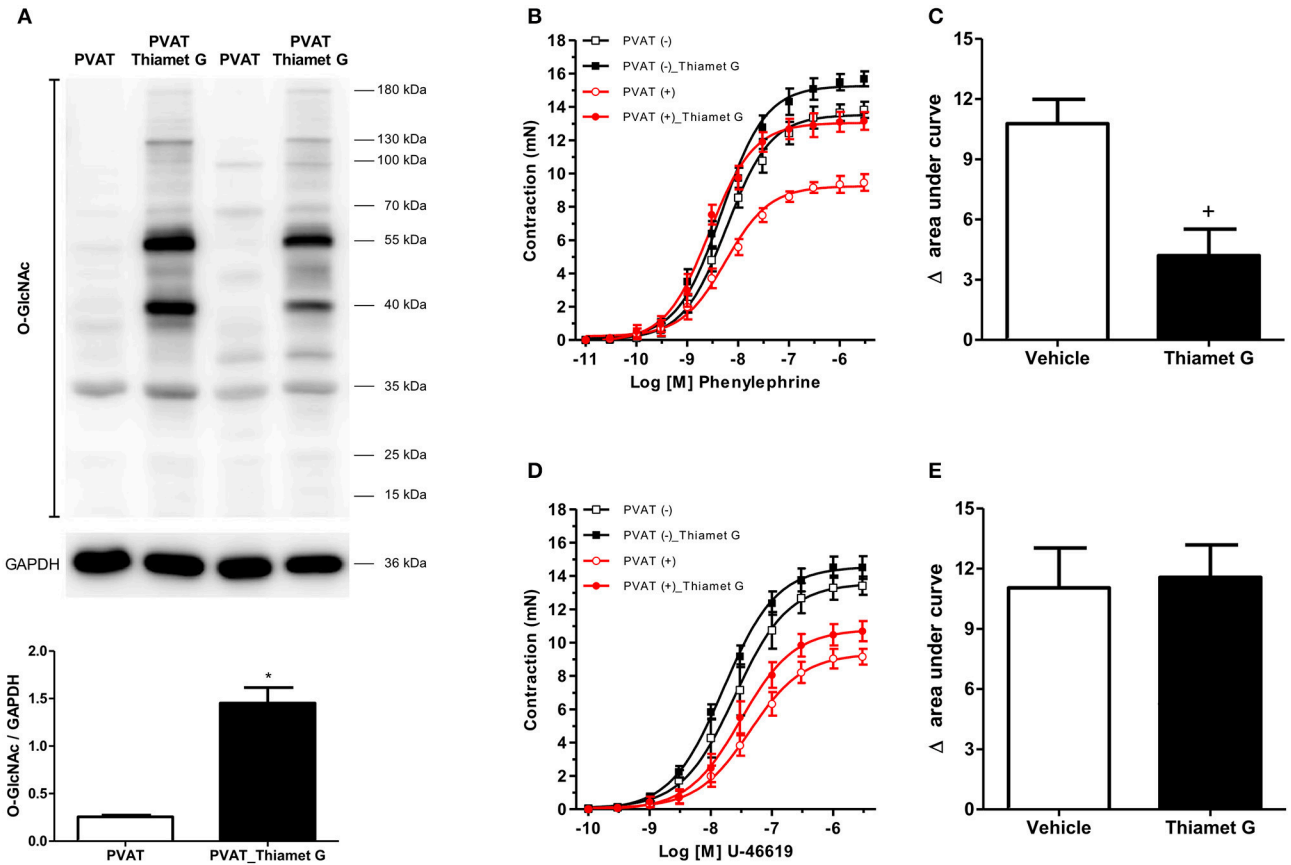

FIGURE 1 | Increased *O*-GlcNAc-modified proteins induce loss of the PVAT anti-contractile effect**. (A)** Expression of *O*-GlcNAc-modified proteins in PVAT incubated with the *O*-GlcNAcase (OGA) inhibitor, Thiamet G (10^{-6} M, for 24 h, $n = 6$) or vehicle ($n = 6$). Concentration-response curves to **(B)** phenylephrine ($n = 7$) and **(D)** thromboxane A_2 receptor agonist, U-46619 ($n = 7$), were performed in endothelium-denuded aortic rings without (–) or with (+) PVAT, incubated with Thiamet G (10^{-6} M, for 24 h) or vehicle. **(C,E)** show the difference (delta) of the areas under the curves to phenylephrine and U-46619, respectively, in the absence and presence of PVAT after incubation with Thiamet G or vehicle. Data are represented as the mean ± SEM. Student's *t*-test: $^{*}p < 0.05$ PVAT_Thiamet *G* vs. PVAT; $^{+}p < 0.05$ Thiamet G vs. Vehicle.

TABLE 1 | pD_2 and Emax (mN) values of phenylephrine and U-46619-induced contraction in thoracic aorta arteries incubated with vehicle or Thiamet G.

	pD_2		Emax	
Groups	**Phenylephrine**	**U-46619**	**Phenylephrine**	**U-46619**
PVAT (–)	8.2 ± 0.05 ($n = 6$)	7.6 ± 0.09 ($n = 7$)	13.5 ± 0.2 ($n = 6$)	13.5 ± 0.5 ($n = 7$)
PVAT (–)_Thiamet G	8.3 ± 0.05 ($n = 6$)	7.7 ± 0.05 ($n = 7$)	15.2 ± 0.2 ($n = 6$)	14.5 ± 0.2 ($n = 7$)
PVAT (+)	8.2 ± 0.07 ($n = 6$)	7.4 ± 0.08 ($n = 7$)	9.2 ± 0.2 ($n = 6$)*	9.3 ± 0.3 ($n = 7$)*
PVAT (+)_Thiamet G	8.6 ± 0.06 ($n = 6$)$^{+}$	7.5 ± 0.08 ($n = 7$)	13.0 ± 0.2 ($n = 6$)$^{+}$	10.8 ± 0.4 ($n = 7$)$^{+}$

*Data represent the mean ± SEM of n experiments. Two-way ANOVA: *p < 0.05 vs. respective PVAT (–); $^{+}p < 0.05$ vs. respective PVAT (+).*

and triglycerides concentrations were determined in serum samples from rats fasted for 12 h, by an enzymatic colorimetric method (Doles®, Brazil). Serum insulin concentration (ng/mL) was determined by radioimmunoassay (Insulin Kit®, Brazil). Insulin sensitivity was calculated using the HOMA-IR index (Homeostasis Model Assessment) (Pan et al., 2015), which takes into account insulin and fasting blood glucose levels, using the following mathematical formula: HOMA-IR = fasting insulin x fasting glucose/22.5. The oral glucose tolerance test (OGTT) was performed to evaluate glucose tolerance. Rats were deprived of food for 6 h. Blood was sampled from the caudal vein immediately before (baseline, t_0) and after (t_{15}, t_{30}, t_{60}, t_{90}, t_{120} minutes) administration of 2 g of glucose/kg by oral gavage.

Assessment of Vascular Function

Thoracic aorta was rapidly removed, transferred to an ice-cold (4°C) Krebs Henseleit modified solution [(in mM) 130 NaCl, 14.9 $NaHCO_3$, 4.7 KCl, 1.18 KH_2PO_4, 1.17 $MgSO_4 \cdot 7H_2O$, 5.5

TABLE 2 | Characteristics of rats fed the Control and High Sugar diets.

	Control 10 Weeks	High sugar 10 Weeks	Control 12 Weeks	High sugar 12 Weeks
Initial body mass (g)	252.6 ± 2.0	254.1 ± 2.3	253.2 ± 2.2	255.3 ± 3.2
Final body mass (g)	469.4 ± 3.0	583.2 ± 3.7^{+}	493.9 ± 3.1	657.5 ± 3.9*
Body mass gain (g)	216.8 ± 2.5	329.1 ± 3.1^{+}	240.7 ± 2.6	402.2 ± 3.1*
Epididymal fat (g)	5.32 ± 0.1	9.57 ± 0.6^{+}	5.89 ± 0.2	11.73 ± 0.6*
Visceral fat (g)	6.87 ± 0.3	12.36 ± 0.5^{+}	7.33 ± 0.1	15.18 ± 0.6*
Retroperitoneal fat (g)	6.36 ± 0.2	11.62 ± 0.4^{+}	7.19 ± 0.2	14.25 ± 0.5*
Adiposity index (%)	3.97 ± 0.1	5.75 ± 0.1^{+}	4.13 ± 0.1	6.26 ± 0.1*
Total cholesterol (mg/dL)	88.7 ± 5.2	113.8 ± 2.1^{+}	90.2 ± 4.8	124.2 ± 3.7*
Triglycerides (mg/dL)	68.2 ± 2.3	83.4 ± 3.1^{+}	67.1 ± 3.9	92.8 ± 2.8*

Data represent the mean ± SEM of n experiments. Two-way ANOVA: $^{+}p < 0.05$ vs. Control 10 Weeks; $^{*}p < 0.05$ vs. Control 12 Weeks.

glucose, 1.56 $CaCl_2 \cdot 2H_2O$ and 0.026 EDTA] gassed with 5% CO_2 / 95% O_2 to maintain a pH of 7.4, and dissected into 3 mm rings whereby perivascular fat and connective tissues were either removed (PVAT–) or left intact (PVAT+). Aortic rings were mounted in a wire myograph to measure isometric tension, as previously described (Costa et al., 2016). Vessels were allowed to equilibrate for about 30 min in Krebs Henseleit solution and baseline tension of 30 mN. After the stabilization period, the arteries were stimulated with Krebs solution containing a high concentration of potassium [K^+ (120 mM)] to evaluate the contractile capacity of the segments. KCl-mediated contraction responses were similar in all experimental conditions (∼35 mN). Endothelial function was assessed by testing the relaxant effect of acetylcholine (ACh, 10^{-6} M) on vessels contracted with phenylephrine (PE, 10^{-7} M). In experiments with endothelium-denuded vessels, aortic rings were subjected to rubbing of the intimal surface. Rings showing a maximum of 5% relaxation in response to ACh were considered to be without endothelium. Cumulative concentration-response curves to PE (10^{-10}-10^{-4} M) and sodium nitroprusside (SNP, 10^{-10}-10^{-4} M) were performed in PVAT (+) or PVAT (–) aortic rings. Contractile responses to PE were also determined after incubation with L-NAME (10^{-4} M), nitric oxide synthase inhibitor, 30 min before adding the contractile agonist. Each vascular preparation was tested with a single agent.

PVAT *ex Vivo* Incubation

PVAT from rats fed the control diet were incubated for 24 h in normoglycemic (5.6 mM glucose) Dulbecco's Modified Eagle Medium (DMEM), in the presence or absence of the OGA inhibitor Thiamet G (10^{-6} M, Okuda, 2017). PVAT from rats fed the control diet were incubated for 3, 6, and 12 h in hyperglycemic (25 mM glucose) DMEM. In this experiment, the control was obtained using PVAT incubated in normoglycemic DMEM for 12 h. In addition, PVAT from rats fed the control diet were incubated for 6 h in hyperglycemic DMEM in the presence or absence of the superoxide anion ($O_2^{\cdot-}$) scavenger Tiron (10^{-4} M, Alves-Lopes et al., 2016). For this condition, the experimental control was PVAT incubated in normoglycemic DMEM for 6 h. During incubations, PVAT was individually maintained in six-well Petri dishes at 37°C and 5% CO_2.

Western Blot Analysis

PVAT from thoracic aorta and visceral adipose tissue from humans were frozen in liquid nitrogen and homogenized in a lysis buffer [50 mM Tris/HCl, 150 mM NaCl, 1% Nonidet P40, 1 mM EDTA, 1 μg/ml leupeptin, 1 μg/ml pepstatin, 1 μg/ml aprotinin, 1 mM sodium orthovanadate, 1 mM phenylmethanesulfonyl fluoride (PMSF), and 1 mM sodium fluoride]. The tissue extracts were centrifuged, and total protein content was quantified using the Bradford method (Bradford, 1976). Proteins (20 μg) were separated by electrophoresis on 10% polyacrylamide gel, and transferred on to nitrocellulose membranes. Non-specific binding sites were blocked with 5% bovine serum albumin (BSA) in Tris buffered saline (TBS) containing 0.1% Tween 20 (for 1 h at 24°C). Membranes were incubated with antibodies (at the indicated dilutions) overnight at 4°C. Antibodies were used as follows: anti-Anti-β-*O*-Linked *N*-Acetylglucosamine (1:5000 dilution; Sigma-Aldrich Inc., Germany), anti-OGA (1:1000 dilution; Sigma-Aldrich Inc., Germany), anti-OGT (1:1000 dilution; Abcam, UK), anti-GAPDH (1:10000 dilution; Sigma-Aldrich Inc., Germany). After incubation with secondary antibodies, signals were obtained by chemiluminescence and quantified densitometrically.

OGA Activity in Rat PVAT and Visceral Adipose Tissue of Humans

The tissue proteins were extracted according to the previous item and quantified using the Bradford method. Proteins (3 μg) were eluted in 100 μL of citrate buffer (0.05 M, pH 5.0). After elution, the OGA substrate 4-Methylumbelliferyl *N*-acetyl-β-D-glucosaminide (4-MUNAG, 300 μg/ml, Sigma-Aldrich Inc., Germany) and OGA inhibitor Thiamet G (10^{-6} M) were added. The reaction occurred in an oven at 37°C for 30 min. Then, the reaction was stopped after addition glycine buffer (0.1 M, pH 12). The breaking of the 4-MUNAG by the OGA emits fluorescence after excitation of 362 nm and emission of 448 nm. The values were expressed in fluorescence relative units through the delta of the reactions in the presence and absence of Thiamet G.

Immunoprecipitation

To evaluate the degree *O*-GlcNAc modification on eNOS, direct immunoprecipitation was performed using magnetic

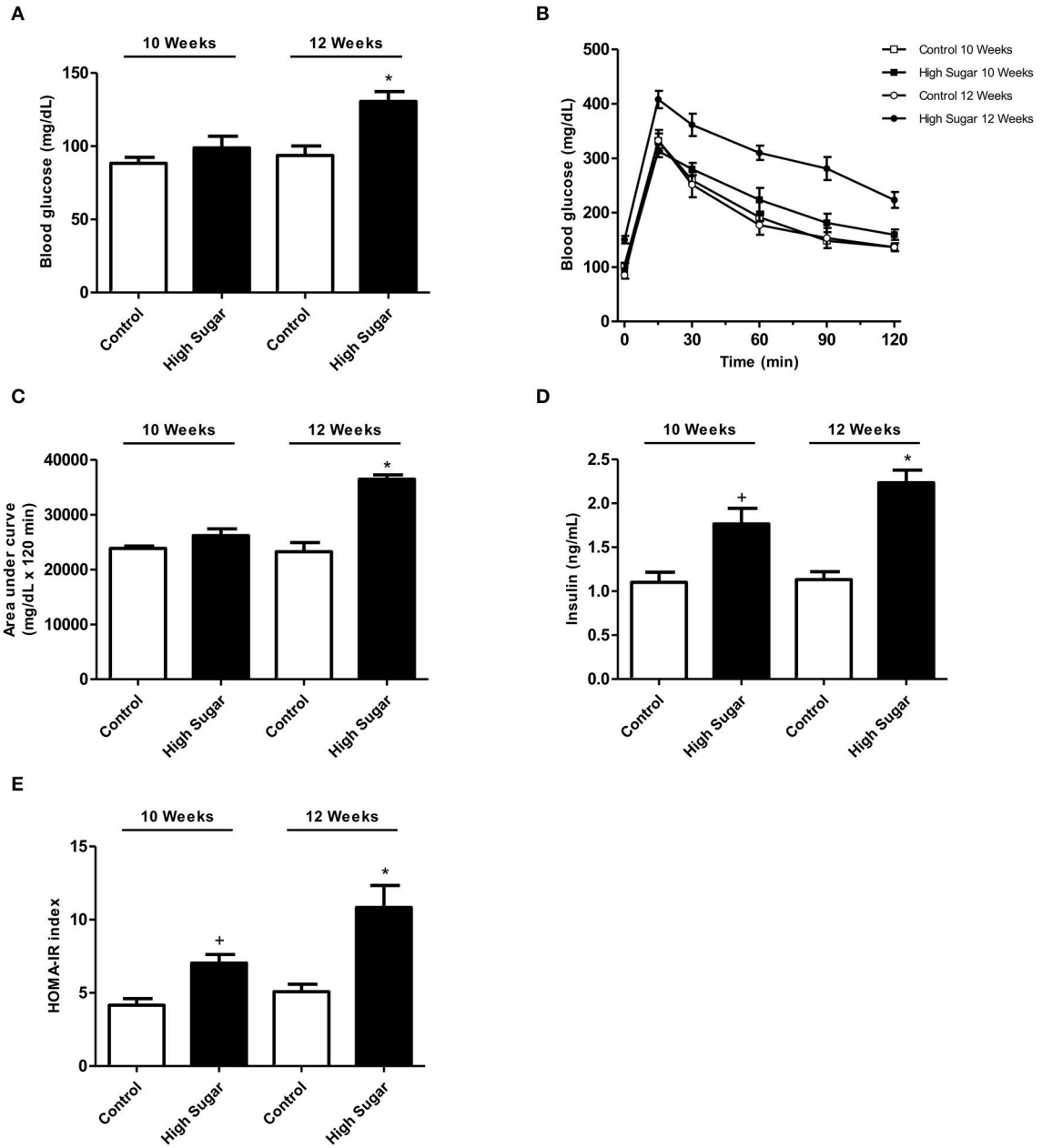

FIGURE 2 | High sugar diet-induced disturbs in the rat glucose metabolism. **(A)** Glucose serum levels in rats fed the control ($n = 8$) or high sugar ($n = 8$) diet for 10 or 12 weeks. **(B)** Glucose serum levels and **(C)** the areas under the curves obtained during the OGTT in rats fed the control ($n = 8$) or high sugar ($n = 8$) diet for 10 or 12 weeks. **(D)** Insulin serum levels in rats fed the control ($n = 8$) or high sugar ($n = 8$) diet for 10 or 12 weeks. **(E)** HOMA-IR index in rats fed with control ($n = 8$) or high sugar ($n = 8$) diet for 10 or 12 weeks. Data are represented as the mean ± SEM. Two-way ANOVA: $^{+}p < 0.05$ High Sugar 10 weeks vs. Control 10 weeks; $^{*}p < 0.05$ High Sugar 12 weeks vs. Control 12 weeks.

beads, according to the manufacturer protocol (PureProteome Protein G Magnetic Beads, LSKMAGG02, Merck-Millipore, UK). Briefly, the bead-antibody complex was formed by incubating 30 μL of beads with 5 μg of anti-eNOS antibody (Sc-376751-Santa Cruz Biotechnology, USA). Subsequently, the bead-antibody complex was added to 500 μg of proteins derived from the total protein extract of the PVAT of the animals. After overnight incubation at 4°C, the bead-antibody-protein complex was precipitated with the aid of the magnetic tube rack (DynaMag TM-2, Invitrogen^{TM}, Thermo Fisher Scientific Inc., UK). Then, proteins were separated by sodium dodecyl sulfate/polyacrylamide gel (8%) electrophoresis (SDS/PAGE), as described in the western blot protocol. Anti-*O*-GlcNAc (O7764, Sigma-Aldrich Inc., Germany) and anti-eNOS (Sc-376751, Santa

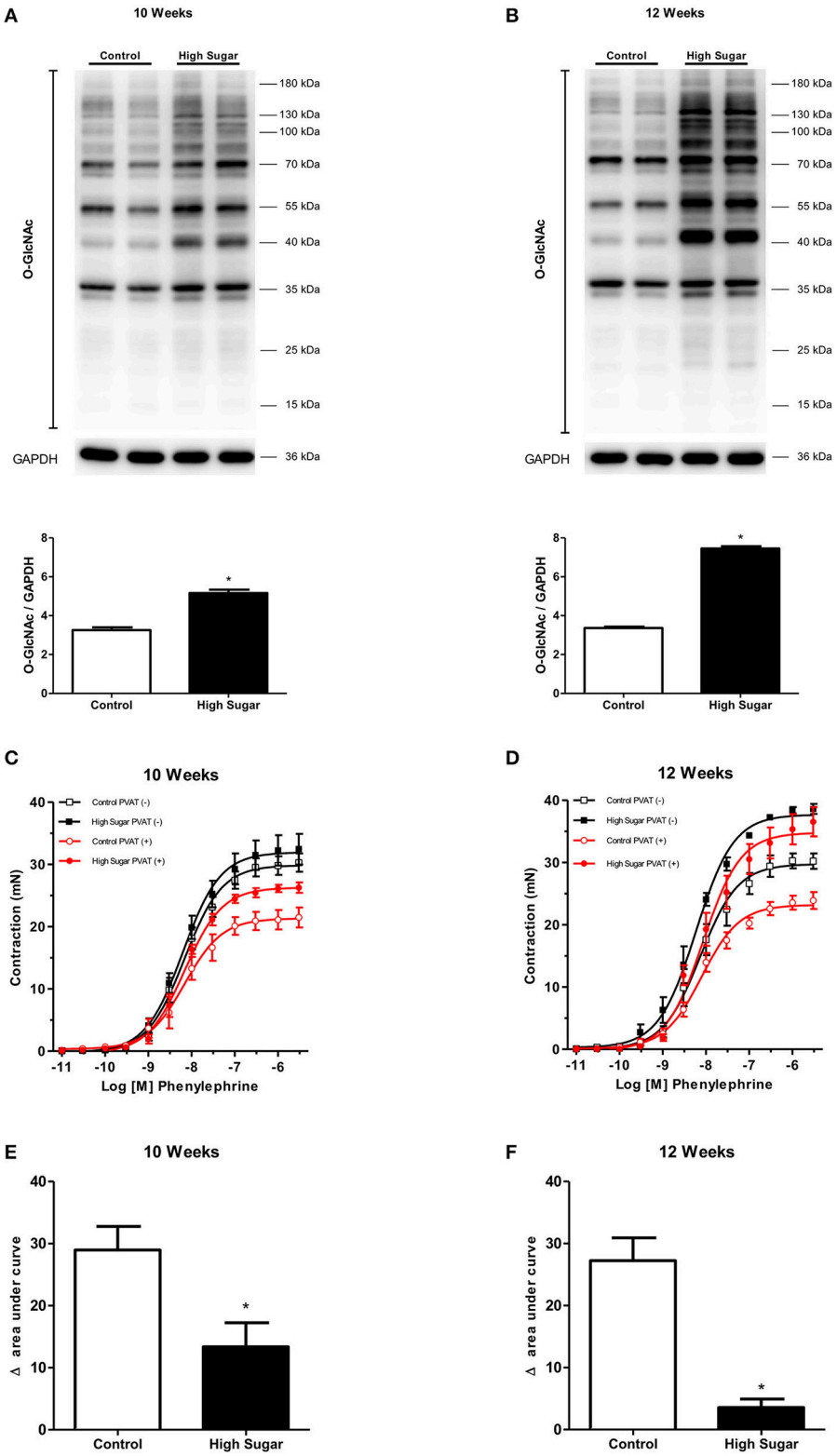

FIGURE 3 | High sugar diet increases *O*-GlcNAc-modified proteins in the PVAT and impairs PVAT anti-contractile effect. Expression of *O*-GlcNAc-modified proteins in thoracic aorta PVAT of rats fed the control ($n = 6$) or high sugar ($n = 6$) diet for **(A)** 10 or **(B)** 12 weeks. Concentration-response curves to phenylephrine were performed in endothelium-denuded aortic rings, without (–) or with (+) PVAT, from rats fed the control ($n = 7$) or high sugar ($n = 7$) diet for **(C)** 10 or **(D)** 12 weeks. **(E,F)** show the delta of the areas under the curves to phenylephrine, in the absence and presence of PVAT, in arteries of rats fed the control or high sugar diet for 10 or 12 weeks, respectively. Data are represented as the mean ± SEM. Student's *t*-test: $^*p < 0.05$ High Sugar vs. Control.

TABLE 3 | pD_2 and Emax (mN) values of phenylephrine-induced contraction in thoracic aorta arteries from Control or High Sugar diet-fed rats.

	pD_2		Emax	
Groups	**10 Weeks**	**12 Weeks**	**10 Weeks**	**12 Weeks**
Control PVAT (–)	8.1 ± 0.06 ($n = 6$)	8.1 ± 0.07 ($n = 6$)	29.8 ± 0.6 ($n = 6$)	29.7 ± 0.8 ($n = 6$)
High Sugar PVAT (–)	8.2 ± 0.07 ($n = 7$)	8.1 ± 0.05 ($n = 7$)	31.9 ± 0.8 ($n = 7$)	37.6 ± 0.6 ($n = 7$)
Control PVAT (+)	8.1 ± 0.09 ($n = 6$)	8.0 ± 0.04 ($n = 6$)	21.3 ± 0.7 ($n = 6$)*	23.1 ± 0.4 ($n = 6$)*
High Sugar PVAT (+)	8.1 ± 0.04 ($n = 7$)	8.3 ± 0.07 ($n = 7$)$^+$	26.2 ± 0.4 ($n = 7$)$^+$	34.7 ± 0.8 ($n = 7$)$^+$

*Data represent the mean ± SEM of n experiments. Two-way ANOVA: *$p < 0.05$ vs. respective Control PVAT (–); $^+p < 0.05$ vs. respective Control PVAT (+).*

Cruz Biotechnology, USA) primary antibodies were used. Protein bands were detected by chemiluminescence reaction (Luminata Forte, WBLUF0100, Merck-Millipore, UK) and the intensity of the bands was evaluated by densitometric analysis using ImageQuant software. The results are expressed by the ratio of the intensity of the *O*-GlcNAc bands to the intensity of the respective bands of the immunoprecipitated eNOS.

Measurement of Reactive Oxygen Species

Dihydroethidium

ROS generation in PVAT was assessed by dihydroethidium (DHE), as previously described (Suzuki et al., 1995). Aortas surrounded by periaortic fat were embedded in medium for frozen tissue specimens to ensure optimal cutting temperature (OCT™) and stored at −80°C. Fresh-frozen specimens were cross-sectioned at 10 μm thickness and placed on slides covered with poly-(L-lysine) solution. The tissue was loaded with the non-selective dye for ROS detection DHE (5×10^{-6} M; for 30 min at 37°C), which was prepared in phosphate buffer 0.1 M. Images were collected on a ZEISS microscope and the results are expressed as fold changes relatively to the control. Fluorescent images were analyzed by measuring the mean optical density of the fluorescence in a computer system (Image J software©) and normalized by the area.

Lucigenin

ROS generation in the PVAT and humans visceral adipose tissue was measured by a luminescence assay using lucigenin as the electron acceptor and NADH as the substrate. Periaortic fat from control and high sugar diet-fed rats was homogenized in assay buffer (50 mM KH_2PO_4, 1 mM EGTA, and 150 mM sucrose, pH 7.4) with a glass-to-glass homogenizer. The assay was performed with 100 μL of sample, lucigenin (5 μM), NADH (0.1 mM), and assay buffer. Luminescence was measured for 30 cycles of 18 s each by a luminometer (Lumistar Galaxy, BMG Labtechnologies, Ortenberg, Germany). Basal readings were obtained prior to the addition of NADH and the reaction was started by the addition of the substrate. Basal and buffer blank values were subtracted from the NADH-derived luminescence. $O_2^{\cdot-}$ was expressed as relative luminescence units (RLU)/mg of protein.

Nitric Oxide Metabolites Levels

PVAT from thoracic aorta and human visceral adipose tissue were immediately frozen in liquid nitrogen, pulverized and homogenized in 20 mM Tris-HCl (pH 7.4). The samples were centrifuged (5,000 × g for 10 min at 4°C) and the total protein content was quantified using the Bradford method. The samples were analyzed in duplicate for nitrite and nitrate (NOx) using ozone-based chemiluminescence assay. Briefly, PVAT samples were treated with cold ethanol (1:2 mesenteric bed to ethanol, for 30 min at −20°C) and centrifuged (4,000 × g for 10 min). NOx levels were measured by injecting 25 μL of supernatant in a container vent glass containing 0.8% of vanadium (III) in HCl (1 N) at 90°C, which reduces NOx into NO gas. A stream of nitrogen was bubbled through the purge vessel containing vanadium (III) with sodium hydroxide [NaOH (1N)], and then through an analyzer (Sievers Nitric Oxide Analyzer® 280, GE Analytical Instruments, Boulder, CO, USA).

Data and Statistical Analyses

Data are expressed as mean ± SEM. Concentration-response curves were fitted using the function Y = Bottom + [Top-Bottom]/[1+10^(LogEC50-X)] into a curve by non-linear regression analysis. The curves were compared using the delta of the areas under curves, maximal response (Emax) and pD_2 (defined as the negative logarithm of the EC_{50} values). The delta of the areas under curves was calculated as the difference between the concentration-response curves in the presence or in the absence of the PVAT and different drugs. Student's *t*-test was used to compare the delta of the areas under curves. Two-way ANOVA with Bonferroni post-test was used to compare Emax, pD_2, biochemical, and high glucose experiments. Mann Whitney test was used to compare groups with $n = 4$. The Prism software, version 5.0 (GraphPad Software Inc., San. Diego, CA, USA) was used to analyze these parameters. N represents the number of animals used. *p*-values < 0.05 were considered significant.

RESULTS

To determine the effects of increased *O*-GlcNAc-modified proteins on PVAT function, *O*-GlcNAcylation of rat thoracic aorta PVAT proteins was induced using Thiamet G (10^{-6} M for 24 h), a potent and selective *O*-GlcNAcase (OGA) inhibitor. Thiamet G significantly increased the expression of *O*-GlcNAc-modified proteins in the PVAT (**Figure 1A**). To determine whether increased levels of *O*-GlcNAc-proteins reduce the PVAT anti-contractile effect, endothelium-denuded thoracic aortic rings with or without PVAT were incubated with Thiamet G (10^{-6} M for 24 h) or vehicle. Subsequently, concentration-response curves to either phenylephrine or the thromboxane A_2 receptor agonist U-46619 were performed. Emax values showed,

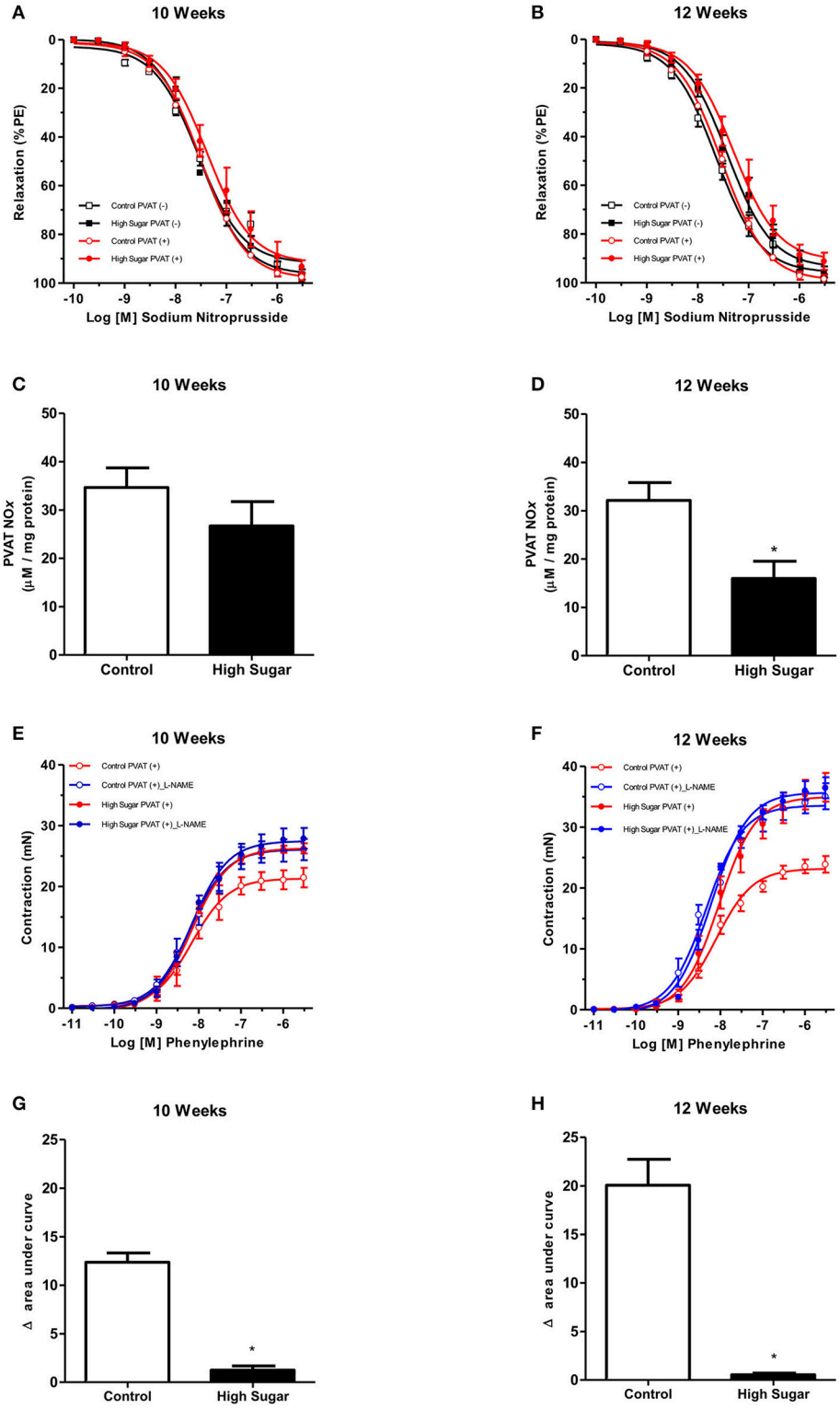

FIGURE 4 | High sugar diet decreases nitric oxide (NO) generation in the PVAT. Concentration-response curves to sodium nitroprusside, a NO donor, were performed in endothelium-denuded aortic rings, without (–) or with (+) PVAT, from rats fed the control ($n = 7$) or high sugar ($n = 7$) diet for **(A)** 10 or **(B)** 12 weeks. Nitrite and nitrate (NOx) formation in the PVAT of rats fed the control ($n = 6$) or high sugar diet ($n = 6$) for **(C)** 10 or **(D)** 12 weeks. Concentration-response curves to phenylephrine were performed in endothelium-denuded aortic rings, without (–) or with (+) PVAT, from rats fed the control ($n = 7$) or high sugar ($n = 7$) diet for **(E)** 10 or **(F)** 12 weeks, incubated with the NO synthase inhibitor, L-NAME (10^{-4} M, for 30 min) or vehicle. **(G,H)** show the delta of the areas under the curves to phenylephrine in the presence of PVAT after incubation with L-NAME or vehicle. Data are represented as the mean ± SEM. Student's *t*-test: $^{*}p < 0.05$ High Sugar vs. Control.

TABLE 4 | pD_2 and Emax (mN) values of sodium nitroprusside-induced relaxation and phenylephrine-induced contraction in thoracic aorta arteries, from Control or High Sugar-fed rats, incubated with vehicle or L-NAME.

	pD_2		Emax	
Groups	**10 Weeks**	**12 Weeks**	**10 Weeks**	**12 Weeks**
Control PVAT (–) *(Sodium nitroprusside)*	7.5 ± 0.05 ($n = 6$)	7.6 ± 0.05 ($n = 6$)	92.8 ± 2.0 ($n = 6$)	95.8 ± 1.9 ($n = 6$)
High Sugar PVAT (–) *(Sodium nitroprusside)*	7.6 ± 0.05 ($n = 7$)	7.4 ± 0.06 ($n = 7$)	96.4 ± 1.9 ($n = 7$)	94.7 ± 2.3 ($n = 7$)
Control PVAT (+) *(Sodium nitroprusside)*	7.4 ± 0.02 ($n = 6$)	7.5 ± 0.02 ($n = 6$)	97.1 ± 1.1 ($n = 6$)	98.1 ± 1.1 ($n = 6$)
High Sugar PVAT (+) *(Sodium nitroprusside)*	7.3 ± 0.08 ($n = 7$)	7.3 ± 0.07 ($n = 7$)	92.7 ± 2.0 ($n = 7$)	92.8 ± 2.9 ($n = 7$)
Control PVAT (+)	8.1 ± 0.09 ($n = 6$)	8.1 ± 0.05 ($n = 6$)	21.3 ± 0.7 ($n = 6$)	23.1 ± 0.4 ($n = 6$)
Control PVAT (+) *(L-NAME)*	8.1 ± 0.08 ($n = 7$)	8.3 ± 0.06 ($n = 7$)	26.1 ± 0.7 ($n = 7$)$^+$	33.5 ± 0.7 ($n = 7$)$^+$
High Sugar PVAT (+)	8.2 ± 0.04 ($n = 6$)	8.0 ± 0.07 ($n = 6$)	26.2 ± 0.4 ($n = 6$)	34.9 ± 0.9 ($n = 6$)
High Sugar PVAT (+) *(L-NAME)*	8.1 ± 0.06 ($n = 7$)	8.2 ± 0.04 ($n = 7$)	27.4 ± 0.6 ($n = 7$)	35.7 ± 0.5 ($n = 7$)

Data represent the mean ± SEM of n experiments. Two-way ANOVA: $^+p < 0.05$ vs. respective Control PVAT (+).

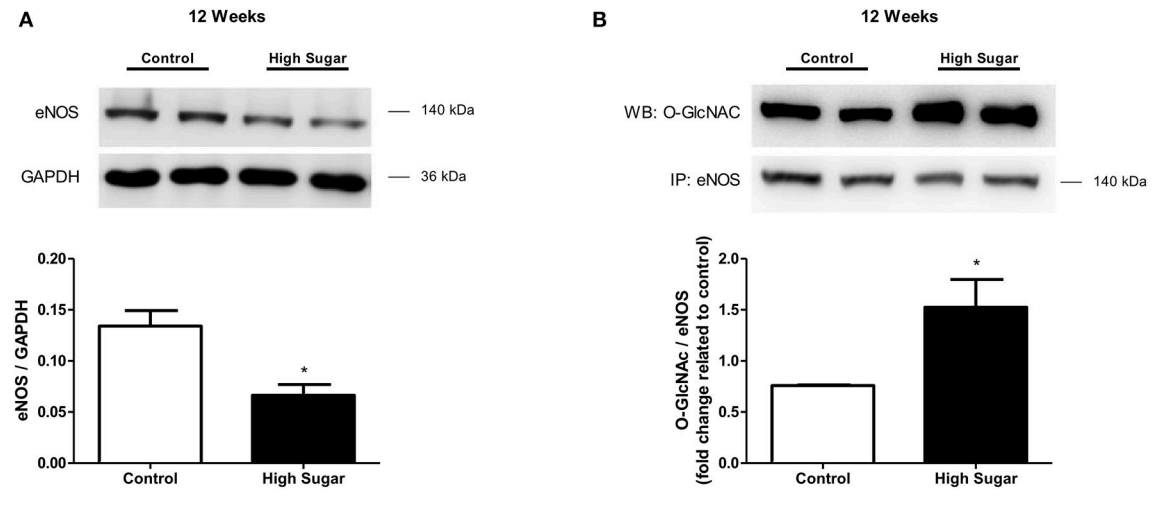

FIGURE 5 | High sugar diet decreases endothelial nitric oxide synthase (eNOS) in the PVAT. **(A)** eNOS protein expression in aortic PVAT from rats fed the control ($n = 4$) or high sugar ($n = 4$) diet for 12 weeks, determined by western blot analysis, and **(B)** *O*-GlcNAc-modified eNOS, determined by immunoprecipitation of eNOS and probing with the anti-*O*-GlcNAc antibody. Data are represented as the mean ± SEM. Mann Whitney test: $^*p < 0.05$ High Sugar *vs.* Control.

as expected, that the presence of PVAT reduced the contraction to phenylephrine and U-46619 in aortic rings incubated with vehicle (**Table 1**). Analysis of the delta of the areas under curves showed that incubation of PVAT-intact aortic rings with Thiamet G decreased the PVAT anti-contractile effect in arteries contracted with phenylephrine (**Figures 1B,C**), but not in arteries contracted with U-46619 (**Figures 1D,E**).

Considering that *O*-GlcNAcylation integrates glucose metabolism with intracellular protein activity and mediates multiple mechanisms of vascular dysfunction in metabolic syndrome, including impaired contractility (Lima et al., 2016), the possible relevance of PVAT *O*-GlcNAcylation following a high sugar diet was assessed. Rats fed the high sugar diet for 10 and 12 weeks exhibited an increase in all anthropometric parameters, total cholesterol and triglycerides (**Table 2**) compared with rats on the control diet. Only rats fed the high sugar diet for 12 weeks showed increased serum glucose levels (**Figure 2A**) and glucose intolerance, determined by the areas under the curves in the OGTT (**Figures 2B,C**). Insulin serum levels (**Figure 2D**) and HOMA-IR index (**Figure 2E**) were increased in rats fed the high sugar diet for 10 and 12 weeks.

To test the hypothesis that the high sugar diet increases PVAT *O*-GlcNAc levels leading to the loss of its anti-contractile effect, the content of *O*-GlcNAc-modified proteins in the PVAT from rats fed either the control or high sugar diet was determined. *O*-GlcNAcylated-proteins content was significantly increased in the PVAT from rats on the high sugar diet for 10 (**Figure 3A**) and 12 (**Figure 3B**) weeks. To determine the effects of high sugar diet on PVAT function, concentration-response curves to phenylephrine were performed in endothelium-denuded aortic rings with or without PVAT. Emax values showed that the presence of PVAT reduced the contraction to phenylephrine in arteries from rats fed the control diet, regardless of the duration of the diet (**Table 3**). Analysis of the delta of the areas under the curves confirmed that high sugar diet decreased the PVAT anti-contractile effect in arteries from rats fed for 10 (**Figures 3C,E**) or 12 (**Figures 3D,F**) weeks.

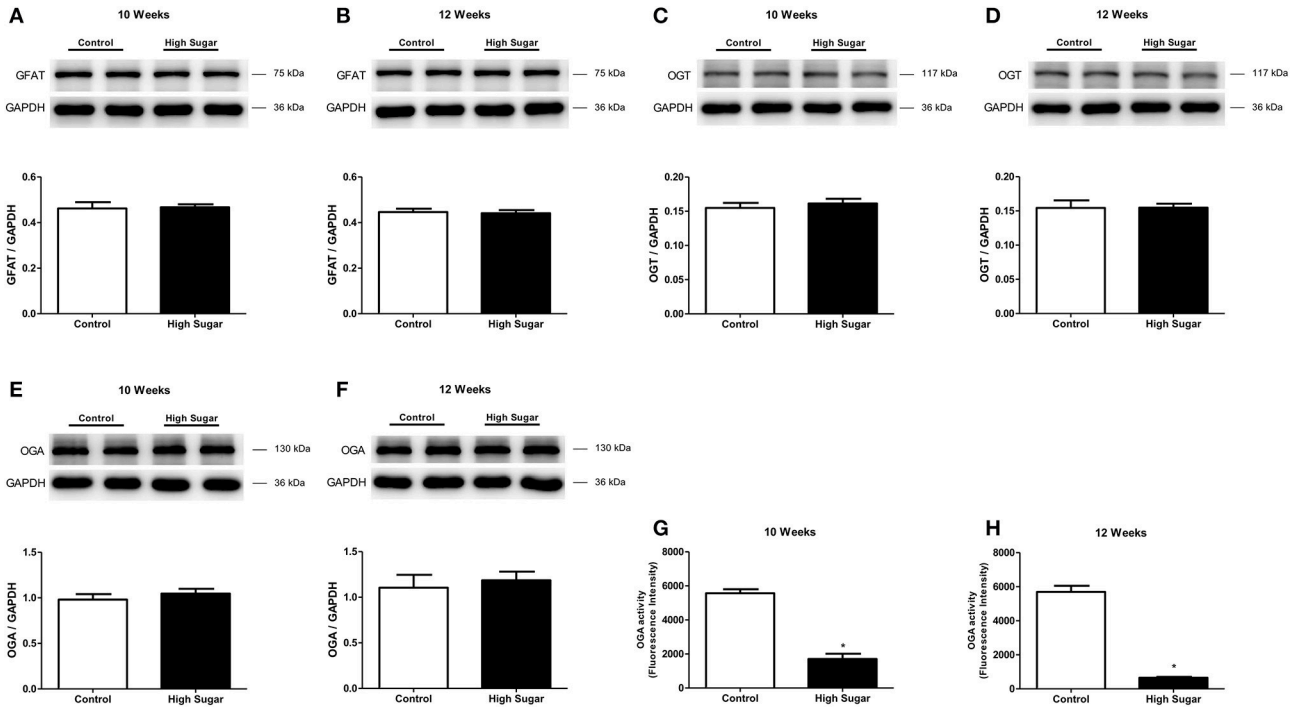

FIGURE 6 | High sugar diet did not alter expression of proteins that regulate the hexosamine pathway, but decreases OGA protein activity. **(A,B)** GFAT, glucosamine-fructose-6-phosphate aminotransferase ($n = 6$); **(C,D)** OGT, *O*-linked *N*-acetylglucosamine (GlcNAc) transferase ($n = 6$); **(E,F)** OGA, *O*-GlcNAcase ($n = 6$) proteins expression, determined by western blot analysis. OGA activity in the PVAT from rats fed the control ($n = 6$) or high sugar ($n = 6$) diet for **(G)** 10 and **(H)** 12 weeks. Data are represented as the mean ± SEM. Student's *t*-test: $^*p < 0.05$ High Sugar vs. Control.

Considering that NO is produced and released by the PVAT and induces relaxation of vascular smooth muscle cells (VSMC), and that PVAT dysfunction can be related to either changes in signaling pathways in the vasculature or to a defective production of NO by the PVAT, the effects of the high sugar diet on sodium nitroprusside (SNP)-induced endothelium-independent vascular relaxation as well as in NO bioavailability were determined. There was no difference in vascular relaxation to SNP in rats fed the high sugar diet either for 10 or 12 weeks (**Figures 4A,B**, **Table 4**), indicating that the high sugar diet does not reduce NO-mediated signaling in VSMC. NO formation in PVAT from rats fed the high sugar diet during 10 weeks was not decreased (**Figure 4C**). However, PVAT from high sugar diet-fed rats for 12 weeks exhibited decreased NO levels (**Figure 4D**). Interestingly, whereas L-NAME produced an upward shift in phenylephrine responses in endothelium-denuded and PVAT-intact aortas from rats fed the control diet, this effect was not observed in aortas from the high sugar-fed group, i.e., the NO synthase inhibitor L-NAME did not further enhance the effects of the high sugar diet [either for 10 weeks (**Figure 4E**, **Table 4**) or 12 weeks (**Figure 4F**, **Table 4**)] on the loss of PVAT anti-contractile effect. These data indicate that the high sugar diet decreases PVAT anti-contractile effect by reducing NO bioavailability (**Figures 4G,H**). Consistent with these results, the expression of endothelial nitric oxide synthase (eNOS) was significantly reduced in the PVAT from high sugar-fed rats (**Figure 5A**) and this change was accompanied by increased eNOS *O*-GlcNAcylation (**Figure 5B**). These results indicate that *O*-GlcNAcylation of eNOS impairs the activity of this enzyme and decreases NO production in PVAT.

The effects of high sugar diet on the expression of proteins that directly regulate the *O*-GlcNAcylation process were also determined. No differences were detected in the PVAT expression of GFAT, the first and rate-limiting enzyme of the hexosamine biosynthesis pathway, between rats that received the control and high sugar diets for 10 (**Figure 6A**) or 12 (**Figure 6B**) weeks. Similarly, there were no differences in the expression of OGT (**Figures 6C,D**) or OGA (**Figures 6E,F**) enzymes in the PVAT from rats fed the control and high sugar diets for 10 or 12 weeks. However, OGA activity was significantly reduced in the PVAT of rats fed the high sugar diet for 10 (**Figure 6G**) and 12 (**Figure 6H**) weeks, suggesting that *O*-GlcNAc elevation in PVAT is a function of decreased OGA activity.

We have recently reported that increased mitochondrial ROS generation mediates the loss of PVAT anti-contractile effects in high-fat diet obese mice (da Costa et al., 2017). To explore the possibility that increased *O*-GlcNAc levels in the PVAT are linked to oxidative stress, we assessed the generation of NADPH-derived $O_2^{\cdot-}$ by the lucigenin-enhanced chemiluminescence and DHE fluorescence techniques. $O_2^{\cdot-}$ production was significantly increased in the PVAT of rats fed the high sugar diet for 12 weeks (**Figures 7A,B**). In view of the pro-oxidative phenotype

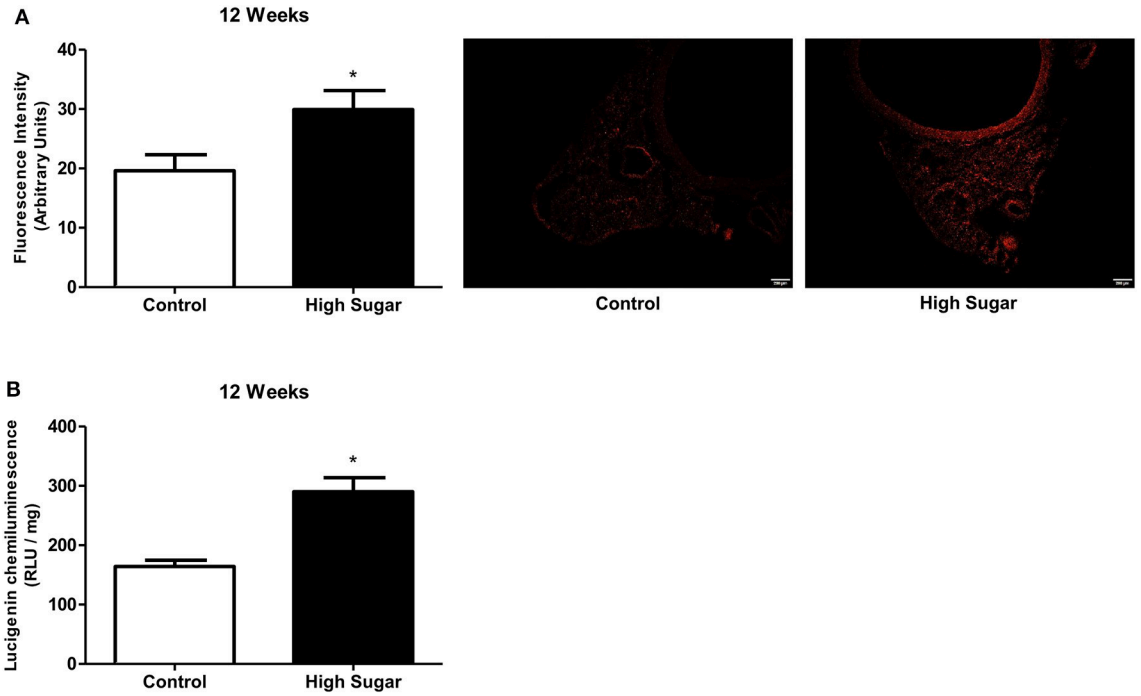

FIGURE 7 | High sugar diet increases reactive oxygen species (ROS) generation in the PVAT. ROS generation, measured **(A)** by DHE (Dihydroethidium) and **(B)** by lucigenin in the PVAT from rats fed the control ($n = 5$) or high sugar ($n = 5$) diet for 12 weeks. Data are represented as the mean ± SEM. Student's *t*-test: $^*p < 0.05$ High Sugar vs. Control.

observed in the PVAT, we hypothesized that the increased flux of glucose through the hexosamine biosynthetic pathway leads to increased *O*-GlcNAc modification of PVAT proteins via increased generation of NADPH-derived $O_2^{\cdot-}$. To verify this hypothesis, PVAT from rats fed the control diet was exposed to high glucose medium for 6 h. Incubation in high glucose medium increased the PVAT content of *O*-GlcNAc-modified proteins, and effect that was attenuated by pre-incubation with Tiron (10^{-4} M) (**Figure 8A**). Similar to what was observed in the PVAT from rats fed the high sugar diet, the high glucose medium increased ROS generation (**Figure 8B**), which was accompanied by a decrease in OGA activity (**Figure 8C**). Reduction of OGA activity was also prevented by Tiron, suggesting that ROS modulate PVAT OGA activity. Finally, high glucose medium-induced modifications were followed by decreased PVAT NO production, which was prevented by the pre-incubation with Tiron (**Figure 8D**).

To determine whether there is a correlation between data from the experimental animal and the clinical onset, visceral adipose tissue samples from normoglycemic (blood glucose mean 92.5 mg/dL) and hyperglycemic (mean blood glucose 173.1 mg/dL) patients were analyzed. Increased levels of *O*-GlcNAc-modified proteins were found in the visceral adipose tissue from hyperglycemic individuals in comparison to samples from normoglycemic subjects. In addition, increased ROS generation (**Figure 9B**) and decreased OGA activity (**Figure 9C**) were detected in the visceral adipose tissue from hyperglycemic patients.

DISCUSSION

PVAT is increasingly recognized as a widespread and relevant tissue in vascular biology as well as an important determinant of the cardiovascular complications associated with obesity and type 2 diabetes (Meijer et al., 2011). However, the molecular mechanisms underlying PVAT dysfunction in these conditions are largely unknown. Increased *O*-GlcNAcylation has been reported in human and animal visceral adipose tissue during pathological conditions such as hypertension, obesity, and type 2 diabetes (Ma and Hart, 2013). Nevertheless, the role of *O*-GlcNAcylation in PVAT dysfunction has not been previously determined. The present study demonstrates that *O*-GlcNAcylation plays a key role on high-sugar diet-induced PVAT dysfunction. Our studies reveal a previously unknown function of *O*-GlcNAcylation in controlling the anti-contractile activity of the PVAT. Chronic hyperglycemia increased ROS production and induced a phenotype of increased *O*-GlcNAcylation and decreased ADRF release, primarily by regulating NO production in the adipocytes (**Figure 10**). These new findings have important implications for prevention and treatment of vascular complications during obesity and other metabolic disorders and might, therefore, underscore O-GlcNAcylation as a target to combat vascular damage.

The results delineate potential negative consequences of increased PVAT *O*-GlcNAcylation in response to chronic hyperglycemia (**Figure 2**). Previous studies have demonstrated that acute increases in O-GlcNAcylation in 3T3-L1 adipocytes

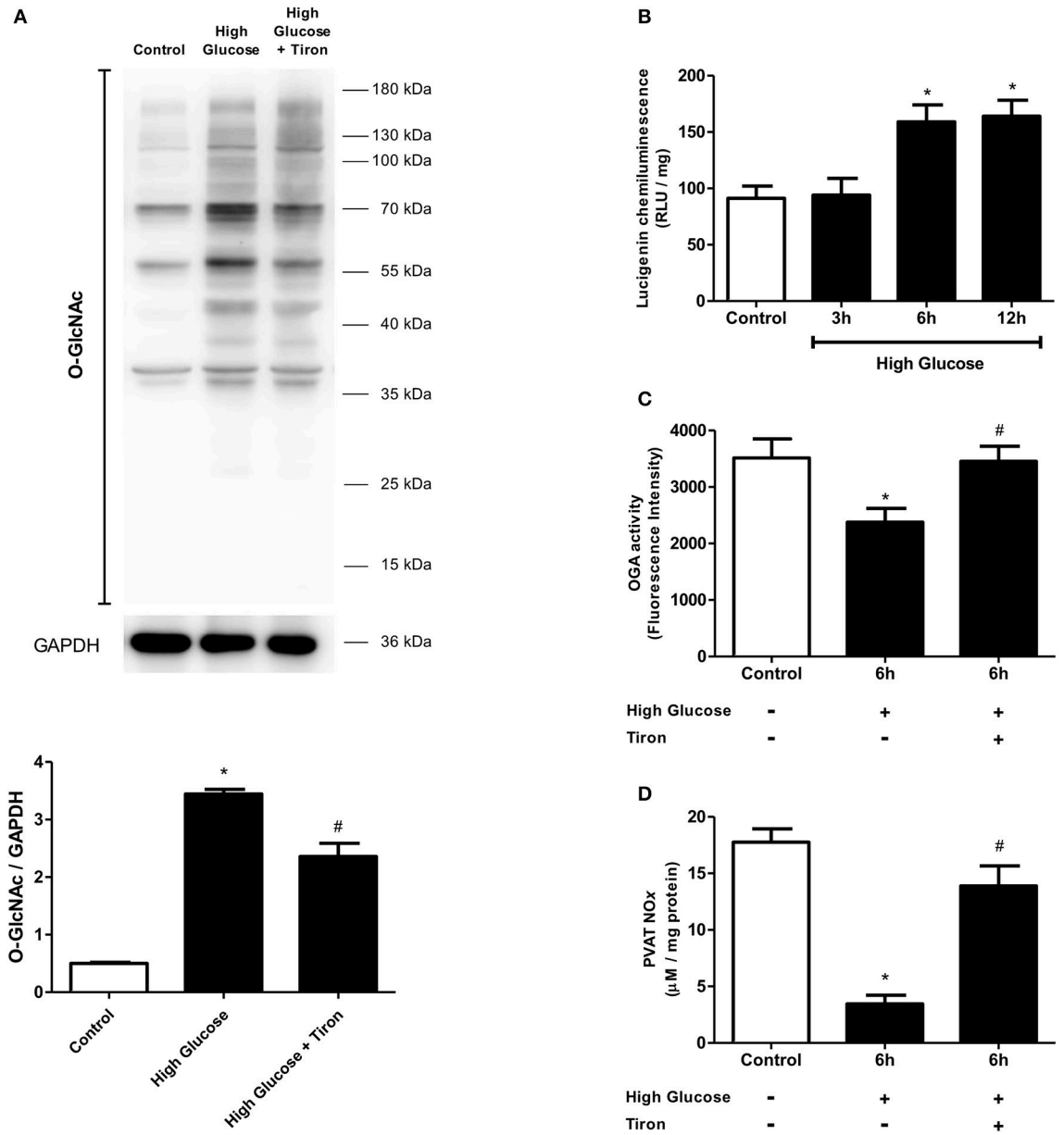

FIGURE 8 | Effect of ROS in *O*-GlcNAcylation processes in PVAT incubated with high glucose medium. **(A)** *O*-GlcNAc-modified protein expression is increased in PVAT incubated with high glucose medium for 6 h and this increase is attenuated by simultaneous incubating with Tiron (10^{-4} M), a superoxide anion scavenger. **(B)** ROS production increases in the PVAT incubated in high glucose medium for 6 and 12 h. The PVAT maintained in high glucose medium for 6 h and incubated with Tiron does not exhibit **(C)** decreased OGA activity or **(D)** decreased NOx production. Data are represented as the mean ± SEM. Two-way ANOVA: $^{*}p < 0.05$ High Glucose vs. Control, $^{\#}p < 0.05$ High Glucose + Tiron vs. High Glucose, $n = 6$ for each experimental group.

treated with PUGNAc lead to insulin resistance (Vosseller et al., 2002). Moreover, a similar phenomenon has been observed in rat skeletal muscle (Arias et al., 2004). However, few studies have examined the function of chronic increases in *O*-GlcNAcylation. Our findings, along with other studies (Medford et al., 2012; Heath et al., 2014), indicate that increased *O*-GlcNAcylation over an extended period, as observed in the later stages of diabetes, may cause adverse complications in the cardiovascular system (**Figure 3**). By using Thiamet-G, a potent and selective OGA inhibitor, our data provide further evidence that increased PVAT *O*-GlcNAcylation impairs the anti-contractile effects to phenylephrine, mediated by this tissue (**Figure 1**). In this case, the use of culture medium to keep the vessels for 24 h (time required to increase *O*-GlcNAc-modified proteins in PVAT) may be considered a methodological limitation. This *ex vivo* period changes the contractile properties when compared to freshly isolated vessels. However, there is no loss of information, since control vessels were also exposed to the same cultivation period.

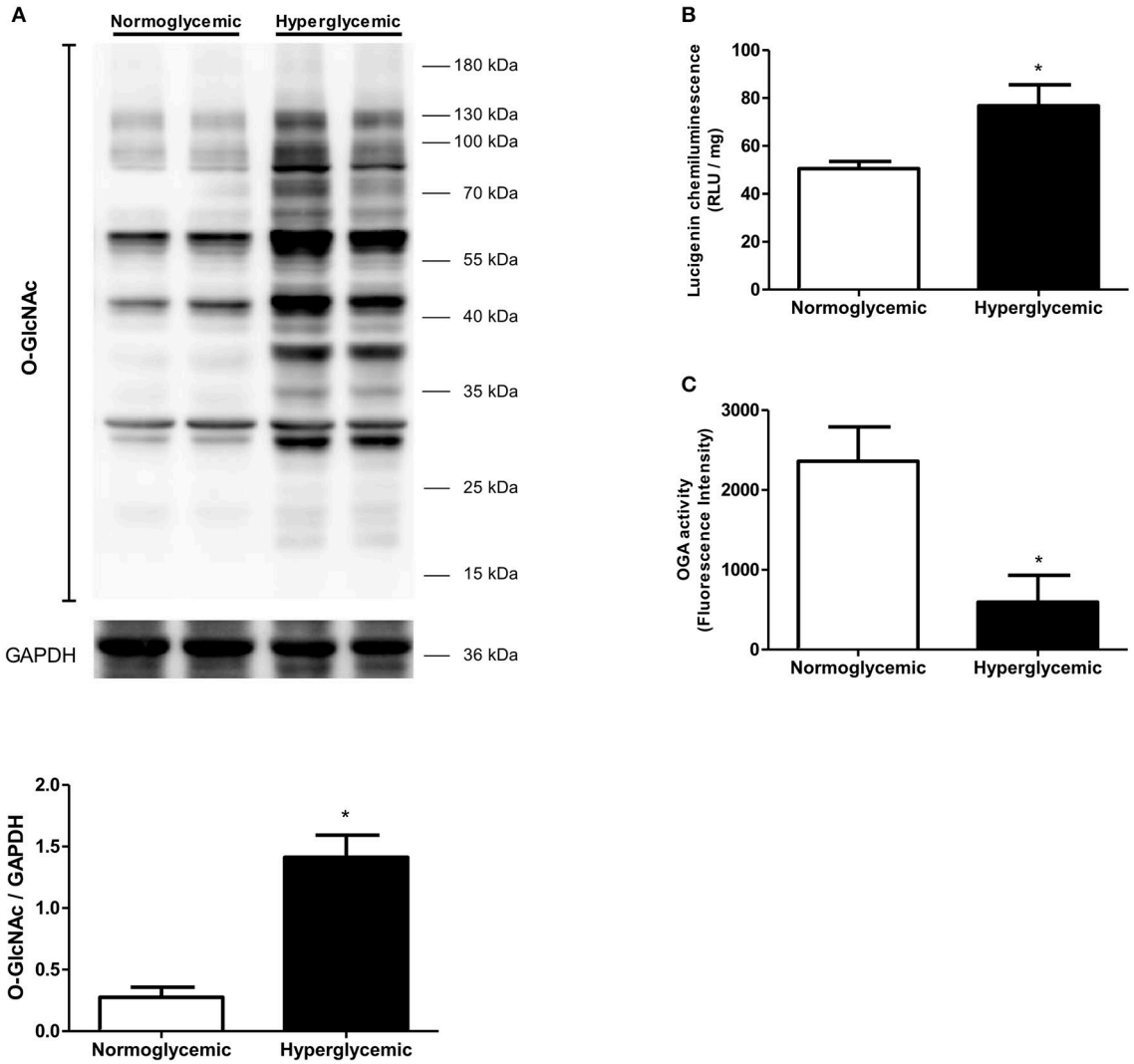

FIGURE 9 | Effect of glycemia on *O*-GlcNAc-modified protein profile in human visceral adipose tissue. **(A)** *O*-GlcNAc-modified protein expression and **(B)** ROS generation are increased whereas **(C)** OGA activity is decreased in the adipose tissue of human with hyperglycemia. Data are represented as the mean ± SEM. Mann Whitney test: $^*p < 0.05$ Hyperglycemic vs. Normoglycemic, $n = 4$ for each group.

Mechanistic studies demonstrated that increased PVAT *O*-GlcNAcylation following chronic hyperglycemia is linked to inhibition of OGA activity. Consistent with clinical observations demonstrating an association between PVAT dysfunction and other vascular complications in obesity and diabetes, our findings demonstrate increased aortic contraction in high sugar-fed rats, which was further worsened in the presence of PVAT (**Figure 3**). Our data also demonstrate increased *O*-GlcNAcylation associated with OGA inhibition in human visceral adipose tissue following long-term hyperglycemic conditions (**Figure 9**). Together, these studies indicate a causative link between increased *O*-GlcNAcylation in the PVAT and hyperglycemia-induced vascular dysfunction.

PVAT from high sugar-fed rats displays a significant reduction in NO production (**Figure 5**) associated with decreased eNOS expression (**Figure 4**). Previous studies have shown eNOS expression in adipose tissues (Ribiere et al., 1996; Victorio et al., 2016) and adipocytes (Ribiere et al., 1996). It is assumed that adipocyte-derived NO is released into the interstitial fluid and diffuses into the capillaries and adjacent arterioles causing vasodilation (Mastronardi et al., 2002). Indeed, enhanced relaxant response of mesenteric arteries and increased leptin-mediated NO production in the mesenteric artery PVAT have been demonstrated at the early phase of diet-induced obesity in C57BL/6J mice (Gil-Ortega et al., 2010). In addition, the studies of Xia et al. confirmed that PVAT-derived NO contributes to acetylcholine-induced vasodilation (Xia et al., 2016). The authors demonstrated that, under diet-induced obesity conditions, eNOS-driven NO production is reduced in the PVAT. In our model, the loss of the PVAT anti-contractile

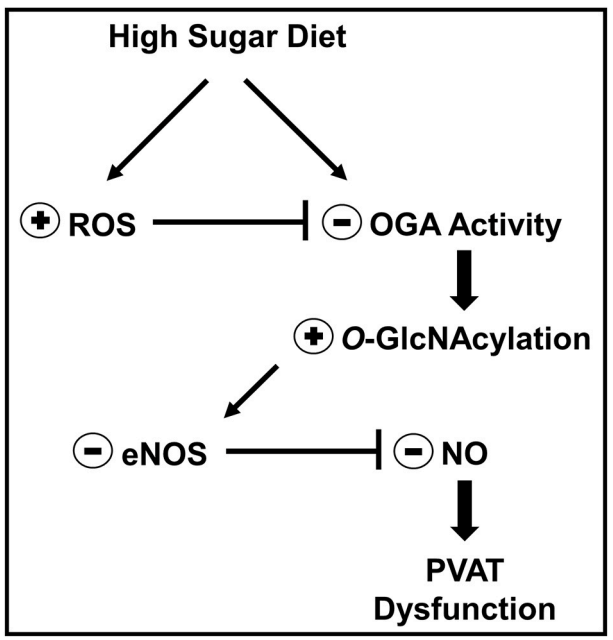

FIGURE 10 | Mechanism proposed to explain how *O*-GlcNAc-modified proteins contribute to high sugar diet-induced PVAT dysfunction. In the context of hyperglycemia, such as in animals fed a high sugar diet or in hyperglycemic patients, increased PVAT ROS generation leads to inhibition of OGA activity and accumulation of *O*-GlcNAc-modified proteins, including eNOS. *O*-GlcNAcylation of eNOS reduces NO production by the enzyme and is linked to PVAT dysfunction.

function in rats fed a high sugar diet was not further modified by eNOS inhibition. Thus, eNOS-derived NO in PVAT plays a major role in the anti-contractile effects mediated by PVAT. The intrinsic relaxant responsiveness of VSMC was preserved, since sodium nitroprusside-induced relaxations were identical despite the loss of eNOS-derived NO in PVAT (**Figure 4**). These data suggest that changes in PVAT anti-contractile effects during hyperglycemia are most likely caused by alterations in PVAT-derived components and not by changes in the VSMC function.

Notably, the present study provides novel mechanisms underlying the regulation of eNOS activity in the PVAT. Although impaired activation of PVAT eNOS and reduction of PVAT-derived NO have been associated with obesity-induced vascular dysfunction, whether eNOS activation in PVAT is regulated directly by *O*-GlcNAcylation is not clear. Our studies have identified that decreased eNOS expression is accompanied by an increase in eNOS *O*-GlcNAcylation, which promotes vascular dysfunction during hyperglycemia (**Figure 5**). Increased *O*-GlcNAcylation of eNOS, which is associated with decreased phosphorylation at Ser^{1177}, the site responsible for activation of the enzyme, has been reported in bovine aortic endothelial cells (Du et al., 2001). The work by Federici et al. (2002) also demonstrated an inverse correlation between eNOS *O*-GlcNAcylation and phosphorylation status in human coronary artery endothelial cells. Furthermore, the authors showed that both hyperglycemia and direct activation of the hexosamine biosynthesis pathway by glucosamine determines reduction in insulin-stimulated phosphorylation of eNOS by increased *O*-GlcNAcylation of key signaling molecules. Interestingly, Musicki et al. (2005) demonstrated that increased *O*-GlcNAcylation of eNOS-Ser^{1177} attenuates shear stress-induced increase in penile blood flow during diabetes. More recently, Beleznai and Bagi (2012) reported that increased *O*-GlcNAcylation contributes to impaired NO-mediated arteriolar dilation following hyperglycemia. Overall, our findings show that increased *O*-GlcNAcylation of eNOS impairs the activity of this enzyme and the subsequent NO production in the PVAT and support the concept that PVAT *O*-GlcNAcylation may be a significant contributing factor to vascular dysfunction in metabolic syndrome.

Apart from inhibiting eNOS, basal *O*-GlcNAcylation may regulate other signaling systems that decrease NO production, such as ROS (Lima et al., 2012). In the present study, acute and chronic high glucose increased PVAT generation of ROS. *O*-GlcNAc may influence the expression or function of a variety of proteins involved in high glucose-induced ROS production. However, it is equally plausible that much of the effect of high glucose levels on PVAT *O*-GlcNAcylation is secondary to the increase in PVAT ROS generation. In addition to modulating the activity of specific intracellular protein kinases and phosphatases (Takakura et al., 1999; Weber et al., 2004), ROS stimulate the hexosamine biosynthetic pathway and, consequently, *O*-GlcNAcylation (Brownlee, 2001). For instance, increased production of mitochondria-derived ROS induces both changes in phosphorylation and *O*-GlcNAcylation of many intracellular proteins (Jones et al., 2008; Laczy et al., 2009). Restoration of both OGA activity and NO production by Tiron (**Figure 8**) further supports a role for ROS-mediated signals in mediating *O*-GlcNAcylation-induced impairment of eNOS activity and vascular dysfunction. The concurrent increase in both ROS generation and *O*-GlcNAcylation clearly demonstrate the reciprocal regulation between *O*-GlcNAcylation and ROS. Nevertheless, our findings, along with the western blot data showing that Tiron only partially reduces PVAT *O*-GlcNAc levels (**Figure 8**), suggest that chronic hyperglycemia increases *O*-GlcNAcylation of target proteins in the PVAT via increased ROS generation.

As discussed above, the different outcomes of reducing ROS formation probably reflect the involvement of different signal transduction pathways in high glucose-treated PVAT. Reinforcing this view, it has been reported that both oxidative stress and high glucose decrease endothelial NO bioavailability, impair vascular relaxation (King, 1996; Creager et al., 2003; Landmesser et al., 2003), and increase *O*-GlcNAcylation (Lima et al., 2012; Ma and Hart, 2013). Further studies are warranted to dissect the precise signaling cascades that are responsible for hyperglycemia-induced *O*-GlcNAcylation of PVAT eNOS. However, the novel regulation of eNOS activation in PVAT by *O*-GlcNAcylation uncovered in this study may not only impact the biological function of this tissue, but also provides novel mechanistic insights into the pathogenesis of hyperglycemia-associated vascular disease.

In summary, the present study demonstrates a novel causative link between chronic increases in *O*-GlcNAcylation of target proteins in the PVAT and hyperglycemia-associated vascular dysfunction. It also provides a novel molecular insight into the mechanism underlying the regulation of eNOS activity, with *O*-GlcNAcylation leading to reduced NO production and PVAT anti-contractile effect. Our studies also reveal a critical interplay between *O*-GlcNAcylation and ROS generation in the PVAT, which mediates high glucose-induced PVAT dysfunction and vascular injury. These findings have determined *O*-GlcNAcylation as a novel contributor to the process of hyperglycemia-induced PVAT dysfunction and identified *O*-GlcNAcylation of eNOS as a possible target for the development of therapies for vascular dysfunction in metabolic syndrome.

AUTHOR CONTRIBUTIONS

RdC, JdS, NdSL, and RT participated in the design of the study; RdC, JdS, JA, TD, DR, and LG conducted the experiments; RT and NdSL contributed new reagents or analytical tools; RdC, JdS, JA, NdSL, and RT performed the data analysis; RdC, JdS, NdSL, and RT wrote the paper.

ACKNOWLEDGMENTS

This work was supported by grants from Fundação de Amparo à Pesquisa do Estado de São Paulo (FAPESP-CRID 2013/08216-2 to RT), Coordenação de Aperfeiçoamento de Pessoal de Nível Superior (CAPES), Conselho Nacional de Desenvolvimento Científico e Tecnológico (CNPq), Brazil.

REFERENCES

Alves-Lopes, R., Neves, K. B., Montezano, A. C., Harvey, A., Carneiro, F. S., Touyz, R. M., et al. (2016). Internal pudental artery dysfunction in diabetes mellitus is mediated by NOX1-derived ROS-, Nrf2-, and Rho kinase-dependent mechanisms. *Hypertension* 68, 1056–1064. doi: 10.1161/HYPERTENSIONAHA.116.07518

Arias, E. B., Kim, J., and Cartee, G. D. (2004). Prolonged incubation in PUGNAc results in increased protein O-Linked glycosylation and insulin resistance in rat skeletal muscle. *Diabetes* 53, 921–930. doi: 10.2337/diabetes.53.4.921

Beleznai, T., and Bagi, Z. (2012). Activation of hexosamine pathway impairs nitric oxide (NO)-dependent arteriolar dilations by increased protein O-GlcNAcylation. *Vascul. Pharmacol.* 56, 115–121. doi: 10.1016/j.vph.2011.11.003

Bradford, M. M. (1976). A rapid and sensitive method for the quantitation of microgram quantities of protein utilizing the principle of protein-dye binding. *Anal. Biochem.* 72, 248–254. doi: 10.1016/0003-2697(76)90527-3

Brownlee, M. (2001). Biochemistry and molecular cell biology of diabetic complications. *Nature* 414, 813–820. doi: 10.1038/414813a

Costa, R. M., Filgueira, F. P., Tostes, R. C., Carvalho, M. H., Akamine, E. H., and Lobato, N. S. (2016). H2O2 generated from mitochondrial electron transport chain in thoracic perivascular adipose tissue is crucial for modulation of vascular smooth muscle contraction. *Vascul. Pharmacol.* 84, 28–37. doi: 10.1016/j.vph.2016.05.008

Creager, M. A., Luscher, T. F., Cosentino, F., and Beckman, J. A. (2003). Diabetes and vascular disease: pathophysiology, clinical consequences, and medical therapy: part I. *Circulation* 108, 1527–1532. doi: 10.1161/01.CIR.0000091257.27563.32

da Costa, R. M., Fais, R. S., Dechandt, C. R. P., Louzada-Junior, P., Alberici, L. C., Lobato, N. S., et al. (2017). Increased mitochondrial ROS generation mediates the loss of the anti-contractile effects of perivascular adipose tissue in high-fat diet obese mice. *Br. J. Pharmacol.* 174, 3527–3541. doi: 10.1111/bph.13687

Du, X. L., Edelstein, D., Dimmeler, S., Ju, Q., Sui, C., and Brownlee, M. (2001). Hyperglycemia inhibits endothelial nitric oxide synthase activity by posttranslational modification at the Akt site. *J. Clin. Invest.* 108, 1341–1348. doi: 10.1172/JCI11235

Farb, M. G., Ganley-Leal, L., Mott, M., Liang, Y., Ercan, B., Widlansky, M. E., et al. (2012). Arteriolar function in visceral adipose tissue is impaired in human obesity. *Arterioscler. Thromb. Vasc. Biol.* 32, 467–473. doi: 10.1161/ATVBAHA.111.235846

Federici, M., Menghini, R., Mauriello, A., Hribal, M. L., Ferrelli, F., Lauro, D., et al. (2002). Insulin-dependent activation of endothelial nitric oxide synthase is impaired by O-linked glycosylation modification of signaling proteins in human coronary endothelial cells. *Circulation* 106, 466–472. doi: 10.1161/01.CIR.0000023043.02648.51

Fernández-Alfonso, M. S., Gil-Ortega, M., García-Prieto, C. F., Aranguez, I., Ruiz-Gayo, M., and Somoza, B. (2013). Mechanisms of perivascular adipose tissue dysfunction in obesity. *Int. J. Endocrinol.* 2013:402053. doi: 10.1155/2013/402053

Gao, Y. J. (2007). Dual modulation of vascular function by perivascular adipose tissue and its potential correlation with adiposity/lipoatrophy-related vascular dysfunction. *Curr. Pharm. Des.* 13, 2185–2192. doi: 10.2174/138161207781039634

Gil-Ortega, M., Stucchi, P., Guzmán-Ruiz, R., Cano, V., Arribas, S., González, M. C., et al. (2010). Adaptative nitric oxide overproduction in perivascular adipose tissue during early diet-induced obesity. *Endocrinology* 151, 3299–3306. doi: 10.1210/en.2009-1464

Hart, G. W., Housley, M. P., and Slawson, C. (2007). Cycling of O-linked beta-N-acetylglucosamine on nucleocytoplasmic proteins. *Nature* 446, 1017–1022. doi: 10.1038/nature05815

Heath, J. M., Sun, Y., Yuan, K., Bradley, W. E., Litovsky, S., Dell'Italia, L. J., et al. (2014). Activation of AKT by O-linked N-acetylglucosamine induces vascular calcification in diabetes mellitus. *Circ. Res.* 114, 1094–1102. doi: 10.1161/CIRCRESAHA.114.302968

Jones, S. P., Zachara, N. E., Ngoh, G. A., Hill, B. G., Teshima, Y., Bhatnagar, A., et al. (2008). Cardioprotection by N-acetylglucosamine linkage to cellular proteins. *Circulation* 117, 1172–1182. doi: 10.1161/CIRCULATIONAHA.107.730515

King, G. L. (1996). The role of hyperglycaemia and hyperinsulinaemia in causing vascular dysfunction in diabetes. *Ann. Med.* 28, 427–432. doi: 10.3109/07853899608999103

Laczy, B., Hill, B. G., Wang, K., Paterson, A. J., White, C. R., Xing, D., et al. (2009). Protein O-GlcNAcylation: a new signaling paradigm for the cardiovascular system. *Am. J. Physiol. Heart Circ. Physiol.* 296, H13–H28. doi: 10.1152/ajpheart.01056.2008

Landmesser, U., Dikalov, S., Price, S. R., McCann, L., Fukai, T., Holland, S. M., et al. (2003). Oxidation of tetrahydrobiopterin leads to uncoupling of endothelial cell nitric oxide synthase in hypertension. *J. Clin. Invest.* 111, 1201–1209. doi: 10.1172/JCI200314172

Lima, V. V., Giachini, F. R., Matsumoto, T., Li, W., Bressan, A. F., Chawla, D., et al. (2016). High-fat diet increases O-GlcNAc levels in cerebral arteries: a link to vascular dysfunction associated with hyperlipidaemia/obesity? *Clin. Sci.* 130, 871–880. doi: 10.1042/CS20150777

Lima, V. V., Rigsby, C. S., Hardy, D. M., Webb, R. C., and Tostes, R. C. (2009). O-GlcNAcylation: a novel post-translational mechanism to alter vascular cellular signaling in health and disease: focus on hypertension. *J. Am. Soc. Hypertens.* 3, 374–387. doi: 10.1016/j.jash.2009.09.004

Lima, V. V., Spitler, K., Choi, H., Webb, R. C., and Tostes, R. C. (2012). O-GlcNAcylation and oxidation of proteins: is signalling in the cardiovascular system becoming sweeter? *Clin. Sci.* 123, 473–486. doi: 10.1042/CS20110638

Lumeng, C. N., Bodzin, J. L., and Saltiel, A. R. (2007). Obesity induces a phenotypic switch in adipose tissue macrophage polarization. *J. Clin. Invest.* 117, 175–184. doi: 10.1172/JCI29881

Ma, J., and Hart, G. W. (2013). Protein O-GlcNAcylation in diabetes and diabetic complications. *Expert Rev. Proteomics* 10, 365–380. doi: 10.1586/14789450.2013.820536

Ma, L., Ma, S., He, H., Yang, D., Chen, X., Luo, Z., et al. (2010). Perivascular fat-mediated vascular dysfunction and remodeling through the AMPK/mTOR pathway in high-fat diet-induced obese rats. *Hypertens. Res.* 33, 446–453. doi: 10.1038/hr.2010.11

Mastronardi, C. A., Yu, W. H., and McCann, S. M. (2002). Resting and circadian release of nitric oxide is controlled by leptin in male rats. *Proc. Natl. Acad. Sci. U.S.A.* 99, 5721–5726. doi: 10.1073/pnas.082098499

Medford, H. M., Chatham, J. C., and Marsh, S. A. (2012). Chronic ingestion of a Western diet increases O-linked-beta-N-acetylglucosamine (O-GlcNAc) protein modification in the rat heart. *Life Sci.* 90, 883–888. doi: 10.1016/j.lfs.2012.04.030

Meijer, R. I., Serne, E. H., Smulders, Y. M., van Hinsbergh, V. W., Yudkin, J. S., and Eringa, E. C. (2011). Perivascular adipose tissue and its role in type 2 diabetes and cardiovascular disease. *Curr. Diab. Rep.* 11, 211–217. doi: 10.1007/s11892-011-0186-y

Musicki, B., Kramer, M. F., Becker, R. E., and Burnett, A. L. (2005). Inactivation of phosphorylated endothelial nitric oxide synthase (Ser-1177) by O-GlcNAc in diabetes-associated erectile dysfunction. *Proc. Natl. Acad. Sci. U.S.A.* 102, 11870–11875. doi: 10.1073/pnas.0502488102

Okuda, T. (2017). PUGNAc treatment provokes globotetraosylceramide accumulation in human umbilical vein endothelial cells. *Biochem. Biophys. Res. Commun.* 487, 76–82. doi: 10.1016/j.bbrc.2017.04.019

Pan, Y., Qiao, Q. Y., Pan, L. H., Zhou, D. C., Hu, C., Gu, H. F., et al. (2015). Losartan reduces insulin resistance by inhibiting oxidative stress and enhancing insulin signaling transduction. *Exp. Clin. Endocrinol. Diabetes* 123, 170–177. doi: 10.1055/s-0034-1395658

Ribiere, C., Jaubert, A. M., Gaudiot, N., Sabourault, D., Marcus, M. L., Boucher, J. L., et al. (1996). White adipose tissue nitric oxide synthase: a potential source for NO production. *Biochem. Biophys. Res. Commun.* 222, 706–712. doi: 10.1006/bbrc.1996.0824

Silva, J. F., Correa, I. C., Diniz, T. F., Lima, P. M., Santos, R. L., Cortes, S. F., et al. (2016). Obesity, inflammation, and exercise training: relative contribution of inos and enos in the modulation of vascular function in the mouse Aorta. *Front. Physiol.* 7:386. doi: 10.3389/fphys.2016.00386

Suzuki, H., Swei, A., Zweifach, B. W., and Schmid-Schönbein, G. W. (1995). *In vivo* evidence for microvascular oxidative stress in spontaneously hypertensive rats. Hydroethidine microfluorography. *Hypertension* 25, 1083–1089. doi: 10.1161/01.HYP.25.5.1083

Szasz, T., and Webb, R. C. (2012). Perivascular adipose tissue: more than just structural support. *Clin. Sci.* 122, 1–12. doi: 10.1042/CS20110151

Takakura, K., Beckman, J. S., MacMillan-Crow, L. A., and Crow, J. P. (1999). Rapid and irreversible inactivation of protein tyrosine phosphatases PTP1B, CD45, and LAR by peroxynitrite. *Arch. Biochem. Biophys.* 369, 197–207. doi: 10.1006/abbi.1999.1374

Victorio, J. A., Fontes, M. T., Rossoni, L. V., and Davel, A. P. (2016). Different anti-contractile function and nitric oxide production of thoracic and abdominal perivascular adipose tissues. *Front. Physiol.* 7:295. doi: 10.3389/fphys.2016.00295

Vosseller, K., Wells, L., Lane, M. D., and Hart, G. W. (2002). Elevated nucleocytoplasmic glycosylation by O-GlcNAc results in insulin resistance associated with defects in Akt activation in 3T3-L1 adipocytes. *Proc. Natl. Acad. Sci. U.S.A.* 99, 5313–5318. doi: 10.1073/pnas.072072399

Weber, D. S., Taniyama, Y., Rocic, P., Seshiah, P. N., Dechert, M. A., Gerthoffer, W. T., et al. (2004). Phosphoinositide-dependent kinase 1 and p21-activated protein kinase mediate reactive oxygen species-dependent regulation of platelet-derived growth factor-induced smooth muscle cell migration. *Circ. Res.* 94, 1219–1226. doi: 10.1161/01.RES.0000126848.54740.4A

Xia, N., Horke, S., Habermeier, A., Closs, E. I., Reifenberg, G., Gericke, A., et al. (2016). Uncoupling of endothelial nitric oxide synthase in perivascular adipose tissue of diet-induced obese mice. *Arterioscler. Thromb. Vasc. Biol.* 36, 78–85. doi: 10.1161/ATVBAHA.115.306263

Xia, N., and Li, H. (2017). The role of perivascular adipose tissue in obesity-induced vascular dysfunction. *Br. J. Pharmacol.* 174, 3425–3442. doi: 10.1111/bph.13650

Conflict of Interest Statement: The authors declare that the research was conducted in the absence of any commercial or financial relationships that could be construed as a potential conflict of interest.

frontiers in Physiology

ORIGINAL RESEARCH
published: 23 March 2018
doi: 10.3389/fphys.2018.00245

Insulin Receptor Substrate 2 Controls Insulin-Mediated Vasoreactivity and Perivascular Adipose Tissue Function in Muscle

Alexander H. Turaihi[1], *Wineke Bakker*[2], *Victor W. M. van Hinsbergh*[1], *Erik H. Serné*[2], *Yvo M. Smulders*[2], *Hans W. M. Niessen*[3] *and Etto C. Eringa*[1]*

[1] *Department of Physiology, Amsterdam Cardiovascular Sciences, VU University Medical Center, Amsterdam, Netherlands,* [2] *Department of Internal Medicine, Amsterdam Cardiovascular Sciences, VU University Medical Center, Amsterdam, Netherlands,* [3] *Department of Pathology and Cardiac Surgery, Amsterdam Cardiovascular Sciences, VU University Medical Center, Amsterdam, Netherlands*

Introduction: Insulin signaling in adipose tissue has been shown to regulate insulin's effects in muscle. In muscle, perivascular adipose tissue (PVAT) and vascular insulin signaling regulate muscle perfusion. Insulin receptor substrate (IRS) 2 has been shown to control adipose tissue function and glucose metabolism, and here we tested the hypothesis that IRS2 mediates insulin's actions on the vessel wall as well as the vasoactive properties of PVAT.

Methods: We studied PVAT and muscle resistance arteries (RA) from littermate $IRS2^{+/+}$ and $IRS2^{-/-}$ mice and vasoreactivity by pressure myography, vascular insulin signaling, adipokine expression, and release and PVAT morphology. As insulin induced constriction of $IRS2^{+/+}$ RA in our mouse model, we also exposed RA's of C57/Bl6 mice to PVAT from $IRS2^{+/+}$ and $IRS2^{-/-}$ littermates to evaluate vasodilator properties of PVAT.

Results: $IRS2^{-/-}$ RA exhibited normal vasomotor function, yet a decreased maximal diameter compared to $IRS2^{+/+}$ RA. $IRS2^{+/+}$ vessels unexpectedly constricted endothelin-dependently in response to insulin, and this effect was absent in $IRS2^{-/-}$ RA due to reduced ERK1/2activation. For evaluation of PVAT function, we also used C57/Bl6 vessels with a neutral basal effect of insulin. In these experiments insulin (10.0 nM) increased diameter in the presence of $IRS2^{+/+}$ PVAT (17 ± 4.8, $p = 0.014$), yet induced a $10 \pm 7.6\%$ decrease in diameter in the presence of $IRS2^{-/-}$ PVAT. Adipocytes in $IRS2^{-/-}$ PVAT (1314 ± 161 μm^2) were larger ($p = 0.0013$) than of $IRS2^{+/+}$ PVAT (915 ± 63 μm^2). Adiponectin, IL-6, PAI-1 secretion were similar between $IRS2^{+/+}$ and $IRS2^{-/-}$ PVAT, as were expression of pro-inflammatory genes (TNF-α, CCL2) and adipokines (adiponectin, leptin, endothelin-1). Insulin-induced AKT phosphorylation in RA was similar in the presence of $IRS2^{-/-}$ and $IRS2^{+/+}$ PVAT.

Conclusion: In muscle, IRS2 regulates both insulin's vasoconstrictor effects, mediating ERK1/2-ET-1 activation, and its vasodilator effects, by mediating the vasodilator effect of PVAT. The regulatory role of IRS2 in PVAT is independent from adiponectin secretion.

Keywords: insulin sensitivity, perivascular adipose tissue, insulin receptor substrate 2, microcirculation, endothelium

OPEN ACCESS

Edited by:
Maik Gollasch,
Charité Universitätsmedizin Berlin, Germany

Reviewed by:
Geraldine Clough,
University of Southampton, United Kingdom
Huige Li,
Johannes Gutenberg-Universität Mainz, Germany

***Correspondence:**
Etto C. Eringa
e.eringa@vumc.nl

Specialty section:
This article was submitted to Vascular Physiology, a section of the journal Frontiers in Physiology

Received: *12 October 2017*
Accepted: *06 March 2018*
Published: *23 March 2018*

Citation:
Turaihi AH, Bakker W, van Hinsbergh VWM, Serné EH, Smulders YM, Niessen HWM and Eringa EC (2018) Insulin Receptor Substrate 2 Controls Insulin-Mediated Vasoreactivity and Perivascular Adipose Tissue Function in Muscle. Front. Physiol. 9:245. doi: 10.3389/fphys.2018.00245

INTRODUCTION

Insulin resistance, obesity and type 2 diabetes (DM2) are increasingly common risk factors for cardiovascular disease (Brownrigg et al., 2016). Resistance to insulin's vasodilator effects is characteristic of insulin resistant and type 2 diabetic subjects (Jiang et al., 1999; Okon et al., 2005), and has been shown to contribute to increased vascular resistance (Woerdeman et al., 2016), defects in organ perfusion and atherosclerosis (Rask-Madsen et al., 2010). As such, understanding and reversing defects in vascular insulin signaling contributes to prevention of cardiovascular complications of obesity and DM2.

After a meal, the physiological rise in plasma insulin levels induces pleiotropic effects on the muscle vasculature (Baron, 1993) to facilitate its access to myocytes. Insulin appearance in skeletal muscle interstitium is the rate limiting step for insulin's metabolic actions that promote glucose disposal (Yang et al., 1989), and therefore insulin access to the muscle interstitium contributes to whole-body insulin sensitivity (Kubota et al., 2011). In muscle microvessels, insulin can induce vasoconstriction through ERK1/2-dependent endothelin-1 (ET-1) production (Eringa et al., 2004) and vasodilatation through insulin receptor substrate1/2 (IRS1/2)- and Akt-dependent nitric oxide (NO) production (Montagnani et al., 2002; Meijer et al., 2015). While insulin's vasodilator actions predominate in normal conditions, insulin's vasoconstrictor effect is dominant in obesity and DM2, as a result of increased ET-1 production and decreased NO production (Lesniewski et al., 2008). The roles of IRS1 and−2 in insulin's vasoconstrictor actions have not been studied.

An important local regulator of insulin's vascular actions is perivascular adipose tissue (PVAT), which surrounds most vessels with an internal diameter $>100\,\mu m$ and consists of adipocytes, inflammatory cells and stem cells (Houben et al., 2012). Anatomical locations of PVAT include the aorta as well as the vascular networks of muscle and the heart (Mazurek et al., 2003; Verlohren et al., 2004; Meijer et al., 2015). PVAT serves as a source of adipokines which exert control over endothelial responses to insulin and other vasoactive stimuli (Greenstein et al., 2009). Understanding the signaling pathway between PVAT and the vasculature potentially uncovers new therapeutic targets to treat disorders such as hypertension and DM2. Resistance to insulin-induced vasodilatation is better understood when taking the continuous interplay between PVAT and the vasculature into consideration. PVAT secretes adiponectin which signals through AMP-activated protein kinase (AMPK) and Akt to stimulate NO production, uncovering insulin-mediated vasodilation (Meijer et al., 2015; de Boer et al., 2016). We have previously shown that PVAT from db/db mice secretes less adiponectin and fails to induce insulin-mediated vasodilation when compared to wild-type PVAT (Meijer et al., 2013). Thus, qualities inherent to PVAT are important in endothelial reactivity to insulin.

Genetic mutations in IRS1 and IRS2 have been associated with DM2 and impaired vascular function (Jiang et al., 1999; Esposito et al., 2003; Bodhini et al., 2007). Aside from its role in insulin signal transduction (Sun et al., 1995), IRS2 functions independently in insulin growth factor-1 (IGF-1) and anti-inflammatory cytokine signaling (O'Connor et al., 2007). Mice lacking IRS2 show insulin resistance and beta-cell failure, resulting in peripheral insulin resistance and DM2 after 8–10 weeks of age (Kubota et al., 2000; Withers et al., 2014).Importantly, IRS2 also regulates endocrine functions of adipose tissue, inhibiting fatty acid synthesis (Previs et al., 2000). Moreover, insulin's effects on adipose tissue have been shown to control glucose uptake in muscle (Abel et al., 2001). Despite the recognition that IRS2 plays an important role in glucose homeostasis and adipose tissue function, the role of IRS2 in PVAT function is unknown.

The aim of this study was to elucidate the role of IRS2 in control of muscle perfusion by insulin and as well as the mechanisms involved. To this end, we used the *ex vivo* pressure myograph to investigate effects of insulin on muscle resistance arteries (RA) in the absence and presence of PVAT.

MATERIALS AND METHODS

Animals

Animal experiments were performed in accordance with the European Community Council Directive 2010/63/EU for laboratory animal care and the Dutch Law on animal experimentation. The experimental protocol was validated and approved by the local committee on animal experimentation of the VU University Medical Center. Male C57Bl/6NCrl mice (further indicated as Bl6) were bred in-house (obtained from Harlan, Horst, the Netherlands). Male $IRS2^{+/+}$ and $IRS2^{-/-}$ mice, on a hybrid background of the Bl6 and SV129 mice strains (Jackson Laboratories, Maine, USA), were obtained by heterozygous breeding. PCR was used to confirm the genotype of the mice as described (Withers et al., 1999) with primers: *5′-GTCATCAGGACATAGCGTTGG-3′,5′-CTTG GCTACCATGTTGTTATTGTC-3′, 5′-AGTTCTGGAGGTTTAC TTTCCTAG-3′*. Sv129 mice (Jackson laboratories, Maine, USA) were used to check for differences in genetic background in insulin responses. Mice were housed in standard cages and were fed chow diet and water *ad libitum*. Mice were sacrificed by isoflurane overdose after overnight fasting at 8 weeks age.

Vasoreactivity Experiments

First-order RA from the gracilis muscle were isolated from lean Bl6, $IRS2^{+/+}$ and $IRS2^{-/-}$ mice after an overnight fast. PVAT surrounding the RA of Bl6, $IRS2^{+/+}$ and $IRS2^{-/-}$ mice was isolated from the section of the RA between its origin at the femoral artery and its first major side branch within the gracilis muscle as described (Meijer et al., 2013). RA's were cannulated in a pressure myograph and studied at a pressure of 80 mmHg and a temperature of 37°C in K-MOPS buffer with a KCl concentration of 25 mM, as described previously (Meijer et al., 2013).

RA's were randomly assigned to incubation either without PVAT ($n = 9$) or with $IRS2^{+/+}$ ($n = 9$) and $IRS2^{-/-}$ PVAT ($n = 10$) with approximately equal amounts PVAT used in each condition. Preconstriction of 40% was achieved with KCl, the inner diameter of RA's was recorded to determine baseline diameter and diameter changes induced by four concentrations of insulin (0.01, 0.1, 1, and 10 nM) (Novorapid;

Novo Nordisk, Bagsværd, Denmark), each exposure being for 30 min. The three lowest insulin concentrations of insulin are within the physiological range, with the third concentration (1 nM) corresponding to postprandial levels, whereas the fourth concentration is pharmacological. Smooth muscle function was tested as KCl-induced vasoconstriction and only vessels which showed a constriction of >40% of their maximal diameters were used for experiments. Endothelial integrity was determined by measuring responses to the endothelium-dependent vasodilator acetylcholine $1*10^{-7}$ M (ACh) and the end of each experiment, an RA failing to achieve at least 10% vasodilation to ACh were excluded from all analyses. The role of ET-1 was assessed by pre-treatment for 30 min with the non-selective ET-1 receptor antagonist (PD142893: 10 μM, Kordia, Leiden, the Netherlands) before the addition of insulin. The vasomotor response to insulin was expressed as a percentage of the baseline diameter, i.e., the vessel diameter immediately before addition of the first concentration of insulin.

Western Blot

Protein analyses were performed by Western blotting, as described (Meijer et al., 2013). Segment of RA from $IRS2^{+/+}$ and $IRS2^{-/-}$ mice were exposed to solvent or to insulin for 15 min at 37°C. In order to study the effects of PVAT on the RA, $IRS2^{+/+}$ and $IRS2^{-/-}$ PVAT were isolated from overnight fasted mice and then incubated in 100 μl MOPS buffer with 1% of *bovine serum albumin (*BSA). PVAT samples were stimulated with either solvent or 10 nM insulin for 30 min in a 96 well-plate. Thereafter, freshly isolated femoral artery segments from fasted 8 week old Bl6 mice were added to the PVAT wells and incubated at 37°C for 15 min. Femoral artery segments were used in order to obtain appropriate amounts of protein for Western blotting. The artery segments were snap frozen in liquid nitrogen and savedat −80°C till further analysis. The protein lysates were stained with a specific primary antibody against Ser 473 phosphorylated Akt (antibodies obtained from Cell Signaling Technology, Boston, MA, USA) and were visualized with a chemiluminescence kit (GE Healthcare, Diegem, Belgium). A specific primary antibody against ERK1/2 (1:1,000; New England Biolabs, Ipswich, USA) was used to examine ERK1/2 activation. Differences in phosphorylated protein of Akt at ser 473 were adjusted for differences in the total Akt protein staining.

Adipokine Secretion

PVAT-conditioned media were prepared and the amount of secreted adipokines were quantified using the mouse magnetic-bead adipokine milliplex multianalyte ELISA kit (Millipore, Amsterdam, the Netherlands) and detected using the Luminex system. Freshly isolated PVAT from fasted $IRS2^{+/+}$ ($n = 7$) and $IRS2^{-/-}$ ($n = 5$) mice in amounts of comparable size were incubated in 100 μl MOPS buffer with 1% of BSA and stimulated with either solvent or 10 nM insulin at 37°C for 45 min in a 96 well-plate. The conditioned media were snap frozen in liquid nitrogen and saved at −80°C till further analysis. Adiponectin, IL-6, Leptin, MCP-1, PAI-1 (Total), Resistin, and TNF-α concentrations in the conditioned media were measured in duplicate and averaged. Data are corrected for the PVAT weight that was used in the incubation.

Real Time Quantitative Polymerase Chain Reaction (qRT-PCR)

Total RNA was extracted from PVAT using a miRCURY RNA isolation kit (Exiqon). PVAT RNA was reversely transcribed and amplified using Ovation PicoSL WTA System V2 (Nugen). Quantitative PCR was performed using a commercial SYBR green mastermix (Biorad) and specific primers (available upon request) for pro-inflammatory genes (TNF-α and CCL2) and adipokines (adiponectin, leptin, and endothelin-1). IRS1 expression was evaluated to check for compensation to IRS2 knockout. Data were corrected for the geometric mean of ribosomal protein S15 (*Rps15*) and expressed relative to the wild type PVAT.

Histology

PVAT surrounding the RA was excised together with part of the underlying muscle and stored overnight in buffered formaldehyde (4%) and embedded in paraffin. For histochemical analysis, slices with a thickness of 5 μm were dewaxed, rehydrated and stained with hematoxylin and eosin (H&E). The cross-sectional area of adipocytes was analyzed in blinded fashion using Image J software.

Blood Pressure and Heart Rate Measurements

Blood pressure and heart rate of $IRS2^{+/+}$ and $IRS2^{-/-}$ were determined under stress-free conditions using radio telemetry as described (Aman et al., 2012).

Statistical Analysis

Values are expressed as mean ± SEM. Steady-state responses are reported as mean change from baseline (percentages) ± SEM. Differences in insulin-induced vasoreactivity were performed using two-way ANOVA. Tukey *post-hoc* test was where appropriate. Differences in IHC analyses and in protein phosphorylation as found by Western blot were determined using unpaired student *t*-test. Phosphorylation was expressed as the fold increase over the unstimulated controls, assigning a value of 1 to the control. qRT-PCR data was log2 transformed before statistical analysis. Differences with $p < 0.05$ were considered statistically significant. Analyses were performed with GraphPad Prism 6.0 (GraphPad software, San Diego, CA, USA).

RESULTS

General Characteristics of $IRS2^{+/+}$ and $IRS2^{-/-}$Mice

$IRS2^{+/+}$ and $IRS2^{-/-}$littermates had similar body weights (23 ± 1 and 24 ± 1 g, respectively, **Table 1**). $IRS2^{-/-}$ mice had higher non-fasting levels of plasma insulin (9 ± 1 vs. 20 ± 2 μU/ml, $p < 0.01$) and exhibited fasting hyperglycemia (5.3 ± 0.57 vs. 12.6 ± 2.7 mMol/l, $p < 0.05$) than $IRS2^{+/+}$. $IRS2^{-/-}$ mice showed a small decrease in blood pressure compare to their $IRS2^{+/+}$ littermates (**Table 1**).

Insulin-Mediated Vasoreactivity in IRS2$^{+/+}$ and IRS2$^{-/-}$ Muscle Resistance Arteries

To gain insight into the role of IRS2 in insulin-dependent vasoreactivity in muscle, we first examined the reactivity of IRS2$^{+/+}$ and IRS2$^{-/-}$ gracilis muscle RA obtained from IRS2$^{+/+}$ and IRS2$^{-/-}$ mice in response to insulin and other vasoactive molecules.IRS2$^{+/+}$ and IRS2$^{-/-}$RA showed normal endothelial and smooth muscle function, as reflected by responses to acetylcholine (**Figure 1A**), sodium nitroprusside (**Figure 1B**), and exogenous ET-1 (**Figure 1C**). The maximal diameter of IRS2$^{-/-}$ RA was reduced compared to IRS2$^{+/+}$ RA (111 ± 6 vs. 127 ± 5 micron, $P < 0.05$), and basal vascular tone in the presence of 25 mM potassium was 34 ± 2% in IRS2$^{+/+}$ and 27 ± 4% in IRS2$^{-/-}$ RA ($P = 0.11$). Unexpectedly, insulin induced vasoconstriction in isolated IRS2$^{+/+}$RA, which was inhibited by the non-selective ET-1 receptor antagonist PD142893 (**Figures 2A,B**). This confirms the critical role of endothelin-1 ininsulin's vasoconstrictor effects, and shows a decreased contribution of NO to insulin-mediated vasoreactivity in IRS2$^{+/+}$ RA. In IRS2$^{-/-}$ mice, no vasoconstrictor response was observed during exposure of the isolated arteries to insulin, nor in the presence of the ET-1 receptor antagonist (**Figure 2B**). Mechanistically, the insulin-induced phosphorylation of ERK1/2 was impaired in IRS2$^{-/-}$ RA compared to IRS2$^{+/+}$ RA (**Figure 2C**), whereas insulin-stimulated activation of Akt was similar (**Figure 2D**). This indicates that the stimulation of ERK1/2-ET-1 activity by insulin requires IRS2.

The observed insulin-induced vasoconstriction of isolated IRS2$^{+/+}$ RA contrasts with the response of C57Bl/6 mice (Meijer et al., 2013), which vasodilate in response to insulin during ET-1 receptor inhibition and during incubation with PVAT of lean Bl6 mice (data not shown). As the IRS2 mice used in this study are bred on a mixed background of the mouse strains C57Bl/6 and SV129, we tested whether the Sv129 background caused the vasoconstrictor response by studying insulin responses of isolated RA from SV129 mice. Insulin indeed induced vasoconstriction in arteries from SV129 mice, while it had no net effect on the diameter of C57Bl/6 RA (Figure S1A). Endothelial function (response to acetylcholine-mediated vasodilation) was not different between the two strains (Figure S1B). Collectively, arteries from different mouse strains can display different responses to insulin. For this reason and to facilitate comparability with other experiments, we proceeded by studying the effect of PVAT obtained from IRS2$^{+/+}$ and IRS2$^{-/-}$ mice on RA's obtained from C57Bl/6 mice. RA's from C57/Bl6 mice had a maximal diameter of 137 ± 5 microns.

TABLE 1 | General characteristics of IRS2-deficient and wild-type littermates at 8 weeks of age.

General characteristics	IRS2$^{+/+}$	IRS2$^{-/-}$	*P*
Body weight (g)	23 ± 1	24 ± 1	0.84
Fasting blood glucose (mMol/l)	5.3 ± 0.5	12.6 ± 2.7	<0.05
Non-fasting blood glucose (mMol/l)	8.7 ± 0.8	12.2 ± 0.9	<0.01
Non-fasting blood insulin ($\mu U/ml$)	9 ± 1	20 ± 2	<0.01
MAP (mm Hg)	115 ± 3	101 ± 5	<0.05
SBP (mm Hg)	127 ± 3	110 ± 6	<0.05
Heart rate (beats per minute)	589 ± 11	553 ± 19	0.08

IRS2$^{-/-}$ had similar body weights and higher levels of insulin and glucose than the IRS2$^{+/+}$ mice. MAP, mean arterial pressure, SBP, systolic blood pressure. Data represent mean ± SEM, IRS2$^{+/+}$N = 10, IRS2$^{-/-}$N = 7.

PVAT From IRS2$^{+/+}$ but Not IRS2$^{-/-}$Mice Uncovers Insulin-Induced Vasodilation in Resistance Arteries

To study the interaction between PVAT and insulin-induced vasoreactivity of isolated muscle RA's, PVAT of IRS2$^{+/+}$ and IRS2$^{-/-}$ littermates was co-incubated with RA's in the pressure myograph for 45 min. Insulin (10 nM) induced vasodilation in the presence of IRS2$^{+/+}$ PVAT (17.2 ± 4.9%, $N = 9$; **Figure 3A**). On the other hand, insulin failed to induce diameter change in arteries incubated with IRS2$^{-/-}$ PVAT (−7.3 ± 4.7%, $N = 10$) or without the presence of PVAT (0.4 ± 4.1%, $N = 9$). Baseline vessel tone was not different in RA's ($n = 28$) in the presence of either IRS2$^{+/+}$ PVAT orIRS2$^{-/-}$ PVAT nor was acetylcholine-induced vasodilation (**Figures 3B**,**C**).

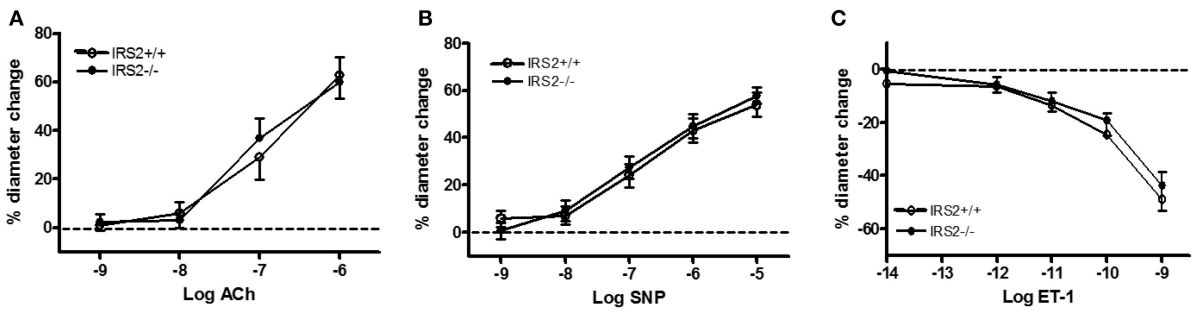

FIGURE 1 | Vasoregulatory responses in resistance arteries of IRS2$^{-/-}$ mice without PVAT. In all experiments on tissues of IRS2$^{-/-}$ mice, their IRS2$^{+/+}$ littermates were the control strain. Acetylcholine, ACh **(A)**; sodium nitroprusside, SNP **(B)** and ET-1 **(C)** were similar in IRS2$^{+/+}$ (○, $n = 5$) and IRS2$^{-/-}$ resistance arteries (●, $n = 6$).

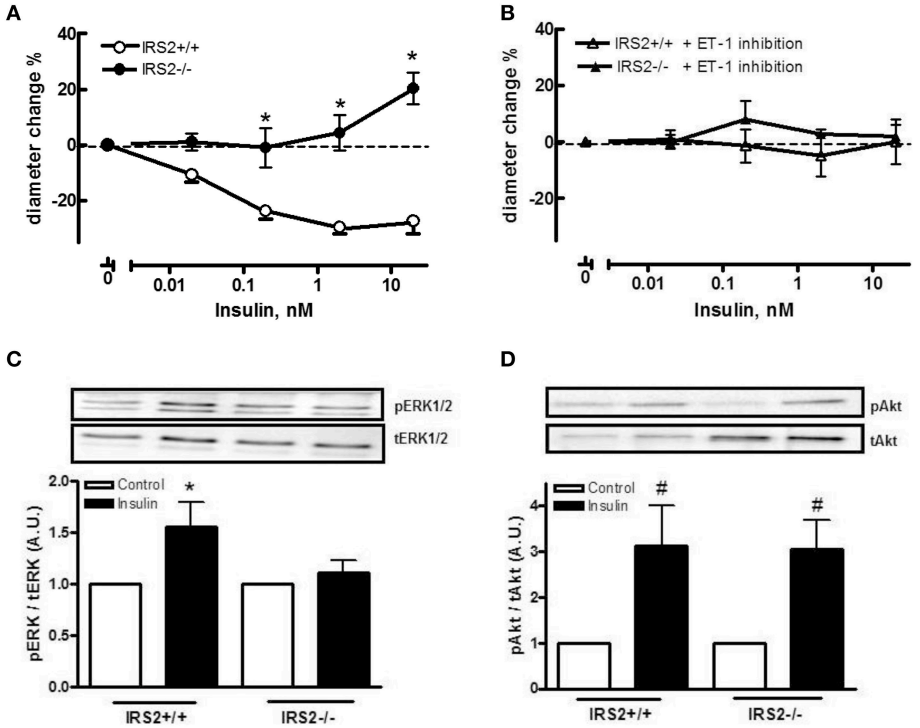

FIGURE 2 | IRS2 mediates insulin-stimulated ERK1/2-ET-1 activity in muscle resistance arteries without PVAT. Responses of $IRS2^{+/+}$ and $IRS2^{-/-}$ RA to insulin **(A)** and during endothelin receptor blockade using PD142893 (10ulMol/l) **(B)**, $n = 5$, $^{*}p < 0.01$ vs. $IRS2^{+/+}$. **(C,D)**: IRS2 deletion decreases insulin-stimulated phosphorylation of ERK1/2, but not of Akt in muscle RA. ERK1/2 and Akt phosphorylation were compared between insulin stimulation (2 nM) (black bars) and the control situation (white bars) in segments of the gracilis RA from $IRS2^{+/+}$ ($n = 8$) and $IRS2^{-/-}$ ($n = 9$) mice, $^{*}p < 0.05$; $^{\#}p < 0.01$ vs. control.

Adipocyte Size Is Increased in PVAT of $IRS2^{-/-}$ Mice

To quantify the effects of IRS2 deletion on the morphology and inflammatory status of PVAT, adipocyte area and macrophage infiltration were investigated. Adipocyte area was significantly ($p = 0.0013$) larger in $IRS2^{-/-}$ PVAT ($1{,}314 \pm 161\ \mu m^2$) compared to $IRS2^{+/+}$ ($915 \pm 63\ \mu m^2$) (**Figure 3D**). Leukocyte infiltration assessed in tissue slices was not quantifiable in PVAT of both genotypes. IRS2 mRNA levels in PVAT were confirmed to be absent in $IRS2^{-/-}$ PVAT (**Figure 4A**). To check for compensation for IRS2 knockout, we measured IRS1 mRNA expression and we found no differences between $IRS^{+/+}$ and $IRS^{-/-}$ PVAT (**Figure 4B**).

Adiponectin Expression and Secretion From $IRS2^{-/-}$ PVAT Are Similar to $IRS2^{+/+}$ PVAT

To elucidate the mechanisms involved in the interaction of intramuscular PVAT with insulin-induced vasoreactivity, we examined the role of several secreted adipokines in this interaction. Adiponectin secretion was similar between $IRS2^{+/+}$ and $IRS2^{-/-}$ PVAT conditioned media (**Figure 5A**), as was Adiponectin mRNA in PVAT between $IRS2^{+/+}$ and $IRS2^{-/-}$ mice (**Figure 4C**). Despite the increase in adipocyte size, leptin expression was similar between $IRS2^{+/+}$ and $IRS2^{-/-}$ PVAT (**Figure 4D**). Other adipokines and inflammatory markers were also studied. Levels of TNF-α and MCP-1 were undetectable in PVAT-conditioned medium (data not shown). Moreover, TNF-α mRNA levels were low in $IRS2^{+/+}$ and $IRS2^{-/-}$ PVAT (**Figure 4E**) while mRNA levels of CCL2 were similar between $IRS2^{+/+}$ and $IRS2^{-/-}$ PVAT (**Figure 4F**). There were no differences between $IRS2^{+/+}$ and $IRS2^{-/-}$ in the amounts of secreted PAI-1, IL-6, Leptin (**Figures 5B,D,E**). Unexpectedly, we found that IRS2 deficiency decreases resistin secretion by PVAT (**Figure 5C**), demonstrating that IRS2 deficiency does alter the secretory function of PVAT.

Normal Phosphorylation of Akt in Response to Insulin in Arteries Incubated With $IRS2^{-/-}$ PVAT

To further study the insulin-induced vasodilator pathway, which is mediated through Akt and eNOS phosphorylation, phosphorylation of Akt was studied in the presence of $IRS2^{+/+}$ and $IRS2^{-/-}$ PVAT. The phosphorylation of Akt in femoral artery segments of C57Bl/6 mice was significantly increased after insulin stimulation in the presence of $IRS2^{+/+}$ as well as $IRS2^{-/-}$ PVAT (**Figure 6**).

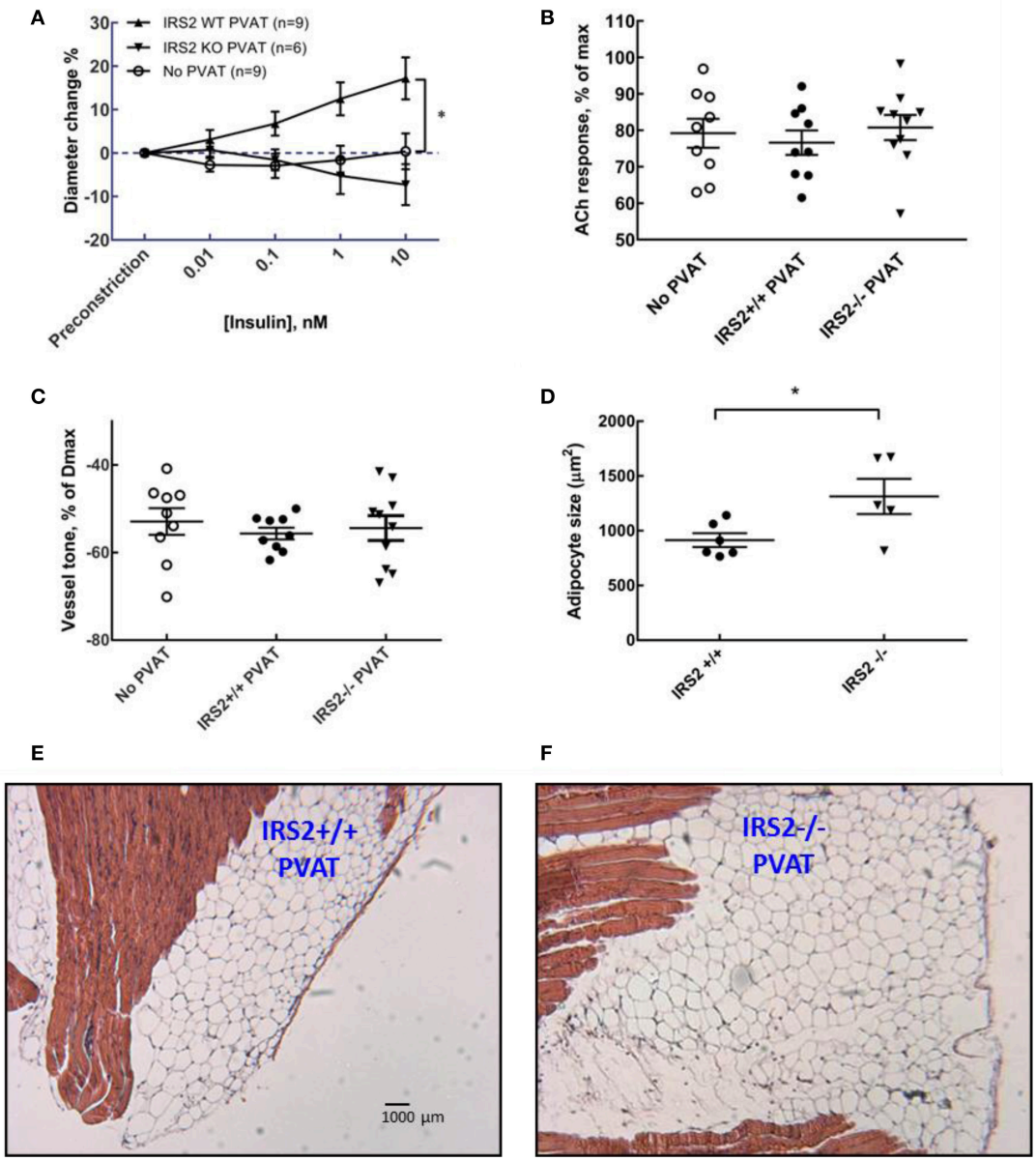

FIGURE 3 | IRS2$^{-/-}$ PVAT does not uncover insulin-mediated vasodilation. **(A)** Arteries obtained from C57/Bl6 mice were incubated with PVAT from IRS2$^{+/+}$ and IRS2$^{-/-}$ littermates and stimulated with increasing doses of insulin. Incubation with IRS2$^{+/+}$ PVAT, allowed the artery to dilate in reaction insulin in dose-dependent manner (17.2 ± 4.9% dilation in response to highest (insulin), $p < 0.0001$, $N = 9$,) while arteries that were incubated with IRS2$^{-/-}$ PVAT or were deprived of PVAT did not react to insulin (−7.3 ± 4.7%, $N = 10$ and 0.4 ± 4.1%, $N = 9$, respectively; $p = 0.17$). Data are presented as mean ± SEM, tested with two-way ANOVA with Tukey *post-hoc* correction. **(B)** At the end of the experiment, endothelial integrity was examined by stimulating the arteries with acetylcholine. All the arteries that were included in the analyses in **(A)** had at least 60% dilation in response to acetylcholine—cutoff point to rule out endothelialdamage. **(C)** PVAT did not affect the percentage of arteriolar preconstriction in the organ bath. **(D)** Adipocyte size in IRS2$^{+/+}$ PVAT (412.1 ± 58.7 μm) are smaller ($p = 0.03$) than adipocytes in IRS2$^{-/-}$ PVAT (914.7 ± 63. 2 μm). Data are presented as mean ± SEM, tested with unpaired *t*-test. **(D,E)**: Morphology of IRS2+/+ and IRS2$^{-/-}$ PVAT at the site of the gracilis resistance artery. **(E,F)** are at the same magnification. M: muscle.

DISCUSSION

The main findings of this study are fourfold: (1) IRS2 in the vessel wall of muscle RA is more involved in the ERK1/2-Endothelin-1 pathway than in the Akt-NO pathway of insulin signaling, (2) IRS2$^{-/-}$ PVAT loses its ability to induce insulin-mediated vasodilation in skeletal muscle RA, (3) this is accompanied by increased adipocyte area in IRS2$^{-/-}$ PVAT with no signs of increased inflammation, (4) adiponectin secretion is similar between IRS2$^{-/-}$ PVAT and wildtype PVAT. A graphical summary of our findings is depicted in **Figure 7**.

It has been shown that IRS2 is a major IRS isoform expressed in endothelial cells (Kubota et al., 2003). In their important work, Kubota et al. (2003) showed that mice lacking

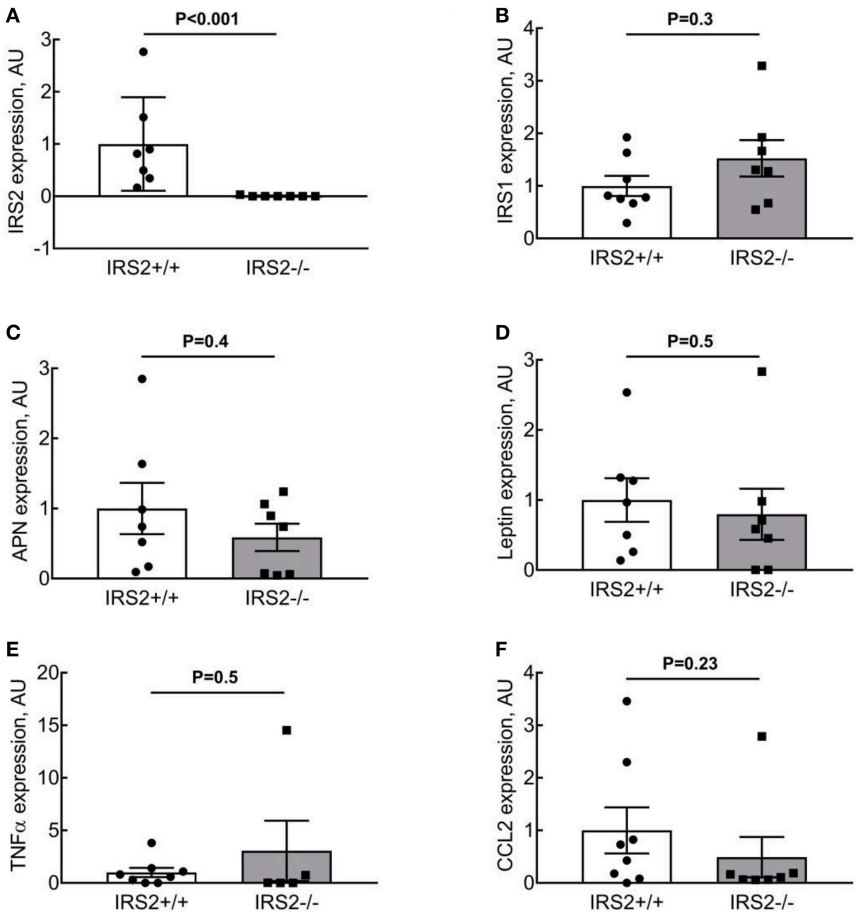

FIGURE 4 | IRS2$^{-/-}$PVAT does not show increased inflammatory gene expression. **(A,B)** IRS expression in IRS2$^{-/-}$ mice. **(C,D)** IRS2 deficiency does not alter adiponectin and leptin expression in PVAT. **(E,F)** IRS2 deficiency does not enhance inflammatory gene expression in PVAT. Data were log-transformed prior to statistical analysis as described in section Methods. APN, Adiponectin.

IRS2 in endothelial cells had impaired insulin-induced eNOS phosphorylation. This resulted in a reduced insulin-mediated microvascular recruitment and a decrease in muscle glucose uptake. Insulin induces a strong vasoconstriction in the IRS2$^{+/+}$ arteries which is completely dependent on ET-1 (**Figure 2**). We found out that this is due the difference in mouse strains as the Sv129-strain is less sensitive to insulin-mediated NO production in the vascular wall (Supplemental Figure S1). Importantly, the arteries that displayed vasoconstriction were in an experimental setup that is deprived of IRS2$^{+/+}$ PVAT. Nevertheless, this insulin-induced vasoconstriction observed in IRS2$^{+/+}$ RA is different than our earlier observations in human and Bl6 arteries that did not show insulin-induced vasoconstriction. Moreover, these arteries showed insulin-mediated vasodilation after preincubation with PVAT from lean mice. This is why we decided to proceed with our experimental set-up using RA obtained from Bl6 mice and constantly comparing the IRS2$^{-/-}$ PVAT with PVAT obtained from their wildtype littermates. We show in our study that the absence of IRS2 in PVAT is sufficient to abrogate the PVAT-assisted insulin-mediated vasodilation of skeletal muscle RA despite the fact that these arteries were functionally normal (**Figure 3A**). In their seminal work, Abel et al. showed that alterations in adipocyte inherent characteristics resulted in a decreased muscle glucose uptake (Abel et al., 2001). This means that adipose tissue is capable of (in)directly altering the capacity of the body to regulate glucose homeostasis. In their study, however, the authors did not specifically examine the function of PVAT in these mice.

Kubota et al. have reported that the expression of IRS2 in endothelial cells is reduced by high fat diet in mice (Kubota et al., 2003). Conditions of calorie excess lead to a low-grade inflammation and production of pro-inflammatory cytokines (TNF-α and IL-6) from adipose tissue (Yudkin et al., 1999, 2005) which inhibits adiponectin secretion (Tilg and Moschen, 2006). Indeed, PVAT anticontractile properties are lost due to inflammation (Greenstein et al., 2009; Withers et al., 2011). After we observed that IRS2$^{-/-}$ PVAT has lost its vasodilatory capacity, we looked at inflammatory signs in this tissue. Literature has shown that, as fat mass increases in obesity, the size of adipocytes increases. In our study, adipocytes in IRS2$^{-/-}$ PVAT were larger than IRS2$^{+/+}$ PVAT (**Figure 3D**). PVAT hypertrophy in IRS2$^{-/-}$ mice may be caused by decreased resistin expression, as resistin

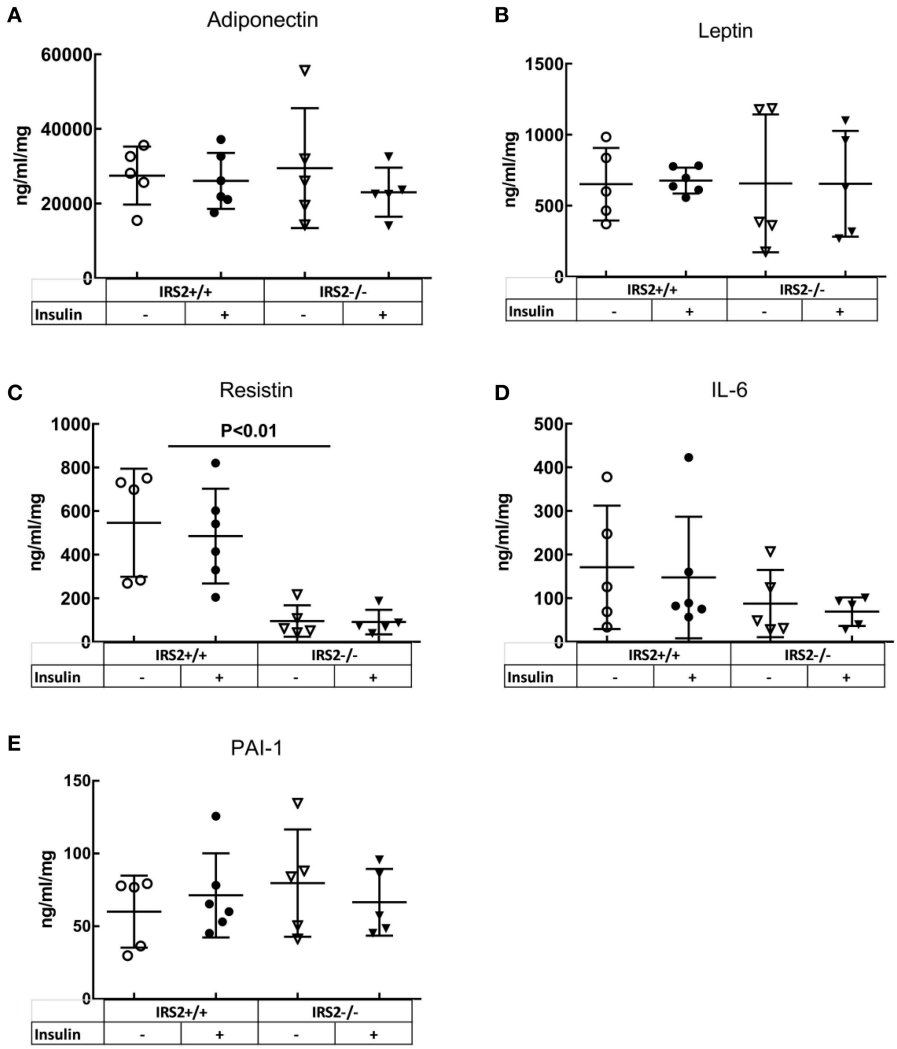

FIGURE 5 | IRS2$^{-/-}$ PVAT secretes equal amounts of Adiponectin compared to wild-type PVAT. There are no significant differences between IRS2$^{+/+}$ and IRS2$^{-/-}$ PVAT in **(A)** adiponectin, **(B)** IL6, **(D)** Leptin, **(E)** PAI-1. **(C)** Resistin secretion is decreasedin IRS2$^{-/-}$ PVAT. Insulin stimulation did not affect the secretion of the measured adipokines. The amounts of MCP-1 and TNF-α were below the detection limitof the assay.

stimulates lipolysis (Ort et al., 2005). (Mita et al., 2011) showed that IRS2-deficient macrophages accumulate in the vascular wall; eventual accumulation in PVAT is expected since PVAT is vascularized. In our study, however, we failed to show signs of inflammation in IRS2$^{-/-}$ PVAT. First, macrophage staining in PVAT samples was not quantifiable because of the small size of PVAT samples and low prevalence of leukocytes (data not shown). Second, there were no differences in IL-6 secretion from IRS2$^{-/-}$ and wildtype PVAT and the concentration of TNF-α was low (**Figure 5**). Third, we did not find differences in CCL2 and TNF-α mRNA expression levels between IRS2$^{-/-}$ and wild-type PVAT. It would be interesting to quantify markers of inflammation in IRS2$^{-/-}$ PVAT obtained from older mice to study age related changes in PVAT in conditions of IRS2 deficiency. However the functional defects of IRS2-deficient PVAT are unlikely to be caused by exaggerated inflammation.

Adiponectin is an important modulator of many metabolic processes and has been shown to increase insulin sensitivity and improve vascular function (Funahashi et al., 1999; Yokota et al., 2000; Laakso, 2001).The concentration of adiponectin is inversely associated with DM2 (Duncan et al., 2004; Luo et al., 2010). Adiponectin binds its receptor and activates AMPKα1α2 which eventually stimulates Akt phosphorylation and NO production (Eringa et al., 2006; de Boer et al., 2016). In the current study, however, we did not see differences in the secretion of adiponectin (**Figure 5A**) or expression levels thereof in IRS2$^{-/-}$ and IRS2$^{+/+}$ PVAT (**Figure 4C**). To confirm this, Akt phosphorylation in wild-type arteries incubated with IRS2-deficient PVAT was comparable to incubation with wild-type PVAT after insulin stimulation (**Figure 6**). The failure of arteries to dilate in response to insulin after incubation with IRS2$^{-/-}$ PVAT despite a normal Akt phosphorylation

prompted us to measure eNOS phosphorylation. However, we were unsuccessful to this end due to the small amounts of eNOS protein in resistancearteries. Collectively, our results suggest that the failure of the vasodilator capacity in IRS2$^{-/-}$ PVAT stems from changes in molecules other than adiponectin that directly affects eNOS phosphorylation. In previous publications, we showed that db/db PVAT has lost its vasodilator capacity which was accompanied by a decreased adiponectin secretion; however, adding recombinant adiponectin to db/db PVAT only partially restored insulin-induced vasodilation, suggesting that other adipokines contribute to PVAT vasodilator capacity (Meijer et al., 2013). Previs et al. have shown that IRS2-deficient adipocytes fail to attenuate lipolysis in response to insulin (Previs et al., 2000). Hence, Free Fatty Acids (FFA) are probable contributors to the impaired vasodilatory capacity of PVAT in IRS2-deficient mice. Moreover, we have previously shown (Bakker et al., 2008) that activation of PKCtheta by the FFA palmitic acid reduces insulin-mediated Akt phosphorylation (Ser(473), which is crucial in insulin-mediated activation of eNOS) while increasing ERK1/2 phosphorylation. Based on our data, we propose the following working hypothesis (depicted in **Figure 7**). In the healthy situation, insulin mediates vasodilation by inducing autophosphorylation of its receptor which results in phosphorylation of IRS-1 and -2 and eventually activating Akt and endothelial Nitric Oxide Synthase (eNOS) to produce NO. The PVAT secretes the necessary adipokines (represented by adiponectin) that enhance NO production in endothelial cells.IRS2-deficient PVAT fails to uncover insulin-mediated vasodilation in muscle RA. Probable mechanisms do not involve adiponectin, but rather involve direct mediators that are released from PVAT (such as FFA) that interact with eNOS to reduce NO production.

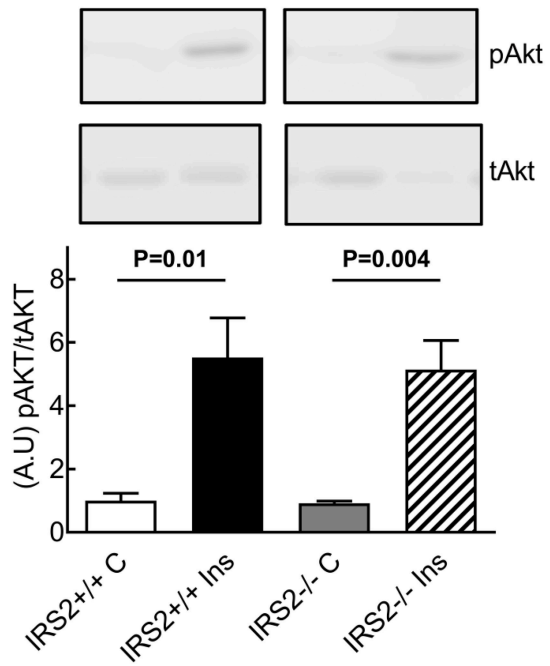

FIGURE 6 | Normal insulin-stimulated phosphorylation of Akt in arteries incubated with IRS2$^{-/-}$ PVAT. Insulin stimulation for 15 min resulted in strong Akt phosphorylation with no differences between incubation with IRS2$^{-/-}$or wildtype PVAT.

Study Limitations

In parallel with the findings of this study, there are a number of limitations that need to be considered. First, at 8 weeks of age, IRS2$^{-/-}$ mice showed hyperinsulinemia and hyperglycemia (**Table 1**). Hence, it is not possible to delineate whether the dysfunction in IRS2$^{-/-}$ PVAT is due to a direct role of IRS2 absence in PVAT signaling or due to an indirect role of the

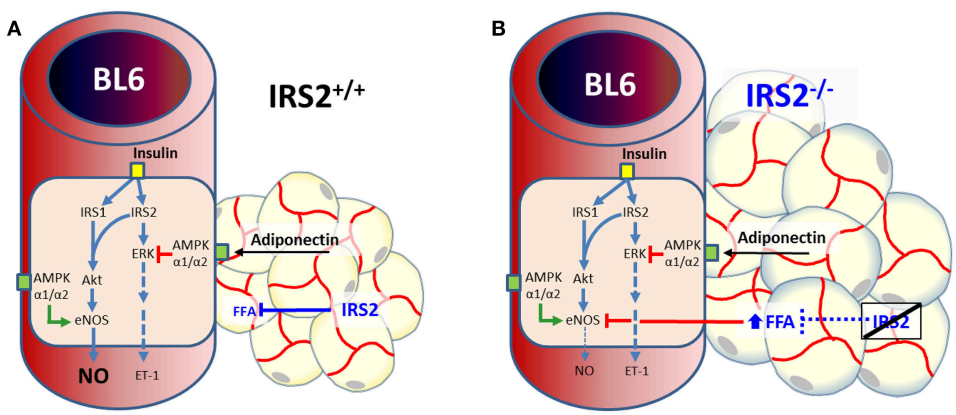

FIGURE 7 | Dual role of IRS2 in regulation of insulin-induced vasoreactivity in muscle. **(A)** In health, insulin induces vasodilation by activating its receptor, resulting in phosphorylation and activation of insulin receptor substrates (IRSs) 1 and 2.both IRS isoforms are involved inAkt and endothelial Nitric Oxide Synthase (eNOS) activation, while IRS2 mediates insulin-induced activation of ERK1/2. Perivascular adipose tissue (PVAT) secretes vasodilator adipokines such adiponectin that reduce endothelin (ET-1) secretion (de Boer et al., 2016) and enhance NO production in endothelial cells through AMPK (Eringa et al., 2010). **(B)** IRS2-deficient PVAT fails to uncover insulin-mediated vasodilation in muscle arteries. Probable mechanisms aredirect mediators that are released from PVAT that interact with eNOS to reduce NO production, such as free fatty acids (FFA) (Previs et al., 2000).

alteredmetabolic milieu. To account for this, we included young (∼8–10 weeks) mice in our study which have minimal to mild whole-body metabolic dysregulation when compared to older IRS2$^{-/-}$ mice. Previously, we have found that short term exposure of muscle RA to 10 mM of glucose does not alter their functional properties (Eringa et al., 2002). Moreover, we made our observation in an *ex vivo* set up wherein the PVAT and the arteries were incubated in a physiological buffer before the start of the experimental measurement. Hence, the indirect effects of whole-body metabolic dysregulation on PVAT phenotype in IRS2$^{-/-}$ mice were kept to a minimum. It should be noted that while hyperglycemia-mediated effects of IRS2 deficiency cannot be fully excluded, these effects are relevant to PVAT dysfunction in DM2. Second, the adipokine secretion pattern or IRS2$^{-/-}$ PVAT observed in this study is highlighted by a paradoxical decrease in resistin secretion. We cannot fully explain this finding, but the low inflammation in IRS2$^{-/-}$ PVAT (**Figures 4E,F**) may contribute as macrophages are an important source of resistin (Qatanani et al., 2009). Third, as the PVAT in our study is missing IRS2 in all of its components (adipocytes, endothelial cells, macrophages), further experiments are needed to decipher the role of IRS2 deletion in the endothelium of PVAT. Lastly, it was not possible to measure the amount of Endothelin-1 released from the cannulated vessels in the organ bath; challenges arose in performing the *in vitro* analyses of this study due to the small amount of PVAT and small-sized arteries obtained from the mice.

In conclusion, we show in this study that in the muscle microcirculation IRS2 directly mediates insulin's vasoconstrictor effects in the vascular wall while indirectly mediating its vasodilator effects by controlling vasodilator actions of PVAT. IRS2 inactivation in PVAT abolishes its vasodilator capacity independently from adiponectin secretion or inflammation in PVAT. Future research should focus on detailed analysis of the PVAT secretome in IRS2-deficient PVAT to gain further insight into adipose tissue dysfunction in insulin-resistant individuals.

AUTHOR CONTRIBUTIONS

AT wrote the manuscript and researched and analyzed data. WB gathered part of the data regarding the IRS2 mouse colony. HN, YS, VvH, and ES supervised, contributed to discussions, and edited the manuscript. EE researched data, supervised, contributed to discussions, and edited the manuscript. EE is the guarantor of this work and, as such, had full access to all the data in the study and takes responsibility for the integrity of the data and the accuracy of the data analysis.

FUNDING

This work was supported by the Netherlands Organization for Scientific Research (VIDI grant 917.133.72).

ACKNOWLEDGMENTS

We acknowledge Zeineb Gam and Elisa Meinster for their dedicated technical assistance in performing the experiments of this study.

SUPPLEMENTARY MATERIAL

The Supplementary Material for this article can be found online at: https://www.frontiersin.org/articles/10.3389/fphys.2018.00245/full#supplementary-material

REFERENCES

Abel, E. D., Peroni, O., Kim, J. K., Kim, Y. B., Boss, O., Hadro, E., et al. (2001). Adipose-selective targeting of the GLUT4 gene impairs insulin action in muscle and liver. *Nature* 409, 729–733. doi: 10.1038/35055575

Aman, J., van Bezu, J., Damanafshan, A., Huveneers, S., Eringa, E. C., Vogel, S. M., et al. (2012). Effective treatment of edema and endothelial barrier dysfunction with imatinib. *Circulation* 126, 2728–2738. doi: 10.1161/CIRCULATIONAHA.112.134304

Bakker, W., Sipkema, P., Stehouwer, C. D., Serne, E. H., Smulders, Y. M., van Hinsbergh, V. W., et al. (2008). Protein kinase C theta activation induces insulin-mediated constriction of muscle resistance arteries. *Diabetes* 57, 706–713. doi: 10.2337/db07-0792

Baron, A. D. (1993). Cardiovascular actions of insulin in humans. Implications for insulin sensitivity and vascular tone. *Baillieres Clin. Endocrinol. Metab.* 7, 961–987. doi: 10.1016/S0950-351X(05)80241-1

Bodhini, D., Radha, V., Deepa, R., Ghosh, S., Majumder, P. P., Rao, M. R., et al. (2007). The G1057D polymorphism of IRS-2 gene and its relationship with obesity in conferring susceptibility to type 2 diabetes in Asian Indians. *Int. J. Obes.* 31, 97–102. doi: 10.1038/sj.ijo.0803356

Brownrigg, J. R., Hughes, C. O., Burleigh, D., Karthikesalingam, A., Patterson, B. O., Holt, P. J., et al. (2016). Microvascular disease and risk of cardiovascular events among individuals with type 2 diabetes: a population-level cohort study. *Lancet Diabetes Endocrinol.* 4, 588–597. doi: 10.1016/S2213-8587(16)30057-2

de Boer, M. P., Meijer, R. I., Richter, E. A., van Nieuw Amerongen, G. P., Sipkema, P., van Poelgeest, E. M., et al. (2016). Globular adiponectin controls insulin-mediated vasoreactivity in muscle through AMPKalpha2. *Vasc. Pharmacol.* 78, 24–35. doi: 10.1016/j.vph.2015.09.002

Duncan, B. B., Schmidt, M. I., Pankow, J. S., Bang, H., Couper, D., Ballantyne, C. M., et al. (2004). Adiponectin and the development of type 2 diabetes: the atherosclerosis risk in communities study. *Diabetes* 53, 2473–2478. doi: 10.2337/diabetes.53.9.2473

Eringa, E. C., Bradley, E. A., Stehouwer, D. A., Korstjens, I., Nieuw Amerongen, G. P., et al. (2010). Activation of AMP-activated protein kinase by 5-Aminoimidazole-4-Carboxamide-1-beta-D-Ribofuranoside in the muscle microcirculation increases nitric oxide synthesis and microvascular perfusion. *Arterioscler. Thromb. Vasc. Biol.* 30, 1137–1142. doi: 10.1161/ATVBAHA.110.204404

Eringa, E. C., Stehouwer, C. D., Merlijn, T., Westerhof, N., and Sipkema, P. (2002). Physiological concentrations of insulin induce endothelin-mediated vasoconstriction during inhibition of NOS or PI3-kinase in skeletal muscle arterioles. *Cardiovasc. Res.* 56, 464–471. doi: 10.1016/S0008-6363(02)00593-X

Eringa, E. C., Stehouwer, C. D., van Nieuw Amerongen, G. P., Ouwehand, L., Westerhof, N., and Sipkema, P. (2004). Vasoconstrictor effects of insulin in skeletal muscle arterioles are mediated by ERK1/2 activation in endothelium. *Am. J. Physiol. Heart Circ. Physiol.* 287, H2043–H2048. doi: 10.1152/ajpheart.00067.2004

Eringa, E. C., Stehouwer, C. D., Walburg, K., Clark, A. D., van Nieuw Amerongen, G. P., Westerhof, N., et al. (2006). Physiological concentrations of insulin induce endothelin-dependent vasoconstriction of skeletal muscle resistance arteries in the presence of tumor necrosis factor-alpha dependence on c-Jun N-terminal kinase. *Arterioscler. Thromb. Vasc. Biol.* 26, 274–280. doi: 10.1161/01.ATV.0000198248.19391.3e

Esposito, D. L., Li, Y., Vanni, C., Mammarella, S., Veschi, S., Della Loggia, F., et al. (2003). A novel T608R missense mutation in insulin receptor substrate-1

identified in a subject with type 2 diabetes impairs metabolic insulin signaling. *J. Clin. Endocrinol. Metab.* 88, 1468–1475. doi: 10.1210/jc.2002-020933

Funahashi, T., Nakamura, T., Shimomura, I., Maeda, K., Kuriyama, H., Takahashi, M., et al. (1999). Role of adipocytokines on the pathogenesis of atherosclerosis in visceral obesity. *Intern. Med.* 38, 202–206. doi: 10.2169/internalmedicine.38.202

Greenstein, A. S., Khavandi, K., Withers, S. B., Sonoyama, K., Clancy, O., Jeziorska, M., et al. (2009). Local inflammation and hypoxia abolish the protective anticontractile properties of perivascular fat in obese patients. *Circulation* 119, 1661–1670. doi: 10.1161/CIRCULATIONAHA.108.821181

Houben, A. J., Eringa, E. C., Jonk, A. M., Serne, E. H., Smulders, Y. M., and Stehouwer, C. D. (2012). Perivascular fat and the microcirculation: relevance to insulin resistance, diabetes, and cardiovascular disease. *Curr. Cardiovasc. Risk Rep.* 6 80–90. doi: 10.1007/s12170-011-0214-0

Jiang, Z. Y., Lin, Y. W., Clemont, A., Feener, E. P., Hein, K. D., Igarashi, M., et al. (1999). Characterization of selective resistance to insulin signaling in the vasculature of obese Zucker (fa/fa) rats. *J. Clin. Invest.* 104, 447–457. doi: 10.1172/JCI5971

Kubota, N., Tobe, K., Terauchi, Y., Eto, K., Yamauchi, T., Suzuki, R., et al. (2000). Disruption of insulin receptor substrate 2 causes type 2 diabetes because of liver insulin resistance and lack of compensatory beta-cell hyperplasia. *Diabetes* 49, 1880–1889. doi: 10.2337/diabetes.49.11.1880

Kubota, T., Kubota, N., Kumagai, H., Yamaguchi, S., Kozono, H., Takahashi, T., et al. (2011). Impaired insulin signaling in endothelial cells reduces insulin-induced glucose uptake by skeletal muscle. *Cell Metab.* 13, 294–307. doi: 10.1016/j.cmet.2011.01.018

Kubota, T., Kubota, N., Moroi, M., Terauchi, Y., Kobayashi, T., Kamata, K., et al. (2003). Lack of insulin receptor substrate-2 causes progressive neointima formation in response to vessel injury. *Circulation* 107, 3073–3080. doi: 10.1161/01.CIR.0000070937.52035.25

Laakso, M. (2001). Cardiovascular disease in type 2 diabetes: challenge for treatment and prevention. *J. Intern. Med.* 249, 225–235. doi: 10.1046/j.1365-2796.2001.00789.x

Lesniewski, L. A., Donato, A. J., Behnke, B. J., Woodman, C. R., Laughlin, M. H., Ray, C. A., et al. (2008). Decreased NO signaling leads to enhanced vasoconstrictor responsiveness in skeletal muscle arterioles of the ZDF rat prior to overt diabetes and hypertension. *Am. J. Physiol. Heart Circ. Physiol.* 294, H1840–H1850. doi: 10.1152/ajpheart.00692.2007

Luo, N., Liu, J., Chung, B. H., Yang, Q., Klein, R. L., Garvey, W. T., et al. (2010). Macrophage adiponectin expression improves insulin sensitivity and protects against inflammation and atherosclerosis. *Diabetes* 59, 791–799. doi: 10.2337/db09-1338

Mazurek, T., Zhang, L., Zalewski, A., Mannion, J. D., Diehl, J. T., Arafat, H., et al. (2003). Human epicardial adipose tissue is a source of inflammatory mediators. *Circulation* 108, 2460–2466. doi: 10.1161/01.CIR.0000099542.57313.C5

Meijer, R. I., Bakker, W., Alta, C. L., Sipkema, P., Yudkin, J. S., Viollet, B., et al. (2013). Perivascular adipose tissue control of insulin-induced vasoreactivity in muscle is impaired in db/db mice. *Diabetes* 62, 590–598. doi: 10.2337/db11-1603

Meijer, R. I., Serne, E. H., Korkmaz, H. I., van der Peet, D. L., de Boer, M. P., Niessen, H. W., et al. (2015). Insulin-induced changes in skeletal muscle microvascular perfusion are dependent upon perivascular adipose tissue in women. *Diabetologia* 58, 1907–1915. doi: 10.1007/s00125-015-3606-8

Mita, T., Azuma, K., Goto, H., Jin, W. L., Arakawa, M., Nomiyama, T., et al. (2011). IRS-2 deficiency in macrophages promotes their accumulation in the vascular wall. *Biochem. Biophys. Res. Commun.* 415, 545–550. doi: 10.1016/j.bbrc.2011.10.086

Montagnani, M., Ravichandran, L. V., Chen, H., Esposito, D. L., and Quon, M. J. (2002). Insulin receptor substrate-1 and phosphoinositide-dependent kinase-1 are required for insulin-stimulated production of nitric oxide in endothelial cells. *Mo. Endocrinol.* 16, 1931–1942. doi: 10.1210/me.2002-0074

O'Connor, J. C., Sherry, C. L., Guest, C. B., and Freund, G. G. (2007). Type 2 diabetes impairs insulin receptor substrate-2-mediated phosphatidylinositol 3-kinase activity in primary macrophages to induce a state of cytokine resistance to IL-4 in association with overexpression of suppressor of cytokine signaling-3. *J. Immunol.* 178, 6886–6893. doi: 10.4049/jimmunol.178.11.6886

Okon, E. B., Chung, W. Y., Rauniyar, P., Padilla, E., Tejerina, T., van Breemen, C. et al (2005). Compromised arterial function in human type 2 diabetic patients. *Diabetes* 54, 2415–2423. doi: 10.2337/diabetes.54.8.2415

Ort, T., Arjona, A. A., MacDougall, J. R., Nelson, P. J., Rothenberg, M. E., Wu, F., et al. (2005). Recombinant human FIZZ3/resistin stimulates lipolysis in cultured human adipocytes, mouse adipose explants, and normal mice. *Endocrinology* 146, 2200–2209. doi: 10.1210/en.2004-1421

Previs, S. F., Withers, D. J., Ren, J. M., White, M. F., and Shulman, G. I. (2000). Contrasting effects of IRS-1 versus IRS-2 gene disruption on carbohydrate and lipid metabolism *in vivo*. *J. Biol. Chem.* 275, 38990–38994. doi: 10.1074/jbc.M006490200

Qatanani, M., Szwergold, N. R., Greaves, D. R., Ahima, R. S., and Lazar, M. A. (2009). Macrophage-derived human resistin exacerbates adipose tissue inflammation and insulin resistance in mice. *J. Clin. Invest.* 119, 531–539. doi: 10.1172/JCI37273

Rask-Madsen, C., Li, Q., Freund, B., Feather, D., Abramov, R., Wu, I. H., et al. (2010). Loss of insulin signaling in vascular endothelial cells accelerates atherosclerosis in apolipoprotein E null mice. *Cell Metab.* 11, 379–389. doi: 10.1016/j.cmet.2010.03.013

Sun, X. J., Wang, L. M., Zhang, Y., Yenush, L., Myers, M. G. Jr., Glasheen, E., et al. (1995). Role of IRS-2 in insulin and cytokine signalling. *Nature* 377, 173–177. doi: 10.1038/377173a0

Tilg, H., and Moschen, A. R. (2006). Adipocytokines: mediators linking adipose tissue, inflammation and immunity. *Nat. Rev. Immunol.* 6, 772–783. doi: 10.1038/nri1937

Verlohren, S., Dubrovska, G., Tsang, S. Y., Essin, K., Luft, F. C., Huang, Y., et al. (2004). Visceral periadventitial adipose tissue regulates arterial tone of mesenteric arteries. *Hypertension* 44, 271–276. doi: 10.1161/01.HYP.0000140058.28994.ec

Withers, D. J., Burks, D. J., Towery, H. H., Altamuro, S. L., Flint, C. L., and White, M. F. (1999). Irs-2 coordinates Igf-1 receptor-mediated beta-cell development and peripheral insulin signalling. *Nat. Genet.* 23, 32–40. doi: 10.1038/12631

Withers, S. B., Agabiti-Rosei, C., Livingstone, D. M., Little, M. C., Aslam, R., Malik, R. A., et al. (2011). Macrophage activation is responsible for loss of anticontractile function in inflamed perivascular fat. *Arterioscler. Thromb. Vasc. Biol.* 31, 908–913. doi: 10.1161/ATVBAHA.110.221705

Withers, S. B., Bussey, C. E., Saxton, S. N., Melrose, H. M., Watkins, A. E., and Heagerty, A. M. (2014). Mechanisms of adiponectin-associated perivascular function in vascular disease. *Arterioscler. Thromb. Vasc. Biol.* 34, 1637–1642. doi: 10.1161/ATVBAHA.114.303031

Woerdeman, J., Meijer, R. I., Eringa, E. C., Hoekstra, T., Smulders, Y. M., and Serne, E. H. (2016). Insulin sensitivity determines effects of insulin and meal ingestion on systemic vascular resistance in healthy subjects. *Microcirculation* 23, 62–68. doi: 10.1111/micc.12258

Yang, Y. J., Hope, I. D., Ader, M., and Bergman, R. N. (1989). Insulin transport across capillaries is rate limiting for insulin action in dogs. *J. Clin. Invest.* 84 1620–1628. doi: 10.1172/JCI114339

Yokota, T., Oritani, K., Takahashi, I., Ishikawa, J., Matsuyama, A., Ouchi, N., et al. (2000). Adiponectin, a new member of the family of soluble defense collagens, negatively regulates the growth of myelomonocytic progenitors and the functions of macrophages. *Blood* 96, 1723–1732.

Yudkin, J. S., Eringa, E., and Stehouwer, C. D. (2005). "Vasocrine" signalling from perivascular fat: a mechanism linking insulin resistance to vascular disease. *Lancet* 365, 1817–1820. doi: 10.1016/S0140-6736(05) 66585-3

Yudkin, J. S., Stehouwer, C. D., Emeis, J. J., and Coppack, S. W. (1999). C-reactive protein in healthy subjects: associations with obesity, insulin resistance, and endothelial dysfunction: a potential role for cytokines originating from adipose tissue? *Arterioscler. Thromb. Vasc. Biol.* 19, 972–978. doi: 10.1161/01.ATV.19.4.972

Conflict of Interest Statement: The authors declare that the research was conducted in the absence of any commercial or financial relationships that could be construed as a potential conflict of interest.

frontiers in Physiology

REVIEW
published: 21 March 2018
doi: 10.3389/fphys.2018.00253

Perivascular Adipose Tissue as a Relevant Fat Depot for Cardiovascular Risk in Obesity

Rafael M. Costa[1], Karla B. Neves[2], Rita C. Tostes[1] and Núbia S. Lobato[3]*

[1] Department of Pharmacology, Ribeirao Preto Medical School, University of São Paulo, Ribeirao Preto, Brazil, [2] Institute of Cardiovascular and Medical Sciences, British Heart Foundation, Glasgow Cardiovascular Research Centre, University of Glasgow, Glasgow, United Kingdom, [3] Institute of Health Sciences, Federal University of Goias, Jatai, Brazil

Obesity is associated with increased risk of premature death, morbidity, and mortality from several cardiovascular diseases (CVDs), including stroke, coronary heart disease (CHD), myocardial infarction, and congestive heart failure. However, this is not a straightforward relationship. Although several studies have substantiated that obesity confers an independent and additive risk of all-cause and cardiovascular death, there is significant variability in these associations, with some lean individuals developing diseases and others remaining healthy despite severe obesity, the so-called metabolically healthy obese. Part of this variability has been attributed to the heterogeneity in both the distribution of body fat and the intrinsic properties of adipose tissue depots, including developmental origin, adipogenic and proliferative capacity, glucose and lipid metabolism, hormonal control, thermogenic ability, and vascularization. In obesity, these depot-specific differences translate into specific fat distribution patterns, which are closely associated with differential cardiometabolic risks. The adventitial fat layer, also known as perivascular adipose tissue (PVAT), is of major importance. Similar to the visceral adipose tissue, PVAT has a pathophysiological role in CVDs. PVAT influences vascular homeostasis by releasing numerous vasoactive factors, cytokines, and adipokines, which can readily target the underlying smooth muscle cell layers, regulating the vascular tone, distribution of blood flow, as well as angiogenesis, inflammatory processes, and redox status. In this review, we summarize the current knowledge and discuss the role of PVAT within the scope of adipose tissue as a major contributing factor to obesity-associated cardiovascular risk. Relevant clinical studies documenting the relationship between PVAT dysfunction and CVD with a focus on potential mechanisms by which PVAT contributes to obesity-related CVDs are pointed out.

Keywords: perivascular adipose tissue, obesity, vascular function, cardiovascular risk, adipokine

OPEN ACCESS

Edited by:
Maik Gollasch,
Charité Universitätsmedizin Berlin, Germany

Reviewed by:
D. Neil Granger,
Louisiana State University Health Sciences Center Shreveport, United States
Geraldine Clough,
University of Southampton, United Kingdom

****Correspondence:***
Rafael M. Costa
rafael.menezess@yahoo.com.br

Specialty section:
This article was submitted to Vascular Physiology, a section of the journal Frontiers in Physiology

Received: *09 December 2017*
Accepted: *06 March 2018*
Published: *21 March 2018*

Citation:
Costa RM, Neves KB, Tostes RC and Lobato NS (2018) Perivascular Adipose Tissue as a Relevant Fat Depot for Cardiovascular Risk in Obesity. Front. Physiol. 9:253. doi: 10.3389/fphys.2018.00253

INTRODUCTION

Obesity is a fast-growing problem that is reaching epidemic magnitudes worldwide, affecting both children and adults (Ogden et al., 2016; Lim et al., 2017). This condition is defined as a disproportionate body weight for height with excessive fat accumulation that is frequently accompanied by mild, chronic, systemic inflammation (Gonzalez-Muniesa et al., 2017).

There is emerging body of scientific, medical, and behavioral data showing that central deposition of adipose tissue is associated with elevated risk of morbidity and mortality due to several cardiovascular complications, including stroke, congestive heart failure, myocardial infarction, and cardiovascular death, and this is independent of the association between obesity and the components of the metabolic syndrome and other cardiovascular risk factors (Arnlöv et al., 2010; Williams et al., 2015). Previous support for this understanding was provided by the American Heart Association in 1998, which has reclassified obesity as a major, modifiable risk factor for coronary heart disease (CHD) (Eckel and Krauss, 1998).

Besides being considered the largest energetic reservoir in the body, white adipose tissue (WAT) has been recognized as a remarkably complex endocrine organ that produces and secretes several substances with endocrine, paracrine, and autocrine functions, acting as a major regulator of systemic energy homeostasis (Rosen and Spiegelman, 2014). In obesity, adipose tissue may become dysfunctional and fail to appropriately expand to store the excess energy. This results in ectopic fat deposition in other tissues that regulate metabolic homeostasis (Tchoukalova et al., 2010). WAT expansion has been associated with numerous local consequences, including inflammation (Apovian et al., 2008), fibrosis (Henegar et al., 2008), hypoxia (Jiang et al., 2011), dysregulated adipokine secretion (Jernås et al., 2006; Skurk et al., 2007), and disrupted mitochondrial function (Heinonen et al., 2015). The whole-body consequences of WAT dysfunction include abnormal glucose and lipid metabolism, insulin resistance, increase in blood pressure, coagulation, fibrinolysis, inflammation, and endothelial dysfunction, all of which provide important mechanisms linking obesity to cardiovascular disease (CVD).

In addition to abdominal adiposity, recent evidence indicates that perivascular adipose tissue (PVAT) produces and releases a wide variety of adipokines and other factors that exert a paracrine influence on the vascular function, not only in veins and conductance arteries, but also in vessels of smaller caliber, which are essential in the regulation of blood pressure (Iozzo, 2011; Aghamohammadzadeh et al., 2012; Malinowski et al., 2013; Szasz et al., 2013). Although PVAT has been considered an inherent component that provides structural support to the vessels, now it is clear that this tissue possesses the dynamic capacity to mobilize near vessels with the potential for cellular communication and control of vascular function (Sacks and Fain, 2007; Chatterjee et al., 2009). Local accumulation of perivascular adipocytes has been consistently associated with the development of cardiometabolic complications in obesity (Chang et al., 2013; Lim and Meigs, 2014). In fact, adipose tissue surrounding the heart has been clinically associated with coronary artery disease (Cheng et al., 2008; Clément et al., 2009; Company et al., 2010), which reinforces the evidence that local adipose tissue accumulation can constitute an important regulator of cardiovascular function and a mediator of the development and progression of CVDs. The present review provides a comprehensive overview on the role of PVAT within the scope of adipose tissue as a major contributing factor to obesity-associated cardiovascular risk. We will also highlight the relevant clinical studies documenting the relationship between PVAT dysfunction and CVD and the potential mechanisms by which PVAT contributes to obesity-related cardiovascular complications.

OBESITY AND CARDIOVASCULAR RISK

Over the past decades, an explosive increase in overweight and obesity prevalence has taken place in most of the high-income countries (Vandevijvere et al., 2015). Several recent reviews have also shown significant increases in the prevalence of these conditions in low- and middle-income countries, affecting both men and women, adults and children (Gupta et al., 2012; Popkin and Slining, 2013; Sayon-Orea et al., 2013; Yatsuya et al., 2014). Although there are great variations in the prevalence and trends of overweight and obesity among different regions, the numbers have been projected to further increase in coming years (Gupta et al., 2012; Popkin and Slining, 2013; Sayon-Orea et al., 2013; Yatsuya et al., 2014; Poobalan and Aucott, 2016). The percentage of adults with a body mass index (BMI) $\geq$25 kg/m^2 between 1980 and 2013 increased in men and women from 28.8% (95% UI: 28.4–29.3) to 36.9% (36.3–37.4), and from 29.8 to 38%, respectively. Among children and adolescents, in 2013, 23.8% (22.9–24.7) of boys and 22.6% (21.7–23.6) of girls were either overweight or obese in developed countries (Ng et al., 2014). The prevalence rate in developing countries elevated from 8.1% (7.7–8.6) to 12.9% (12.3–13.5) for boys and from 8.4% (8.1–8.8) to 13.4% (13.0–13.9) in girls, in 2013. The World Health Organization (WHO) estimated that more than 2.1 billion adults were overweight or obese globally in 2014. By 2030, estimations predict that 57.8% of the adult population will have a BMI of 25 kg/m^2 or higher (Kelly et al., 2008; Finkelstein et al., 2012). As such, the adverse health consequences of obesity, particularly the burden of CVDs are expected to increase in coming years.

In adults, obesity generally presents as an excess of body weight and adipose tissue, which is clinically assessed by the BMI, calculated by the weight in kilograms divided by the height in square meters (Garrow and Webster, 1985). The idea that BMI is associated with higher all-cause morbidity/mortality risk is supported by a wealth of epidemiological and clinical data (Borrell and Samuel, 2014; Yang et al., 2016; Kong et al., 2017). However, a recent comprehensive estimation, resulting from a systematic review on the association of all-cause mortality in adults with BMI categories used in the United States and internationally, demonstrated that while grades 2 and 3 obesity are both associated with significantly higher all-cause mortality, overweight (defined as a BMI of 25 – <30) is associated with significantly lower overall mortality relative to the normal weight category. Furthermore, the authors did not find significant excess mortality associated with grade 1 obesity (BMI of 30 – <35) (Flegal et al., 2013), suggesting that cardiovascular risk and mortality are not simply associated with the amount of adipose tissue.

Adipose tissue is dispersed throughout the body in discrete depots ranging from 5 to 60% of total body weight (Cinti, 2001). More than 80% of the tissue is found subcutaneously, mainly

in the abdominal, gluteal and femoral areas. Visceral adipose tissue and smaller depots close to organs represent the remaining 10–20% of total body fat in men and 5–10% in women (Lee et al., 2013). It has become increasingly evident that the regional body fat distribution, the size of each depot, the depot-related differences in adipose tissue function, and the balance between them are important for the individual cardiometabolic risk. For example, a peripheral adiposity in upper and lower extremities is favorable while the truncal adipose tissue deposition, which includes subcutaneous fat in thoracic and abdominal region and the fat in intrathoracic and intraabdominal regions, is detrimental and associated with increased mortality (Garg, 2004; McLaughlin et al., 2011). Moreover, for any given BMI-value, there is significant variability with some lean individuals developing disease and others exhibiting a better metabolic profile than expected for their adiposity profile (Samocha-Bonet et al., 2012). Lapidus et al. in 1980s, reported a stronger association of waist-to-hip circumference ratio, which reflects abdominal fat, with a 12-year incidence of myocardial infarction, angina pectoris, stroke, and death, when compared to other anthropometric measures (Lapidus et al., 1984). Subsequently, many clinical studies have established the superior capability of waist-to-hip ratio measure to predict CVD risk when compared to BMI.

The large-scale randomized factorial clinical trial study ADVANCE (Action in Diabetes and Vascular disease: Preterax and Diamicron-MR Controlled Evaluation) examined the relative importance of different adiposity markers in predicting CVD risk in a population of individuals with type 2 diabetes (Czernichow et al., 2011). After 9.1 years of follow up, investigators reported that waist-to-hip ratio is the best predictor of cardiovascular events and mortality in patients with type-2-diabetes while the BMI is the worst. The INTERHEART study, a large multiethnic case-control study of acute myocardial infarction, also evidenced a greater contribution for waist-to-hip ratios accounting for most of the risk of myocardial infarction when compared to BMI, in both sexes and at all ages (Yusuf et al., 2004). A meta-analysis using data pooled from 15 prospective studies that included more than 258,000 subjects reported a progressive increase in cardiovascular risk accompanying the increase in waist circumference and waist-to-hip ratios (de Koning et al., 2007). Specifically, every 1 cm of increase in waist circumference was associated with a 2% increased relative risk of cardiovascular event and a 0.01 increase in waist-to-hip ratio was associated with a 5% increase in risk of future CVD for both men and women. The Nurses' Health Study, one of the largest and longest studies to date that measured abdominal obesity, confirmed these findings using the waist circumference measure (Zhang et al., 2008). The investigators reported that during 16 years of follow-up in US women, elevated waist circumference was associated with significantly increased CVD mortality even among normal-weight women.

As obesity is strongly linked to comorbid conditions, including type 2 diabetes, hypertension, hypercholesterolemia, hypertriglyceridemia, and non-alcoholic fatty liver disease, these risk factors have been considered important intermediate steps in the causal relationship between obesity and CVD risk. From this perspective, there has been considerable debate about whether the adjustment for these risk factors in statistical models is necessary for the true absolute risk predicting CVD risk or whether such adjustments, rather than controlling for, may increase the overall risk of bias. In fact, the increased cardiovascular risk attributed to weight gain persists even after adjustment for the frequently observed co-existing risk factors. In 1983, a 26-year follow-up of participants in the Framingham Heart Study reported that this risk was particularly apparent for heart failure, but it was also identified with CHD, stroke, and death from CVD. Kenchaiah and colleagues also provided unequivocal evidence in 2002, using updated Framingham data. According to authors, approximately 11% of heart failure cases among men and 14% among women are attributable to obesity alone, suggesting that efforts to promote optimal body weight may reduce the risk of heart failure (Kenchaiah et al., 2002). A careful review of these studies further supports the idea that composition of adipose tissue is important for cardiovascular risk stratification and characterizes visceral adipose tissue as an incomparable pathogenic depot that confers risk beyond its contribution to overall adiposity. These constraints that govern the outcomes of obesity are described in a recent review by Mahmood et al. (2014) and emphasizes the importance of adipose tissue depots as potential components in assessing and predicting cardiometabolic risk.

SYSTEMIC ADIPOSE TISSUE DYSFUNCTION AND VASCULAR FUNCTION IN OBESITY

The WAT is no longer considered to be only a passive tissue for the storage of excess energy in the form of fat. There is now compelling evidence that this tissue acts as an endocrine organ that produces and releases biologically active compounds that regulate metabolic and cardiovascular homeostasis and undergoes pathological expansion during obesity (Waki and Tontonoz, 2007; Coelho et al., 2013). In addition to the better-known WAT, mammals also exhibit brown adipose tissue (BAT). Functional BAT in adult humans is localized to areas close to the clavicular, periaortic, cervical, and suprarenal regions (Cypess et al., 2009). BAT is an energy-expending organ that produces heat, and it is essential for adaptive thermogenesis. Adipocytes from BAT possess large numbers of mitochondria that contain a unique protein called uncoupling protein 1 (UCP1), which is a proton channel within the inner mitochondrial membrane involved in the dissipation of the proton motive force that is normally used to drive the synthesis of cellular ATP. Consequently, the energy in the mitochondrial electrochemical gradient is released in the form of heat (Cannon and Nedergaard, 2004). Indeed, evidence from clinical and experimental studies indicate that BAT activation increases thermogenesis (Lidell and Enerback, 2010). Recent reports have also unequivocally demonstrated that BAT exerts significant impact on whole-body energy homeostasis and that its activity profoundly influences body weight (Fruhbeck et al., 2009). In fact, overweight and obesity have been associated with lower BAT

activity (Vijgen et al., 2011), which is increased after weight loss (Vijgen et al., 2012). Together with data obtained from rodent models (Vegiopoulos et al., 2010; Seale et al., 2011; Kiefer et al., 2012), these reports have drawn attention to BAT as an attractive target for the treatment of obesity and associated metabolic diseases. Hence, potent or permanent interventions targeting on induction of brown phenotype in adipose tissue depots will facilitate long term studies to investigate their precise role in driving metabolic diseases and to determine their potential to attenuate cardiovascular risk. However, it is discernible that such a critical approach will require layers of specificity, beyond the targeting of individual components of WAT, considering the possibility that factors involved in browning of specific adipose tissue depots may not share similar regulatory network.

A highly relevant factor for the understanding of the cardiovascular impact of increased adipose tissue mass is the recognition that adipocytes are endocrine and paracrine determinants of vascular function. The great question that arises from these observations is how excessive accumulation of adipose tissue could lead to the development of such dysfunction even at a distance. The answer to this question is provided by the evidence that adipose tissue is involved in the production of various proteins, collectively called adipokines (including chemokines, cytokines, and hormones) (Kershaw and Flier, 2004), which are secreted into the circulatory system and act in several physiological processes, including energy balance, immune responses, blood pressure, vascular homeostasis and angiogenesis, glucose and lipid metabolism, and even insulin sensitivity (Prins, 2002), all of which may contribute to the elevated cardiovascular risk associated with obesity (Weyer et al., 2000; Wang et al., 2005). The positive energy balance induces an expansion and remodeling of the adipose tissue that is initially driven by adipocyte hyperplasia mediated by the recruitment and proliferation of adipogenic progenitors followed by an increase in adipocyte hypertrophy (Hausman et al., 2001; Spalding et al., 2008), which lead to dysregulated secretion of adipokines and increased release of free fatty acids (**Figure 1**).

Although the altered secretory function of adipose tissue is consistent with the idea that chronic obesity-related low-grade inflammation in adipose tissue is involved in the metabolic complications of obesity, it is important to consider that adipocytes in adipose tissue are not the only culprit. Regardless of the mechanisms of adipose tissue expansion, positive energy balance eventually leads to necrotic and/or apoptotic cell death and this is paralleled by quantitative and qualitative changes in the cellular composition and the phenotype of individual cells within adipose tissue (Weisberg et al., 2003). For example, adipose tissue from obese individuals is infiltrated by numerous activated macrophages, leading to increases in both absolute macrophage number and the relative level of macrophage-to-adipocyte ratio. In addition to this quantitative change, the macrophage phenotype is also altered by the obesity state. Macrophages that accumulate in adipose tissue of obese organisms tend to express genes associated with increased production of pro-inflammatory cytokines, express inducible nitric oxide synthase (iNOS), and produce high levels of reactive oxygen species (ROS), and nitrogen intermediates (Lumeng et al., 2007). Thus, it has become evident that interactions between the different cell types from enlarged and inflamed adipose tissue contribute to its overall impact on obesity-related disorders. In fact, some evidence exists that the release of some adipokines is even higher from the cells of the stroma-vascular fraction than from adipocytes (Chavey et al., 2009; Hamaguchi et al., 2012).

Adipose tissue dysfunction may also promote a state of systemic endothelial cell activation through the endocrine actions of inflammatory adipokines (Skurk et al., 2007; Dulloo et al., 2010). The impact of these adipokines on vascular function is not limited to the momentary regulation of the release of endothelium-derived vasoactive factors or regulation of vascular smooth muscle tone. Some adipokines may also profoundly affect local growth, migration, and inflammatory processes (Miao and Li, 2012). Obviously, these variety of products secreted by the adipose tissue, without even reporting the entirety of released adipokines, have provided promising possibilities for identifying novel biomarkers associated with obesity and the cardiovascular complications associated with this condition (Bagi et al., 2012; Barton et al., 2012). Although these studies set several adipokines into their functional context enhancing our current knowledge of the endocrine function of the adipose tissue, the identified proteins must be further validated regarding their expression, secretion and function. Translation of protein profiling results into clinical use will contribute to validate novel adipokines potentially representing a link between obesity and human disease. In this regard, studies must move from characterizing protein abundances to elaboration of their functional effects within cellular networks. However, since human genetic variability is estimated to contribute variations in the capacity of different adipose tissue depots to store and release fatty acids and to produce adipokines (White and Tchoukalova, 2014), and many of the direct genetic achievements are still being investigated for their causal impact on phenotypic outcomes, it is prudent to interpret both positive and negative results with caution. Integrated approaches including the analysis of multiple scientific fields will certainly enhance the understanding of this new physiological concept of interorgan crosstalk in the context of obesity.

PERIVASCULAR ADIPOSE TISSUE EFFECTS ON VASCULAR FUNCTION

Besides the endocrine role of adipose tissue, mediated by adipokines, a major emerging concept indicates that ectopic fat depots surrounding the heart and almost all systemic blood vessels, can also directly affect the cardiovascular function (Chang et al., 2013). These include: the PVAT, that is, the fat immediately adjacent to the adventitia of almost all arteries; the epicardial adipose tissue, which refers to the fat depot laying on the surface of the myocardium surrounding the coronary arteries; and the pericardial adipose tissue, the fat depot located between the visceral and parietal pericardium (Iozzo, 2011). Notably, this anatomical proximity of PVAT has an enormous influence on the cardiovascular system and highly vascularized

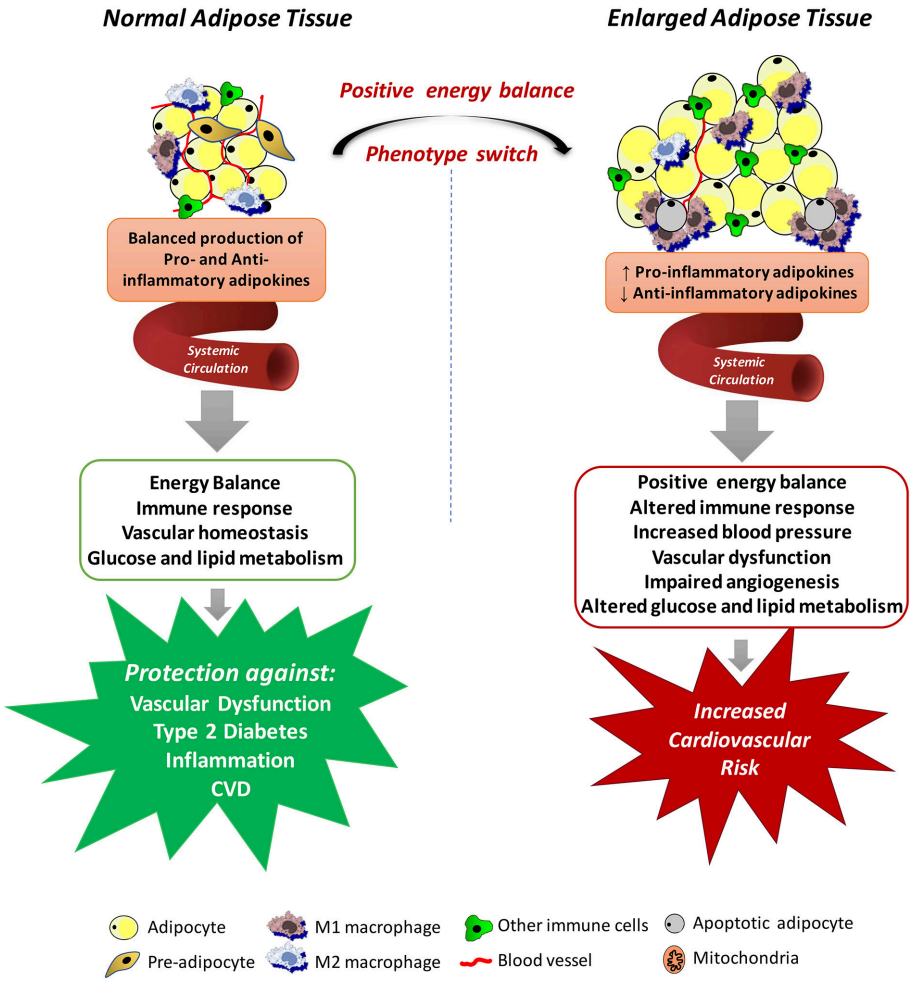

FIGURE 1 | Mechanisms by which systemic adipose tissue dysfunction could lead to the development of vascular dysfunction in obesity. Adipose tissue produces various chemokines, cytokines and hormones, which are secreted into the circulatory system and act in several physiological processes, including energy balance, immune responses, blood pressure, vascular homeostasis and angiogenesis, glucose and lipid metabolism. Expansion of the adipose tissue leads to necrotic and/or apoptotic cell death and this is paralleled by infiltration of activated macrophages, increased production of pro-inflammatory adipokines and reactive oxygen species, promoting a state of systemic endothelial cell activation and vascular dysfunction, all of which may contribute to the elevated cardiovascular risk associated with obesity.

organs (e.g., the kidney). In fact, over the past years, clinical and experimental evidence accumulated recognizing that PVAT not only stores triacylglycerols/triglycerides and free fatty acids, participating in energy metabolism, but also secretes a wide variety of biologically active molecules, including adipokines, such as leptin, adiponectin, chemerin, visfatin, resistin, tumor necrosis factor alpha (TNF-α), interleukin-6 (IL-6), interleukin-18 (IL-8), monocyte chemoattractant protein-1 (MCP-1), and plasminogen activator inhibitor 1 (PAI-1), which modulate vascular tone (Maenhaut and Van de Voorde, 2011), smooth muscle cells migration and proliferation (Miao and Li, 2012), neointimal hyperplasia and formation (Takaoka et al., 2010; Schroeter et al., 2013), inflammatory responses and oxidative stress (Salgado-Somoza et al., 2010). Most of these properties converge on endocrine-related effects, but also on a direct, paracrine influence in CVD, not only on large arteries and veins, but also in small and resistance vessels, and skeletal muscle microvessels, considered to be of greatest importance in blood pressure regulation, as has been reviewed elsewhere (Szasz et al., 2013; Xia and Li, 2017).

The structural and physiological characteristics of PVAT vary according to its location. In the mesenteric arteries, PVAT resembles WAT, with less differentiated adipocytes, poor vascularization, a specific profile of cytokines production/secretion, and contains infiltrates of macrophages, fibroblasts and cells of the immune system (Guzik et al., 2013). On the other hand, recent studies have demonstrated that PVAT of the thoracic aorta exhibits features that resemble BAT rather than WAT (Fitzgibbons et al., 2011; Chang et al., 2012), including expression of genes highly or solely expressed in the BAT, the presence of multilocular adipocytes and high abundance of mitochondria. Like BAT, PVAT is activated by cold and generates

heat. Interestingly, the cold-induced activation of thermogenesis in PVAT is accompanied by attenuation of the atherosclerotic process in apolipoprotein E deficient mice ($ApoE^{-/-}$), whereas such protection is lost in mice where PVAT is absent (Chang et al., 2012), indicating that the thermogenic properties of PVAT also mediate its vascular protective effects.

Consistent with the findings that thoracic aorta PVAT shares common characteristics with BAT, our group has recently demonstrated a potential role of mitochondria in periaortic adipose tissue as a source of mediators that could be involved in the modulation of vascular contraction along with the PVAT-derived relaxing factors (Costa et al., 2016). These are all exciting developments that have the potential to provide insight into new aspects of the specific nature and function of different adipose tissue depots while also places PVAT as a promising component of investigation regarding brown fat and its potential beneficial effects, including those on the vasculature. Further work is required to resolve interesting questions raised by these findings: are the precursor components of PVAT adipocytes distinct from those of white or BAT? Although the morphology and mRNA/protein profile of PVAT is evocative of classic BAT, is this tissue a true BAT? Recent studies have illustrated a remarkable possibility that the origin of PVAT adipocytes may so far be distinct from either white or brown adipocytes. Using a vascular smooth muscle cell (VSMC)-specific nuclear receptor activated by peroxisome proliferator-γ (PPARγ) deletion, Chang group generated mice completely devoid of PVAT in the aortic and mesenteric regions while both interscapular BAT and gonadal/inguinal/subcutaneous WAT remained intact, indicating that BAT, WAT, and PVAT have different origins (Chang et al., 2012). In this regard, the previous observation of Chatterjee's group demonstrated that *in vitro* differentiated human coronary artery perivascular adipocytes exhibit a distinct state of adipogenic differentiation and adipokine secretion when compared with adipocytes from subcutaneous or visceral adipose depots (Chatterjee et al., 2009), suggesting that PVAT exhibit a unique gene expression profile that underlies its role in vascular function. Although these well-established strategies provide extremely promising prospects, an unresolved question is the relative contribution of different brown and brown-like fat depots to metabolic and CVD in humans. Whether PVAT thermogenesis can be targeted for therapeutic purposes needs to be determined. It also seems clear that understanding the differences between PVAT depots, specifically, the functional analysis of bioenergetics in this tissue and its impact on systemic metabolism is a very promising approach in the context of metabolism and the etiology of the spectrum of cardiometabolic disorders.

The concept that PVAT influences vascular function, particularly contractile responses, dates from at least as early as the 1990s, when Soltis and Cassis described that PVAT retained and impaired the diffusion of pharmacological agents, justifying a reduction in the contractile response observed in vessels with this tissue (Soltis and Cassis, 1991). However, subsequent studies using several agonists of low retention in adipocytes also demonstrated such a decrease (Gollasch and Dubrovska, 2004). Löhn and his colleagues found that the vascular responses to angiotensin II (Ang II), serotonin (5-HT), and phenylephrine (PE) are reduced in intact aortas with PVAT, suggesting that periaortic adipose tissue regulates vascular tone by the release of transferable adventitia-derived relaxing factors (ADRF), now defined as PVAT-derived relaxant factors (PVRF) (Lohn et al., 2002). The anti-contractile effect of PVRFs under physiological conditions has been described in several species and is mediated by different mechanisms depending on the vascular bed. Convincing evidence has demonstrated that VSMC potassium (K^+) channels play a critical role in mediating the relaxation responses to PVRFs. The study of Löhn showed that the anti-contractile effect of periadventitial fat was reduced by inhibition of ATP-dependent K^+ channels and by the tyrosine kinase inhibitor genistein (Lohn et al., 2002). Following these findings, subsequent studies demonstrated that PVAT-derived transferable factors produce vasorelaxation by opening of voltage-dependent K^+ (Kv) channels (Dubrovska et al., 2004; Verlohren et al., 2004; Gao et al., 2005; Fesus et al., 2007). Schleifenbaum's group further explored the involvement of the Kv-subfamily on PVRFs actions. The authors demonstrated that the voltage-activated family of K^+ channels KCNQ (Kv7), which are not targeted by endothelium-derived relaxing factors (EDRF), play significant role in the vasorelaxation induced by PVRFs, which is at least in part mediated or modulated by hydrogen sulfide (H_2S). Although the KCNQ channel subtype involved in the PVRF effects has not been identified so far and clear evidence for direct activation of KCNQ channels by PVRF is still missing, the opening of these channels by pharmacological agents restores the diminished anti-contractile effects of perivascular fat in spontaneously hypertensive rats, thus suggesting its pivotal role in perivascular regulation of vascular tone (Schleifenbaum et al., 2010).

Although we are unable to cover the topic in detail in this manuscript, it is important to note that many other mechanisms involved in PVRF-induced anti-contractile effects have been described. Lu and collaborators, by using inferior vena cava rings in the absence and presence of PVAT and endothelium, found that endothelium removal abolishes PVAT anti-contractile response. The same group of researchers has suggested that PVAT releases Ang 1–7, which, by acting on receptors in the endothelium, leads to nitric oxide (NO) release and activation of Kv channels with subsequent vascular relaxation (Lu et al., 2011). PVRF may also act through endothelium-independent mechanisms involving hydrogen peroxide (H_2O_2) production and subsequent activation of guanylyl cyclase (sGC) (Gao et al., 2007).

In addition to the vasodilator effects, there is also considerable evidence of contractile function mediated by PVAT. Soltis and Cassis reported the critical role of adipocyte-derived Ang II in PVAT-mediated potentiation of electrical stimulation-induced contraction in rat mesenteric arteries (Soltis and Cassis, 1991). This effect was subsequently shown *in vivo* systemically in rat mesenteric PVAT (Lu et al., 2010). Gao et al. also reported that PVAT enhances the contractile response of mesenteric arteries to perivascular nerve stimulation through superoxide anion (O_2^-) production (Gao et al., 2006). The study of Payne documented that PVAT impairs coronary endothelial function in response to

bradykinin both *in vitro* and *in vivo*, implicating local adipose tissue in the initiation and pathogenesis of coronary vascular disease (Payne et al., 2008). In particular, the authors documented that adipose tissue-derived factors diminish endothelial NO production through the direct inhibition of the enzyme NOS. Following these findings, the authors demonstrated that periadventitial adipose tissue-derived factors impair coronary endothelial NO production via a PKC-β-dependent, site-specific phosphorylation of endothelial NOS (eNOS) at Thr^{495} (Payne et al., 2009). Some adipose tissue-derived factors, such as leptin (Knudson et al., 2005), resistin (Dick et al., 2006), and TNF-α (Picchi et al., 2006), secreted under conditions of inflammation, can also attenuate vasodilatation, and these factors are produced by PVAT.

In the last years, several studies identified additional components involved in the contractile effects of PVAT, which have been reported especially in the context of obesity and CVD. One example of this is the study of Meyer's group, which demonstrated that PVAT controls arterial smooth muscle tone by releasing an "adipocyte-derived contracting factor" (ADCF) formed by cyclooxygenase (COX), which mediates the contractile effects of PVAT in obesity (Meyer et al., 2013). Another powerful example is the work of Watts et al. illuminating a potential role for the adipokine chemerin as an endogenous mediator that is responsible for vasoconstriction in obesity (Watts et al., 2013). In line with these observations, our group demonstrated that incubation of isolated vessels with chemerin for 24 h increases arterial sensitivity to endothelin-1 (Lobato et al., 2012). Thus, it is clear that PVAT is a complex, active organ with several functions beyond mechanical protection for the underlying vasculature and the current literature provides substantial evidence that this tissue produces many putative vasoactive factors that may influence vascular function and obesity-related vascular injury. However, most of these characterization studies have been carried out on vessel rings isolated from animal models, in the presence or absence of the PVAT layer. This poses an important and unresolved question regarding how much of these results can be translated *in vivo*, especially concerning human physiology. A thoughtful consideration of the implications of manipulating PVAT function to treat chronic vascular diseases is therefore warranted.

PERIVASCULAR ADIPOSE TISSUE DYSFUNCTION AS A MAJOR CONTRIBUTING FACTOR TO OBESITY-ASSOCIATED VASCULAR DYSFUNCTION

As the understanding of the molecular mechanisms that underlie the connections between PVAT and vascular function progress, the ultimate goal is to establish the integrated role of this vascular component for obesity-related vascular dysfunction. Like observed with the total adipose tissue, PVAT mass is increased throughout the vasculature in both animal models and humans with obesity (Greenstein et al., 2009; Marchesi et al., 2009; Ketonen et al., 2010; Lehman et al., 2010). Considering that the anti-contractile influence of PVAT is directly dependent on its volume (Verlohren et al., 2004; Gao et al., 2006), it would be discernible that such an increase would be associated with enhancement of PVAT anti-contractile effects. However, available support for our understanding of the connection between PVAT and vascular dysfunction in obesity comes from the findings that obesity is associated with structural and functional changes in PVAT, leading to an imbalance in favor of vasoconstrictor and pro-inflammatory substances, as well as changes in the signaling pathways in the vessel and that this condition interferes with vascular function (**Figure 2**). Numerous studies have since validated this postulate (reviewed in Xia and Li, 2017). In line with this observation, Gao et al. (2005) demonstrated that increased adiposity causes an alteration in the modulatory function of PVAT on vascular relaxation response. New Zealand Obese (NZO) mice, which present most symptoms of the metabolic syndrome and a greater amount of PVAT, also show a reduction in the anti-contractile effect of PVAT (Fesus et al., 2007). Higher periaortic fat mass in rats treated for 6 months with high fat diet (HFD) lead to reduced endothelium-dependent relaxation due to downregulation of AMP-activated protein kinase (AMPK) and eNOS in the aorta with a concurrent upregulation of the mTOR ripamycin target, which negatively regulates the AMPK-eNOS pathway (Ma et al., 2010). Another important milestone toward our basic understanding of the relationship between PVAT dysfunction and obesity-associated vascular dysfunction was the demonstration of changes in the proteomic profile of 186 proteins in PVAT of coronary arteries, which correlate with increased contractile effect and the activation of calcium (Ca^{2+})-dependent signaling pathways in VSMCs from Ossabaw pigs (Owen et al., 2013).

These considerations aside, the diverse aspects of PVAT influence on vascular dysfunction in obesity could be also framed by examining its high relationship with oxidative stress. ROS, such as O_2^- and H_2O_2, play important roles in the modulation of vascular function by the PVAT. H_2O_2 is a vasoactive substance that induces both contractile and relaxing responses by different mechanisms depending on its concentration, the type and contraction state of the vessel, and the animal species. H_2O_2-induced relaxation may be endothelium dependent as a result of increased NO release secondary to K^+ channel activation. In addition, H_2O_2 induces endothelium-independent relaxation through the direct opening of K^+ channels in VSMC, by the oxidation of its cysteine residues, as well as by the direct activation of the sGC enzyme (Ardanaz and Pagano, 2006). The contractile effect mediated by H_2O_2 occurs due to the direct activation of the enzyme COX and an increase of intracellular Ca^{2+}. Evidence indicates that ROS accumulation activates contraction pathways related to MAPKs, with increased ERK 1/2 phosphorylation (Peters et al., 2000). In addition, H_2O_2 activates the Rho kinase pathway, favoring vascular contraction (Ardanaz and Pagano, 2006). In fact, the Rho kinase pathway is important not only in the contraction of VSMC, but also in increased proliferation and cell migration, which has attracted much attention in relation to its role in the pathogenesis of CVDs (Loirand et al., 2006). Considering that O_2^- induces vascular contraction while H_2O_2 has dual effects, the final result of the

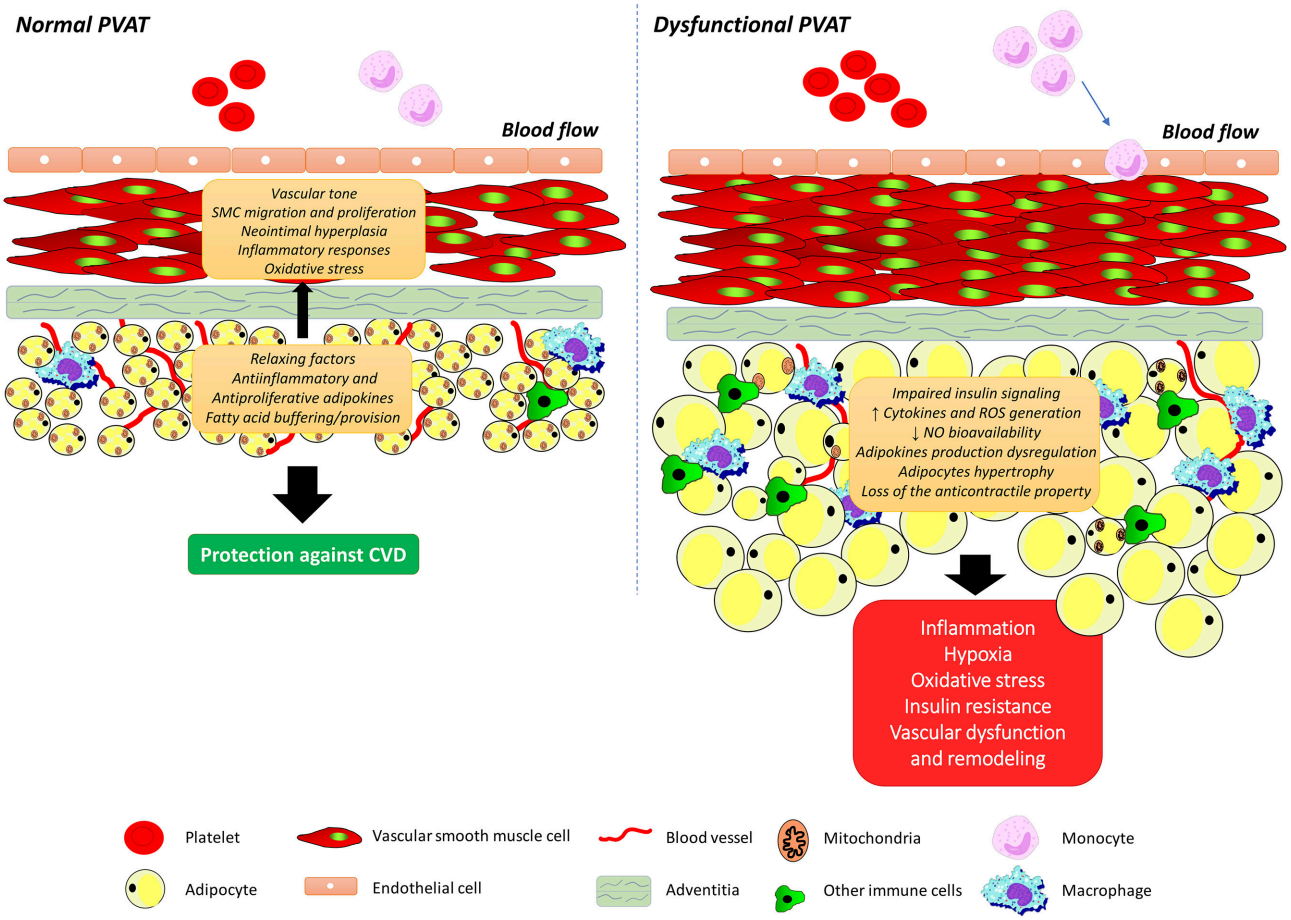

FIGURE 2 | Perivascular adipose tissue dysfunction and obesity-associated vascular dysfunction**.** Perivascular adipose tissue (PVAT) secretes a wide variety of biologically active molecules, including the adipokines, which modulate vascular tone, smooth muscle cells migration and proliferation, neointimal hyperplasia, inflammatory responses, and oxidative stress. Obesity is associated with structural and functional changes in PVAT, leading to an imbalance in favor of vasoconstrictor and pro-inflammatory substances, adipocytes hypertrophy as well as changes in insulin signaling pathways. SMC, smooth muscle cell; ROS, reactive oxygen species; NO, nitric oxide.

action of these ROS will depend on the relative balance between the production and the release of these factors by the PVAT. Ketonen et al. demonstrated in C57BL/6J mice fed a HFD that the reduction in endothelium-dependent relaxation occurs due to oxidative stress in PVAT, characterized by an increase in O_2^- and H_2O_2 production (Ketonen et al., 2010).

The NAD(P)H oxidase, which is the major source of O_2^- in the vasculature, is expressed in PVAT of rat mesenteric arteries and contributes to increased contractile response to perivascular nerve stimulation (Gao et al., 2006). Indeed, the expression of p67phox subunit of the NAD(P)H oxidase complex is increased in periaortic adipose tissue from short-term fed HFD obese mice (60% cal from fat) and this is accompanied by enhancement of both O_2^- and H_2O_2 levels (Ketonen et al., 2010). Increased NAD(P)H oxidase activity and O_2^- production associated with decreased expression of total SOD activity and extracellular superoxide dismutase (ecSOD) were described in the PVAT of these animals. The changes were accompanied by a reduction in eNOS expression and NO production in the PVAT (Gil-Ortega et al., 2014). Similarly, in NZO mice, increased O_2^- formation and reduced SOD expression in PVAT contribute to vascular dysfunction by reducing the anti-contractile effect of this tissue (Marchesi et al., 2009). Gil-Ortega et al. reported that long-term HFD induces substantial reduction in ec-SOD expression and total SOD activity, an increase of NOX activity and O_2^- release from the mesenteric PVAT, suggesting that the imbalance between antioxidant and pro-oxidant mechanisms in PVAT might contribute to vascular oxidative stress, thus aggravating endothelial dysfunction (Gil-Ortega et al., 2014). Marchesi et al. have also shown that the loss of PVAT anti-contractile properties in NZO mice might be associated with increase in both O_2^- and NAD(P)H oxidase activity (Marchesi et al., 2009). Uncoupling of eNOS in PVAT, which contributes not only to increase ROS formation but also to decrease NO bioavailability, was also recently described as a novel mechanism underlying the vascular dysfunction in diet-induced obesity (Xia et al., 2016).

The mitochondrial electron transport chain (mETC), a significant source of ROS, has also been pointed as an integral

component implicated in the physiological regulation of vascular function by PVAT. We recently showed that O_2^- production from the mETC is increased in PVAT during norepinephrine (NE)-induced aortic muscle contraction. O_2^- is subsequently dismutated to H_2O_2 by manganese SOD (Mn-SOD), which, in turn, modulates VSMC contraction (Costa et al., 2016). Following these findings, we next provided unequivocal evidence linking mitochondria to PVAT-associated oxidative stress and the subsequent loss of the PVAT anti-contractile effects observed in experimental obesity (da Costa et al., 2017). Under these conditions, the increase in PVAT-mediated ROS generation becomes an important sign of increased vascular contraction. As PVAT has a similar phenotype to BAT, including the expression of UCP-1, which is necessary for non-shivering thermogenesis, as discussed above, and considering that local energy metabolism induced by changes in temperature affects vascular function and atherogenesis (Brown et al., 2014), it can be proposed that increased energy production in PVAT under obesity condition also affects vessel biology favoring the development of CVD.

Structural and functional modifications of PVAT in obesity can also induce vascular remodeling. Periaortic adipocytes significantly increase the growth rate of aortic smooth muscle cells from aged and obese Wistar Kyoto rats supplemented with HFD. This effect is abolished in the presence of proteinase K, but is maintained in the presence of filtered proteins with a molecular mass less than 100 kDa, indicating that PVAT releases soluble proteins that stimulate growth of VSMCs, which can further aggravate aging- and obesity-associated vascular diseases (Barandier et al., 2005). Finally, the paracrine actions of factors produced and released by PVAT can also change vascular insulin sensitivity (Meijer et al., 2013). Although the prospective association between PVAT dysfunction and diabetes has not been demonstrated so far, this possibility has been previously postulated by Yudkin et al. and remarkably illustrated by several subsequent studies (Yudkin et al., 2005). Meijer's group showed that local depots of PVAT, which surround resistance arteries in the muscle microcirculation, controls vascular responses to insulin through adiponectin secretion and subsequent activation of AMPK signaling (Meijer et al., 2013). The expression of adiponectin is significantly lower in the epicardial adipose tissue isolated from patients with CAD (Iacobellis et al., 2005). In humans, PVAT accumulation around the brachial artery was negatively correlated with insulin sensitivity and the post-ischaemic increase in blood flow. The association was independent of the presence of other cardiovascular risk factors, including age, sex, liver fat, BMI, and visceral adipose tissue (Rittig et al., 2008). Additionally, PVAT from obese mice inhibits insulin-induced vasodilatation, which can be restored by inhibition of the inflammatory kinase Jun NH (2)-terminal kinase (JNK) (Meijer et al., 2013). JNK may directly induce insulin resistance by a mechanism that involves phosphorylation of the insulin receptor substrate (IRS) 1, blocking the transduction signal produced by the insulin receptor (Sabio et al., 2008). Studies in humans and animal models have demonstrated an important upstream role of this protein in integrating inflammatory and metabolic function that were recently reviewed elsewhere (Hotamisligil, 2017).

These findings, in addition to the observations that local accumulation of adipose tissue is consistently related to decreased flow-mediated vasodilation (Albu et al., 2005), fasting insulin levels and insulin resistance in humans (Rittig et al., 2008), support the involvement PVAT-derived factors as paracrine, rather than endocrine mediators of both microvascular dysfunction and insulin resistance in obesity. There is also tremendous redundancy in these pathways that support the view that the association between PVAT and cardiometabolic risk factors might not simply be the consequence of overall adiposity, but potentially constitutes an additional risk factor. Considering that hyperglycemia and hyperinsulinemia can also directly impair vascular function and consequently glucose disposal, it is also possible to suggest a vicious cycle of PVAT dysfunction that contributes to and is exacerbated by the impairment in insulin homeostasis.

INFLAMMATION IN PERIVASCULAR ADIPOSE TISSUE: THE LINK BETWEEN OBESITY AND CARDIOVASCULAR DISEASE?

In the last decades obesity has been associated with a moderate degree of inflammation in adipose tissue, a condition that results from chronic activation of the innate immune system. This type of inflammation, called metaflammation or metabolic inflammation is free of pathogens and orchestrated by metabolic cells in response to excess nutrients and energy (Hotamisligil, 2017). Initial support for this understanding came from the following observations: macrophages-derived TNF-α induces insulin resistance in adipocytes (Pekala et al., 1983); adipose tissue from obese individuals displays increased expression of inflammatory mediators (Hotamisligil et al., 1993; Uysal et al., 1997); and inflammation promotes disturbances in glucose metabolism. It is relevant to emphasize here the first demonstrations that macrophage infiltration occurs into the adipose tissue in obesity (Weisberg et al., 2003; Xu et al., 2003). These findings were the basis for elucidating the involvement of adipose tissue macrophages as direct modulators of metabolism, and led to the observations that the increased free fatty acids exposure in obesity promotes the polarization of macrophages resident in the adipose tissue toward a pro-inflammatory (M1-polarized) phenotype which can activate inflammatory pathways and impair insulin signaling (Hevener et al., 2007; Lumeng et al., 2007; Nguyen et al., 2007). The molecular mechanisms underlying these events include epigenomic alterations that determine macrophage sensitivity to metabolically driven inflammatory (metaflammatory) signals (Fan et al., 2016), and additional macrophage-secreted products, including the potent and pleiotropic immune mediator TNF-α, which attenuates insulin signaling in adipocytes (Li et al., 2016). Many other immune cells including dendritic cells, mast cells, eosinophils, and lymphoid cells also contribute to metabolic tissue homeostasis and to the control of glucose metabolism. Regarding the initiation of metaflammation, an emerging concept is that adipocyte hypertrophy causes local

hypoxia, which, in turn, causes infiltration of macrophages and other immune cells ($CD4^+$ and $CD8^+$ T cells, natural killer T cells, and mast cells) in visceral adipose tissue (Roemeling-van Rhijn et al., 2013). This increase in cells of the immune system along with the proinflammatory cytokines in adipocytes may negatively regulate PPARγ activity, which is essential for both adipogenesis and maintenance of the tissue gene expression (Guri et al., 2008).

Intermittent inflammatory processes have also been observed in PVAT. These include increased migration of immune cells, altered production of pro- and anti-inflammatory cytokines, adipokines, and lipid mediators, as well as signaling through a plethora of immune receptors and intracellular signaling molecules. Importantly, this entire cascade and mediators have now provided highly promising evidence that PVAT inflammation plays a key role at various stages of CVD. One powerful example of this is the recent work illuminating a role for perivascular inflammation as an alteration that precedes atherosclerotic plaque formation and even the development of endothelial dysfunction and oxidative stress in $ApoE^{-/-}$ mice (Skiba et al., 2017). Specifically, the authors found increased leukocyte infiltration in the perivascular tissue when compared to the vessel wall. Furthermore, it was demonstrated that PVAT or adventitial inflammation and infiltration with macrophages and T cells precede not only significant atherosclerotic plaque development, but also the impairment of endothelium-dependent NO bioavailability. In support of this finding, it was previously shown that major risk factors for atherosclerosis, including hypertension, hyperlipidemia or ty 2 diabetes promote perivascular inflammation before and during development of atherosclerosis (Galkina et al., 2006; Galkina and Ley, 2009; Sagan et al., 2012; Guzik et al., 2013).

Molecular mechanisms linking PVAT inflammation in obesity to CVD indicate several key components. These may include chemotactic migration of PVAT immune cells into adventitia, with release of cytokines, which can alter vascular function (Mikolajczyk et al., 2016). In this regard, it was previously demonstrated that human PVAT exhibits a strong chemotactic activity on monocytes, granulocytes, and T lymphocytes that is mainly mediated by the secretion of IL-8 and MCP-1, which are known proatherogenic chemokines and their production is increased in obesity. These mediators are likely to contribute to the infiltration of leukocytes at the interface between PVAT and adventitia of atherosclerotic aortas (Henrichot et al., 2005). Visceral adipose tissue accumulation also promotes an increase in the secretion of angiopoietin-like protein 2 (Angptl2), a pro-inflammatory factor derived from adipocytes and considered a key mediator of chronic adipose tissue inflammation and obesity-related systemic insulin resistance (Tabata et al., 2009). In fact, Angptl2 secreted by PVAT accelerates neointimal formation after endovascular injury in mice by increasing inflammation-related gene expression and by accelerating extracellular matrix degradation (Tian et al., 2013). In line with these experimental findings, the authors provided relevant clinical data that strongly suggest that PVAT-secreted Angptl2 plays a significant role in accelerating vascular inflammation by cooperating with pro-inflammatory TNF-α or counteracting the anti-inflammatory activity of adiponectin, potentially leading to development of atherosclerosis in humans (Tian et al., 2013).

PVAT inflammation may also be associated with altered release of adipokines and other adipocyte-derived relaxing factors (Antonopoulos et al., 2015; Woodward et al., 2017). Initial support for this understanding came from the findings that perivascular adipocytes from human and mice without atherosclerotic disease exhibit a heightened proinflammatory state and reduced adipocytic differentiation under basal conditions as compared with adipocytes derived from subcutaneous and visceral adipose depots, and that high-fat feeding causes further reductions in adipocyte-associated gene expression while upregulates proinflammatory gene expression (Chatterjee et al., 2009). Specifically, secretion of the anti-inflammatory adipokine adiponectin is markedly reduced, whereas that of proinflammatory cytokines IL-6, IL-8, and MCP-1, is markedly increased in perivascular adipocytes. These changes have also direct effects on the PVAT vasoactive properties, as evidenced in animal and human small-artery studies, where hypoxia and inflammation were shown to attenuate the local vasoactive properties of PVAT by oxidative stress (Greenstein et al., 2009).

In addition to the previously-mentioned adipokines, chemerin, a secreted protein originally revealed as a chemoattractant molecule for immature dendritic cells and macrophages (Wittamer et al., 2003) is now considered a novel adipokine that regulates adipogenesis, adipocyte metabolism (Bozaoglu et al., 2007; Goralski et al., 2007) and inflammation (Parolini et al., 2007; Cash et al., 2010). Chemerin acts through CMKLR1 (chemokine-like receptor 1) or ChemR23 (chemerin receptor 23), which is expressed in macrophages, dendritic cells, adipocytes and vascular cells (Zabel et al., 2005, 2006; Parolini et al., 2007). Chemerin is considered a biomarker for adiposity since its plasma levels strongly associate with BMI and is linked to obesity and metabolic syndrome, a cluster of metabolic disorders that increase the risk for diabetes and CVD (Bozaoglu et al., 2009; Li et al., 2014). Furthermore, serum chemerin levels are significantly elevated in morbidly obese patients and reduced with the weight loss after bariatric surgery. The strong decrease of chemerin after surgery was associated with an improvement in insulin sensitivity and blood glucose, which further support the key role of this adipokine in mediating metabolic alterations in obesity (Ress et al., 2010; Sell et al., 2010). Animal studies reported the parallel findings that knockout mice for the primary receptor for chemerin, ChemR23, exhibit reduced food consumption, weight gain, and adiposity (Ernst et al., 2012). Consistent with this phenotype, ChemR23 knockout mice also displayed lower fasting blood glucose and serum insulin levels.

Recent observations have also shown that chemerin is highly expressed in PVAT. Spiroglou et al. first detected chemerin expression in epicardial and periaortic adipose tissue and demonstrated a positive correlation of this adipokine with both aortic and coronary atherosclerosis (Spiroglou et al., 2010). Most recently, Watts and her co-workers reported that chemerin produced by periaortic PVAT stimulates vascular contraction through the receptor typically attributed to function only in immune cells. Moreover, arteries from

obese or hypertensive mice or obese humans with dysfunctional endothelium demonstrated amplified contractions in response to chemerin (Watts et al., 2013). Although there is no empirical evidence linking specific chemerin signaling pathways with the PVAT inflammation, a bulk of animal and human studies exploring the immune functions of chemerin make this a very plausible possibility. CMKLR1 is expressed in several immune cell types known to accumulate in obese adipose tissue (Wittamer et al., 2003; Parolini et al., 2007; Cash et al., 2010). Sell and collaborators demonstrated that chemerin activates the NF-κB pathway and impairs glucose uptake in skeletal muscle cells (Sell et al., 2010). In human endothelial cells, it was shown a significant upregulation of chemerin receptor by pro-inflammatory cytokines such as TNF-α, IL-1β, and IL-6 (Kaur et al., 2010). Accordingly, circulating levels of chemerin are elevated in diseases associated with chronic inflammation, including obesity and the metabolic syndrome (Wittamer et al., 2003; Bozaoglu et al., 2009; Li et al., 2014). Our recent studies also point to a role of chemerin in regulating inflammatory processes. Chemerin was shown to decrease NO-dependent cGMP signaling, thereby reducing vascular relaxation in rat aorta, an effect related to increased generation of O_2^-, an important mediator of inflammation (Neves et al., 2014). In line with these findings, we demonstrated that chemerin, through Nox activation and redox-sensitive MAPKs signaling, exerts proapoptotic, proinflammatory, and proliferative effects in human vascular cells (Neves et al., 2015).

Taken together, these findings not only provide multiple layers of potential mediators for the inflammatory component of PVAT in obesity but also clearly demonstrate that bidirectional interactions between that the systemic metabolic inflammation and local immune components are critical considerations in determining the physiological and pathological vascular outcomes associated with obesity. The proximity of PVAT as a rich source of proinflammatory cytokines and other mediators together with the associated alterations in this tissue support the concept that specific changes of local adipose tissue depots contribute to disease processes in the neighboring vessel wall.

CLINICAL MEASURE OF PERIVASCULAR ADIPOSE TISSUE IN OBESITY-ASSOCIATED CARDIOVASCULAR RISK ASSESSMENT: FINDING THE POINT

Some of the initial thoughts and considerations of the reciprocal relationship between PVAT and risk factors for CVD have been provided by clinical findings showing an association between both perivascular and epicardial adipose tissue with the main anthropometric and clinical parameters of the metabolic syndrome (Iacobellis et al., 2003b). In fact, a very good correlation is observed between epicardial adipose tissue, assessed by echocardiography, and waist circumference, diastolic blood pressure, fasting plasma insulin, LDL cholesterol, and plasma adiponectin (Iacobellis et al., 2003b). Importantly, the association of insulin sensitivity and low adiponectin levels with the epicardial fat thickness is independent of BMI, suggesting that PVAT assessment might provide a more sensitive and more specific measure of the true visceral fat content (Iacobellis et al., 2003a). In support of these findings, a recent meta-analysis of published reports concluded that echocardiographic epicardial adipose thickness is significantly higher in patients with metabolic syndrome than in those without it (Pierdomenico et al., 2013).

Echocardiographic evaluation of epicardial adipose tissue thickness is considered a very reliable method to measure visceral adiposity, as first proposed and validated by Iacobellis et al. (2005). It is also relatively cheap and easy to perform as a screening test for assessment of patients suspected to be at risk for cardiovascular or metabolic outcomes. However, the technic provides only measurements of the regional thickness of epicardial adipose tissue and presents the risk to confuse pericardial fluid with adipose tissue since the fluid also shows up as relatively echo-free on an echocardiograph (Singh et al., 2007). The advances in imaging technology have enabled a more direct quantitative assessment of the local fat depots and have also been the basis for investigations into the possibility that PVAT acts as direct modulator of metabolism and cardiovascular function. From this perspective, clinical findings showed that volumetric quantification of epicardial and peri-coronary adipose tissue thickness by computed tomography, which provides a more accurate assessment due to its higher spatial resolution, is also positively related with parameters of obesity, such as BMI, waist circumference and the abdominal visceral adipose tissue mass (Gorter et al., 2008). In line with this, PVAT thickness, measured by computed tomography in the areas of right coronary artery, left anterior descending artery and left circumflex coronary artery is positively associated with waist circumference, waist-to-hip ratio, BMI, blood glucose, triglycerides, and systolic blood pressure. Epicardial adipose tissue is also linked to coronary calcification, a known marker of coronary atherosclerosis (de Vos et al., 2008).

In agreement with the above observations, abdominal periaortic adipose tissue and thoracic periaortic adipose tissue volume, measured by computed tomography, are consistently correlated with visceral abdominal fat, subcutaneous abdominal fat, waist circumference, and BMI in a random subset of participants from the Framingham Heart Study (Schlett et al., 2009). Thanassoulis et al. extended these findings by showing that both thoracic and abdominal periaortic adipose tissue volumes, measured using the same approach, are associated with higher aortic dimensions even after adjustment for other vascular and metabolic risk factors including global measures of obesity such as BMI (Thanassoulis et al., 2012). By contrast, the study of Rosito et al. found no significant associations between pericardial fat and CVD risk factors compared with visceral fat when both were considered in the same model. Nevertheless, the authors evidenced strong correlations between pericardial fat volume and metabolic risk factors even after adjusting for many potential confounders, including age, smoking, alcohol use, and physical activity. Furthermore, pericardial fat was found to be associated with coronary artery Ca^{2+} and abdominal aortic Ca^{2+} even after

metabolic risk factors and visceral adipose tissue were accounted for, which is consistent with the postulation that pericardial fat may in fact exert a harmful perivascular effect on the coronary arteries (Rosito et al., 2008).

SUMMARY

There is tremendous wealth in the mechanisms that support the understanding of the relationship between excess adiposity and cardiovascular risk. The strongest evidence comes from the observations of basic science and translational studies regarding important physiological process that occur in adipose tissue and deleterious effects of relevant importance on vascular complications. It is interesting to consider the role that adipokines play among the mechanisms whereby adipocytes influence vascular function. However, there is considerably more work to be performed in both basic science and clinical areas to understand and reduce the enhanced CVD risk that is evident in the obese state. Clearly, these intriguing observations are not sufficient to answer the question whether increased PVAT mass represents a surrogate marker of cardiovascular risk or an independent pathogenic variable. However, outcome studies need to establish whether PVAT depots have prognostic significance and may therefore provide additional evidence for a causal relationship. Although the reduction of whole-body fat would be ideal among individuals who have obesity, a thoughtful consideration of the additional benefits of targeting fat depots at specific locations in individuals at greater cardiometabolic risk represents an alternative approach.

Further dissection of the vascular signaling pathways altered by PVAT-derived factors will likely reveal functional strategies for suppressing the negative effects of abnormal adipose tissue excess on CVD complications without altering the beneficial effects of normal fat depots. The challenges remaining in this field can be identified in two different areas. How does structural and functional changes of PVAT start in obesity and at what point does it become detrimental? What are the appropriate model systems and paths to elucidate the unknown mechanisms to prevent or treat human CVD? Regarding the contribution of new characterized adipokines, there are also several interesting and emerging concepts. Given these challenges, and the need for therapeutic approaches that do not permanently interfere with entire physiological effects of the PVAT, conveying the experimental insights into successful clinical interventions will require collaborative and diverse cross studies, new experimental approaches and integration of genetic variations with other environmental modifiers to establish links with complex cardiovascular phenotypes and facilitate successful translation to human disease.

AUTHOR CONTRIBUTIONS

RC, KN, RT, and NL equally contributed to the conception of paper, drafting the manuscript, and approved its final version.

REFERENCES

Aghamohammadzadeh, R., Withers, S., Lynch, F., Greenstein, A., Malik, R., and Heagerty, A. (2012). Perivascular adipose tissue from human systemic and coronary vessels: the emergence of a new pharmacotherapeutic target. *Br. J. Pharmacol.* 165, 670–682. doi: 10.1111/j.1476-5381.2011.01479.x

Albu, J. B., Kovera, A. J., Allen, L., Wainwright, M., Berk, E., Raja-Khan, N., et al. (2005). Independent association of insulin resistance with larger amounts of intermuscular adipose tissue and a greater acute insulin response to glucose in African American than in white nondiabetic women. *Am. J. Clin. Nutr.* 82, 1210–1217. doi: 10.1093/ajcn/82.6.1210

Antonopoulos, A. S., Margaritis, M., Coutinho, P., Shirodaria, C., Psarros, C., Herdman, L., et al. (2015). Adiponectin as a link between type 2 diabetes and vascular NADPH oxidase activity in the human arterial wall: the regulatory role of perivascular adipose tissue. *Diabetes* 64, 2207–2219. doi: 10.2337/db14-1011

Apovian, C. M., Bigornia, S., Mott, M., Meyers, M. R., Ulloor, J., Gagua, M., et al. (2008). Adipose macrophage infiltration is associated with insulin resistance and vascular endothelial dysfunction in obese subjects. *Arterioscler. Thromb. Vasc. Biol.* 28, 1654–1659. doi: 10.1161/ATVBAHA.108.170316

Ardanaz, N., and Pagano, P. J. (2006). Hydrogen peroxide as a paracrine vascular mediator: regulation and signaling leading to dysfunction. *Exp. Biol. Med.* 231, 237–251. doi: 10.1177/153537020623100302

Arnlöv, J., Ingelsson, E., Sundström, J., and Lind, L. (2010). Impact of body mass index and the metabolic syndrome on the risk of cardiovascular disease and death in middle-aged men. *Circulation* 121, 230–236. doi: 10.1161/CIRCULATIONAHA.109.887521

Bagi, Z., Feher, A., and Cassuto, J. (2012). Microvascular responsiveness in obesity: implications for therapeutic intervention. *Br. J. Pharmacol.* 165, 544–560. doi: 10.1111/j.1476-5381.2011.01606.x

Barandier, C., Montani, J. P., and Yang, Z. (2005). Mature adipocytes and perivascular adipose tissue stimulate vascular smooth muscle cell proliferation: effects of aging and obesity. *Am. J. Physiol. Heart Circ. Physiol.* 289, H1807–H1813. doi: 10.1152/ajpheart.01259.2004

Barton, M., Baretella, O., and Meyer, M. R. (2012). Obesity and risk of vascular disease: importance of endothelium-dependent vasoconstriction. *Br. J. Pharmacol.* 165, 591–602. doi: 10.1111/j.1476-5381.2011.01472.x

Borrell, L. N., and Samuel, L. (2014). Body mass index categories and mortality risk in US adults: the effect of overweight and obesity on advancing death. *Am. J. Public Health* 104, 512–519. doi: 10.2105/AJPH.2013.301597

Bozaoglu, K., Bolton, K., McMillan, J., Zimmet, P., Jowett, J., Collier, G., et al. (2007). Chemerin is a novel adipokine associated with obesity and metabolic syndrome. *Endocrinology* 148, 4687–4694. doi: 10.1210/en.2007-0175

Bozaoglu, K., Segal, D., Shields, K. A., Cummings, N., Curran, J. E., Comuzzie, A. G., et al. (2009). Chemerin is associated with metabolic syndrome phenotypes in a Mexican-American population. *J. Clin. Endocrinol. Metab.* 94, 3085–3088. doi: 10.1210/jc.2008-1833

Brown, N. K., Zhou, Z., Zhang, J., Zeng, R., Wu, J., Eitzman, D., et al. (2014). Perivascular adipose tissue in vascular function and disease: a review of current research and animal models. *Arterioscler. Throm. Vasc. Biol.* 34, 1621–1630. doi: 10.1161/ATVBAHA.114.303029

Cannon, B., and Nedergaard, J. (2004). Brown adipose tissue: function and physiological significance. *Physiol. Rev.* 84, 277–359. doi: 10.1152/physrev.00015.2003

Cash, J. L., Christian, A. R., and Greaves, D. R. (2010). Chemerin peptides promote phagocytosis in a ChemR23- and Syk-dependent manner. *J. Immunol.* 184, 5315–5324. doi: 10.4049/jimmunol.0903378

Chang, L., Milton, H., Eitzman, D. T., and Chen, Y. E. (2013). Paradoxical roles of perivascular adipose tissue in atherosclerosis and hypertension. *Circ. J.* 77, 11–18. doi: 10.1253/circj.CJ-12-1393

Chang, L., Villacorta, L., Li, R., Hamblin, M., Xu, W., Dou, C., et al. (2012). Loss of perivascular adipose tissue on peroxisome proliferator-activated receptor-gamma deletion in smooth muscle cells impairs intravascular thermoregulation and enhances atherosclerosis. *Circulation* 126, 1067–1078. doi: 10.1161/CIRCULATIONAHA.112.104489

Chatterjee, T. K., Stoll, L. L., Denning, G. M., Harrelson, A., Blomkalns, A., L., Idelman, G., et al. (2009). Proinflammatory phenotype of perivascular adipocytes: influence of high-fat feeding. *Circ. Res.* 104, 541–549. doi: 10.1161/CIRCRESAHA.108.182998

Chavey, C., Lazennec, G., Lagarrigue, S., Clapé, C., Iankova, I., Teyssier, J., et al. (2009). CXC ligand 5 is an adipose-tissue derived factor that links obesity to insulin resistance. *Cell Metab.* 9, 339–349. doi: 10.1016/j.cmet.2009.03.002

Cheng, K. H., Chu, C. S., Lee, K., T., Lin, T. H., Hsieh, C. C., Chiu, C. C., et al. (2008). Adipocytokines and proinflammatory mediators from abdominal and epicardial adipose tissue in patients with coronary artery disease. *Int. J. Obes.* 32, 268–274. doi: 10.1038/sj.ijo.0803726

Cinti, S. (2001). The adipose organ: morphological perspectives of adipose tissues. *Proc. Nutr. Soc.* 60, 319–328. doi: 10.1079/PNS200192

Clément, K., Basdevant, A., and Dutour, A. (2009). Weight of pericardial fat on coronaropathy. *Arterioscler. Thromb. Vasc. Biol.* 29, 615–616. doi: 10.1161/ATVBAHA.108.182907

Coelho, M., Oliveira, T., and Fernandes, R. (2013). Biochemistry of adipose tissue: an endocrine organ. *Arch. Med. Sci.* 9, 191–200. doi: 10.5114/aoms.2013.33181

Company, J. M., Booth, F. W., Laughlin, M. H., Arce-Esquivel, A. A., Sacks, H., S., Bahouth, S., W., et al. (2010). Epicardial fat gene expression after aerobic exercise training in pigs with coronary atherosclerosis: relationship to visceral and subcutaneous fat. *J. Appl. Physiol.* 109, 1904–1912. doi: 10.1152/japplphysiol.00621.2010

Costa, R. M., Filgueira, F. P., Tostes, R. C., Carvalho, M. H., Akamine, E. H., and Lobato, N. S. (2016). H_2O_2 generated from mitochondrial electron transport chain in thoracic perivascular adipose tissue is crucial for modulation of vascular smooth muscle contraction. *Vascul. Pharmacol.* 84, 28–37. doi: 10.1016/j.vph.2016.05.008

Cypess, A. M., Lehman, S., Williams, G., Tal, I., Rodman, D., Goldfine, A. B., et al. (2009). Identification and importance of brown adipose tissue in adult humans. *N. Engl. J. Med.* 360, 1509–1517. doi: 10.1056/NEJMoa0810780

Czernichow, S., Kengne, A. P., Huxley, R. R., Batty, G. D., de Galan, B., Grobbee, D., et al. (2011). Comparison of waist-to-hip ratio and other obesity indices as predictors of cardiovascular disease risk in people with type-2 diabetes: a prospective cohort study from advance. *Eur. J. Cardiovasc. Prev. Rehabil.* 18, 312–319. doi: 10.1097/HJR.0b013e32833c1aa3

da Costa, R. M., Fais, R. S., Dechandt, C. R. P., Louzada-Junior, P., Alberici, L. C., Lobato, N. S. et al. (2017). Increased mitochondrial ROS generation mediates the loss of the anti-contractile effects of perivascular adipose tissue in high-fat diet obese mice. *Br. J. Pharmacol.* 174, 3527–3541. doi: 10.1111/bph.13687

de Koning, L., Merchant, A. T., Pogue, J., and Anand, S. S. (2007). Waist circumference and waist-to-hip ratio as predictors of cardiovascular events: meta-regression analysis of prospective studies. *Eur. Heart J.* 28, 850–856. doi: 10.1093/eurheartj/ehm026

de Vos, A. M., Prokop, M., Roos, C. J., Meijs, M. F., van der Schouw, Y. T., Rutten, A., et al. (2008). Peri-coronary epicardial adipose tissue is related to cardiovascular risk factors and coronary artery calcification in post-menopausal women. *Eur. Heart J.* 29, 777–783. doi: 10.1093/eurheartj/ehm564

Dick, G. M., Katz, P. S., Farias, M. III., Morris, M., James, J., Knudson, J. D., et al. (2006). Resistin impairs endothelium-dependent dilation to bradykinin, but not acetylcholine, in the coronary circulation. *Am. J. Physiol. Heart Circ. Physiol.* 291, H2997–H3002. doi: 10.1152/ajpheart.01035.2005

Dubrovska, G., Verlohren, S., Luft, F. C., and Gollasch, M. (2004). Mechanisms of ADRF release from rat aortic adventitial adipose tissue. *Am. J. Physiol. Heart Circ. Physiol.* 286, H1107–H1113. doi: 10.1152/ajpheart.00656.2003

Dulloo, A. G., Jacquet, J., Solinas, G., Montani, J. P., and Schutz, Y. (2010). Body composition phenotypes in pathways to obesity and the metabolic syndrome. *Int. J. Obes.* 34(Suppl. 2), S4–S17. doi: 10.1038/ijo.2010.234

Eckel, R. H., and Krauss, R. M. (1998). American Heart Association call to action: obesity as a major risk factor for coronary heart disease. AHA nutrition committee. *Circulation* 97, 2099–2100. doi: 10.1161/01.CIR.97.21.2099

Ernst, M. C., Haidl, I. D., Zúñiga, L. A., Dranse, H. J., Rourke, J. L., Zabel, B. A., et al. (2012). Disruption of the chemokine-like receptor-1 (CMKLR1) gene is associated with reduced adiposity and glucose intolerance. *Endocrinology* 153, 672–682. doi: 10.1210/en.2011-1490

Fan, R., Toubal, A., Goñi, S., Drareni, K., Huang, Z., Alzaid, F., et al. (2016). Loss of the co-repressor GPS2 sensitizes macrophage activation upon metabolic stress induced by obesity and type 2 diabetes. *Nat. Med.* 22, 780–791. doi: 10.1038/nm.4114

Fésüs, G., Dubrovska, G., Gorzelniak, K., Kluge, R., Huang, Y., Luft, F. C., et al. (2007). Adiponectin is a novel humoral vasodilator. *Cardiovasc. Res.* 75, 719–727. doi: 10.1016/j.cardiores.2007.05.025

Finkelstein, E. A., Khavjou, O. A., Thompson, H., Trogdon, J. G., Pan, L., Sherry, B., et al. (2012). Obesity and severe obesity forecasts through 2030. *Am. J. Prev. Med.* 42, 563–570. doi: 10.1016/j.amepre.2011.10.026

Fitzgibbons, T. P., Kogan, S., Aouadi, M., Hendricks, G. M., Straubhaar, J., and Czech, M., P. (2011). Similarity of mouse perivascular and brown adipose tissues and their resistance to diet-induced inflammation. *Am. J. Physiol. Heart Circ. Physiol.* 301, H1425–1437. doi: 10.1152/ajpheart.00376.2011

Flegal, K. M., Kit, B. K., Orpana, H., and Graubard, B. I. (2013). Association of all-cause mortality with overweight and obesity using standard body mass index categories: a systematic review and meta-analysis. *JAMA* 309, 71–82. doi: 10.1001/jama.2012.113905

Frühbeck, G., Becerril, S., Sáinz, N., Garrastachu, P., and García-Velloso, M. J. (2009). BAT: a new target for human obesity? *Trends Pharmacol. Sci.* 30, 387–396. doi: 10.1016/j.tips.2009.05.003

Galkina, E., and Ley, K. (2009). Immune and inflammatory mechanisms of atherosclerosis (*). *Annu. Rev. Immunol.* 27, 165–197. doi: 10.1146/annurev.immunol.021908.132620

Galkina, E., Kadl, A., Sanders, J., Varughese, D., Sarembock, I. J., and Ley, K. (2006). Lymphocyte recruitment into the aortic wall before and during development of atherosclerosis is partially L-selectin dependent. *J. Exp. Med.* 203, 1273–1282. doi: 10.1084/jem.20052205

Gao, Y. J., Lu, C., Su, L. Y., Sharma, A. M., and Lee, R. M. (2007). Modulation of vascular function by perivascular adipose tissue: the role of endothelium and hydrogen peroxide. *Br. J. Pharmacol.* 151, 323–331. doi: 10.1038/sj.bjp.0707228

Gao, Y. J., Takemori, K., Su, L. Y., An, W. S., Lu, C., and Sharma, A. M. (2006). Perivascular adipose tissue promotes vasoconstriction: the role of superoxide anion. *Cardiovasc. Res.* 71, 363–373. doi: 10.1016/j.cardiores.2006.03.013

Gao, Y. J., Zeng, Z. H., Teoh, K., Sharma, A. M., Abouzahr, L., Cybulsky, I., et al. (2005). Perivascular adipose tissue modulates vascular function in the human internal thoracic artery. *J. Thorac. Cardiovasc. Surg.* 130, 1130–1136. doi: 10.1016/j.jtcvs.2005.05.028

Garg, A. (2004). Regional adiposity and insulin resistance. *J. Clin. Endocrinol. Metab.* 89, 4206–4210. doi: 10.1210/jc.2004-0631

Garrow, J. S., and Webster, J. (1985). Quetelet's index (W/H2) as a measure of fatness. *Int. J. Obes.* 9, 147–153.

Gil-Ortega, M., Condezo-Hoyos, L., García-Prieto, C. F., Arribas, S. M., González, M. C., Aranguez, I., et al. (2014). Imbalance between pro and anti-oxidant mechanisms in perivascular adipose tissue aggravates long-term high-fat diet-derived endothelial dysfunction. *PLoS ONE* 9:e95312. doi: 10.1371/journal.pone.0095312

Gollasch, M., and Dubrovska, G. (2004). Paracrine role for periadventitial adipose tissue in the regulation of arterial tone. *Trends Pharmacol. Sci.* 25, 647–653. doi: 10.1016/j.tips.2004.10.005

Gonzalez-Muniesa, P., Martinez-Gonzalez, M. A., Hu, F. B., Despres, J. P., Matsuzawa, Y., Loos, R. J. F., et al. (2017). Obesity. *Nat. Rev. Dis. Primers* 3, 17034. doi: 10.1038/nrdp.2017.34

Goralski, K. B., McCarthy, T. C., Hanniman, E. A., Zabel, B. A., Butcher, E. C., Parlee, S. D., et al. (2007). Chemerin, a novel adipokine that regulates adipogenesis and adipocyte metabolism. *J. Biol. Chem.* 282, 28175–28188. doi: 10.1074/jbc.M700793200

Gorter, P. M., van Lindert, A. S., de Vos, A. M., Meijs, M. F., van der Graaf, Y., Doevendans, P. A., et al. (2008). Quantification of epicardial and peri-coronary fat using cardiac computed tomography; reproducibility and relation with obesity and metabolic syndrome in patients suspected of coronary artery disease. *Atherosclerosis* 197, 896–903. doi: 10.1016/j.atherosclerosis.2007.08.016

Greenstein, A. S., Khavandi, K., Withers, S. B., Sonoyama, K., Clancy, O., Jeziorska, M., et al. (2009). Local inflammation and hypoxia abolish the protective anticontractile properties of perivascular fat in obese patients. *Circulation* 119, 1661–1670. doi: 10.1161/CIRCULATIONAHA.108.821181

Gupta, N., Goel, K., Shah, P., and Misra, A. (2012). Childhood obesity in developing countries: epidemiology, determinants, and prevention. *Endocr. Rev.* 33, 48–70. doi: 10.1210/er.2010-0028

Guri, A. J., Hontecillas, R., Ferrer, G., Casagran, O., Wankhade, U., Noble, A. M., et al. (2008). Loss of PPAR gamma in immune cells impairs the ability of abscisic acid to improve insulin sensitivity by suppressing monocyte chemoattractant protein-1 expression and macrophage infiltration into white adipose tissue. *J. Nutr. Biochem.* 19, 216–228. doi: 10.1016/j.jnutbio.2007.02.010

Guzik, B., Sagan, A., Ludew, D., Mrowiecki, W., Chwała, M., Bujak-Gizycka, B., et al. (2013). Mechanisms of oxidative stress in human aortic aneurysms–association with clinical risk factors for atherosclerosis and disease severity. *Int. J. Cardiol.* 168, 2389–2396. doi: 10.1016/j.ijcard.2013.01.278

Hamaguchi, K., Itabashi, A., Kuroe, Y., Nakano, M., Fujimoto, E., Kato, T., et al. (2012). Analysis of adipose tissues and stromal vascular cells in a murine arthritis model. *Metab. Clin. Exp.* 61, 1687–1695. doi: 10.1016/j.metabol.2012.05.018

Hausman, D. B., DiGirolamo, M., Bartness, T. J., Hausman, G., J., and Martin, R., J. (2001). The biology of white adipocyte proliferation. *Obes. Rev.* 2, 239–254. doi: 10.1046/j.1467-789X.2001.00042.x

Heinonen, S., Buzkova, J., Muniandy, M., Kaksonen, R., Ollikainen, M., Ismail, K., et al. (2015). Impaired mitochondrial biogenesis in adipose tissue in acquired obesity. *Diabetes* 64, 3135–3145. doi: 10.2337/db14-1937

Henegar, C., Tordjman, J., Achard, V., Lacasa, D., Cremer, I., Guerre-Millo, M., et al. (2008). Adipose tissue transcriptomic signature highlights the pathological relevance of extracellular matrix in human obesity. *Genome Biol.* 9:R14. doi: 10.1186/gb-2008-9-1-r14

Henrichot, E., Juge-Aubry, C. E., Pernin, A., Pache, J. C., Velebit, V., Dayer, J. M., et al. (2005). Production of chemokines by perivascular adipose tissue: a role in the pathogenesis of atherosclerosis? *Arterioscler. Thromb. Vasc. Biol.* 25, 2594–2599. doi: 10.1161/01.ATV.0000188508.40052.35

Hevener, A. L., Olefsky, J. M., Reichart, D., Nguyen, M. T., Bandyopadyhay, G., Leung, H. Y., et al. (2007). Macrophage PPAR gamma is required for normal skeletal muscle and hepatic insulin sensitivity and full antidiabetic effects of thiazolidinediones. *J. Clin. Invest.* 117, 1658–1669. doi: 10.1172/JCI31561

Hotamisligil, G. S. (2017). Inflammation, metaflammation and immunometabolic disorders. *Nature* 542, 177–185. doi: 10.1038/nature21363

Hotamisligil, G. S., Shargill, N. S., and Spiegelman, B. M. (1993). Adipose expression of tumor necrosis factor-alpha: direct role in obesity-linked insulin resistance. *Science* 259, 87–91. doi: 10.1126/science.7678183

Iacobellis, G., Assael, F., Ribaudo, M. C., Zappaterreno, A., Alessi, G., Di Mario, U., et al. (2003a). Epicardial fat from echocardiography: a new method for visceral adipose tissue prediction. *Obes. Res.* 11, 304–310. doi: 10.1038/oby.2003.45

Iacobellis, G., Pistilli, D., Gucciardo, M., Leonetti, F., Miraldi, F., Brancaccio, G., et al. (2005). Adiponectin expression in human epicardial adipose tissue *in vivo* is lower in patients with coronary artery disease. *Cytokine* 29, 251–255. doi: 10.1016/j.cyto.2004.11.002

Iacobellis, G., Ribaudo, M. C., Assael, F., Vecci, E., Tiberti, C., Zappaterreno, A., et al. (2003b). Echocardiographic epicardial adipose tissue is related to anthropometric and clinical parameters of metabolic syndrome: a new indicator of cardiovascular risk. *J. Clin. Endocrinol. Metab.* 88, 5163–5168. doi: 10.1210/jc.2003-030698

Iozzo, P. (2011). Myocardial, perivascular, and epicardial fat. *Diabetes Care* 34(Suppl. 2), S371–379. doi: 10.2337/dc11-s250

Jernås, M., Palming, J., Sjöholm, K., Jennische, E., Svensson, P. A., Gabrielsson, B. G., et al. (2006). Separation of human adipocytes by size: hypertrophic fat cells display distinct gene expression. *FASEB J.* 20, 1540–1542. doi: 10.1096/fj.05-5678fje

Jiang, C., Qu, A., Matsubara, T., Chanturiya, T., Jou, W., Gavrilova, O., et al. (2011). Disruption of hypoxia-inducible factor 1 in adipocytes improves insulin sensitivity and decreases adiposity in high-fat diet-fed mice. *Diabetes* 60, 2484–2495. doi: 10.2337/db11-0174

Kaur, J., Adya, R., Tan, B. K., Chen, J., and Randeva, H., S. (2010). Identification of chemerin receptor (ChemR23) in human endothelial cells: chemerin-induced endothelial angiogenesis. *Biochem. Biophys. Res. Commun.* 391, 1762–1768. doi: 10.1016/j.bbrc.2009.12.150

Kelly, T., Yang, W., Chen, C. S., Reynolds, K., and He, J. (2008). Global burden of obesity in 2005 and projections to 2030. *Int. J. Obes.* 32, 1431–1437. doi: 10.1038/ijo.2008.102

Kenchaiah, S., Evans, J. C., Levy, D., Wilson, P. W., Benjamin, E. J., Larson, M. G., et al. (2002). Obesity and the risk of heart failure. *N. Engl. J. Med.* 347, 305–313. doi: 10.1056/NEJMoa020245

Kershaw, E. E., and Flier, J. S. (2004). Adipose tissue as an endocrine organ. *J. Clin. Endocrinol. Metab.* 89, 2548–2556. doi: 10.1210/jc.2004-0395

Ketonen, J., Shi, J., Martonen, E., and Mervaala, E. (2010). Periadventitial adipose tissue promotes endothelial dysfunction via oxidative stress in diet-induced obese C57Bl/6 mice. *Circ. J.* 74, 1479–1487. doi: 10.1253/circj.CJ-09-0661

Kiefer, F. W., Vernochet, C., O'Brien, P., Spoerl, S., Brown, J. D., Nallamshetty, S., et al. (2012). Retinaldehyde dehydrogenase 1 regulates a thermogenic program in white adipose tissue. *Nat. Med.* 18, 918–925. doi: 10.1038/nm.2757

Knudson, J. D., Dincer, U. D., Zhang, C., Swafford, A. N. Jr., Koshida, R., Picchi, A., et al. (2005). Leptin receptors are expressed in coronary arteries, and hyperleptinemia causes significant coronary endothelial dysfunction. *Am. J. Physiol. Heart Circ. Physiol.* 289, H48–H56. doi: 10.1152/ajpheart.01159.2004

Kong, K. A., Park, J., Hong, S. H., Hong, Y. S., Sung, Y. A., and Lee, H. (2017). Associations between body mass index and mortality or cardiovascular events in a general Korean population. *PLoS ONE* 12:e0185024. doi: 10.1371/journal.pone.0185024

Lapidus, L., Bengtsson, C., Larsson, B., Pennert, K., Rybo, E., and Sjöström, L. (1984). Distribution of adipose tissue and risk of cardiovascular disease and death: a 12 year follow up of participants in the population study of women in Gothenburg, Sweden. *Br. Med. J.* 289, 1257–1261. doi: 10.1136/bmj.289.6454.1257

Lee, M. J., Wu, Y., and Fried, S. K. (2013). Adipose tissue heterogeneity: implication of depot differences in adipose tissue for obesity complications. *Mol. Aspects Med.* 34, 1–11. doi: 10.1016/j.mam.2012.10.001

Lehman, S. J., Massaro, J. M., Schlett, C. L., O'Donnell, C. J., Hoffmann, U., and Fox, C. S. (2010). Peri-aortic fat, cardiovascular disease risk factors, and aortic calcification: the Framingham Heart Study. *Atherosclerosis* 210, 656–661. doi: 10.1016/j.atherosclerosis.2010.01.007

Li, P., Liu, S., Lu, M., Bandyopadhyay, G., Oh, D., Imamura, T., et al. (2016). Hematopoietic-derived galectin-3 causes cellular and systemic insulin resistance. *Cell* 167, 973-984 e912. doi: 10.1016/j.cell.2016.10.025

Li, Y., Shi, B., and Li, S. (2014). Association between serum chemerin concentrations and clinical indices in obesity or metabolic syndrome: a meta-analysis. *PLoS ONE* 9:e113915. doi: 10.1371/journal.pone.0113915

Lidell, M. E., and Enerbäck, S. (2010). Brown adipose tissue–a new role in humans? *Nat. Rev. Endocrinol.* 6, 319–325. doi: 10.1038/nrendo.2010.64

Lim, S., and Meigs, J. B. (2014). Links between ectopic fat and vascular disease in humans. *Arterioscler. Thromb. Vasc. Biol.* 34, 1820–1826. doi: 10.1161/ATVBAHA.114.303035

Lim, Y. M., Song, S., and Song, W. O. (2017). Prevalence and determinants of overweight and obesity in children and adolescents from migrant and seasonal farmworker families in the United States-a systematic review and qualitative assessment. *Nutrients* 9:188. doi: 10.3390/nu9030188

Lobato, N. S., Neves, K. B., Filgueira, F. P., Fortes, Z. B., Carvalho, M. H., Webb, R. C., et al. (2012). The adipokine chemerin augments vascular reactivity to contractile stimuli via activation of the MEK-ERK1/2 pathway. *Life Sci.* 91, 600–606. doi: 10.1016/j.lfs.2012.04.013

Löhn, M., Dubrovska, G., Lauterbach, B., Luft, F. C., Gollasch, M., and Sharma, A. M. (2002). Periadventitial fat releases a vascular relaxing factor. *FASEB J.* 16, 1057–1063. doi: 10.1096/fj.02-0024com

Loirand, G., Guérin, P., and Pacaud, P. (2006). Rho kinases in cardiovascular physiology and pathophysiology. *Circ. Res.* 98, 322–334. doi: 10.1161/01.RES.0000201960.04223.3c

Lu, C., Su, L. Y., Lee, R. M., and Gao, Y. J. (2010). Mechanisms for perivascular adipose tissue-mediated potentiation of vascular contraction to perivascular neuronal stimulation: the role of adipocyte-derived angiotensin II. *Eur. J. Pharmacol.* 634, 107–112. doi: 10.1016/j.ejphar.2010.02.006

Lu, C., Zhao, A. X., Gao, Y. J., and Lee, R. M. (2011). Modulation of vein function by perivascular adipose tissue. *Eur. J. Pharmacol.* 657, 111–116. doi: 10.1016/j.ejphar.2010.12.028

Lumeng, C. N., Bodzin, J. L., and Saltiel, A. R. (2007). Obesity induces a phenotypic switch in adipose tissue macrophage polarization. *J. Clin. Invest.* 117, 175–184. doi: 10.1172/JCI29881

Ma, L., Ma, S., He, H., Yang, D., Chen, X., Luo, Z., et al. (2010). Perivascular fat-mediated vascular dysfunction and remodeling through the AMPK/mTOR pathway in high-fat diet-induced obese rats. *Hypertens. Res.* 33, 446–453. doi: 10.1038/hr.2010.11

Maenhaut, N., and Van de Voorde, J. (2011). Regulation of vascular tone by adipocytes. *BMC Med.* 9:25. doi: 10.1186/1741-7015-9-25

Mahmood, S. S., Levy, D., Vasan, R. S., and Wang, T. J. (2014). The Framingham Heart Study and the epidemiology of cardiovascular disease: a historical perspective. *Lancet* 383, 999–1008. doi: 10.1016/S0140-6736(13)61752-3

Malinowski, M., Deja, M. A., Janusiewicz, P., Golba, K. S., Roleder, T., and Wos, S. (2013). Mechanisms of vasodilatatory effect of perivascular tissue of human internal thoracic artery. *J. Physiol. Pharmacol.* 64, 309–316.

Marchesi, C., Ebrahimian, T., Angulo, O., Paradis, P., and Schiffrin, E. L. (2009). Endothelial nitric oxide synthase uncoupling and perivascular adipose oxidative stress and inflammation contribute to vascular dysfunction in a rodent model of metabolic syndrome. *Hypertension* 54, 1384–1392. doi: 10.1161/HYPERTENSIONAHA.109.138305

McLaughlin, T., Lamendola, C., Liu, A., and Abbasi, F. (2011). Preferential fat deposition in subcutaneous versus visceral depots is associated with insulin sensitivity. *J. Clin. Endocrinol. Metab.* 96, E1756–E1760. doi: 10.1210/jc.2011-0615

Meijer, R. I., Bakker, W., Alta, C. L., Sipkema, P., Yudkin, J. S., Viollet, B., et al. (2013). Perivascular adipose tissue control of insulin-induced vasoreactivity in muscle is impaired in db/db mice. *Diabetes* 62, 590–598. doi: 10.2337/db11-1603

Meyer, M. R., Fredette, N. C., Barton, M., and Prossnitz, E. R. (2013). Regulation of vascular smooth muscle tone by adipose-derived contracting factor. *PLoS ONE* 8:e79245. doi: 10.1371/journal.pone.0079245

Miao, C. Y., and Li, Z. Y. (2012). The role of perivascular adipose tissue in vascular smooth muscle cell growth. *Br. J. Pharmacol.* 165, 643–658. doi: 10.1111/j.1476-5381.2011.01404.x

Mikolajczyk, T. P., Nosalski, R., Szczepaniak, P., Budzyn, K., Osmenda, G., Skiba, D., et al. (2016). Role of chemokine RANTES in the regulation of perivascular inflammation, T-cell accumulation, and vascular dysfunction in hypertension. *FASEB J.* 30, 1987–1999. doi: 10.1096/fj.201500088R

Neves, K. B., Lobato, N. S., Lopes, R. A., Filgueira, F. P., Zanotto, C. Z., Oliveira, A. M., et al. (2014). Chemerin reduces vascular nitric oxide/cGMP signalling in rat aorta: a link to vascular dysfunction in obesity? *Clin. Sci.* 127, 111–122. doi: 10.1042/CS20130286

Neves, K. B., Nguyen Dinh Cat, A., Lopes, R. A., Rios, F. J., Anagnostopoulou, A., Lobato, N. S., et al. (2015). Chemerin regulates crosstalk between adipocytes and vascular cells through Nox. *Hypertension* 66, 657–666. doi: 10.1161/HYPERTENSIONAHA.115.05616

Ng, M., Fleming, T., Robinson, M., Thomson, B., Graetz, N., Margono, C., et al. (2014). Global, regional, and national prevalence of overweight and obesity in children and adults during 1980-2013, a systematic analysis for the global burden of Disease Study 2013. *Lancet* 384, 766–781. doi: 10.1016/S0140-6736(14)60460-8

Nguyen, M. T., Favelyukis, S., Nguyen, A. K., Reichart, D., Scott, P. A., Jenn, A., et al. (2007). A subpopulation of macrophages infiltrates hypertrophic adipose tissue and is activated by free fatty acids via Toll-like receptors 2 and 4 and JNK-dependent pathways. *J. Biol. Chem.* 282, 35279–35292. doi: 10.1074/jbc.M706762200

Ogden, C. L., Carroll, M. D., Lawman, H. G., Fryar, C. D., Kruszon-Moran, D., Kit, B. K., et al. (2016). Trends in obesity prevalence among children and adolescents in the United States, 1988-1994 through 2013-2014. *JAMA* 315, 2292–2299. doi: 10.1001/jama.2016.6361

Owen, M. K., Witzmann, F. A., McKenney, M. L., Lai, X., Berwick, Z. C., Moberly, S. P., et al. (2013). Perivascular adipose tissue potentiates contraction of coronary vascular smooth muscle: influence of obesity. *Circulation* 128, 9–18. doi: 10.1161/CIRCULATIONAHA.112.001238

Parolini, S., Santoro, A., Marcenaro, E., Luini, W., Massardi, L., Facchetti, F., et al. (2007). The role of chemerin in the colocalization of NK and dendritic cell subsets into inflamed tissues. *Blood* 109, 3625–3632. doi: 10.1182/blood-2006-08-038844

Payne, G. A., Bohlen, H. G., Dincer, U. D., Borbouse, L., and Tune, J., D. (2009). Periadventitial adipose tissue impairs coronary endothelial function via PKC-beta-dependent phosphorylation of nitric oxide synthase. *Am. J. Physiol. Heart Circ. Physiol.* 297, H460–H465. doi: 10.1152/ajpheart.00116.2009

Payne, G. A., Borbouse, L., Bratz, I. N., Roell, W. C., Bohlen, H. G., Dick, G. M., et al. (2008). Endogenous adipose-derived factors diminish coronary endothelial function via inhibition of nitric oxide synthase. *Microcirculation* 15, 417–426. doi: 10.1080/10739680701858447

Pekala, P., Kawakami, M., Vine, W., Lane, M. D., and Cerami, A. (1983). Studies of insulin resistance in adipocytes induced by macrophage mediator. *J. Exp. Med.* 157, 1360–1365. doi: 10.1084/jem.157.4.1360

Peters, S. L., Mathy, M. J., Pfaffendorf, M., and van Zwieten, P. A. (2000). Reactive oxygen species-induced aortic vasoconstriction and deterioration of functional integrity. *Naunyn Schmiedebergs Arch. Pharmacol.* 361, 127–133. doi: 10.1007/s002109900148

Picchi, A., Gao, X., Belmadani, S., Potter, B. J., Focardi, M., Chilian, W. M., et al. (2006). Tumor necrosis factor-alpha induces endothelial dysfunction in the prediabetic metabolic syndrome. *Circ. Res.* 99, 69–77. doi: 10.1161/01.RES.0000229685.37402.80

Pierdomenico, S. D., Pierdomenico, A. M., Cuccurullo, F., and Iacobellis, G. (2013). Meta-analysis of the relation of echocardiographic epicardial adipose tissue thickness and the metabolic syndrome. *Am. J. Cardiol.* 111, 73–78. doi: 10.1016/j.amjcard.2012.08.044

Poobalan, A., and Aucott, L. (2016). Obesity among young adults in developing countries: a systematic overview. *Curr. Obes. Rep.* 5, 2–13. doi: 10.1007/s13679-016-0187-x

Popkin, B. M., and Slining, M. M. (2013). New dynamics in global obesity facing low- and middle-income countries. *Obes. Rev.* 14(Suppl. 2), 11–20. doi: 10.1111/obr.12102

Prins, J. B. (2002). Adipose tissue as an endocrine organ. *Best Pract. Res. Clin. Endocrinol. Metab.* 16, 639–651. doi: 10.1053/beem.2002.0222

Ress, C., Tschoner, A., Engl, J., Klaus, A., Tilg, H., Ebenbichler, C. F., et al. (2010). Effect of bariatric surgery on circulating chemerin levels. *Eur. J. Clin. Invest.* 40, 277–280. doi: 10.1111/j.1365-2362.2010.02255.x

Rittig, K., Staib, K., Machann, J., Bottcher, M., Peter, A., Schick, F., et al. (2008). Perivascular fatty tissue at the brachial artery is linked to insulin resistance but not to local endothelial dysfunction. *Diabetologia* 51, 2093–2099. doi: 10.1007/s00125-008-1128-3

Roemeling-van Rhijn, M., Mensah, F. K., Korevaar, S. S., Leijs, M. J., van Osch, G. J., Ijzermans, J. N., et al. (2013). Effects of Hypoxia on the immunomodulatory properties of adipose tissue-derived mesenchymal stem cells. *Front. Immunol.* 4:203. doi: 10.3389/fimmu.2013.00203

Rosen, E. D., and Spiegelman, B. M. (2014). What we talk about when we talk about fat. *Cell* 156, 20–44. doi: 10.1016/j.cell.2013.12.012

Rosito, G. A., Massaro, J. M., Hoffmann, U., Ruberg, F. L., Mahabadi, A. A., Vasan, R. S., et al. (2008). Pericardial fat, visceral abdominal fat, cardiovascular disease risk factors, and vascular calcification in a community-based sample: the Framingham Heart Study. *Circulation* 117, 605–613. doi: 10.1161/CIRCULATIONAHA.107.743062

Sabio, G., Das, M., Mora, A., Zhang, Z., Jun, J. Y., Ko, H. J., et al. (2008). A stress signaling pathway in adipose tissue regulates hepatic insulin resistance. *Science* 322, 1539–1543. doi: 10.1126/science.1160794

Sacks, H. S., and Fain, J. N. (2007). Human epicardial adipose tissue: a review. *Am. Heart J.* 153, 907–917. doi: 10.1016/j.ahj.2007.03.019

Sagan, A., Mrowiecki, W., Mikolajczyk, T. P., Urbanski, K., Siedlinski, M., Nosalski, R., et al. (2012). Local inflammation is associated with aortic thrombus formation in abdominal aortic aneurysms. relationship to clinical risk factors. *Thromb. Haemost* 108, 812–823. doi: 10.1160/TH12-05-0339

Salgado-Somoza, A., Teijeira-Fernández, E., Fernández, A. L., González-Juanatey, J. R., and Eiras, S. (2010). Proteomic analysis of epicardial and subcutaneous adipose tissue reveals differences in proteins involved in oxidative stress. *Am. J. Physiol. Heart Circ. Physiol.* 299, H202–H209. doi: 10.1152/ajpheart.00120.2010

Samocha-Bonet, D., Chisholm, D. J., Tonks, K., Campbell, L. V., and Greenfield, J. R. (2012). Insulin-sensitive obesity in humans - a favorable fat phenotype? *Trends Endocrinol. Metab.* 23, 116–124. doi: 10.1016/j.tem.2011.12.005

Sayón-Orea, C., Bes-Rastrollo, M., Carlos, S., Beunza, J. J., Basterra-Gortari, F. J., and Martínez-González, M. A. (2013). Association between sleeping hours and siesta and the risk of obesity: the SUN Mediterranean Cohort. *Obes. Facts* 6, 337–347. doi: 10.1159/000354746

Schleifenbaum, J., Köhn, C., Voblova, N., Dubrovska, G., Zavarirskaya, O., Gloe, T., et al. (2010). Systemic peripheral artery relaxation by KCNQ channel openers and hydrogen sulfide. *J. Hypertens.* 28, 1875–1882. doi: 10.1097/HJH.0b013e32833c20d5

Schlett, C. L., Massaro, J. M., Lehman, S. J., Bamberg, F., O'Donnell, C. J., Fox, C. S., et al. (2009). Novel measurements of periaortic adipose tissue in comparison to anthropometric measures of obesity, and abdominal adipose tissue. *Int. J. Obes.* 33, 226–232. doi: 10.1038/ijo.2008.267

Schroeter, M. R., Eschholz, N., Herzberg, S., Jerchel, I., Leifheit-Nestler, M., Czepluch, F. S., et al. (2013). Leptin-dependent and leptin-independent paracrine effects of perivascular adipose tissue on neointima formation. *Arterioscler. Thromb. Vasc. Biol.* 33, 980–987. doi: 10.1161/ATVBAHA.113.301393

Seale, P., Conroe, H. M., Estall, J., Kajimura, S., Frontini, A., Ishibashi, J., et al. (2011). Prdm16 determines the thermogenic program of subcutaneous white adipose tissue in mice. *J. Clin. Invest.* 121, 96–105. doi: 10.1172/JCI44271

Sell, H., Divoux, A., Poitou, C., Basdevant, A., Bouillot, J. L., Bedossa, P., et al. (2010). Chemerin correlates with markers for fatty liver in morbidly obese patients and strongly decreases after weight loss induced by bariatric surgery. *J. Clin. Endocrinol. Metab.* 95, 2892–2896. doi: 10.1210/jc.2009-2374

Singh, N., Singh, H., Khanijoun, H. K., and Iacobellis, G. (2007). Echocardiographic assessment of epicardial adipose tissue–a marker of visceral adiposity. *Mcgill J. Med.* 10, 26–30.

Skiba, D. S., Nosalski, R., Mikolajczyk, T. P., Siedlinski, M., Rios, F. J., Montezano, A. C., et al. (2017). Anti-atherosclerotic effect of the angiotensin 1-7 mimetic AVE0991 is mediated by inhibition of perivascular and plaque inflammation in early atherosclerosis. *Br. J. Pharmacol.* 174, 4055–4069. doi: 10.1111/bph.13685

Skurk, T., Alberti-Huber, C., Herder, C., and Hauner, H. (2007). Relationship between adipocyte size and adipokine expression and secretion. *J. Clin. Endocrinol. Metab.* 92, 1023–1033. doi: 10.1210/jc.2006-1055

Soltis, E. E., and Cassis, L. A. (1991). Influence of perivascular adipose tissue on rat aortic smooth muscle responsiveness. *Clin. Exp. Hypertens. A* 13, 277–296. doi: 10.3109/10641969109042063

Spalding, K. L., Arner, E., Westermark, P. O., Bernard, S., Buchholz, B. A., Bergmann, O., et al. (2008). Dynamics of fat cell turnover in humans. *Nature* 453, 783–787. doi: 10.1038/nature06902

Spiroglou, S. G., Kostopoulos, C. G., Varakis, J. N., and Papadaki, H. H. (2010). Adipokines in periaortic and epicardial adipose tissue: differential expression and relation to atherosclerosis. *J. Atheroscler. Thromb.* 17, 115–130. doi: 10.5551/jat.1735

Szasz, T., Bomfim, G. F., and Webb, R. C. (2013). The influence of perivascular adipose tissue on vascular homeostasis. *Vasc. Health Risk Manag.* 9, 105–116. doi: 10.2147/VHRM.S33760

Tabata, M., Kadomatsu, T., Fukuhara, S., Miyata, K., Ito, Y., Endo, M., et al. (2009). Angiopoietin-like protein 2 promotes chronic adipose tissue inflammation and obesity-related systemic insulin resistance. *Cell Metab.* 10, 178–188. doi: 10.1016/j.cmet.2009.08.003

Takaoka, M., Suzuki, H., Shioda, S., Sekikawa, K., Saito, Y., Nagai, R., et al. (2010). Endovascular injury induces rapid phenotypic changes in perivascular adipose tissue. *Arterioscler. Thromb. Vasc. Biol.* 30, 1576–1582. doi: 10.1161/ATVBAHA.110.207175

Tchoukalova, Y. D., Votruba, S. B., Tchkonia, T., Giorgadze, N., Kirkland, J. L., and Jensen, M., D. (2010). Regional differences in cellular mechanisms of adipose tissue gain with overfeeding. *Proc. Natl. Acad. Sci. U.S.A.* 107, 18226–18231. doi: 10.1073/pnas.1005259107

Thanassoulis, G., Massaro, J. M., Corsini, E., Rogers, I., Schlett, C. L., Meigs, J. B., et al. (2012). Periaortic adipose tissue and aortic dimensions in the Framingham Heart Study. *J. Am. Heart Assoc.* 1:e000885. doi: 10.1161/JAHA.112.000885

Tian, Z., Miyata, K., Tazume, H., Sakaguchi, H., Kadomatsu, T., Horio, E., et al. (2013). Perivascular adipose tissue-secreted angiopoietin-like protein 2 (Angptl2) accelerates neointimal hyperplasia after endovascular injury. *J. Mol. Cell. Cardiol.* 57: 1–12. doi: 10.1016/j.yjmcc.2013.01.004

Uysal, K. T., Wiesbrock, S. M., Marino, M. W., and Hotamisligil, G. S. (1997). Protection from obesity-induced insulin resistance in mice lacking TNF-alpha function. *Nature* 389, 610–614. doi: 10.1038/39335

Vandevijvere, S., Chow, C. C., Hall, K. D., Umali, E., and Swinburn, B. A. (2015). Increased food energy supply as a major driver of the obesity epidemic: a global analysis. *Bull. World Health Organ.* 93, 446–456. doi: 10.2471/BLT.14.150565

Vegiopoulos, A., Müller-Decker, K., Strzoda, D., Schmitt, I., Chichelnitskiy, E., Ostertag, A., et al. (2010). Cyclooxygenase-2 controls energy homeostasis in mice by *de novo* recruitment of brown adipocytes. *Science* 328, 1158–1161. doi: 10.1126/science.1186034

Verlohren, S., Dubrovska, G., Tsang, S. Y., Essin, K., Luft, F. C., Huang, Y., et al. (2004). Visceral periadventitial adipose tissue regulates arterial tone of mesenteric arteries. *Hypertension* 44, 271–276. doi: 10.1161/01.HYP.0000140058.28994.ec

Vijgen, G. H., Bouvy, N. D., Teule, G. J., Brans, B., Hoeks, J., Schrauwen, P., et al. (2012). Increase in brown adipose tissue activity after weight loss in morbidly obese subjects. *J. Clin. Endocrinol. Metab.* 97, E1229–E1233. doi: 10.1210/jc.2012-1289

Vijgen, G. H., Bouvy, N. D., Teule, G. J., Brans, B., Schrauwen, P., and van Marken Lichtenbelt, W. D. (2011). Brown adipose tissue in morbidly obese subjects. *PLoS ONE* 6:e17247. doi: 10.1371/journal.pone.0017247

Waki, H., and Tontonoz, P. (2007). Endocrine functions of adipose tissue. *Annu. Rev. Pathol.* 2, 31–56. doi: 10.1146/annurev.pathol.2.010506.091859

Wang, Y., Rimm, E. B., Stampfer, M. J., Willett, W. C., and Hu, F. B. (2005). Comparison of abdominal adiposity and overall obesity in predicting risk of type 2 diabetes among men. *Am. J. Clin. Nutr.* 81, 555–563. doi: 10.1093/ajcn/81.3.555

Watts, S. W., Dorrance, A. M., Penfold, M. E., Rourke, J. L., Sinal, C. J., Seitz, B., et al. (2013). Chemerin connects fat to arterial contraction. *Arterioscler. Thromb. Vasc. Biol.* 33, 1320–1328. doi: 10.1161/ATVBAHA.113.301476

Weisberg, S. P., McCann, D., Desai, M., Rosenbaum, M., Leibel, R. L., and Ferrante, A. W. Jr. (2003). Obesity is associated with macrophage accumulation in adipose tissue. *J. Clin. Invest.* 112, 1796–1808. doi: 10.1172/JCI200319246

Weyer, C., Foley, J. E., Bogardus, C., Tataranni, P. A., and Pratley, R. E. (2000). Enlarged subcutaneous abdominal adipocyte size, but not obesity itself, predicts type II diabetes independent of insulin resistance. *Diabetologia* 43, 1498–1506. doi: 10.1007/s001250051560

White, U. A., and Tchoukalova, Y. D. (2014). Sex dimorphism and depot differences in adipose tissue function. *Biochim. Biophys. Acta* 1842, 377–392. doi: 10.1016/j.bbadis.2013.05.006

Williams, E. P., Mesidor, M., Winters, K., Dubbert, P. M., and Wyatt, S. B. (2015). Overweight and obesity: prevalence, consequences, and causes of a growing public health problem. *Curr. Obes. Rep.* 4, 363–370. doi: 10.1007/s13679-015-0169-4

Wittamer, V., Franssen, J. D., Vulcano, M., Mirjolet, J. F., Le Poul, E., Migeotte, I., et al. (2003). Specific recruitment of antigen-presenting cells by chemerin, a novel processed ligand from human inflammatory fluids. *J. Exp. Med.* 198, 977–985. doi: 10.1084/jem.20030382

Woodward, L., Akoumianakis, I., and Antoniades, C. (2017). Unravelling the adiponectin paradox: novel roles of adiponectin in the regulation of cardiovascular disease. *Br. J. Pharmacol.* 174, 4007–4020. doi: 10.1111/bph.13619

Xia, N., and Li, H. (2017). The role of perivascular adipose tissue in obesity-induced vascular dysfunction. *Br. J. Pharmacol.* 174, 3425–3442. doi: 10.1111/bph.13650

Xia, N., Horke, S., Habermeier, A., Closs, E. I., Reifenberg, G., Gericke, A., et al. (2016). Uncoupling of endothelial nitric oxide synthase in perivascular adipose tissue of diet-induced obese mice. *Arterioscler. Thromb. Vasc. Biol.* 36, 78–85. doi: 10.1161/ATVBAHA.115.306263

Xu, H., Barnes, G. T., Yang, Q., Tan, G., Yang, D., Chou, C. J., et al. (2003). Chronic inflammation in fat plays a crucial role in the development of obesity-related insulin resistance. *J. Clin. Invest.* 112, 1821–1830. doi: 10.1172/JCI200319451

Yang, W., Li, J. P., Zhang, Y., Fan, F. F., Xu, X., P., Wang, B. Y., et al. (2016). Association between body mass index and all-cause mortality in hypertensive adults: results from the China stroke primary prevention trial (CSPPT). *Nutrients* 8:384. doi: 10.3390/nu8060384

Yatsuya, H., Li, Y., Hilawe, E. H., Ota, A., Wang, C., Chiang, C., et al. (2014). Global trend in overweight and obesity and its association with cardiovascular disease incidence. *Circ. J.* 78, 2807–2818. doi: 10.1253/circj.CJ-14-0850

Yudkin, J. S., Eringa, E., and Stehouwer, C. D. (2005). Vasocrine signalling from perivascular fat: a mechanism linking insulin resistance to vascular disease. *Lancet* 365, 1817–1820. doi: 10.1016/S0140-6736(05)66585-3

Yusuf, S., Hawken, S., Ounpuu, S., Dans, T., Avezum, A., Lanas, F., et al. (2004). Effect of potentially modifiable risk factors associated with myocardial infarction in 52 countries (the INTERHEART study): case-control study. *Lancet* 364, 937–952. doi: 10.1016/S0140-6736(04)17018-9

Zabel, B. A., Ohyama, T., Zuniga, L., Kim, J. Y., Johnston, B., Allen, S. J., et al. (2006). Chemokine-like receptor 1 expression by macrophages *in vivo*: regulation by TGF-beta and TLR ligands. *Exp. Hematol.* 34, 1106–1114. doi: 10.1016/j.exphem.2006.03.011

Zabel, B. A., Silverio, A. M., and Butcher, E. C. (2005). Chemokine-like receptor 1 expression and chemerin-directed chemotaxis distinguish plasmacytoid from myeloid dendritic cells in human blood. *J. Immunol.* 174, 244–251. doi: 10.4049/jimmunol.174.1.244

Zhang, C., Rexrode, K. M., van Dam, R. M., Li, T. Y., and Hu, F. B. (2008). Abdominal obesity and the risk of all-cause, cardiovascular, and cancer mortality: sixteen years of follow-up in US women. *Circulation* 117, 1658–1667. doi: 10.1161/CIRCULATIONAHA.107.739714

Conflict of Interest Statement: The authors declare that the research was conducted in the absence of any commercial or financial relationships that could be construed as a potential conflict of interest.

frontiers in Physiology

ORIGINAL RESEARCH
published: 19 March 2018
doi: 10.3389/fphys.2018.00229

Protective Role of Perivascular Adipose Tissue in Endothelial Dysfunction and Insulin-Induced Vasodilatation of Hypercholesterolemic LDL Receptor-Deficient Mice

*Natali Baltieri, Daniele M. Guizoni, Jamaira A. Victorio and Ana P. Davel**

Department of Structural and Functional Biology, Institute of Biology, University of Campinas, Campinas, Brazil

OPEN ACCESS

Edited by:
Stephanie W. Watts, Michigan State University, United States

Reviewed by:
A. Elizabeth Linder, Universidade Federal de Santa Catarina, Brazil
Philip Aaronson, King's College London, United Kingdom

***Correspondence:**
Ana P. Davel
anadavel@unicamp.br

Specialty section:
This article was submitted to Vascular Physiology, a section of the journal Frontiers in Physiology

Received: *07 December 2017*
Accepted: *01 March 2018*
Published: *19 March 2018*

Citation:
Baltieri N, Guizoni DM, Victorio JA and Davel AP (2018) Protective Role of Perivascular Adipose Tissue in Endothelial Dysfunction and Insulin-Induced Vasodilatation of Hypercholesterolemic LDL Receptor-Deficient Mice. Front. Physiol. 9:229. doi: 10.3389/fphys.2018.00229

Background: Endothelial dysfunction plays a pivotal role in the initiation of atherosclerosis. Vascular insulin resistance might contribute to a reduction in endothelial nitric oxide (NO) production, leading to impaired endothelium-dependent relaxation in cardiometabolic diseases. Because perivascular adipose tissue (PVAT) controls endothelial function and NO bioavailability, we hypothesized a role for this fat deposit in the vascular complications associated with the initial stages of atherosclerosis. Therefore, we investigated the potential involvement of PVAT in the early endothelial dysfunction in hypercholesterolemic LDL receptor knockout mice (LDLr-KO).

Methods: Thoracic aortas with and without PVAT were isolated from 4-month-old C57BL/6J (WT) and LDLr-KO mice. The contribution of PVAT to relaxation responses to acetylcholine, insulin, and sodium nitroprusside was investigated. Western blotting was used to examine endothelial NO synthase (eNOS) and adiponectin expression, as well the insulin signaling pathway in aortic PVAT.

Results: PVAT-free aortas of LDLr-KO mice exhibited impaired acetylcholine- and insulin-induced relaxation compared with those of WT mice. Both vasodilatory responses were restored by the presence of PVAT in LDLr-KO mice, associated with enhanced acetylcholine-induced NO levels. PVAT did not change vasodilatory responses to acetylcholine and insulin in WT mice, while vascular relaxation evoked by the NO donor sodium nitroprusside was not modified by either genotype or PVAT. The expression of insulin receptor substrate-1 (IRS-1), phosphatidylinositol 3-kinase (PI3K), AKT, ERK1/2, phosphorylation of AKT (Ser473) and ERK1/2 (Thr202/Tyr204), and adiponectin was similar in the PVAT of WT and LDLr-KO mice, suggesting no changes in PVAT insulin signaling. However, eNOS expression was enhanced in the PVAT of LDLr-KO mice, while eNOS expression was less abundant in PVAT-free aortas.

Conclusion: These results suggest that elevated eNOS-derived NO production in aortic PVAT might be a compensatory mechanism for the endothelial dysfunction and impaired vasodilator action of insulin in hypercholesterolemic LDLr-deficient mice. This protective effect may limit the progression of atherosclerosis in genetic hypercholesterolemia in the absence of an atherogenic diet.

Keywords: perivascular adipose tissue, endothelium, LDL receptor deficiency, hypercholesterolemia, nitric oxide, insulin, adiponectin

INTRODUCTION

Hypercholesterolemia is the main risk factor for the development of atherosclerosis by enhancing low-density lipoprotein (LDL) retention within the vessel wall (Stapleton et al., 2010). Atherosclerosis is a progressive disease in which inflammation, fat deposits, and cells and extracellular matrix accumulation in the artery result in the occlusion of the vessel lumen, underlying a major cause of clinical cardiovascular events worldwide (World Health Organization, 2014; Mozaffarian et al., 2016). One of the initial steps of the atherosclerotic process is the development of endothelial dysfunction, which precedes atherosclerosis development in humans (Guzik et al., 2000; Heitzer et al., 2001).

LDL receptor knockout mice (LDLr-KO) is a model of human familial hypercholesterolemia (FH). Although young adult LDLr-KO mice fed with standard low-fat diet only develop small spontaneous atherosclerotic lesions in the aortic root (Dorighello et al., 2016, 2017), these animals present impaired endothelium-dependent relaxation in the aorta (Rabelo et al., 2003; Langbein et al., 2015; Guizoni et al., 2016). This finding is consistent with reduced endothelium-dependent vasodilation in human hypercholesterolemia (Creager et al., 1990, 1992). In this model of genetic hypercholesterolemia, endothelial dysfunction is associated with the reduced gene and protein expression of endothelial nitric oxide synthase (eNOS) (Guizoni et al., 2016; Langbein et al., 2016), and reduced dimerization of this enzyme, resulting in impaired endothelial nitric oxide (NO) release (Guizoni et al., 2016).

Nitric oxide (NO) is an endothelium-derived vasodilator factor with antiatherogenic properties, including the inhibition of platelets, and monocyte adhesion to the endothelium, platelet aggregation, smooth muscle proliferation, and oxidation of LDL (Vanhoutte, 2003). Consistently, the administration of L-arginine, as eNOS substrate and NO precursor, improves the endothelial function in hypercholesterolemic patients (Creager et al., 1992; Siasos et al., 2007), whereas the lack of NO accelerates the progression of atherosclerosis (Kauser et al., 2000). Genetic hypercholesterolemia is also associated with the impaired secretion of insulin (Souza et al., 2013), a hormone stimulating NO production (Potenza et al., 2009). In addition to endothelium-derived NO, NO release from perivascular adipose tissue (PVAT) has recently been demonstrated as an important adipocyte-derived relaxation factor (ADRF) in the aorta (Victorio et al., 2016; Xia et al., 2016), but whether or not changes in PVAT eNOS function are involved in hypercholesterolemia-induced vascular dysfunction remains unknown.

Perivascular adipose tissue (PVAT) surrounds most blood vessels and releases numerous factors and adipokines with paracrine effects on both vascular structure and function (Akoumianakis et al., 2017). Higher levels of proinflammatory adipocytokines and lower levels of adiponectin were found within the PVAT after artery injury (Takaoka et al., 2010), and an inflamed PVAT results in neointima formation (Moe et al., 2013). In addition, increased amounts of angiogenic factors release by PVAT may have a pathological relevance for atherosclerosis development (Chang et al., 2013). However, the thermogenic properties of PVAT have been demonstrated as anti-atherogenic (Chang et al., 2012; Brown et al., 2014). Nevertheless, the role of PVAT in the development and progression of this vascular disease is still unclear. Because PVAT regulates endothelial function and NO bioavailability, we hypothesized a role for this fat deposit in the vascular complications associated with the initial stages of atherosclerosis. Therefore, the present study was designed to evaluate the potential influence of PVAT in the early endothelial dysfunction of hypercholesterolemic LDLr-KO mice.

MATERIALS AND METHODS

Animals

LDL receptor knockout (LDLr-KO) mice and respective C57BL6/J wild-type (WT) mice were purchased from the Jackson Laboratory, and the strains are maintained by breeding at the Multidisciplinary Center for Biological Research (CEMIB-UNICAMP, Campinas, SP, Brazil) with genotypic control. The mice were housed at 22 ± 1°C on a 12:12 h light:dark cycle with free access to a standard rodent chow diet (Nuvital CR1, Colombo, Paraná, Brazil) and water. At 4 months old, the mice were weighted and anesthetized with urethane (5 g/kg body weight, i.p.) to collect blood samples and isolate thoracic aorta.

All experimental protocols were approved (protocol # 3639-1) by the Ethics Committee on Animal Use of the University of Campinas (CEUA-UNICAMP, Campinas-SP, Brazil) and carried out in accordance with the ethical principles for animal experimentation adopted by the Brazilian Society of Laboratory Animal Science (SBCAL/COBEA).

Plasma Biochemical Analysis

Blood samples were obtained from the tail vein for blood glucose measurement (Accu-Chek Advantage, Roche Diagnostics, Sao Paulo, Brazil). Subsequently, the mice were anesthetized (5 g/kg

of urethane, i.p.), and blood samples were collected by cardiac puncture and centrifuged (8,000 g for 15 min at 4°C); the serum supernatants were subsequently collected for biochemical analysis. Total cholesterol and triglyceride levels were measured using standard commercial kits (Chod-Pap, Roche Diagnostic GmbH, Mannheim, Germany).

Vascular Reactivity in the Presence or Absence of PVAT

The thoracic aorta was isolated and cut into cylindrical segments (∼2 mm in length) with or without surrounding PVAT. The segments were mounted in a tissue chamber bath (Panlab Harvard Apparatus, Cornellà-Barcelona, Spain) containing Krebs–Henseleit solution (in mM: 118 NaCl, 4.7 KCl, 25 NaHCO3, 2.5 CaCl2-2H2O, 1.2 KH2PO4, 1.2 MgSO4-7H2O,11 glucose and 0.01 EDTA; pH = 7.4, 37°C) with a resting tension of 0.5 g stabilized for 1 h, as previously demonstrated (Davel et al., 2012; Guizoni et al., 2016). Subsequently, aortic rings were exposed to 125 mM of KCl to test vascular integrity and assess maximal contraction, and no differences were found among groups (data not shown). Following washing, the aortic rings were contracted with a submaximal concentration of the thromboxane A2 receptor agonist (U-46619, 70% of maximal contraction to 125 mM of KCl) and relaxation curves to acetylcholine (0.1 nmol/L to 10 μmol/L, Sigma-Aldrich, Saint Louis, MO, USA), insulin (0.1 to 10 nmol/L, Humulin® R - rDNA origin, Lilly USA, Indianapolis, USA), or the NO-donor sodium nitroprusside (1 pmol/L to 0.1 μmol/L Sigma-Aldrich, Saint Louis, MO, USA) were performed.

PVAT Homogenization and Western Blotting

Thoracic aorta and respective PVAT were separately pulverized in N2 liquid and homogenized in cold RIPA lysis buffer (Merck Millipore, Billerica, MA, USA) containing PMSF (1 mM), Na3VO4 (1 mM) and 2 μL/mL of protease inhibitor cocktail (PIC, Sigma-Aldrich) to obtain total protein extract (Victorio et al., 2016). The proteins were quantified using the BCA Protein Assay Kit (Thermo Fisher Scientific Inc.) to determine the protein concentration values of the samples (PVAT: $WT = 4.49 \pm 2.94$ and LDLr-KO $= 5.74 \pm 1.98$ mg/ml; aorta: $WT = 6.13 \pm 3.09$ and LDLr-KO $= 7.46 \pm 1.98$ mg/ml). Then, 40 μg of PVAT or aorta extracts and the 1 μL of plasma were electrophoretically separated on 7.5 or 12% acrylamide SDS–PAGE and then transferred to PVDF membranes using a Mini Trans-Blot Cell system. Non-specific binding sites were blocked with 5% non-fat milk solution, and then the membranes were incubated for 12 h at 4°C with the following primary antibodies: anti-insulin receptor substrate-1 (IRS-1), anti-p85 subunit of phosphatidylinositol 3 kinase (PI3K), anti-Akt1/2/3, anti-phospho (Ser473)-Akt1/2/3 (1:1,000; Santa Cruz Biotechnology), anti-eNOS (1:1,000; BD Transduction, Franklin Lakes, NJ, USA), anti-ERK1/2, anti-phospho (Thr202/Tyr204)-ERK1/2 (1:1,000; Cell Signaling, Danvers, MA, USA), and anti-adiponectin (1.5 μg/mL, Novus Biologicals, Littleton, CO, USA). Additionally, α-tubulin (1:1,000; Santa Cruz Biotechnology) was used as an internal control protein for PVAT, α-actin (1:1,000; Abcam, Cambridge, MA, USA) was used as an internal control protein for aorta, and Ponceau S staining for adiponectin expression in plasma and PVAT. After washing (10 mM of Tris, 100 mM of NaCl and 0.1% Tween-20), the membranes were incubated for 90 min with the specific secondary antibody conjugated to peroxidase. Immunocomplexes were detected using a luminol peroxidase chemiluminescence kit (ECL Plus, Amersham) and visualized using photographic film (Hyperfilm ECL, Amersham) in a dark room. The intensity of the immunoblots was quantified using ImageJ 1.46p software (National Institutes of Health, Bethesda, MD, USA).

PVAT NO Release

NO in PVAT was detected with 4,5-diaminofluorescein diacetate (DAF-2 DA) (Xia et al., 2016). Aortic PVAT cryostat sections (20 μm) were loaded with DAF-2 DA (8 μM) in the presence of acetylcholine (10 μM) at 37°C for 30 min. Then, fluorescence imaging was performed with a microscope (Eclipse Ti-S, Nikon, Tokyo, Japan) equipped with a fluorescence filter. DAF-2 DA was excited by an interference filter at 465–495 nm, and fluorescence emitted between 515 and 555 nm was collected (Zhou and He, 2011). The images captured under a 10X objective were analyzed using ImageJ 1.46p software (National Institutes of Health), the mean optical density of the fluorescence was measured, and the results were normalized by the PVAT area (μm^2). Fluorescence intensity was quantified by the subtraction of acetylcholine-treated samples from basal conditions.

Statistical Analysis

Data were expressed as the means ± SEM. Two-way ANOVA was used to analyze the vasorelaxation response curves. When ANOVA showed a significant effect, Bonferroni's *post-hoc* test was used to compare individual means. Unpaired Student's *t*-test was used for two-group comparisons. For each concentration-response curve, R_{max} and the negative logarithm of the concentration of the agonist that produced half of R_{max} ($-\text{LogEC}_{50}$) were calculated using non-linear regression analysis. GraphPad Prim Software 5.0 (San Diego, CA, EUA) was used for statistical analysis and $-\text{LogEC}_{50}$ and R_{max} calculation. $P < 0.05$ values were considered significant.

TABLE 1 | Body weight and total serum cholesterol, triglycerides, and glycemia in wild-type (WT) and LDLr knockout mice (LDLr-KO).

	WT	LDLr-KO
Body weight (g)	28 ± 0.6	27 ± 0.6
Blood glucose (mg/dL)	135 ± 14	143 ± 23
Total cholesterol (mg/dL)	84.6 ± 4.6	262.3 ± 14.3*
Triglycerides (mg/dL)	54.3 ± 4.1	145.4 ± 11.5*

*Data are expressed as mean ± SEM (N = 10–14). Unpaired Student's t-test: *P < 0.05 vs. WT.*

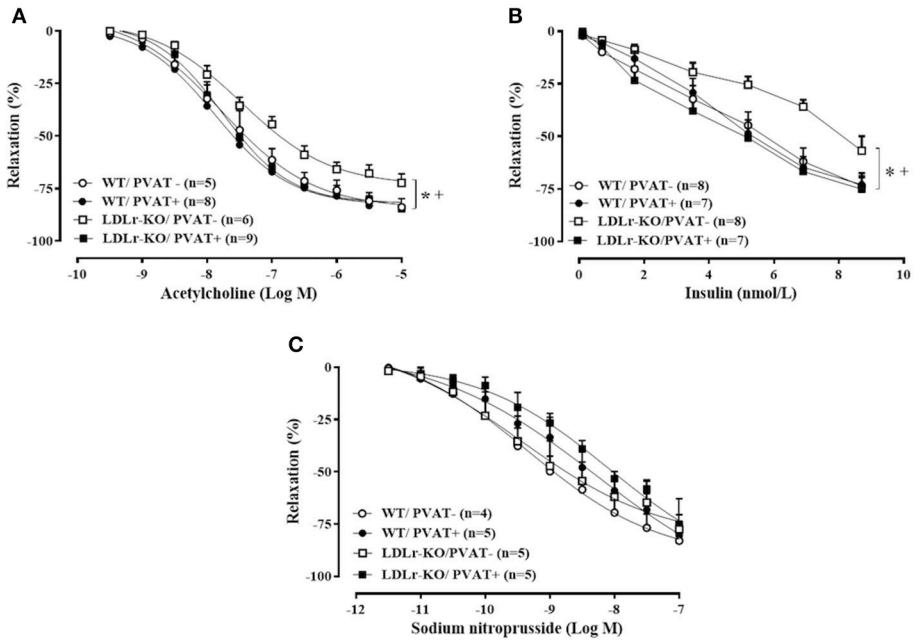

FIGURE 1 | Perivascular adipose tissue (PVAT) avoids endothelial dysfunction in LDLr knockout mice. Relaxation curves to acetylcholine **(A)**, insulin **(B)**, and sodium nitroprusside **(C)** in aortic rings with (+) and without (–) PVAT from wild-type (WT; circles) and LDLr knockout mice (LDLr-KO; squares). Two-way ANOVA, $P < 0.05$: * vs. WT/PVAT–; $^{+}$ vs. LDLr-KO/PVAT+.

RESULTS

As expected, LDLr-KO mice exhibited dyslipidemia characterized by elevated plasma levels of total cholesterol and triglycerides (Bonfleur et al., 2011), with no changes in blood glucose or body weight (**Table 1**).

The vascular reactivity study revealed an impaired relaxation to acetylcholine and insulin in aorta of LDLr-KO mice in the absence of PVAT (**Figures 1A,B**), with a reduced R_{max} to both agonists (**Table 2**). These data suggest an impaired endothelial vasodilatory response and vascular insulin resistance. However, the presence of PVAT prevented the impaired vasodilatory response to both acetylcholine and insulin in LDLr-KO associated with increased R_{max} while not affecting vasorelaxation in WT (**Figures 1A,B**; **Table 2**). Changes in acetylcholine- and insulin-induced relaxation were not the result of a smooth muscle defect, as the relaxation response to the NO donor sodium nitroprusside was similar between WT and LDLr-KO mice, with or without PVAT (**Figure 1C**, **Table 2**).

Considering that NO is the main endothelium-derived vasodilator factor mediating acetylcholine- and insulin-induced relaxation in the murine aorta (Wu et al., 1994), we investigated vascular and PVAT eNOS expression. Interestingly, while eNOS expression was reduced in aortic tissue from LDLr-KO mice (**Figure 2A**), aortic PVAT showed more abundant eNOS expression (**Figure 2B**), associated with enhanced PVAT NO levels (**Figure 2C**). These data suggest increased eNOS-derived NO production as a mechanism involved in the protective effect of aortic PVAT in dyslipidemic LDLr-KO mice.

TABLE 2 | Maximal relaxation response (R_{max}) and potency for acetylcholine, insulin, and sodium nitroprusside in aortas with (+) or without (–) perivascular adipose tissue (PVAT) from wild-type (WT) and LDLr knockout mice (LDLr-KO).

	WT		LDLr-KO	
	PVAT–	PVAT+	PVAT–	PVAT+
ACETYLCHOLINE				
R_{max} (%)	84 ± 4.1	87 ± 3.9	70 ± 4.7*	85 ± 1.3^{+}
$-LogEC_{50}$	7.67 ± 0.16	7.81 ± 0.16	7.37 ± 0.14	7.74 ± 0.11
INSULIN				
R_{max} (%)	76 ± 3.9	73 ± 4.0	57 ± 6.9*	76 ± 4.1^{+}
$-LogEC_{50}$	8.39 ± 0.06	8.39 ± 0.05	8.30 ± 0.03	8.48 ± 0.09
SODIUM NITROPRUSSIDE				
R_{max} (%)	83 ± 4.9	80 ± 6.9	78 ± 14.7	75 ± 4.8
$-LogEC_{50}$	9.33 ± 0.49	9.04 ± 0.17	9.15 ± 0.28	8.51 ± 0.08

*Data are expressed as mean ± SEM (N = 4–9). 2-way ANOVA followed by Bonferroni's post-hoc test, $P < 0.05$. * vs. WT/PVAT-; + vs. LDLr-KO/PVAT–.*

To investigate insulin signaling in PVAT, we evaluated the protein expression of IRS-1, PI3K, and total and phosphorylated Akt and ERK. However, as shown in **Figure 3**, no differences between groups were observed.

Finally, because adiponectin is an important adipokine that stimulates NO production and facilitates endothelium-dependent relaxation (Margaritis et al., 2013), we examined PVAT and circulating adiponectin expression (**Figures 4A,B**). No significant changes were found between WT and LDLr-KO mice.

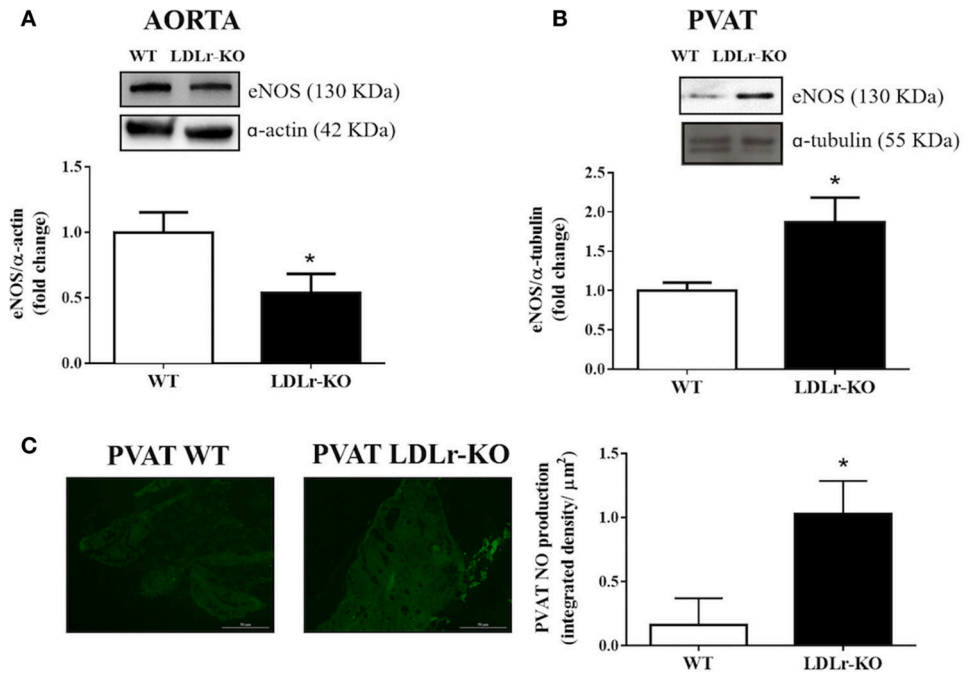

FIGURE 2 | eNOS expression is reduced in aorta while is increased in perivascular adipose tissue (PVAT) of LDLr knockout mice. Aortic **(A)** and PVAT **(B)** eNOS expression in wild-type (WT) and LDLr knockout (LDLr-KO) mice. Representative blots are shown at the top of the graphs. **(C)** Representative images and the quantification of PVAT NO production determined by DAF-2 DA fluorescence intensity in response to acetylcholine in WT and LDLr-KO mice. Student's *t*-test, $^*P < 0.05$ vs. WT.

DISCUSSION

The results from the present study showed that in LDLr-KO mice, the presence of PVAT protected against impaired endothelium-dependent relaxation to acetylcholine and insulin, in association with enhanced eNOS protein expression and NO levels in thoracic aortic PVAT. Since this genetic model of FH exhibited only small aortic-root lesions in mice maintained on a standard low-fat diet (Dorighello et al., 2016), these data reveal a protective role for PVAT in an early phase of vascular injury induced by hypercholesterolemia.

We (Guizoni et al., 2016) and others (Rabelo et al., 2003; Langbein et al., 2015) have demonstrated a slight but significant reduction in acetylcholine-induced relaxation in LDLr-KO mice, as evidenced by a reduced maximal response to this agonist (Hofmann et al., 2017). Similarly, we found a reduced maximal relaxation to acetylcholine in aorta without PVAT from LDLr-KO fed a standard diet, indicating endothelial dysfunction in this genetic model of FH. This endothelial dysfunction became more evident in the presence of high fat/high cholesterol diets or the upregulation of lectin-like oxidized LDLr-1 (LOX-1) (Hofmann et al., 2017). However, Western-type diets also induced a range of secondary factors, such as inflammation, insulin resistance, and obesity, which synergistically interact to increase atherosclerosis. A high-fat diet per se upregulates proinflammatory gene expression in PVAT depots (Chatterjee et al., 2009). Inflamed fat surrounding the vessels resulted in enhanced atherosclerotic lesions and exacerbated endothelial dysfunction (Öhman et al., 2011). Therefore, PVAT may have pathological relevance in advanced atherosclerosis, contributing to plaque complications (Chang et al., 2013). In the present study, we investigated the role of PVAT in endothelium-dependent relaxation in the early stages of vascular injury in LDLr-KO mice fed a standard diet. Interestingly, the presence of PVAT improved relaxation responses to acetylcholine and insulin in the aortas of LDLr-KO mice, suggesting a protective role for this tissue in the present genetic model of FH by improving endothelial function. In healthy mouse aorta, the presence of PVAT did not affect the endothelium-dependent relaxation induced by acetylcholine, as previously demonstrated (Ketonen et al., 2010; Li et al., 2011).

Gil-Ortega et al. (2010) showed adaptive NO overproduction in PVAT during the initial steps of high-fat diet-induced obesity in mice. PVAT-derived NO may contribute to the anticontractile effect of PVAT independently of the endothelium (Aghamohammadzadeh et al., 2016). Since eNOS is expressed in aortic endothelium and PVAT (Victorio et al., 2016; Xia et al., 2016), we investigated whether the protective role of PVAT in endothelium-dependent relaxation responses in LDLr-KO mice was associated with changes in eNOS expression. The results demonstrated reduced eNOS expression in the vascular wall of LDLr-KO mice, as previously demonstrated, associated with reduced NO production (Guizoni et al., 2016). Lower eNOS and nNOS activation is also related to

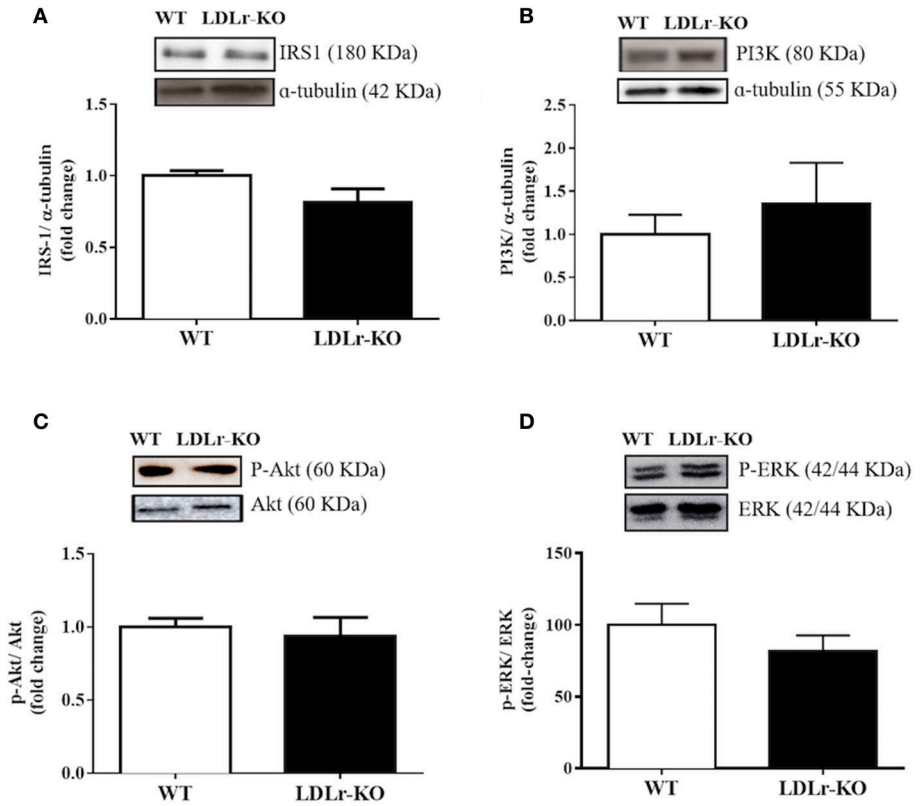

FIGURE 3 | Vascular insulin signaling has not changed in perivascular adipose tissue (PVAT) of LDLr knockout mice. Protein expression of IRS-1 **(A)**, p85 subunit of PI3K **(B)**, p-Akt/Akt ratio **(C)**, and p-ERK/ERK ratio **(D)** in PVAT from wild-type (WT) and LDLr knockout (LDLr-KO) mice. Representative blots are shown at the top of the graphs.

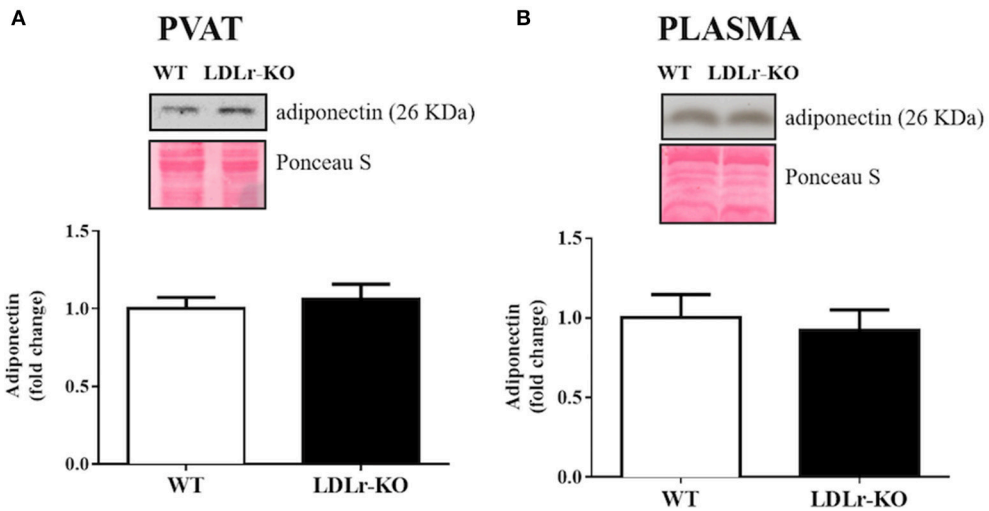

FIGURE 4 | Circulating and perivascular adiponectin expression. Protein expression of adiponectin in aortic perivascular adipose tissue (PVAT) **(A)** and in plasma **(B)** from wild-type (WT), and LDLr knockout (LDLr-KO) mice. Representative blots are shown at the top of the graphs.

endothelial dysfunction in apolipoprotein E-deficient mice (Capettini et al., 2011). In accordance with these data, lower NO production is observed in endothelial cells exposed to the serum of hypercholesterolemic patients (Feron et al., 1999). However, in contrast to lower endothelial eNOS expression in the vessel wall, increased eNOS expression

and NO levels were observed in the aortic PVAT of LDLr-KO mice. Therefore, higher eNOS-derived NO production in surrounding fat may be the mechanism enhancing endothelium-dependent relaxation in the aortas of LDLr-KO mice.

In addition to reduced relaxation to acetylcholine, the aortas from LDLr-KO mice without PVAT exhibited impaired relaxation to insulin. Insulin is an important stimulus in endothelial cells for eNOS-derived NO production (Potenza et al., 2009). Therefore, lower eNOS expression in the vascular wall should be a mechanism involved in the impaired relaxation to this hormone in hypercholesterolemic mice. Since relaxation response to sodium nitroprusside was not different among groups, changes in smooth muscle responsiveness may not be involved in the reduced vasodilatory responses observed in LDLr-KO mice. High plasma levels of cholesterol in LDLr-KO mice impairs beta-cell pancreatic function reducing insulin secretion, even in the absence of metabolic factors induced by Western-type diets, suggesting that genetic hypercholesterolemia increases the risk of diabetes development (Bonfleur et al., 2011; Souza et al., 2013). This finding is consistent with the slight increase in fasted plasma glucose previously observed in LDLr-KO mice (Bonfleur et al., 2011; Souza et al., 2013), although we did not find significant differences in non-fasted animals. In the present study, the reduced vasodilatory effect of insulin suggests vascular insulin resistance. Insulin enhances the expression and activity of eNOS in endothelial cells by upregulating the PI3K/Akt pathway, which induced endothelium-dependent relaxation (Montagnani et al., 2002; Potenza et al., 2009). However, hyperinsulinemia and insulin resistance favor the insulin-dependent activation of MAP-kinases (MAPK), which is associated with the elevated expression of proinflammatory and atherogenic factors (Eringa et al., 2004; Cersosimo et al., 2012; da Silva Franco et al., 2017). The presence of PVAT prevented the reduced insulin-induced relaxation in aorta of LDLr-KO mice. Thus, we hypothesized that an enhanced insulin signaling in PVAT could be a mechanism opposing the vascular insulin resistance in these animals. However, no differences were found for IRS-1, PI3K, and phosphorylated and total Akt and ERK, suggesting that this signaling pathway may not be involved in the protective effect of PVAT. However, we cannot exclude changes in the insulin molecular pathway, other than those evaluated in the present study.

Adiponectin has been described as an ADRF with antiatherogenic properties (Fésüs et al., 2007; Li et al., 2015). The upregulation of adiponectin is observed in PVAT of internal mammary arteries of obese patients with coronary artery disease and might reflect a compensatory mechanism to preserve endothelial function (Cybularz et al., 2017), as previously demonstrated in obese diabetic mice (Liu et al., 2014). In addition, adiponectin improves insulin sensitivity in major insulin target tissues (Ruan and Dong, 2016) and enhances NO production through eNOS activation via PI3K/Akt phosphorylation and eNOS coupling by increasing BH_4 bioavailability (Margaritis et al., 2013). Thus, we investigated the expression of adiponectin in PVAT and plasma. However, no differences were observed between WT and LDLr-KO mice, suggesting that the effect of PVAT on improving endothelial function in LDLr-KO mice is not associated with modifications of local or circulating levels of this ADRF.

Thoracic PVAT acts as a buffer against toxic levels of fatty acids in arterial circulation and clears fatty acids via inducing thermogenesis (van Dam et al., 2017). Interestingly, enhanced thermogenic activity of PVAT improves endothelial function by inducing the increased release of prostacyclin, whereas impaired PVAT thermogenesis causes atherosclerosis (Chang et al., 2012). Therefore, PVAT adaptive thermogenesis has a beneficial impact on endothelial function protecting against vascular injury. We cannot exclude that this protection exerted by PVAT on endothelial function could be lost in aging. One limitation of the present study is that we did not evaluate PVAT thermogenesis, which is a potential mechanism of endothelial protection in standard-diet fed LDLr-KO mice, as Western-type diets induced whitening and impaired thermogenesis in PVAT (Chang et al., 2013). Recently, Srikakulapu et al. (2017) demonstrated that harboring of B-1 cells by PVAT provides atheroprotection to the aorta, suggesting an additional mechanism for the beneficial role of PVAT in the vasculature.

CONCLUSION

Taken together, the results of the present study suggest that aortic PVAT is protective for endothelial dysfunction in LDLr-KO mice, a genetic model of FH. Therefore, this adaptive mechanism in PVAT may protect endothelial function and maintain normal endothelium-dependent relaxation in the early stages of atherosclerotic disease.

ETHICS STATEMENT

All experimental protocols were approved (protocol # 3639-1) by the Ethics Committee on Animal Use of the University of Campinas (CEUA-UNICAMP, Campinas-SP, Brazil) and carried out in accordance with the ethical principles for animal experimentation adopted by the Brazilian Society of Laboratory Animal Science (SBCAL/COBEA).

AUTHOR CONTRIBUTIONS

NB designed and executed the experiments, analyzed the data, wrote the manuscript. DG assisted in the experiments, data analysis and interpretation, read and revised the manuscript. JV performed DAF-2 DA fluorescence analysis. AD conceived the study, guided the experimental design, data analysis and interpretation, read and revised the manuscript.

FUNDING

This work was supported by grant from Sao Paulo Research Foundation - FAPESP (#2014/22506-6 and # 2016/14461-8).

REFERENCES

Aghamohammadzadeh, R., Unwin, R. D., Greenstein, A. S., and Heagerty, A. M. (2016). Effects of obesity on perivascular adipose tissue vasorelaxant function: nitric oxide, inflammation and elevated systemic blood pressure. *J. Vasc. Res.* 52, 299–305. doi: 10.1159/000443885

Akoumianakis, I., Tarun, A., and Antoniades, C. (2017). Perivascular adipose tissue as a regulator of vascular disease pathogenesis: identifying novel therapeutic targets. *Br. J. Pharmacol.* 174, 3411–3424. doi: 10.1111/bph.13666

Bonfleur, M. L., Ribeiro, R. A., Balbo, S. L., Vanzela, E. C., Carneiro, E. M., de Oliveira, H. C., et al. (2011). Lower expression of PKAα impairs insulin secretion in islets isolated from low-density lipoprotein receptor ($LDLR^{-/-}$) knockout mice. *Metabolism* 60, 1158–1164. doi: 10.1016/j.metabol.2010.12.010

Brown, N. K., Zhou, Z., Zhang, J., Zeng, R., Wu, J., Eitzman, D. T., et al. (2014). Perivascular adipose tissue in vascular function and disease: a review of current research and animal models. *Arterioscler. Thromb. Vasc. Biol.* 34, 1621–1630. doi: 10.1161/ATVBAHA.114.303029

Capettini, L. S., Cortes, S. F., Silva, J. F., Alvarez-Leite, J. I., and Lemos, V. S. (2011). Decreased production of neuronal NOS-derived hydrogen peroxide contributes to endothelial dysfunction in atherosclerosis. *Br. J. Pharmacol.* 164, 1738–1748. doi: 10.1111/j.1476-5381.2011.01500.x

Cersosimo, E., Xu, X., and Musi, N. (2012). Potential role of insulin signaling on vascular smooth muscle cell migration, proliferation, and inflammation pathways. *Am. J. Physiol. Cell Physiol.* 302, C652–C657. doi: 10.1152/ajpcell.00022.2011

Chang, L., Milton, H., Eitzman, D. T., and Chen, Y. E. (2013). Paradoxical roles of perivascular adipose tissue in atherosclerosis and hypertension. *Circ. J.* 77, 11–18. doi: 10.1253/circj.CJ-12-1393

Chang, L., Villacorta, L., Li, R., Hamblin, M., Xu, W., Dou, C., et al. (2012). Loss of perivascular adipose tissue on peroxisome proliferator-activated receptor-γ deletion in smooth muscle cells impairs intravascular thermoregulation and enhances atherosclerosis. *Circulation* 126, 1067–1078. doi: 10.1161/CIRCULATIONAHA.112.104489

Chatterjee, T. K., Stoll, L. L., Denning, G. M., Harrelson, A., Blomkalns, A. L., Idelman, G., et al. (2009). Proinflammatory phenotype of perivascular adipocytes: influence of high-fat feeding. *Circ. Res.* 104, 541–549. doi: 10.1161/CIRCRESAHA.108.182998

Creager, M. A., Cooke, J. P., Mendelsohn, M. E., Gallagher, S. J., Coleman, S. M., Loscalzo, J., et al. (1990). Impaired vasodilation of forearm resistance vessels in hypercholesterolemic humans. *J. Clin. Invest.* 86, 228–234. doi: 10.1172/JCI114688

Creager, M. A., Gallagher, S. J., Girerd, X. J., Coleman, S. M., Dzau, V. J., and Cooke, J. P. (1992). L-arginine improves endothelium-dependent vasodilation in hypercholesterolemic humans. *J. Clin. Invest.* 90, 1248–1253. doi: 10.1172/JCI115987

Cybularz, M., Langbein, H., Zatschler, B., Brunssen, C., Deussen, A., Matschke, K., et al. (2017). Endothelial function and gene expression in perivascular adipose tissue from internal mammary arteries of obese patients with coronary artery disease. *Atheroscler. Suppl.* 30, 149–158. doi: 10.1016/j.atherosclerosissup.2017.05.042

da Silva Franco, N., Lubaczeuski, C., Guizoni, D. M., Victorio, J. A., Santos-Silva, J. C., Brum, P. C., et al. (2017). Propranolol treatment lowers blood pressure, reduces vascular inflammatory markers and improves endothelial function in obese mice. *Pharmacol. Res.* 122, 35–45. doi: 10.1016/j.phrs.2017.05.018

Davel, A. P., Ceravolo, G. S., Wenceslau, C. F., Carvalho, M. H., Brum, P. C., and Rossoni, L. V. (2012). Increased vascular contractility and oxidative stress in β2-Adrenoceptor knockout mice: the role of NADPH oxidase. *J. Vasc. Res.* 49, 342–352. doi: 10.1159/000337486

Dorighello, G. G., Paim, B. A., Kiihl, S. F., Ferreira, M. S., Catharino, R. R., Vercesi, A. E., et al. (2016). Correlation between mitochondrial reactive oxygen and severity of atherosclerosis. *Oxidative Med. Cell. Longev.* 2016:7843685. doi: 10.1155/2016/7843685

Dorighello, G. G., Paim, B. A., Leite, A. C., Vercesi, A. E., and Oliveira, H. C. (2017). Spontaneous experimental atherosclerosis in hypercholesterolemic mice advances with ageing and correlates with mitochondrial reactive oxygen species. *Exp. Gerontol.* doi: 10.1016/j.exger.2017.02.010. [Epub ahead of print].

Eringa, E. C., Stehouwer, C. D., van Nieuw Amerongen, G. P., Ouwehand, L., Westerhof, N., and Sipkema, P. (2004). Vasoconstrictor effects of insulin in skeletal muscle arterioles are mediated by ERK1/2 activation in endothelium. *Am. J. Physiol. Heart Circ. Physiol.* 287, H2043–H2048. doi: 10.1152/ajpheart.00067.2004

Feron, O., Dessy, C., Moniotte, S., Desager, J. P., and Balligand, J. L. (1999). Hypercholesterolemia decreases nitric oxide production by promoting the interaction of caveolin and endothelial nitric oxide synthase. *J. Clin. Invest.* 103, 897–905. doi: 10.1172/JCI4829

Fésüs, G., Dubroska, G., Gorzelnial, K., Kluge, R., Huang, Y., Luft, F. C., et al. (2007). Adiponectin is a novel humoral vasodilator. *Cardiovasc. Res.* 75, 719–727. doi: 10.1016/j.cardiores.2007.05.025

Gil-Ortega, M., Stucchi, P., Guzmán-Ruiz, R., Cano, V., Arribas, S., González, M. C., et al. (2010). Adaptative nitric oxide overproduction in perivascular adipose tissue during early diet-induced obesity. *Endocrinology* 151, 3299–3306. doi: 10.1210/en.2009-1464

Guizoni, D. M., Dorighello, G. G., Oliveira, H. C., Delbin, M. A., Krieger, M. H., and Davel, A. P. (2016). Aerobic exercise training protects against endothelial dysfunction by increasing nitric oxide and hydrogen peroxide production in LDL receptor-deficient mice. *J. Transl. Med.* 14:213. doi: 10.1186/s12967-016-0972-z

Guzik, T. J., West, N. E., Black, E., McDonald, D., Ratnatunga, C., Pillai, R., et al. (2000). Vascular superoxide production by NAD(P)H oxidase: association with endothelial dysfunction and clinical risk factors. *Circ. Res.* 86, e85–e90. doi: 10.1161/01.RES.86.9.e85

Heitzer, T., Schlinzig, T., Krohn, K., Meinertz, T., and Münzel, T. (2001). Endothelial dysfunction, oxidative stress, and risk of cardiovascular events in patients with coronary artery disease. *Circulation* 104, 2673–2678. doi: 10.1161/hc4601.099485

Hofmann, A., Brunssen, C., Poitz, D. M., Langbein, H., Strasser, R. H., Henle, T., et al. (2017). Lectin-like oxidized low-density lipoprotein receptor-1 promotes endothelial dysfunction in LDL receptor knockout background. *Atheroscler. Suppl.* 30, 294–302. doi: 10.1016/j.atherosclerosissup.2017.05.020

Kauser, K., da Cunha, V., Fitch, R., Mallari, C., and Rubanyi, G. M. (2000). Role of endogenous nitric oxide in progression of atherosclerosis in apolipoprotein E-deficient mice. *Am. J. Physiol. Heart Circ. Physiol.* 278, H1679–H1685. doi: 10.1152/ajpheart.2000.278.5.H1679

Ketonen, J., Shi, J., Martonen, E., and Mervaala, E. (2010). Periadventitial adipose tissue promotes endothelial dysfunction via oxidative stress in diet-induced obese C57Bl/6 mice. *Circ. J.* 74,1479–1487. doi: 10.1253/circj.CJ-09-0661

Langbein, H., Brunssen, C., Hofmann, A., Cimalla, P., Brux, M., Bornstein, S. R., et al. (2016). NADPH oxidase 4 protects against development of endothelial dysfunction and atherosclerosis in LDL receptor deficient mice. *Eur. Heart J.* 37, 1753–1761. doi: 10.1093/eurheartj/ehv564

Langbein, H., Hofmann, A., Brunssen, C., Goettsch, W., and Morawietz, H. (2015). Impact of high-fat diet and voluntary running on body weight and endothelial function in LDL receptor knockout mice. *Atheroscler. Suppl.* 18, 59–66. doi: 10.1016/j.atherosclerosissup.2015.02.010

Li, C., Wang, Z., Wang, C., Ma, Q., and Zhao, Y. (2015). Perivascular adipose tissue-derived adiponectin inhibits collar-induced carotid atherosclerosis by promoting macrophage autophagy. *PLoS ONE* 10:e0124031. doi: 10.1371/journal.pone.0124031

Li, Y., Mihara, K., Saifeddine, M., Krawetz, A., Lau, D. C., Li, H., et al. (2011). Perivascular adipose tissue-derived relaxation factors: release by peptide agonists via proteinase-activated receptor-2 (PAR2) and non-PAR2 mechanisms. *Br. J. Pharmacol.* 164, 1990–2002. doi: 10.1111/j.1476-5381.2011.01501.x

Liu, Y., Li, D., Zhang, Y., Sun, R., and Xia, M. (2014). Anthocyanin increases adiponectin secretion and protects against diabetes-related endothelial dysfunction. *Am. J. Physiol. Endocrinol. Metab.* 306, E975–E988. doi: 10.1152/ajpendo.00699.2013

Margaritis, M., Antonopoulos, A. S., Digby, J., Lee, R., Reilly, S., Coutinho, P., et al. (2013). Interactions between vascular wall and perivascular adipose tissue reveal novel roles for adiponectin in the regulation of endothelial nitric oxide synthase function in human vessels. *Circulation* 127, 2209–2221. doi: 10.1161/CIRCULATIONAHA.112.001133

Moe, K. T., Naylynn, T. M., Yin, N. O., Khairunnisa, K., Allen, J. C., Wong, M. C., et al. (2013). Tumor necrosis factor-alpha induces aortic intima-media

thickening via perivascular adipose tissue inflammation. *J. Vasc. Res.* 50, 228–237. doi: 10.1159/000350542

Montagnani, M., Ravichandran, L. V., Chen, H., Esposito, D. L., and Quon, M. J. (2002). Insulin receptor substrate-1 and phosphoinositide-dependent kinase-1 are required for insulin-stimulated production of nitric oxide in endothelial cells. *Mol. Endocrinol.* 16, 1931–1942. doi: 10.1210/me.2002-0074

Mozaffarian, D., Benjamin, E. J., Go, A. S., Arnett, D. K., Blaha, M. J., Cushman, M., et al. (2016). Heart disease and stroke statistics-2016 update: a report from the American Heart Association. *Circulation* 133, e38–360. doi: 10.1161/CIR.0000000000000366

Öhman, M. K., Luo, W., Wang, H., Guo, C., Abdallah, W., Russo, H. M., et al. (2011). Perivascular visceral adipose tissue induces atherosclerosis in apolipoprotein E deficient mice. *Atherosclerosis* 219, 33–39. doi: 10.1016/j.atherosclerosis.2011.07.012

Potenza, M. A., Addabbo, F., and Montagnani, M. (2009). Vascular actions of insulin with implications for endothelial dysfunction. *Am. J. Physiol. Endocrinol. Metab.* 297, E568–E577. doi: 10.1152/ajpendo.00297.2009

Rabelo, L. A., Cortes, S. F., Alvarez-Leite, J. I., and Lemos, V. S. (2003). Endothelium dysfunction in LDL receptor knockout mice: a role for H_2O_2. *Br. J. Pharmacol.* 138, 1215–1220. doi: 10.1038/sj.bjp.0705164

Ruan, H., and Dong, L. Q. (2016). Adiponectin signaling and function in insulin target tissues. *J. Mol. Cell Biol.* 8, 101–109. doi: 10.1093/jmcb/mjw014

Siasos, G., Tousoulis, D., Antoniades, C., Stefanadi, E., and Stefanadis, C. (2007). L-Arginine, the substrate for NO synthesis: an alternative treatment for premature atherosclerosis? *Int. J. Cardiol.* 116, 300–308. doi: 10.1016/j.ijcard.2006.04.062

Souza, J. C., Vanzela, E. C., Ribeiro, R. A., Rezende, L. F., de Oliveira, C. A., Carneiro, E. M., et al. (2013). Cholesterol reduction ameliorates glucose-induced calcium handling and insulin secretion in islets from low-density lipoprotein receptor knockout mice. *Biochim. Biophys. Acta* 1831, 769–775. doi: 10.1016/j.bbalip.2012.12.013

Srikakulapu, P., Upadhye, A., Rosenfeld, S. M., Marshall, M. A., McSkimming, C., and Hickman, A. W. (2017). Perivascular adipose tissue harbors atheroprotective IgM-producing B cells. *Front Physiol.* 8:719. doi: 10.3389/fphys.2017.00719

Stapleton, P. A., Goodwill, A. G., James, M. E., Brock, R. W., and Frisbee, J. C. (2010). Hypercholesterolemia and microvascular dysfunction: interventional strategies. *J. Inflamm.* 7:54. doi: 10.1186/1476-9255-7-54

Takaoka, M., Suzuki, H., Shioda, S., Sekikawa, K., Saito, Y., Nagai, R., et al. (2010). Endovascular injury induces rapid phenotypic changes in perivascular adipose tissue. *Arterioscler. Thromb. Vasc. Biol.* 30, 1576–1582. doi: 10.1161/ATVBAHA.110.207175

van Dam, A. D., Boon, M. R., Berbée, J. F. P., Rensen, P. C. N., and van Harmelen, V. (2017). Targeting white, brown and perivascular adipose tissue in atherosclerosis development. *Eur. J. Pharmacol.* 816, 82–92. doi: 10.1016/j.ejphar.2017.03.051

Vanhoutte, P. M. (2003). Endothelial control of vasomotor function: from health to coronary disease. *Circ. J.* 67, 572–575. doi: 10.1253/circj.67.572

Victorio, J. A., Fontes, M. T., Rossoni, L. V., and Davel, A. P. (2016). Different anti-contractile function and nitric oxide production of thoracic and abdominal perivascular adipose tissues. *Front. Physiol.* 7:295. doi: 10.3389/fphys.2016.00295

World Health Organization (2014). *The Top 10 Causes of Death. Fact Sheet N° 310.* Available online at: http://www.whoint/mediacentre/factsheets/fs310/en/index.html

Wu, H. Y., Jeng, Y. Y., Yue, C. J., Chyu, K. Y., Hsueh, W. A., and Chan, T. M. (1994). Endothelial-dependent vascular effects of insulin and insulin-like growth factor I in the perfused rat mesenteric artery and aortic ring. *Diabetes* 43, 1027–1032. doi: 10.2337/diab.43.8.1027

Xia, N., Horke, S., Habermeier, A., Closs, E. I., Reifenberg, G., Gericke, A., et al. (2016). Uncoupling of endothelial nitric oxide synthase in perivascular adipose tissue of diet-induced obese mice. *Arterioscler. Thromb. Vasc. Biol.* 36, 78–85. doi: 10.1161/ATVBAHA.115.306263

Zhou, X., and He, P. (2011). Improved measurements of intracellular nitric oxide in intact microvessels using 4,5-diaminofluorescein diacetate. *Am. J. Physiol. Heart Circ. Physiol.* 301, H108–H114. doi: 10.1152/ajpheart.00195.2011

Conflict of Interest Statement: The authors declare that the research was conducted in the absence of any commercial or financial relationships that could be construed as a potential conflict of interest.

frontiers in Physiology

REVIEW
published: 13 February 2018
doi: 10.3389/fphys.2018.00003

Roles of Perivascular Adipose Tissue in the Pathogenesis of Atherosclerosis

Kimie Tanaka[1] *and Masataka Sata*[2]*

[1] Division for Health Service Promotion, The University of Tokyo, Tokyo, Japan, [2] Department of Cardiovascular Medicine, Institute of Biomedical Sciences, Tokushima University Graduate School, Tokushima, Japan

Traditionally, it is believed that white adipose tissues serve as energy storage, heat insulation, and mechanical cushion, whereas non-shivering thermogenesis occurs in brown adipose tissue. Recent evidence revealed that adipose tissue secretes many types of cytokines, called as adipocytokines, which modulate glucose metabolism, lipid profile, appetite, fibrinolysis, blood pressure, and inflammation. Most of the arteries are surrounded by perivascular adipose tissue (PVAT). PVAT has been thought to be simply a structurally supportive tissue for vasculature. However, recent studies showed that PVAT influences vasodilation and vasocontraction, suggesting that PVAT regulates vascular tone and diameter. Adipocytokines secreted from PVAT appear to have direct access to the adjacent arterial wall by diffusion or via vasa vasorum. In fact, PVAT around atherosclerotic lesions and mechanically-injured arteries displayed inflammatory cytokine profiles, suggesting that PVAT functions to promote vascular lesion formation. Many clinical studies revealed that increased accumulation of epicardial adipose tissue (EAT), which surrounds coronary arteries, is associated with coronary artery disease. In this review article, we will summarize recent findings about potential roles of PVAT in the pathogenesis of atherosclerosis, particularly focusing on a series of basic and clinical studies from our laboratory.

Keywords: perivascular adipose tissue, atherosclerosis, epicardial adipose tissue, inflammation, adipocytokine

OPEN ACCESS

Edited by:
Stephanie W. Watts,
Michigan State University,
United States

Reviewed by:
Irena Levitan,
University of Illinois at Chicago,
United States
Klaus Ley,
La Jolla Institute for Allergy and Immunology (LJI), United States

***Correspondence:**
Masataka Sata
masataka.sata@tokushima-u.ac.jp

Specialty section:
This article was submitted to Vascular Physiology, a section of the journal Frontiers in Physiology

Received: *30 September 2017*
Accepted: *03 January 2018*
Published: *13 February 2018*

Citation:
Tanaka K and Sata M (2018) Roles of Perivascular Adipose Tissue in the Pathogenesis of Atherosclerosis. Front. Physiol. 9:3. doi: 10.3389/fphys.2018.00003

PERIVASCULAR ADIPOSE TISSUE AND ADIPOCYTOKINES

It has been believed that atherosclerotic process is initiated by endothelial injury, followed by inflammatory cells infiltration into the subendothelial layer. Thus, inflammation spreads from the inside toward the outside of the artery (Ross, 1999). On the other hand, it is assumed that inflammatory process also progresses from the outside toward the inside. Most of the arteries surrounded by perivascular adipose tissue (PVAT). Aorta has abundant PVAT (Szasz et al., 2013), while PVAT is not detected around cerebral arteries and microvessels. There is no distinct borderline between arterial adventitia and PVAT. PVAT has been considered as simply a supporting organ of vasculature.

In 1991, Soltis and Cassis demonstrated that perivascular adipose tissue significantly influences vascular responsiveness to contractile stimuli using rat aortic rings with or without surrounding adipose tissues (Soltis and Cassis, 1991). This study suggested that PVAT potentially serves as a regulator of vascular responsiveness (Soltis and Cassis, 1991). Recently, adipose tissue have received a lot of attention as endocrine organ. It was reported that adipocytes secrete numerous kinds of

inflammatory and anti-inflammatory cytokines, called as "adipocytokines," such as tumor necrosis factor (TNF)-α and adiponectin (Matsuzawa et al., 2004). Analyses of human samples showed that PVAT around the coronary arteries, like other adipose tissues, expresses inflammatory cytokines, and chemokines (Mazurek et al., 2003; Henrichot et al., 2005). It was also reported that PVAT secretes reactive oxygen spices, nitric oxide, angiotensin II, and free fatty acid (Szasz et al., 2013). Adipocytokines secreted from PVAT appear to have direct access to the adjacent arterial wall via diffusion or vasa vasorum (Sacks and Fain, 2007; Tanaka et al., 2011) (**Figure 1**).

INFLUENCE OF PVAT ON ENDOTHELIAL FUNCTION AND VASCULAR LESION FORMATION: LESSONS FROM ANIMAL MODELS

We evaluated whether inflammation in PVAT affects the lesion formation after a mechanical vascular injury in murine femoral artery (Takaoka et al., 2009) (**Figure 2**). Wild-type (C57BL/6) mice received either a standard chow diet or a high-fat high-sucrose (HF/HS) diet. The body weight of the wild-type mice increased by 54% with a HF/HS feeding. The number of macrophages accumulated in PVAT increased by HF/HS diet. Expression of adiponectin was down-regulated, while expression of inflammatory cytokines was up-regulated in PVAT of mice fed on HF/HS diet. A wire was inserted into the femoral artery of mice to induce endothelial denudation and over-dilatation of the femoral artery. The changes in cytokine expression in PVAT around the injured artery was associated with exaggerated neointima formation at 4 weeks after the injury, suggesting that PVAT influences pathological vascular remodeling in response to mechanical vascular injury.

We also investigated an atheroprotective role of healthy PVAT by removing PVAT in mice fed on a standard diet. Removal of healthy PVAT markedly enhanced neointima formation, which was attenuated by transplantation of subcutaneous fat tissues from the mice fed on a standard diet. The results suggest an atheroprotective role of healthy PVAT. On the other hand, transplantation of subcutaneous fat from the obese mice or visceral fat failed to show atheroprotective effect. To investigate the local effects of PVAT adiponectin on vascular remodeling, recombinant adiponectin was delivered locally to the adventitial space in adiponectin-deficient mice, using gelatin hydrogel. Four weeks after endovascular injury, neointima formation was reduced by perivascular delivery of adiponectin. Taken together, it was suggested that PVAT functions to prevent lesion formation by secreting atheroprotective adipokines, such as adiponectin. However, obesity alters adipocytokine expression profiles of PVAT, resulting in enhanced neointima formation after vascular injury (Takaoka et al., 2009).

We also reported that mechanical endovascular injury alters adipocytokine expression in PVAT (Takaoka et al., 2010). A wire was inserted into the femoral artery of mice to induce endothelial denudation and over-dilatation. We found that this mechanical

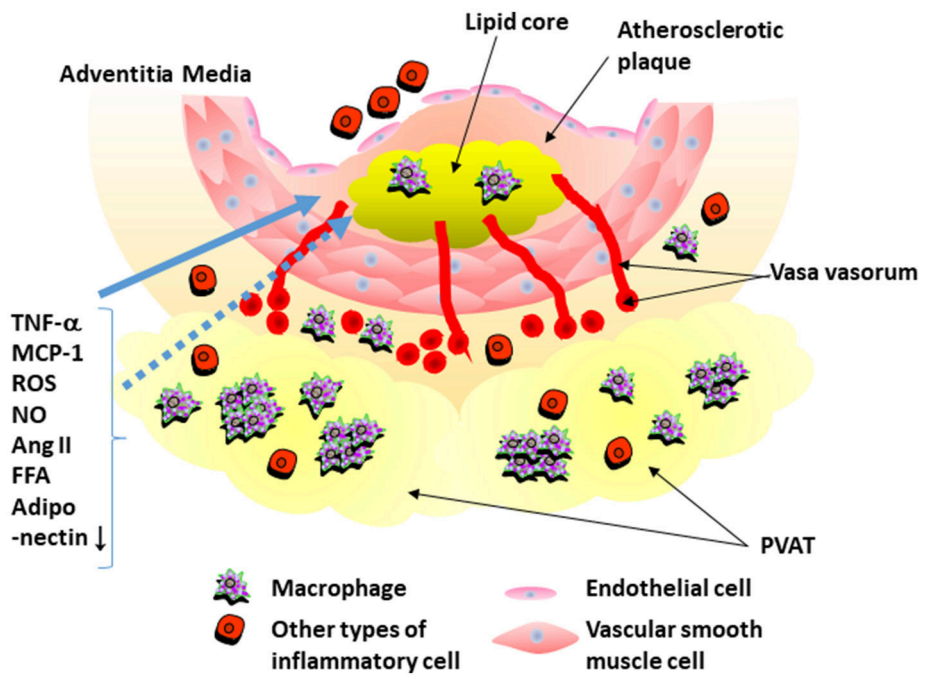

FIGURE 1 | Interaction of perivascular adipose tissue and atherosclerotic plaque. Perivascular adipose tissue (PVAT) secretes inflammatory cytokines that recruit inflammatory cells into PVAT. PVAT also secrets reactive oxygen spices (ROS), nitric oxide (NO), angiotensin II, and free fatty acid (FFA). Expression of adiponectin is decreased in PVAT around atherosclerotic plaque. Adipocytokines secreted from PVAT appear to have direct access to the adjacent arterial wall by diffusion or via vasa vasorum. TNF-α, tumor necrosis factor-α; Ang II, angiotensin II; MCP-1, monocyte chemoattractant protein-1.

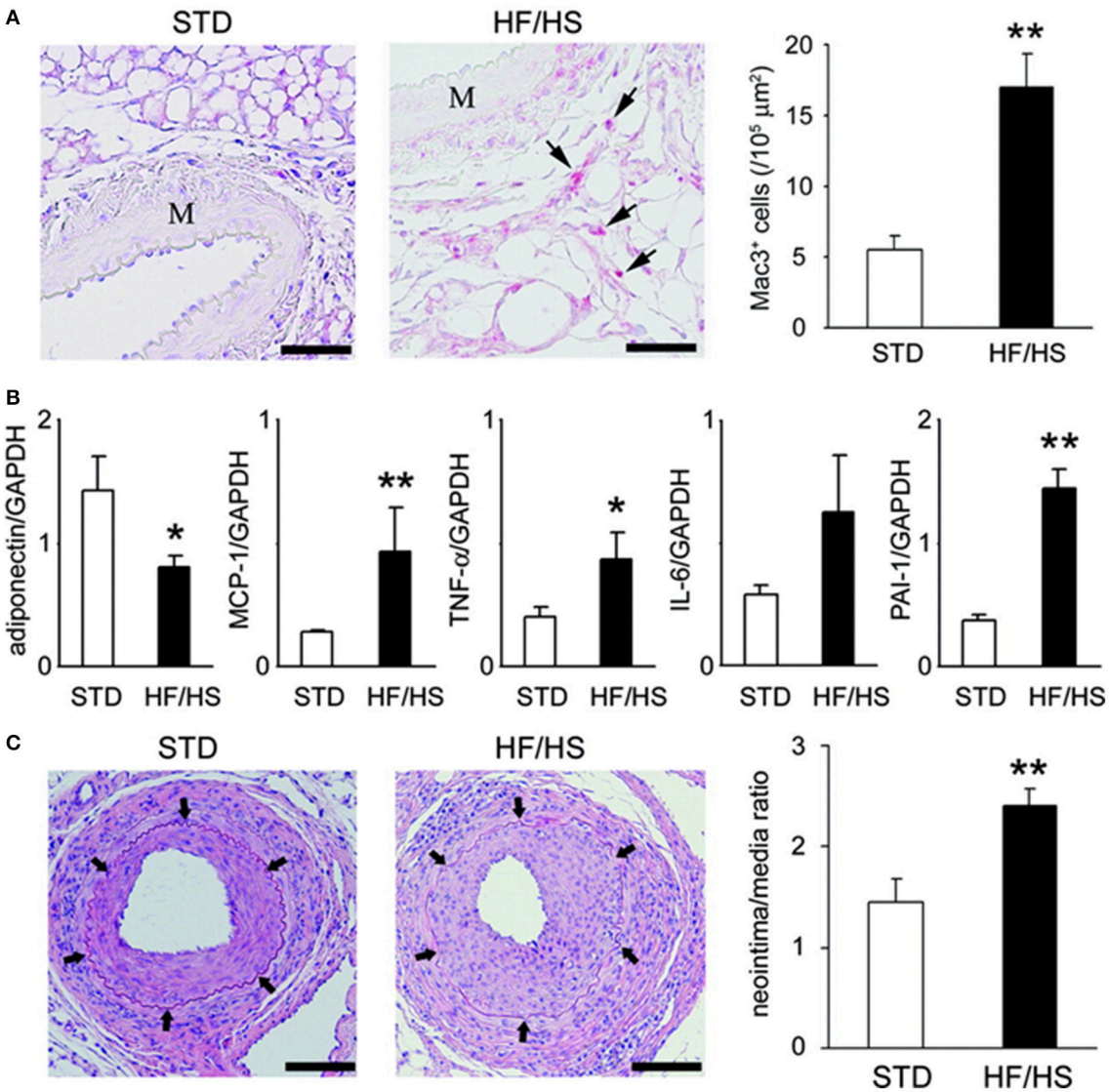

FIGURE 2 | Obesity-induced inflammatory changes in periadventitial fat enhanced neointimal hyperplasia. **(A)** Obesity-induced accumulation of inflammatory cells in periadventitial fat. Immunohistochemical analysis showed accumulation of Mac3-positive macrophages (arrows) within periadventitial fat in obese mice. Scale bar: 50 μm. Results are expressed as mean ± SEM. $^{**}P < 0.01$. M indicates media of femoral artery. **(B)** Expression of mRNA in periadventitial fat around femoral artery from STD (standard diet) ($n = 6$) and HF/HS (high fat/high sucrose diet) WT C57BL6 mice. Expression level was assessed by real-time PCR normalized to each GAPDH level. Results are expressed as means ± SEM. $^{*}P < 0.05$, $^{**}P < 0.01$. **(C)** Hematoxylin/eosin-stained sections of femoral arteries from mice fed on STD or HF/HS diet 4 weeks after endovascular injury. Arrows indicate internal elastic lamina. Scale bar: 100 μm. Morphometric analysis of injured femoral arteries in lean ($n = 7$) and obese ($n = 6$) mice 4 weeks after wire-induced injury. Results are expressed as means ± SEM. $^{**}P < 0.01$. All figures are cited from the reference (Takaoka et al., 2009) with permission.

injury up-regulated inflammatory cytokines and down-regulated adiponectin in PVAT. These changes were attenuated in TNF-α knockout mice, suggesting that TNF-α is important to transmit endovascular injury to adipocytokine changes in PVAT (Takaoka et al., 2010).

Consistent with our studies, others reported that PVAT plays a role in the pathogenesis of vascular lesion formation. Ketonen et al. reported that obesity-induced endothelial dysfunction is caused by increased oxidative stress and enhanced expression of inflammatory cytokine in PVAT (Ketonen et al., 2010). Manka et al. reported that transplantation of PVAT from obese mice to low-density lipoprotein receptor knockout mice enhanced lesion formation with increased inflammatory cell infiltration and pathological angiogenesis in adventitia. Theses pathological effects of PVAT transplantation was attenuated when PVAT from monocyte chemoattractant protein-1 (MCP-1)-deficient mice was transplanted. These results suggest that PVAT promotes vascular lesion formation through MCP-1-dependent mechanisms (Manka et al., 2014). These animal studies indicate that obesity increases expression of inflammatory adipocytokines

in PVAT, leading to endothelial dysfunction and enhanced vascular lesion formation.

POSSIBLE ROLES OF EPICARDIAL ADIPOSE TISSUE IN THE PATHOGENESIS OF HUMAN CORONARY ARTERY DISEASE

Epicardial adipose tissue (EAT) is assumed to secrete abundant cytokines to the adjacent coronary artery (Sacks and Fain, 2007). For example, in the patients undergoing coronary artery bypass graft (CABG) surgery, it was reported that EAT abundantly expressed interleukin (IL)-1β, IL-6, TNF-α, and MCP-1 compared to their subcutaneous adipose tissue (Mazurek et al., 2003). Baker et al. reported that the expression of adiponectin mRNA was significantly lower in EAT than in gluteal and abdominal adipose tissues (Baker et al., 2006).

However, it remains to be elucidated whether the potential role of chronic inflammation in EAT plays a role in the pathogenesis of coronary artery disease (CAD). Therefore, we analyzed EAT obtained during cardiac surgery (Hirata et al., 2011a,b). EAT and subcutaneous adipose tissue (SCAT) were obtained from 38 CAD patients undergoing CABG and 40 non-CAD patients undergoing valvular surgery (Hirata et al., 2011b). Expressions of IL-6 and TNF-α were significantly increased in EAT of the CAD group compared to that of the non-CAD group. There was no significant difference between the CAD and the non-CAD groups in the expression of adipocytokines in SCAT. To investigate the mechanisms by which expression of inflammatory cytokines is elevated in EAT of the CAD patients, we performed immunohistochemistry against CD68, a marker for all types of macrophages, CD11c, a marker for inflammatory M1 macrophage (Lumeng et al., 2007), and CD206, a marker for anti-inflammatory M2 macrophage (Bourlier et al., 2008) (**Figure 3**). CD68 positive macrophages were significantly increased in EAT of the CAD group. The ratio of CD11c/CD68-positive cells was significantly increased, and the ratio of CD206/CD68-positive cells was significantly decreased in EAT in the CAD group. These data demonstrate relative increase of M1 macrophages and relative decrease of M2 macrophages in EAT in the CAD group. The ratio of M1/M2 macrophages showed positive correlation with the severity of CAD as determined by Gensini score (Gensini, 1983). These results suggested that the chronic inflammation and macrophage polarization in EAT would play a pathological role in human coronary atherosclerosis.

Recently, it was reported that the expression of omentin was detected in EAT. Omentin, also known as interectin-1, is one of the recently identified adipocytokines (Harada et al., 2016). Omentin is expressed abundantly in omentum adipose tissue and is considered to have cardiovascular protective effects like adiponectin. It is known that omentin expression decreases in the milieus of diabetes mellitus or obesity (Shibata et al., 2017). Harada et al. analyzed EAT and SCAT from 15 non-obese CAD patients and 10 non-obese and non-CAD patients. Omentin expression increased in the EAT of non-obese CAD patients, despite a decrease in plasma levels. These results indicated that

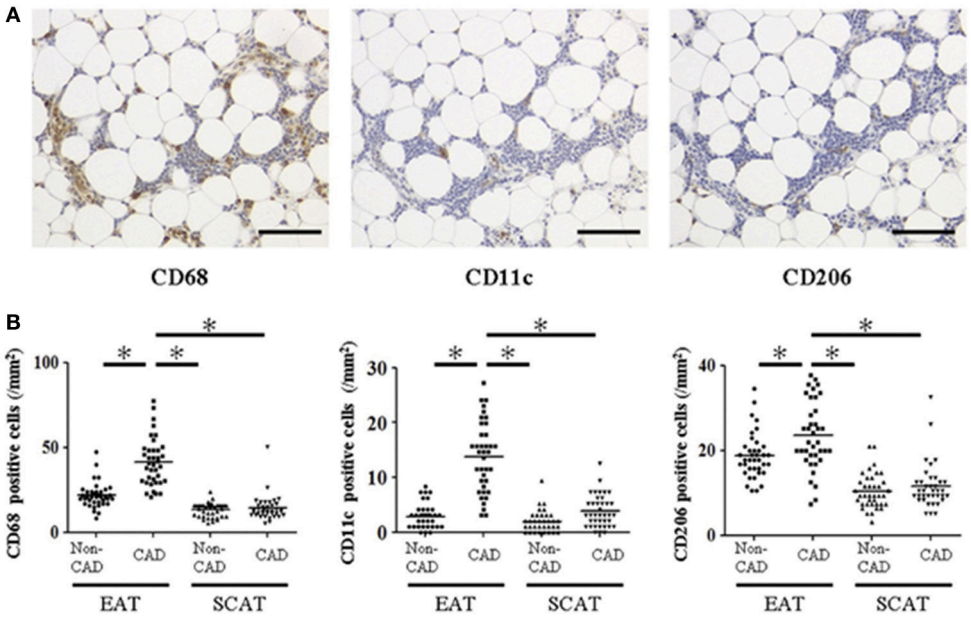

FIGURE 3 | Macrophage infiltration in human epicardial adipose tissue and subcutaneous adipose tissue. **(A)** Representative images of immunohistochemical staining showing accumulation of CD68-, CD11c-, and CD206-positive cells in epicardial adipose tissue (EAT) of coronary artery disease (CAD) patient. Scale bar = 100 μm. **(B)** Cell count of accumulating macrophages. Each point represents the cell count of infiltrating macrophages (/mm^2). Bar indicates mean. *$p < 0.05$. SCAT, subcutaneous adipose tissue. All figures are cited from the reference (Hirata et al., 2011b) with permission.

omentin expression in EAT may play a certain role in the pathogenesis of CAD (Harada et al., 2016).

EPICARDIAL ADIPOSE TISSUE VOLUME AND CORONARY ARTERY DISEASE

More than 200 years ago, an autopsy report of the case of a patient, who died in 1801, already described that CAD was combined with unusual accumulation of fat about the heart (Warren, 1962). Recently, many groups including us suggested that CAD is associated with increased EAT volume (Dagvasumberel et al., 2012). EAT volume can be quantified by coronary CT, echocardiography and MRI (magnetic resonance imaging). Konishi et al. measured "pericardial adipose tissue" volume by 64-slice CT, and suggested that CAD is more highly associated with pericardial fat volume than abdominal obesity (Konishi et al., 2010). Other studies also suggested that EAT volume may predict the severity of coronary atherosclerotic lesions and the clinical prognoses (Dagvasumberel et al., 2012). Moreover, a recent study indicated that EAT volume predicts fatal and non-fatal cardiac events independently of the classical coronary risk factors (Mahabadi et al., 2013). We also investigated the impact of EAT volume on CAD (Dagvasumberel et al., 2012). Multivariate analysis indicated that EAT volume index [EAT volume/body surface area (BSA)] were significant CAD predictors in men, whereas BMI, age, presence of hypertension, diabetes mellitus, and hyperlipidemia were not associated with the presence of CAD.

Previous studies suggested that increased visceral adipose tissue (VAT) is associated with CAD. For example, the prospective long-term follow-up of the Framingham Heart Study showed that VAT was an independent predictor of incident of cardiovascular disease (Britton et al., 2013). Accumulating evidence suggests that inflammatory cells can be observed in VAT than in SCAT and that VAT secretes more inflammatory adipocytokines than SCAT (Ibrahim, 2010). It is also suggested that VAT adipocytes plays more important roles in the pathogenesis of insulin resistance than SCAT adipocytes does (Ibrahim, 2010). Thus, it is likely that VAT influences vascular function and atherosclerosis than SCAT does.

We collected EAT and SCAT from 50 CAD patients and 50 non-CAD patients who underwent elective cardiac surgery. We evaluated the polarity of the accumulated macrophages in adipose tissue by immunohistochemical staining with the antibodies for CD68, CD11c, and CD206 and compared them with EAT volume index (**Figure 4**) (Shimabukuro et al., 2013). We found that EAT volume index was a significant prognostic factor to predict CAD. There were positive correlations between EAT volume index and the numbers of CD68 and CD11c positive M1 macrophage, and the expressions of inflammatory cytokines such as IL-1β, and negatively correlated with adiponectin expression in EAT (Shimabukuro et al., 2013). A multivariate analysis model revealed that number of CD68 (+) cells and IL-1β, and adiponectin expression in EAT strongly predicted CAD. These results indicated that EAT volume, macrophage infiltration, and adipocytokine signals in EAT are closely associated with CAD and that EAT volume and adipocytokine imbalance play critical roles in the pathogenesis of human coronary atherosclerosis.

Recent reports suggested that EAT accumulation is associated with not only coronary artery disease but also atrial fibrillation (AF) (Soeki and Sata, 2012). In Framingham heart cohort, EAT volume was measured by CT in 3217 subjects, and it was suggested that EAT volume was an independent risk factor of AF after adjusting other risk factors such as hypertension, PR interval, and body mass index (BMI) (Thanassoulis et al., 2010). Another study demonstrated that peri-atrial EAT volume was associated with new-onset AF in patients with CAD, independent of enlargement of the left atrium (Nakanishi et al., 2012). It is assumed that inflammatory cytokines secreted from peri-atrial EAT promote fibrotic remodeling of atrial myocardium, leading to AF (Hatem et al., 2016).

HOW TO EVALUATE EPICARDIAL ADIPOSITY?

Although many groups have investigated correlation between the EAT volume and coronary atherosclerotic lesions, there might be a confusion in definition of fat depots around the heart (Yamada and Sata, 2015). EAT, or subepicardial adipose tissue, located inside the parietal pericardium, have a direct contact with coronary artery (**Figure 5**). On the other hand, adipose tissue located outside the parietal pericardium is called as paracardial adipose tissue (PAT). PAT is also called as thoracic or intrathoracic adipose tissue. There is a difference in the definition of "pericardial adipose tissue." In some studies, PAT was described as "pericardial adipose tissue," whereas EAT or EAT together with PAT were described as "pericardial adipose tissue" in other studies (Yamada and Sata, 2015). EAT shares coronary circulation with cardiac myocardium, while PAT is perfused by non-coronary source. Thus, EAT and PAT are distinct fats with different impacts on coronary atherosclerosis (Yamada and Sata, 2015). We would like to define that "pericardial adipose tissue" means "epicardial adipose tissue" plus "paracardial adipose tissue."

To evaluate EAT accumulation, different groups use EAT volume (Konishi et al., 2010; Mahabadi et al., 2013) or EAT volume index, which is EAT volume divided by BSA. We found that the EAT volume was higher in men than in women, but the mean EAT volume/height and EAT volume/BSA were comparable (Dagvasumberel et al., 2012). Therefore, it is likely that EAT volume index might be a preferable parameter (Shimabukuro et al., 2013).

El Khoudary et al. assessed whether volumes of heart fat depots (EAT and PAT) were associated with coronary artery calcification (CAC) in women at midlife and whether these associations were modified by menopausal status and estradiol levels (El Khoudary et al., 2017). Volumes of PAT and EAT increased after menopause. Of note, estradiol decline was associated with PAT volume, but not EAT volume, suggesting that menopause has something to do with PAT accumulation. CAC measures were associate with EAT volume. Menopausal status or

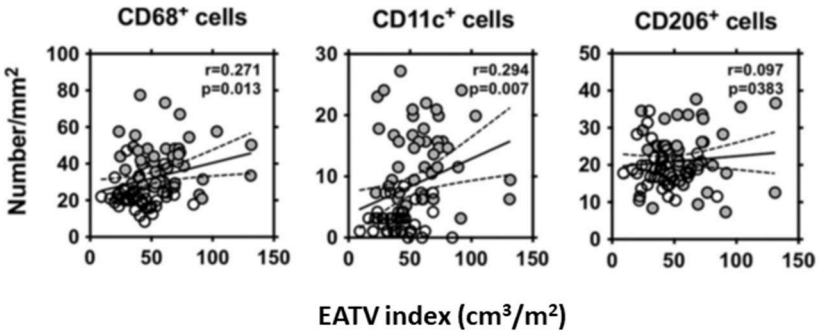

FIGURE 4 | Correlation between the EAT volume index and the number of CD68+, CD11c+, and CD206+ cells in EAT. The EAT volume index was positively correlated with the numbers of CD68+, and CD11c+ cells in EAT in the patients who underwent non-coronary (○) or coronary (•) surgery. Liner regression analysis was made in a combined group, including non-coronary artery disease (CAD) and CAD subjects. *R* and *P*-values are shown. EATV index, epicardial adipose tissue volume index. All figures cited from the reference (Shimabukuro et al., 2013) with permission.

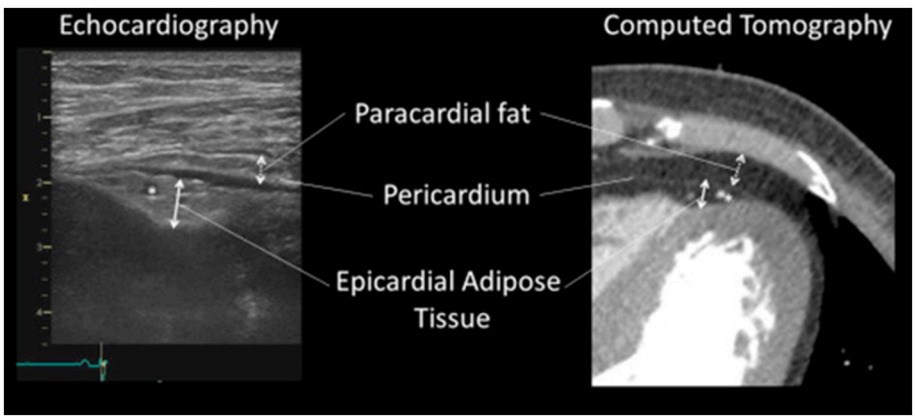

FIGURE 5 | Identification of epicardial adipose tissue and paracardial adipose tissue. Identification of epicardial adipose tissue and paracardial adipose tissue by echocardiography **(Left)** and contrast enhanced 320-slice multi-detector computed tomography **(Right)**. The asterisks (*) indicate left descending coronary artery. "Pericardial adipose tissue" includes both epicardial adipose tissue (located within or deep into the pericardium) and paracardial adipose tissue (located superficial to the pericardium). Sometimes, pericardial adipose tissue is referred to as paracardial adipose tissue. All figures cited from the reference (Yamada and Sata, 2015) without modification.

estradiol did not modify this association. In contrast, menopausal status significantly modified association between PAT and CAC measures. It was reported that PAT might be a risk factor for coronary artery disease in menopausal women. It was suggested that PAT depot need to be monitored and would be a target for intervention in women at midlife (El Khoudary et al., 2017).

Many groups measured EAT thickness using echocardiography and reported that EAT thickness was greater in CAD patients than in non-CAD patients (Iacobellis, 2015). Recently, we developed a new method to evaluate EAT thickness (Hirata et al., 2015). We evaluated EAT thickness at anterior interventricular groove (EAT-AIG) and at anterior right ventricle (EAT-RV) of 311 patients by echocardiography using a high frequency linear probe. EAT-AIG had a strong correlation with EAT volume evaluated by coronary CT. Both EAT-AIG and EAT-RV of CAD patients were greater than those of non-CAD patients. EAT-AIG was more strongly correlated with CAD as determined by the receiver operating characteristics curve analysis. It was suggested that we may be able to predict CAD with high sensitivity and specificity by evaluating EAT thickness by the non-invasive echocardiography using the high frequent linear probe (Hirata et al., 2015).

Nerlekar at al. performed meta-analysis to assess the association between EAT and high-risk plaque (HRP) (Nerlekar et al., 2017). Nine studies (n = 3,772 patients) were included with seven measuring EAT volume by CT and two measuring EAT thickness by echocardiography. Increase in EAT volume or thickness was associated with the presence of HRP. Increasing EAT volume has a significant association with HRP. However, EAT thickness had no significant association with HRP. This analysis included only two studies evaluating EAT thickness by echocardiography. Further investigation is required to establish clinical significance of evaluating EAT thickness to predict the existence of HRP.

Besides coronary CT and echocardiography, it was reported that EAT volume can be evaluated by MRI (Levelt et al., 2016).

There is no standard method to evaluate EAT volume to predict coronary atherosclerosis disease. It is hoped that EAT can be evaluated precisely and easily using appropriate modalities.

CAN PVAT BE REDUCED TO PREVENT CARDIOVASCULAR EVENTS?

It is very important to clarify whether modification of life-style or medication can reduce PVAT, leading to phenotypic improvement of inflammatory PVAT. It was reported that EAT was decreased by aerobic exercise for 12 weeks in obese middle-aged men (Kim et al., 1985). Interestingly, reduction in EAT volume showed linear correlation with reduction in VAT volume (Kim et al., 1985).

In a sub-analysis of BELLES (Beyond Endorsed Lipid Lowering with Electron Beam Tomography Scanning) trial, in which the effect of the moderate and the aggressive doses of statin therapy to coronary calcification were tested in 615 hyperlipidemic post-menopausal women, EAT volume was measured by CT in the intensive therapy group (atorvastatin 80 mg) and the moderate therapy group (pravastatin 40 mg). One year later, reduction of EAT volume was observed in the intensive and the moderate therapy groups. Decrease in EAT volume was statistically significant in the intensive therapy group, but not in the moderate therapy group. Interestingly, EAT volume reduction showed no correlation with the degree of lipid lowering. These results suggested that, in post-menopausal women, statin therapy decreased EAT volume especially in the intensive therapy group and that the effect of statin was not associated with the LDL lowering effect. Anti-inflammatory pleiotropic effects of statin might be related to this effect (Alexopoulos et al., 2013).

Recently, it was reported that sodium-glucose co-transporter 2 (SGLT2) inhibitors (ipragliflozin, luseogliflozin, and canagliflozin) reduced the EAT (Bouchi et al., 2017; Fukuda et al., 2017; Yagi et al., 2017) as well as the abdominal visceral fat (Tosaki et al., 2017) in type 2 diabetes patients. Recent randomized clinical trials showed that use of SGLT2 inhibitors (canagliflozin and empagliflozin) decreases mortality and morbidity of cardiovascular diseases in diabetic patients (Zinman et al., 2015; Neal et al., 2017). If SGLT2 inhibitors can decrease EAT volume as well as other adipose tissues, it is assumed that reduction in EAT could lead to cardiovascular protective effects by SGLT2 inhibitors, which have been proved by recent randomized clinical trials (Heerspink et al., 2016; Rajasekeran et al., 2016).

It remains to be clarified whether the decrease of EAT by any therapeutic interventions can inhibit progression of coronary lesions or the occurrence of coronary events. Further studies will clarify whether reduction in EAT volume could be a therapeutic target to prevent cardiovascular events.

CONCLUSIONS

PVAT has been considered to secrete humoral factors, influencing the function and the lesion formation of the adjacent artery. EAT volume can be measured by CT, echocardiography and MRI, which are commonly used in clinical practices. Numerous imaging studies suggested that increased EAT volume is associated with CAD. Almost all the data presented is correlative. It remains to be elucidated whether the reduction of EAT volume would be effective in prevention of cardiovascular events. Future studies will clarify more in detail the roles of PVAT in the pathogenesis of CAD. EAT would be a useful biomarker in the diagnosis of CAD and would be a good therapeutic target.

DISCLOSURES

MS received research funding from Takeda, Tanabe-Mitsubishi, Astellas, Daiichi-Sankyo, MSD, Bayer Healthcare, and Ono, and lecture fees from Takeda, Boehringer Ingelheim, Bayer Healthcare, Mochida, Astellas, Tanabe-Mitsubishi, Novartis, AstraZeneca, MSD, and Shionogi. The Department of Cardio-Diabetes Medicine, Tokushima University Graduate School, is supported in part by unrestricted research grants from Boehringer Ingelheim, Tanabe-Mitsubishi, Kowa, and Actelion.

AUTHOR CONTRIBUTIONS

All authors listed have made a substantial, direct and intellectual contribution to the work, and approved it for publication.

FUNDING

This work was partially supported by Japan Society for the Promotion of Science KAKENHI Grants (Number 26461141 to KT and Number 16H05299 & 26248050 to MS) and grants from The Vehicle Racing Commemorative Foundation (KT and MS), Mitsui Sumitomo Insurance Welfare Foundation (KT), The Uehara Memorial Foundation (MS), and Takeda Science Foundation (MS).

ACKNOWLEDGMENTS

The authors thank Hiromi Kato, Yumi Sugawara, Yumiko Saga, Shintaro Okamoto, and Etsuko Uematsu for their technical assistance.

REFERENCES

Alexopoulos, N., Melek, B. H., Arepalli, C. D., Hartlage, G. R., Chen, Z., Kim, S., et al. (2013). Effect of intensive versus moderate lipid-lowering therapy on epicardial adipose tissue in hyperlipidemic post-menopausal women: a substudy of the BELLES trial (Beyond Endorsed Lipid Lowering with EBT Scanning). *J. Am. Coll. Cardiol.* 61, 1956–1961. doi: 10.1016/j.jacc.2012.12.051

Baker, A. R., Silva, N. F., Quinn, D. W., Harte, A. L., Pagano, D., Bonser, R. S., et al. (2006). Human epicardial adipose tissue expresses a pathogenic profile of adipocytokines in patients with cardiovascular disease. *Cardiovasc. Diabetol.* 5:1. doi: 10.1186/1475-2840-5-1

Bouchi, R., Terashima, M., Sasahara, Y., Asakawa, M., Fukuda, T., Takeuchi, T., et al. (2017). Luseogliflozin reduces epicardial fat accumulation in

patients with type 2 diabetes: a pilot study. *Cardiovasc. Diabetol.* 16:32. doi: 10.1186/s12933-017-0516-8

Bourlier, V., Zakaroff-Girard, A., Miranville, A., De Barros, S., Maumus, M., Sengenes, C., et al. (2008). Remodeling phenotype of human subcutaneous adipose tissue macrophages. *Circulation* 117, 806–815. doi: 10.1161/CIRCULATIONAHA.107.724096

Britton, K. A., Massaro, J. M., Murabito, J. M., Kreger, B. E., Hoffmann, U., and Fox, C. S. (2013). Body fat distribution, incident cardiovascular disease, cancer, and all-cause mortality. *J. Am. Coll. Cardiol.* 62, 921–925. doi: 10.1016/j.jacc.2013.06.027

Dagvasumberel, M., Shimabukuro, M., Nishiuchi, T., Ueno, J., Takao, S., Fukuda, D., et al. (2012). Gender disparities in the association between epicardial adipose tissue volume and coronary atherosclerosis: a 3-dimensional cardiac computed tomography imaging study in Japanese subjects. *Cardiovasc. Diabetol.* 11:106. doi: 10.1186/1475-2840-11-106

El Khoudary, S. R., Shields, K. J., Janssen, I., Budoff, M. J., Everson-Rose, S. A., Powell, L. H., et al. (2017). Postmenopausal women with greater paracardial fat have more coronary artery calcification than premenopausal women: the study of women's health across the nation (SWAN) cardiovascular fat ancillary study. *J. Am. Heart Assoc.* 6:e004545. doi: 10.1161/JAHA.116.004545

Fukuda, T., Bouchi, R., Terashima, M., Sasahara, Y., Asakawa, M., Takeuchi, T., et al. (2017). Ipragliflozin reduces epicardial fat accumulation in non-obese Type 2 diabetic patients with visceral obesity: a pilot study. *Diabetes Ther.* 8, 851–861. doi: 10.1007/s13300-017-0279-y

Gensini, G. G. (1983). A more meaningful scoring system for determining the severity of coronary heart disease. *Am. J. Cardiol.* 51:606. doi: 10.1016/S0002-9149(83)80105-2

Harada, K., Shibata, R., Ouchi, N., Tokuda, Y., Funakubo, H., Suzuki, M., et al. (2016). Increased expression of the adipocytokine omentin in the epicardial adipose tissue of coronary artery disease patients. *Atherosclerosis* 251, 299–304. doi: 10.1016/j.atherosclerosis.2016.07.003

Hatem, S. N., Redheuil, A., and Gandjbakhch, E. (2016). Cardiac adipose tissue and atrial fibrillation: the perils of adiposity. *Cardiovasc. Res.* 109, 502–509. doi: 10.1093/cvr/cvw001

Heerspink, H. J., Perkins, B. A., Fitchett, D. H., Husain, M., and Cherney, D. Z. (2016). Sodium glucose cotransporter 2 inhibitors in the treatment of diabetes mellitus: cardiovascular and kidney effects, potential mechanisms, and clinical applications. *Circulation* 134, 752–772. doi: 10.1161/CIRCULATIONAHA.116.021887

Henrichot, E., Juge-Aubry, C. E., Pernin, A., Pache, J. C., Velebit, V., Dayer, J. M., et al. (2005). Production of chemokines by perivascular adipose tissue: a role in the pathogenesis of atherosclerosis? *Arterioscler. Thromb. Vasc. Biol.* 25, 2594–2599. doi: 10.1161/01.ATV.0000188508.40052.35

Hirata, Y., Kurobe, H., Akaike, M., Chikugo, F., Hori, T., Bando, Y., et al. (2011a). Enhanced inflammation in epicardial fat in patients with coronary artery disease. *Int. Heart J.* 52, 139–142. doi: 10.1536/ihj.52.139

Hirata, Y., Tabata, M., Kurobe, H., Motoki, T., Akaike, M., Nishio, C., et al. (2011b). Coronary atherosclerosis is associated with macrophage polarization in epicardial adipose tissue. *J. Am. Coll. Cardiol.* 58, 248–255. doi: 10.1016/j.jacc.2011.01.048

Hirata, Y., Yamada, H., Kusunose, K., Iwase, T., Nishio, S., Hayashi, S., et al. (2015). Clinical utility of measuring epicardial adipose tissue thickness with echocardiography using a high-frequency linear probe in patients with coronary artery disease. *J. Am. Soc. Echocardiogr.* 28, 1240–1246.e1. doi: 10.1016/j.echo.2015.07.006

Iacobellis, G. (2015). Local and systemic effects of the multifaceted epicardial adipose tissue depot. *Nat. Rev. Endocrinol.* 11, 363–371. doi: 10.1038/nrendo.2015.58

Ibrahim, M. M. (2010). Subcutaneous and visceral adipose tissue: structural and functional differences. *Obes. Rev.* 11, 11–18. doi: 10.1111/j.1467-789X.2009.00623.x

Ketonen, J., Shi, J., Martonen, E., and Mervaala, E. (2010). Periadventitial adipose tissue promotes endothelial dysfunction via oxidative stress in diet-induced obese C57Bl/6 mice. *Circ. J.* 74, 1479–1487. doi: 10.1253/circj.CJ-09-0661

Kim, M. K., Tomita, T., Kim, M. J., Sasai, H., Maeda, S., and Tanaka, K. (1985). Aerobic exercise training reduces epicardial fat in obese men. *J. Appl. Physiol.* 106, 5–11. doi: 10.1152/japplphysiol.90756.2008

Konishi, M., Sugiyama, S., Sugamura, K., Nozaki, T., Ohba, K., Matsubara, J., et al. (2010). Association of pericardial fat accumulation rather than abdominal obesity with coronary atherosclerotic plaque formation in patients with suspected coronary artery disease. *Atherosclerosis* 209, 573–578. doi: 10.1016/j.atherosclerosis.2009.10.008

Levelt, E., Pavlides, M., Banerjee, R., Mahmod, M., Kelly, C., Sellwood, J., et al. (2016). Ectopic and visceral fat deposition in lean and obese patients with Type 2 diabetes. *J. Am. Coll. Cardiol.* 68, 53–63. doi: 10.1016/j.jacc.2016.03.597

Lumeng, C. N., Bodzin, J. L., and Saltiel, A. R. (2007). Obesity induces a phenotypic switch in adipose tissue macrophage polarization. *J. Clin. Invest.* 117, 175–184. doi: 10.1172/JCI29881

Mahabadi, A. A., Berg, M. H., Lehmann, N., Kälsch, H., Bauer, M., Kara, K., et al. (2013). Association of epicardial fat with cardiovascular risk factors and incident myocardial infarction in the general population: the Heinz Nixdorf Recall Study. *J. Am. Coll. Cardiol.* 61, 1388–1395. doi: 10.1016/j.jacc.2012.11.062

Manka, D., Chatterjee, T. K., Stoll, L. L., Basford, J. E., Konaniah, E. S., Srinivasan, R., et al. (2014). Transplanted perivascular adipose tissue accelerates injury-induced neointimal hyperplasia: role of monocyte chemoattractant protein-1. *Arterioscler. Thromb. Vasc. Biol.* 34, 1723–1730. doi: 10.1161/ATVBAHA.114.303983

Matsuzawa, Y., Funahashi, T., Kihara, S., and Shimomura, I. (2004). Adiponectin and metabolic syndrome. *Arterioscler. Thromb. Vasc. Biol.* 24, 29–33. doi: 10.1161/01.ATV.0000099786.99623.EF

Mazurek, T., Zhang, L., Zalewski, A., Mannion, J. D., Diehl, J. T., Arafat, H., et al. (2003). Human epicardial adipose tissue is a source of inflammatory mediators. *Circulation* 108, 2460–2466. doi: 10.1161/01.CIR.0000099542.57313.C5

Nakanishi, K., Fukuda, S., Tanaka, A., Otsuka, K., Sakamoto, M., Taguchi, H., et al. (2012). Peri-atrial epicardial adipose tissue is associated with new-onset nonvalvular atrial fibrillation. *Circ. J.* 76, 2748–2754. doi: 10.1253/circj.CJ-12-0637

Neal, B., Perkovic, V., Mahaffey, K. W., de Zeeuw, D., Fulcher, G., Erondu, N., et al. (2017). Canagliflozin and cardiovascular and renal events in type 2 diabetes. *N. Engl. J. Med.* 377, 644–657. doi: 10.1056/NEJMoa1611925

Nerlekar, N., Brown, A. J., Muthalaly, R. G., Talman, A., Hettige, T., Cameron, J. D., et al. (2017). Association of epicardial adipose tissue and high-risk plaque characteristics: a systematic review and meta-analysis. *J. Am. Heart Assoc.* 6:e006379. doi: 10.1161/JAHA.117.006379

Rajasekeran, H., Lytvyn, Y., and Cherney, D. Z. (2016). Sodium-glucose cotransporter 2 inhibition and cardiovascular risk reduction in patients with type 2 diabetes: the emerging role of natriuresis. *Kidney Int.* 89, 524–526. doi: 10.1016/j.kint.2015.12.038

Ross, R. (1999). Atherosclerosis–an inflammatory disease. *N. Engl. J. Med.* 340, 115–126. doi: 10.1056/NEJM199901143400207

Sacks, H. S., and Fain, J. N. (2007). Human epicardial adipose tissue: a review. *Am. Heart J.* 153, 907–917. doi: 10.1016/j.ahj.2007.03.019

Shibata, R., Ouchi, N., Ohashi, K., and Murohara, T. (2017). The role of adipokines in cardiovascular disease. *J. Cardiol.* 70, 329–334. doi: 10.1016/j.jjcc.2017.02.006

Shimabukuro, M., Hirata, Y., Tabata, M., Dagvasumberel, M., Sato, H., Kurobe, H., et al. (2013). Epicardial adipose tissue volume and adipocytokine imbalance are strongly linked to human coronary atherosclerosis. *Arterioscler. Thromb. Vasc. Biol.* 33, 1077–1084. doi: 10.1161/ATVBAHA.112.300829

Soeki, T., and Sata, M. (2012). Role of epicardial adipose tissue in atrial fibrillation. *Circ. J.* 76, 2738–2739. doi: 10.1253/circj.CJ-12-1283

Soltis, E. E., and Cassis, L. A. (1991). Influence of perivascular adipose tissue on rat aortic smooth muscle responsiveness. *Clin. Exp. Hypertens. A* 13, 277–296. doi: 10.3109/10641969109042063

Szasz, T., Bomfim, G. F., and Webb, R. C. (2013). The influence of perivascular adipose tissue on vascular homeostasis. *Vasc. Health Risk Manag.* 9, 105–116. doi: 10.2147/VHRM.S33760

Takaoka, M., Nagata, D., Kihara, S., Shimomura, I., Kimura, Y., Tabata, Y., et al. (2009). Periadventitial adipose tissue plays a critical role in vascular remodeling. *Circ. Res.* 105, 906–911. doi: 10.1161/CIRCRESAHA.109.199653

Takaoka, M., Suzuki, H., Shioda, S., Sekikawa, K., Saito, Y., Nagai, R., et al. (2010). Endovascular injury induces rapid phenotypic changes in perivascular adipose tissue. *Arterioscler. Thromb. Vasc. Biol.* 30, 1576–1582. doi: 10.1161/ATVBAHA.110.207175

Tanaka, K., Nagata, D., Hirata, Y., Tabata, Y., Nagai, R., and Sata, M. (2011). Augmented angiogenesis in adventitia promotes growth of atherosclerotic plaque in apolipoprotein E-deficient mice. *Atherosclerosis* 215, 366–373. doi: 10.1016/j.atherosclerosis.2011.01.016

Thanassoulis, G., Massaro, J. M., O'Donnell, C. J., Hoffmann, U., Levy, D., Ellinor, P. T., et al. (2010). Pericardial fat is associated with prevalent atrial fibrillation: the Framingham Heart Study. *Circ. Arrhythm. Electrophysiol.* 3, 345–350. doi: 10.1161/CIRCEP.109.912055

Tosaki, T., Kamiya, H., Himeno, T., Kato, Y., Kondo, M., Toyota, K., et al. (2017). Sodium-glucose Co-transporter 2 inhibitors reduce the abdominal visceral fat area and may influence the renal function in patients with type 2 diabetes. *Intern. Med.* 56, 597–604. doi: 10.2169/internalmedicine.56.7196

Warren, J. (1962). Remarks on angina pectoris. *N. Engl. J. Med.* 266, 3–7. doi: 10.1056/NEJM196201042660101

Yagi, S., Hirata, Y., Ise, T., Kusunose, K., Yamada, H., Fukuda, D., et al. (2017). Canagliflozin reduces epicardial fat in patients with type 2 diabetes mellitus. *Diabetol. Metab. Syndr.* 9:78. doi: 10.1186/s13098-017-0275-4

Yamada, H., and Sata, M. (2015). Role of pericardial fat: the good, the bad and the ugly. *J. Cardiol.* 65, 2–4. doi: 10.1016/j.jjcc.2014.07.004

Zinman, B., Wanner, C., Lachin, J. M., Fitchett, D., Bluhmki, E., Hantel, S., et al. (2015). Empagliflozin, cardiovascular outcomes, and mortality in type 2 diabetes. *N. Engl. J. Med.* 373, 2117–2128. doi: 10.1056/NEJMoa 1504720

Conflict of Interest Statement: The authors declare that the research was conducted in the absence of any commercial or financial relationships that could be construed as a potential conflict of interest.

frontiers in Physiology

ORIGINAL RESEARCH
published: 09 February 2018
doi: 10.3389/fphys.2018.00051

High Fat Diet Attenuates the Anticontractile Activity of Aortic PVAT via a Mechanism Involving AMPK and Reduced Adiponectin Secretion

*Tarek A. M. Almabrouk[1,2], Anna D. White[1], Azizah B. Ugusman[1,3], Dominik S. Skiba[1,4], Omar J. Katwan[1,5], Husam Alganga[1,2], Tomasz J. Guzik[1,4], Rhian M. Touyz[1], Ian P. Salt[1] and Simon Kennedy[1]**

[1] Institute of Cardiovascular and Medical Sciences, College of Medical, Veterinary and Life Sciences, University of Glasgow, Glasgow, United Kingdom, [2] Medical School, University of Zawia, Zawia, Libya, [3] Department of Physiology, National University of Malaysia Medical Centre, Kuala Lumpur, Malaysia, [4] Jagiellonian University College of Medicine, Krakow, Poland, [5] Department of Biochemistry, College of Medicine, University of Diyala, Baqubah, Iraq

OPEN ACCESS

Edited by:
Stephanie W. Watts,
Michigan State University,
United States

Reviewed by:
María S. Fernández-Alfonso,
Complutense University of Madrid,
Spain
Jianbo Wu,
University of Missouri, United States

***Correspondence:**
Simon Kennedy
simon.kennedy@glasgow.ac.uk

Specialty section:
This article was submitted to Vascular Physiology, a section of the journal Frontiers in Physiology

Received: 21 September 2017
Accepted: 16 January 2018
Published: 09 February 2018

Citation:
Almabrouk TAM, White AD, Ugusman AB, Skiba DS, Katwan OJ, Alganga H, Guzik TJ, Touyz RM, Salt IP and Kennedy S (2018) High Fat Diet Attenuates the Anticontractile Activity of Aortic PVAT via a Mechanism Involving AMPK and Reduced Adiponectin Secretion. Front. Physiol. 9:51. doi: 10.3389/fphys.2018.00051

Background and aim: Perivascular adipose tissue (PVAT) positively regulates vascular function through production of factors such as adiponectin but this effect is attenuated in obesity. The enzyme AMP-activated protein kinase (AMPK) is present in PVAT and is implicated in mediating the vascular effects of adiponectin. In this study, we investigated the effect of an obesogenic high fat diet (HFD) on aortic PVAT and whether any changes involved AMPK.

Methods: Wild type Sv129 (WT) and AMPKα1 knockout (KO) mice aged 8 weeks were fed normal diet (ND) or HFD (42% kcal fat) for 12 weeks. Adiponectin production by PVAT was assessed by ELISA and AMPK expression studied using immunoblotting. Macrophages in PVAT were identified using immunohistochemistry and markers of M1 and M2 macrophage subtypes evaluated using real time-qPCR. Vascular responses were measured in endothelium-denuded aortic rings with or without attached PVAT. Carotid wire injury was performed and PVAT inflammation studied 7 days later.

Key results: Aortic PVAT from KO and WT mice was morphologically indistinct but KO PVAT had more infiltrating macrophages. HFD caused an increased infiltration of macrophages in WT mice with increased expression of the M1 macrophage markers *Nos2* and *Il1b* and the M2 marker *Chil3*. In WT mice, HFD reduced the anticontractile effect of PVAT as well as reducing adiponectin secretion and AMPK phosphorylation. PVAT from KO mice on ND had significantly reduced adiponectin secretion and no anticontractile effect and feeding HFD did not alter this. Wire injury induced macrophage infiltration of PVAT but did not cause further infiltration in KO mice.

Conclusions: High-fat diet causes an inflammatory infiltrate, reduced AMPK phosphorylation and attenuates the anticontractile effect of murine aortic PVAT. Mice lacking AMPKα1 phenocopy many of the changes in wild-type aortic PVAT after HFD, suggesting that AMPK may protect the vessel against deleterious changes in response to HFD.

Keywords: perivascular adipose tissue, AMPK, high-fat diet, adiponectin, anticontractile effect

INTRODUCTION

Obesity is an independent risk factor for the development of cardiovascular diseases including coronary artery disease, hypertension, atherosclerosis, and heart failure (Poirier et al., 2006). It has been reported that the risk of cardiovascular disease is four times higher in obese than normal weight people (Manson et al., 1995). Understanding the correlation between obesity and cardiovascular risk has focussed on studying the effect of changes in particular fat depots throughout the body and in this regard, the perivascular adipose tissue (PVAT), which surrounds most blood vessels and regulates vascular function, would appear to be of particular importance. PVAT is an endocrine tissue that produces many active molecules termed adipocytokines (Almabrouk et al., 2014) and in healthy subjects, PVAT exhibits an anticontractile effect via release of PVAT-derived relaxing factors (Aghamohammadzadeh et al., 2012). Studies have shown that PVAT attenuates vascular contraction in multiple vascular beds including coronary vessels (Aghamohammadzadeh et al., 2012), rat aorta (Löhn et al., 2002; Dubrovska et al., 2004), and rat mesenteric arteries (Verlohren et al., 2004) and there are multiple PVAT-derived agents which have been proposed to underlie this anticontractile effect including adiponectin (Fesus et al., 2007), NO (Gil-Ortega et al., 2014) and H_2O_2 (Gao et al., 2007).

As obesity is associated with an increased PVAT mass, it would be intuitive to expect an increased anticontractile effect of the PVAT due to enhanced release of PVAT-derived relaxing factors. However, obesity triggers structural and functional changes in PVAT which contribute to a loss or attenuation of the anticontractile effect, which in similarity to *endothelial dysfunction* has been termed *PVAT dysfunction* (Guzik et al., 2006). This may be by virtue of increased oxidative stress (Ketonen et al., 2010; Rebolledo et al., 2010; Gil-Ortega et al., 2014), hypoxia and inflammation (Greenstein et al., 2009) within the adipose tissue leading to dysfunctional adipokine release (Maenhaut et al., 2010; Gu and Xu, 2013). Although it has been shown that the anti-contractile activity of PVAT is attenuated in obese patients and animal models (Greenstein et al., 2009), the underlying mechanism of PVAT dysfunction remains elusive.

The enzyme AMP-activated protein kinase (AMPK) maintains energy homoeostasis (Carling et al., 2011) and is involved in regulation of glucose, lipid, and protein metabolism (Hardie, 2011). AMPK is activated by reduced cellular energy charge, such as that occurring in hypoxia, hypoglycaemia, and ischaemia, leading to increased phosphorylation of the catalytic AMPKα subunit at Thr172. Activated AMPK subsequently phosphorylates a number of metabolic enzymes leading to normalization of ATP levels (Bijland et al., 2013; Salt and Hardie, 2017). In addition to the well-characterized metabolic actions of AMPK, it is increasingly clear that AMPK plays an important role in the maintenance of vascular health (Salt and Hardie, 2017). Interestingly, in adipose tissue the activity of AMPK is diminished in obesity and metabolic syndrome (Ruderman et al., 2013) while in fat-fed rats, the AMPK/mTOR pathway may contribute to PVAT-mediated vascular dysfunction and remodeling (Ma et al., 2010). Adiponectin, the most abundant adipokine generated by PVAT (Fesus et al., 2007), may exert its anticontractile effect through hyperpolarisation of vascular smooth muscle cells (VSMCs) via AMPK (Weston et al., 2013), and in HFD-fed obese rats, adiponectin improves endothelial dysfunction in the aorta via AMPK activation and eNOS phosphorylation (Deng et al., 2010). Thus, reduced AMPK activity or expression in obesity could underlie the loss of the anticontractile effect of PVAT. Indeed, in a previous study, we demonstrated that aortic PVAT from mice globally deficient in AMPKα1 did not exert an anticontractile effect and this correlated with reduced adiponectin secretion (Almabrouk et al., 2017). However, whether AMPK reduction is also affecting adiponectin release from PVAT in HFD-fed animals remains unclear.

The effect of diet-induced obesity on AMPK has most frequently been studied at the level of the endothelium and VSMCs (Ma et al., 2009, 2010). These studies have yielded consistent results, showing that AMPK acts as a protective mechanism against diet-induced obesity. For example, fructose-fed rats exhibit dysfunction of adipocytokine expression in PVAT and loss of endothelium-dependent vasodilation which can be reversed by activating AMPK (Sun et al., 2014). In fat-fed rats, treatment with a steroid sapogenin (diosgenin) enhanced AMPK phosphorylation in PVAT and reduced inflammatory markers, an effect reversed by AMPK knockdown using siRNA (Chen et al., 2016). A recent study by Zaborska et al. demonstrated that the male offspring of female rats fed a HFD during pregnancy and lactation had dysfunctional mesenteric PVAT which correlated with reduced AMPK activity in the PVAT and reduced NO bioavailability (Zaborska et al., 2016). In a further study by the same group it was found that O-GlcNAcylation was the likely cause of reduced AMPK activity and that the anticontractile effect of PVAT could be recovered by activating AMPK (Zaborska et al., 2017). However, to date, few studies have addressed how HFD modulates the anticontractile activity of PVAT independent of the endothelium and the role of AMPK in this effect. We hypothesized that AMPK expressed in PVAT would act as a protective mechanism to reduce some of the deleterious effects of high fat diet (HFD) on vascular function.

METHODS

Animal Model

Mice used in this study were housed in single-sex groups of 5–6 mice per cage at the Central Research Facility at the University of Glasgow and kept on 12 h cycles of light and dark and at ambient temperature. Wild type (Sv129-WT) mice were purchased from Harlan Laboratories (Oxon, UK). AMPKα1 KO mice were kindly supplied by Benoit Viollet (Institut Cochin, Paris, France) and the generation of these animals has been described before (Jørgensen et al., 2004). All animal experiments were performed in accordance with the United Kingdom Home Office Legislation under the Animals (Scientific Procedure) Act 1986 (project licenses 60/4224 and 70/8572 which were approved by the Glasgow University Animal Welfare and Ethical Review Board) and guidelines from Directive 2010/63/EU of the European Parliament on the protection of animals used for scientific purposes.

In all experiments, age-matched male and female WT and KO mice were used as preliminary experiments demonstrated no gender difference in aortic responses to contractile and relaxant agents (data not shown). WT and KO mice were randomly divided into two groups and fed either a normal diet [ND; $n = 14$(WT) and $n = 14$(KO)] or a high fat diet [HFD; $n = 15$(WT) and $n = 15$(KO)] for 12 weeks starting at 8 weeks of age. The high-fat diet (Western RD) was purchased from SDS (SDS diets, U.K) and contained: fat 21.4%, protein 17.5% and carbohydrate 50% (42% kcal fat). Body weight was monitored weekly and blood pressure (BP) was measured every 4 weeks using tail cuff plethysmography (Visitech systems, North Carolina, USA). Food intake was assessed by weighing the remaining food in the hopper of each cage. At the end of 12 weeks mice were fasted for 16 h before a glucose tolerance test (Mancini et al., 2017) and were then euthanised by a rising concentration of CO_2. Blood was obtained by cardiac puncture and blood glucose measured using a portable glucose monitoring system (Ascensia CONTOUR blood glucose monitoring system, Bayer HealthCare). Serum insulin concentration was determined using a rat/mouse insulin ELISA kit (Millipore) according to the manufacturer's instructions in which the absorbance at 485 nm was determined using a FLUOstar OPTIMA microplate reader (BMG Labtech, Germany). Mean absorbance was determined from duplicate samples and concentration calculated by comparison to the standard curve.

For experiments involving the analysis of tissues, the thoracic aorta and spleen (used as a positive control) were removed and placed in ice-cold oxygenated (95% O_2:5% CO_2) Krebs' solution of the following composition: 118 mM NaCl, 4.7 mM KCl, 1.2 mM $MgSO_4$, 25 mM $NaHCO_3$, 1.03 mM KH_2PO_4, 11 mM glucose, and 2.5 mM $CaCl_2$.

Histological Analysis

To determine the effect of HFD on PVAT morphology, freshly isolated thoracic aortae with intact PVAT from WT and KO mice were placed in 10% zinc formalin and fixed overnight. Arteries were processed through a gradient of alcohols to Histoclear and embedded vertically in paraffin wax before being sectioned on a microtome at 5 μm. Haematoxylin and eosin staining was performed and sections visualized by light microscopy.

Immunohistochemistry using rat anti-MAC2 (#CL8942AP, Cedarlane, UK), rabbit anti-AMPKα (#ab131512, Abcam) and anti-phospho-AMPKα Thr172 (#2535, Cell Signaling Technology) antibodies was utilized to detect the presence of inflammatory cells as well as the effect of HFD on AMPK phosphorylation. In brief, aortic rings and spleens from WT and KO mice fed ND or HFD were fixed overnight in 10% acetic zinc formalin. Sections (5 μm) on slides were deparaffinised and endogenous peroxidase activity blocked by immersing in 3% (v/v) H_2O_2 in methanol for 20 min. Non-specific antibody binding was blocked using 10% non-immune goat serum (Histostain Plus bulk kit blocking solution, Invitrogen) or normal rabbit serum (Vector labs; MAC2 antibody) for 1 h at room temperature and primary antibodies were then added overnight at 4°C. Antibodies were diluted in 1% (w/v) BSA in PBS and used at a concentration of 1:5000 (MAC2) or 1:100 (phospho-AMPKα). Secondary antibody (rabbit anti rat, Vector Labs, UK or biotinylated anti-rabbit, Histostain bulk kit) was incubated for 1 h at room temperature and antibody binding was visualized using DAB (3,3′ diaminobenzidine) chromogenic substrate (Vector Laboratories) and haematoxylin counter stain. Sections were photographed using AxioVision microscope software (Zeiss, Germany).

Real-Time PCR

Expression of M1 and M2 macrophage markers and adiponectin mRNAs in the PVAT was evaluated using real-time PCR as described elsewhere (Skiba et al., 2017). Briefly, total RNA was obtained from PVAT samples using RNeasy Lipid Tissue Mini Kit (Qiagen) and measured by Nanodrop 2000 (Thermo Fisher Scientific). Reverse transcription of 1 μg RNA was performed using High Capacity cDNA Reverse Transcription Kit (Applied Biosystems). mRNA expression of chosen genes in PVAT was analyzed using TaqMan® probes and TaqMan® Real-Time PCR Master Mix (Thermo Fisher Scientific). Expression of mRNA for *Tnf-α* and housekeeping gene *Gapdh* were analyzed using Fast SYBR® Green Master Mix (Thermo Fisher Scientific) and primers (Eurofins) shown in Supplementary Table 1. Reactions were prepared and run on 384-well plates on the QuantStudio™ 7 Flex Real-Time PCR System using a standard protocol and mRNA expression was analyzed using QuantStudio™ Real-Time PCR Software. All data were normalized to levels of *Gapdh* mRNA and relative quantification was calculated as $2^{-\Delta Ct}$. Details of the probes and primers used are listed in Supplementary Table 1.

Protein Expression/Immunoblotting

Samples of thoracic aortic PVAT were dissected, weighed and lysed as previously described (Almabrouk et al., 2017). The protein content of WT and KO PVAT lysates derived from mice fed either ND or HFD was calculated by Coomassie Plus Protein Assay Reagent (Perbio, USA) against a BSA standard curve. Protein samples were resolved by SDS-PAGE, transferred to nitrocellulose membranes and incubated overnight at 4°C with mouse anti-GAPDH (Ambion AM4300) antibodies, or rabbit anti-AMPKα (Cell Signaling Technology #2603), anti-phospho-AMPK Thr172 (Cell Signaling Technology #2535), anti-acetyl CoA carboxylase (ACC) (Cell Signaling Technology #3676) and anti-phospho-ACC Ser79 (Cell Signaling Technology #3661) antibodies. All primary antibodies were diluted 1:1000 in 50% (v/v) TBS, 50% (v/v) Odyssey®-Block (LI-COR, USA). Immunolabelled proteins were visualized using infrared dye-labeled secondary antibodies and an Odyssey Sa Infrared Imaging System (LI-COR, USA).

Adiponectin Elisa

To examine the effect of HFD on adiponectin release from PVAT, conditioned media samples from WT and KO PVAT from ND and HFD groups were prepared according to the method of Almabrouk et al. (2017). Briefly, PVATs (20 mg) were isolated, weighed and incubated in 1 ml of aerating Krebs' solution at 37°C. Adiponectin content of the conditioned media were analyzed by adiponectin/Acrp30 Quantikine ELISA Kit

(MRP300, R&D systems, Abingdon, Oxfordshire). Adiponectin was detected as a colourimetric reaction product by measuring absorbance of the ELISA plate at 450 nm with wavelength correction using a FLUOstar OPTIMA microplate reader (BMG Labtech, Germany). The mean absorbances for the samples were measured in duplicate and the adiponectin concentration was determined by comparison with the standard curve.

Small Vessel Wire Myography

WT and KO thoracic aortae from ND and HFD groups were cut into 2 mm rings with some rings cleaned of PVAT, and others left with the PVAT intact. In all experiments, the endothelium was removed by gently rubbing the interior of the vessel with fine wire and its absence was confirmed by lack of vasodilation (<10%) in response to 10^{-6} M acetylcholine. Artery rings were mounted on two stainless steel pins in a four channel wire myograph (Danish Myo Technology). Vessels were incubated in Krebs' at 37°C and gassed continuously with 95% O_2 and 5% CO_2. Rings were set at a pre-determined optimum resting force of 9.8 mN (Weingärtner et al., 2015) and allowed to equilibrate for 30 min prior to use. After calibration, arterial rings were challenged by addition of 40 mM KCl to sensitize the vessels and then contracted using 30 nM 9,11-dideoxy-9α,11α-methanoepoxy PGF2α (U46619, Tocris) before commencing experiments. Cumulative concentration–response curves to the K^+ channel opener cromakalim (1×10^{-9} to 1×10^{-6} M; Sigma-Aldrich, Poole, UK), added at 10 min intervals were constructed. Data were expressed as a percentage loss of U46619-induced tone.

Mouse Carotid Artery Injury

To further investigate the role of AMPK in the PVAT on vessel inflammation, we used the mouse carotid wire injury model; characterized by endothelial denudation and infiltration of inflammatory cells throughout the vessel wall (Tennant et al., 2008; Greig et al., 2015). Briefly, mice ($n = 5$ WT and $n = 4$ KO fed on normal chow) were anesthetized and maintained on 1% isoflurane throughout. The left carotid artery was surgically exposed and injured luminally in WT and AMPKα1 KO mice using a flexible nylon wire. Animals were recovered with suitable analgesic cover and kept for 7 days. The right carotid artery served as a non-injured contralateral control. Arteries were removed, fixed, and processed for histological analysis and ICC as already outlined.

Statistical Analysis

All results are expressed as mean ± standard error of the mean (SEM) where n represents the number of experiments performed or number of mice used. Data were analyzed with GraphPad Prism 5.0 software. When comparing two or more variables two-way ANOVA (analysis of variance) tests were used. When comparing two or more data groups (contraction data), two-way ANOVA followed by Newman–Keuls post hoc test was used. In all cases, a p-value of <0.05 was considered statistically significant.

RESULTS

Effect of HFD on Weight, Food Intake, and Blood Pressure

At the end of the 12 week period of feeding there was a significant increase in body weight in WT mice on HFD compared to mice fed ND (Figure S1A). Fasting blood glucose and plasma insulin measured at the end of the study period both showed a tendency toward an increase in the WT HFD group, as did incremental area under the curve (AUC) following the glucose tolerance test (**Table 1** and Figures S1C,D). In the KO mice, weight gain following HFD was similar to that observed in WT mice (Figure S1A). Similarly, fasting blood glucose, plasma insulin (**Table 1**) and incremental AUC following a GTT were no different from the values seen in WT mice fed either diet. Systolic blood pressure was unchanged in any group over the course of the 12 week study period (Figure S1B).

PVAT Morphology and Inflammation

In haematoxylin and eosin stained samples of thoracic aortic PVAT from both WT and KO mice, the PVAT was composed of adipocytes with the morphological features of brown adipose tissue (BAT). After 12 weeks of HFD, the PVAT did not appear grossly altered although there were some cells containing larger lipid droplets with the appearance of white adipocytes (**Figure 1**). Immunohistochemistry for the macrophage marker MAC2 was used to identify the effect of HFD on monocyte/macrophage numbers within the PVAT. In WT mice, there was very little positive MAC2 staining within the PVAT after 12 weeks of ND but this was significantly increased in mice fed HFD (**Figure 2**). In KO mice fed ND, there was significantly more positive MAC2 staining compared to WT mice on ND, indicating that lack of AMPKα1 increases monocyte/macrophage numbers within PVAT and that AMPK may protect against deleterious changes in immune cell infiltration in PVAT. In KO mice fed HFD, there was no further increase in MAC2 staining (**Figure 2**). To study macrophage phenotype in more detail, real-time PCR was used to identify mRNA levels of markers of M1 and M2 macrophages in homogenized samples of PVAT. In WT mice fed HFD there was an increased expression of some M1 macrophage marker mRNAs (*Nos2* and *Il1b*; **Figures 3A,B**) while others (*Il12a*) remained unchanged (**Figure 3C**). Interestingly, KO mice fed ND exhibited increased *Nos2* when compared to WT mice fed ND. HFD did not cause any further increase in these markers in KO mice (**Figures 3A,B**). Within the M2

TABLE 1 | Effect of 12 weeks of high fat diet (HFD) on plasma glucose, insulin and AUC following a glucose tolerance test.

Parameter	WT ND ($n = 10$)	WT HFD ($n = 11$)	KO ND ($n = 10$)	KO HFD ($n = 11$)
Blood glucose (mmol/l)	3.8 ± 0.3	4.7 ± 0.6	4.1 ± 0.3	4.9 ± 0.6
Insulin (ng/ml)	0.6 ± 0.04	0.9 ± 0.1	0.6 ± 0.03	0.7 ± 0.03
GTT (AUC)	1035 ± 91.66	1187 ± 141.4	1046 ± 97.88	1220 ± 131.3

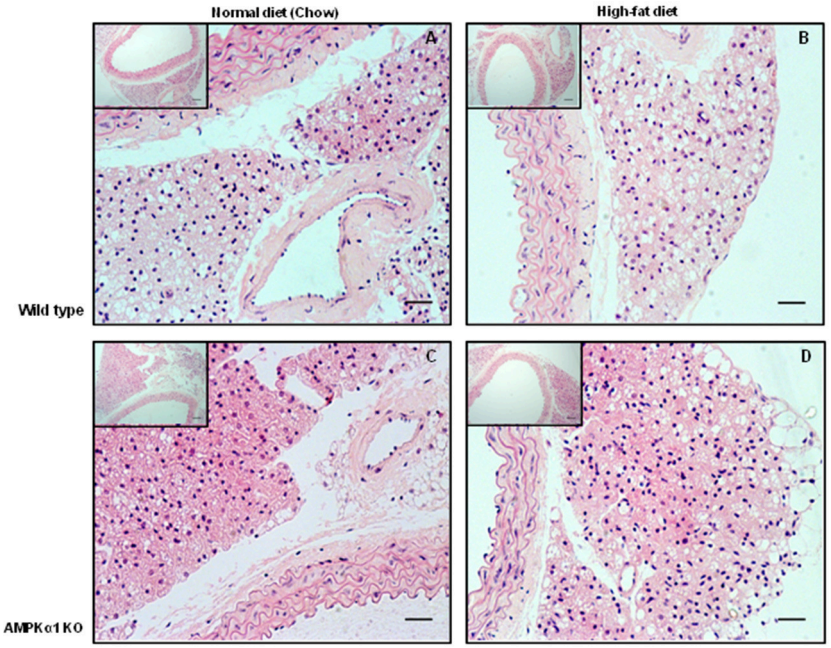

FIGURE 1 | Effect of 12 weeks high-fat diet on thoracic aorta PVAT. Aortic rings from wild type mice **(A,B)** and AMPKα1 knockout mice **(C,D)** were harvested from mice fed normal diet (chow) or high fat diet and stained with H&E. Nuclei appear blue/purple whereas cytoplasm is stained pink. Scale bar = 20 μm. Representative images of $n = 5$ separate animals per group.

markers, levels of *Chil3* mRNA were increased in WT mice after 12 weeks of HFD (**Figure 3D**), while *Arg1* mRNA remained unchanged (**Figure 3E**). Levels of *Tnf-α* were not changed in KO mice compared to WT mice and HFD had no significant effect (**Figure 3F**).

AMPK Levels and Phosphorylation in PVAT

In WT mice, staining for phospho-AMPKα Thr172 was found throughout the PVAT surrounding the aorta. HFD did not appear to alter staining intensity noticeably. In the KO mice, staining intensity for phospho-AMPKα Thr172 was markedly lower compared to the WT and HFD did not change the apparent intensity of the staining (**Figure 4A**). Immunoblotting was used to quantify the levels of phosphorylated AMPKα and the AMPK substrate, ACC in homogenized PVAT samples (**Figure 4B**). Compared to WT mice fed ND, mice fed HFD exhibited reduced levels of phosphorylated AMPKα without altering total levels of AMPKα relative to GAPDH (**Figures 4C,D**). Furthermore, PVAT homogenates from WT mice fed HFD exhibited a tendency toward reduced phosphorylated ACC relative to total ACC compared with WT mice fed ND, yet, this did not achieve statistical significance (**Figure 4E**). As expected, KO mice on either diet exhibited markedly reduced levels of AMPKα and phosphorylated AMPKα (**Figures 4C,D**). Furthermore, this was associated with reduced AMPK activity as assessed by ACC phosphorylation relative to total ACC (**Figure 4E**), without altering total ACC levels (**Figure 4F**).

Adiponectin Production by PVAT

HFD caused a significant reduction (∼70%) in the adiponectin content of conditioned media (CM) collected from PVAT of WT mice compared to mice fed ND (**Figure 5A**). CM from KO mice fed ND had significantly lower adiponectin content compared to WT mice, yet HFD caused no further alteration of adiponectin levels in CM from PVAT of KO mice (**Figure 5A**). To further investigate the changes in adiponectin caused by HFD, RT-PCR was used to quantify adiponectin mRNA expression. In WT mice, feeding HFD for 12 weeks had no effect on adiponectin mRNA expression (**Figure 5B**) and in KO mice, expression was not significantly different compared to WT mice and feeding HFD had no effect. This suggests that HFD or AMPKα1 knockout significantly attenuates adiponectin secretion by the PVAT without affecting gene expression.

Anticontractile Effect of PVAT and Importance of AMPK

The presence or absence of the vascular endothelium did not affect the contractile response to U46619 in WT or KO aortic rings (data not shown). In endothelium-denuded vessels, the contraction of WT aorta without PVAT to 30 nM U46619 was 1.2 ± 0.3 g ($n = 7$) and this was not significantly affected by 12 weeks of HFD (**Figure 6A**). Similarly, in WT vessels with intact PVAT, contraction to 30 nM U46619 was unaffected by HFD (1.4 ± 0.3 g; $n = 6$ vs. 1.1 ± 0.1 g; **Figure 6A**). KO mice showed a similar contraction in response to U46619 and this was unaffected following HFD in rings either with or without intact PVAT (**Figure 6C**).

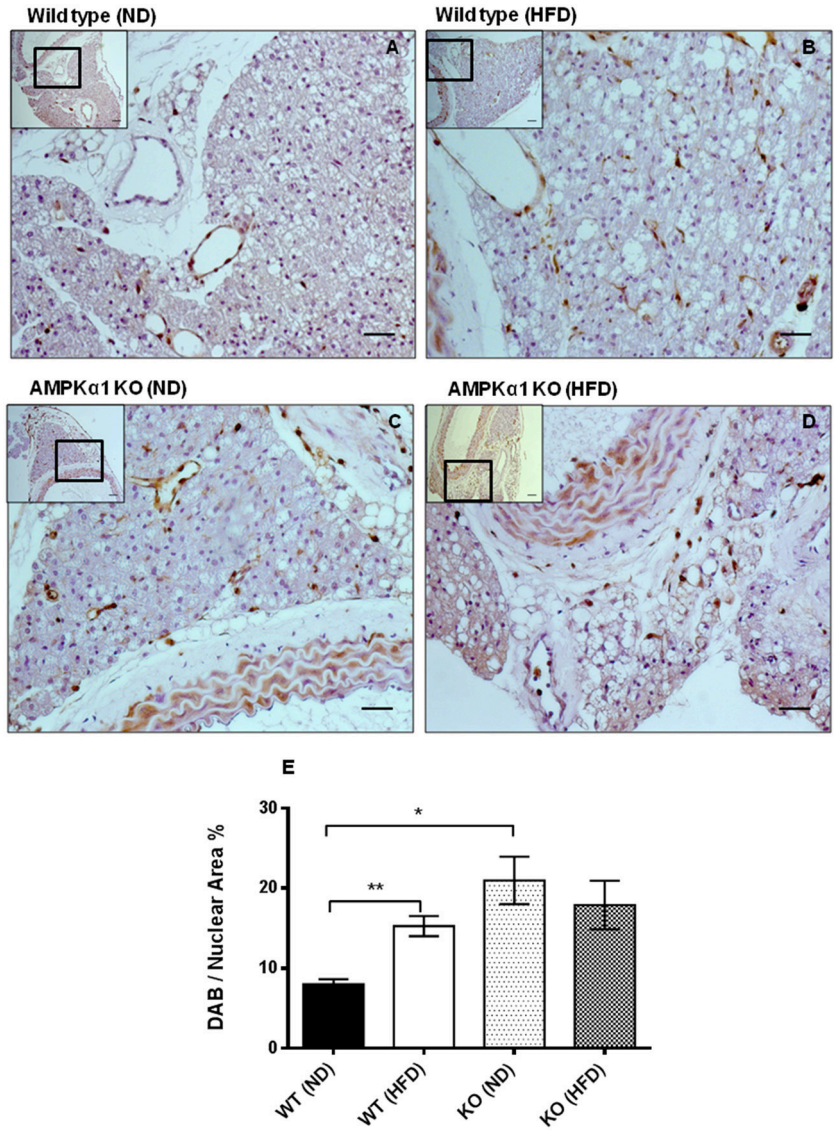

FIGURE 2 | Effect of high-fat diet on macrophage marker (MAC2) expression in thoracic aortic PVAT. Aortic rings from wild type mice **(A,B)** and AMPKα1 knockout mice **(C,D)** were harvested from mice fed normal diet (ND) **(A,C)** or high fat diet (HFD) **(B,D)** and immunostained with anti-MAC2 antibody with haematoxylin counterstain. Scale bar = 20μm. Images shown are representative of at least $n = 5$ separate animals per group. **(E)** Histogram showing quantitation of immunostaining data. Data were expressed as percentage of stained cells to total nuclear area in the section. $^{**}p < 0.01$ vs WT (ND); $^{*}p < 0.05$ vs WT (ND).

In WT mice, the maximum relaxation to cromakalim was significantly increased in aortic rings with intact PVAT (83.3 ± 3.6%, $n = 7$ vs. 27.6 ± 2.8%, $n = 7$; $p < 0.05$). After 12 weeks of HFD, the maximal relaxation to cromakalim in aortic rings with intact PVAT was significantly attenuated (around 30%) compared to mice fed ND (**Figure 6B**) while in aortic rings without PVAT, the diet had no effect on relaxation, suggesting it is dysfunction of the PVAT caused by HFD which attenuates the anticontractile effect. In the AMPKα1 KO mice fed normal diet, the anticontractile effect of the PVAT was absent and maximal responses to cromakalim were not significantly different between vessels with or without intact PVAT. In KO mice fed HFD, there was no significant change in the relaxation to cromakalim (**Figure 6C**).

Carotid Injury—Effect on Inflammation in PVAT

We next sought to investigate if vascular injury exerts effects on PVAT and if this is mediated by AMPK. Using the carotid artery wire injury model we examined whether PVAT lacking AMPKα1 responded differently to vascular injury and associated vessel inflammation. PVAT surrounding the carotid artery appeared very similar to that surrounding the thoracic aorta. Haematoxylin and eosin staining revealed that WT

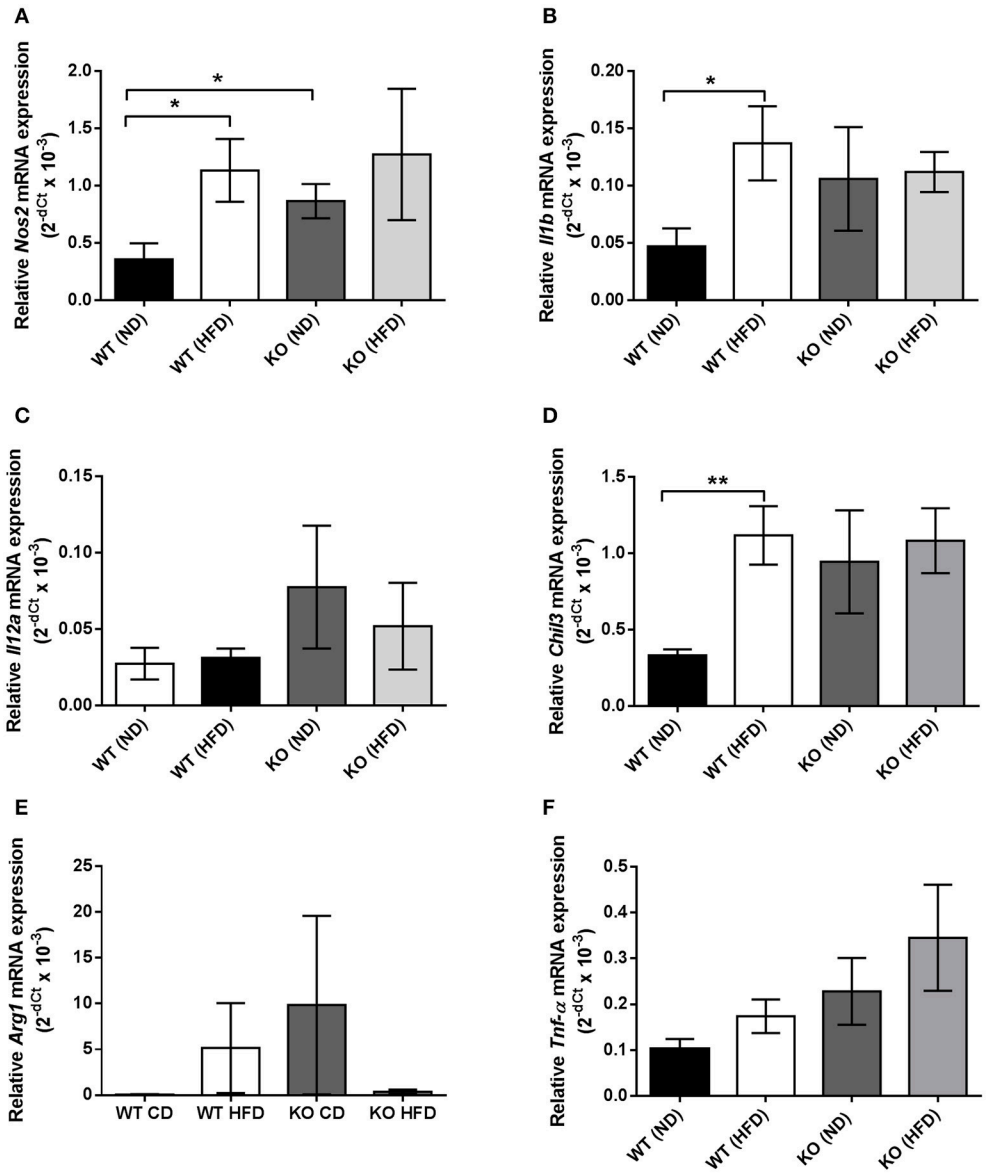

FIGURE 3 | Quantification of macrophage marker expression within thoracic PVAT samples using RT-PCR. **(A,B)**, HFD significantly raised mRNA expression of M1 markers *Nos2* and *Il1b*, encoding iNOS and IL-1β in WT PVAT but had no effect in PVAT from AMPK α1 KO mice. KO PVAT had a higher expression of iNOS compared to WT PVAT in mice fed ND. **(C)** Expression of *Il12a*, encoding IL-12 was unchanged following HFD in either WT or KO mice. **(D)** HFD also significantly increased expression of the M2 marker *Chil3*, encoding YM1 in WT but not KO mice. **(E)** Expression of the M2 marker *Arg1*, encoding arginase was unchanged following HFD in either WT or KO mice. Similarly, expression of *Tnf-α*, encoding TNF-α was unchanged following HFD in either WT or KO mice **(F)**. Values are expressed as means ± SEM, $n = 4$ for all groups; $^{*}p < 0.05$ and $^{**}p < 0.01$ vs. WT (ND). iNOS- inducible nitric oxide synthase; IL-1β- interleukin 1β; YM1, Beta-N-acetylhexosaminidase.

PVAT consisted of adipocytes with the characteristic multiple lipid vacuoles and central nuclei which is characteristic of brown adipocytes and this was similar in the wire injured left carotid samples (**Figures 7A,B**). In KO mice, the PVAT had a similar BAT-like appearance and this was unchanged 7 days after wire injury (**Figures 7C,D**). Immunohistochemistry using the antibody against MAC2 showed significant macrophage infiltration in WT injured carotid arteries in comparison with the control right carotid (**Figure 7E**). In KO mice, there was a trend toward greater MAC2 expression in the PVAT of the non-injured vessels but there was no significant increase caused by wire injury (**Figure 7E**).

DISCUSSION

This study investigated the effect of HFD on PVAT regulation of conduit artery tone in WT and AMPKα1 KO mice. One of the novel findings of this study was that the anticontractile effect of PVAT in aortic rings with no endothelium was significantly

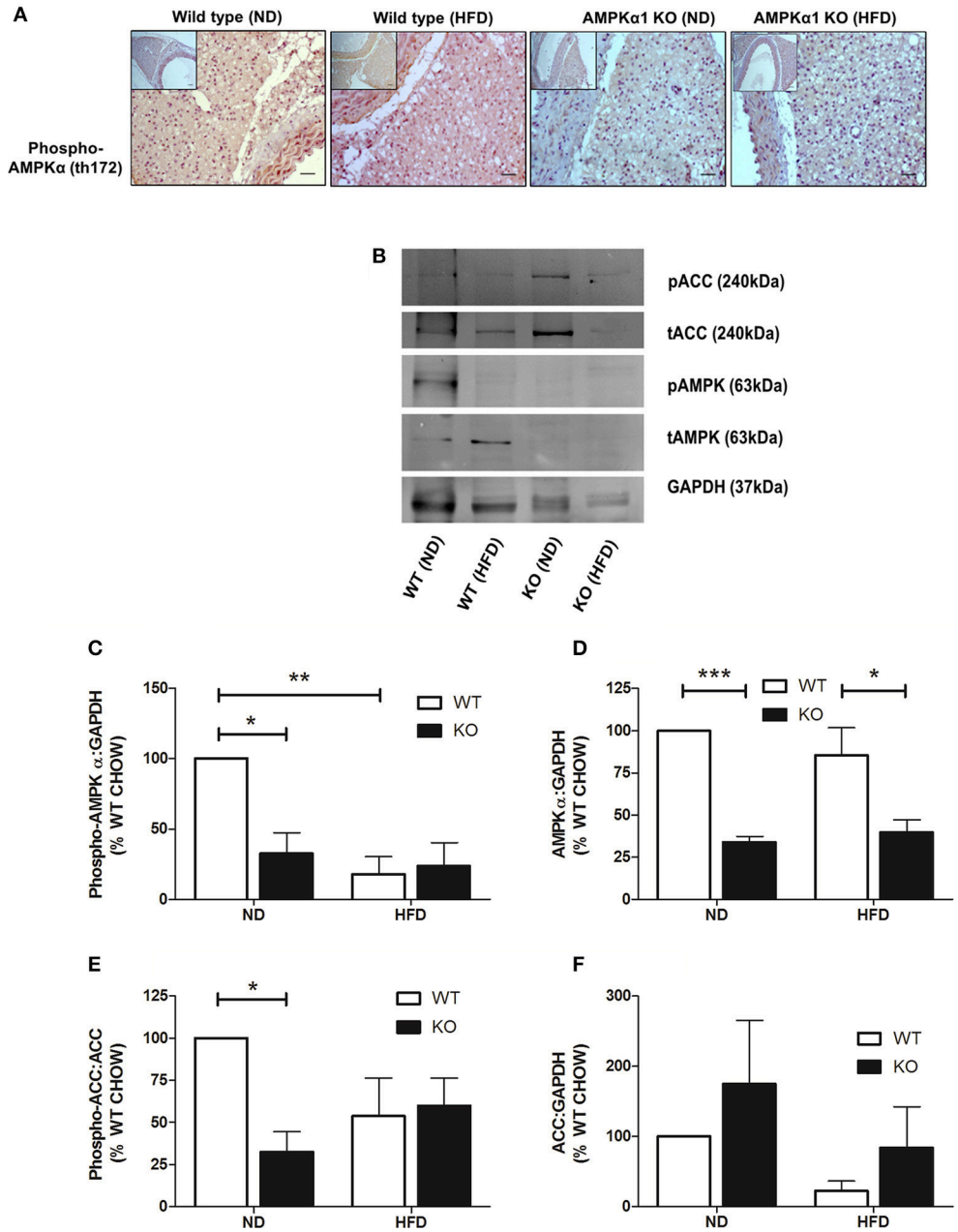

FIGURE 4 | Effect of HFD on levels and phosphorylation of AMPK in PVAT. Sections of thoracic aorta from WT and KO mice on normal or high-fat diet were probed using anti-phospho-AMPKα Thr172 antibodies **(A)**. There was significantly less staining in KO tissue compared to WT but feeding high-fat diet had no obvious effect on phospho-AMPKα levels. Scale bar = 20μm, representative images of at least $n = 3$ separate mice per group. **(C–F)** lysates of PVAT from WT and KO mice fed ND and HFD were immunoblotted with the indicated antibodies. **(B)** Representative immunoblots. **(C–F)** Quantitative analysis of immunoblots, expressed as the ratio of phosphorylated AMPKα **(C),** AMPKα **(D),** and total ACC **(F)** relative to GAPDH. **(E)** Quantitative analysis of phosphorylation of the AMPK substrate, ACC, relative to total ACC levels. $^{*}p < 0.05$, $^{**}p < 0.01$or $^{***}p < 0.001$ vs. WT (ND), $n = 3$ for all data sets.

diminished in WT mice fed a HFD compared to those maintained on chow diet. The loss of anti-contractile function could be due in part to a reduction in PVAT-derived adiponectin release caused by AMPK dysfunction and/or inflammation within the PVAT. This is supported by data obtained in the AMPKα1 KO mouse which displayed dysfunctional aortic PVAT with increased macrophage infiltration and a lack of anticontractile activity even in the absence of HFD.

Both WT and KO animals fed the HFD gained weight to a greater extent than those fed normal diet; indicative of the obesogenic nature of the diet. However, other cardiometabolic parameters such as plasma insulin and glucose as well as systolic

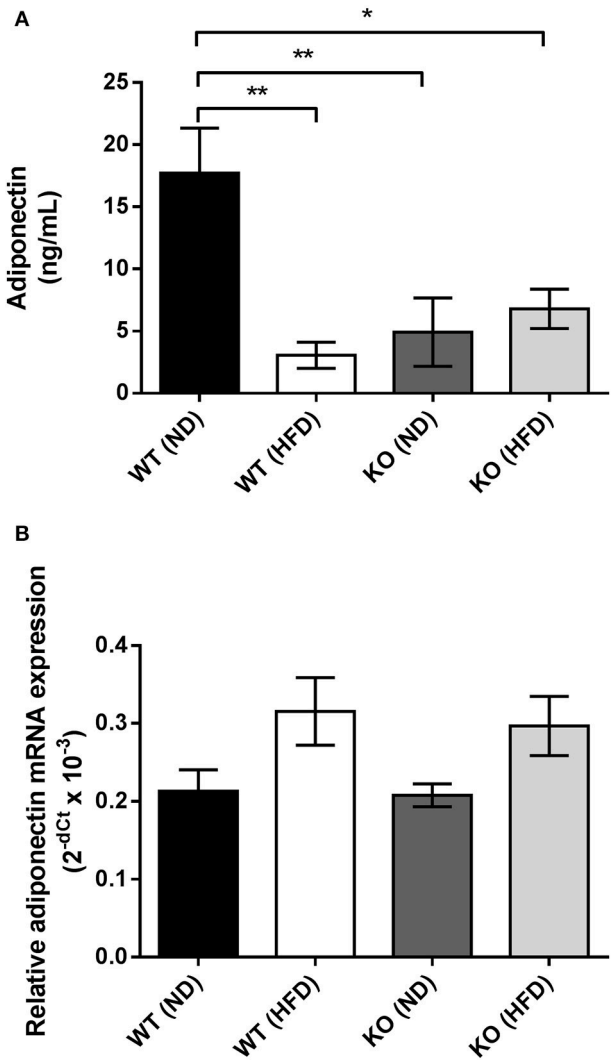

FIGURE 5 | Effect of HFD on adiponectin secretion and mRNA expression in PVAT. **(A)** Conditioned medium was collected from WT and KO PVAT from mice fed ND or HFD and adiponectin levels assessed by ELISA ($n = 6$ for all groups). *$p < 0.05$ and **$p < 0.01$ vs. WT ND. **(B)** Adiponectin mRNA expression was assessed by qPCR in samples of aortic PVAT from WT and KO fed either ND or HFD ($n = 4$ for all groups). No significant changes in adiponectin gene expression were detected.

arterial blood pressure were not significantly elevated in either of the HFD groups compared to groups fed the normal diet. This is in contrast with a previous study in mice on a 54% kcal fat diet for only 8 weeks (da Silva Franco et al., 2017). In terms of plasma glucose and insulin, most studies report a rise induced by HFD, even after only 4 weeks of feeding (Guilford et al., 2017), but others have found no change after 6 weeks (60% kcal of fat diet; Zhang et al., 2017). Our study used a diet with a lower percentage of kcal as fat (42%) and we cannot rule out changes occurring if feeding duration was increased beyond 12 weeks as both plasma insulin and glucose showed trends toward an increase in both HFD groups. However, it is clear that knockout of the AMPKα1 gene did not affect the cardiometabolic paramaters or the morphological appearance of the PVAT.

The mechanisms underlying the effect of AMPK in regulating adipose tissue mass are poorly characterized. Adipose tissue mass expansion occurs as a consequence of either an increase in adipocyte number as a result of enhanced adipogenesis, an increase in cell size due to fat deposition in pre-existing cells, or a combination of both. It has been reported that the increase in adipose tissue mass in AMPKα2 knockout mice was due to an increased triglyceride accumulation in the pre-existing adipocytes rather than an increase in cell number or differentiation as no changes in the expression of adipocyte transcription factors, PPARγ, C/EBPα, or the mature adipocyte markers, including aFABP/aP2, were reported (Villena et al., 2004). The model used in the current study is a global AMPKα1 knockout mouse and there was no evidence of increased adipose tissue mass and KO animals on the HFD gained weight at the same rate as the WT mice. Weight gain and development of obesity is dependent on energy balance.

The main focus of this study was the effect of HFD on aortic PVAT and here, HFD caused a marked increase in the number of macrophages in WT mice as detected by the MAC2 marker (**Figure 2**). The gross morphological appearance of the PVAT was not different between WT and KO groups but 12 weeks of HFD did cause the appearance of some adipocytes with larger lipid droplets in the PVAT (**Figure 1**) and this is likely related to an overall increase in the adiposity of the fat-fed animals as evidenced by the weight gain. RT-PCR was used to differentiate between M1 and M2 type macrophages within the PVAT. In the WT group, the HFD increased the expression of M1 markers (iNOS and IL-1β) in comparison with ND fed mice. M1 macrophages have pro-inflammatory and anti-angiogenic properties and generation of inflammatory cytokines within the PVAT may play a role in the adipose tissue microenvironment and affect generation of adipokines such as adiponectin. Indeed a recent study also found increases in the PVAT content of M1 macrophages in the ApoE$^{-/-}$ mouse model of atherosclerosis, suggesting that macrophage polarization in the artery wall can drive vascular disease (Skiba et al., 2017). In the KO mouse there was a significantly increased expression of iNOS but HFD did not cause any further increase in the these markers and this may be indicative of the already inflamed PVAT in the KO or that AMPKα1 is necessary for macrophage polarization. In support of this, rats with chronic kidney disease have reduced AMPK activity in macrophages which disturbs macrophage polarization and this can be restored by activating AMPK (Li et al., 2015). Another possibility is that adipokines produced by the PVAT can affect macrophage polarization. Indeed, human adipocyte-conditioned media was found to modulate the expression profile of macrophages via AMPK activation and expression of angiotensin-converting enzyme (ACE) (Kohlstedt et al., 2011). However, it should be noted that one M2 marker was also raised in WT mice fed HFD which could suggest recruitment of both M1 and M2 macrophages rather than unequivocal polarization toward an M1 phenotype. This may also be supported by the fact that the expression data are not normalized to a general macrophage marker, thus the

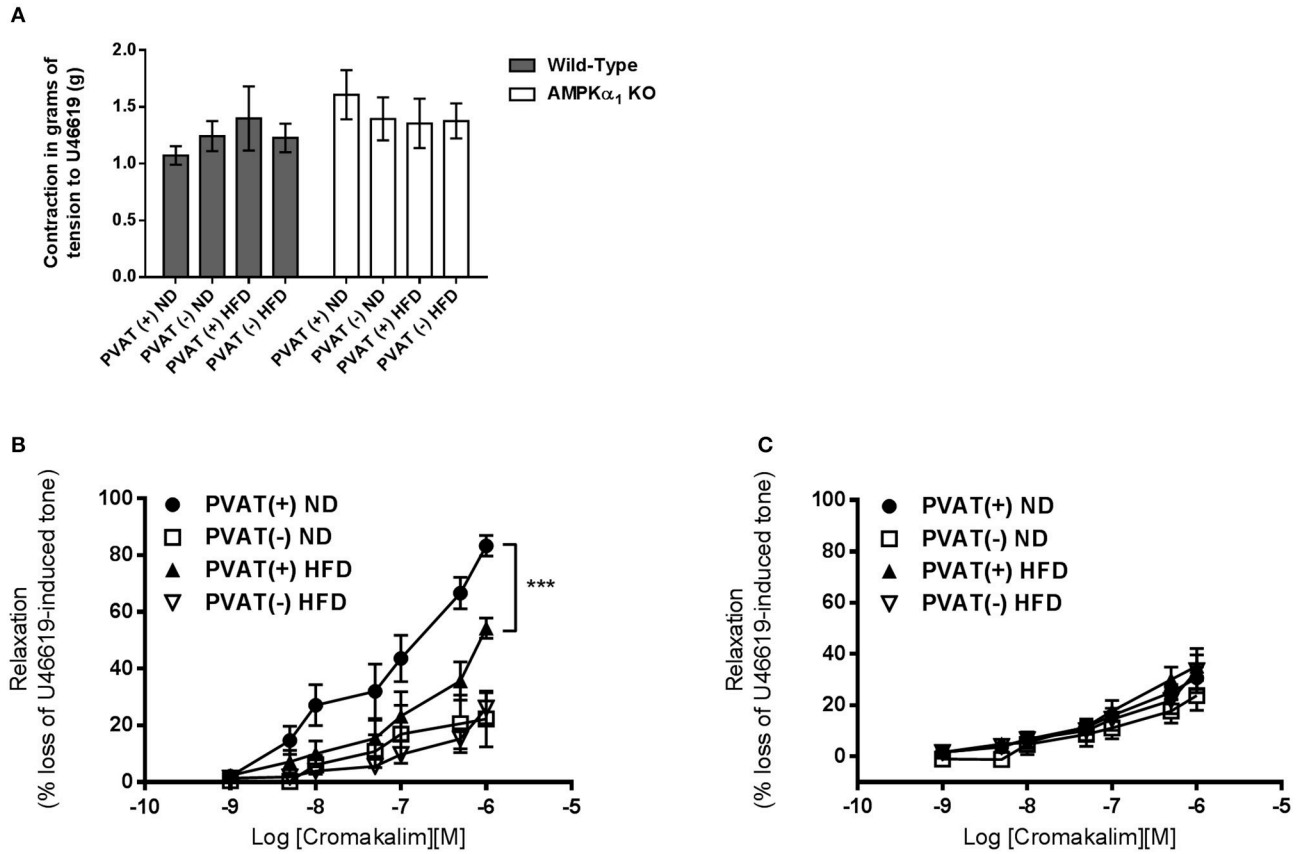

FIGURE 6 | Effect of HFD on the anticontractile effect of aortic PVAT. **(A)** There was no significant difference in contractile force in response to 30nM U46619 in rings from WT or KO mice and this was not influenced by 12 weeks of HFD or the presence or absence of intact PVAT on the artery ring. Dose response curves to cromakalim were constructed in preconstricted aortic rings from WT mice **(B)** or AMPKα1 knockout mice **(C)**. All rings were denuded of endothelium and either had PVAT removed (–) or left intact (+). Intact PVAT had an anticontractile effect in WT mice which was attenuated by high fat diet feeding. HFD had no effect on relaxation in rings without attached PVAT **(A)**. In KO mice, the PVAT did not have an anticontractile effect and HFD did not alter this **(B)**. ***$p < 0.001$ vs. PVAT(–) (ND); $n = 6–7$.

increased expression of some of these markers could simply be due to the larger number of macrophages present in the WT PVAT following HFD and further work is required to study this in more detail.

To investigate this further, we measured adiponectin production in adipocyte-conditioned media from aortic PVAT and also studied AMPK levels in homogenized PVAT samples to assess if this was affected by the HFD and if it could underlie the inflammatory changes. Previous studies have shown that even very short periods of HFD cause a rise in the inflammatory adipocytokine leptin and chemokine MIP1α concomitant with a decrease in the expression of adiponectin, PPARγ, and FABP4 (Chatterjee et al., 2009). The data presented here also show a clear and significant reduction in adiponectin secretion caused by HFD in the WT mouse (**Figure 5A**) but with no significant change in adiponectin gene expression (**Figure 5B**), suggesting a deficiency in gene translation or adiponectin secretion caused by HFD. In agreement with our results Ketonen et al. also found no change in adiponectin mRNA expression in thoracic PVAT even after 8 months of 60% kcal fat diet in C57BL6/J mice (Ketonen et al., 2010).

Several lines of evidence report that AMPK may regulate adiponectin secretion by the PVAT via suppression of inflammatory cytokines such as TNF-α and IL-6 (Lihn et al., 2004; Tsuchida et al., 2005; Sell et al., 2006). Activation of AMPK with AICAR in human adipose tissue was associated with degradation of TNF-α and increased adiponectin gene expression (Lihn et al., 2004) while TNF-α and IL-6 are known to have inhibitory effects on adiponectin gene expression and release (Fasshauer et al., 2002, 2003). Moreover, TNF-α has been suggested to play a central role in regulating adiponectin levels (Greenberg et al., 1991) and suppressing TNF-α protein may be involved in the up-regulation of adiponectin mRNA levels (Lihn et al., 2004). Sell et al. reported activation of AMPK by AICAR and troglitazone was associated with reduction of IL-6, IL-8, MIP-1α/β, and MCP-1 and upregulation of adiponectin expression (Sell et al., 2006). Similar findings demonstrate that the expression of inflammatory genes including TNF-α, MCP-1, and macrophage antigen-1 in WAT was reduced in response to PPARα agonist rosiglitazone (Tsuchida et al., 2005). Thus, in the current study, the increase in the expression of macrophage markers and reduced adiponectin secretion reported in fat-fed

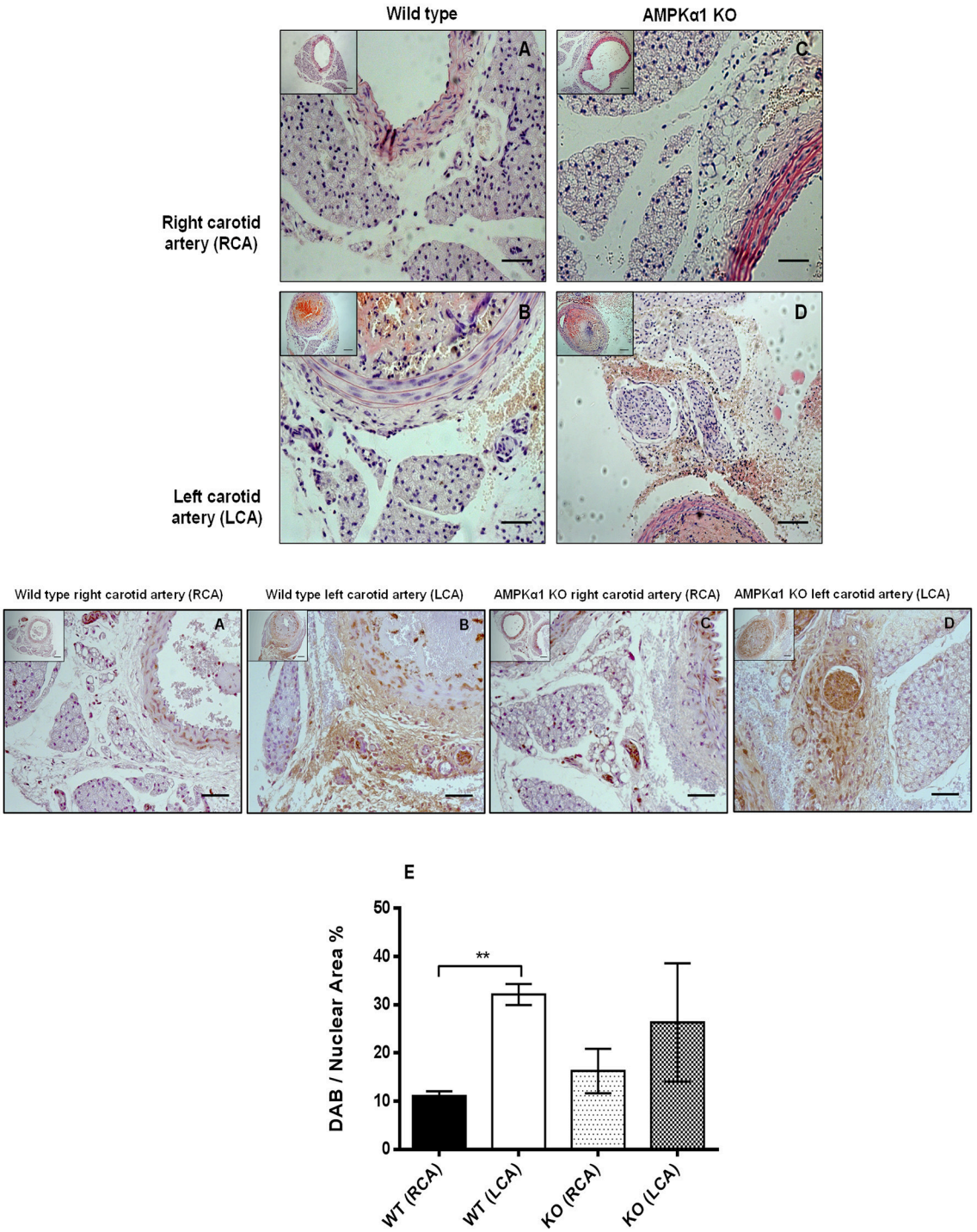

FIGURE 7 | Effect of wire injury on carotid PVAT morphology and inflammation in WT and AMPKα1 KO mice. **(A–D)** haematoxylin and eosin stained sections harvested from WT and KO right carotid arteries (non-injured) and left carotid arteries (injured). Representative images from $n = 4–5$ separate animals are shown. There were no obvious differences in PVAT morphology caused by wire injury in either the WT or KO mice. Scale bar; 20 μm. Middle panel- representative WT and KO right and left carotid arteries with intact PVAT stained with anti- MAC2 antibody and counterstained with haematoxylin. Wire injury caused a dramatic increase in MAC2 expression in the PVAT of WT carotid arteries. In KO mice, there was a trend toward increased MAC2 expression in the non-injured vessels and also in the injured vessels compared to WT mice but this failed to reach significance. **(E)** Histogram showing quantification of MAC2 staining calculated as percentage of stained cells to total nuclear area in the section. $^{**}p < 0.001$ vs. WT RCA.

WT and KO animals may be due to reduced AMPK activity leading to upregulation of inflammatory cytokines such as TNF-α and IL-6 and downregulation of adiponectin secretion by the PVAT. Indeed, in WT animals fed HFD, there was a significant reduction in activating Thr172 phosphorylation of AMPK, without any change in overall AMPK levels (**Figure 4C**). This indicates a reduction in AMPK activity as a result of feeding HFD and interestingly, this was phenocopied in animals lacking AMPKα1.

Functionally, we hypothesized that HFD may impair vessel relaxation. In a previous study we showed that PVAT exerts an anticontractile effect in murine aorta and that this is lost in AMPKα1 KO mice due to PVAT dysfunction with reduced adiponectin secretion in the KO mouse (Almabrouk et al., 2017). Indeed, in that study we found that the presence of PVAT also caused a slight reduction in contraction of WT but not KO aortic rings in response to the thromboxane agonist U46619. This was not replicated here and feeding either WT or KO mice HFD had no effect on contraction to U46619 (**Figure 6A**). However, in common with our previous study, presence of PVAT increased relaxation to cromakalim in WT but not KO aortic rings. Here we extend these findings to demonstrate that the anticontractile effects of PVAT can be attenuated in WT mice by 12 weeks of HFD (**Figure 6**). In vessels lacking PVAT, HFD had no significant effect on relaxation to the endothelium-independent vasodilator cromakalim and this was the case in both WT and KO mice. However, in vessels with intact PVAT, HFD attenuated relaxation in the WT group but not the KO group. This strongly suggests that the effect of HFD in WT mice was on the PVAT rather than on the medial VSMCs. Since the anticontractile effect was absent in KO mice, and unaffected by HFD, it also seems likely that AMPK within the PVAT is involved in mediating the anticontractile response, likely via generation of adiponectin which is a vasodilator in mouse aorta (Almabrouk et al., 2017). However, it must be noted that there are other targets of AMPK in addition to adiponectin and these cannot be ruled out from involvement in the loss of the anticontractile effect of PVAT in HFD-fed mice.

These results are consistent with previous studies reporting that PVAT-mediated anticontractile effect is impaired in HFD models (Nakagawa et al., 2002; Gao et al., 2005; Fesus et al., 2007; Greenstein et al., 2009; Marchesi et al., 2009; Ma et al., 2010; Payne et al., 2010; Owen et al., 2013). Gao et al. reported that the effect is lost in obese rats due to reduced release of relaxing factors despite the increased amount of PVAT around rat aorta (Gao et al., 2005). A loss of the anticontractile effect of PVAT was also reported in obese New Zealand mice (NZO), a model which is characterized by metabolic syndrome and larger amounts of PVAT. This was suggested to be due to changes in the expression of PVAT-derived factors other than adiponectin (Fesus et al., 2007). In the Ossabaw swine model of obesity there was an up-regulation of 186 PVAT-derived proteins associated with increased coronary contractility and these included transforming protein RhoA and calpastatin (Owen et al., 2013). HFD-induced obesity likely impairs PVAT-mediated anticontractile effects by promoting a marked proinflammatory shift in cytokines and chemokines associated with oxidative stress in the PVAT (Bailey-Downs et al., 2013). Although it wasn't studied here, PVAT inflammation and oxidative stress can also lead to endothelial dysfunction with decreased NO bioavailability and increased superoxide generation by uncoupled endothelial NO synthase in PVAT (Marchesi et al., 2009).

Since we found reduced AMPK activity in the PVAT of mice fed HFD it is tempting to speculate that AMPK acts as a protective mechanism against inflammation and loss of PVAT anticontractile function and that this effect is overcome in HFD-induced obesity. Indeed, AMPK activation inhibits multiple pro-inflammatory signaling pathways in cultured adipocytes (Mancini et al., 2017). Additionally, in KO mice, the PVAT already showed increased MAC2 expression following ND and HFD had no additional effect. These results further support the protective anti-inflammatory role of AMPK in PVAT. The absence of any difference between ND and HFD groups in the KO mice may be due to the fact that the PVAT of KO mice is already maximally infiltrated or perhaps as a result of a compensation mechanism by AMPKα2 complexes in the PVAT which prevent or modulate further inflammatory cell infiltration and this requires further investigation. Other stimuli which induce vascular inflammation also lack an effect in the AMPKα1 KO mouse and here we demonstrate that in the mouse carotid artery injury model. While injury to the WT carotid caused a strong infiltration of macrophages 7 days after injury, the KO carotid PVAT already had a trend toward increased macrophage infiltration and wire injury did not affect this; suggesting that the activity of AMPK in the PVAT prevents the PVAT becoming inflamed.

CONCLUSION

In conclusion, HFD is associated with increased macrophage infiltration and polarization toward the M1 inflammatory phenotype, reduced AMPK activity and reduced adiponectin secretion by thoracic PVAT. These changes likely underlie the loss of the anti-contractile activity of the PVAT. Vascular AMPK, and in particular AMPK expressed in the PVAT may therefore protect the vessel against deleterious changes in response to HFD and may be a target to treat vessel inflammation seen in many cardiovascular diseases.

AUTHOR CONTRIBUTIONS

TA, AW, AU, DS, HA, and OK: conducted the experiments, collected and analyzed the data and prepared the figures; TA: drafted sections of the paper; IS, RT, and SK: conceived and planned the experiments; SK: prepared the final version of the manuscript and SK, RT, TG, and IS: proof read the final version of the manuscript.

ACKNOWLEDGMENTS

The authors gratefully acknowledge support from Zawia University (Libya) and the Ministry of Higher Education (Libya) in the form of a Ph.D. Studentship awarded to

TA, AU was supported by a visiting scholarship from the National University of Malaysia and Ministry of Higher Education Malaysia. DS was supported by Mobilnosc Plus (1300/1/MOB/IV/2015/0). This work was also supported by an equipment grant (BDA11/0004309 to IS) and Sir George Alberti Fellowship (BDA13/0004652 to AW) from Diabetes UK. RT is supported by a BHF Chair (CH/12/29762). Some of the data in this paper has previously been published as part of a Ph.D. thesis submitted by TA to Glasgow University. It has not been published elsewhere and the thesis is available online: http://encore.lib.gla.ac.uk/iii/encore/record/C__Rb3271692.

SUPPLEMENTARY MATERIAL

The Supplementary Material for this article can be found online at: https://www.frontiersin.org/articles/10.3389/fphys.2018.00051/full#supplementary-material

REFERENCES

Aghamohammadzadeh, R., Withers, S., Lynch, F., Greenstein, A., Malik, R., and Heagerty, A. (2012). Perivascular adipose tissue from human systemic and coronary vessels: the emergence of a new pharmacotherapeutic target. *Br. J. Pharmacol.* 165, 670–682. doi: 10.1111/j.1476-5381.2011.01479.x

Almabrouk, T. A., Ewart, M. A., Salt, I. P., and Kennedy, S. (2014). Perivascular fat, AMP-activated protein kinase and vascular diseases. *Br. J. Pharmacol.* 171, 595–617. doi: 10.1111/bph.12479

Almabrouk, T. A. M. (2017). *Role of AMP-Protein Kinase (AMPK) in Regulation of Perivascular Adipose Tissue (PVAT) Function*. Ph.D. thesis, University of Glasgow. Available online at: http://encore.lib.gla.ac.uk/iii/encore/record/C__Rb3271692

Almabrouk, T. A., Ugusman, A. B., Katwan, O. J., Salt, I. P., and Kennedy, S. (2017). Deletion of AMPKalpha1 attenuates the anticontractile effect of perivascular adipose tissue (PVAT) and reduces adiponectin release. *Br. J. Pharmacol.* 174, 3398–3410. doi: 10.1111/bph.13633

Bailey-Downs, L. C., Tucsek, Z., Toth, P., Sosnowska, D., Gautam, T., Sonntag, W. E., et al. (2013). Aging exacerbates obesity-induced oxidative stress and inflammation in perivascular adipose tissue in mice: a paracrine mechanism contributing to vascular redox dysregulation and inflammation. *J. Gerontol. A Biol. Sci. Med. Sci.* 68, 780–792. doi: 10.1093/gerona/gls238

Bijland, S., Mancini, S. J., and Salt, I. P. (2013). Role of AMP-activated protein kinase in adipose tissue metabolism and inflammation. *Clin. Sci.* 124, 491–507. doi: 10.1042/CS20120536

Carling, D., Mayer, F. V., Sanders, M. J., and Gamblin, S. J. (2011). AMP-activated protein kinase: nature's energy sensor. *Nat. Chem. Biol.* 7, 512–518. doi: 10.1038/nchembio.610

Chatterjee, T. K., Stoll, L. L., Denning, G. M., Harrelson, A., Blomkalns, A. L., Idelman, G., et al. (2009). Proinflammatory phenotype of perivascular adipocytes: influence of high-fat feeding. *Circ. Res.* 104, 541–549. doi: 10.1161/CIRCRESAHA.108.182998

Chen, Y., Xu, X., Zhang, Y., Liu, K., Huang, F., Liu, B., et al. (2016). Diosgenin regulates adipokine expression in perivascular adipose tissue and ameliorates endothelial dysfunction via regulation of AMPK. *J. Steroid Biochem. Mol. Biol.* 155, 155–165. doi: 10.1016/j.jsbmb.2015.07.005

da Silva Franco, N., Lubaczeuski, C., Guizoni, D. M., Victorio, J. A., Santos-Silva, J. C., Brum, P. C., et al. (2017). Propranolol treatment lowers blood pressure, reduces vascular inflammatory markers and improves endothelial function in obese mice. *Pharmacol. Res.* 122, 35–45. doi: 10.1016/j.phrs.2017.05.018

Deng, G., Long, Y., Yu, Y. R., and Li, M. R. (2010). Adiponectin directly improves endothelial dysfunction in obese rats through the AMPK-eNOS Pathway. *Int. J. Obes.* 34, 165–171. doi: 10.1038/ijo.2009.205

Dubrovska, G., Verlohren, S., Luft, F. C., and Gollasch, M. (2004). Mechanisms of ADRF release from rat aortic adventitial adipose tissue. *Am. J. Physiol. Heart Circ. Physiol.* 286, H1107–H1113. doi: 10.1152/ajpheart.00656.2003

Fasshauer, M., Klein, J., Neumann, S., Eszlinger, M., and Paschke, R. (2002). Hormonal regulation of adiponectin gene expression in 3T3-L1 adipocytes. *Biochem. Biophys. Res. Commun.* 290, 1084–1089. doi: 10.1006/bbrc.2001.6307

Fasshauer, M., Kralisch, S., Klier, M., Lossner, U., Bluher, M., Klein, J., et al. (2003). Adiponectin gene expression and secretion is inhibited by interleukin-6 in 3T3-L1 adipocytes. *Biochem. Biophys. Res. Commun.* 301, 1045–1050. doi: 10.1016/S0006-291X(03)00090-1

Fésüs, G., Dubrovska, G., Gorzelniak, K., Kluge, R., Huang, Y., Luft, F. C., et al. (2007). Adiponectin is a novel humoral vasodilator. *Cardiovasc. Res.* 75, 719–727. doi: 10.1016/j.cardiores.2007.05.025

Gao, Y. J., Holloway, A. C., Zeng, Z. H., Lim, G. E., Petrik, J. J., Foster, W. G., et al. (2005). Prenatal exposure to nicotine causes postnatal obesity and altered perivascular adipose tissue function. *Obes. Res.* 13, 687–692. doi: 10.1038/oby.2005.77

Gao, Y. J., Lu, C., Su, L. Y., Sharma, A. M., and Lee, R. M. (2007). Modulation of vascular function by perivascular adipose tissue: the role of endothelium and hydrogen peroxide. *Br. J. Pharmacol.* 151, 323–331. doi: 10.1038/sj.bjp.0707228

Gil-Ortega, M., Condezo-Hoyos, L., García-Prieto, C. F., Arribas, S. M., González, M. C., Aranguez, I., et al. (2014). Imbalance between pro and anti-oxidant mechanisms in perivascular adipose tissue aggravates long-term high-fat diet-derived endothelial dysfunction. *PLoS ONE* 9:e95312. doi: 10.1371/journal.pone.0095312

Greenberg, A. S., Egan, J. J., Wek, S. A., Garty, N. B., Blanchette-Mackie, E. J., and Londos, C. (1991). Perilipin, a major hormonally regulated adipocyte-specific phosphoprotein associated with the periphery of lipid storage droplets. *J. Biol. Chem.* 266, 11341–11346.

Greenstein, A. S., Khavandi, K., Withers, S. B., Sonoyama, K., Clancy, O., Jeziorska, M., et al. (2009). Local inflammation and hypoxia abolish the protective anticontractile properties of perivascular fat in obese patients. *Circulation* 119, 1661–1670. doi: 10.1161/CIRCULATIONAHA.108.821181

Greig, F. H., Hutchison, L., Spickett, C. M., and Kennedy, S. (2015). Differential effects of chlorinated and oxidized phospholipids in vascular tissue: implications for neointima formation. *Clin. Sci.* 128, 579–592. doi: 10.1042/CS20140578

Gu, P., and Xu, A. (2013). Interplay between adipose tissue and blood vessels in obesity and vascular dysfunction. *Rev. Endocr. Metab. Disord.* 14, 49–58. doi: 10.1007/s11154-012-9230-8

Guilford, B. L., Parson, J. C., Grote, C. W., Vick, S. N., Ryals, J. M., and Wright, D. E. (2017). Increased FNDC5 is associated with insulin resistance in high fat-fed mice. *Physiol. Rep.* 5:e13319. doi: 10.14814/phy2.13319

Guzik, T. J., Mangalat, D., and Korbut, R. (2006). Adipocytokines - novel link between inflammation and vascular function? *J. Physiol. Pharmacol.* 57, 505–528.

Hardie, D. G. (2011). AMP-activated protein kinase: an energy sensor that regulates all aspects of cell function. *Genes Dev.* 25, 1895–1908. doi: 10.1101/gad.17420111

Jørgensen, S. B., Viollet, B., Andreelli, F., Frøsig, C., Birk, J. B., Schjerling, P., et al. (2004). Knockout of the α2 but Not α1 5′-AMP-activated protein kinase isoform abolishes 5-Aminoimidazole-4-carboxamide-1-β-4-ribofuranosidebut not contraction-induced glucose uptake in skeletal muscle. *J. Biol. Chem.* 279, 1070–1079. doi: 10.1074/jbc.M306205200

Ketonen, J., Shi, J., Martonen, E., and Mervaala, E. (2010). Periadventitial adipose tissue promotes endothelial dysfunction via oxidative stress in diet-induced obese C57Bl/6 mice. *Circ. J.* 74, 1479–1487. doi: 10.1253/circj.CJ-09-0661

Kohlstedt, K., Trouvain, C., Namgaladze, D., and Fleming, I. (2011). Adipocyte-derived lipids increase angiotensin-converting enzyme (ACE) expression and modulate macrophage phenotype. *Basic Res. Cardiol.* 106, 205–215. doi: 10.1007/s00395-010-0137-9

Li, C., Ding, X. Y., Xiang, D. M., Xu, J., Huang, X. L., Hou, F. F., et al. (2015). Enhanced M1 and impaired M2 macrophage polarization and reduced

mitochondrial biogenesis via inhibition of AMP kinase in chronic kidney disease. *Cell. Physiol. Biochem.* 36, 358–372. doi: 10.1159/000430106

Lihn, A. S., Jessen, N., Pedersen, S. B., Lund, S., and Richelsen, B. (2004). AICAR stimulates adiponectin and inhibits cytokines in adipose tissue. *Biochem. Biophys. Res. Commun.* 316, 853–858. doi: 10.1016/j.bbrc.2004.02.139

Löhn, M., Dubrovska, G., Lauterbach, B., Luft, F. C., Gollasch, M., and Sharma, A. M. (2002). Periadventitial fat releases a vascular relaxing factor. *FASEB J.* 16, 1057–1063. doi: 10.1096/fj.02-0024com

Ma, L., Ma, S., He, H., Yang, D., Chen, X., Luo, Z., et al. (2010). Perivascular fat-mediated vascular dysfunction and remodeling through the AMPK/mTOR pathway in high-fat diet-induced obese rats. *Hypertens. Res.* 33, 446–453. doi: 10.1038/hr.2010.11

Ma, S. T., Chen, X. P., Yang, D. C., Yan, Z. C., Liu, D. Y., and Zhu, Z. M. (2009). Perivascular fat mediated vascular dysfunction and remodeling via the AMPK/mTOR pathway in high fat diet-induced obese rats. *Int. J. Cardiol.* 137:S116. doi: 10.1016/j.ijcard.2009.09.393

Maenhaut, N., Boydens, C., and Van de Voorde, J. (2010). Hypoxia enhances the relaxing influence of perivascular adipose tissue in isolated mice aorta. *Eur. J. Pharmacol.* 641, 207–212. doi: 10.1016/j.ejphar.2010.05.058

Mancini, S. J., White, A. D., Bijland, S., Rutherford, C., Graham, D., Richter, E. A., et al. (2017). Activation of AMP-activated protein kinase rapidly suppresses multiple pro-inflammatory pathways in adipocytes including IL-1 receptor-associated kinase-4 phosphorylation. *Mol. Cell. Endocrinol.* 440, 44–56. doi: 10.1016/j.mce.2016.11.010

Manson, J. E., Willett, W. C., Stampfer, M. J., Colditz, G. A., Hunter, D. J., Hankinson, S. E., et al. (1995). Body weight and mortality among women. *N. Engl. J. Med.* 333, 677–685. doi: 10.1056/NEJM199509143331101

Marchesi, C., Ebrahimian, T., Angulo, O., Paradis, P., and Schiffrin, E. L. (2009). Endothelial nitric oxide synthase uncoupling and perivascular adipose oxidative stress and inflammation contribute to vascular dysfunction in a rodent model of metabolic syndrome. *Hypertension* 54, 1384–1392. doi: 10.1161/HYPERTENSIONAHA.109.138305

Nakagawa, K., Higashi, Y., Sasaki, S., Oshima, T., Matsuura, H., and Chayama, K. (2002). Leptin causes vasodilation in humans. *Hypertens. Res.* 25, 161–165. doi: 10.1291/hypres.25.161

Owen, M. K., Witzmann, F. A., Mckenney, M. L., Lai, X., Berwick, Z. C., Moberly, S. P., et al. (2013). Perivascular adipose tissue potentiates contraction of coronary vascular smooth muscle: influence of obesity. *Circulation* 128, 9–18. doi: 10.1161/CIRCULATIONAHA.112.001238

Payne, G. A., Borbouse, L., Kumar, S., Neeb, Z., Alloosh, M., Sturek, M., et al. (2010). Epicardial perivascular adipose-derived leptin exacerbates coronary endothelial dysfunction in metabolic syndrome via a protein kinase C-beta pathway. *Arterioscler. Thromb. Vasc. Biol.* 30, 1711–1717. doi: 10.1161/ATVBAHA.110.210070

Poirier, P., Giles, T. D., Bray, G. A., Hong, Y., Stern, J. S., Pi-Sunyer, F. X., et al. (2006). Obesity and cardiovascular disease: pathophysiology, evaluation, and effect of weight loss. *Arterioscler. Thromb. Vasc. Biol.* 26, 968–976. doi: 10.1161/01.ATV.0000216787.85457.f3

Rebolledo, A., Rebolledo, O. R., Marra, C. A., García, M. E., Roldán Palomo, A. R., Rimorini, L., et al. (2010). Early alterations in vascular contractility associated to changes in fatty acid composition and oxidative stress markers in perivascular adipose tissue. *Cardiovasc. Diabetol.* 9:65. doi: 10.1186/1475-2840-9-65

Ruderman, N. B., Carling, D., Prentki, M., and Cacicedo, J. M. (2013). AMPK, insulin resistance, and the metabolic syndrome. *J. Clin. Invest.* 123, 2764–2772. doi: 10.1172/JCI67227

Salt, I. P., and Hardie, D. G. (2017). AMP_activated protein kinase: an ubiquitous signaling pathway with key roles in the cardiovascular system. *Circ. Res.* 120, 1825–1841. doi: 10.1161/CIRCRESAHA.117.309633

Sell, H., Dietze-Schroeder, D., Eckardt, K., and Eckel, J. (2006). Cytokine secretion by human adipocytes is differentially regulated by adiponectin, AICAR, and troglitazone. *Biochem. Biophys. Res. Commun.* 343, 700–706. doi: 10.1016/j.bbrc.2006.03.010

Skiba, D. S., Nosalski, R., Mikolajczyk, T. P., Siedlinski, M., Rios, F. J., Montezano, A. C., et al. (2017). Anti-atherosclerotic effect of the angiotensin 1-7 mimetic AVE0991 is mediated by inhibition of perivascular and plaque inflammation in early atherosclerosis. *Br. J. Pharmacol.* 174, 4055–4069. doi: 10.1111/bph.13685

Sun, Y., Li, J., Xiao, N., Wang, M., Kou, J., Qi, L., et al. (2014). Pharmacological activation of AMPK ameliorates perivascular adipose/endothelial dysfunction in a manner interdependent on AMPK and SIRT1. *Pharmacol. Res.* 89, 19–28. doi: 10.1016/j.phrs.2014.07.006

Tennant, G. M., Wadsworth, R. M., and Kennedy, S. (2008). PAR-2 mediates increased inflammatory cell adhesion and neointima formation following vascular injury in the mouse. *Atherosclerosis* 198, 57–64. doi: 10.1016/j.atherosclerosis.2007.09.043

Tsuchida, A., Yamauchi, T., Takekawa, S., Hada, Y., Ito, Y., Maki, T., et al. (2005). Peroxisome proliferator–activated receptor (PPAR)α activation increases adiponectin receptors and reduces obesity-related inflammation in adipose tissue. Comparison of activation of PPARα, PPARγ, and their combination. *Diabetes* 54, 3358–3370. doi: 10.2337/diabetes.54.12.3358

Verlohren, S., Dubrovska, G., Tsang, S. Y., Essin, K., Luft, F. C., Huang, Y., et al. (2004). Visceral periadventitial adipose tissue regulates arterial tone of mesenteric arteries. *Hypertension* 44, 271–276. doi: 10.1161/01.HYP.0000140058.28994.ec

Villena, J. A., Viollet, B., Andreelli, F., Kahn, A., Vaulont, S., and Sul, H. S. (2004). Induced adiposity and adipocyte hypertrophy in mice lacking the AMP-activated protein kinase-alpha2 subunit. *Diabetes* 53, 2242–2249. doi: 10.2337/diabetes.53.9.2242

Weingärtner, O., Husche, C., Schött, H. F., Speer, T., Böhm, M., Miller, C. M., et al. (2015). Vascular effects of oxysterols and oxyphytosterols in apoE–/– mice. *Atherosclerosis* 240, 73–79. doi: 10.1016/j.atherosclerosis.2015.02.032

Weston, A. H., Egner, I., Dong, Y., Porter, E. L., Heagerty, A. M., and Edwards, G. (2013). Stimulated release of a hyperpolarizing factor (ADHF) from mesenteric artery perivascular adipose tissue: involvement of myocyte BKCa channels and adiponectin. *Br. J. Pharmacol.* 169, 1500–1509. doi: 10.1111/bph.12157

Zaborska, K. E., Edwards, G., Austin, C., and Wareing, M. (2017). The role of O-GlcNAcylation in perivascular adipose tissue dysfunction of offspring of high-fat diet-fed rats. *J. Vasc. Res.* 54, 79–91. doi: 10.1159/000458422

Zaborska, K. E., Wareing, M., Edwards, G., and Austin, C. (2016). Loss of anti-contractile effect of perivascular adipose tissue in offspring of obese rats. *Int. J. Obes.* 40, 1205–1214. doi: 10.1038/ijo.2016.62

Zhang, Y., Zhang, C., Li, H., and Hou, J. (2017). Down-regulation of vascular PPAR-γ contributes to endothelial dysfunction in high-fat diet-induced obese mice exposed to chronic intermittent hypoxia. *Biochem. Biophys. Res. Commun.* 492, 243–248 doi: 10.1016/j.bbrc.2017.08.058

Conflict of Interest Statement: The authors declare that the research was conducted in the absence of any commercial or financial relationships that could be construed as a potential conflict of interest.

frontiers in Physiology

REVIEW
published: 06 February 2018
doi: 10.3389/fphys.2018.00070

PVAT and Its Relation to Brown, Beige, and White Adipose Tissue in Development and Function

*Staffan Hildebrand, Jasmin Stümer and Alexander Pfeifer**

Institute of Pharmacology and Toxicology, University Hospital Bonn, University of Bonn, Bonn, Germany

Adipose tissue is commonly categorized into three types with distinct functions, phenotypes, and anatomical localizations. White adipose tissue (WAT) is the major energy store; the largest depots of WAT are found in subcutaneous or intravisceral sites. Brown adipose tissue (BAT) is responsible for energy dissipation during cold-exposure (i.e., non-shivering thermogenesis) and is primarily located in the interscapular region. Beige or brite (brown-in-white) adipose tissue can be found interspersed in WAT and can attain a brown-like phenotype. These three types of tissues also have endocrine functions and play major roles in whole body metabolism especially in obesity and its co-morbidities, such as cardiovascular disease. Over the last years, perivascular adipose tissue (PVAT) has emerged as an adipose organ with endocrine and paracrine functions. Pro and anti-inflammatory agents released by PVAT affect vascular health, and are implicated in the inflammatory aspects of atherosclerosis. PVAT shares several of the defining characteristics of brown adipose tissue, including its cellular morphology and expression of thermogenic genes characteristic for brown adipocytes. However, PVATs from different vessels are phenotypically different, and significant developmental differences exist between PVAT and other adipose tissues. Whether PVAT represents classical BAT, beige adipose tissue, or WAT with changing characteristics, is unclear. In this review, we summarize the current knowledge on how PVAT relates to other types of adipose tissue, both in terms of functionality, developmental origins, and its role in obesity-related cardiovascular disease and inflammation.

Keywords: PVAT, perivascular, adipose tissue, BAT, inflammation, cardiovascular disease

OPEN ACCESS

Edited by:
Maik Gollasch,
Charité Universitätsmedizin Berlin, Germany

Reviewed by:
Bradley S. Fleenor,
Ball State University, United States
Keshari Thakali,
University of Arkansas for Medical Sciences, United States

****Correspondence:***
Alexander Pfeifer
alexander.pfeifer@uni-bonn.de

Specialty section:
This article was submitted to Vascular Physiology, a section of the journal Frontiers in Physiology

Received: *21 November 2017*
Accepted: *19 January 2018*
Published: *06 February 2018*

Citation:
Hildebrand S, Stümer J and Pfeifer A (2018) PVAT and Its Relation to Brown, Beige, and White Adipose Tissue in Development and Function. Front. Physiol. 9:70. doi: 10.3389/fphys.2018.00070

INTRODUCTION

During the last decades, the prevalence of obesity has reached pandemic dimensions, doubling since 1990. In 2015, over 600 million obese adults and over 100 million obese children were reported worldwide (Afshin et al., 2017). Obesity is characterized by a high body mass index (BMI) $\geq$30. Overweight and obesity are associated with several severe comorbidities, such as cardiovascular disease, type 2 diabetes mellitus, and certain types of cancer (Chen et al., 2016). Importantly, more than two thirds of the deaths related to overweight and obesity were caused by cardiovascular disease (CVD) (Afshin et al., 2017) showing the importance of vascular disease in metabolic disorders. The defining trait in obesity is the abnormal increase in WAT mass with adipocyte hypertrophy and hyperplasia, brought on by an imbalance between energy intake and energy consumption leading to energy overload. This can result in hypertriglyceridemia, insulin

resistance, and chronic low-grade inflammation first of the adipose tissue and then throughout the whole body (Czech et al., 1977; Hotamisligil, 2006; Guilherme et al., 2008).

In mammals, there are three types of adipose tissues: white, brown and beige. These tissues have distinct functions and consequently have different morphology, protein expression patterns, and developmental origin (Pfeifer and Hoffmann, 2015). The function of white adipose tissue (WAT) is to store energy in the form of lipids, which can be released to fuel other tissues. On the other hand, brown adipose tissue (BAT) has unique thermogenic properties and is a vital organ for maintaining body temperature in smaller mammals and human infants with a high surface-to-volume ratio. Beige or brite (brown-in-white) fat is predominantly found interspersed in WAT depots, but can acquire a brown-like phenotype upon cold exposure or pharmacological stimulation (Chen et al., 2016). In mice, subcutaneous WAT (SAT) has the highest capacity for "browning" or "beiging" (Chen et al., 2016). **Figure 1** shows a simplified schematic of the different (murine) adipose tissues discussed in this review.

Perivascular adipose tissue (PVAT) is the fat surrounding the blood vessels, directly adjacent to the vascular wall, and was considered for long time to serve only structural, vessel-supporting purposes. As fat in general is now well known to be a secretory organ, PVAT is today also recognized to be an endocrine organ, actively releasing bioactive molecules such as pro- and anti-inflammatory cytokines and vasoactive substances (**Figure 2**; Soltis and Cassis, 1991; Gollasch and Dubrovska, 2004; Gao et al., 2007; Britton and Fox, 2011). Over the last years, several studies have been conducted comparing PVAT to other adipose tissues, such as classical BAT and WAT, which we try to summarize in this review. Obesity is associated with an increased risk for CVD and with remodeling of the adipose tissues, both WAT and BAT (Fantuzzi and Mazzone, 2007; Berbée et al., 2015). Given the proximity of PVAT to the vasculature, we also aim to compare the potential impact of PVAT on CVD and vice-versa.

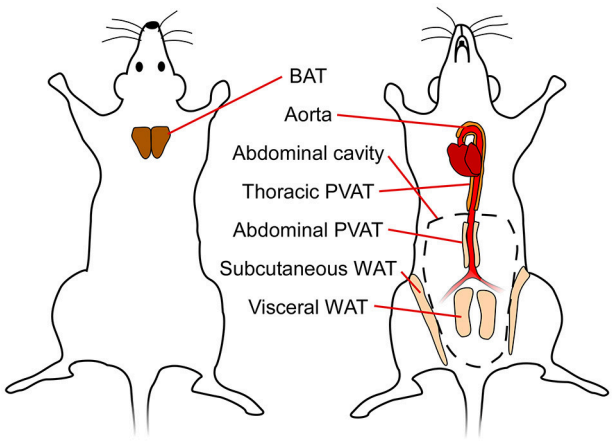

FIGURE 1 | Simplified schematic showing different adipose tissue depots in mice. BAT, brown adipose tissue; WAT, white adipose tissue; PVAT, perivascular adipose tissue.

White Adipose Tissue

WAT makes up the main mass of adipose tissue in human adults, and represents 10-20 percent of body weight in healthy subjects. WAT is widely distributed through the whole body and is located mainly in subcutaneous regions and surrounding internal organs (visceral adipose tissue, VAT) (Chen et al., 2017). WAT is well known as the major organ to store energy in form of triacylglycerols (TAG), which can be mobilized via lipolysis whenever energy is needed. Lipolysis is initiated by norepinephrine binding to beta-adrenergic receptors. This initiates the production of cyclic adenosine-monophosphate (cAMP), the second messenger which activates hormone sensitive lipase via protein kinase A (PKA), resulting in the release of free fatty acids from stored TAG (Duncan et al., 2007).

Morphologically, white adipocytes contain a single, big lipid droplet occupying most of the cytoplasm, and a peripheral nucleus, which leads to a typical signet ring appearance. WAT also has important endocrine functions secreting hormones and cytokines such as leptin, adiponectin, tumor-necrosis factor α (TNFα) and interleukin-6 (IL-6) (Chen et al., 2017). Adipogenic differentiation of white adipocytes is regulated by several known transcription factors including CCAAT/enhancer-binding-proteins C/EBPβ and C/EBPδ, which in turn regulate expression of peroxisome proliferator-activated factor gamma (PPARγ) and C/EBPα. Together, C/EBPα and PPARγ regulate gene transcription and promote differentiation of adipocytes during late WAT adipogenesis (Barak et al., 1999; Rosen et al., 1999; Rosen and MacDougald, 2006; Hudak and Sul, 2013).

Brown Adipose Tissue

BAT plays a crucial role in generating heat via non-shivering thermogenesis (NST) in newborn humans. NST is achieved through the expression of the mitochondrial protein uncoupling protein-1 (UCP-1), which uncouples the respiratory chain and causes a leak of protons across the mitochondrial membrane (Cannon and Nedergaard, 2004; Pfeifer and Hoffmann, 2015). This process results in the generation of heat instead of adenosine triphosphate (ATP), and is initiated by activation of β-3 adrenergic receptors (β3-AR) and adenosine A_{2A} receptors expressed on brown adipocytes (Lowell and Flier, 1997; Gnad et al., 2014). In contrast to white adipocytes, brown adipocytes contain many small lipid droplets leading to a multilocular histological appearance. Furthermore, brown adipocytes contain densely packed mitochondria needed for efficient NST, and is highly vascularised, which taken together causes the characteristic brown color.

Several factors that regulate BAT development have been identified, such as PPARγ, peroxisome proliferator-activated receptor gamma coactivator 1-alpha (PGC-1α), orexin, and bone morphogenic factor 7 (BMP7) (Tseng et al., 2008; Hondares et al., 2011; Cohen et al., 2014).

Nowadays, it is well established that not only newborns but also human adults have depots of BAT that are metabolically active during cold exposure. BAT in human adults is mainly found in the supraclavicular, neck, perirenal and mediastinal region (Nedergaard et al., 2007; Cypess et al., 2009; van Marken Lichtenbelt et al., 2009). These findings are is also in agreement

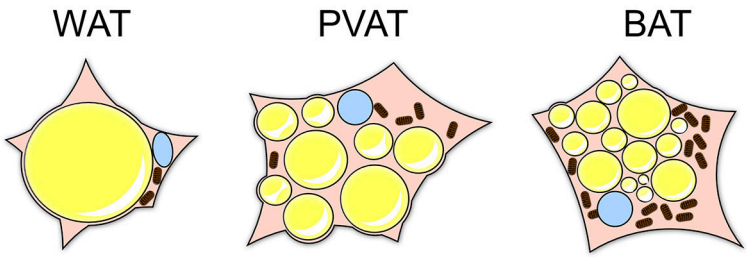

	WAT	PVAT	BAT
Lipid content	Very high, single droplet	High, multiple lipid droplets	High, multiple lipid droplets
Mitochondrial content	Low	High	Very high
UCP1 expression	Very low	Dependent on tissue localization	High
Vascularization	Adequate, compromised in obesity	In direct contact with adventitia of blood vessels	Highly perfused
Function	Storage of lipids, endocrine function	Thermogenesis, regulation of vascular tone	Thermogenesis
Location	Subcutaneous or intra-abdominal	Around blood vessels	Mainly inter- and subscapular
Response to HFD	Hypertrophy, hyperplasia, inflammation (depot dependent)	Some hypertrophy in thoracic PVAT, Hypertrophy, whitening and inflammation in abdominal PVAT	Some hypertrophy

FIGURE 2 | Overview of the characteristics of different adipose tissues. BAT, brown adipose tissue; WAT, white adipose tisse; PVAT, perivascular adipose tissue; HFD, high-fat diet; UCP1, uncoupling protein 1.

with earlier post mortem investigations of human adults tissue showing that BAT can be found in deeper regions of the human body, where it might act as a thermogenic protection for internal organs (Heaton, 1972). Interestingly, studies in human adults have demonstrated a reduced BAT activity in obese and overweight subjects. Conversely, BAT mass positively correlates with resting metabolic rate (van Marken Lichtenbelt et al., 2009). During obesity, the adipocytes in interscapular BAT seem to adopt a white-like phenotype, with increased lipid accumulation (Shimizu et al., 2014).

In summary, the presence of active BAT in human adults makes this special type of fat an interesting target for new therapeutic approaches to tackle obesity.

Beige Adipose Tissue

In response to cold exposure, WAT can adopt a brown-like phenotype in a process called "browning." During browning, UCP-1-expressing brown-like adipocytes, with a high number of mitochondria and multilocular lipid droplets, appear (Lo and Sun, 2013; Pfeifer and Hoffmann, 2015; Chen et al., 2016). These so called beige or brite (brown-in-white) cells also express a number of characteristic markers, such as CD137, Tbx1, and Cited-1 (Harms and Seale, 2013). The capacity for browning varies between the different WAT depots, with SAT being more prone to browning than VAT (Seale et al., 2011). This probably owes mainly to differential expression of PR domain containing 16 (PRDM16) in SAT and VAT. PRDM16 is critical for phenotypic maintenance of classical BAT, and is more highly expressed in SAT than VAT (Seale et al., 2011). Importantly, ablation of PRDM16 in adipocytes disrupts browning of SAT upon cold exposure (Cohen et al., 2014). The interconversion of adipocytes has been reported to be possible in both directions: white adipocytes gain a beige/brite phenotype during cold exposure, and return to a white adipocyte-like appearance after removal of the cold stimulus (Rosenwald et al., 2013).

PVAT AS BROWN ADIPOSE TISSUE

Similarities and Differences between PVAT vs. BAT, WAT, or Beige Fat

Several reports (Gálvez-Prieto et al., 2008; Police et al., 2009; Fitzgibbons et al., 2011) indicate that depending on the localization, PVAT can resemble either WAT or BAT. Thoracic periaortic adipose tissue is morphologically similar to BAT, with adipocytes that have a multilocular appearance and round nuclei (Fitzgibbons et al., 2011). A direct comparison of gene expression of thoracic PVAT, interscapular BAT and WAT from mice revealed that only 228 genes (i.e. 0.79%) were significantly different between thoracic PVAT and classical BAT (Fitzgibbons et al., 2011). Interestingly, there was no significant difference in the expression levels of the genes known to be typically expressed in classical BAT, such as *Cidea*, *Ucp-1*, or *PPARγ* (Fitzgibbons et al., 2011). Furthermore, proteomic analysis shows striking similarities in protein expression between periaortic adipose tissue and classical BAT, but not WAT (Chang et al., 2012).

In contrast to beige adipose tissue, thoracic PVAT maintains a BAT-like phenotype in the absence of activating stimuli. Furthermore, perivascular adipocytes do not undergo significant

whitening during high fat diet (HFD) feeding, which is characteristic of BAT (Fitzgibbons et al., 2011). These findings suggest that, from a morphological and functional standpoint, thoracic PVAT more closely resembles classical BAT than beige fat.

Functionally, PVAT also exhibits important similarities with BAT. Chang et al. created a PVAT-deficient mouse by knocking out PPARγ in smooth muscle cells, and were able to show that PVAT significantly contributes to maintaining intravascular temperature during cold exposure. While PVAT activation could not completely rescue the reduction in intravascular temperature caused by resection of BAT, mice lacking both BAT and PVAT had significantly lower intravascular temperature than mice lacking only BAT (Chang et al., 2012).

However, there are also reports characterizing PVAT as WAT or WAT-like (Omar et al., 2014). This discrepancy appears to derive from the anatomical localization of the PVAT. In contrast to thoracic PVAT, the adipose tissue surrounding the abdominal aorta appears to be similar to WAT. In obese mice, the abdominal PVAT has been described to have a white-like phenotype with a primarily unilocular appearance (Police et al., 2009). Additionally, the mesenteric PVAT has been described to be similar to WAT with large lipid droplets and low expression levels of UCP-1 (Gálvez-Prieto et al., 2008).

Together, these data suggest that the functional phenotype of PVAT is directly linked with its anatomical localization. Thoracic PVAT is phenotypically close to BAT, and shares its unique functional characteristics. Abdominal PVAT, on the other hand, has been described to closely resemble WAT, and has a similar role in obesity-induced inflammatory responses. Furthermore, PVAT does not seem to share the dynamic properties of beige fat: thoracic PVAT displays a BAT-like phenotype without external stimuli, and does not readily lose this phenotype in diet-induced obesity.

Developmental Differences between PVAT, BAT, WAT, and Beige Fat

While the phenotype of thoracic PVAT may be almost indistinguishable from BAT, the question whether or not it is classical BAT is still not solved. On the other hand, location of PVAT might determine its color/phenotype: some parts of PVAT, e.g., abdominal PVAT, have been reported to resemble WAT (Police et al., 2009; Gálvez-Prieto et al., 2012). During embryogenesis, the mesodermal germ layer gives rise to mesenchymal progenitors that in turn differentiate into all types of adipocyte precursor cells. However, over the last decade, it has become increasingly clear that adipocytes of different adipose tissue depots are derived from precursor cells of distinct lineages. This notion is underlined by the fact that mature adipocytes of different depots appear at different times during embryogenesis (Xue et al., 2007; Wang et al., 2013; Hong et al., 2015). Functional mature brown adipocytes in the interscapular region are necessary for temperature homeostasis immediately at birth, and consequently start developing around 4 days prior to birth (Xue et al., 2007). White adipocytes mostly develop after birth, although significant differences exist between WAT tissues in different depots. This was recently demonstrated by Wang et al., who used an inducible adipocyte labeling system based on the adiponectin promoter to track adipogenesis *in vivo* (Wang et al., 2013). In this study, visceral adipocytes were found to start developing postnatally, while subcutaneous adipocytes initiated differentiation in the embryo (around E16) (Wang et al., 2013). The latter finding is also corroborated by another study, where flow cytometry and histological analysis revealed a subcutaneous population of lipid-lacking perilipin$^+$/adiponectin$^+$ preadipocytes appearing at E16.5 (Hong et al., 2015). Considering the phenotypical differences between PVAT surrounding different vessels, it is plausible that location-specific differences in PVAT development also exist.

Aside from the temporal regulation of adipocyte differentiation, differences can also be found in the progenitor cells themselves that give rise to mature adipocytes of different depots. *De novo* adipogenesis of white fat occurs close to blood vessels, and several studies have demonstrated that white adipocytes develop from perivascular platelet-derived growth factor α-expressing (Pdgfrα$^+$) progenitor cells (Berry and Rodeheffer, 2013; Hong et al., 2015; Sun et al., 2017). However, adipocyte progenitors cannot be identified solely based on Pdgfrα expression, as not all vascular Pdgfrα$^+$ cells are adipogenic (Berry and Rodeheffer, 2013). Other studies have shown that the vascular fraction capable of *in vitro* adipogenesis is CD31$^-$CD34$^+$, which is an antigen signature that matches adventitial fibroblasts rather than endothelial or mural cells (Guimaraes-Camboa and Evans, 2017; Hepler and Gupta, 2017). White adipocytes that develop in adulthood, e.g., during obesity-induced WAT hyperplasia, likely have a different origin. Here, mature adipocytes derive from specialized mural Pdgfrβ$^+$ precursor cells residing in the blood vessels of adipose tissue, although the exact identity of these cells is unknown (Jiang et al., 2014; Vishvanath et al., 2016).

On the other hand, brown adipocytes appear to stem from myogenic progenitors, and indeed share many characteristics with skeletal muscle cells, such as a similar transcriptome and mitochondrial proteome (Forner et al., 2009). The myogenic transcription factors paired box protein Pax-3 and 7 (Pax3, Pax7), as well as myogenic factor 5 (Myf5), are activated during the early development of brown adipocytes from mesenchymal stem cells (Lepper and Fan, 2010; Sanchez-Gurmaches and Guertin, 2014). From these Myf5$^+$Pax3$^+$Pax7$^+$ precursors, brown preadipocytes become committed to the brown fat lineage through activation of BMP7 (Park et al., 2013). An earlier study identified PRDM16 as a key determinant of brown adipocyte commitment during development (Seale et al., 2008), but more recent investigations suggest that PRDM16 primarily maintains the BAT phenotype postnatally (Harms et al., 2014). The myogenic lineage described above may not be accurate for all BAT depots, as a recent study, in which detailed lineage analysis were performed, revealed that only the major depots (inter- and subscapular) of BAT are exclusively derived from Myf5$^+$Pax3$^+$ precursors. Furthermore, the myogenic lineage may also not be unique to BAT (Sanchez-Gurmaches and Guertin, 2014): some WAT depots are in fact derived solely from Myf5$^+$ cells (Sanchez-Gurmaches and Guertin, 2014). This suggests that certain canonical BAT

lineage markers may correlate more closely to anatomical localization of the tissue during development, rather than functionality.

Beige cells are often described as inducible brown adipocytes, although there is no consensus concerning the embryonic origin of beige adipocytes (Pfeifer and Hoffmann, 2015). Four possible lineages of beige adipocyte development have been suggested: (1) transdifferentiation of mature white adipocytes (Himms-Hagen et al., 2000; Vitali et al., 2012), (2) maturation of brown preadipocytes already existing in WAT (Wang et al., 2014), (3) differentiation and maturation of pre-existing white preadipocytes (Seale et al., 2008), or (4) differentiation from vascular precursors, similarly to what occurs during WAT hyperplasia (Long et al., 2014). In fact, the amounting data from recent studies suggest that all these pathways could contribute to beige adipocyte development, depending on tissue depot and stimuli (Harms and Seale, 2013). While transdifferentiation of mature adipocytes probably only takes place on a low scale (Harms and Seale, 2013), beige adipocytes can arise from brown-like preadipocytes ($Myf5^+$) or white-like preadipocytes ($Myf5^-$) depending on the developmental origin of the depot in question (Sanchez-Gurmaches et al., 2012). However, it is not presently clear whether this diverging lineage translates into functional differences. Furthermore, prolonged cold exposure in rodents (>2 weeks) leads to beige adipogenesis from the same mural $Pdgfr\beta^+$ precursor population that is responsible for diet-induced WAT hyperplasia (Vishvanath et al., 2016).

Perivascular fat does not share the myogenic lineage of classical brown fat. Rather, PVAT seems to share a developmental origin with vascular smooth muscle (mural) cells. Chang and colleagues deleted the master regulator of adipogenesis PPARγ in smooth muscle by crossing SM22α-Cre mice with $PPAR\gamma^{flox/flox}$ mice (Chang et al., 2012). This resulted in a complete loss of PVAT, but no change in either WAT or BAT development. The expression of SM22α in mesenchymal cells proximal to the aorta during early embryogenesis might suggest that PVAT development is initiated during embryonic development, which would distinguish it from other mural-derived adipose tissues (Li et al., 1996). However, further investigation is needed to clarify this.

Additionally, thoracic PVAT cells originate from $Myf5^-$ precursors, further separating them from intrascapular classical brown adipocytes (Sanchez-Gurmaches and Guertin, 2014). Thoracic PVAT also seems to develop differently in males and females: a majority of periaortic adipocytes in females originate from $Pax3^+$ precursors, while all periaortic adipocytes in males arise from $Pax3^-$ cells. In contrast, 99–100% of all interscapular and subscapular brown adipocytes from both genders are derived from $Pax3^+$ precursors (Sanchez-Gurmaches and Guertin, 2014). In summary, these data suggest that the functional differences between thoracic PVAT and BAT are almost negligible. In contrast, abdominal PVAT has been suggested to closely resemble WAT (Police et al., 2009; Gálvez-Prieto et al., 2012). PVAT might be categorized as a fourth type of fat tissue which seems to be developmentally different from BAT, WAT, and beige fat.

PVAT IN OBESITY-RELATED VASCULAR DISEASE

Atherosclerosis

CVD is the leading cause of mortality globally, and is responsible for almost a third of all deaths world-wide (WHO, 2017). The underlying cause of CVD is atherosclerosis, the thickening and hardening of arterial walls because of: (1) endothelial dysfunction, (2) retention and accumulation of low-density lipoprotein (LDL) particles and immune cells in the tunica intima, and (3) proliferation and migration of intimal smooth muscle cells. If unaddressed, this condition can progress to various life-threatening conditions such as thrombosis, myocardial infarction, and stroke (Lusis, 2000).

Inflammation is intimately linked with atherosclerosis. The initial step in atherogenesis is endothelial dysfunction, leading to increased retention of LDL particles in the subendothelial space. The retained particles are then modified in various ways (e.g., oxidation and glycation), which turns them into auto-antigens, inducing a low-grade inflammation (Rader and Daugherty, 2008; Tabas et al., 2015). The inflammatory response activates endothelial cells, leading to increased adhesion and infiltration and monocytes (Madamanchi et al., 2005; Tabas et al., 2015). Intra-intimal differentiation of monocytes into macrophages plays a key role in atherogenesis, and accumulation of the modified LDL particles in these macrophages eventually turns them into the foam cells that are characteristic of atherosclerosis (Tabas et al., 2015). The adaptive immune system is also important for atherogenesis. T-cells and B-cells infiltrate the intima following endothelial cell activation, and have both been demonstrated to regulate the progression of atherosclerosis (Ammirati et al., 2015). Immunodeficiency in mice reduces plaque formation, and reconstituting $CD4^+$ T-cells in *scid/scid* mice increases it (Dansky et al., 1997; Zhou et al., 2000). Furthermore, selective depletion of $CD4^+$ T-cells using antibodies reduces fatty streak formation in early atherogenesis (Emeson et al., 1996). On the other hand, B-cell depletion by splenectomy increases atherogenesis, and subsequent B-cell transfer from donor mice decreases it, possibly through regulation of T-cell activity (Caligiuri et al., 2002).

PVAT and Inflammation

While conventional monocyte and T-cell infiltration occurs from the luminal side of the vessel wall, accumulating evidence also suggests that adventitia plays an important role in vascular inflammation. T-cells, B-cells, monocytes, and mature macrophages all reside in the adventitia of diseased vessels (Maiellaro and Taylor, 2007), the former two exceeding their corresponding numbers in the intima of $ApoE^{-/-}$ mice up to 80-fold. Furthermore, adventitial vasa vasorum neovascularisation has been shown to precede endothelial dysfunction in hypercholesterolemic pigs (Herrmann et al., 2001). This suggests that immune cell infiltration occurs not only from the luminal side of the vessel (inside-out), but also from the adventitial side (outside-in) (Kawabe and Hasebe, 2014). Considering this, the role of PVAT in arterial inflammation is

of great interest due to its location to the vessel wall, especially considering the lack of a fascia separating the PVAT from the adventitia. This direct contact enables significant paracrine signaling from PVAT to the vessel wall, and PVAT is indeed known to release numerous paracrine factors that influence the vessel in terms of both inflammation and contractility. Pro- and anti-inflammatory agents released by PVAT include leptin (Gálvez-Prieto et al., 2012; Li et al., 2014), adiponectin (Lynch et al., 2013; Antonopoulos et al., 2015), resistin (Park et al., 2014), TNF-α (DeVallance et al., 2016), MCP-1 (Manka et al., 2014), TGF-β (Chatterjee et al., 2013), angiopoietin-like protein 2 (Angptl2) (Tian et al., 2013), and IL-6 (Du et al., 2015), all of which are known to influence the progression of atherosclerosis in some way:

Adenoviral overexpression of leptin in PVAT promotes neointima formation, and transplantation of PVAT from HFD-fed obese mice, but not leptin-deficient *ob/ob* mice, to injured vessels increases neointima formation (Schroeter et al., 2013). Additionally, vascular smooth muscle cells (VSMCs) incubated with conditioned medium from the PVAT of HFD-fed rats increased leptin-dependent switching to the proliferative, synthetic phenotype characteristic of VSMCs in the neointima (Li et al., 2014).

Adiponectin is widely described as anti-inflammatory and protective against atherosclerosis (Xita and Tsatsoulis, 2012; Antonopoulos et al., 2015). Adiponectin-deficient mice have pronounced neointima formation upon wire injury, which can be rescued by local administration of recombinant adiponectin to the adventitial region of the injured vessels (Takaoka et al., 2009). This suggests that adiponectin secreted from PVAT may be protective against neointimal hyperplasia.

PVAT-derived resistin has not been directly shown to influence atherosclerosis, but does increase the expression of osteopontin in VSMCs (Park et al., 2014), which in turn has been implicated in VSMC proliferation and restenosis (Panda et al., 1997; Shimizu et al., 2004).

The effect of PVAT on intimal VSMC infiltration has also been investigated after transplantation of thoracic PVAT to wire-injured carotid arteries, where the presence of PVAT accelerated neointimal formation in an MCP-1 dependent manner (Manka et al., 2014). Interestingly, MCP-1 did not influence the infiltration of macrophages. MCP-1 has also been shown to stimulate VSMC proliferation *in vitro* (Viedt et al., 2002).

Moreover, inflamed PVAT increases VSMC proliferation in a TGF-β dependent manner, suggesting that TGF-β released from PVAT can potentiate neointima formation (Moe et al., 2013) The PVAT transplantation approach has also been used to study the effects of PVAT-derived Angptl2 on the progression of neointimal hyperplasia after endovascular injury (Tian et al., 2013). Here, PVAT from mice over-expressing Angptl2 accelerate neointima formation, while PVAT from Angptl2$^{-/-}$ mice attenuated it. One should note, however, that the role of VSMC migration and proliferation in atherosclerosis is still debated (Bennett et al., 2016). Recent studies suggest that proliferation of VSMC is mainly protective, stabilizing the late-stage plaque rather than contributing to its formation (Bennett et al., 2016). Experiments in which PVAT has been replaced by other adipose tissue depots also hint to the similarities in paracrine signaling between PVAT and WAT. Two studies have examined the effects of replacing femoral PVAT with VAT and SAT, respectively, on neointimal formation (Takaoka et al., 2009; Tian et al., 2013). Interestingly, both studies arrived at the same result: removal of PVAT exacerbates neointimal hyperplasia, and transplantation of either VAT or SAT attenuates this effect (Takaoka et al., 2009; Tian et al., 2013). These studies corroborate previous reports that femoral PVAT is similar to WAT (Brown et al., 2014).

TNF-α and IL-6 are also known to accelerate atherogenesis, although evidence of PVAT directly affecting neointima formation via these molecules is lacking (Moe et al., 2013; Hartman and Frishman, 2014). The role of IL-6 seems to be dose-dependent: several studies have confirmed the pro-inflammatory effects of IL-6 in atherosclerosis models (Hartman and Frishman, 2014), but a complete loss of IL-6 increases plaque formation and serum cholesterol levels in ApoE$^{-/-}$ mice (Schieffer et al., 2004).

Under homeostatic conditions, the anti-inflammatory effects of PVAT predominate, and secretion of pro-inflammatory paracrine agents is relatively low (Police et al., 2009; Fitzgibbons and Czech, 2014). In hypertriglyceridemia and obesity, however, there is significant upregulation of several pro-inflammatory chemokines and macrophage markers in both thoracic and abdominal PVAT (Police et al., 2009). The inflammatory response in thoracic PVAT, however, is quite low in comparison to abdominal PVAT, further supporting the notion that thoracic and abdominal PVAT closely resemble BAT and WAT, respectively (Police et al., 2009; Padilla et al., 2013).

The BAT-like phenotype of thoracic PVAT may also influence the progression of atherosclerosis in an inflammation-independent manner. Cold exposure activates both BAT and thoracic PVAT (Chang et al., 2012), initiating thermogenesis via mitochondrial uncoupling. The high requirement for fuel in this process leads to a dramatic increase in the uptake of circulating triglycerides into BAT, greatly reducing the levels of serum lipoprotein particles in both genetic and diet-induced models of obesity (Bartelt et al., 2011). In fact, activation of BAT has been shown to directly protect from atherogenesis through this mechanism in a recent study (Berbée et al., 2015). Interestingly, this study also addressed lipid uptake into PVAT during stimulation with the β3-AR agonist CL316243. Treatment with the agonist significantly increased uptake of lipids from the circulation in manner similar to BAT (Berbée et al., 2015), suggesting that cold exposure could also lead to an amelioration of diet-induced hypertriglyceridemia through PVAT activation, which in turn would slow the progression of atherosclerosis. Interestingly, activation of PVAT through cold exposure has been shown to reduce the expression of pro-inflammatory markers in ferrets, indicating a possible therapeutic role of PVAT in atherosclerosis and other inflammatory vascular diseases (Reynés et al., 2017).

The effects of aging also highlight the phenotypical differences between thoracic and abdominal PVAT. Padilla et al. investigated the expression of several inflammation-related genes in adipose tissues of young and old rats. Although neither thoracic nor abdominal PVAT showed any strong age-related increase in

any of the analyzed inflammation markers, basal expression of almost all analyzed inflammatory markers was increased in abdominal compared to thoracic PVAT (Padilla et al., 2013). Moreover, abdominal, but not thoracic, PVAT of older rats had higher level of CD11α and FoxP3, indicating increased immune cell infiltration (Padilla et al., 2013). Bailey-Downs et al. also studied the combined effects of aging and HFD on inflammation in thoracic PVAT in mice (Bailey-Downs et al., 2013). Conditioned medium containing the secretome from PVAT excised from young or old mice fed either HFD or control diet (CD) was applied to aortic segments, and the inflammatory response of the vessels were analyzed. Interestingly, segments incubated with the conditioned medium from HFD-PVAT had higher levels of TNFα and IL-6 expression than segments incubated with conditioned medium from CD-PVAT (Bailey-Downs et al., 2013). Analysis of the PVAT itself after HFD or CD feeding did not reveal any significant increase in macrophage infiltration. This may indicate that while HFD does not necessarily lead to an increased state of inflammation in thoracic PVAT itself, it may contribute to inflammation in the vessel wall through paracrine signaling. In this study, aging strongly exacerbated the effects of HFD, both in terms of vessel inflammation and macrophage infiltration in PVAT (Bailey-Downs et al., 2013).

PVAT and ROS Production

Recently, a role for PVAT in regulating reactive oxygen species (ROS) production in vessels was described. ROS production by NADPH oxidases is a critical step for the development of endothelial dysfunction in several pathologies, including diabetes, atherosclerosis, and aging (Guzik et al., 2000; Guzik and Harrison, 2006). Analysis of the internal mammary arteries and the adjacent PVAT in a cohort of 386 patients revealed a strong correlation of insulin resistance and type 2 diabetes, with both lower serum adiponectin levels and increased O_2^- production in the vascular wall. Additionally, artery segments incubated with adiponectin had significantly reduced vascular NADPH-dependent O_2^- production, and scavenging O_2^- radicals reduced adiponectin expression in PVAT. This study indicates that PVAT can detect ROS production in its adjacent artery, and in turn reduce it by increasing adiponectin expression (Antonopoulos et al., 2015).

ROS production in PVAT has also been implicated in obesity. Aortic PVAT from mice fed a HFD showed an increased TNF-α mediated ROS production, with increased contractile tone of the underlying vessel (Ketonen et al., 2010; da Costa et al., 2017). ROS production in thoracic PVAT following HFD is also known to be exacerbated by aging (Bailey-Downs et al., 2013). Whether or not this HFD-induced ROS production is partly responsible for the progression of e.g., atherosclerosis has not been directly studied.

PVAT in Hypertension

Hypertension is a common complication of obesity and affects almost 60% of obese individuals (Must et al., 1999). While the development of hypertension in obesity is multifactorial, it can partly be ascribed to the endocrine effects of adipose tissue (Sharma et al., 2001; Re, 2009). In obesity, WAT releases several factors that are known to affect vascular tone and blood pressure (Yiannikouris et al., 2010). These include leptin (Bravo et al., 2006), angiotensin II (Schütten et al., 2017), non-esterified fatty acids (NEFAs) (Sarafidis and Bakris, 2007), adiponectin (Ohashi et al., 2011), and resistin (Zhang et al., 2017). Interestingly, all these factors have been shown to be released from PVAT (see also above) (Lu et al., 2010; Gálvez-Prieto et al., 2012; Campia et al., 2014; Park et al., 2014; Antonopoulos et al., 2015). While this could indicate that PVAT is similar to WAT in terms of its regulation of hypertension, studies examining the role of BAT in hypertension are lacking. Furthermore, in some studies examining the release of the above mentioned factors, it is not immediately clear which type of PVAT was studied, making a thorough comparative analysis impossible (Gálvez-Prieto et al., 2012; Park et al., 2014). PVAT also releases numerous factors that directly affect vascular tone in a paracrine fashion, including norepinephrine, nitric oxide, hydrogen sulfide, and methyl palmitate (Lee et al., 2011; Chang et al., 2013). However, relating the release of these factors from PVAT to the effects of WAT on systemic vascular tone in obesity is not meaningful.

OUTLOOK

As the obesity pandemic continues to grow, there is an urgent need for effective pharmacological treatment of both the underlying causes and the associated comorbidities. Understanding the basic biology of the implicated tissues, as well as the pathological alterations and processes, is essential for the development of new therapeutic strategies. So far, the understanding of the role of PVAT in vascular disease is in its infancy, but recent studies indicate that several features of PVAT could have positive effects on the progression of atherosclerosis and endothelial dysfunction in various ways.

While the origin of PVAT seems to be different from BAT, their phenotypes appear almost indistinguishable, both in thermogenic properties and resistance to diet-induced inflammation. The thermogenic capacity of thoracic PVAT, for example, could prove useful in regulating energy expenditure, and should be investigated for a potential role in the treatment of energy balance-related diseases such as obesity and diabetes. Phenotypically and functionally, it is tempting to categorize thoracic PVAT as BAT, and abdominal and femoral PVAT as WAT. However, the developmental origins of PVAT seem to differ from both BAT and WAT, although this remains to be fully elucidated. In summary, the available evidence points to clear differences between PVAT and other adipose tissues. Thus, PVAT might be regarded as neither BAT nor WAT, but rather as a distinct type of adipose tissue.

AUTHOR CONTRIBUTIONS

All authors listed have made a substantial, direct and intellectual contribution to the work, and approved it for publication.

FUNDING

JS was supported by the BONFOR research commission of the Medical Faculty, University of Bonn.

REFERENCES

Afshin, A., Forouzanfar, M. H., Reitsma, M. B., Sur, P., Estep, K., Lee, A., et al. (2017). Health effects of overweight and obesity in 195 countries over 25 years. *N. Engl. J. Med.* 377, 13–27. 173–187. doi: 10.1056/NEJMoa1614362

Ammirati, E., Moroni, F., Magnoni, M., and Camici, P. G. (2015). The role of T and B cells in human atherosclerosis and atherothrombosis. *Clin. Exp. Immunol.* 179, 173–187. doi: 10.1111/cei.12477

Antonopoulos, A. S., Margaritis, M., Coutinho, P., Shirodaria, C., Psarros, C., Herdman, L., et al. (2015). Adiponectin as a link between type 2 diabetes and vascular NADPH oxidase activity in the human arterial wall: the regulatory role of perivascular adipose tissue. *Diabetes* 64, 2207–2219. doi: 10.2337/db14-1011

Bailey-Downs, L. C., Tucsek, Z., Toth, P., Sosnowska, D., Gautam, T., Sonntag, W. E., et al. (2013). Aging exacerbates obesity-induced oxidative stress and inflammation in perivascular adipose tissue in mice: a paracrine mechanism contributing to vascular redox dysregulation and inflammation. *J. Gerontol. A Biol. Sci. Med. Sci.* 68, 780–792. doi: 10.1093/gerona/gls238

Barak, Y., Nelson, M. C., Ong, E. S., Jones, Y. Z., Ruiz-Lozano, P., Chien, K. R., et al. (1999). PPAR gamma is required for placental, cardiac, and adipose tissue development. *Mol. Cell* 4, 585–595. doi: 10.1016/S1097-2765(00)80209-9

Bartelt, A., Bruns, O. T., Reimer, R., Hohenberg, H., Ittrich, H., Peldschus, K., et al. (2011). Brown adipose tissue activity controls triglyceride clearance. *Nat. Med.* 17, 200–205. doi: 10.1038/nm.2297

Bennett, M. R., Sinha, S., and Owens, G. K. (2016). Vascular smooth muscle cells in Atherosclerosis. *Circ. Res.* 118, 692–702. doi: 10.1161/CIRCRESAHA.115.306361

Berbée, J. F., Boon, M. R., Khedoe, P. P., Bartelt, A., Schlein, C., Worthmann, A., et al. (2015). Brown fat activation reduces hypercholesterolaemia and protects from atherosclerosis development. *Nat. Commun.* 6:6356. doi: 10.1038/ncomms7356

Berry, R., and Rodeheffer, M. S. (2013). Characterization of the adipocyte cellular lineage *in vivo*. *Nat. Cell Biol.* 15, 302–308. doi: 10.1038/ncb2696

Bravo, P. E., Morse, S., Borne, D. M., Aguilar, E. A., and Reisin, E. (2006). Leptin and hypertension in obesity. *Vasc. Health Risk Manag.* 2, 163–169. doi: 10.2147/vhrm.2006.2.2.163

Britton, K. A., and Fox, C. S. (2011). Perivascular adipose tissue and vascular disease. *Clin. Lipidol.* 6, 79–91. doi: 10.2217/clp.10.89

Brown, N. K., Zhou, Z., Zhang, J., Zeng, R., Wu, J., Eitzman, D. T., et al. (2014). Perivascular adipose tissue in vascular function and disease: a review of current research and animal models. *Arterioscler. Thromb. Vasc. Biol.* 34, 1621–1630. doi: 10.1161/ATVBAHA.114.303029

Caligiuri, G., Nicoletti, A., Poirier, B., and Hansson, G. K. (2002). Protective immunity against atherosclerosis carried by B cells of hypercholesterolemic mice. *J. Clin. Invest.* 109, 745–753. doi: 10.1172/JCI7272

Campia, U., Tesauro, M., Di Daniele, N., and Cardillo, C. (2014). The vascular endothelin system in obesity and type 2 diabetes: pathophysiology and therapeutic implications. *Life Sci.* 118, 149–155. doi: 10.1016/j.lfs.2014.02.028

Cannon, B., and Nedergaard, J. (2004). Brown adipose tissue: function and physiological significance. *Physiol. Rev.* 84, 277–359. doi: 10.1152/physrev.00015.2003

Chang, L., Milton, H., Eitzman, D. T., and Chen, Y. E. (2013). Paradoxical roles of perivascular adipose tissue in atherosclerosis and hypertension. *Circ. J.* 77, 11–18. doi: 10.1253/circj.CJ-12-1393

Chang, L., Villacorta, L., Li, R., Hamblin, M., Xu, W., Dou, C., et al. (2012). Loss of perivascular adipose tissue on peroxisome proliferator-activated receptor-gamma deletion in smooth muscle cells impairs intravascular thermoregulation and enhances atherosclerosis. *Circulation* 126, 1067–1078. doi: 10.1161/CIRCULATIONAHA.112.104489

Chatterjee, T. K., Aronow, B. J., Tong, W. S., Manka, D., Tang, Y., Bogdanov, V. Y., et al. (2013). Human coronary artery perivascular adipocytes overexpress genes responsible for regulating vascular morphology, inflammation, and hemostasis. *Physiol. Genomics.* 45, 697–709. doi: 10.1152/physiolgenomics.00042.2013

Chen, Y., Pan, R., and Pfeifer, A. (2016). Fat tissues, the brite and the dark sides. *Pflugers Arch.* 468, 1803–1807. doi: 10.1007/s00424-016-1884-8

Chen, Y., Pan, R., and Pfeifer, A. (2017). Regulation of brown and beige fat by microRNAs. *Pharmacol. Ther.* 170, 1–7. doi: 10.1016/j.pharmthera.2016.10.004

Cohen, P., Levy, J. D., Zhang, Y., Frontini, A., Kolodin, D. P., Svensson, K. J., et al. (2014). Ablation of PRDM16 and beige adipose causes metabolic dysfunction and a subcutaneous to visceral fat switch. *Cell* 156, 304–316. doi: 10.1016/j.cell.2013.12.021

Cypess, A. M., Lehman, S., Williams, G., Tal, I., Rodman, D., Goldfine, A. B., et al. (2009). Identification and importance of brown adipose tissue in adult humans. *N. Engl. J. Med.* 360, 1509–1517. doi: 10.1056/NEJMoa0810780

Czech, M. P., Richardson, D. K., and Smith, C. J. (1977). Biochemical basis of fat cell insulin resistance in obese rodents and man. *Metab. Clin. Exp.* 26, 1057–1078. doi: 10.1016/0026-0495(77)90024-5

da Costa, R. M., Fais, R. S., Dechandt, R. P. C., Louzada-Junior, P., Alberici, L. C., Lobato, N. S., et al. (2017). Increased mitochondrial ROS generation mediates the loss of the anti-contractile effects of perivascular adipose tissue in high-fat diet obese mice. *Br. J. Pharmacol.* 174, 3527–3541. doi: 10.1111/bph.13687

Dansky, H. M., Charlton, S. A., Harper, M. M., and Smith, J. D. (1997). T and B lymphocytes play a minor role in atherosclerotic plaque formation in the apolipoprotein E-deficient mouse. *Proc. Natl. Acad. Sci. U.S.A.* 94, 4642–4646. doi: 10.1073/pnas.94.9.4642

DeVallance, E., Branyan, K., Lemaster, K., Brooks, S., Asano, S., Skinner, R., et al. (2016). Perivascular adipose tissue derived TNF α neutralization recovers aortic function in metabolic syndrome. *FASEB J.* 30:1282.7. doi: 10.1096/fasebj.30.1_supplement.1282.7

Du, B., Ouyang, A., Eng, J. S., and Fleenor, B. S. (2015). Aortic perivascular adipose-derived interleukin-6 contributes to arterial stiffness in low-density lipoprotein receptor deficient mice. *Am. J. Physiol. Heart Circ. Physiol.* 308, H1382–H1390. doi: 10.1152/ajpheart.00712.2014

Duncan, R. E., Ahmadian, M., Jaworski, K., Sarkadi-Nagy, E., and Sul, H. S. (2007). Regulation of lipolysis in adipocytes. *Annu. Rev. Nutr.* 27, 79–101. doi: 10.1146/annurev.nutr.27.061406.093734

Emeson, E. E., Shen, M. L., Bell, C. G., and Qureshi, A. (1996). Inhibition of atherosclerosis in CD4 T-cell-ablated and nude (nu/nu) C57BL/6 hyperlipidemic mice. *Am. J. Pathol.* 149, 675–685.

Fantuzzi, G., and Mazzone, T. (2007). Adipose tissue and atherosclerosis: exploring the connection. *Arterioscler. Thromb. Vasc. Biol.* 27, 996–1003. doi: 10.1161/ATVBAHA.106.131755

Fitzgibbons, T. P., and Czech, M. P. (2014). Epicardial and perivascular adipose tissues and their influence on cardiovascular disease: basic mechanisms and clinical associations. *J. Am. Heart Assoc.* 3:e000582. doi: 10.1161/JAHA.113.000582

Fitzgibbons, T. P., Kogan, S., Aouadi, M., Hendricks, G. M., Straubhaar, J., and Czech, M. P. (2011). Similarity of mouse perivascular and brown adipose tissues and their resistance to diet-induced inflammation. *Am. J. Physiol. Heart Circ. Physiol.* 301, H1425–H1437. doi: 10.1152/ajpheart.00376.2011

Forner, F., Kumar, C., Luber, C. A., Fromme, T., Klingenspor, M., and Mann, M. (2009). Proteome differences between brown and white fat mitochondria reveal specialized metabolic functions. *Cell Metab.* 10, 324–335. doi: 10.1016/j.cmet.2009.08.014

Gálvez-Prieto, B., Bolbrinker, J., Stucchi, P., de Las Heras, A. I., Merino, B., Arribas, S. et al. (2008). Comparative expression analysis of the renin-angiotensin system components between white and brown perivascular adipose tissue. *J. Endocrinol.* 197, 55–64. doi: 10.1677/JOE-07-0284

Gálvez-Prieto, B., Somoza, B., Gil-Ortega, M., García-Prieto, C. F., de Las Heras, A. I., González, M. C., et al. (2012). Anticontractile effect of perivascular adipose tissue and leptin are reduced in hypertension. *Front. Pharmacol.* 3:103. doi: 10.3389/fphar.2012.00103

Gao, Y. J., Lu, C., Su, L. Y., Sharma, A. M., and Lee, R. M. (2007). Modulation of vascular function by perivascular adipose tissue: the role of endothelium and hydrogen peroxide. *Br. J. Pharmacol.* 151, 323–331. doi: 10.1038/sj.bjp.0707228

Gnad, T., Scheibler, S., von Kügelgen, I., Scheele, C., Kilić, A., Glöde, A., et al. (2014). Adenosine activates brown adipose tissue and recruits beige adipocytes via A2A receptors. *Nature.* 516, 395–399. doi: 10.1038/nature13816

Gollasch, M., and Dubrovska, G. (2004). Paracrine role for periadventitial adipose tissue in the regulation of arterial tone. *Trends Pharmacol. Sci.* 25, 647–653. doi: 10.1016/j.tips.2004.10.005

Guilherme, A., Virbasius, J. V., Puri, V., and Czech, M. P. (2008). Adipocyte dysfunctions linking obesity to insulin resistance and type 2 diabetes. *Nat. Rev. Mol. Cell Biol.* 9, 367–377. doi: 10.1038/nrm2391

Guimaraes-Camboa, N., and Evans, S. M. (2017). Are perivascular adipocyte progenitors mural cells or adventitial fibroblasts? *Cell Stem Cell* 20, 587–589. doi: 10.1016/j.stem.2017.04.010

Guzik, T. J., and Harrison, D. G. (2006). Vascular NADPH oxidases as drug targets for novel antioxidant strategies. *Drug Discov. Today* 11, 524–533. doi: 10.1016/j.drudis.2006.04.003

Guzik, T. J., West, N. E., Black, E., McDonald, D., Ratnatunga, C., Pillai, R., et al. (2000). Vascular superoxide production by NAD(P)H oxidase: association with endothelial dysfunction and clinical risk factors. *Circ. Res.* 86, E85–E90. doi: 10.1161/01.RES.86.9.e85

Harms, M. J., Ishibashi, J., Wang, W., Lim, H. W., Goyama, S., Sato, T., et al. (2014). Prdm16 is required for the maintenance of brown adipocyte identity and function in adult mice. *Cell Metab.* 19, 593–604. doi: 10.1016/j.cmet.2014.03.007

Harms, M., and Seale, P. (2013). Brown and beige fat: development, function and therapeutic potential. *Nat. Med.* 19, 1252–1263. doi: 10.1038/nm.3361

Hartman, J., and Frishman, W. H. (2014). Inflammation and atherosclerosis: a review of the role of interleukin-6 in the development of atherosclerosis and the potential for targeted drug therapy. *Cardiol. Rev.* 22, 147–151. doi: 10.1097/CRD.0000000000000021

Heaton, J. M. (1972). Distribution of Brown Adipose-Tissue in Human. *J. Anat.* 112(Pt 1), 35–39.

Hepler, C., and Gupta, R. K. (2017). The expanding problem of adipose depot remodeling and postnatal adipocyte progenitor recruitment. *Mol. Cell. Endocrinol.* 445, 95–108. doi: 10.1016/j.mce.2016.10.011

Herrmann, J., Lerman, L. O., Rodriguez-Porcel, M., D. R., Holmes Jr, Richardson, D. M., Ritman, E. L., et al. (2001). Coronary vasa vasorum neovascularization precedes epicardial endothelial dysfunction in experimental hypercholesterolemia. *Cardiovasc. Res.* 51, 762–766. doi: 10.1016/S0008-6363(01)00347-9

Himms-Hagen, J., Melnyk, A., Zingaretti, M. C., Ceresi, E., Barbatelli, G., and Cinti, S. (2000). Multilocular fat cells in WAT of CL-316243-treated rats derive directly from white adipocytes. *Am. J. Physiol. Cell Physiol.* 279, C670–C681.doi: 10.1152/ajpcell.2000.279.3.C670

Hondares, E., Rosell, M., Diaz-Delfin, J., Olmos, Y., Monsalve, M., Iglesias, R., et al. (2011). Peroxisome proliferator-activated receptor alpha (PPAR alpha) induces PPAR gamma coactivator 1 alpha (PGC-1 alpha) gene expression and contributes to thermogenic activation of brown fat INVOLVEMENT OF PRDM16. *J. Biol. Chem.* 286, 43112–43122. doi: 10.1074/jbc.M111.252775

Hong, K. Y., Bae, H., Park, I., Park, D. Y., Kim, K. H., Kubota, Y., et al. (2015). Perilipin^{+} embryonic preadipocytes actively proliferate along growing vasculatures for adipose expansion. *Development* 142, 2623–2632. doi: 10.1242/dev.125336

Hotamisligil, G. S. (2006). Inflammation and metabolic disorders. *Nature*. 444, 860–867. doi: 10.1038/nature05485

Hudak, C. S., and Sul, H. S. (2013). Pref-1, a gatekeeper of adipogenesis. *Front. Endocrinol.* 4:79. doi: 10.3389/fendo.2013.00079

Jiang, Y., Berry, D. C., Tang, W., and Graff, J. M. (2014). Independent stem cell lineages regulate adipose organogenesis and adipose homeostasis. *Cell Rep.* 9, 1007–1022. doi: 10.1016/j.celrep.2014.09.049

Kawabe, J., and Hasebe, N. (2014). Role of the vasa vasorum and vascular resident stem cells in atherosclerosis. *Biomed Res. Int.* 2014:701571. doi: 10.1155/2014/701571

Ketonen, J., Shi, J., Martonen, E., and Mervaala, E. (2010). Periadventitial adipose tissue promotes endothelial dysfunction via oxidative stress in diet-induced obese C57Bl/6 mice. *Circ J.* 74, 1479–1487. doi: 10.1253/circj.CJ-09-0661

Lee, Y. C., Chang, H. H., Chiang, C. L., Liu, C. H., Yeh, J. I., Chen, M. F., et al. (2011). Role of perivascular adipose tissue-derived methyl palmitate in vascular tone regulation and pathogenesis of hypertension. *Circulation* 124, 1160–1171. doi: 10.1161/CIRCULATIONAHA.111.027375

Lepper, C., and Fan, C. M. (2010). Inducible lineage tracing of Pax7-descendant cells reveals embryonic origin of adult satellite cells. *Genesis* 48, 424–436. doi: 10.1002/dvg.20630

Li, H., Wang, Y. P., Zhang, L. N., and Tian, G. (2014). Perivascular adipose tissue-derived leptin promotes vascular smooth muscle cell phenotypic switching via p38 mitogen-activated protein kinase in metabolic syndrome rats. *Exp. Biol. Med.* 239, 954–965. doi: 10.1177/1535370214527903

Li, L., Miano, J. M., Mercer, B., and Olson, E. N. (1996). Expression of the SM22alpha promoter in transgenic mice provides evidence for distinct transcriptional regulatory programs in vascular and visceral smooth muscle cells. *J. Cell Biol.* 132, 849–859. doi: 10.1083/jcb.132.5.849

Lo, K. A., and Sun, L. (2013). Turning WAT into BAT: a review on regulators controlling the browning of white adipocytes. *Biosci. Rep.* 33, 711–719. doi: 10.1042/BSR20130046

Long, J. Z., Svensson, K. J., Tsai, L., Zeng, X., Roh, H. C., Kong, X., et al. (2014). A smooth muscle-like origin for beige adipocytes. *Cell Metab.* 19, 810–820. doi: 10.1016/j.cmet.2014.03.025

Lowell, B. B., and Flier, J. S. (1997). Brown adipose tissue, beta 3-adrenergic receptors, and obesity. *Annu. Rev. Med.* 48, 307–316. doi: 10.1146/annurev.med.48.1.307

Lu, C., Su, L. Y., Lee, R. M., and Gao, Y. J. (2010). Mechanisms for perivascular adipose tissue-mediated potentiation of vascular contraction to perivascular neuronal stimulation: the role of adipocyte-derived angiotensin II. *Eur. J. Pharmacol.* 634, 107–112. doi: 10.1016/j.ejphar.2010.02.006

Lusis, A. J. (2000). Atherosclerosis. *Nature* 407, 233–241. doi: 10.1038/35025203

Lynch, F. M., Withers, S. B., Yao, Z., Werner, M. E., Edwards, G., Weston, A. H., et al. (2013). Perivascular adipose tissue-derived adiponectin activates BK(Ca) channels to induce anticontractile responses. *Am. J. Physiol. Heart Circ. Physiol.* 304, H786–H795. doi: 10.1152/ajpheart.00697.2012.

Madamanchi, N. R., Vendrov, A., and Runge, M. S. (2005). Oxidative stress and vascular disease. *Arterioscler. Thromb. Vasc. Biol.* 25, 29–38. doi: 10.1161/01.ATV.0000150649.39934.13

Maiellaro, K., and Taylor, W. R. (2007). The role of the adventitia in vascular inflammation. *Cardiovasc. Res.* 75, 640–648. doi: 10.1016/j.cardiores.2007.06.023

Manka, D., Chatterjee, T. K., Stoll, L. L., Basford, J. E., Konaniah, E. S., Srinivasan, R., et al. (2014). Transplanted perivascular adipose tissue accelerates injury-induced neointimal hyperplasia: role of monocyte chemoattractant protein-1. *Arterioscler. Thromb. Vasc. Biol.* 34, 1723–1730. doi: 10.1161/ATVBAHA.114.303983

Moe, K. T., Naylynn, T. M., Yin, N. O., Khairunnisa, K., Allen, J. C., Wong, M. C., et al. (2013). Tumor necrosis factor-alpha induces aortic intima-media thickening via perivascular adipose tissue inflammation. *J. Vasc. Res.* 50, 228–237. doi: 10.1159/000350542

Must, A., Spadano, J., Coakley, E. H., Field, A. E., Colditz, G., and Dietz, W. H. (1999). The disease burden associated with overweight and obesity. *JAMA* 282, 1523–1529. doi: 10.1001/jama.282.16.1523

Nedergaard, J., Bengtsson, T., and Cannon, B. (2007). Unexpected evidence for active brown adipose tissue in adult humans. *Am. J. Physiol. Endocrinol. Metab.* 293, E444–E452. doi: 10.1152/ajpendo.00691.2006

Ohashi, K., Ouchi, N., and Matsuzawa, Y. (2011). Adiponectin and hypertension. *Am. J. Hypertens.* 24, 263–269. doi: 10.1038/ajh.2010.216

Omar, A., Chatterjee, T. K., Tang, Y. L., Hui, D. Y., and Weintraub, N. L. (2014). Proinflammatory phenotype of perivascular adipocytes. *Arterioscler. Thromb. Vasc. Biol.* 34, 1631–1636. doi: 10.1161/ATVBAHA.114.303030

Padilla, J., Jenkins, N. T., Vieira-Potter, V. J., and Laughlin, M. H. (2013). Divergent phenotype of rat thoracic and abdominal perivascular adipose tissues. *Am. J. Physiol. Regul. Integr. Comp. Physiol.* 304, R543–R552. doi: 10.1152/ajpregu.00567.2012

Panda, D., Kundu, G. C., Lee, B. I., Peri, A., Fohl, D., Chackalaparampil, I., et al. (1997). Potential roles of osteopontin and alphaVbeta3 integrin in the development of coronary artery restenosis after angioplasty. *Proc. Natl. Acad. Sci. U.S.A.* 94, 9308–9313. doi: 10.1073/pnas.94.17.9308

Park, J. H., Kang, H. J., Kang, S. I., Lee, J. E., Hur, J., Ge, K., et al. (2013). A multifunctional protein, EWS, is essential for early brown fat lineage determination. *Dev. Cell* 26, 393–404. doi: 10.1016/j.devcel.2013.07.002

Park, S. Y., Kim, K. H., Seo, K. W., Bae, J. U., Kim, Y. H., Lee, S. J., et al. (2014). Resistin derived from diabetic perivascular adipose tissue up-regulates vascular expression of osteopontin via the AP-1 signalling pathway. *J. Pathol.* 232, 87–97. doi: 10.1002/path.4286

Pfeifer, A., and Hoffmann, L. S. (2015). Brown, beige, and white: the new color code of fat and its pharmacological implications. *Annu. Rev. Pharmacol. Toxicol.* 55, 207–227. doi: 10.1146/annurev-pharmtox-010814-124346

Police, S. B., Thatcher, S. E., Charnigo, R., Daugherty, A., and Cassis, L. A. (2009). Obesity promotes inflammation in periaortic adipose tissue and angiotensin II-induced abdominal aortic aneurysm formation. *Arterioscler. Thromb. Vasc. Biol.* 29, 1458–1464. doi: 10.1161/ATVBAHA.109.192658

Rader, D. J., and Daugherty, A. (2008). Translating molecular discoveries into new therapies for atherosclerosis. *Nature* 451, 904–913. doi: 10.1038/nature06796

Re, R. N. (2009). Obesity-related hypertension. *Ochsner. J.* 9, 133–136.

Reynés, B., van Schothorst, E. M., García-Ruiz, E., Keijer, J., Palou, A., and Oliver, P. (2017). Cold exposure down-regulates immune response pathways in ferret aortic perivascular adipose tissue. *Thromb. Haemost.* 117, 981–991. doi: 10.1160/TH16-12-0931

Rosen, E. D., and MacDougald, O. A. (2006). Adipocyte differentiation from the inside out. *Nat. Rev. Mol. Cell Biol.* 7, 885–896. doi: 10.1038/nrm2066

Rosen, E. D., Sarraf, P., Troy, A. E., Bradwin, G., Moore, K., Milstone, D. S., et al. (1999). PPAR gamma is required for the differentiation of adipose tissue *in vivo* and *in vitro*. *Mol. Cell.* 4, 611–617. doi: 10.1016/S1097-2765(00)80211-7

Rosenwald, M., Perdikari, A., Rülicke, T., and Wolfrum, C. (2013). Bi-directional interconversion of brite and white adipocytes. *Nat. Cell Biol.* 15, 659–667. doi: 10.1038/ncb2740

Sanchez-Gurmaches, J., and Guertin, D. A. (2014). Adipocytes arise from multiple lineages that are heterogeneously and dynamically distributed. *Nat. Commun.* 5:4099. doi: 10.1038/ncomms5099

Sanchez-Gurmaches, J., Hung, C. M., Sparks, C. A., Tang, Y., Li, H., and Guertin, D. A. (2012). PTEN loss in the Myf5 lineage redistributes body fat and reveals subsets of white adipocytes that arise from Myf5 precursors. *Cell Metab.* 16, 348–362. doi: 10.1016/j.cmet.2012.08.003

Sarafidis, P. A., and Bakris, G. L. (2007). Non-esterified fatty acids and blood pressure elevation: a mechanism for hypertension in subjects with obesity/insulin resistance? *J. Hum. Hypertens.* 21, 12–19. doi: 10.1038/sj.jhh.1002103

Schieffer, B., Selle, T., Hilfiker, A., Hilfiker-Kleiner, D., Grote, K., Tietge, U. J., et al. (2004). Impact of interleukin-6 on plaque development and morphology in experimental atherosclerosis. *Circulation* 110, 3493–3500. doi: 10.1161/01.CIR.0000148135.08582.97

Schroeter, M. R., Eschholz, N., Herzberg, S., Jerchel, I., Leifheit-Nestler, M., Czepluch, F. S., et al. (2013). Leptin-dependent and leptin-independent paracrine effects of perivascular adipose tissue on neointima formation. *Arterioscler. Thromb. Vasc. Biol.* 33, 980–987. doi: 10.1161/ATVBAHA.113.301393

Schütten, M. T., Houben, A. J., de Leeuw, P. W., and Stehouwer, C. D. (2017). The Link between adipose tissue renin-angiotensin-aldosterone system signaling and obesity-associated hypertension. *Physiology* 32, 197–209. doi: 10.1152/physiol.00037.2016

Seale, P., Bjork, B., Yang, W. L., Kajimura, S., Chin, S., Kuang, S. H., et al. (2008). PRDM16 controls a brown fat/skeletal muscle switch. *Nature* 454, 961–967. doi: 10.1038/nature07182

Seale, P., Conroe, H. M., Estall, J., Kajimura, S., Frontini, A., Ishibashi, J., et al. (2011). Prdm16 determines the thermogenic program of subcutaneous white adipose tissue in mice. *J. Clin. Invest.* 121, 96–105. doi: 10.1172/JCI44271

Sharma, A. M., Engeli, S., and Pischon, T. (2001). New developments in mechanisms of obesity-induced hypertension: role of adipose tissue. *Curr. Hypertens. Rep.* 3, 152–156. doi: 10.1007/s11906-001-0030-x

Shimizu, H., Takahashi, M., Takeda, S., Inoue, S., Fujishiro, J., Hakamata, Y., et al. (2004). Mycophenolate mofetil prevents transplant arteriosclerosis by direct inhibition of vascular smooth muscle cell proliferation. *Transplantation* 77, 1661–1667. doi: 10.1097/01.TP.0000127592.13707.B6

Shimizu, I., Aprahamian, T., Kikuchi, R., Shimizu, A., Papanicolaou, K. N., MacLauchlan, S., et al. (2014). Vascular rarefaction mediates whitening of brown fat in obesity. *J. Clin. Invest.* 124, 2099–2112. doi: 10.1172/JCI71643

Soltis, E. E., and Cassis, L. A. (1991). Influence of perivascular adipose-tissue on rat aortic smooth-muscle responsiveness. *Clin. Exp. Hypertens. Part A-Theory Prac.* 13, 277–296. doi: 10.3109/10641969109042063

Sun, C., Berry, W. L., and Olson, L. E. (2017). PDGFRalpha controls the balance of stromal and adipogenic cells during adipose tissue organogenesis. *Development* 144, 83–94. doi: 10.1242/dev.135962

Tabas, I., García-Cardeña, G., and Owens, G. K. (2015). Recent insights into the cellular biology of atherosclerosis. *J. Cell Biol.* 209, 13–22. doi: 10.1083/jcb.201412052

Takaoka, M., Nagata, D., Kihara, S., Shimomura, I., Kimura, Y., Tabata, Y., et al. (2009). Periadventitial adipose tissue plays a critical role in vascular remodeling. *Circ. Res.* 105, 906–911. doi: 10.1161/CIRCRESAHA.109.199653

Tian, Z., Miyata, K., Tazume, H., Sakaguchi, H., Kadomatsu, T., Horio, E., et al. (2013). Perivascular adipose tissue-secreted angiopoietin-like protein 2 (Angptl2) accelerates neointimal hyperplasia after endovascular injury. *J. Mol. Cell. Cardiol.* 57, 1–12. doi: 10.1016/j.yjmcc.2013.01.004

Tseng, Y. H., Kokkotou, E., Schulz, T. J., Huang, T. L., Winnay, J. N., Taniguchi, C. M., et al. (2008). New role of bone morphogenetic protein 7 in brown adipogenesis and energy expenditure. *Nature* 454, 1000–1004. doi: 10.1038/nature07221

van Marken Lichtenbelt, W. D., Vanhommerig, J. W., Smulders, N. M., Drossaerts, J. M., Kemerink, G. J., Bouvy, N. D. et al. (2009). Cold-activated brown adipose tissue in healthy men. *N. Engl. J. Med.* 360, 1500–1508. doi: 10.1056/NEJMoa0808718

Viedt, C., Vogel, J., Athanasiou, T., Shen, W., Orth, S. R., Kübler, W., et al. (2002). Monocyte chemoattractant protein-1 induces proliferation and interleukin-6 production in human smooth muscle cells by differential activation of nuclear factor-kappaB and activator protein-1. *Arterioscler. Thromb. Vasc. Biol.* 22, 914–920. doi: 10.1161/01.ATV.0000019009.73586.7F

Vishvanath, L., MacPherson, K. A., Hepler, C., Wang, Q. A., Shao, M., Spurgin, S. B., et al. (2016). Pdgfrbeta+ mural preadipocytes contribute to adipocyte hyperplasia induced by high-fat-diet feeding and prolonged cold exposure in adult mice. *Cell Metab.* 23, 350–359. doi: 10.1016/j.cmet.2015.10.018

Vitali, A., Murano, I., Zingaretti, M. C., Frontini, A., Ricquier, D., and Cinti, S. (2012). The adipose organ of obesity-prone C57BL/6J mice is composed of mixed white and brown adipocytes. *J. Lipid Res.* 53, 619–629. doi: 10.1194/jlr.M018846

Wang, Q. A., Tao, C., Gupta, R. K., and Scherer, P. E. (2013). Tracking adipogenesis during white adipose tissue development, expansion and regeneration. *Nat. Med.* 19, 1338–1344. doi: 10.1038/nm.3324

Wang, W., Kissig, M., Rajakumari, S., Huang, L., Lim, H. W., Won, K. J., et al. (2014). Ebf2 is a selective marker of brown and beige adipogenic precursor cells. *Proc. Natl. Acad. Sci. U.S.A.* 111, 14466–14471. doi: 10.1073/pnas.1412685111

WHO (2017). *Cardiovascular Diseases (CVDs) Fact Sheet*. Available online at: http://www.who.int/mediacentre/factsheets/fs317/en/ (Acessed Nov 18, 2017).

Xita, N., and Tsatsoulis, A. (2012). Adiponectin in diabetes mellitus. *Curr. Med. Chem.* 19, 5451–5458. doi: 10.2174/092986712803833182

Xue, B., Rim, J. S., Hogan, J. C., Coulter, A. A., Koza, R. A., and Kozak, L. P. (2007). Genetic variability affects the development of brown adipocytes in white fat but not in interscapular brown fat. *J. Lipid Res.* 48, 41–51. doi: 10.1194/jlr.M600287-JLR200

Yiannikouris, F., Gupte, M., Putnam, K., and Cassis, L. (2010). Adipokines and blood pressure control. *Curr. Opin. Nephrol. Hypertens.* 19, 195–200. doi: 10.1097/MNH.0b013e3283366cd0

Zhang, Y., Li, Y., Yu, L., and Zhou, L. (2017). Association between serum resistin concentration and hypertension: a systematic review and meta-analysis. *Oncotarget* 8, 41529–41537. doi: 10.18632/oncotarget.17561

Zhou, X., Nicoletti, A., Elhage, R., and Hansson, G. K. (2000). Transfer of $CD4^+$ T cells aggravates atherosclerosis in immunodeficient apolipoprotein E knockout mice. *Circulation* 102, 2919–2922. doi: 10.1161/01.CIR.102.24.2919

Conflict of Interest Statement: The authors declare that the research was conducted in the absence of any commercial or financial relationships that could be construed as a potential conflict of interest.

frontiers in Physiology

ORIGINAL RESEARCH
published: 12 January 2018
doi: 10.3389/fphys.2017.01135

Increased Contractile Function of Human Saphenous Vein Grafts Harvested by "No-Touch" Technique

*Lene P. Vestergaard[1], Leila Benhassen[1,2], Ivy S. Modrau[2], Frank de Paoli[1,2] and Ebbe Boedtkjer[1]**

[1] Department of Biomedicine, Aarhus University, Aarhus, Denmark, [2] Department of Cardiothoracic Surgery, Aarhus University Hospital, Aarhus, Denmark

Saphenous vein grafts are the most common conduits used for coronary artery bypass grafting (CABG); however, no more than 60% of vein grafts remain open after 10 years and graft failure is associated with poor clinical outcome. The "no-touch" harvesting technique—where a sheet of perivascular tissue is retained around the vein—improves graft patency to over 80% after 16 years of follow-up, but the mechanism for the improved patency rate is unclear. In this study, we investigated acute functional differences between vein grafts harvested conventionally and by "no-touch" technique and explored the importance of perivascular tissue for reducing surgical trauma, minimizing excessive distension, and releasing vasoactive paracrine factors. Segments of human saphenous veins were obtained from CABG surgery and their functional properties investigated by isometric and isobaric myography. We found a broad diameter-tension relationship for human saphenous veins, with peak capacity for active tension development at diameters corresponding to transmural pressures around 60 mmHg. Across the investigated transmural pressure range between 10 and 120 mmHg, maximal tension development was higher for "no-touch" compared to conventionally harvested saphenous veins. Contractile responses to serotonin, noradrenaline, and depolarization induced with elevated extracellular [K^+] were significantly larger for saphenous veins harvested by "no-touch" compared to conventional technique. Conventional vein grafts are routinely pressurized manually in order to test for leaks; however, avoiding this distension procedure did not change the acute contractile function of the conventionally excised saphenous veins. In contrast, even though surgical removal of perivascular tissue during conventional harvesting was associated with a substantial decrease in force development, removal of perivascular tissue by careful dissection under a stereomicroscope only marginally affected contractile responses of veins harvested by "no-touch" technique. In conclusion, we show that saphenous veins harvested by "no-touch" technique have greater contractile capacity than veins harvested by conventional technique. The different capacity for smooth muscle contraction is not due to vasoactive substances released by the perivascular tissue. Instead, we propose that the larger tension development of saphenous veins harvested by "no-touch" technique reflects reduced surgical damage, which may have long-term consequences that contribute to the superior graft patency.

Keywords: coronary artery disease, coronary artery bypass grafting, perivascular adipose tissue, saphenous vein, vasoconstriction

OPEN ACCESS

Edited by:
Maik Gollasch, Charité Universitätsmedizin Berlin, Germany

Reviewed by:
María S. Fernández-Alfonso, Complutense University of Madrid, Spain
Robert Feil, Universität Tübingen, Germany

***Correspondence:**
Ebbe Boedtkjer
eb@biomed.au.dk

Specialty section:
This article was submitted to Vascular Physiology, a section of the journal Frontiers in Physiology

Received: *29 September 2017*
Accepted: *22 December 2017*
Published: *12 January 2018*

Citation:
Vestergaard LP, Benhassen L, Modrau IS, de Paoli F and Boedtkjer E (2018) Increased Contractile Function of Human Saphenous Vein Grafts Harvested by "No-Touch" Technique. Front. Physiol. 8:1135. doi: 10.3389/fphys.2017.01135

INTRODUCTION

The long-term success of coronary artery bypass grafting (CABG) is negatively influenced by graft failure (Lopes et al., 2012; Blachutzik et al., 2016). Patency of conventionally harvested saphenous vein grafts is 80–90% 1 year after the CABG procedure and decreases to no more than 60% after 10 years (Campeau et al., 1979; Fitzgibbon et al., 1996; Harskamp et al., 2013a; de Vries et al., 2016). The left internal thoracic artery is considered first choice conduit because of prolonged high patency (Otsuka et al., 2013) but equivalent results (e.g., 83% patency after 16 years) can be achieved with saphenous vein grafts harvested by so-called "no-touch" technique (Souza et al., 2001, 2006; Johansson et al., 2009; Samano et al., 2015). When "no-touch" vein grafts are excised, a sheet of perivascular tissue is retained around the vein (Souza, 1996). Suggestions have been made that improved integrity of the endothelial and medial smooth muscle cell layers (Ahmed et al., 2004; Vasilakis et al., 2004; Loesch et al., 2006), higher expression and activity of endothelial NO synthase (Tsui et al., 2001; Dashwood et al., 2009), greater density of vasa vasorum (Dreifaldt et al., 2011), and paracrine release of vasoactive substances from the perivascular tissue (Fernández-Alfonso et al., 2017) contribute to the superior patency of "no-touch" compared to conventional saphenous vein grafts. Nevertheless, the impact of perivascular tissue and harvesting techniques on the pathophysiology of graft occlusion is still not well-understood.

Vein grafts used for CABG surgery experience dramatic changes in mechanical forces—in particular increased transmural pressure and linear velocity of the blood—when they are transplanted from the venous to the arterial circulation. Elevated shear stress and circumferential wall stress of arteries compared to veins of equal caliber are important factors that influence vessel wall remodeling and neointima formation (Fitts et al., 2014). Increased physiological shear stress—which is typically 10–70 dynes/cm^2 in arteries compared to 1–5 dynes/cm^2 in veins (dela Paz and D'Amore, 2009; Fitts et al., 2014)—usually leads to outward remodeling. However, damaged endothelial cell layer caused by excessive physical forces can lead to endothelial dysfunction or even allow shear forces to act directly on the smooth muscle cells (Fry, 1969; Fitts et al., 2014). The mechanotransduction pathways and pathophysiological consequences of increased mechanical stress remain controversial and may depend on the flow pattern, but effects of shear stress on smooth muscle cell phenotype (i.e., shift from contractile to synthetic phenotype) and proliferation have been demonstrated and may contribute to inward remodeling and luminal obstruction of transplanted vein grafts (Kipshidze et al., 2004; Shi and Tarbell, 2011). It is well-accepted that surgical procedures and graft characteristics affect the rate of graft failure (Harskamp et al., 2013b), and it is expected that long-term patency is improved if the transplanted graft is functionally and structurally intact at the time of anastomosis.

In addition to providing structural support, the secretory activity of perivascular tissue can have functional implications for the vascular wall (Fernández-Alfonso, 2004). Crosstalk between perivascular tissue and resistance arteries in many vascular beds contributes to metabolic regulation of blood flow whereby local perfusion is adjusted to the metabolic demand. Proposed paracrine factors released from perivascular tissue include NO, leptin, adiponectin, prostanoids, angiotensin 1–7, and hydrogen sulfide (Simonsen and Boedtkjer, 2016), which in addition to vasomotor effects may modify the structure of the blood vessel wall, for instance, through changes in cell migration, proliferation, and apoptosis. Perivascular cardiomyocyte-rich tissue surrounding coronary arteries modifies both vasocontraction and—relaxation (Aalbaek et al., 2015). Even though the cause-effect relationship is still unclear, the relevance of altered crosstalk between perivascular tissue and cells of the vascular wall for disease is supported by altered anti-contractile influences of perivascular tissue in models of type 2 diabetes (Bonde et al., 2017), obesity (Yudkin et al., 2005; Greenstein et al., 2009; Aghamohammadzadeh et al., 2013), inflammation (Bhattacharya et al., 2013), and hypertension (Li et al., 2013).

There is evidence for structural damage to the vascular wall of conventionally harvested vein grafts (Ahmed et al., 2004; Loesch et al., 2006). However, functional evidence of altered vasomotor performance has not been provided and consequences of different harvesting techniques for the vasomotor function of excised grafts have not been systematically evaluated. In the current study, we hypothesized that harvest of saphenous vein grafts by "no-touch" technique improves the immediate contractile function because (a) the adherent perivascular tissue releases vasoactive paracrine factors that modify smooth muscle contractions or (b) the atraumatic "no-touch" surgical technique reduces damage and preserves smooth muscle contractile capacity. We find that saphenous vein grafts harvested by "no-touch" technique have increased capacity for force generation and that this greater contractile function is unrelated to acute release of paracrine factors from the perivascular tissue. We propose that improved graft viability with associated greater dynamic range of tone regulation contributes to the superior long-term patency of "no-touch" vein grafts used for CABG surgery.

MATERIALS AND METHODS

"No-touch" vein harvest technique was implemented at Aarhus University Hospital in 2011, 5 years prior to the present study. All conduits were harvested by the same team of cardiac surgeons experienced in both "no-touch" and conventional harvest techniques. The study was carried out in accordance with Danish legislation and the protocol approved by the Mid-Jutland Regional Committee on Health Research Ethics (enquiry no. 167/2017). According to Danish legislation, written informed consent was not required because the procedures involve excess resected tissue from a surgical procedure where all post-surgical tissue and data handling was anonymized.

Conventional Harvesting Technique

The saphenous vein was exposed by a longitudinal incision through the skin, the perivascular tissue stripped from the adventitial layer, and all side branches divided between clips or ligatures. The saphenous vein was removed and distended

manually with a 10-mL syringe containing heparin-saline—0.90% (weight/volume) aqueous NaCl solution containing 50 IU/mL heparin—to check for leaks. Attention was paid not to overdistend the vein. After distension, the vein graft was stored in heparin-saline at room temperature until anastomosis.

"No-Touch" Harvesting Technique

The course of the saphenous vein was delineated with a marker on the overlying skin using B-mode ultrasonography and a longitudinal incision was made through the skin until the saphenous vein was visualized. The saphenous vein was excised with adherent perivascular tissue along the whole circumference and all side branches were divided between clips or ligatures. At the surgeons discretion, one of two approaches was now chosen: the vein was either (a) stored at room temperature in papaverine-containing, heparinized autologous blood solution —60 mL blood added 1,000 IU heparin and 60 mg papaverine—until it was connected to the aortic cannula and perfused through the arterial line, or (b) manually distended and stored at room temperature in the papaverine-containing, heparinized autologous blood solution until anastomosis. Attention was paid not to overdistend the vein.

Isometric Myography

The vein segments investigated for contractile function were stored only very briefly (typically, a few minutes) in the above-mentioned heparin-saline or autologous blood solution. The vein segments were then transferred to chilled physiological saline solutions (PSS) and transported (∼20 min duration) on ice to the laboratory at Aarhus University for analysis of contractile function. Two millimeter long segments of saphenous vein grafts were mounted in 4-channel wire myographs (610 M; DMT, Aarhus Denmark) on 100-μm tungsten pins either with the amount of associated perivascular tissue provided by the surgeons or after the perivascular tissue was removed by microdissection under a stereomicroscope (Zeiss, Germany). The time for transport and subsequent handling of veins was similar for veins harvested by conventional and "no-touch" technique. Diameter-tension relationships were established by first stretching the relaxed veins under continuous force recordings to diameters corresponding to fixed transmural pressures, and then trigger maximal active tension with 125 mM extracellular K^+ and 10 μM serotonin. Concentration-response relationships to noradrenaline, serotonin, and extracellular K^+ were established in veins that—when fully relaxed—were normalized to an internal diameter corresponding to a transmural pressure of either 20 mmHg (representative of the venous circulation) or 100 mmHg (representative of the arterial circulation; Mulvany and Halpern, 1977). When the vein segments were set to new diameters by moving the myograph pins apart, stretch-induced damage was avoided by first allowing time for full relaxation in Ca^{2+}-free PSS containing 10 μM sodium nitroprusside (SNP). Under these conditions, the equivalent transmural pressure was calculated based on LaPlace's law.

Isobaric Myography

Saphenous vein segments were microdissected free from surrounding perivascular tissue and mounted with ligatures on two silicone tubes in a pressure myograph (110P; DMT). The inner diameter *(ID)* of the vein segments was visualized and recorded with MyoVIEW 3.2 software (DMT). Vasoconstriction was evaluated during cumulative application of serotonin at transmural pressures of 20 and 100 mmHg. The fully relaxed diameter ($ID_{passive}$) was recorded by exposing the veins to Ca^{2+}-free PSS containing 5 mM EGTA and 10 μM papaverine. For each condition, we calculated: Active tone = ($ID_{passive}$-ID_{active})/$ID_{passive}$, where all diameters correspond to the same transmural pressure.

Composition of Solutions

The PSS used for evaluation of venous contractile function had the following composition (in mM): NaCl 119, $CaCl_2$ 1.6, KCl 4.7, $MgSO_4$ 1.7, $NaHCO_3$ 22, KH_2PO_4 1.18, EDTA 0.026, and glucose 5.5. PSS with high [K^+] was produced by equimolar substitution of KCl for NaCl. All solutions were titrated to pH 7.4 at 37°C after vigorous bubbling with a gas mixture of 5% CO_2/balance air.

Statistics

Data are expressed as mean ± SEM; *n* equals number of patients. Probability (*P*) values <0.05 were considered statistically significant. One or two vessel segments from each patient were investigated for each condition; if two vessel segments from the same patient were tested, the average value was used to represent that patient in subsequent statistical analyses to ensure that values within each group were independent. Diameter-tension and concentration-response relationships were fitted to second order polynomial and sigmoidal functions, respectively, and compared between experimental conditions with extra sum-of-squares *F*-tests. The effects of two variables on a third variable, measured multiple times for each patient, were evaluated by repeated measures two-way ANOVA followed by Sidak's post-tests. Statistical analyses were performed using Microsoft Excel 2010 and GraphPad Prism 7.03 software.

RESULTS

Saphenous Veins Have Broad Diameter-Tension Relationships and Maximal Active Tension Development Is Increased in "No-Touch" Veins

Initially, we determined the relationship between the degree of passive stretch and the capacity of the harvested vein grafts for maximal active tension development. The saphenous vein segments were relaxed and stepwise stretched in Ca^{2+}-free PSS with 10 μM SNP; and at each progressively larger diameter, the capacity for maximal active force development—after washout of SNP and return of extracellular Ca^{2+}–was tested by exposure to 125 mM extracellular K^+ and 10 μM serotonin. An original trace showing the protocol is provided in **Figure 1A**. The passive diameters were converted to equivalent transmural pressures using LaPlace's law. As

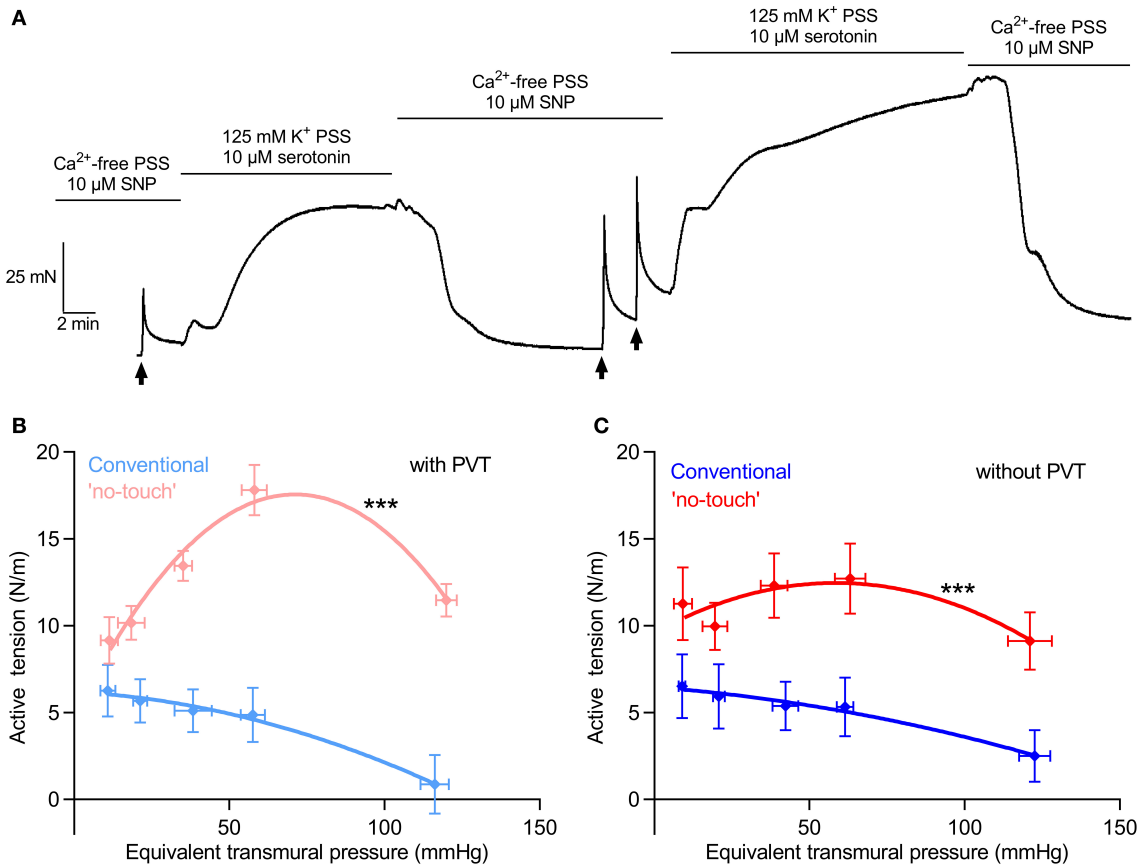

FIGURE 1 | Saphenous veins have a broad diameter-tension relationship and the capacity for maximal tension development is increased in "no-touch" veins. **(A)** Original force trace showing the protocol used for establishing the diameter-tension relationship for saphenous vein grafts. The arrows indicate time points where the micrometer screw is turned to stretch the vein to a larger diameter. The protocol was repeated multiple times to cover the pressure interval between 10 and 120 mmHg. **(B,C)**. Maximal active tension development plotted as function of the equivalent passive transmural pressure for vein graft segments surrounded by the amount of perivascular tissue (PVT) retained by the surgeon (**B**, $n = 8$–11) and after removal of PVT by careful dissection under a stereomicroscope (**C**, $n = 8$–11). The curves are results of second order polynomial fits and we compare them by extra sum-of-squares F-tests. $^{***}P < 0.05$ *vs.* Conventional.

shown in **Figure 1B**, the "no-touch" saphenous veins showed peak active tension development at diameters equivalent to around 60 mmHg, and relatively small decreases in capacity for active tension development were observed when the passive diameter was increased or decreased within the broad interval corresponding to transmural pressures between 20 and 120 mmHg. Striking differences in maximal active tension development were observed between veins harvested by "no-touch" and conventional technique: at its peak, maximal tension development was 3-fold larger in "no-touch" than conventional vein grafts (**Figure 1B**).

To investigate whether the difference in maximal tension development was due to vasoactive paracrine factors released from the perivascular tissue, we next carefully removed the perivascular tissue from the "no-touch" vein grafts by microdissection under a stereomicroscope. Any small amount of perivascular tissue remaining on the conventionally harvested vein grafts was removed in a similar manner. We saw a small, yet significant ($P < 0.05$, extra sum-of-squares F-test), reduction in vasocontractile capacity when the perivascular tissue was carefully removed by microdissection (compare **Figures 1B,C**). Notably, the difference in maximal active tension development between the veins harvested by "no-touch" and conventional technique was also evident after the perivascular tissue had been removed (**Figure 1C**). These findings support that possible vasomotor effects of paracrine factors released from the perivascular tissue are not the main causes of the acute difference in vasocontractile function observed between veins harvested by "no-touch" and conventional technique.

Isometric Vasocontraction at "Venous" and "Arterial" Transmural Pressures Is Not Affected by Microdissection of Perivascular Tissue

To further explore whether paracrine factors released from the perivascular tissue surrounding saphenous veins have vasomotor effects, veins harvested by "no-touch" technique were each cut into two segments: one was investigated as supplied from the surgeon whereas the perivascular tissue was

carefully removed from the other by microdissection under a stereomicroscope. The veins were mounted for isometric investigation and stretched to internal diameters corresponding to typical mean venous and arterial transmural pressures of 20 and 100 mmHg, respectively. The acute removal of perivascular tissue had no significant effect on the concentration-dependent vasoconstrictor response elicited by serotonin (**Figure 2A**) or the sympathetic neurotransmitter noradrenaline (**Figure 2B**). Responses to elevated extracellular $[K^+]$—applied in order to bypass receptor activation and investigate the response to direct depolarization of vascular smooth muscle cells—also did not differ between "no-touch" veins with and without perivascular tissue (**Figure 2C**). Responses to elevated extracellular $[K^+]$ were evaluated in the presence of 1 μM α-receptor antagonist phentolamine in order to block effects of noradrenaline released from perivascular nerve endings in response to depolarization. These findings are consistent with the diameter-tension relationships (**Figure 1**) and support that the differences in vasocontractile function between veins harvested by conventional and "no-touch" technique are not explained by acute vasomotor effects of paracrine factors released from the perivascular tissue.

Isometric Vasocontraction Is Increased in Veins Harvested by "No-Touch" Technique

We next microdissected and mounted saphenous vein segments harvested by "no-touch" and conventional technique in wire myographs to compare their contractile function. The concentration-dependent tension development in response to serotonin (**Figure 3A**) and noradrenaline (**Figure 3B**) was greater in veins harvested by "no-touch" technique than in veins harvested by conventional technique; although for noradrenaline, the difference between the harvesting procedures was evident only when veins were normalized to a transmural pressure of 20 mmHg. Saphenous veins harvested by "no-touch" technique also produced stronger contractions than veins harvested by conventional technique when exposed to stepwise increments in extracellular $[K^+]$ (**Figure 3C**).

Endothelium-Dependent Vasorelaxation Is Modest in Vein Grafts and Unaffected by Harvest Procedure

In order to evaluate the function of the endothelium, we next tested vasorelaxation of serotonin-pre-contracted veins in response to methacholine. When veins were pre-contracted with 10 μM serotonin, they relaxed on average <10% upon application of methacholine (**Figure 4**), which is in agreement with previous observations (Wise et al., 2015). Although there was a tendency toward improved vasorelaxation of veins harvested by "no-touch" compared to conventional technique, this did not reach statistical significance ($P = 0.09$), see **Figure 4**.

Isobaric Vasoconstriction Is Increased in Veins Harvested by "No-Touch" Technique

To further support the greater vasomotor responses of "no-touch" saphenous veins, we next mounted veins—microdissected free from perivascular tissue—in pressure myographs and exposed them to transmural pressures of 20 or 100 mmHg. At 20 mmHg, veins harvested by "no-touch" technique produced stronger vasoconstriction in response to serotonin than veins harvested by conventional technique (**Figure 5**). Active tone development was much attenuated at a transmural pressure of 100 mmHg; and at this higher pressure, no difference was observed between veins excised by the two different harvesting techniques (**Figure 5**).

Avoiding Manual Distension of Conventionally Harvested Vein Grafts Does Not Recover Tension Development

As part of the harvest procedure, vein grafts are pressurized to check for leaks. We investigated if the reduced vasocontraction

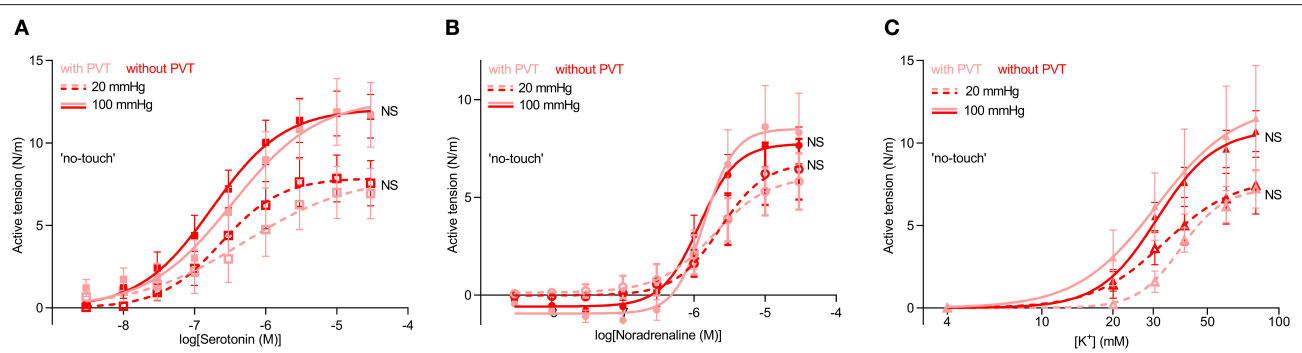

FIGURE 2 | Vasocontraction of saphenous veins harvested by "no-touch" technique is not affected by removal of perivascular tissue (PVT) by microdissection. **(A–C)** Vasocontractile responses to serotonin (**A**, $n = 8$–9), noradrenaline (**B**, $n = 8$–9), and elevated extracellular $[K^+]$ (**C**, $n = 7$–8). Experiments involving elevated extracellular $[K^+]$ were performed in the presence of 1 μM phentolamine in order to inhibit effects of noradrenaline released from perivascular nerve endings in response to depolarization. 20 and 100 mmHg refer to the equivalent transmural pressures at which the veins were investigated. The curves are the results of least-squares fits to sigmoidal functions, and we compare them using extra sum-of-squares *F*-tests. NS: not significantly different vs. with PVT.

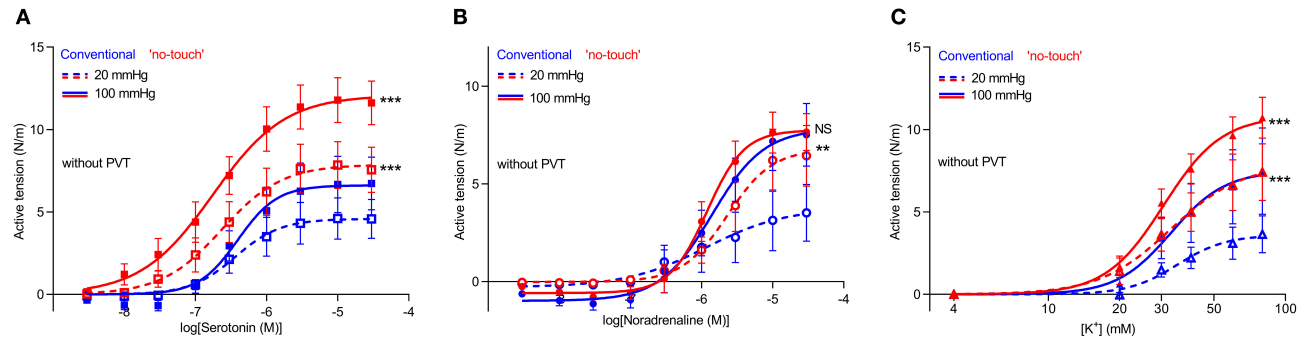

FIGURE 3 | Vasocontraction in response to noradrenaline, serotonin and depolarization with elevated [K^+] is increased in saphenous veins harvested by "no-touch" technique. **(A–C)** Vasocontractile responses to serotonin (**A**, $n = 6–9$), noradrenaline (**B**, $n = 6–9$), and elevated extracellular [K^+] (**C**, $n = 7–8$). 20 and 100 mmHg refer to the equivalent transmural pressures at which the veins were investigated. Experiments involving elevated extracellular [K^+] were performed in the presence of 1 μM phentolamine in order to inhibit effects of noradrenaline released from perivascular nerve endings in response to depolarization. The data relating to "no-touch" veins are replotted from **Figure 2** to ease interpretations. The curves are the results of least-squares fits to sigmoidal functions, and we compare them using extra sum-of-squares *F*-tests. $^{**}P < 0.01$, $^{***}P < 0.001$, NS: not significantly different vs. Conventional.

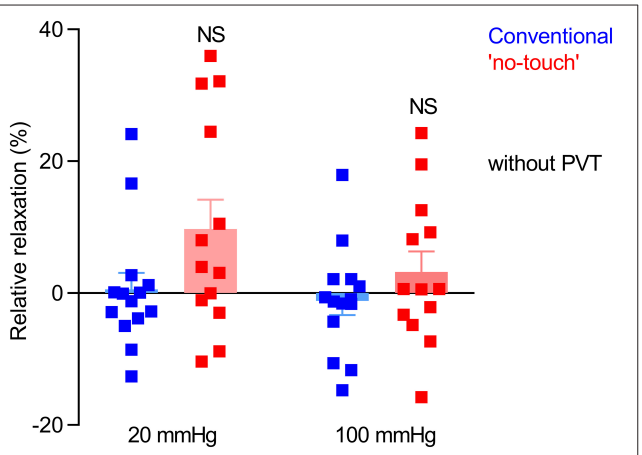

FIGURE 4 | Endothelium-dependent vasorelaxation is modest and variable in vein grafts and not significantly different between veins harvested by conventional and "no-touch" technique. The vein grafts ($n = 13–14$) were stretched to an internal diameter corresponding to a transmural pressure of 20 or 100 mmHg, pre-contracted with 10 μM serotonin, and exposed to 10 μM methacholine. The data are compared by repeated measures two-way ANOVA followed by Sidak's post-test. NS: not significantly different vs. Conventional.

of conventionally harvested veins compared to veins harvested by "no-touch" technique is explained by damage during this manual distension, which could be exacerbated in veins lacking the structural support from the perivascular tissue. To explore this possibility, we investigated a subset of veins harvested by conventional technique, except that one segment of the vein was not exposed to manual distension. Avoiding manual graft distension did not increase contractile responses of conventionally harvested veins during stimulation with serotonin (**Figure 6A**), noradrenaline (**Figure 6B**) or elevated extracellular [K^+] (**Figure 6C**). Based on these findings, we conclude that damage during manual distension is not responsible for the lower vasocontraction of conventionally harvested vein grafts.

DISCUSSION

A series of well-designed and well-conducted randomized clinical trials from a single center in Sweden with up to 16 years of angiographic follow-up provides strong evidence of superior patency rates of "no-touch" compared to conventional saphenous vein grafts (Souza et al., 2001, 2006; Johansson et al., 2009; Samano et al., 2015). The current study evaluates whether the acute vasomotor function of "no-touch" saphenous vein grafts differs from that of conventionally harvested vein grafts and was conducted in order to identify functional properties that might help to understand the improved patency.

Our studies show that saphenous veins harvested by "no-touch" technique have greater contractile capacity than equivalent grafts harvested by conventional technique (**Figures 1**, **3**, **5**). The stronger contractions—evident under both isometric (**Figures 1**, **3**) and isobaric (**Figure 5**) experimental conditions—are observed in response to the vascular agonists serotonin and noradrenaline (**Figures 3A,B**, **5**) and also when smooth muscle cell membrane depolarization is induced by elevating extracellular [K^+] (**Figure 3C**).

Vasoactive effects of paracrine factors released from perivascular tissue have been described for multiple arterial preparations from humans and rodents (Gollasch, 2012) and in rat inferior vena cava (Lu et al., 2011). In contrast, we find that removal of the perivascular tissue surrounding human saphenous vein segments only has marginal acute effects on their contractile properties (**Figures 1**, **2**) suggesting that the perivascular adipose tissue surrounding saphenous veins has very little net vasomotor effect. This is in congruence with a rather loose association between the perivascular tissue and the saphenous veins compared, for instance, to coronary arteries. Nevertheless, additional studies are required to determine whether the perivascular tissue is important for long-term graft patency.

Because the greater capacity for vasocontraction of "no-touch" relative to conventional vein grafts is evident also after

the perivascular tissue has been removed by microdissection (**Figures 1**, **2**, **3**, **5**), our studies suggest that the sheath of perivascular tissue is important for atraumatic excision and handling rather than as a source of paracrine secretion. It is commonly observed that stretch or forceful dilation of contracted blood vessels damages their function; and to minimize this effect, vasodilators (e.g., papaverine) are routinely used during CABG graft harvesting (He et al., 1993). In the investigated saphenous vein segments, we observed that if veins were not fully relaxed during the normalization procedure or during the passive stretch component of the diameter-tension protocol, they immediately lost contractile function. Thus, our findings are consistent with the perivascular tissue being critical for permitting the surgeon to avoid directly grasping the vein with surgical instruments that can lead to cell damage and associated vasospasm (Souza and Samano, 2016; Fernández-Alfonso et al., 2017), and protecting against direct damage induced by sharp dissection during stripping of conventional vein grafts.

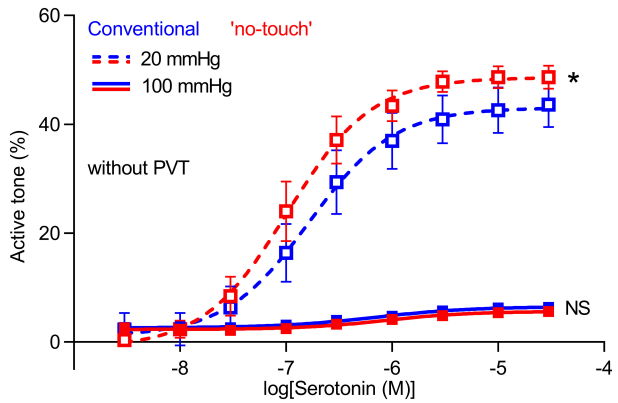

FIGURE 5 | Isobaric vasoconstriction is increased in "no-touch" vein grafts. Veins harvested by "no-touch" ($n = 7$) and conventional ($n = 7$) technique were constricted with serotonin at transmural pressures of 20 and 100 mmHg. The curves are the results of least-squares fits to sigmoidal functions, and we compare them using extra sum-of-squares F-tests. *$P < 0.05$, NS: not significantly different vs. Conventional.

The proposed importance of the perivascular tissue as a mechanical shield against surgical handling suggests that the amount of retained perivascular tissue can be reduced to a thin sheath, which will minimize the size of the surgical wound on the harvest site and the risk of wound infection. Infection is a challenge of the open surgical techniques compared to endoscopic harvesting techniques (Kopjar et al., 2016; Souza and Samano, 2016). Still, clinical verification of the amount of perivascular tissue necessary for improved long-term graft function and clinical outcome is necessary as there is currently no direct evidence that the capacity for vein graft contraction is causatively related to its long-term patency.

Venous transmural pressure in healthy humans is typically around 20 mmHg but can increase to around 60 mmHg during sustained upright posture or in patients with insufficient venous valve function (Koster et al., 2013). Maximal active tension development at transmural pressures higher than the physiological level (**Figure 1**) provides basis for a Starling-like mechanism that will limit vein compliance during combined venous build-up of blood and activation of venous smooth muscle cells. The increased active tension development will support local intravascular pressure increases that can facilitate return of blood to the heart through the valve-containing venous circulation.

Previous studies have shown that the storage conditions used between harvest and implantation can affect the quality of CABG vein grafts. In particular, endothelium-dependent vasorelaxation has been found improved by storage in buffered salt solutions (Wise et al., 2015). In the current study, the excised grafts were stored for a few minutes in the storage solution used for the surgical procedure (i.e., heparin-saline or

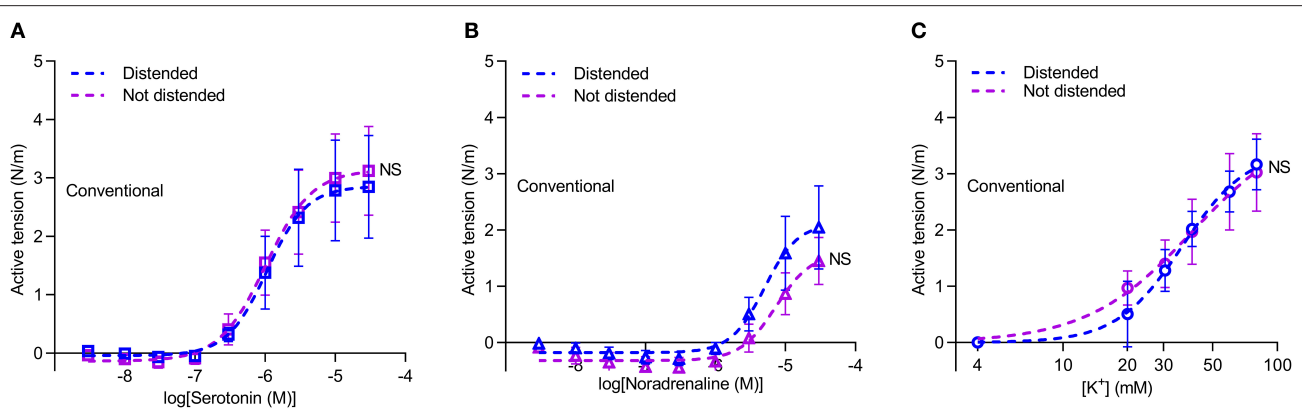

FIGURE 6 | Avoiding distension of conventional vein grafts does not lead to larger contractions. **(A–C)** Vasocontraction in response to serotonin (**A**, $n = 7$), noradrenaline (**B**, $n = 6$) and elevated extracellular [K^+] (**C**, $n = 6$). Arteries were normalized to an internal diameter corresponding to a transmural pressure of 20 mmHg. Experiments involving elevated extracellular [K^+] were performed in the presence of 1 μM phentolamine in order to inhibit effects of noradrenaline released from perivascular nerve endings in response to depolarization. The curves are the results of least-squares fits to sigmoidal functions, and we compare them using extra sum-of-squares F-tests. NS: not significantly different vs. Distended Conventional veins.

heparinized papaverine-containing autologous blood solution) before they were transferred to a buffered salt solution (i.e., PSS) that was used for transport, dissection, and experiments. Using buffered salt solution for storage and handling, we avoid that variation in storage conditions differentially affect the function of vein grafts harvested by conventional and "no-touch" technique.

Although we primarily consider the enhanced contractile capacity of "no-touch" vein grafts an important sign of improved viability, the greater capacity for vasocontraction also provides enhanced ability for dynamic regulation of precapillary resistance, local perfusion, and capillary pressure. A greater viability of the medial vascular smooth muscle cells of "no-touch" vein grafts is consistent with previous histological investigations (Ahmed et al., 2004; Vasilakis et al., 2004; Loesch et al., 2006). Because cell damage in the vascular wall is associated with structural disintegration and platelet deposition, it is expected that improved graft viability in the acute phase can reduce long-term graft failure.

In conclusion, we demonstrate for the first time that saphenous vein grafts harvested by "no-touch" technique have stronger vasocontractile capacity than vein grafts harvested by conventional technique. In the "no-touch" veins, the increase in active tension development at transmural pressures higher than the physiological level provides basis for a Starling-like mechanism that could limit build-up of blood and counteract edema formation. Whereas, acute vasomotor effects of paracrine factors released from the perivascular tissue were negligible, our findings support that the atraumatic "no-touch" surgical technique improves graft viability, which is consistent with the greater long-term patency.

AUTHOR CONTRIBUTIONS

IM, FdP, and EB: conceived the project; LV and LB: performed and analyzed experiments; All authors contributed to the design of experiments and interpretation of data; EB: wrote the manuscript; All authors revised the manuscript and accepted the final version.

FUNDING

This study was supported by the Danish Heart Foundation (grant no. 14-R97-A5321-22809 to EB) and the MEMBRANES research center at Aarhus University.

ACKNOWLEDGMENTS

The authors would like to thank Filip Aalbæk for his initial contribution to establishing the procedure for sampling and analysis of vein graft segments. We are grateful to the nurses and surgeons at the Department of Cardiothoracic Surgery at Aarhus University Hospital for their collaboration and support of this study.

REFERENCES

Aalbaek, F., Bonde, L., Kim, S., and Boedtkjer, E. (2015). Perivascular tissue inhibits rho-kinase-dependent smooth muscle Ca^{2+} sensitivity and endothelium-dependent H_2S signalling in rat coronary arteries. *J. Physiol.* 593, 4747–4764.doi: 10.1113/JP271006

Aghamohammadzadeh, R., Greenstein, A. S., Yadav, R., Jeziorska, M., Hama, S., Soltani, F., et al. (2013). Effects of bariatric surgery on human small artery function: evidence for reduction in perivascular adipocyte inflammation and the restoration of normal anticontractile activity despite persistent obesity. *J. Am. Coll. Cardiol.* 62, 128–135.doi: 10.1016/j.jacc.2013.04.027

Ahmed, S. R., Johansson, B. L., Karlsson, M. G., Souza, D. S. R., Dashwood, M. R., and Loesch, A. (2004). Human saphenous vein and coronary bypass surgery: ultrastructural aspects of conventional and "no-touch" vein graft preparations. *Histol. Histopathol.* 19, 421–433. doi: 10.14670/HH-19.421

Bhattacharya, I., Drägert, K., Albert, V., Contassot, E., Damjanovic, M., Hagiwara, A., et al. (2013). Rictor in perivascular adipose tissue controls vascular function by regulating inflammatory molecule expression. *Arterioscler. Thromb. Vasc. Biol.* 33, 2105–2111.doi: 10.1161/ATVBAHA.112.301001

Blachutzik, F., Achenbach, S., Troebs, M., Roether, J., Nef, H., Hamm, C., et al. (2016). Angiographic findings and revascularization success in patients with acute myocardial infarction and previous coronary bypass grafting. *Am. J. Cardiol.* 118, 473–476.doi: 10.1016/j.amjcard.2016.05.040

Bonde, L., Shokouh, P., Jeppesen, P. B., and Boedtkjer, E. (2017). Crosstalk between cardiomyocyte-rich perivascular tissue and coronary arteries is reduced in the zucker diabetic fatty rat model of type 2 diabetes mellitus. *Acta Physiol.* 219, 227–238.doi: 10.1111/apha.12685

Campeau, L., Lespérance, J., Hermann, J., Corbara, F., Grondin, C. M., and Bourassa, M. G. (1979). Loss of the improvement of angina between 1 and 7 years after aortocoronary bypass surgery: correlations with changes in vein grafts and in coronary arteries. *Circulation* 60, 1–5.doi: 10.1161/01.CIR.60.2.1

Dashwood, M. R., Savage, K., Tsui, J. C., Dooley, A., Shaw, S. G., Fernandez Alfonso, M. S., et al. (2009). Retaining perivascular tissue of human saphenous vein grafts protects against surgical and distension-induced damage and preserves endothelial nitric oxide synthase and nitric oxide synthase activity. *J. Thorac. Cardiovasc. Surg.* 138, 334–340.doi: 10.1016/j.jtcvs.2008.11.060

de Vries, M. R., Simons, K. H., Jukema, J. W., Braun, J., and Quax, P. H. A. (2016). Vein graft failure: from pathophysiology to clinical outcomes. *Nat. Rev. Cardiol.* 13, 451–470.doi: 10.1038/nrcardio.2016.76

dela Paz, N. G., and D'Amore, P. A. (2009). Arterial versus venous endothelial cells. *Cell Tissue Res.* 335, 5–16.doi: 10.1007/s00441-008-0706-5

Dreifaldt, M., Souza, D. S. R., Loesch, A., Muddle, J. R., Karlsson, M. G., Filbey, D., et al. (2011). The "no-touch" harvesting technique for vein grafts in coronary artery bypass surgery preserves an intact vasa vasorum. *J. Thorac. Cardiovasc. Surg.* 141, 145–150.doi: 10.1016/j.jtcvs.2010.02.005

Fernández-Alfonso, M. S., Gil-Ortega, M., Aranguez, I., Souza, D., Dreifaldt, M., Somoza, B., et al. (2017). Role of PVAT in coronary atherosclerosis and vein graft patency: friend or foe? *Br. J. Pharmacol.* 174, 3561–3572. doi: 10.1111/bph.13734.

Fernández-Alfonso, M. S. (2004). Regulation of vascular tone. *Hypertension* 44, 255–256.doi: 10.1161/01.HYP.0000140056.64321.f9

Fitts, M. K., Pike, D. B., Anderson, K., and Shiu, Y.T. (2014). Hemodynamic shear stress and endothelial dysfunction in hemodialysis access. *Open Urol. Nephrol. J.* 7, 33–44.doi: 10.2174/1874303X01407010033

Fitzgibbon, G. M., Kafka, H. P., Leach, A. J., Keon, W. J., Hooper, G. D., and Burton, J. R. (1996). Coronary bypass graft fate and patient outcome: angiographic follow-up of 5,065 grafts related to survival and reoperation in 1,388 patients during 25 years. *J .Am. Coll. Cardiol.* 28, 616–626.doi: 10.1016/0735-1097(96)00206-9

Fry, D. L. (1969). Certain histological and chemical responses of the vascular interface to acutely induced mechanical stress in the aorta of the dog. *Circ. Res.* 24, 93–108.doi: 10.1161/01.RES.24.1.93

Gollasch, M. (2012). Vasodilator signals from perivascular adipose tissue. *Br. J. Pharmacol.* 165, 633–642.doi: 10.1111/j.1476-5381.2011.01430.x

Greenstein, A. S., Khavandi, K., Withers, S. B., Sonoyama, K., Clancy, O., Jeziorska, M., et al. (2009). Local inflammation and hypoxia abolish the protective anticontractile properties of perivascular fat in obese patients. *Circulation* 119, 1661–1670.doi: 10.1161/CIRCULATIONAHA.108.821181

Harskamp, R. E., Lopes, R. D., Baisden, C. E., de Winter, R. J., and Alexander, J. H. (2013a). Saphenous vein graft failure after coronary artery bypass surgery: pathophysiology, management, and future directions. *Ann Surg.* 257, 824–833.doi: 10.1097/SLA.0b013e318288c38d

Harskamp, R. E., Williams, J. B., Hill, R. C., de Winter, R. J., Alexander, J. H., and Lopes, R. D. (2013b). Saphenous vein graft failure and clinical outcomes: toward a surrogate end point in patients following coronary artery bypass surgery? *Am. Hear. J.* 165, 639–643.doi: 10.1016/j.ahj.2013.01.019

He, G. W., Rosenfeldt, F. L., and Angus, J. A. (1993). Pharmacological relaxation of the saphenous vein during harvesting for coronary artery bypass grafting. *Ann. Thorac. Surg.* 55, 1210–1217.doi: 10.1016/0003-4975(93)90036-H

Johansson, B. L., Souza, D. S. R., Bodin, L., Filbey, D., and Bojö, L. (2009). No touch vein harvesting technique for CABG improves the long-term clinical outcome. *Scand. Cardiovasc. J.* 43, 63–68.doi: 10.1080/14017430802140104

Kipshidze, N., Dangas, G., Tsapenko, M., Moses, J., Leon, M. B., Kutryk, M., et al. (2004). Role of the endothelium in modulating neointimal formation. *J. Am. Coll. Cardiol.* 44, 733–739.doi: 10.1016/j.jacc.2004.04.048

Kopjar, T., Dashwood, M. R., and Biocina, B. (2016). Is local wound infection rate more important than long-term graft patency in coronary artery bypass grafting? *J. Thorac. Cardiovasc. Surg.* 151, 275. doi: 10.1016/j.jtcvs.2015.09.066

Koster, M., Amann-Vesti, B. R., Husmann, M., Jacomella, V., Meier, T. O., Jeanneret, C., et al. (2013). Non-invasive pressure measurement of the great saphenous vein in healthy controls and patients with venous insufficiency. *Clin. Hemorheol. Microcirc.* 54, 325–332. doi: 10.3233/CH-131737.

Li, R., Andersen, I., Aleke, J., Golubinskaya, V., Gustafsson, H., and Nilsson, H. (2013). Reduced anti-contractile effect of perivascular adipose tissue on mesenteric small arteries from spontaneously hypertensive rats: role of Kv7 channels. *Eur. J. Pharmacol.* 698, 310–315.doi: 10.1016/j.ejphar.2012.09.026

Loesch, A., Dashwood, M. R., and Souza, D. S. R. (2006). Does the method of harvesting the saphenous vein for coronary artery bypass surgery affect venous smooth muscle cells? iNOS immunolabelling and ultrastructural findings. *Int. J. Surg.* 4, 20–29.doi: 10.1016/j.ijsu.2005.11.002

Lopes, R. D., Mehta, R. H., Hafley, G. E., Williams, J. B., Mack, M. J., Peterson, E. D., et al. (2012). Relationship between vein graft failure and subsequent clinical outcomes after coronary artery bypass surgery. *Circulation*. 125, 749–756.doi: 10.1161/CIRCULATIONAHA.111.040311

Lu, C., Zhao, A. X., Gao, Y.-J., and Lee, R. M. (2011). Modulation of vein function by perivascular adipose tissue. *Eur. J. Pharmacol.* 657, 111–116.doi: 10.1016/j.ejphar.2010.12.028

Mulvany, M. J., and Halpern, W. (1977). Contractile properties of small arterial resistance vessels in spontaneously hypertensive and normotensive rats. *Circ. Res.* 41, 19–26.doi: 10.1161/01.RES.41.1.19

Otsuka, F., Yahagi, K., Sakakura, K., and Virmani, R. (2013). Why is the mammary artery so special and what protects it from atherosclerosis? *Ann. Cardiothorac Surg.* 2, 519–526. doi: 10.3978/j.issn.2225-319X.2013.07.06

Samano, N., Geijer, H., Liden, M., Fremes, S., Bodin, L., and Souza, D. (2015). The no-touch saphenous vein for coronary artery bypass grafting maintains a patency, after 16 years, comparable to the left internal thoracic artery: a randomized trial. *J. Thorac. Cardiovasc. Surg.* 150, 880–888.doi: 10.1016/j.jtcvs.2015.07.027

Shi, Z.-D., and Tarbell, J. M. (2011). Fluid flow mechanotransduction in vascular smooth muscle cells and fibroblasts. *Ann. Biomed. Eng.* 39, 1608–1619.doi: 10.1007/s10439-011-0309-2

Simonsen, U., and Boedtkjer, E. (2016). New roles of factors from perivascular tissue in regulation of vascular tone. *Acta. Physiol.* 216, 159–162.doi: 10.1111/apha.12620

Souza, D., and Samano, N. (2016). Long-term patency versus leg wound healing in coronary artery bypass surgery: surgical aspects of the no-touch harvesting technique. *J. Thorac. Cardiovasc. Surg.* 151, 276.doi: 10.1016/j.jtcvs.2015.10.025

Souza, D. S. R., Bomfim, V., Skoglund, H., Dashwood, M. R., Borowiec, J. W., Bodin, L., et al. (2001). High early patency of saphenous vein graft for coronary artery bypass harvested with surrounding tissue. *Ann. Thorac. Surg.* 71, 797–800.doi: 10.1016/S0003-4975(00)02508-X

Souza, D. S., Johansson, B., Bojö, L., Karlsson, R., Geijer, H., Filbey, D., et al. (2006). Harvesting the saphenous vein with surrounding tissue for CABG provides long-term graft patency comparable to the left internal thoracic artery: results of a randomized longitudinal trial. *J. Thorac. Cardiovasc. Surg.* 132, 373.e5–378.e5. doi: 10.1016/j.jtcvs.2006.04.002

Souza, D. (1996). A new no-touch preparation technique: technical notes. *Scand. J. Thoracic. Cardiovasc. Surg.* 30, 41–44.doi: 10.3109/14017439609107239

Tsui, J. C., Souza, D. S., Filbey, D., Bomfim, V., and Dashwood, M. R. (2001). Preserved endothelial integrity and nitric oxide synthase in saphenous vein grafts harvested by a "no-touch" technique. *Br. J. Surg.* 88, 1209–1215.doi: 10.1046/j.0007-1323.2001.01855.x

Vasilakis, V., Dashwood, M. R., Souza, D. S. R., and Loesch, A. (2004). Human saphenous vein and coronary bypass surgery: scanning electron microscopy of conventional and "no-touch" vein grafts. *Vasc. Dis. Prev.* 1, 133–139.doi: 10.2174/1567270043405204

Wise, E. S., Hocking, K. M., Eagle, S., Absi, T., Komalavilas, P., Cheung-Flynn, J., et al. (2015). Preservation solution impacts physiologic function and cellular viability of human saphenous vein graft. *Surgery* 158, 537–546.doi: 10.1016/j.surg.2015.03.036

Yudkin, J. S., Eringa, E., and Stehouwer, C. D. (2005). "Vasocrine" signalling from perivascular fat: a mechanism linking insulin resistance to vascular disease. *Lancet* 365, 1817–1820. doi: 10.1016/S0140-6736(05)66585-3

Conflict of Interest Statement: The authors declare that the research was conducted in the absence of any commercial or financial relationships that could be construed as a potential conflict of interest.

frontiers in Physiology

ORIGINAL RESEARCH
published: 19 December 2017
doi: 10.3389/fphys.2017.01032

MitoNEET in Perivascular Adipose Tissue Blunts Atherosclerosis under Mild Cold Condition in Mice

Wenhao Xiong[1,2], Xiangjie Zhao[2], Minerva T. Garcia-Barrio[2], Jifeng Zhang[2], Jiandie Lin[3], Y. Eugene Chen[4], Zhisheng Jiang[1] and Lin Chang[2]**

[1] Key Laboratory for Atherosclerology of Hunan Province, Institute of Cardiovascular Disease, University of South China, Hengyang, China, [2] Cardiovascular Research Center, University of Michigan, Ann Arbor, MI, United States, [3] Life Science Institute, University of Michigan, Ann Arbor, MI, United States, [4] Department of Cardiac Surgery, University of Michigan, Ann Arbor, MI, United States

Background: Perivascular adipose tissue (PVAT), which surrounds most vessels, is de facto a distinct functional vascular layer actively contributing to vascular function and dysfunction. PVAT contributes to aortic remodeling by producing and releasing a large number of undetermined or less characterized factors that could target endothelial cells and vascular smooth muscle cells, and herein contribute to the maintenance of vessel homeostasis. Loss of PVAT in mice enhances atherosclerosis, but a causal relationship between PVAT and atherosclerosis and the possible underlying mechanisms remain to be addressed. The CDGSH iron sulfur domain 1 protein (referred to as mitoNEET), a mitochondrial outer membrane protein, regulates oxidative capacity and adipose tissue browning. The roles of mitoNEET in PVAT, especially in the development of atherosclerosis, are unknown.

Methods: The brown adipocyte-specific mitoNEET transgenic mice were subjected to cold environmental stimulus. The metabolic rates and PVAT-dependent thermogenesis were investigated. Additionally, the brown adipocyte-specific mitoNEET transgenic mice were cross-bred with ApoE knockout mice. The ensuing mice were subsequently subjected to cold environmental stimulus and high cholesterol diet challenge for 3 months. The development of atherosclerosis was investigated.

Results: Our data show that mitoNEET mRNA was downregulated in PVAT of both peroxisome proliferator-activated receptor gamma coactivator 1-alpha (Pgc1α)- and beta (Pgc1β)-knockout mice which are sensitive to cold. MitoNEET expression was higher in PVAT of wild type mice and increased upon cold stimulus. Transgenic mice with overexpression of mitoNEET in PVAT were cold resistant, and showed increased expression of thermogenic genes. ApoE knockout mice with mitoNEET overexpression in PVAT showed significant downregulation of inflammatory genes and showed reduced atherosclerosis development upon high fat diet feeding when kept in a 16°C environment.

Conclusion: mitoNEET in PVAT is associated with PVAT-dependent thermogenesis and prevents atherosclerosis development. The results of this study provide new insights on PVAT and mitoNEET biology and atherosclerosis in cardiovascular diseases.

Keywords: Cisd1, mitoNEET, perivascular adipose tissue, atherosclerosis, mitochondria

OPEN ACCESS

Edited by:
Stephanie W. Watts, Michigan State University, United States

Reviewed by:
Erik Nicolaas Theodorus Petrus Bakker, University of Amsterdam, Netherlands
Suowen Xu, University of Rochester, United States

***Correspondence:**
Zhisheng Jiang
zsjiang2005@126.com
Lin Chang
lincha@med.umich.edu

Specialty section:
This article was submitted to This article was submitted to Vascular Physiology, a specialty of Frontiers in Physiology, a section of the journal Frontiers in Physiology

Received: *30 September 2017*
Accepted: *28 November 2017*
Published: *19 December 2017*

Citation:
Xiong W, Zhao X, Garcia-Barrio MT, Zhang J, Lin J, Chen YE, Jiang Z and Chang L (2017) MitoNEET in Perivascular Adipose Tissue Blunts Atherosclerosis under Mild Cold Condition in Mice. Front. Physiol. 8:1032. doi: 10.3389/fphys.2017.01032

INTRODUCTION

The major adipose tissue in humans is white adipose tissue (WAT). Although long believed that brown adipose tissue (BAT) only existed in infants, the existence of a functional BAT is now accepted in the clavicular, cervical, suprarenal, and periaortic regions of adult humans (Nedergaard et al., 2007, 2010). WAT and BAT exhibit distinct functions. WAT has been recognized as a tissue for energy storage (Kim and Moustaid-Moussa, 2000) and related to cardiovascular diseases (CVDs), while the main function of BAT is to generate heat and energy expenditure (Smith and Horwitz, 1969). Studies using mouse models demonstrated that activation of BAT by cold temperature enhances clearance of plasma lipids and prevents the development of atherosclerosis (Bartelt et al., 2011). Additionally, WAT can be converted to "beige" fat (between WAT and BAT) by cold stimuli or hormones such as irisin (Zhang et al., 2014), FGF21 (Fisher et al., 2012), etc. Also, beige can be converted to WAT (Cohen et al., 2014). Beige adipocytes have a gene expression pattern distinct from either WAT or BAT and promote energy expenditure due to existence of uncoupling protein-1 (UCP-1) in the mitochondria, similarly to classic brown adipocytes (Wu et al., 2012). Recent strategies for "browning" WAT via cold stimuli or hormones significantly enhanced thermogenesis and may aid in prevention of obesity and related CVDs. Additionally, not all adipose tissue expansion is necessarily associated with pathological changes. The concept of the "metabolically healthy obese" state (Ruderman et al., 1981) suggests that some individuals can preserve systemic insulin sensitivity on the basis of "healthy" adipose tissue expansion (Sun et al., 2011). One example is that of thiazolidinediones (TZDs), the insulin-sensitizers known to affect the morphology of adipose tissue while improving insulin sensitivity. Both in humans and experimental animals, TZDs increase the number of small adipocytes and decrease large adipocytes (Hallakou et al., 1997; Okuno et al., 1998; Boden et al., 2003). TZDs have favorable effects on atherosclerosis in patients with type 2 diabetes mellitus (Ryan et al., 2007; Yu et al., 2007; Harashima et al., 2009; Kiyici et al., 2009).

PVAT is the adipose tissue surrounding most vessels. The PVAT of rodents is similar to BAT (Chang et al., 2012b). We previously demonstrated that one major physiological function of PVAT is thermogenesis in response to cold stimuli (Chang et al., 2012b). The intrinsic characteristic of energy expenditure of brown or beige adipocytes highlights the potential importance of PVAT as a target for the treatment of obesity and related CVDs (Chang et al., 2017). Our previous study demonstrated that donor PVAT from healthy mice ameliorates the endothelial dysfunction of aging recipient mice (Chang et al., 2012b) and that cold exposure inhibits atherosclerosis and improves endothelial function in mice with intact PVAT but not in mice lacking PVAT. Thus, our published data strongly suggest that PVAT metabolism is highly related to atherosclerosis.

MitoNEET, a mitochondrial outer membrane protein necessary for energy metabolism, was identified as an additional target of TZDs (Colca et al., 2004; Wiley et al., 2007a,b). Adipocyte specific overexpression of mitoNEET driven by the aP2 promoter induces severe obesity in ob/ob mice. Surprisingly, the adipocyte size was normal in the mitoNEET transgenic ob/ob mice despite accumulation of fat mass, suggesting that mitoNEET is able to convert hypertrophic fat to hyperplastic fat in ob/ob mice (Kusminski et al., 2012). Our study shows that mitoNEET expression is dramatically reduced in PVAT of *Pgc1α* or *Pgc1β* knockout mice which exhibit impaired PVAT thermogenesis. Thus, we hypothesize that mitoNEET is a critical mediator to maintain PVAT thermogenesis and protects against atherosclerosis. In this study, we document that the mice with specific overexpression of mitoNEET in brown adipocytes (mitoNEET-Tg) are cold resistant and partially resistant to the development of atherosclerosis in an ApoE knockout background.

MATERIALS AND METHODS

Animals

Transgenic mice with brown adipocyte-specific overexpression of mitoNEET (mitoNEET-Tg) in a C57BL/6J background were generated to express human mitoNEET driven by the mouse *Ucp-1* promoter. Littermate mice without the human mitoNEET transgene served as wild type control mice. For the atherosclerosis study, mitoNEET-Tg mice were crossed with ApoE knockout (ApoE KO) mice (Stock# 002052, Jackson Laboratory) to obtain ApoE knockout mitoNEET-Tg mice (ApoE/mitoNEET-Tg). The offspring were genotyped by PCR analysis of DNA obtained from tail-snip biopsies using transgene-specific oligonucleotide primers for human mitoNEET and ApoE knockout. We selected two groups of mice for this study: (1) ApoE homozygous and positive for human mitoNEET, and (2) littermate control mice with a genotype of ApoE homozygous and negative for human mitoNEET. All experiments were conducted in 8-week-old male mice. The study protocol was approved by the Animal Research Ethics Committee of the University of Michigan.

Surgical Removal of the Interscapular BAT

Mice were anesthetized by isoflurane inhalation and fixed face down on a surgical heating pad (37°C). The subscapular hair was removed, and a 1 cm long incision on the midline skin was made to expose the interscapular BAT. Next, the intact BAT was completely separated from the interscapular trigonal pyramidal region. The vessels supplying blood to BAT and the neighboring cells at the trigonal pyramidal bottom were cauterized using an electronic cauterizer to permanently block bleeding and BAT regeneration after the BAT removal procedure. The skin wound was closed using wound clips. The mice were allowed to recover for 1 week at room temperature (22°C) before initiating the temperature, energy expenditure and atherosclerosis studies at 16°C (Chang et al., 2012b).

Wireless Measurements of Body Temperature Using Implanted Probes

The mice were anesthetized by isoflurane inhalation. The neck hair was removed, and the skin was opened. A temperature monitoring microchip (Bio Medic Data Systems, 12 mm long and

2 mm in diameter) was surgically implanted in the subcutaneous area. After 3 days' recovery from the surgery, the temperature was manually recorded by remotely scanning the animal using a handheld reader system (DAS-7007R, Bio Medic Data Systems) at 9 a.m., 12 p.m., and 4 p.m. daily.

Measurement of Intravascular Temperature in Mice

Intravascular temperature was monitored using a T-type thermocouple probe (ADInstruments MLT1405) which was inserted into the thoracic aorta through the left carotid artery of mice under anesthesia induced by isoflurane inhalation (Chang et al., 2012b). The thermocouple probe was connected to a data acquisition system (AdInstruments Powerlab) to monitor the temperature inside of aortic lumen. During the procedure, the mice were lying on their backs on a 35°C warm pad with constant inhalation of isoflurane, and cold stimulation was performed by submerging the tail and hind feet in 4°C water with the researcher blinded to the genotype of mice.

Energy Expenditure Assay in Mice

Oxygen consumption (VO_2), carbon dioxide production (VCO_2), spontaneous motor activity and food intake were measured using the Comprehensive Laboratory Monitoring System (CLAMS, Columbus Instruments), an integrated open-circuit calorimeter equipped with an optical beam activity monitoring device. Mice were individually placed into the sealed chambers ($7.9'' \times 4'' \times 5''$) with free access to food and water. To determine the energy expenditure in mice upon acute cold exposure, the study was carried out in an experimentation room set at 22 or 4°C with 12-12 h (6:00 p.m.∼6:00 a.m.) dark-light cycles. The measurements were carried out continuously for 48 h at 22 or 4°C. Mice were provided food and water through the feeding and drinking devices located inside the chamber without nesting material due to the fact that it blocks the beams that track activity. The amount of food consumed by each animal was monitored through a precision balance attached below the chamber. The body composition data were measured using an NMR analyzer when conscious mice were placed individually into the measuring tube with a minimum restrain. Total energy expenditure was calculated based on the values of VO_2, VCO_2, and the protein breakdown (Riachi et al., 2004).

Atherosclerosis Study

For atherosclerosis experiments, 8-week-old male ApoE KO and ApoE/mitoNEET-Tg mice were fed a high-cholesterol diet (Harlan, TD.88137) for 3 months in a cold-temperature chamber (16°C) with a 12-h:12-h light-dark cycle and free access to water and diet as in our previous study (Chang et al., 2012b). Afterwards, the animals were sacrificed with excess CO_2. After collection of plasma, the mice were perfused with 20 ml normal saline solution through the heart, followed by 20 ml 37% formalin. The mice were fixed with formalin and the whole aortic tree was dissected under a surgical microscope. Next, the aortic trees were stained with Oil Red O solution (0.2% Oil Red O (w/v) in 3.5:1 of methanol:1N NaOH) for 50 min, followed by 70% ethanol for 30 min. Afterwards, the aortic trees were kept in ddH_2O. The attached connective tissues around the aortic trees were cleaned and pinned on a plate containing paraffin wax, and then the aorta was longitudinally opened with a Vannas scissor to expose the atherosclerotic lesions. The pictures of whole aortic trees were obtained using a digital camera, and the atherosclerotic lesion areas were calculated by an Image software (Meta Imaging Series 7.0, Molecular Devices, LLC).

Histological Analysis

Adipose tissues were harvested from mice that were anesthetized and fixed overnight via transcardial perfusion with 4% paraformaldehyde (pH 8.0). After dehydration, the samples were embedded in paraffin wax according to standard laboratory procedures. Sections of 5 μm were stained with H&E for routine histopathological examination with light microscopy.

Quantitative Real-Time Reverse-Transcriptase Polymerase Chain Reaction (QT-PCR) and Western Blot

The mice were housed at 4°C for 24 h, 16°C for 1 week or 3 months. The tissues indicated in the figures were harvested and frozen in liquid nitrogen for mRNA and protein analysis. Total RNA was isolated from tissues using TRIzol reagent (Invitrogen). The mRNA levels were measured by QT-PCR using a Bio-Rad thermocycler and a SYBR green kit (Bio-Rad). The mouse primers used for each gene were, respectively, as follows:

Ucp-1: 5′-AAAAACAGAAGGATTGCCGAAACT-3′ and 5′-TAAGCATTGTAGGTCCCCGTGTAG-3′;

Cidea: 5′-CTGTCGCCAAGGTCGGGTCAAG-3′ and 5′-CGAAAAGGGCGAGCTGGATGTAT-3′;

Pgc-1α: 5′-CTCCTCCCACAACTCCTCCTCATA-3′ and 5′-GGGCCGTTTAGTCTTCCTTTCCTC-3′;

Pgc-1β: 5′-CTACCGCCTGGCCATACCTGTCA-3′ and 5′-CTCCTCATCTTCCTCCCGCTTTTG-3′;

IL-6: 5′-TTCCCTACTTCACAAGTC-3′ and 5′-GTACAAAGCTCATGGAGA-3′;

TNF-α: 5′-CTCAGATCATCTTCTCAA-3′ and 5′-GGTTTGCCGAGTAGATCT-3′;

Mcp-1: 5′-CACCAGCACCAGCCAACTCTCACT-3′ and 5′-CATTCCTTCTTGGGGTCAGCACAG-3′;

Ckb: 5′-CCTGCTTCGTCCGGCATC-3′ and 5′-GTCCAAAGTAAAGCCGCTCG-3′;

Macrod1: 5′-ATTGTCAACGCTGCCAACAG-3′ and 5′-TTCTGTAGGGTGCGGCATTC-3′;

Fabp3: 5′-CAGGTGGCTAGCATGACCAA-3′ and 5′-ATGAGTTTGCCTCCGTCCAG-3′;

Idh2: 5′-TGTATCCATGGCCTCAGCAA-3′ and 5′-TGCCATGTACAGAGTACCCAC-3′;

Klf2: 5′-TAAAGGCGCATCTGCGTACA-3′ and 5′-GTGGCACTGAAAGGGTCTGT-3′.

The proteins in tissues were extracted by T-PER tissue protein extraction reagent (Thermo Scientific 78510) as indicated in the instructions manual. Protein separation by electrophoresis using 10% SDS-PAGE gels for 1 h at 150V in Tris/Glycine/SDS electrophoresis buffer (25 mM Tris, 190 mM glycine and 0.1%

SDS) was performed on 30 μg protein/well in loading buffer (4% SDS, 10% 2-mercaptoethanol, 20% glycerol, 0.004% bromophenol blue and 0.125M Tris-HCl) after boiling at 100°C for 10 min. Proteins were transferred to a nitrocellulose membrane in transfer buffer (25 mM Tris, 190 mM glycine and 20% methanol) at 40V overnight at 4°C. The membrane was rinsed in TBST buffer (20 mM Tris pH7.5, 150 mM NaCl, 0.1% Tween 20) 3 times at room temperature. MitoNEET protein levels were detected by overnight incubation at 4°C in 5% milk containing 1:1000 anti-mitoNEET antibody (ProteintechTM Cat#: 16006-1-AP). Then the membrane was rinsed in TBST buffer, and incubated with Goat anti-Rabbit IgG antibody (IRDye680LT) for 2 h at room temperature. The blot image was captured and analyzed by BioRad LI-COR system.

Statistical Analysis

All data were evaluated with a 2-tailed, unpaired Student's *t*-test or compared by one-way ANOVA followed by Newman-Keuls and were expressed as mean ± SD. A value of $p < 0.05$ was considered statistically significant.

RESULTS

MitoNEET Is Reduced in PVAT of *Pgc1α and Pgc1β* Knockout Mice

Prior studies indicated that the characteristics of PVAT in mice make it almost identical to interscapular BAT (Fitzgibbons et al., 2011; Chang et al., 2012b). Thus, we reasoned that thermogenesis would be one of the properties of PVAT. Our previous study demonstrated that mice lacking PVAT had lower intravascular temperature in response to cold stimuli (Chang et al., 2012b). Since *Pgc1α* and *Pgc1β* are well-known nuclear receptor coactivators critically involved in BAT thermogenesis (Spiegelman, 2007a,b), we performed RNA deep sequencing analysis in PVAT of *Pgc1α* and *Pgc1β* knockout (KO) mice to screen for factors related to thermogenesis in PVAT. Firstly, we confirmed that *Pgc1α* mRNA or *Pgc1β* mRNA is efficiently deleted in both PVAT and BAT of *Pgc1α* KO (**Figure 1A**) or *Pgc1β* KO mice (**Figure 1B**), respectively. To investigate whether *Pgc1α* or *Pgc1β* in PVAT contribute to PVAT thermogenesis, we measured the intravascular temperature of *Pgc1α* or *Pgc1β* KO mice upon cold stimulus for 90 s. As shown in **Figure 1C**, upon 4°C cold stimulus, the intravascular temperatures in all mice are gradually reduced. However, the intravascular temperature of both *Pgc1α* or *Pgc1β* KO mice drops faster than that of wild type mice. After just 30 s of cold stimulus, the average temperature in thoracic aorta of wild type mice dropped 0.05 ± 0.03°C, while it dropped 0.13 ± 0.04°C and 0.12 ± 0.05°C in the aorta of *Pgc1α* KO and Pgc1β KO mice, respectively. After 60 s of cold stimulus it further dropped to a differential of 0.28 ± 0.05°C and 0.30 ± 0.07°C in *Pgc1α* KO and *Pgc1β* KO mice respectively vs. 0.10 ± 0.03°C in wild type mice. At the endpoint of cold exposure, 90 s, the average temperature in thoracic aorta of wild type mice is reduced 0.19 ± 0.03°C while it is reduced 0.44 ± 0.11°C in *Pgc1α* KO mice and 0.48 ± 0.14°C in *Pgc1β* KO mice (**Figure 1C**). These data indicate that deleting *Pgc1α* or *Pgc1β* in PVAT might contribute to the hypothermic phenotype independent of BAT. To investigate the common thermogenic genes, which might represent a cross point between *Pgc1α* and *Pgc1β* in terms of their shared thermogenic mechanisms, we compared the genes in PVAT of *Pgc1α* and *Pgc1β* showing a 1.5-fold change when compared to PVAT of wild type mice. About 37 genes are reduced in PVAT of *Pgc1α* KO mice, while about 112 genes are reduced in PVAT of *Pgc1β* KO mice. Among them, only 8 genes [*Ivns1abp*, *Ckb*, *Macrod1*, *Fabp3*, *Lmpdh1*, *Idh2*, *Klf2* and *Cisd1* (mitoNEET)], which might be directly involved as effectors of thermogenic mechanisms, are reduced in PVAT of both *Pgc1α* and *Pgc1β* KO mice (**Figure 1D**), consistent with known functions of these genes in thermogenesis and lipid metabolism in adipose tissue (Banerjee et al., 2003; Chen et al., 2011; Vergnes et al., 2011; Van der Zee, 2013; Lee et al., 2016). Using real-time PCR, we confirmed that 6 of 8 genes were down-regulated in PVAT of both *Pgc1α* and *Pgc1β* KO mice (**Suppl. Figure IA**, **Figure 1E**). MitoNEET protein levels were also significantly reduced in PVAT of *Pgc1α* and *Pgc1β* KO mice (**Figure 1F**). Although all the common differentially regulated genes might be critical for thermogenesis, we focused on mitoNEET in this study because mitoNEET is located on the mitochondrial membrane, making it a likely direct effector, and it is involved in WAT browning (Kusminski et al., 2014). Also, compared with WAT, mitoNEET mRNA levels in PVAT and BAT are about 15-fold higher, respectively (**Figure 2A**). These data suggest that mitoNEET in brown-like PVAT might be directly involved in the regulation of PVAT-dependent thermogenesis.

MitoNEET Is Up-Regulated in Brown-Like Adipocytes upon Cold Stimulus

Next, we investigated whether mitoNEET is associated with thermogenesis. Even though mitoNEET is also highly expressed in mitochondria-rich organs such as skeletal muscle, heart and brain, however, upon cold stimulus, mitoNEET expression is not increased in those three tissues (**Suppl. Figure I**) while it is significantly increased in PVAT and BAT (**Figures 2B,C**). Despite of subcutaneous WAT (sWAT) being recognized as an Ucp1-positive beige adipose tissue, the mitoNEET mRNA in sWAT is comparable with that in pure gonadal WAT (gWAT) (**Figure 2A**). Consistently, the increase in mitoNEET levels in sWAT is not as marked as in PVAT and BAT (**Figures 2B,C**) upon 24 h cold stimulus. These data suggested that mitoNEET in brown-like PVAT might be strongly associated with cold-induced thermogenesis.

Mice with MitoNEET Overexpression in Brown Adipocytes Are Cold Resistant

To investigate whether mitoNEET in brown adipocytes regulates thermogenesis, we generated mice with brown adipocyte-specific overexpression of human mitoNEET (mitoNEET-Tg) driven by the *Ucp-1* promoter using the strategy outlined in **Figure 3A**. Western blot confirms that mitoNEET is specifically overexpressed in PVAT and BAT (**Figure 3B**), but not in subcutaneous and gonadal WAT (**Suppl. Figure IIA**). Overexpression of mitoNEET in brown adipocytes does not

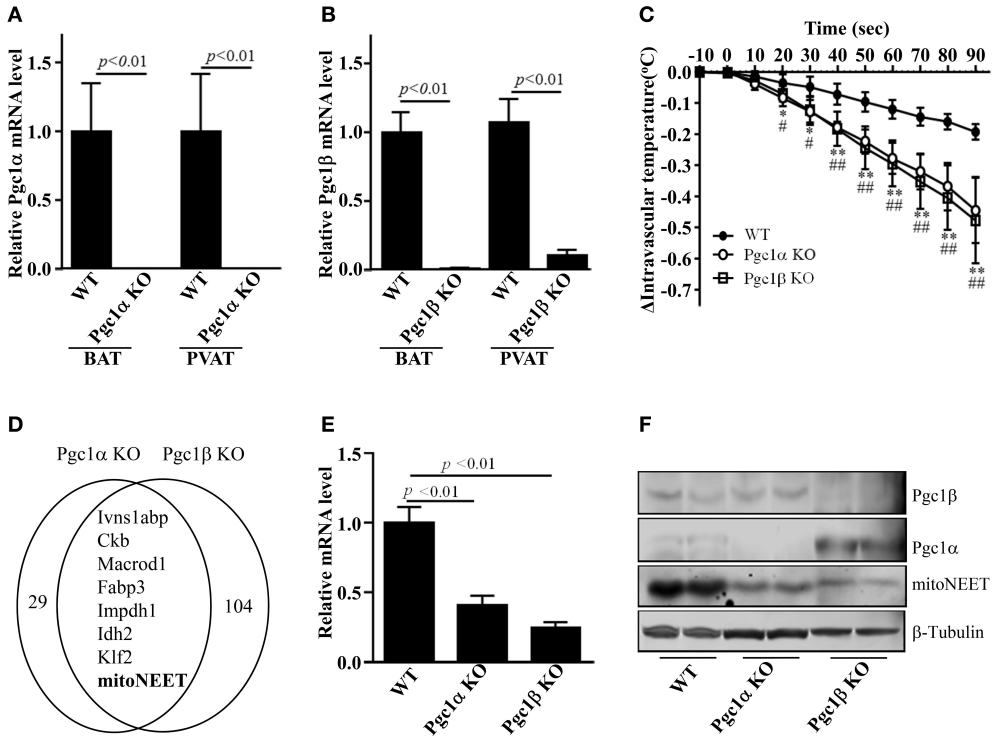

FIGURE 1 | mitoNEET is reduced in PVAT of *Pgc1* knockout mice. Real-time PCR shows *Pgc1α* mRNA levels in BAT and PVAT of *Pgc1α* knockout mice (Pgc1α KO) **(A)**, and *Pgc1β* mRNA levels in BAT and PVAT of *Pgc1β* knockout mice (Pgc1β KO) **(B)**. The relative mRNA levels were normalized by 18S, respectively. Data shown are mean ± SD. $n = 5$ mice/group. **(C)** Intravascular (thoracic aorta) temperature in anesthetized wild type (WT), *Pgc1α* KO and *Pgc1β* KO mice in response to 4°C stimuli. The lag time reflects the time of dipping of the hind feet and tail in 4°C cold water. The zero represents the start time point of immersion in the cold water. Data shown are mean ± SD. $n = 6$ mice/group.*$p < 0.05$ Pgc1α KO vs. WT, **$p < 0.01$ Pgc1α KO vs. WT; $^{\#}p < 0.05$ Pgc1β KO vs. WT, $^{\#\#}p < 0.01$ Pgc1β KO vs. WT. **(D)** RNA deep sequencing identified eight common downregulated genes in PVAT of both *Pgc1α* KO and *Pgc1β* KO mice, as indicated in the Venn diagrams. **(E)** mitoNEET mRNA levels in PVAT of *Pgc1α* KO and *Pgc1β* KO mice. The relative mitoNEET mRNA level was normalized by 18S, respectively. Data shown are mean ± *SD*. $n = 5$ mice/group. **(F)** Western blots show Pgc1α, Pgc1β and mitoNEET protein levels in PVAT of WT, Pgc1α KO and Pgc1β KO mice, $n = 2$ mice/group.

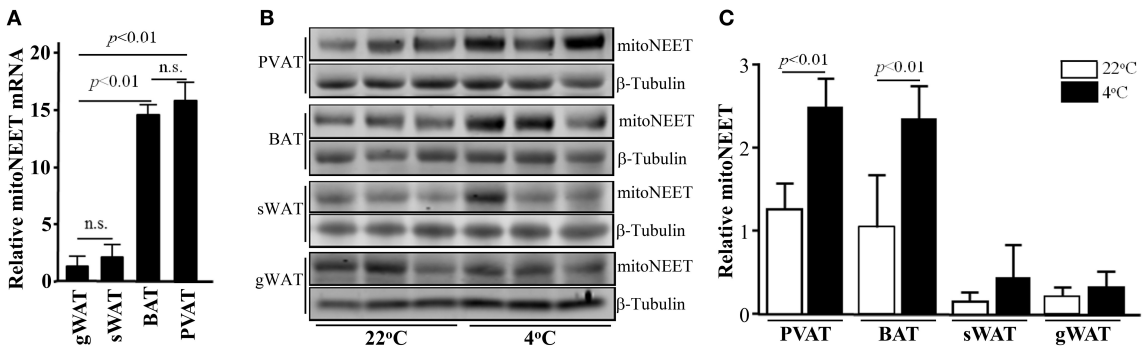

FIGURE 2 | mitoNEET is up-regulated in PVAT upon cold stimuli. **(A)** mitoNEET mRNA levels in BAT, PVAT, gonadal WAT (gWAT), and subcutaneous WAT (sWAT) in 10-week old C57BL/6J mice which were housed at 22°C. The relative mitoNEET mRNA level was normalized by 18S, and the expression level of mitoNEET mRNA in gWAT was set as 1. Data shown are mean ± *SD*. $n = 5$ mice/group. **(B)** Western blots show mitoNEET protein levels in PVAT, BAT, sWAT, and gWAT at 22°C and after 24-h 4°C cold stimuli. $n = 3$ mice per temperature condition. **(C)** Quantitative data of blots in **(B)** expressed as the ratio of densitometry of mitoNEET/β-Tubulin. Data shown as mean ± *SD* of 3 blots either at 22°C or 4°C.

affect the morphology of interscapular BAT, PVAT and aorta (**Figure 3C**), or of subcutaneous and gonadal WAT (**Suppl. Figure IIB**). Next, we investigated whether mitoNEET overexpression in brown adipocytes enhances thermogenesis in mice. As shown in **Figure 3D**, in a 22°C environment, the body temperatures are comparable between wild type and

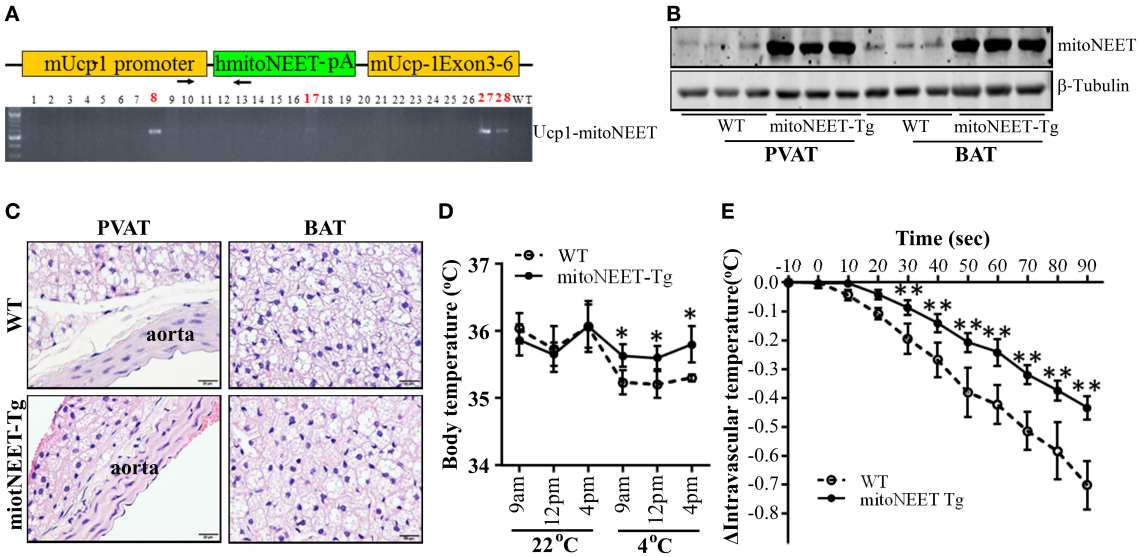

FIGURE 3 | Cold tolerance in mitoNEET-Tg mice**. (A)** Schema of the construct used for generating transgenic mice with brown adipocyte-specific overexpression of the human mitoNEET driven by the mouse Ucp-1 promoter (top). Identification of four human mitoNEET positive founders in the C57BL/6J background (#8, #17, #27, and #28) were identified (bottom). The transgenic mice used in this study are from #8 line. **(B)** Western blot shows that mitoNEET is overexpressed in PVAT and BAT of the transgenic mice. **(C)** Representative H.E. staining showing the morphology of thoracic aortic PVAT and interscapular BAT in 10-week old wild type and mitoNEET-Tg mice. Magnification bar = 20 μm. **(D)** Body temperature of conscious wild type and mitoNEET-Tg mice in response to 4°C stimuli. The body temperatures were collected at 9 a.m., 12 p.m., and 4 p.m. when the mice were housed either in a 22°C or a 4°C chamber. Data shown as mean ± SD, $n = 5$ mice per group,*$p < 0.05$ vs. WT mice. **(E)** Intravascular (thoracic aorta) temperature in the anesthetized mice with interscapular BAT removal was recorded for 90 s as described in Materials and Methods Section. Data shown as mean ± SD. $n = 6$ mice/group.**$p < 0.01$ vs. WT.

mitoNEET-Tg mice. However, when the mice are placed in a 4°C environment, the body temperature is significantly reduced in the wild type animals while the mitoNEET-Tg mice are able to maintain the body temperature, suggesting that mitoNEET in brown adipocytes is able to prevent the temperature reduction observed in the wild type animals upon transfer to the cold environment. To exclude the potential contribution of BAT to intravascular temperature, we surgically removed the interscapular BAT in both the wild type and mitoNEET-Tg mice and measured the intravascular temperature in mice under anesthesia. As shown in **Figure 3E**, by immersing the hind feet and tail of mice with 4°C cold water, the reduction rate of intravascular temperatures of mitoNEET-Tg mice is slower than that of wild type mice. After 90 s of cold stimulation, the intravascular temperature in wild type mice dropped by 0.70 ± 0.08°C, while it only dropped by 0.44 ± 0.04°C in mitoNEET-Tg mice. Consistently, in mice housed in a mild cold environment (16°C) as a challenge for 1-week, the mRNA levels related to thermogenesis-associated genes such as *Ucp1*, *Cidea*, *Evolv3*, *Dio2*, and *Pgc1α* are increased in the PVAT of mitoNEET-Tg mice when compared with those in PVAT of wild type mice (**Figure 4**) while the adipogenic *aP2* remains unchanged. These genes, except for *Evolv3* are not increased in gWAT (**Suppl. Figure IIIA**). The increased expression of thermogenesis-associated genes in PVAT was also confirmed in the mitoNEET-Tg mice line originated from founder #27 (**Suppl. Figure IIIB**), ruling out an insertional effect in the #8 founder. These data further confirm that mitoNEET in PVAT positively contributes to cold-induced thermogenesis independently of the presence of BAT.

Overexpression of MitoNEET in PVAT Increases Whole Body Metabolism

Next, we studied whether overexpression of mitoNEET in PVAT from mice with BAT removed promotes energy expenditure. Our results indicate that overexpression of mitoNEET in brown adipocytes does not affect the food intake (**Figure 5A**), body composition (**Figure 5B**) and total locomotor activity (**Figure 5C**) when the mice were housed in a 22°C environment. Additionally, there are no statistical differences in energy expenditure at room temperature, between that of wild type and mitoNEET-Tg mice (**Figure 5D**). Consistently, O_2 consumption (**Figure 5E**) and CO_2 production (**Figure 5F**) are comparable between wild type and mitoNEET-Tg mice at that temperature. When mice were housed at 4°C, the cold stimulus increases comparably the food intake and reduces fluid percentage and total locomotor activity of both wild type and mitoNEET-Tg mice (**Figures 5A–C**), indicating that overexpression of mitoNEET in PVAT does not change the food intake, body composition and movement behaviors of mice. However, when challenged with 4°C cold stimulus, both O_2 consumption (**Figure 5E**) and CO_2 production (**Figure 5F**) are significantly increased in the mitoNEET-Tg mice. Consistently, the energy expenditure (**Figure 5D**) was also significantly increased at 4°C in mitoNEET-Tg mice when compared with wild type mice, suggesting

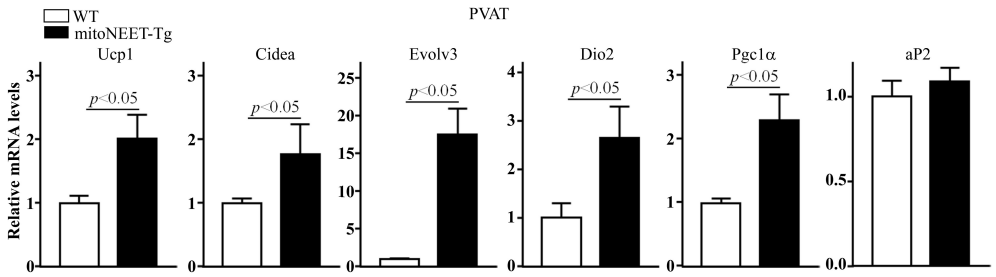

FIGURE 4 | Increase in thermogenesis-related genes in PVAT of mitoNEET-Tg mice. RT-PCR was used to determine the mRNA levels (relative to 18S) of thermogenesis-related genes in PVAT of wild type and mitoNEET-Tg mice housed at 16°C for 1-week. Data shown as mean ± SD. $n = 6$ mice/group.

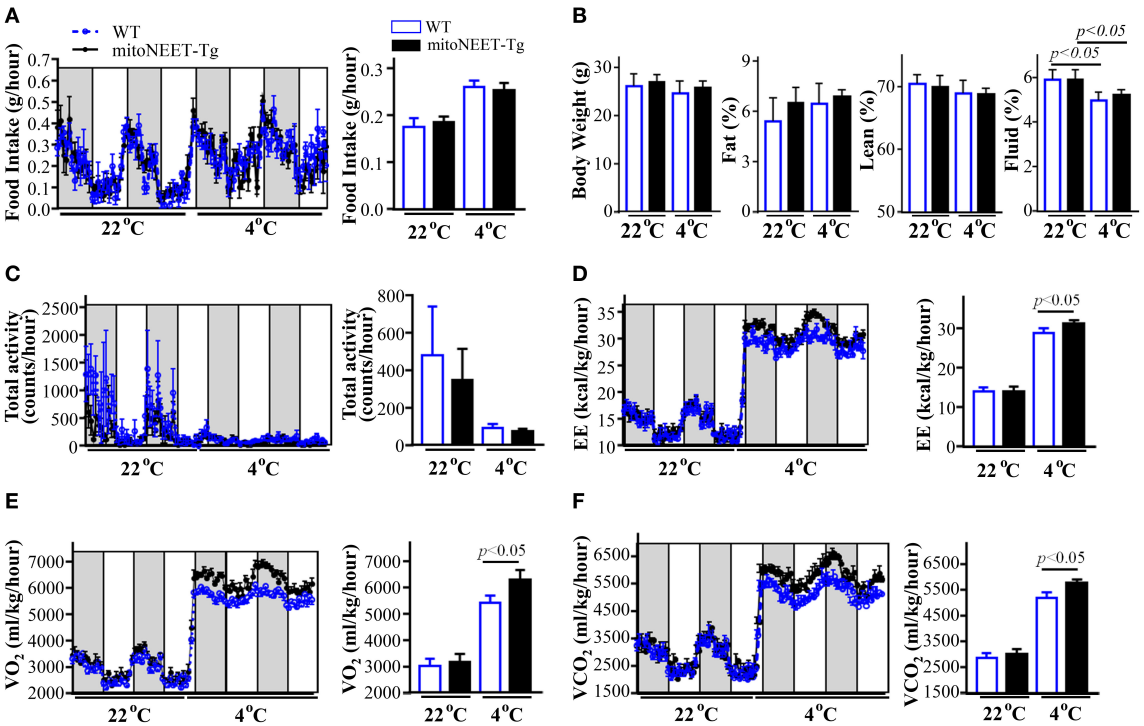

FIGURE 5 | Energy expenditure in mitoNEET-Tg mice. Wild type and mitoNEET-Tg mice with interscapular BAT removed were single-housed in metabolic cages. The food intake **(A)**, body weight and body composition **(B)**, total locomotor activity **(C)**, energy expenditure **(D)**, oxygen consumption **(E)** and carbon dioxide production **(F)** were recorded when the chamber temperatures were adjusted to 22°C or 4°C. Data shown as mean ± S.E.M ($n = 6$) and histogram figures are the 24-h average.

that mitoNEET in PVAT is involved in cold-induced energy expenditure.

Overexpression of MitoNEET in PVAT Attenuates the Development of Atherosclerosis in Mice

Since acute 4°C cold exposure enhanced thermogenesis and energy expenditure in mitoNEET-Tg mice, we investigated the effects of overexpression of mitoNEET in PVAT on atherosclerosis when the interscapular BAT was removed and the mice were housed in a mild cold 16°C environment for 3 months. As shown in **Figure 6A**, after 16°C exposure and high cholesterol diet feeding for 3 months, ApoE/mitoNEET-Tg mice show higher expression of thermogenesis-related genes such as *Ucp-1, Cidea, Cox8b, Evolv3,* and *Pgc1a* in PVAT than those in the PVAT of ApoE knockout mice. Consistently, *en face* staining of lipid-rich lesions from mouse aortas showed that the total lesion area was significantly lower in aortas from ApoE/mitoNEET-Tg than those from ApoE knockout mice (**Figures 6B,C**), indicating that overexpression of mitoNEET in PVAT inhibits atherosclerosis in mild cold conditions. However, the body weights (**Figure 6D**) are comparable between ApoE knockout mice with and without mitoNEET overexpression in PVAT after 16°C exposure for 3 months. Compared to ApoE knockout mice, the total plasma cholesterol and triglyceride levels in

ApoE/mitoNEET-Tg mice are significantly reduced in mild cold conditions (**Figure 6E**), suggesting increased lipid clearance. Remarkably, overexpression of mitoNEET significantly reduced the expression of the pro-inflammatory genes *IL-1β, IL-6, Mcp-1*, and *TNFα* in PVAT of ApoE/mitoNEET-Tg mice (**Figure 6F**). Consistently, the macrophage infiltration is significantly reduced in PVAT of ApoE/mitoNEET-Tg mice (**Figures 6G,H**). Taken together, these data indicate that increased levels of mitoNEET in PVAT reduce the development of atherosclerosis.

DISCUSSION

Decreasing the environmental temperature initiates BAT-adaptive thermogenesis in mammals due to uncoupled ATP generation by *Ucp1* in the mitochondria and dissipates energy in the form of heat (Enerback et al., 1997; Lee et al., 2014). Because of their high expression levels in BAT, *Pgc-1* coactivators are well-established markers of BAT. *Pgc1α* and *Pgc1β* are transcriptional coactivators which recruit nuclear receptors or transcription factors to regulate transcription of downstream genes in the nucleus and the mitochondria (Kadlec et al., 2016), and play an absolutely essential and complementary function in mitochondrial biogenesis and thermogenesis in BAT (Puigserver et al., 1998; Lelliott et al., 2006; Uldry et al., 2006). Therefore, we compared the common genes in PVAT found down-regulated in both *Pgc1α* and *Pgc1β* deficient mice, which might represent key points of commonality in the thermogenesis roles of both *Pgc-1* coactivators. Our study here indicates that mitoNEET is one of the molecules which are highly down-regulated in PVAT in both *Pgc1α* and *Pgc1β* deficient mice. MitoNEET, a dimeric mitochondrial outer membrane protein, is a key regulator of mitochondrial function and lipid homeostasis. Loss of mitoNEET in cells decreases cellular respiration because of reduction in the total cellular mitochondrial volume, suggesting that mitoNEET plays critical roles in controlling mitochondrial homeostasis (Vernay et al., 2017). In adipocytes, mitoNEET reduces β-oxidation rates by inhibiting mitochondrial iron transport into the matrix. Interestingly, adipocyte-specific overexpression of mitoNEET driven by the *aP2* promoter enhances lipid uptake

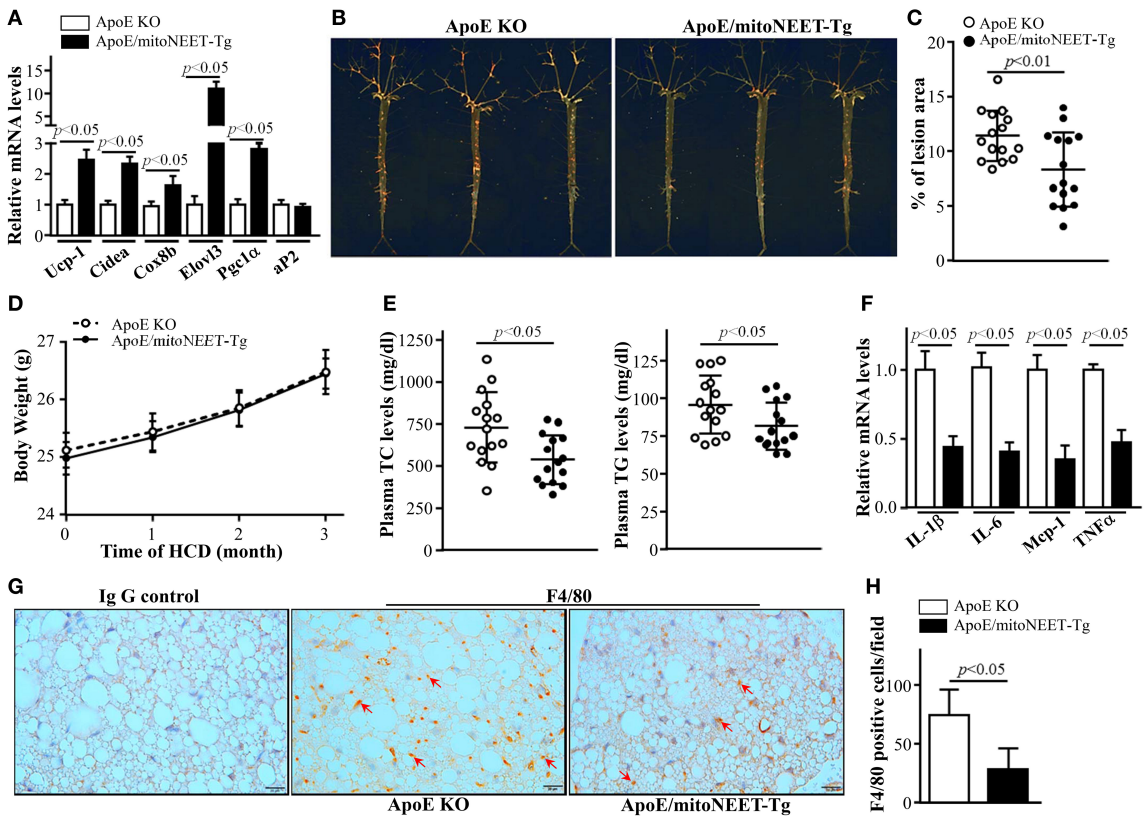

FIGURE 6 | Atherosclerosis in mitoNEET-Tg mice. Twelve-week-old ApoE KO and ApoE/mitoNEET-Tg mice were housed at and fed a high cholesterol diet (HCD) at 16°C for 3 months. **(A)** mRNA levels of thermogenesis genes in PVAT of mice at the end-point of the atherosclerosis study. Data shown are mean ± S.E.M. $n = 5$–6 in each group. **(B)** Representative Oil Red O staining showing atherosclerotic lesions in whole aortic trees. **(C)** Quantitative analysis of the ratio of atherosclerotic lesion area to total aortic tree area. Data shown are mean ± SD. $n = 15$ in each group. **(D)** Body weights of mice during mild cold challenge. Data shown are mean ± S.E.M. $n = 15$ in each group. **(E)** Plasma total cholesterol and triglyceride levels in ApoE knockout and ApoE/mitoNEET-Tg mice at the end-point of the HCD challenge at 16°C for 3 months. Data shown are mean ± SD. $n = 15$ in each group. **(F)** mRNA levels of inflammatory genes in PVAT of mice at the end-point of HCD challenge at 16°C for 3 months. Data shown are mean ± S.E.M. $n = 5$–6 in each group. **(G)** Macrophage infiltration detected by F4/80 staining (brown) in PVAT of mice at the end-point of HCD challenge at 16°C for 3 months. **(H)** Quantitative data of F4/80 positive cells in **(G)**. Data shown are mean ± SD. $n = 6$ in each group.

and leads to benign adipose tissue hyperplasia. Despite the severe obesity resulting from mitoNEET overexpression in ob/ob mice, the insulin sensitivity is preserved (Kusminski et al., 2012). Therefore, mitoNEET might be a potential therapeutic target for diabetes. Additionally, beside its positive impact on lipid and carbohydrate homeostasis by altering mitochondrial matrix iron metabolism, mitoNEET in subcutaneous WAT of mice upregulates a browning signature program (Kusminski et al., 2014). Recently, browning of WAT is passionately recognized as a new strategy for treatment of diabetes and CVDs. Importantly, we documented that mitoNEET is highly expressed in brown-like PVAT and BAT when compared to WAT. Cold exposure significantly increases mitoNEET expression in PVAT and BAT, but not in WAT and other mitochondria-rich organs such as skeletal muscle, heart and brain, suggesting that mitoNEET expression is highly and directly associated with thermogenesis in brown adipocytes. These findings are consistent with the possibility that PVAT could undergo heat generation upon cold stimulus and prompted our further characterization of the role of this gene in PVAT.

Impaired energy metabolism in the blood vessels is believed to be associated with atherogenesis (Mayr et al., 2005). Environmental temperature influences the energy metabolism in the body (Balogh et al., 1952). Even though exposure of mice to 4°C enhances thermogenesis, long-term (8 weeks) 4°C exposure promotes atherosclerotic plaque growth and instability due to Ucp1-dependent lipolysis of adipose tissues (Dong et al., 2013). On the other hand, as PVAT has a phenotype similar to BAT (Fitzgibbons et al., 2011; Chang et al., 2012b), the heat generation in PVAT is critical to the maintenance of intravascular temperature (Chang et al., 2012b). In humans, an intravascular temperature gradient exists, with the temperature increasing in large veins (surrounded by PVAT) as blood approaches the heart (Robinson, 1952), although it is not yet known if this function is associated with PVAT. We previously showed that, consistent with a potential activation of PVAT metabolism during cold-induced thermogenesis, the presence of PVAT in ApoE knockout mice on a high-fat diet and housed in a mild cold temperature (16°C) facility prevented atherosclerosis compared to mice housed at room temperature (22°C) (Chang et al., 2012b). PVAT-free mice housed in similar cold conditions did not have comparable reductions in atherosclerosis, underscoring the necessity of PVAT for this phenotype. Yet, the factors contributing to those phenotypes are still unknown. Here we found that overexpression of mitoNEET in PVAT up-regulates expression of thermogenic genes such as *Ucp-1*, *Cidea*, *Dio2* and *Pgc1α*, etc. in cold conditions. Consistently, mitoNEET-Tg mice (when the BAT was surgically removed) are cold tolerant, indicating that mitoNEET in PVAT contributes to thermogenesis. Indeed, in our study, we found that mitoNEET-Tg mice housed in 4°C environment increased systemic metabolic activity. Also, housing mitoNEET-Tg mice at 16°C for 3-months significantly reduced the development of atherosclerosis when compared with ApoE knockout mice. Importantly, plasma triglyceride levels in mitoNEET-Tg mice were reduced at 16°C, suggesting that the increased metabolic activity of PVAT in mitoNEET-Tg mice may result in increased lipid clearance from the vasculature, thereby contributing to reduced atherogenesis. Indeed, activation of BAT (Bartelt et al., 2011) and PVAT (Chang et al., 2012a) in rodents results in reduced plasma lipid levels. In humans, studies have reported that individuals living in cold climates have active BAT in the peri-aortic region of adults (van Marken Lichtenbelt et al., 2009). However, it is yet unclear if cold exposure in humans activates PVAT thermogenesis leading to protection from atherosclerosis. Exposure to both heat and cold are associated with increased incidences of mortality from heart attacks in humans (Taggart et al., 1972; Sheldahl et al., 1992) although we still need carefully-controlled epidemiological studies to determine if cold exposure is beneficial in preventing the development of atherosclerosis.

PVAT is closely involved in vascular inflammation. The PVAT-resident and -recruited inflammatory cells have been hypothesized to be responsible for vascular diseases (Okamoto et al., 2001). It is believed that the inflammatory response in the vasculature is a key step toward atherosclerosis. Indeed, high-fat diet feeding induces a pro-inflammatory phenotype in the PVAT of mice (Chatterjee et al., 2009). Actually, compared with subcutaneous and visceral adipose tissues, PVAT has less-differentiated adipocytes with more basal inflammatory signature, and lower expression of adiponectin and higher of inflammatory factors such as *IL-6*, *IL-8*, and *MCP-1* (Chatterjee et al., 2009). Indeed, accumulation of inflammatory cells in the PVAT in human atherosclerotic aortas indicates that PVAT recruits pro-inflammatory cells in atherogenesis and is primed for inflammatory responses (Henrichot et al., 2005). Transplant of pro-inflammatory visceral WAT results in atherosclerotic lesions and increased inflammatory markers, compared to transplantation of non-inflammatory subcutaneous WAT (Ohman et al., 2008, 2011). A postmortem study also found that the PVAT mass was positively correlated with atherosclerotic plaque size in atherosclerosis patients (Verhagen et al., 2012). Therefore, an inflammatory PVAT plays pro-atherosclerotic roles. Surprisingly, our data uncovered that expression of inflammatory factors such as *IL-6* and *Mcp-1* is reduced in PVAT of mitoNEET-Tg mice, suggesting an anti-inflammatory role for mitoNEET likely contributing further to the atheroprotective phenotype. Indeed, macrophage infiltration was reduced in the mitoNEET-Tg mice.

Taken together, our study demonstrates that mitoNEET in PVAT plays a key role in intravascular thermoregulation. mitoNEET in PVAT prevents temperature loss in the vasculature upon cold temperature challenge. Of great importance, we show that mitoNEET in PVAT reduces the burden of atherosclerosis, making it an attractive target for clinical intervention, and establishes the notion of a direct beneficial impact of mitoNEET in PVAT to reduce cardiovascular diseases.

AUTHOR CONTRIBUTIONS

WX, XZ, JZ, and LC designed and performed the experiments; JL provided Pgc1α and Pgc1β knockout mice; LC, YC, ZJ, analyzed the data; LC and MG-B wrote the paper.

FUNDING

This work was supported by NIH grants HL122664-01 (to LC), HL088391 (to YC), and the National Natural Science Foundation of China 81670429 (to ZJ).

SUPPLEMENTARY MATERIAL

The Supplementary Material for this article can be found online at: https://www.frontiersin.org/articles/10.3389/fphys.2017.01032/full#supplementary-material

Suppl. Figure I | *Pgc1*-associated genes and mitoNEET levels in different organs. **(A)** mRNA levels *Ckb, MacroD1, Fabp3, Idh2*, *and Klf2* in PVAT of *Pgc1α* KO and *Pgc1β* KO mice. The relative mRNA level of each gene was normalized by 18S, respectively. Data shown are mean ± SD. $n = 5$ mice/group. **(B)** Representative blot shows mitoNEET protein levels in PVAT, BAT, gWAT, skeletal muscle, heart and brain in 10-week old C57BL/6J mice which were housed at 22°C or 4°C for 24 h. Quantification of mitoNEET levels in each tissue, normalized by β-actin. mitoNEET level in each tissue at 22°C was set as 100%. Quantification for PVAT, BAT, and WAT was calculated from two independent blots, and muscle, heart and brain were from one blot. Data shown as mean ± S.E.M.

Suppl. Figure II | Brown adipocyte-specific mitoNEET overexpression mice. **(A)** Representative blot showing mitoNEET protein levels in adipose tissues in 10-week old wild type and mitoNEET-Tg mice. **(B)** Representative H.E. staining showing morphology of subcutaneous and gonadal BAT in 10-week old wild type and mitoNEET-Tg mice. Magnification bar = 20 μm.

Suppl. Figure III | Increased in thermogenesis-related genes in gWAT and PVAT of mitoNEET-Tg mice. **(A)** MitoNEET-Tg mice were housed at 16°C for 1-week. RT-PCR was used to determine the mRNA levels (relative to 18S) of thermogenesis-related genes in gonadal WAT. Data shown as mean ± SD. $n = 6$ mice/group. **(B)** MitoNEET-Tg mice from line #27 were housed at 16°C for 1-week. RT-PCR was used to determine the mRNA levels (relative to 18S) of thermogenesis-related genes in PVAT. Data shown as mean ± SD. $n = 6$ mice/group.

REFERENCES

Balogh, L., Donhoffer, S., Mestyan, G., Pap, T., and Toth, I. (1952). The effect of environmental temperature on the O2-consumption and body temperature of rats under the acute action of some drugs affecting energy exchange and body temperature. *Acta Physiol. Acad. Sci. Hung.* 3, 367–375.

Banerjee, S. S., Feinberg, M. W., Watanabe, M., Gray, S., Haspel, R. L., Denkinger, D. J., et al. (2003). The Kruppel-like factor KLF2 inhibits peroxisome proliferator-activated receptor-gamma expression and adipogenesis. *J. Biol. Chem.* 278, 2581–2584. doi: 10.1074/jbc.M210859200

Bartelt, A., Bruns, O. T., Reimer, R., Hohenberg, H., Ittrich, H., Peldschus, K., et al. (2011). Brown adipose tissue activity controls triglyceride clearance. *Nat. Med.* 17, 200–205. doi: 10.1038/nm.2297

Boden, G., Cheung, P., Mozzoli, M., and Fried, S. K. (2003). Effect of thiazolidinediones on glucose and fatty acid metabolism in patients with type 2 diabetes. *Metab. Clin. Exp.* 52, 753–759. doi: 10.1016/S0026-0495(03)00055-6

Chang, L., Garcia-Barrio, M. T., and Chen, Y. E. (2017). Brown adipose tissue, not just a heater. *Arterioscler. Thromb. Vasc. Biol.* 37, 389–391. doi: 10.1161/ATVBAHA.116.308909

Chang, L., Milton, H., Eitzman, D. T., and Chen, Y. E. (2012a). Paradoxical roles of perivascular adipose tissue in atherosclerosis and hypertension. *Circ. J.* 77, 11–18. doi: 10.1253/circj.CJ-12-1393

Chang, L., Villacorta, L., Li, R., Hamblin, M., Xu, W., Dou, C., et al. (2012b). Loss of perivascular adipose tissue on peroxisome proliferator-activated receptor-gamma deletion in smooth muscle cells impairs intravascular thermoregulation and enhances atherosclerosis. *Circulation* 126, 1067–1078. doi: 10.1161/CIRCULATIONAHA.112.104489

Chatterjee, T. K., Stoll, L. L., Denning, G. M., Harrelson, A., Blomkalns, A. L., Idelman, G., et al. (2009). Proinflammatory phenotype of perivascular adipocytes: influence of high-fat feeding. *Circ. Res.* 104, 541–549. doi: 10.1161/CIRCRESAHA.108.182998

Chen, D., Vollmar, M., Rossi, M. N., Phillips, C., Kraehenbuehl, R., Slade, D., et al. (2011). Identification of macrodomain proteins as novel O-acetyl-ADP-ribose deacetylases. *J. Biol. Chem.* 286, 13261–13271. doi: 10.1074/jbc.M110.206771

Cohen, P., Levy, J. D., Zhang, Y., Frontini, A., Kolodin, D. P., Svensson, K. J., et al. (2014). Ablation of PRDM16 and beige adipose causes metabolic dysfunction and a subcutaneous to visceral fat switch. *Cell* 156, 304–316. doi: 10.1016/j.cell.2013.12.021

Colca, J. R., McDonald, W. G., Waldon, D. J., Leone, J. W., Lull, J. M., Bannow, C. A., et al. (2004). Identification of a novel mitochondrial protein ("mitoNEET") cross-linked specifically by a thiazolidinedione photoprobe. *Am. J. Physiol. Endocrinol. Metab.* 286, E252–E260. doi: 10.1152/ajpendo.00424.2003

Dong, M., Yang, X., Lim, S., Cao, Z., Honek, J., Lu, H., et al. (2013). Cold exposure promotes atherosclerotic plaque growth and instability via UCP1-dependent lipolysis. *Cell Metab.* 18, 118–129. doi: 10.1016/j.cmet.2013.06.003

Enerback, S., Jacobsson, A., Simpson, E. M., Guerra, C., Yamashita, H., Harper, M. E., et al. (1997). Mice lacking mitochondrial uncoupling protein are cold-sensitive but not obese. *Nature* 387, 90–94. doi: 10.1038/387090a0

Fisher, F. M., Kleiner, S., Douris, N., Fox, E. C., Mepani, R. J., Verdeguer, F., et al. (2012). FGF21 regulates PGC-1alpha and browning of white adipose tissues in adaptive thermogenesis. *Genes Dev.* 26, 271–281. doi: 10.1101/gad.177857.111

Fitzgibbons, T. P., Kogan, S., Aouadi, M., Hendricks, G. M., Straubhaar, J., and Czech, M. P. (2011). Similarity of mouse perivascular and brown adipose tissues and their resistance to diet-induced inflammation. *Am. J. Physiol. Heart Circ. Physiol.* 301, H1425–H1437. doi: 10.1152/ajpheart.00376.2011

Hallakou, S., Doare, L., Foufelle, F., Kergoat, M., Guerre-Millo, M., Berthault, M. F., et al. (1997). Pioglitazone induces *in vivo* adipocyte differentiation in the obese Zucker fa/fa rat. *Diabetes* 46, 1393–1399. doi: 10.2337/diabetes.46.9.1393

Harashima, K., Hayashi, J., Miwa, T., and Tsunoda, T. (2009). Long-term pioglitazone therapy improves arterial stiffness in patients with type 2 diabetes mellitus. *Metab. Clin. Exp.* 58, 739–745. doi: 10.1016/j.metabol.2008.09.015

Henrichot, E., Juge-Aubry, C. E., Pernin, A., Pache, J. C., Velebit, V., Dayer, J. M., et al. (2005). Production of chemokines by perivascular adipose tissue: a role in the pathogenesis of atherosclerosis? *Arterioscler. Thromb. Vasc. Biol.* 25, 2594–2599. doi: 10.1161/01.ATV.0000188508.40052.35

Kadlec, A. O., Chabowski, D. S., Ait-Aissa, K., and Gutterman, D. D. (2016). Role of PGC-1alpha in vascular regulation: implications for atherosclerosis. *Arterioscler. Thromb. Vasc. Biol.* 36, 1467–1474. doi: 10.1161/ATVBAHA.116.307123

Kim, S., and Moustaid-Moussa, N. (2000). Secretory, endocrine and autocrine/paracrine function of the adipocyte. *J. Nutr.* 130, 3110S−3115S.

Kiyici, S., Ersoy, C., Kaderli, A., Fazlioglu, M., Budak, F., Duran, C., et al. (2009). Effect of rosiglitazone, metformin and medical nutrition treatment on arterial stiffness, serum MMP-9 and MCP-1 levels in drug naive type 2 diabetic patients. *Diabetes Res. Clin. Pract.* 86, 44–50. doi: 10.1016/j.diabres.2009.07.004

Kusminski, C. M., Holland, W. L., Sun, K., Park, J., Spurgin, S. B., Lin, Y., et al. (2012). MitoNEET-driven alterations in adipocyte mitochondrial activity reveal a crucial adaptive process that preserves insulin sensitivity in obesity. *Nat. Med.* 18, 1539–1549. doi: 10.1038/nm.2899

Kusminski, C. M., Park, J., and Scherer, P. E. (2014). MitoNEET-mediated effects on browning of white adipose tissue. *Nat. Commun.* 5:3962. doi: 10.1038/ncomms4962

Lee, S. J., Kim, S. H., Park, K. M., Lee, J. H., and Park, J. W. (2016). Increased obesity resistance and insulin sensitivity in mice lacking the isocitrate dehydrogenase 2 gene. *Free Radic. Biol. Med.* 99, 179–188. doi: 10.1016/j.freeradbiomed.2016.08.011

Lee, Y. H., Jung, Y. S., and Choi, D. (2014). Recent advance in brown adipose physiology and its therapeutic potential. *Exp. Mol. Med.* 46:e78. doi: 10.1038/emm.2013.163

Lelliott, C. J., Medina-Gomez, G., Petrovic, N., Kis, A., Feldmann, H. M., Bjursell, M., et al. (2006). Ablation of PGC-1beta results in defective mitochondrial

activity, thermogenesis, hepatic function, and cardiac performance. *PLoS Biol.* 4:e369. doi: 10.1371/journal.pbio.0040369

Mayr, M., Chung, Y. L., Mayr, U., Yin, X., Ly, L., Troy, H., et al. (2005). Proteomic and metabolomic analyses of atherosclerotic vessels from apolipoprotein E-deficient mice reveal alterations in inflammation, oxidative stress, and energy metabolism. *Arterioscler. Thromb. Vasc. Biol.* 25, 2135–2142. doi: 10.1161/01.ATV.0000183928.25844.f6

Nedergaard, J., Bengtsson, T., and Cannon, B. (2007). Unexpected evidence for active brown adipose tissue in adult humans. *Am. J. Physiol. Endocrinol. Metab.* 293, E444–E452. doi: 10.1152/ajpendo.00691.2006

Nedergaard, J., Bengtsson, T., and Cannon, B. (2010). Three years with adult human brown adipose tissue. *Ann. N.Y. Acad. Sci.* 1212, E20–E36. doi: 10.1111/j.1749-6632.2010.05905.x

Ohman, M. K., Luo, W., Wang, H., Guo, C., Abdallah, W., Russo, H. M., et al. (2011). Perivascular visceral adipose tissue induces atherosclerosis in apolipoprotein E deficient mice. *Atherosclerosis* 219, 33–39. doi: 10.1016/j.atherosclerosis.2011.07.012

Ohman, M. K., Shen, Y., Obimba, C. I., Wright, A. P., Warnock, M., Lawrence, D. A., et al. (2008). Visceral adipose tissue inflammation accelerates atherosclerosis in apolipoprotein E-deficient mice. *Circulation* 117, 798–805. doi: 10.1161/CIRCULATIONAHA.107.717595

Okamoto, E., Couse, T., De Leon, H., Vinten-Johansen, J., Goodman, R. B., Scott, N. A., et al. (2001). Perivascular inflammation after balloon angioplasty of porcine coronary arteries. *Circulation* 104, 2228–2235. doi: 10.1161/hc4301.097195

Okuno, A., Tamemoto, H., Tobe, K., Ueki, K., Mori, Y., Iwamoto, K., et al. (1998). Troglitazone increases the number of small adipocytes without the change of white adipose tissue mass in obese Zucker rats. *J. Clin. Invest.* 101, 1354–1361. doi: 10.1172/JCI1235

Puigserver, P., Wu, Z., Park, C. W., Graves, R., Wright, M., and Spiegelman, B. M. (1998). A cold-inducible coactivator of nuclear receptors linked to adaptive thermogenesis. *Cell* 92, 829–839. doi: 10.1016/S0092-8674(00)81410-5

Riachi, M., Himms-Hagen, J., and Harper, M. E. (2004). Percent relative cumulative frequency analysis in indirect calorimetry: application to studies of transgenic mice. *Can. J. Physiol. Pharmacol.* 82, 1075–1083. doi: 10.1139/y04-117

Robinson, S. (1952). Physiological effects of heat and cold. *Annu. Rev. Physiol.* 14, 73–96. doi: 10.1146/annurev.ph.14.030152.000445

Ruderman, N. B., Schneider, S. H., and Berchtold, P. (1981). The "metabolically-obese," normal-weight individual. *Am. J. Clin. Nutr.* 34, 1617–1621.

Ryan, K. E., McCance, D. R., Powell, L., McMahon, R., and Trimble, E. R. (2007). Fenofibrate and pioglitazone improve endothelial function and reduce arterial stiffness in obese glucose tolerant men. *Atherosclerosis* 194, e123–e130. doi: 10.1016/j.atherosclerosis.2006.11.007

Sheldahl, L. M., Wilke, N. A., Dougherty, S., and Tristani, F. E. (1992). Cardiac response to combined moderate heat and exercise in men with coronary artery disease. *Am. J. Cardiol.* 70, 186–191. doi: 10.1016/0002-9149(92)91273-7

Smith, R. E., and Horwitz, B. A. (1969). Brown fat and thermogenesis. *Physiol. Rev.* 49, 330–425.

Spiegelman, B. M. (2007a). Transcriptional control of energy homeostasis through the PGC1 coactivators. *Novartis Found. Symp.* 286, 3–6. discusssion: 6–12, 162–163, 196–203.

Spiegelman, B. M. (2007b). Transcriptional control of mitochondrial energy metabolism through the PGC1 coactivators. *Novartis Found. Symp.* 287, 60–63. discussion 63–69.

Sun, K., Kusminski, C. M., and Scherer, P. E. (2011). Adipose tissue remodeling and obesity. *J. Clin. Invest.* 121, 2094–2101. doi: 10.1172/JCI45887

Taggart, P., Parkinson, P., and Carruthers, M. (1972). Cardiac responses to thermal, physical, and emotional stress. *Br. Med. J.* 3, 71–76. doi: 10.1136/bmj.3.5818.71

Uldry, M., Yang, W., St-Pierre, J., Lin, J., Seale, P., and Spiegelman, B. M. (2006). Complementary action of the PGC-1 coactivators in mitochondrial biogenesis and brown fat differentiation. *Cell Metab.* 3, 333–341. doi: 10.1016/j.cmet.2006.04.002

Van der Zee, C. E. (2013). Hypothalamic plasticity of neuropeptide Y is lacking in brain-type creatine kinase double knockout mice with defective thermoregulation. *Eur. J. Pharmacol.* 719, 137–144. doi: 10.1016/j.ejphar.2013.07.027

van Marken Lichtenbelt, W. D., Vanhommerig, J. W., Smulders, N. M., Drossaerts, J. M., Kemerink, G. J., Bouvy, N. D., et al. (2009). Cold-activated brown adipose tissue in healthy men. *N. Engl. J. Med.* 360, 1500–1508. doi: 10.1056/NEJMoa0808718

Vergnes, L., Chin, R., Young, S. G., and Reue, K. (2011). Heart-type fatty acid-binding protein is essential for efficient brown adipose tissue fatty acid oxidation and cold tolerance. *J. Biol. Chem.* 286, 380–390. doi: 10.1074/jbc.M110.184754

Verhagen, S. N., Vink, A., van der Graaf, Y., and Visseren, F. L. (2012). Coronary perivascular adipose tissue characteristics are related to atherosclerotic plaque size and composition. A post-mortem study. *Atherosclerosis* 225, 99–104. doi: 10.1016/j.atherosclerosis.2012.08.031

Vernay, A., Marchetti, A., Sabra, A., Jauslin, T. N., Rosselin, M., Scherer, P. E., et al. (2017). MitoNEET-dependent formation of intermitochondrial junctions. *Proc. Natl. Acad. Sci. U.S.A.* 114, 8277–8282. doi: 10.1073/pnas.1706643114

Wiley, S. E., Murphy, A. N., Ross, S. A., van der Geer, P., and Dixon, J. E. (2007a). MitoNEET is an iron-containing outer mitochondrial membrane protein that regulates oxidative capacity. *Proc. Natl. Acad. Sci. U.S.A.* 104, 5318–5323. doi: 10.1073/pnas.0701078104

Wiley, S. E., Paddock, M. L., Abresch, E. C., Gross, L., van der Geer, P., Nechushtai, R., et al. (2007b). The outer mitochondrial membrane protein mitoNEET contains a novel redox-active 2Fe-2S cluster. *J. Biol. Chem.* 282, 23745–23749. doi: 10.1074/jbc.C700107200

Wu, J., Bostrom, P., Sparks, L. M., Ye, L., Choi, J. H., Giang, A. H., et al. (2012). Beige adipocytes are a distinct type of thermogenic fat cell in mouse and human. *Cell* 150, 366–376. doi: 10.1016/j.cell.2012.05.016

Yu, J., Jin, N., Wang, G., Zhang, F., Mao, J., and Wang, X. (2007). Peroxisome proliferator-activated receptor gamma agonist improves arterial stiffness in patients with type 2 diabetes mellitus and coronary artery disease. *Metab. Clin. Exp.* 56, 1396–1401. doi: 10.1016/j.metabol.2007.05.011

Zhang, Y., Li, R., Meng, Y., Li, S., Donelan, W., Zhao, Y., et al. (2014). Irisin stimulates browning of white adipocytes through mitogen-activated protein kinase p38 MAP kinase and ERK MAP kinase signaling. *Diabetes* 63, 514–525. doi: 10.2337/db13-1106

Conflict of Interest Statement: The authors declare that the research was conducted in the absence of any commercial or financial relationships that could be construed as a potential conflict of interest.

frontiers in Physiology

OPINION
published: 04 December 2017
doi: 10.3389/fphys.2017.00990

Accuracy and Artistry in Anatomical Illustration of Perivascular Adipose Tissue

Caroline M. Pond [1, 2*]

[1] School of Life, Health and Chemical Sciences, The Open University, Milton Keynes, United Kingdom, [2] Department of Zoology, Oxford University, Oxford, United Kingdom

Keywords: Rembrandt, Leonardo da Vinci, Vesalius, anatomy tables, blood vessels, lymph nodes and vessels, site-specific properties, paracrine interactions

Research into the physiology and evolution of perivascular adipose tissue was delayed until the 1990s because the subtle influence of anatomical illustrations misled biologists.

Leonardo da Vinci's magnificent drawings, based on dissections of up to 300 human and animal cadavers, started a fashion for gross anatomy as fine art (Kemp, 2010). The many hitherto unknown details thus displayed were admired by sixteenth century cognoscenti throughout Western Europe. They presented anatomy as functional, orderly, and rational, in keeping with Renaissance values, but did not include adipose tissue around vessels or muscles (**Figure 1A**). Thirty years later, Vesalius studied the internal anatomy, particularly vascular systems (Vesalius, 1543), of mostly young, mostly male criminals, many executed after a period of imprisonment or other deprivation. Such subjects were probably lean, perhaps emaciated, so it is easy to understand why the spectacular and, in most respects, impressively accurate illustrations of his research followed da Vinci's habit of omitting adipose tissue (**Figure 1B**), promoting artistic clarity over biological accuracy.

A century after Vesalius, professional anatomists habitually improved the clarity of drawings and models by showing "important structures" dissected "free" from associated tissues. Ever more ingenious and expensive forms of anatomical illustration were developed for the amusement and erudition of wealthy intellectuals, including wooden boards to which preserved human veins, arteries, and nerves were affixed in their natural configuration (**Figure 1C**). By the seventeenth century, such anatomy tables were not only studied by scientists and physicians but became fashionable as curiosities (Kemp, 2010), especially in Italy. The diarist, traveler and gardener John Evelyn purchased a set in 1646 from Padua University dissectors, and brought them to London, where they were held privately for 150 years before being donated to a medical institution.

The production and display of anatomy tables had little impact on practical surgery (Kemp, 2010), which was still mainly a skill acquired through apprenticeship and experience with only a smattering of formal education. Much of the information they conveyed was irrelevant to their work that was, until anesthetics and antiseptics were invented two centuries later, mostly on limbs and superficial tissues. Opening the trunk was too dangerous, so surgeons were not concerned with the thoracic and abdominal vessels that were the most challenging to prepare and thus most impressive to artists and intellectuals.

While such anatomical illustration prevailed, a young painter struggling to gain status in Amsterdam's competitive art market depicted the tissues of the human arm as they really are (**Figure 1E**). In Rembrandt's 1,632 masterpiece, the "white" adipose tissue is yellow, as it always is in people (and other terrestrial vertebrates) whose diet is rich in carotenes, non-digestible plant pigments abundant in buttercup, dandelion etc. The color indicates that Adriaen Adriaenszoon's criminal career had been lucrative enough to provide plenty of carotene-rich beef, butter, and eggs, and that incarceration on a prison diet of bread and herring heads had not lasted long enough for significant depletion of his storage lipids. That artistic observation triumphed over contemporary conventions to produce a lesson in anatomical accuracy is sobering for all physicians and scientists.

OPEN ACCESS

Edited by:
Maik Gollasch, Charité Universitätsmedizin Berlin, Germany

Reviewed by:
María S. Fernández-Alfonso, Complutense University of Madrid, Spain
Dmitry Tsvetkov, Universität Tübingen, Germany

***Correspondence:**
Caroline M. Pond
c.m.pond@open.ac.uk

Specialty section:
This article was submitted to Vascular Physiology, a section of the journal Frontiers in Physiology

Received: *19 September 2017*
Accepted: *17 November 2017*
Published: *04 December 2017*

Citation:
Pond CM (2017) Accuracy and Artistry in Anatomical Illustration of Perivascular Adipose Tissue. Front. Physiol. 8:990. doi: 10.3389/fphys.2017.00990

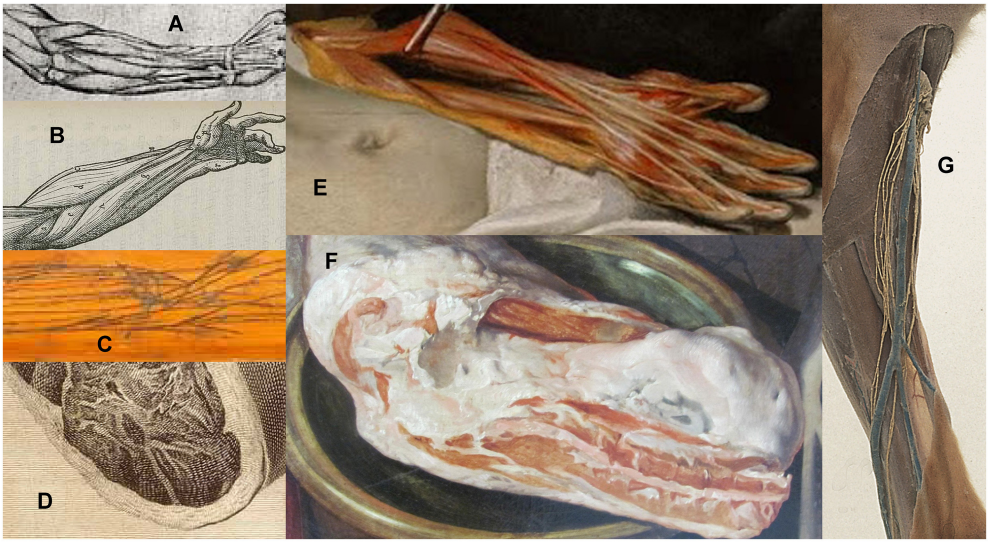

FIGURE 1 | "White" adipose tissue: omitted from human forearm by **(A)** Leonardo da Vinci, c. 1510, **(B)** Vesalius 1543, **(C)** anatomy table; depicted in details from **(D)** woman's thigh in Plate VI, van Riemsdyk (Hunter, 1774), **(E)** man's arm in *The Anatomy Lesson of Dr. Nicolaes Tulp*, Rembrandt 1632, **(F)** pork in *The Four Elements: Fire*, Beuckelaer 1570. **(G)** prosection showing dog popliteal lymphatics and blood vessels (Royal College of Surgeons, $C19th).

Another century of advances in science and artistic realism are evident in the gynecological illustrations created by Jan van Riemsdyk for the Scottish physician and researcher, Hunter (1774). They were less coy about showing superficial and even intermuscular adipose tissue (**Figure 1D**) in the abdomen and thighs of their young female subjects, in whom these depots are always present, sometimes massive, but not on vessels.

Although adipose tissue on animal carcasses featured widely, and accurately, in paintings from the sixteenth century onwards (**Figure 1F**), human and comparative anatomists still regarded it as too inconsistent and inconsequential to be worthy of topographic, functional or evolutionary study. It was always dissected off vessels and lymph nodes in pickled prosections (**Figure 1G**). Illustrations in all editions of *Grey's Anatomy* from 1858 until the 1970s omit adipose tissue, though its presence is sometimes mentioned briefly in the text [Grey, 1901 (reprinted 1974)]. The artist and comparative anatomist Edwin Goodrich excluded it entirely from all his precise, detailed drawings (Goodrich, 1930). Even the modern popular presenter of anatomy, Gunther von Hagens, dissects off all adipose tissue before plastination.

These illustrators' intentions were reasonable: perivascular adipose tissue obscures anatomists' view of the vasculature. But its absence subliminally suggests that the heart, blood, and lymph vessels should be neatly sheathed in "tunics" not clad in "adventitious" adipose tissue that is at best irrelevant to vascular function, perhaps aberrant or detrimental. Microscopy using histological procedures that dissolve lipids, leaving "empty" adipocytes, further promoted the concept of "walls" around all but the smallest blood vessels and implied that all adipocytes are similar, without site-specific properties or interactions with contiguous tissues.

By the 1990s, the biochemical diversity of mammalian adipose tissues was recognized, including endocrine signaling, cytokine synthesis and reception, thermogenesis, fatty acid sorting as well as lipid storage (Pond, 2017). Studies of lymph nodes in neonatal guinea-pigs (Gyllensten, 1950) noted that they attach firmly to the surrounding adipose tissue early in development, but functional interpretation of adipocytes' anatomical relations was delayed until paracrine interactions with blood vessels (Soltis and Cassis, 1991) and lymph nodes (Pond and Mattacks, 1995, 1998) and vessels (Dixon, 2010) were demonstrated.

Paracrine interactions and diverse site-specific properties of adipose tissue were an important evolutionary advance that appeared early in mammalian evolution (Pond, 2003), facilitating the integration of competing metabolic demands of exercise, thermogenesis, efficient digestive and immune systems, and lactation (Pond, 2017). By explaining the molecular mechanisms involved, this Frontiers Research Topic should remedy the anatomists' oversight.

AUTHOR CONTRIBUTIONS

The author confirms being the sole contributor of this work and approved it for publication.

REFERENCES

Dixon, J. B. (2010). Lymphatic lipid transport: sewer or subway. *Trends Endocrinol. Metab*. 21, 480–487. doi: 10.1016/j.tem.2010.04.003

Goodrich, E. S. (1930). *Studies on the Structure and Development of Vertebrates*. London: Macmillan.

Grey, H. (1901 reprinted 1974). *Anatomy, Descriptive and Surgical*. Philadelphia, PA: Running Press.

Gyllensten, L. (1950). The postnatal histogenesis of the lymphatic system of guinea-pigs. *Acta Anat*. 10, 130–160. doi: 10.1159/000140458

Hunter, W. (1774). *Anatomia Humani Gravidi Uteri (Anatomy of the Human Gravid Uterus Exhibited in Figures)*. Birmingham: John Baskerville.

Kemp, M. (2010). Style and non-style in anatomical illustration: from renaissance humanism to Henry Gray. *J. Anat*. 216, 192–208. doi: 10.1111/j.1469-7580.2009.01181.x

Pond, C. M. (2003). Paracrine interactions of mammalian adipose tissue. *J. Exp. Zool*. 295A, 99–110. doi: 10.1002/jez.a.10215

Pond, C. M. (2017). "The evolution of mammalian adipose tissues," In *Adipose Tissue Biology*, ed M. E. Symonds (New York, NY; Heidelberg: Springer Science) 1–59.

Pond, C. M., and Mattacks, C. A. (1995). Interactions between adipose tissue around lymph nodes and lymphoid cells *in vitro*. *J. Lipid Res*. 36, 2219–2231.

Pond, C. M., and Mattacks, C. A. (1998). *In vivo* evidence for the involvement of the adipose tissue surrounding lymph nodes in immune responses. *Immunol. Lett*. 63, 159–167. doi: 10.1016/S0165-2478(98)00074-1

Soltis, E. E., and Cassis, L. A. (1991). Influence of perivascular adipose tissue on rat aortic smooth muscle responsiveness. *Clin. Exp. Hypertens. A* 13, 277–296. doi: 10.3109/10641969109042063

Vesalius, A. (1543). *De Humani Corporis Fabrica Libri Septem (On the Fabric of the Human Body in Seven Books)*. Padua: School of Medicine.

Conflict of Interest Statement: The author declares that the research was conducted in the absence of any commercial or financial relationships that could be construed as a potential conflict of interest.

frontiers in Physiology

REVIEW
published: 28 November 2017
doi: 10.3389/fphys.2017.00969

The Role of Perivascular Adipose Tissue in Non-atherosclerotic Vascular Disease

*Tetsuo Horimatsu, Ha Won Kim and Neal L. Weintraub**

Division of Cardiology, Department of Medicine, Vascular Biology Center, Medical College of Georgia at Augusta University, Augusta, GA, United States

Perivascular adipose tissue (PVAT) surrounds most large blood vessels and plays an important role in vascular homeostasis. PVAT releases various chemokines and adipocytokines, functioning in an endocrine and paracrine manner to regulate vascular signaling and inflammation. Mounting evidence suggests that PVAT plays an important role in atherosclerosis and hypertension; however, the role of PVAT in non-atherosclerotic vascular diseases, including neointimal formation, aortic aneurysm, arterial stiffness and vasculitis, has received far less attention. Increasing evidence suggests that PVAT responds to mechanical endovascular injury and regulates the subsequent formation of neointima via factors that promote smooth muscle cell growth, adventitial inflammation and neovascularization. Circumstantial evidence also links PVAT to the pathogenesis of aortic aneurysms and vasculitic syndromes, such as Takayasu's arteritis, where infiltration and migration of inflammatory cells from PVAT into the vascular wall may play a contributory role. Moreover, in obesity, PVAT has been implicated to promote stiffness of elastic arteries via the production of reactive oxygen species. This review will discuss the growing body of data and mechanisms linking PVAT to the pathogenesis of non-atherosclerotic vascular diseases in experimental animal models and in humans.

Keywords: perivascular adipose tissue, neointimal formation, aortic aneurysm, arterial stiffness, vasculitis

OPEN ACCESS

Edited by:
Luis A. Martinez-Lemus, University of Missouri, United States

Reviewed by:
Jaume Padilla, University of Missouri, United States
Anthony Michael Heagerty, University of Manchester, United Kingdom

****Correspondence:***
Neal L. Weintraub
nweintraub@augusta.edu

Specialty section:
This article was submitted to Vascular Physiology, a section of the journal Frontiers in Physiology

Received: *27 September 2017*
Accepted: *14 November 2017*
Published: *28 November 2017*

Citation:
Horimatsu T, Kim HW and Weintraub NL (2017) The Role of Perivascular Adipose Tissue in Non-atherosclerotic Vascular Disease. Front. Physiol. 8:969. doi: 10.3389/fphys.2017.00969

KEY CONCEPTS

- Accumulating data suggest that PVAT plays an important role not only in atherosclerosis and hypertension, but also in non-atherosclerotic vascular diseases.
- Phenotypic changes in PVAT after vascular injury promote release of adipocytokines that can regulate inflammation, VSMC proliferation and neovascularization, thereby contributing to neointimal formation.
- Phenotypic changes in PVAT in response to high fat diet or smoking may promote vascular inflammation, ROS production, VSMC phenotype switching and matrix degradation to augment AAA formation.
- Inflamed PVAT is associated with arterial stiffness and vasculitis; however, direct evidence of a pathologic role of PVAT is lacking.
- Much of the available data linking PVAT to non-atherosclerotic vascular diseases is associative rather than direct in nature due to the challenges in developing specific experimental models to test the impact of PVAT on these disease states.

INTRODUCTION

Perivascular (PV) adipose tissue (PVAT) surrounds most large blood vessels except the cerebral vasculature, juxtaposed to the vascular adventitia and devoid of an anatomical barrier. The absence of an anatomic barrier suggests that mediators such as adipokines and cytokines released from PVAT can readily gain access into the blood vessel wall. Traditionally, PVAT had been thought to simply provide structural support for blood vessels; however, over the past two decades, it has become recognized as a physiologically and metabolically active endocrine tissue with important effects on vascular function and disease (Verhagen and Visseren, 2011; Fitzgibbons and Czech, 2014).

The bulk of adipose tissue present in adult animals is white adipose tissue (WAT) contained in visceral and subcutaneous depots, which is designed for energy storage and mobilization. By contrast, depending on the anatomic location, PVAT exhibits features of both white and brown adipose tissue (BAT), the latter of which is specialized for thermogenic energy expenditure (Brown et al., 2014). Mature adipocytes within visceral and subcutaneous adipose depots are thought to originate from precursor cells with distinct embryologic lineages (Tchkonia et al., 2007), and PV adipocytes may be distinct from other adipocytes by virture of their putative origin from vascular smooth muscle cell (VSMC) progenitors (Cai et al., 2011; Chang et al., 2012). Although adult human coronary PVAT exhibits the morphology of WAT, the PV adipocytes contained in this depot are more heterogeneous in shape and smaller in size and exhibit a reduced state of adipogenic differentiation as compared with adipocytes residing in subcutaneous and perirenal adipose depots derived from the same subjects (Chatterjee et al., 2009). Like other adipose tissues, human coronary PVAT secretes both pro-inflammatory and anti-inflammatory adipocytokines and chemokines; however, the balance is strongly shifted toward inflammation via elevated secretion of cytokines such as interleukin (IL)-6, IL-8, and in particular, monocyte chemoattractant protein (MCP)-1, concomitant with reduced secretion of anti-inflammatory adiponectin (Chatterjee et al., 2009). In rodents, the gene expression profile of thoracic aortic PVAT is similar to that of BAT (Fitzgibbons et al., 2011; Padilla et al., 2013), while PVAT surrounding the abdominal aorta contains a mixture of WAT and BAT; in contrast, mesenteric, carotid, and femoral PVAT exhibit a purely WAT phenotype. These findings suggest that PVAT exhibits considerable phenotypic heterogeneity depending on its anatomic location.

Given these unique features of PV adipocytes and PVAT, there is great interest in understanding their role in vascular function and disease. In animal models, PVAT has been reported to possess both protective and detrimental effects on vascular function, depending on the experimental model and associated pathological states such as obesity and metabolic disease, which impact the production and/or bioactivity of vasoactive factors and inflammatory mediators. Mounting evidence also suggests that dysfunctional PVAT plays an important role in atherosclerosis and hypertension, in part by promoting insulin resistance and metabolic disease (Eringa et al., 2007). On the other hand, the brown-like function of PVAT can elicit favorable metabolic effects associated with non-shivering thermogenesis and combustion of fatty acids to ameliorate atherosclerosis (Chang et al., 2012). Recent emerging data suggest that PVAT may also modulate non-atherosclerotic vascular diseases, including neointimal formation, aortic aneurysm, arterial stiffness and vasculitis. It is important to point out that much of the available data in non-atherosclerotic diseases is associative rather than direct in nature due to the challenges in developing specific experimental models to test the impact of PVAT on these disease states. This article will review the available evidence and putative mechanisms linking PVAT and non-atherosclerotic vascular diseases.

PVAT AND NEOINTIMAL FORMATION

Pathogenesis of Neointimal Formation

Neointimal formation is initiated by mechanical injury to the arterial endothelium, followed by local inflammatory cell recruitment, production of chemokines and growth factors that promote migration of VSMCs and adventitial fibroblasts into the intimal layer, and neovascularization (Goel et al., 2012). VSMCs robustly proliferate in the intima and deposit extracellular matrix, in a process analogous to scar formation. PVAT releases a variety of adipokines and cytokines that potentially can regulate multiple steps of neointimal formation. In lean mice, adiponectin produced by PVAT exerts anti-inflammatory effects to attenuate neointimal formation (Matsuda et al., 2002). In contrast, Wang et al. reported that visfatin, a PVAT-produced adipocytokine with important effects on glucose metabolism, stimulates VSMC proliferation (Wang et al., 2009). Leptin is an adipocyte-derived hormone with pro-inflammatory effects whose expression in PVAT is increased in obesity. Using an adenoviral vector, Schroeter et al. locally overexpressed leptin in the carotid artery after vascular injury and detected a significant increase in luminal stenosis and the intima-to-media ratio (serum leptin levels were similar among the groups) (Schroeter et al., 2013). The investigators further demonstrated that recombinant human leptin significantly increased VSMC proliferation *in vitro*, suggesting that PVAT could promote neointimal formation through local leptin production. PVAT-derived leptin was also associated with VSMC phenotypic switching to a synthetic phenotype via activation of the p38 mitogen-activated protein kinase (MAPK) signaling pathway (Shin et al., 2005; Li et al., 2014). Like leptin, expression of the pro-inflammatory chemokine MCP-1 is upregulated in PVAT in obesity, and MCP-1 also promotes VSMC proliferation (Aiello et al., 1999). The role of MCP-1 released from PVAT in neointimal formation will be discussed in depth in section Experimental Evidence Demonstrating That PVAT Can Modulate Neointimal Formation.

Endothelial dysfunction is associated with reduced nitric oxide (NO) production through impaired endothelial NO synthase (eNOS) activity, and eNOS gene deletion promoted inward vascular remodeling and enhanced neointimal formation after external carotid artery ligation (Rudic et al., 1998). Furthermore, eNOS deletion induced the expression of stromal

cell-derived factor-1α, which plays an important role in recruitment of VSMC progenitor cells into the neointima (Zhang et al., 2006). PVAT was reported to induce endothelial dysfunction via protein kinase C-β dependent phosphorylation and inactivation of eNOS (Payne et al., 2009). PVAT also may inhibit endothelial NO production through increased expression of caveolin-1, which negatively regulates eNOS via interruption of calcium/calmodulin signaling (Lee et al., 2014). These data suggest that PVAT can promote endothelial dysfunction by impaired NO signaling, thus contributing to neointimal formation.

Adventitial fibroblasts and myofibroblasts directly migrate into the arterial neointima after endovascular injury. Ruan et al. investigated the role of PVAT-derived factors in the regulation of adventitial fibroblast activation and demonstrated that PVAT-derived complement 3 is required for adventitial fibroblast migration and adventitial remodeling in deoxycorticosterone acetate-salt hypertensive rats (Ruan et al., 2010). This suggests an important role of PVAT in promoting fibroblast activation and migration during neointimal formation.

Adventitial neovascularization is associated with vascular restenosis after balloon arterial injury. These neovessels can serve as conduits for inflammatory cell trafficking into the injured blood vessel, and rupture of the neovessels can potentially promote intraplaque hemorrhage leading to acute vascular occlusion (Chen et al., 2016). Human coronary PV adipocytes were demonstrated to secrete higher levels of biologically active pro-angiogenic factors than subcutaneous adipocytes, suggesting a potential role in regulating neovascularization following vascular injury (Chatterjee et al., 2013). Indeed, PV transplantation of epididymal adipose tissue to the ligated carotid artery in mice resulted in a 3 fold increase in *vasa vasorum* density, implying a potential role for PVAT in promoting plaque neovascularization (Tanaka et al., 2015). In humans, the release of pro-angiogenic vascular endothelial growth factor (VEGF) from PVAT of type 2 diabetics was significantly higher than that from PVAT of non-diabetic subjects or from subcutaneous adipose tissue of diabetics (Schlich et al., 2013). Moreover, conditioned medium from PVAT of type 2 diabetic patients induced potent effects on VSMC proliferation, suggesting that dysfunctional PVAT could play an important role in promoting both neovascularization and vascular restenosis in diabetic patients.

Effects of Mechanical Injury on PVAT

While endovascular injury originates in the endothelium, its impact is felt throughout the blood vessel wall, including the adventitia and PV adipocytes. Indeed, mechanical arterial injury induces histological and phenotypic changes locally in PVAT surrounding the injured artery (Okamoto et al., 2001; Rajsheker et al., 2010; Takaoka et al., 2010). Inflammatory leukocytes were detected in PVAT just 1 day after balloon injury in pig coronary arteries, and mRNA expression of vascular cell adhesion molecule (VCAM)-1 was increased in PVAT at 3 days after injury (Okamoto et al., 2001). In the rat wire injury model, F4/80-positive macrophages and CD3-positive T cells were observed to accumulate in PVAT after endovascular injury. In addition, MCP-1 and IL-6 were upregulated in PVAT 1 day after endovascular injury, which was attenuated in tumor necrosis factor (TNF)-α knockout mice (Takaoka et al., 2010), suggesting that mechanical vascular injury is associated with activation of discreet inflammatory pathways in PVAT.

Interestingly, inflammatory changes in PVAT in humans may be detectable using computerized tomography (CT) imaging (Antonopoulos et al., 2017). In this study, the authors demonstrated that the degree of coronary PVAT inflammation correlated with the fat attenuation index (FAI), reflecting changes in the balance between lipid and aqueous phase due to alterations in adipocyte size and lipid content. FAI in PVAT distinguished vulnerable atheromatous plaques causing acute myocardial infarction from stable or previously stented plaques. These findings suggest that biological and phenotypic characteristics of PVAT can change dynamically in response to spontaneous lesion destabilization and mechanical injury. Moreover, PV FAI may be a promising noninvasive method to dynamically monitor vascular inflammation and the extent of underlying vascular disease.

Caveats Associated with Experimental Models Employed to Test the Role of PVAT in Neointimal Formation

To test the role of PVAT in vascular disease, animal models that spontaneously lack PVAT merit consideration, including the A-ZIP/F-1 mouse, the FATATTAC mouse, and the SMPG knockout mouse (Moitra et al., 1998; Pajvani et al., 2005; Chang et al., 2012). Amongst these models, only the SMPG knockout mouse (generated by breeding PPARγ-floxed mice with SM22α-Cre mice) is selectively devoid of PVAT rather than generally lipodystrophic. However, loss of PPARγ expression in VSMCs in these mice may complicate the vascular phenotype (Chang et al., 2012). Surgical models involving removal of endogenous PVAT and/or transplantation of adipose tissue to the arterial wall have also been developed (Takaoka et al., 2009; Öhman et al., 2011; Tian et al., 2013). However, these surgical models pose major technical challenges given the minute size of this adipose depot in mice, the potential for non-specific arterial injury, and/or confounding systemic metabolic effects if a large enough quantity of fat is transplanted. Moreover, most studies have transplanted subcutaneous or epididymal fat, which differs phenotypically from PVAT, to the vascular wall (Takaoka et al., 2009; Öhman et al., 2011; Tian et al., 2013). These technical and methodological nuances must be carefully considered when drawing conclusions from experimental studies probing the role of PVAT in neointimal hyperplasia and other vascular diseases.

Experimental Evidence Demonstrating That PVAT Can Modulate Neointimal Formation

The impact of adipose tissue removal and transplantation on neointimal formation has been examined in experimental animal models using either PVAT (directly) or subcutaneous/visceral adipose tissue (indirectly). Takaoka et al. investigated the impact of diet-induced obesity on inflammatory responses in PVAT and

its subsequent role in the development of neointimal formation (Takaoka et al., 2009). The investigators performed femoral wire injury in mice in the presence or absence of endogenous PVAT. Then, 10 mg of visceral (epididymal) or subcutaneous fat tissue was harvested from wild-type mice fed a chow diet or high fat/high sucrose diet and transplanted around the wire-injured femoral artery. Notably, removal of PVAT enhanced neointimal formation after vascular wire injury, which was attenuated by transplantation of subcutaneous adipose tissue from mice fed a normal chow diet. Transplanting subcutaneous adipose tissue from adiponectin-deficient mice significantly enhanced lesion formation, which was abrogated by local application of recombinant adiponectin to the periadventitial area (Matsuda et al., 2002). In contrast, transplanting epididymal fat, or subcutaneous fat from mice fed a high fat/high sucrose diet, failed to attenuate neointimal formation. These data suggest that periadventitial fat can protect against neointimal formation after angioplasty under physiological conditions through production of adiponectin; the extent to which surgical manipulation vs. removal of PVAT *per se* augmented wire injury, however, is unclear.

Tian et al. reported that PVAT-derived angiopoietin-like protein (Angptl) 2, an adipose tissue-derived pro-inflammatory factor, augments neointimal formation after endovascular injury (Tian et al., 2013). In this study, 10 mg of epididymal adipose tissue was harvested from Angptl2 knockout mice or wild-type mice and transplanted around the wire-injured femoral arteries (note that the expression of Angptl2 in visceral adipose tissue was reportedly comparable with that in PVAT surrounding the femoral artery). Compared with transplantation of adipose tissue from wild-type mice, transplantation of adipose tissue from Angptl2-deficient mice led to decreased neointimal formation following endovascular injury. Expression of TNF-α and IL-1β in adipose tissue from Angptl2 knockout mice was significantly decreased, in conjunction with fewer accumulating macrophages. In addition, vascular matrix metalloproteinase (MMP)-2 activity was diminished by transplanting adipose tissue from Angptl2 knockout mice. Conversely, transplantation of visceral adipose tissue harvested from transgenic mice overexpressing Angptl2 aggravated neointimal formation in response to endovascular injury, in conjunction with increased inflammatory marker expression and MMP-2 activity. While these findings suggest that Angptl2 expression in transplanted PVAT promotes neointimal formation by augmenting adipose tissue inflammation and extracellular matrix degradation, the transplanted adipose tissues were subcutaneous or visceral in origin, and thus may not directly inform the role of PVAT.

Manka et al. provided direct evidence that PVAT contributes to the vascular response to wire injury, at least in part through an MCP-1-dependent mechanism (Manka et al., 2014). Transplanting PVAT (2-3 mg) from wild-type mice to the carotid artery (which is normally devoid of PVAT) exacerbated neointimal formation following wire injury. The transplanted PVAT augmented accumulation of VSMCs in the neointima and promoted adventitial inflammation and angiogenesis. Notably, transplantation of subcutaneous adipose tissue had no effect in this model. Interestingly, the enhanced neointimal formation and adventitial angiogenesis, but not the adventitial inflammation, were prevented by transplanting PVAT from MCP-1 knockout mice. These findings imply an important role for MCP-1 produced by PVAT in neointimal formation and suggest that molecular imaging of MCP-1 in PVAT could be a promising strategy to quantify the risk of restenosis following arterial injury. Moreover, therapeutically targeting MCP-1 in PVAT might be an effective strategy to prevent restenosis in selected patients.

Summary of the Role of PVAT in Neointimal Formation

PVAT can modulate numerous pathways linked to the pathogenesis of neointimal formation (**Figure 1**). Accumulating data suggest that phenotypic changes in PVAT occur soon after vascular injury, thereby leading to changes in expression and release of various inflammatory chemokines, cytokines and adipokines that can regulate inflammation, VSMC proliferation, neovascularization, etc. Experimental approaches employing PVAT removal and/or adipose tissue transplantation *in vivo* have been developed to directly or indirectly examine the role of PVAT in neointimal formation. The available data suggest that PVAT can either modulate or mediate neointimal formation, depending on the particular model and underlying metabolic state. However, the current experimental models are technically challenging and have limitations, so our understanding of the role of PVAT in regulating neointimal formation remains incomplete.

PVAT AND AORTIC ANEURYSM

Pathogenesis of Abdominal Aortic Aneurysms (AAAs)

AAAs account for over 13,000 deaths annually in the United States and about 25,000 AAA repairs are performed each year (Thompson, 2002). Only ∼25% of patients with aortic rupture survive to surgery, with an additional 50% mortality following surgery (Lederle et al., 2002). AAAs are characterized by localized structural deterioration of the aortic wall, leading to progressive aortic dilation and rupture. Key pathological features of AAAs include pronounced inflammatory cell infiltration, oxidative stress, MMP activation, and VSMC apoptosis and phenotype switching, which cumulatively lead to degradation of extracellular matrix, loss of structural integrity, and weakening of the aortic wall (Kuivaniemi et al., 2015). The inflammation in AAAs extends throughout the vessel wall to the adventitia, which has raised interest in the potential role of PVAT in AAA pathogenesis. Smoking, the most significant risk factor for AAAs (Vardulaki et al., 2000), has been shown to accentuate the pro-inflammatory status of PVAT by enhancing expression and activity of the $P2X_7R$-inflammasome complex (Rossi et al., 2014). Wang et al. investigated the levels of inflammatory adipokines produced by PVAT-derived mature adipocytes cultured alone or under nicotine stimulation. Nicotine reduced adiponectin secretion while activating pro-inflammatory nuclear factor (NF)-kB and pro-inflammatory cytokine expression (Wang

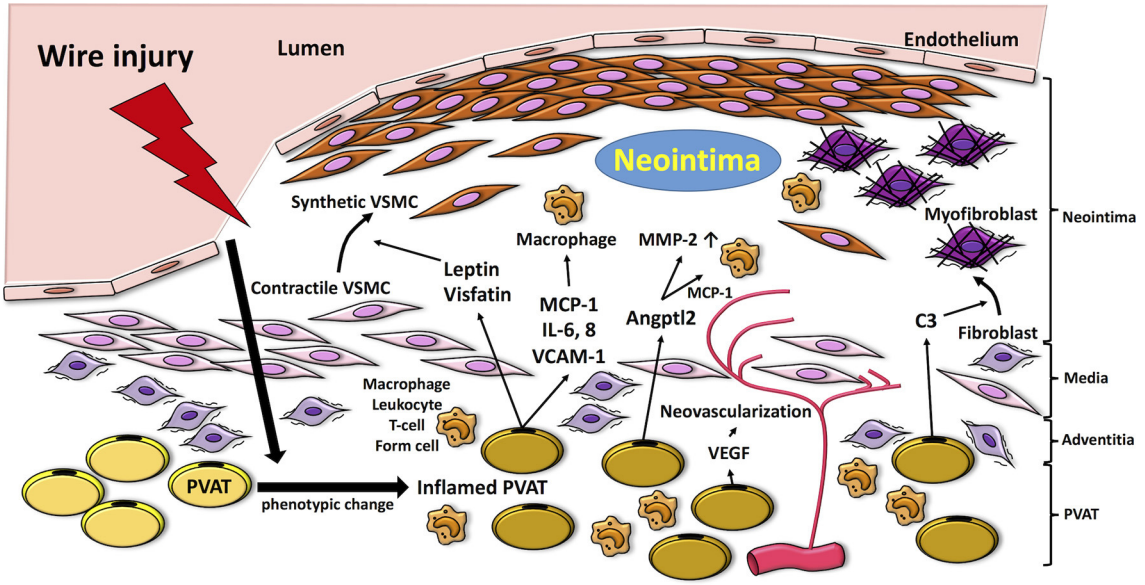

FIGURE 1 | Proposed mechanisms by which PVAT modulates pathways linked to the pathogenesis of neointimal formation. Vascular injury induces inflammation in PVAT, which produces adipocytokines such as MCP-1, IL-6, and VCAM-1 and fosters recruitment of inflammatory cells (i.e., macrophages, neutrophils, T cells) into the vascular adventitia. Release of adipocytokines and chemokines, such as leptin and visfatin, from inflamed PVAT enhances phenotype switching of VSMCs, which proliferate and migrate to the neointima. Moreover, PVAT-medicated Angptl2 elevates MMP-2, and MCP-1 expression. PVAT-derived complement 3 induces adventitial fibroblast migration to neointima. VEGF released from PVAT also contributes to adventitial neovascularization. MCP-1, monocyte chemoattractant protein-1; IL-6, interleukin-6; VCAM-1; vascular cell adhesion molecule-1; VEGF, vascular endothelial growth factor; MMP-2, matrix metalloprotenease-2; VSMC, vascular smooth muscle cell; Angptl2, angiopoietin-like protein 2; C3, complement 3.

et al., 2016), further suggesting a link between smoking, PVAT inflammation and AAA pathogenesis.

MMP production by inflammatory cells and VSMCs is fundamental to the pathogenesis of AAAs (Busuttil et al., 1982; Brophy et al., 1991; Kuivaniemi et al., 2015). As mentioned previously, Angptl2 deficiency in transplanted PVAT was reported to attenuate vascular MMP-2 activity and extracellular matrix degradation (Tian et al., 2013). Kurobe et al. also demonstrated that MMP-2 expression in PVAT was significantly decreased by systemic treatment with eplerenone, a selective mineralocorticoid receptor antagonist, which concomitantly inhibited AAA formation (Kurobe et al., 2013). These studies suggest that PVAT-derived MMP-2 could potentially play a role in AAA pathogenesis or progression.

In healthy blood vessels, VSMCs are quiescent and exhibit a contractile or differentiated phenotype, characterized by high level expression of differentiation markers such as α-smooth muscle actin (SMA) and smooth muscle myosin heavy chain (SM-MHC). During pathogenic conditions, VSMCs exhibit phenotype switching, characterized by increased proliferation, decreased expression of differentiation markers, and dysregulated synthesis of extracellular matrix components. Phenotypic switching of VSMCs in the context of elastase-induced aortic aneurysms in rats was reported (Ailawadi et al., 2009; Mao et al., 2015). As mentioned previously, Li et al. showed that PVAT-derived leptin promotes VSMC phenotypic switching through the p38 MAPK-dependent pathway in rats with metabolic syndrome (Li et al., 2014), suggesting that the paracrine action of PVAT-derived adipokines could potentially regulate AAA pathogenesis by promoting VSMC phenotypic switching.

Anatomic and Biological Changes in PVAT Associated with AAA

Obesity is a risk factor for AAA (Cronin et al., 2013). Like other adipose depots, PVAT expands and becomes more pro-inflammatory during obesity. The quantity of PVAT around the thoracic and abdominal aorta, assessed by CT imaging, was reported to be positively associated with aneurysm diameter in the Framingham Heart Study (Thanassoulis et al., 2012), supporting the notion that local fat depots may contribute to aortic remodeling in human AAAs. Folkesson et al. studied the characteristics of PVAT adjacent to human AAAs in patients undergoing elective surgical repair (Folkesson et al., 2017). They demonstrated that AAAs are surrounded by abundant PVAT enriched in inflammatory cells (neutrophils, macrophages, mast cells, and T cells) and proteases (cathepsin K and S). Moreover, pro-inflammatory IL-6 expression was increased in PVAT by 4-fold as compared to intima/media of the AAA tissues. These data suggest that PVAT could contribute to inflammation in the adjacent aneurysmal aortic wall.

PVAT, like other adipose depots, is richly endowed with mesenchymal stem cells contained in the stromovascular fraction. Stem cells isolated from adipose tissues and implanted

into experimentally-generated AAAs in pigs were demonstrated to stabilize the aneurysm, promote fibrosis, blunt inflammation, and induce elastin fiber regeneration (Riera del Moral et al., 2015). Whether the endogenous mesenchymal stem cells contained in PVAT could produce beneficial effects in AAAs is unknown and worthy of investigation. Nevertheless, this observation raises the possibility that PVAT could play a complex and multi-faceted role in modulating AAAs.

Experimental Evidence That PVAT Can Modulate AAAs

To elucidate the mechanisms of AAA formation, several animal models [i.e., chronic infusion of angiotensin II (AngII), local elastase infusion, and adventitial exposure of calcium chloride] are widely employed (Daugherty and Cassis, 1999; Chiou et al., 2001; Trachet et al., 2015) which exhibit features similar to human AAAs, including inflammatory cell infiltration, VSMC apoptosis and elastin fragmentation. Using the AngII model of AAA formation, Police et al. reported that PVAT surrounding the abdominal aorta exhibited increased numbers of F4/80 positive macrophages and expression of MCP-1 and its receptor, CCR2, as compared to that surrounding the thoracic aorta (Police et al., 2009). Co-localization of PVAT inflammation with AAAs in this model suggests a contributory role in AAA pathogenesis, although this was not directly tested in the study. Gao et al. (2012) reported that high fat diet feeding resulted in endothelial nitric oxide synthase (eNOS) uncoupling in PVAT in obese mice in conjunction with AAA formation, further suggesting a role for obesity-related PVAT dysfunction in the pathogenesis of AAAs.

The recruitment of monocytes to the adventitia, and their subsequent differentiation into CD14-expressing macrophages by IL-6, plays a critical role in aortic aneurysm pathogenesis (Tieu et al., 2009). Notably, soluble CD14 concentrations in plasma were higher in AAA patients compared with controls, and deletion of CD14 reduced AAA formation in mice, suggesting a causal role for this innate immune signaling molecule in AAA pathogenesis (Blomkalns et al., 2013). Moreover, incubation of THP-1 monocytic cells with conditioned medium from PVAT resulted in upregulated CD14 expression and enhanced migration, suggesting that PVAT-derived pro-inflammatory cytokines may promote adventitial macrophage activation in AAAs.

Reactive oxygen species (ROS) are associated with vascular wall remodeling in AAAs (Emeto et al., 2016; Siu et al., 2017). Endothelin (ET)-1 plays a role in vascular ROS production and inflammation, and increased levels of ET-1 are associated with the formation of AAAs (Treska et al., 1999; Flondell-Sité et al., 2010). Li et al. reported that 8 weeks of high fat diet feeding induced AAAs in hyperlipidemic mice overexpressing ET-1 selectively in endothelium (eET-1) as compared to control mice. Levels of ROS and inflammatory cells (monocyte/macrophages and CD4 positive T cells) accumulating in PVAT were significantly higher in eET-1 mice than in control mice, suggesting that ET-1-dependent induction of oxidative stress and inflammatory responses in PVAT might contribute to AAA formation (Li et al., 2013).

Sakaue et al. investigated the impact of deletion of the angiotensin II type 1a (AT_{1a}) receptor in visceral adipose tissue transplanted to the abdominal aorta on AAA formation in hyperlipidemic mice (Sakaue et al., 2017). The authors transplanted 50 mg of visceral (epididymal) adipose tissue from wild-type or AT_{1a} knockout mice fed a high fat diet to the peri-abdominal aorta of recipient mice, which were then infused with AngII. AAA formation was markedly attenuated in mice that were transplanted with adipose tissue lacking AT_{1a} expression compared with control. Activities of MMP-2/MMP-9, and accumulation of F4/80-positive macrophages, were significantly lower than in mice transplanted with visceral adipose tissue from wild-type mice, suggesting that AT_{1a} receptor expression in PVAT can promote macrophage accumulation and MMP activity leading to AAA formation. However, a sham control group was not included in the study, so it is not possible to determine whether adipose tissue transplantation alone modulated AAAs. Moreover, epididymal adipose tissue rather than authentic PVAT was transplanted; thus, further studies are needed to clarify the direct effects of PVAT transplantation on AAA formation. Based on the available data, the potential role of PVAT in AAAs is illustrated in **Figure 2**.

PVAT AND ARTERIAL STIFFNESS

Arterial stiffness is an independent predictor of cardiovascular events, such as heart failure, myocardial infarction, stroke, and kidney dysfunction (Hashimoto and Ito, 2011, 2013; Karras et al., 2012; Kitzman et al., 2013). Increased risk of cardiovascular disease with aging and the metabolic syndrome is in part attributable to arterial stiffening, as assessed by aortic pulse wave velocity in the clinical setting. Aortic stiffness is predominately determined by the balance and cross-linking status of extracellular matrix proteins, such as collagen and elastin, in the arterial wall (Prockop and Kivirikko, 1995; Debelle and Tamburro, 1999). Collagen type 1 is a key load-bearing collagen isoform whose increased expression is positively associated with aortic stiffness. Conversely, expression of elastin, a protein that provides elasticity to arteries, is inversely associated with aortic stiffness. Data in humans indicate that aortic stiffness is positively correlated with the quantity of associated PVAT, independent of body-mass index (Britton et al., 2013).

Experimental studies have begun to elucidate potential mechanisms whereby PVAT may modulate vascular stiffness. IL-6 is a pro-inflammatory cytokine secreted in higher concentrations from PVAT compared with other fat depots, and PVAT-derived IL-6 is associated with an increase in aortic stiffness. In addition, IL-6 concentration is related to pulse wave velocity in humans (Schnabel et al., 2008). Du et al. investigated whether aortic PVAT from hyperlipidemic mice promotes aortic stiffness and remodeling via PVAT-derived IL-6 secretion (Du et al., 2015), assessing intrinsic mechanical stiffness in aortic segments *in vivo* by aortic pulse wave velocity and by *ex vivo* techniques. Compared to wild-type mice, the hyperlipidemic mice exhibited increased aortic pulse wave velocity and intrinsic mechanical stiffness that was associated with higher expression

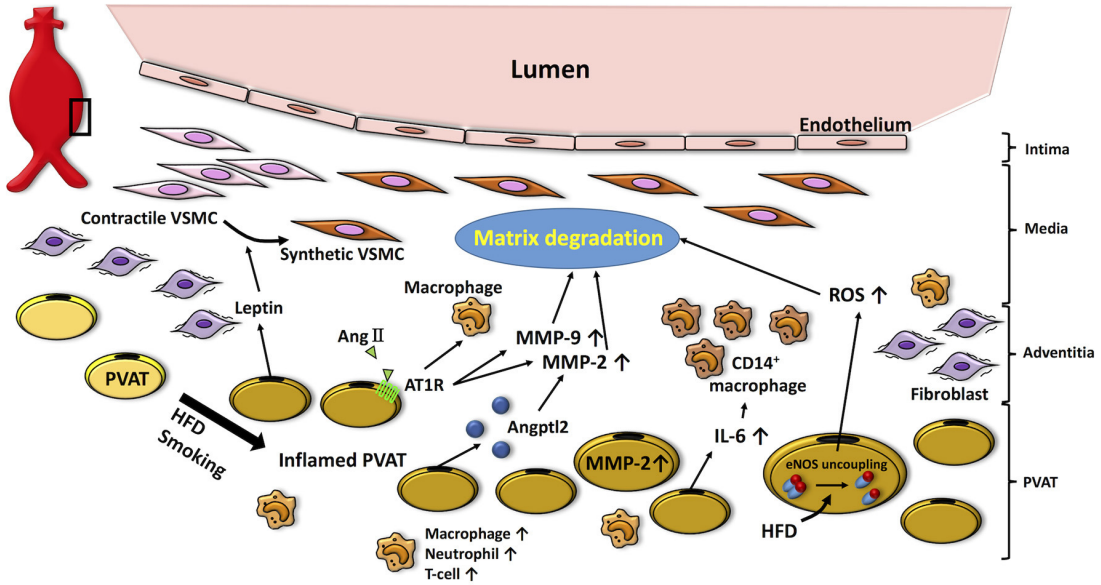

FIGURE 2 | Potential role of PVAT in the pathogenesis of AAA. High fat diet- or smoking-induced PVAT inflammation promotes infiltration of inflammatory cells (i.e., macrophages, neutrophils, T cells), which facilitates matrix fragmentation through increases in MMP expression and activity. Moreover, adipocytokines (i.e., leptin) produced by PVAT induce VSMC phenotype switching associated with aneurysm disease. Inflamed PVAT also increases inflammatory cytokines (i.e., IL-6) and ROS, which further contributes to oxidative stress and matrix degradation in the vascular wall. HFD, high fat diet; AngII, angiotensin II; AT1R, angiotensin II type 1a receptor; Angptl2, angiopoietin-like protein 2; MMP, matrix metalloprotenease; IL-6, interleukin-6; ROS, reactive oxygen species; VSMC, vascular smooth muscle cell.

of collagen type 1 and advanced glycation end products. Importantly, IL-6 secretion from PVAT of hyperlipidemic mice exceeded that of wild-type mice, and the enhanced intrinsic mechanical stiffness was reversed by a neutralizing antibody to IL-6 in hyperlipidemic mice. These data suggest that dysfunctional PVAT can promote intrinsic mechanical stiffening and matrix remodeling via enhanced IL-6 secretion.

Deficiency of lysyl oxidase, a copper-dependent amine oxidase, promotes fragmentation of elastic fibers (Chen et al., 2013). Chen et al. reported that mediators released from PVAT attenuate lysyl oxidase activity, thereby promoting elastin fragmentation and aortic stiffening. Thus, PVAT accumulation potentially may impair elastic fiber stability via several mechanisms to contribute to aortic stiffness.

To investigate the modulatory role of PVAT in arterial stiffness, PVAT was transplanted from young mice (4–6 months), old mice (26–28 months), or old mice treated with tempol (a superoxide dismutase mimetic) onto the abdominal aorta of young recipient mice (Fleenor et al., 2014). Eight weeks post PVAT transplantation, the young recipient mice transplanted with PVAT from old mice had greater aortic stiffness *in vivo* (increased aortic pulse wave velocity) and *ex vivo* (intrinsic mechanical stiffness) compared with those transplanted with PVAT from young donors. The PVAT of old mice contained higher levels of superoxide as compared with that of young mice, and tempol both normalized superoxide levels and abolished the enhanced aortic stiffness caused by transplantation of aged PVAT. Mechanistically, transplantation of aged PVAT led to increased expression of adventitial collagen type 1, which was likewise normalized by tempol treatment. These findings suggest that oxidative stress in PVAT can promote age-related aortic stiffness via the increased expression of collagen type 1, which potentially can be abrogated by targeted antioxidant therapy to PVAT.

PVAT AND VASCULITIC SYNDROMES

Vasculitides represent a heterogeneous group of complex disorders characterized by acute and chronic inflammatory lesions of the vascular wall. As in both atherosclerosis and AAAs, macrophage infiltration is a critical component of vasculitides (Hansson and Hermansson, 2011), and is especially prominent in the adventitia. Granuloma formation is a typical finding in several vasculitides (Hilhorst et al., 2014). Lymphocytes and dendritic cells are enriched in these granulomas, which also contain neutrophils, eosinophils, and B cells. Infiltration of inflammatory cells within PVAT has also been demonstrated in vasculitic syndromes (Jakob et al., 1990; Wagner et al., 1996; Hollan et al., 2008). While several studies have demonstrated an association between PVAT and various vasculitides, direct evidence of a pathogenic role of PVAT is lacking, however.

Takayasu arteritis (TA) is a primary inflammatory disease of large elastic arteries such as the aorta and its major branches, with prominent accumulation of granulomas. TA is prevalent in young women and is more frequent in Asian countries compared to Europe and North America (Richards et al., 2010). The disease is characterized by an acute phase of constitutional symptoms followed by a vascular phase leading to arterial stenosis, occlusion and occasionally aneurysm formation. TA is diagnosed by typical clinical features and demonstrated narrowing of the aorta or its branches near their origin by conventional

CT or CT angiography, magnetic resonance angiography, or ultrasonography (Choe et al., 2000; Gotway et al., 2005). Autopsy studies have described the inflammatory lesions as a nodular fibrosis that develops in the media and adventitia, extending into the *vasa vasorum*, along with intimal thickening (NASU, 1963; Hotchi, 1992; Matsunaga et al., 1998). Interestingly, TA patients have a greater prevalence of metabolic syndrome and higher levels of leptin and resistin, associated with upregulated inflammatory markers such as pentraxins-3 (Kawanami et al., 2004), compared to age-matched controls (Yilmaz et al., 2012; da Silva et al., 2013). Pentraxin-3 is considered to be a reliable activity marker of TA (Dagna et al., 2011). Lower levels of adiponectin were detected in TA patients with metabolic syndrome compared with those without metabolic syndrome. Given that the vessels afflicted with TA are highly endowed with PVAT, it is tempting to speculate that PVAT may contribute to local inflammation of the vascular wall in TA, but definitive evidence is lacking. Analysis of CT scans in patients with TA to quantify the FAI in PVAT could help to define its utility as a marker of PV inflammation and local disease activity in these patients.

CONCLUSIONS

A growing body of data support linkages between PVAT and non-atherosclerotic vascular diseases, including neointimal hyperplasia, aortic aneurysm, arterial stiffness, and vasculitic syndromes, in experimental animal models and in humans. These diseases are all associated with vascular wall inflammation that may be modulated by adipocytokines produced by PVAT. Moreover, mediators produced by PVAT can also regulate VSMC proliferation, matrix degradation, and neovascularization associated with these diseases. The extent to which PVAT is a mediator vs. a marker of non-atherosclerotic vascular disease, or even a promoter of vascular health, remains to be determined. The commonly employed animal models used to examine the role of PVAT in vascular diseases suffer from technical limitations and confounding variables that may complicate data interpretation. Development of more robust animal models is clearly needed to advance our understanding of the role of PVAT in non-atherosclerotic vascular diseases. Exciting new data in humans suggest that imaging PVAT may prove useful to uncover its potential role in vascular diseases and perhaps even to direct new therapeutic approaches.

AUTHOR CONTRIBUTIONS

All authors listed, have made substantial, direct and intellectual contribution to the work, and approved it for publication.

ACKNOWLEDGMENTS

This study was supported by NIH grants HL126949 and HL112640 (NW).

REFERENCES

Aiello, R. J., Bourassa, P. A., Lindsey, S., Weng, W., Natoli, E., Rollins, B. J., et al. (1999). Monocyte chemoattractant protein-1 accelerates atherosclerosis in apolipoprotein E-deficient mice. *Arterioscler. Thromb. Vasc. Biol.* 19, 1518–1525. doi: 10.1161/01.ATV.19.6.1518

Ailawadi, G., Moehle, C. W., Pei, H., Walton, S. P., Yang, Z., Kron, I. L., et al. (2009). Smooth muscle phenotypic modulation is an early event in aortic aneurysms. *J. Thorac. Cardiovasc. Surg.* 138, 1392–1399. doi: 10.1016/j.jtcvs.2009.07.075

Antonopoulos, A. S., Sanna, F., Sabharwal, N., Thomas, S., Oikonomou, E. K., Herdman, L., et al. (2017). Detecting human coronary inflammation by imaging perivascular fat. *Sci. Transl. Med.* 9:eaal2658. doi: 10.1126/scitranslmed.aal2658

Blomkalns, A. L., Gavrila, D., Thomas, M., Neltner, B. S., Blanco, V. M., Benjamin, S. B., et al. (2013). CD14 directs adventitial macrophage precursor recruitment: role in early abdominal aortic aneurysm formation. *J. Am. Heart Assoc.* 2:e000065. doi: 10.1161/JAHA.112.000065

Britton, K. A., Wang, N., Palmisano, J., Corsini, E., Schlett, C. L., Hoffmann, U., et al. (2013). Thoracic periaortic and visceral adipose tissue and their cross-sectional associations with measures of vascular function. *Obesity* 21, 1496–1503. doi: 10.1002/oby.20166

Brophy, C. M., Reilly, J. M., Smith, G. J., and Tilson, M. D. (1991). The role of inflammation in nonspecific abdominal aortic aneurysm disease. *Ann. Vasc. Surg.* 5, 229–233. doi: 10.1007/BF02329378

Brown, N. K., Zhou, Z., Zhang, J., Zeng, R., Wu, J., Eitzman, D. T., et al. (2014). Perivascular adipose tissue in vascular function and disease: a review of current research and animal models. *Arterioscler. Thromb. Vasc. Biol.* 34, 1621–1630. doi: 10.1161/ATVBAHA.114.303029

Busuttil, R. W., Rinderbriecht, H., Flesher, A., and Carmack, C. (1982). Elastase activity: the role of elastase in aortic aneurysm formation. *J. Surg. Res.* 32, 214–217. doi: 10.1016/0022-4804(82)90093-2

Cai, X., Lin, Y., Hauschka, P. V., and Grottkau, B. E. (2011). Adipose stem cells originate from perivascular cells. *Biol. Cell* 103, 435–447. doi: 10.1042/BC20110033

Chang, L., Villacorta, L., Li, R., Hamblin, M., Xu, W., Dou, C., et al. (2012). Loss of perivascular adipose tissue on peroxisome proliferator-activated receptor-gamma deletion in smooth muscle cells impairs intravascular thermoregulation and enhances atherosclerosis. *Circulation* 126, 1067–1078. doi: 10.1161/CIRCULATIONAHA.112.104489

Chatterjee, T. K., Aronow, B. J., Tong, W. S., Manka, D., Tang, Y., Bogdanov, V. Y., et al. (2013). Human coronary artery perivascular adipocytes overexpress genes responsible for regulating vascular morphology, inflammation, and hemostasis. *Physiol. Genomics* 45, 697–709. doi: 10.1152/physiolgenomics.00042.2013

Chatterjee, T. K., Stoll, L. L., Denning, G. M., Harrelson, A., Blomkalns, A. L., Idelman, G., et al. (2009). Proinflammatory phenotype of perivascular adipocytes: influence of high-fat feeding. *Circ. Res.* 104, 541–549. doi: 10.1161/CIRCRESAHA.108.182998

Chen, J. Y., Tsai, P. J., Tai, H. C., Tsai, R. L., Chang, Y. T., Wang, M. C., et al. (2013). Increased aortic stiffness and attenuated lysyl oxidase activity in obesity significance. *Arterioscler. Thromb. Vasc. Biol.* 33, 839–846. doi: 10.1161/ATVBAHA.112.300036

Chen, Y. C., Huang, A. L., Kyaw, T. S., Bobik, A., and Peter, K. (2016). Atherosclerotic plaque rupture: identifying the straw that breaks the camel's back. *Arterioscler. Thromb. Vasc. Biol.* 36, e63–e72. doi: 10.1161/ATVBAHA.116.307993

Chiou, A. C., Chiu, B., and Pearce, W. H. (2001). Murine aortic aneurysm produced by periarterial application of calcium chloride. *J. Surg. Res.* 99, 371–376. doi: 10.1006/jsre.2001.6207

Choe, Y. H., Han, B. K., Koh, E. M., Kim, D. K., Do, Y. S., and Lee, W. R. (2000). Takayasu's arteritis: assessment of disease activity with contrast-enhanced

MR imaging. *AJR Am. J. Roentgenol.* 175, 505–511. doi: 10.2214/ajr.175.2.1750505

Cronin, O., Walker, P. J., and Golledge, J. (2013). The association of obesity with abdominal aortic aneurysm presence and growth. *Atherosclerosis* 226, 321–327. doi: 10.1016/j.atherosclerosis.2012.10.041

da Silva, T. F., Levy-Neto, M., Bonfá, E., and Pereira, R. M. (2013). High prevalence of metabolic syndrome in Takayasu arteritis: increased cardiovascular risk and lower adiponectin serum levels. *J. Rheumatol.* 40, 1897–1904. doi: 10.3899/jrheum.130162

Dagna, L., Salvo, F., Tiraboschi, M., Bozzolo, E. P., Franchini, S., Doglioni, C., et al. (2011). Pentraxin-3 as a marker of disease activity in Takayasu arteritis. *Ann. Intern. Med.* 155, 425–433. doi: 10.7326/0003-4819-155-7-201110040-00005

Daugherty, A., and Cassis, L. (1999). Chronic angiotensin II infusion promotes atherogenesis in low density lipoprotein receptor -/- mice. *Ann. N. Y. Acad. Sci.* 892, 108–118. doi: 10.1111/j.1749-6632.1999.tb07789.x

Debelle, L., and Tamburro, A. M. (1999). Elastin: molecular description and function. *Int. J. Biochem. Cell Biol.* 31, 261–272. doi: 10.1016/S1357-2725(98)00098-3

Du, B., Ouyang, A., Eng, J. S., and Fleenor, B. S. (2015). Aortic perivascular adipose-derived interleukin-6 contributes to arterial stiffness in low-density lipoprotein receptor deficient mice. *Am. J. Physiol. Heart Circ. Physiol.* 308, H1382–H1390. doi: 10.1152/ajpheart.00712.2014

Emeto, T. I., Moxon, J. V., Au, M., and Golledge, J. (2016). Oxidative stress and abdominal aortic aneurysm: potential treatment targets. *Clin. Sci.* 130, 301–315. doi: 10.1042/CS20150547

Eringa, E. C., Bakker, W., Smulders, Y. M., Serné, E. H., Yudkin, J. S., and Stehouwer, C. D. (2007). Regulation of vascular function and insulin sensitivity by adipose tissue: focus on perivascular adipose tissue. *Microcirculation* 14, 389–402. doi: 10.1080/10739680701303584

Fitzgibbons, T. P., and Czech, M. P. (2014). Epicardial and perivascular adipose tissues and their influence on cardiovascular disease: basic mechanisms and clinical associations. *J. Am. Heart Assoc.* 3:e000582. doi: 10.1161/JAHA.113.000582

Fitzgibbons, T. P., Kogan, S., Aouadi, M., Hendricks, G. M., Straubhaar, J., and Czech, M. P. (2011). Similarity of mouse perivascular and brown adipose tissues and their resistance to diet-induced inflammation. *Am. J. Physiol. Circ. Physiol.* 301, H1425–H1437. doi: 10.1152/ajpheart.00376.2011

Fleenor, B. S., Eng, J. S., Sindler, A. L., Pham, B. T., Kloor, J. D., and Seals, D. R. (2014). Superoxide signaling in perivascular adipose tissue promotes age-related artery stiffness. *Aging Cell* 13, 576–578. doi: 10.1111/acel.12196

Flondell-Sité, D., Lindblad, B., and Gottsäter, A. (2010). High levels of endothelin (ET)-1 and aneurysm diameter independently predict growth of stable abdominal aortic aneurysms. *Angiology* 61, 324–328. doi: 10.1177/0003319709344190

Folkesson, M., Vorkapic, E., Gulbins, E., Japtok, L., Kleuser, B., Welander, M., et al. (2017). Inflammatory cells, ceramides, and expression of proteases in perivascular adipose tissue adjacent to human abdominal aortic aneurysms. *J. Vasc. Surg.* 65, 1171–1179. doi: 10.1016/j.jvs.2015.12.056

Gao, L., Siu, K. L., Chalupsky, K., Nguyen, A., Chen, P., Weintraub, N. L., et al. (2012). Role of uncoupled endothelial nitric oxide synthase in abdominal aortic aneurysm formation. *Hypertension* 59, 158–166. doi: 10.1161/HYPERTENSIONAHA.111.181644

Goel, S. A., Guo, L. W., Liu, B., and Kent, K. C. (2012). Mechanisms of post-intervention arterial remodelling. *Cardiovasc. Res.* 96, 363–371. doi: 10.1093/cvr/cvs276

Gotway, M. B., Araoz, P. A., Macedo, T. A., Stanson, A. W., Higgins, C. B., Ring, E. J., et al. (2005). Imaging findings in Takayasu's arteritis. *AJR Am. J. Roentgenol.* 184, 1945–1950. doi: 10.2214/ajr.184.6.01841945

Hansson, G. K., and Hermansson, A. (2011). The immune system in atherosclerosis. *Nat. Immunol.* 12, 204–212. doi: 10.1038/ni.2001

Hashimoto, J., and Ito, S. (2011). Central pulse pressure and aortic stiffness determine renal hemodynamics: pathophysiological implication for microalbuminuria in hypertension. *Hypertension* 58, 839–846. doi: 10.1161/HYPERTENSIONAHA.111.177469

Hashimoto, J., and Ito, S. (2013). Aortic stiffness determines diastolic blood flow reversal in the descending thoracic aorta: potential implication for retrograde embolic stroke in hypertension. *Hypertension* 62, 542–549. doi: 10.1161/HYPERTENSIONAHA.113.01318

Hilhorst, M., Shirai, T., Berry, G., Goronzy, J. J., and Weyand, C. M. (2014). T cell-macrophage interactions and granuloma formation in vasculitis. *Front. Immunol.* 5:432. doi: 10.3389/fimmu.2014.00432

Hollan, I., Prayson, R., Saatvedt, K., Almdahl, S. M., Nossent, H. C., Mikkelsen, K., et al. (2008). Inflammatory cell infiltrates in vessels with different susceptibility to atherosclerosis in rheumatic and non-rheumatic patients: a controlled study of biopsy specimens obtained at coronary artery surgery. *Circ. J.* 72, 1986–1992. doi: 10.1253/circj.CJ-08-0473

Hotchi, M. (1992). Pathological studies on Takayasu arteritis. *Heart Vessels Suppl.* 7, 11–17. doi: 10.1007/BF01744538

Jakob, H., Volb, R., Stangl, G., Reifart, N., Rumpelt, H. J., and Oelert, H. (1990). Surgical correction of a severely obstructed pulmonary in Takayasu's arteritis. *Eur. J. Cardiothorac. Surg.* 4, 456–458. doi: 10.1016/1010-7940(90)90079-F

Karras, A., Haymann, J. P., Bozec, E., Metzger, M., Jacquot, C., Maruani, G., et al. (2012). Large artery stiffening and remodeling are independently associated with all-cause mortality and cardiovascular events in chronic kidney disease. *Hypertension* 60, 1451–1457. doi: 10.1161/HYPERTENSIONAHA.112.197210

Kawanami, D., Maemura, K., Takeda, N., Harada, T., Nojiri, T., Imai, Y., et al. (2004). Direct reciprocal effects of resistin and adiponectin on vascular endothelial cells: a new insight into adipocytokine-endothelial cell interactions. *Biochem. Biophys. Res. Commun.* 314, 415–419. doi: 10.1016/j.bbrc.2003.12.104

Kitzman, D. W., Herrington, D. M., Brubaker, P. H., Moore, J. B., Eggebeen, J., and Haykowsky, M. J. (2013). Carotid arterial stiffness and its relationship to exercise intolerance in older patients with heart failure and preserved ejection fraction. *Hypertension* 61, 112–119. doi: 10.1161/HYPERTENSIONAHA.111.00163

Kuivaniemi, H., Ryer, E. J., Elmore, J. R., and Tromp, G. (2015). Understanding the pathogenesis of abdominal aortic aneurysms. *Expert Rev. Cardiovasc. Ther.* 13, 975–987. doi: 10.1586/14779072.2015.1074861

Kurobe, H., Hirata, Y., Matsuoka, Y., Sugasawa, N., Higashida, M., Nakayama, T., et al. (2013). Protective effects of selective mineralocorticoid receptor antagonist against aortic aneurysm progression in a novel murine model. *J. Surg. Res.* 185, 455–462. doi: 10.1016/j.jss.2013.05.002

Lederle, F. A., Johnson, G. R., Wilson, S. E., Ballard, D. J., Jordan, W. D. Jr., Blebea, J., et al. (2002). Rupture rate of large abdominal aortic aneurysms in patients refusing or unfit for elective repair. *JAMA* 287, 2968–2972. doi: 10.1001/jama.287.22.2968

Lee, M. H., Chen, S. J., Tsao, C. M., and Wu, C. C. (2014). Perivascular adipose tissue inhibits endothelial function of rat aortas via caveolin-1. *PLoS ONE* 9:e99947. doi: 10.1371/journal.pone.0099947

Li, H., Wang, Y. P., Zhang, L. N., and Tian, G. (2014). Perivascular adipose tissue-derived leptin promotes vascular smooth muscle cell phenotypic switching via p38 mitogen-activated protein kinase in metabolic syndrome rats. *Exp. Biol. Med.* 239, 954–965. doi: 10.1177/1535370214527903

Li, M. W., Mian, M. O., Barhoumi, T., Rehman, A., Mann, K., Paradis, P., et al. (2013). Endothelin-1 overexpression exacerbates atherosclerosis and induces aortic aneurysms in apolipoprotein E knockout mice. *Arterioscler. Thromb. Vasc. Biol.* 33, 2306–2315. doi: 10.1161/ATVBAHA.113.302028

Manka, D., Chatterjee, T. K., Stoll, L. L., Basford, J. E., Konaniah, E. S., Srinivasan, R., et al. (2014). Transplanted perivascular adipose tissue accelerates injury-induced neointimal hyperplasia: role of monocyte chemoattractant protein-1. *Arterioscler. Thromb. Vasc. Biol.* 34, 1723–1730. doi: 10.1161/ATVBAHA.114.303983

Mao, N., Gu, T., Shi, E., Zhang, G., Yu, L., and Wang, C. (2015). Phenotypic switching of vascular smooth muscle cells in animal model of rat thoracic aortic aneurysm. *Interact. Cardiovasc. Thorac. Surg.* 21, 62–70. doi: 10.1093/icvts/ivv074

Matsuda, M., Shimomura, I., Sata, M., Arita, Y., Nishida, M., Maeda, N., et al. (2002). Role of adiponectin in preventing vascular stenosis The missing link of adipo-vascular axis. *J. Biol. Chem.* 277, 37487–37491. doi: 10.1074/jbc.M206083200

Matsunaga, N., Hayashi, K., Sakamoto, I., Matsuoka, Y., Ogawa, Y., Honjo, K., et al. (1998). Takayasu arteritis: MR manifestations and diagnosis of acute and chronic phase. *J. Magn. Reson. Imaging* 8, 406–414. doi: 10.1002/jmri.1880080221

Moitra, J., Mason, M. M., Olive, M., Krylov, D., Gavrilova, O., Marcus-Samuels, B., et al. (1998). Life without white fat: a transgenic mouse. *Genes Dev.* 12, 3168–3181. doi: 10.1101/gad.12.20.3168

NASU, T. (1963). Pathology of pulseless disease: a systematic study and critical review of twenty-one autopsy cases reported in Japan. *Angiology* 14, 225–242. doi: 10.1177/000331976301400502

Öhman, M. M., Luo, W., Wang, H., Guo, C., and Abdallah, W., Russo, H., et al. (2011). Perivascular visceral adipose tissue induces atherosclerosis in apolipoprotein E deficient mice. *Atherosclerosis* 219, 33–39. doi: 10.1016/j.atherosclerosis.2011.07.012

Okamoto, E., Couse, T., De Leon, H., Vinten-Johansen, J., Goodman, R. B., Scott, N. A., et al. (2001). Perivascular inflammation after balloon angioplasty of porcine coronary arteries. *Circulation* 104, 2228–2235. doi: 10.1161/hc4301.097195

Padilla, J., Jenkins, N. T., Vieira-Potter, V. J., and Laughlin, M. H. (2013). Divergent phenotype of rat thoracic and abdominal perivascular adipose tissue. *Am. J. Physiol. Regul. Integr. Comp. Physiol.* 304, R543–552. doi: 10.1152/ajpregu.00567.2012

Pajvani, U. B., Trujillo, M. E., Combs, T. P., Iyengar, P., Jelicks, L., Roth, K. A., et al. (2005). Fat apoptosis through targeted activation of caspase 8: a new mouse model of inducible and reversible lipoatrophy. *Nat. Med.* 11, 797–803. doi: 10.1038/nm1262

Payne, G. A., Bohlen, H. G., Dincer, U. D., Borbouse, L., and Tune, J. D. (2009). Periadventitial adipose tissue impairs coronary endothelial function via PKC-beta-dependent phosphorylation of nitric oxide synthase. *Am. J. Physiol. Heart Circ. Physiol.* 297, H460–H465. doi: 10.1152/ajpheart.00116.2009

Police, S. B., Thatcher, S. E., Charnigo, R., Daugherty, A., and Cassis, L. A. (2009). Obesity promotes inflammation in periaortic adipose tissue and angiotensin II-induced abdominal aortic aneurysm formation. *Arterioscler. Thromb. Vasc. Biol.* 29, 1458–1464. doi: 10.1161/ATVBAHA.109.192658

Prockop, D. J., and Kivirikko, K. I. (1995). Collagens: molecular biology, diseases, and potentials for therapy. *Annu. Rev. Biochem.* 64, 403–434. doi: 10.1146/annurev.bi.64.070195.002155

Rajsheker, S., Manka, D., Blomkalns, A. L., Chatterjee, T. K., Stoll, L. L., and Weintraub, N. L. (2010). Crosstalk between perivascular adipose tissue and blood vessels. *Curr. Opin. Pharmacol.* 10, 191–196. doi: 10.1016/j.coph.2009.11.005

Richards, B. L., March, L., and Gabriel, S. E. (2010). Epidemiology of large-vessel vasculidities. *Best Pract. Res. Clin. Rheumatol.* 24, 871–883. doi: 10.1016/j.berh.2010.10.008

Riera del Moral, L., Largo, C., Ramirez, J. R., Vega Clemente, L., Fernández Heredero, A., Riera de Cubas, L., et al. (2015). Potential of mesenchymal stem cell in stabilization of abdominal aortic aneurysm sac. *J. Surg. Res.* 195, 325–333. doi: 10.1016/j.jss.2014.12.020

Rossi, C., Santini, E., Chiarugi, M., Salvati, A., Comassi, M., Vitolo, E., et al. (2014). The complex P2X7 receptor/inflammasome in perivascular fat tissue of heavy smokers. *Eur. J. Clin. Invest.* 44, 295–302. doi: 10.1111/eci.12232

Ruan, C. C., Zhu, D. L., Chen, Q. Z., Chen, J., Guo, S. J., Li, X. D., et al. (2010). Perivascular adipose tissue-derived complement 3 is required for adventitial fibroblast functions and adventitial remodeling in deoxycorticosterone acetate-salt hypertensive rats. *Arterioscler. Thromb. Vasc. Biol.* 30, 2568–2574. doi: 10.1161/ATVBAHA.110.215525

Rudic, R. D., Shesely, E. G., Maeda, N., Smithies, O., Segal, S. S., and Sessa, W. C. (1998). Direct evidence for the importance of endothelium-derived nitric oxide in vascular remodeling. *J. Clin. Invest.* 101, 731–736. doi: 10.1172/JCI1699

Sakaue, T., Suzuki, J., Hamaguchi, M., Suehiro, C., Tanino, A., Nagao, T., et al. (2017). Perivascular adipose tissue angiotensin II type 1 receptor promotes vascular inflammation and aneurysm formation. *Hypertension* 70, 780–789. doi: 10.1161/HYPERTENSIONAHA.117.09512

Schlich, R., Willems, M., Greulich, S., Ruppe, F., Knoefel, W. T., Ouwens, D. M., et al. (2013). VEGF in the crosstalk between human adipocytes and smooth muscle cells: depot-specific release from visceral and perivascular adipose tissue. *Mediators Inflamm.* 2013:982458. doi: 10.1155/2013/982458

Schnabel, R., Larson, M. G., Dupuis, J., Lunetta, K. L., Lipinska, I., Meigs, J. B., et al. (2008). Relations of inflammatory biomarkers and common genetic variants with arterial stiffness and wave reflection. *Hypertension* 51, 1651–1657. doi: 10.1161/HYPERTENSIONAHA.107.105668

Schroeter, M. R., Eschholz, N., Herzberg, S., Jerchel, I., Leifheit-Nestler, M., Czepluch, F. S., et al. (2013). Leptin-Dependent and Leptin-Independent paracrine effects of perivascular adipose tissue on neointima formationsignificance. *Arterioscler. Thromb. Vasc. Biol.* 33, 980–987. doi: 10.1161/ATVBAHA.113.301393

Shin, H. J., Oh, J., Kang, S. M., Lee, J. H., Shin, M. J., Hwang, K. C., et al. (2005). Leptin induces hypertrophy via p38 mitogen-activated protein kinase in rat vascular smooth muscle cells. *Biochem. Biophys. Res. Commun.* 329, 18–24. doi: 10.1016/j.bbrc.2004.12.195

Siu, K. L., Li, Q., Zhang, Y., Guo, J., Youn, J. Y., Du, J., et al. (2017). NOX isoforms in the development of abdominal aortic aneurysm. *Redox. Biol.* 11, 118–125. doi: 10.1016/j.redox.2016.11.002

Takaoka, M., Nagata, D., Kihara, S., Shimomura, I., Kimura, Y., Tabata, Y., et al. (2009). Periadventitial adipose tissue plays a critical role in vascular remodeling. *Circ. Res.* 105, 906–911. doi: 10.1161/CIRCRESAHA.109.199653

Takaoka, M., Suzuki, H., Shioda, S., Sekikawa, K., Saito, Y., Nagai, R., et al. (2010). Endovascular injury induces rapid phenotypic changes in perivascular adipose tissue. *Arterioscler. Thromb. Vasc. Biol.* 30, 1576–1582. doi: 10.1161/ATVBAHA.110.207175

Tanaka, K., Komuro, I., and Sata, M. (2015). Vascular cells originating from perivascular adipose tissue contribute to vasa vasorum neovascularization in atherosclerosis. *Circulation* 132:A14910. Abstract retrieved from abstracts in American Heart Association (Accession No. 14910).

Tchkonia, T., Lenburg, M., Thomou, T., Giorgadze, N., Frampton, G., Pirtskhalava, T., et al. (2007). Identification of depot-specific human fat cell progenitors through distinct expression profiles and developmental gene patterns. *Am. J. Physiol. Endocrinol. Metab.* 292, E298–E307 doi: 10.1152/ajpendo.00202.2006

Thanassoulis, G., Massaro, J. M., Corsini, E., Rogers, I., Schlett, C. L., Meigs, J. B., et al. (2012). Periaortic adipose tissue and aortic dimensions in the Framingham Heart Study. *J. Am. Heart Assoc.* 1:e000885. doi: 10.1161/JAHA.112.000885

Thompson, R. W. (2002). Detection and management of small aortic aneurysms. *N. Engl. J. Med.* 346, 1484–1486. doi: 10.1056/NEJM200205093461910

Tian, Z., Miyata, K., Tazume, H., Sakaguchi, H., Kadomatsu, T., Horio, E., et al. (2013). Perivascular adipose tissue-secreted angiopoietin-like protein 2 (Angptl2) accelerates neointimal hyperplasia after endovascular injury. *J. Mol. Cell. Cardiol.* 57, 1–12. doi: 10.1016/j.yjmcc.2013.01.004

Tieu, B. C., Lee, C., Sun, H., Lejeune, W., Recinos, A., Ju, X., et al. (2009). An adventitial IL-6/MCP1 amplification loop accelerates macrophage-mediated vascular inflammation leading to aortic dissection in mice. *J. Clin. Invest.* 119, 3637–3651. doi: 10.1172/JCI38308

Trachet, B., Fraga-Silva, R. A., Piersigilli, A., Tedgui, A., Sordet-Dessimoz, J., Astolfo, A., et al. (2015). Dissecting abdominal aortic aneurysm in Ang II-infused mice: suprarenal branch ruptures and apparent luminal dilatation. *Cardiovasc. Res.* 105, 213–222. doi: 10.1093/cvr/cvu257

Treska, V., Wenham, P. W., Valenta, J., Topolcan, O., and Pecen, L. (1999). Plasma endothelin levels in patients with abdominal aortic aneurysms. *Eur. J. Vasc. Endovasc. Surg.* 17, 424–428. doi: 10.1053/ejvs.1998.0800

Vardulaki, K. A., Walker, N. M., Day, N. E., Duffy, S. W., Ashton, H. A., and Scott, R. A. (2000). Quantifying the risks of hypertension, age, sex and smoking in patients with abdominal aortic aneurysm. *Br. J. Surg.* 87, 195–200 doi: 10.1046/j.1365-2168.2000.01353.x

Verhagen, S. N., and Visseren, F. L. (2011). Perivascular adipose tissue as a cause of atherosclerosis. *Atherosclerosis* 214, 3–10. doi: 10.1016/j.atherosclerosis.2010.05.034

Wagner, A. D., Björnsson, J., Bartley, G. B., Goronzy, J. J., and Weyand, C. M. (1996). Interferon-gamma-producing T cells in giant cell vasculitis represent a minority of tissue-infiltrating cells and are located distant from the site of pathology. *Am. J. Pathol.* 148, 1925–1933.

Wang, C. N., Yang, G. H., Wang, Z. Q., Liu, C. W., Li, T. J., Lai, Z. C., et al. (2016). Role of perivascular adipose tissue in nicotine-induced endothelial cell inflammatory responses. *Mol. Med. Rep.* 14, 5713–5718. doi: 10.3892/mmr.2016.5934

Wang, P., Xu, T. Y., Guan, Y. F., Su, D. F., Fan, G. R., and Miao, C. Y. (2009). Perivascular adipose tissue-derived visfatin is a vascular smooth muscle cell

growth factor: role of nicotinamide mononucleotide. *Cardiovasc. Res.* 81, 370–380. doi: 10.1093/cvr/cvn288

Yilmaz, H., Gerdan, V., Kozaci, D., Solmaz, D., Akar, S., Can, G., et al. (2012). Ghrelin and adipokines as circulating markers of disease activity in patients with Takayasu arteritis. *Arthritis Res. Ther.* 14:R272. doi: 10.1186/ar4120

Zhang, L. N., Wilson, D. W., Cunha, V. D., Sullivan, M. E., Vergona, R., Rutledge, J. C., et al. (2006). Endothelial NO synthase deficiency promotes smooth muscle progenitor cells in association with upregulation of stromal cell-derived factor-1α in a mouse model of carotid artery ligation. *Arterioscler. Thromb. Vasc. Biol.* 26, 765–772. doi: 10.1161/01.ATV.0000207319.28254.8c

Conflict of Interest Statement: The authors declare that the research was conducted in the absence of any commercial or financial relationships that could be construed as a potential conflict of interest.

The reviewer JP and handling Editor declared their shared affiliation.

frontiers in Physiology

ORIGINAL RESEARCH
published: 22 September 2017
doi: 10.3389/fphys.2017.00719

Perivascular Adipose Tissue Harbors Atheroprotective IgM-Producing B Cells

Prasad Srikakulapu[1], Aditi Upadhye[1], Sam M. Rosenfeld[1], Melissa A. Marshall[1], Chantel McSkimming[1], Alexandra W. Hickman[2], Ileana S. Mauldin[2], Gorav Ailawadi[2], M. Beatriz S. Lopes[3], Angela M. Taylor[4] and Coleen A. McNamara[1, 4]**

[1] Cardiovascular Research Center, University of Virginia, Charlottesville, VA, United States, [2] Department of Surgery, University of Virginia, Charlottesville, VA, United States, [3] Department of Pathology and Neurological Surgery, University of Virginia, Charlottesville, VA, United States, [4] Department of Medicine, Division of Cardiovascular Medicine, University of Virginia, Charlottesville, VA, United States

OPEN ACCESS

Edited by:
Stephanie W. Watts, Michigan State University, United States

Reviewed by:
Keshari Thakali, University of Arkansas for Medical Sciences, United States
Bradley S. Fleenor, Ball State University, United States

***Correspondence:**
Prasad Srikakulapu
ps5fj@virginia.edu
Coleen A. McNamara
cam8c@virginia.edu

Specialty section:
This article was submitted to Vascular Physiology, a section of the journal Frontiers in Physiology

Received: *03 July 2017*
Accepted: *05 September 2017*
Published: *22 September 2017*

Citation:
Srikakulapu P, Upadhye A, Rosenfeld SM, Marshall MA, McSkimming C, Hickman AW, Mauldin IS, Ailawadi G, Lopes MBS, Taylor AM and McNamara CA (2017) Perivascular Adipose Tissue Harbors Atheroprotective IgM-Producing B Cells. Front. Physiol. 8:719. doi: 10.3389/fphys.2017.00719

Adipose tissue surrounding major arteries (Perivascular adipose tissue or PVAT) has long been thought to exist to provide vessel support and insulation. Emerging evidence suggests that PVAT regulates artery physiology and pathology, such as, promoting atherosclerosis development through local production of inflammatory cytokines. Yet the immune subtypes in PVAT that regulate inflammation are poorly characterized. B cells have emerged as important immune cells in the regulation of visceral adipose tissue inflammation and atherosclerosis. B cell-mediated effects on atherosclerosis are subset-dependent with B-1 cells attenuating and B-2 cells aggravating atherosclerosis. While mechanisms whereby B-2 cells aggravate atherosclerosis are less clear, production of immunoglobulin type M (IgM) antibodies is thought to be a major mechanism whereby B-1 cells limit atherosclerosis development. B-1 cell-derived IgM to oxidation specific epitopes (OSE) on low density lipoproteins (LDL) blocks oxidized LDL-induced inflammatory cytokine production and foam cell formation. However, whether PVAT contains B-1 cells and whether atheroprotective IgM is produced in PVAT is unknown. Results of the present study provide clear evidence that the majority of B cells in and around the aorta are derived from PVAT. Interestingly, a large proportion of these B cells belong to the B-1 subset with the B-1/B-2 ratio being 10-fold higher in PVAT relative to spleen and bone marrow. Moreover, PVAT contains significantly greater numbers of IgM secreting cells than the aorta. ApoE$^{-/-}$ mice with B cell-specific knockout of the gene encoding the helix-loop-helix factor Id3, known to have attenuated diet-induced atherosclerosis, have increased numbers of B-1b cells and increased IgM secreting cells in PVAT relative to littermate controls. Immunostaining of PVAT on human coronary arteries identified fat associated lymphoid clusters (FALCs) harboring high numbers of B cells, and flow cytometry demonstrated the presence of T cells and B cells including B-1 cells. Taken together, these results provide evidence that murine and human PVAT harbor B-1 cells and suggest that local IgM production may serve to provide atheroprotection.

Keywords: B cells, IgM, atherosclerosis, inflammation, perivascular adipose tissue, fat associated lymphoid clusters

INTRODUCTION

Atherosclerosis, a chronic inflammatory disease of arteries, is the major underlying cause of cardiovascular disease (CVD). Atherosclerosis develops when low density lipoprotein (LDL) enters the artery wall, becomes oxidized. Products of oxidized lipids are highly reactive and modify self-molecules, thereby generating structural neo-epitopes that are recognized by receptors of the immune system, including scavenger receptors on macrophages leading to foam cell formation. These neo-epitopes are termed oxidation specific epitopes (OSEs) and represent a common set of epitopes present on various oxidatively modified self-proteins and lipids (Chou et al., 2008; Miller et al., 2011). OSEs, including oxidized phospholipids (OxPLs) and malondialdehyde (MDA)-modified amino groups, have also been documented on the surface of apoptotic cells and microvesicles (Chang et al., 2004; Miller et al., 2011; Tsiantoulas et al., 2015). Oxidized LDL (OxLDL) and foam cells promote inflammatory cytokine production and endothelial cell adhesion molecule expression, leading to recruitment of inflammatory cells such as, monocytes, T cells, natural killer cells, natural killer T cells, and dendritic cells into the intima, fueling lesion formation (Hansson and Hermansson, 2011; Wigren et al., 2012; Binder et al., 2016).

B cells have emerged as important immune cells in the regulation of atherosclerosis. B cells regulate immune responses by secreting antibodies and cytokines (Srikakulapu and McNamara, 2017) and can be divided into B-1 and B-2 subtypes. B-2 cells are abundant in secondary lymphoid organs (SLOs), play a major role in adaptive immune responses and are thought to promote atherosclerosis. In contrast, B-1 cells, the major source for natural IgM secretion in the body (Corte-Real et al., 2009; Holodick et al., 2010; Choi et al., 2012), produce IgM to OSE on OxLDL and provide innate immune protection from diet-induced atherosclerosis in mice (Kyaw et al., 2011; Rosenfeld et al., 2015).

Obesity is an important risk factor for CVD. Notably, obesity-induced metabolic dysfunction in adipose tissue depots is linked to inflammation (Fuster et al., 2016). Macrophages infiltrate expanding adipose tissue in response to chemokines produced by adipose tissue in high fat diet-fed mice (Amano et al., 2014; Bai and Sun, 2015; Kaplan et al., 2015), and promote further inflammation through the production of inflammatory cytokines. B-1 and B-2 cells are also present in murine and human adipose tissues and have recently been found to produce immunoglobulins within viceral and subcutanoues adipose tissues, suggesting a mechanism whereby they may participate in regulation of adipose tissue inflammation (Winer et al., 2011; Harmon et al., 2016). B-1 cells in visceral adipose tissue attenuated high fat diet-induced macrophage production of inflammatory cytokines such as, tumor necrosis factor-alpha (TNFα) and monocyte chemoattractant protein-1 (MCP-1) (Harmon et al., 2016). We identified Inhibitor of differentiation-3 (Id3), a basic helix-loop-helix (bHLH) protein that inhibits E-proteins binding to DNA to regulate transcription as an inhibitor of B-1 cell number and IgM production in visceral adipose tissue (Harmon et al., 2016).

In addition to subcutaneous and visceral adipose tissue, adipose tissue surrounds major blood vessels and is called perivascular adipose tissue (PVAT). Historically, PVAT has been thought to function in blood vessel support. However, emerging literature support a role for PVAT in other biological processes such as, maintaining vasomotar tone (Nosalski and Guzik, 2017). Moreover, PVAT contains immune cells such as, macrophages, T cell subsets, NK cells, and dendritic cells (Guzik et al., 2007; Chan et al., 2012; Moore et al., 2015; Wensveen et al., 2015; Mikolajczyk et al., 2016), produces both pro-inflammatory and anti-inflammatory cytokines and has been shown to regulate atherosclerosis in mice (Gustafson, 2010; Rajsheker et al., 2010; Manka et al., 2014). Recently, Moro K et al, discovered lymphoid aggregates in the adipose tissue of normal healthy mice, termed fat associated lymphoid clusters (FALCs) (Moro et al., 2010). Recently, Newland SA et al, have shown the presence of FALCs in peri-aortic adipose tissue of 80 weeks old $ApoE^{-/-}$ mice and these FALCs harbored high numbers of B cells and T cells (Newland et al., 2017). Consistent with these murine findings, PVAT adjacent to human atherosclerotic arteries is more inflamed than PVAT adjacent to normal arteries (Henrichot et al., 2005). Yet, whether FALCs are available in human PVAT near coronary arteries is unknown. We hypothesized that B-1 cells are present in mouse and human PVAT and produce anti-inflammatory IgM in this depot. We further hypothesized that Id3 is an important regulatory factor for B-1 accumulation in PVAT.

In this study, we characterized B cell composition in murine and human PVAT. We provide the first evidence that PVAT contains the majority of artery-associated B cells at homeostasis and in response to Western diet (WD). Moreover, in comparison to other B cell niches, PVAT contains an enriched population of B-1 cell subsets that produce IgM to OSE. Furthermore, we identified Id3 as a critical transcription factor regulating PVAT B-1b cell number. Taken together with previous studies implicating B-1 cells in inhibiting inflammation and providing atheroprotection (Rosenfeld et al., 2015; Harmon et al., 2016), these results suggest that mechanisms to boost B-1b cell antibody production in the PVAT may have important therapeutic implications in early prevention of atherosclerosis.

MATERIALS AND METHODS

Animals

All animal protocols were approved by the Animal Care and Use Committee at the University of Virginia. Apolipoprotein E deficient ($ApoE^{-/-}$) mice were purchased from Jackson Laboratory and maintained in our animal facility (University of Virginia). $Id3^{fl/fl}$ mice were a generous gift from Dr. Yuan Zhang (Duke University). $CD19^{Cre/+}$ mice were provided by Timothy Bender (University of Virginia). $Id3^{fl/fl}$ mice were bred to the $ApoE^{-/-}$ line and then with $CD19^{Cre/+}$ mice to develop B cell specific Id3 knockouts and littermate controls ($ApoE^{-/-}Id3^{WT}$: $ApoE^{-/-}.CD19^{+/+}.Id3^{fl/fl}$ and $ApoE^{-/-}Id3^{BKO}$: $ApoE^{-/-}.CD19^{Cre/+}.Id3^{fl/fl}$) as previously described (Perry et al., 2013). All purchased mice were on C57BL/6J background and those bred were backcrossed

to C57BL/6J mice for 10 generations. All mice were given water *ad libitum* and standard chow diet (Tekland, 7012). Mice were euthanized with CO_2 inhalation. Young (8–10 weeks) male mice were used for all experiments except for atherosclerosis studies. For atherosclerosis studies, $ApoE^{-/-}$ mice were maintained on WD (42% fat, Tekland, 88137) for 12 weeks.

Human Samples

Patients were recruited through the Heart Transplantation Surgery Clinic at the University of Virginia. This study was carried out in accordance with the recommendations of the National Commission for the Protection of Human Subjects of Biomedical and Behavioral Research, Institutional Review Board for Health Sciences Research (IRB-HSR) at the University of Virginia with written informed consent from all subjects. All patients provided informed written consent prior to participation in this study. The protocol was approved by the IRB-HSR at the University of Virginia. Right coronary artery (RCA) and left anterior descending (LAD) artery and PVAT around RCA and LAD were collected from explanted heart. RCA and LAD arteries were collected for IHC experiments. The stromal vascular fraction was isolated from PVAT around coronary arteries, as described in detail below, for flow cytometry analysis. Peripheral blood mononuclear cells (PBMC) were additionally isolated from whole blood for flow cytometry experiments.

Flow Cytometry

Spleen and bone marrow (BM) cells were harvested and single cell suspensions were prepared as previously described (Srikakulapu et al., 2016). In brief, cell suspension from spleen was prepared using a 70 μm cell strainer and mashing spleen with a syringe plunger, and dissolved in FACS buffer. To isolate BM cells, femur and tibia were collected and flushed with FACS buffer. Spleen and BM samples were re-suspended in erythrocyte lysis buffer and washed. To harvest aorta and PVAT, first, para aortic lymph nodes were carefully removed and then aorta was carefully harvested without having any contamination of PVAT. Aorta and PVAT were collected into 5 ml FACS tubes separately, 2 ml of freshly prepared enzyme cocktail mixture [Collagenase I (450 U/ml) (Sigma), Collagenase XI (125 U/ml) (Sigma), Hyaluronidase I (60 U/ml) (Sigma), DNase (60 U/ml) (Sigma) in PBS with 20 mM HEPES] was added per sample. Samples were chopped into small pieces and then incubated in a shaking incubator at 37°C for 45 min to obtain single cell suspensions. Cells were blocked for Fc receptors by Fc block (CD16/32) for 10 min on ice, and were stained for cell surface markers using fluorescently conjugated antibodies for 30 min on ice. After washing and centrifugation, cells were stained with streptavidin—APC eFluor 780 for 15 min on ice. Cells were washed in PBS and stained with a fixable live/dead stain diluted in PBS for 15 min on ice and then fixed in 2% PFA in PBS for 10 min at room temperature prior to re-suspending in FACS buffer (PBS containing 1% BSA and 0.05% NaN_3) or sorting buffer (PBS containing 1% BSA) for cell sorting experiments. Flow cytometry antibodies: CD45 (30-F11), CD19 (1D3), B220/CD45R (RA3-6B2), CD5 (53-7.3), CD43 (S7), IgD (11-26.2a), and IgM (II/41, R6-60.2) were purchased from eBioscience, BD Bioscience, and Biolegend. Live/Dead discrimination was determined by LIVE/DEAD fixable yellow staining (Invitrogen) or DAPI (Sigma-Aldrich). Flow cytometry for human PBMCs was performed as published before (Rosenfeld et al., 2015). Human fat (PVAT) was processed as published before (Zimmerlin et al., 2011). In brief, PVAT was placed in PBS supplemented with 5.5 mM glucose and 50 μg/ml gentamicin and processed immediately. One gram of PVAT was minced and digested in 3 ml digestion buffer [PBS + 1% BSA (Gemini) + 2.5 g/L Collagenase II (Worthington)] in a shaking incubator at 37°C for 15 min. After digestion, enzyme reaction was stopped by adding PBS containing 0.1% BSA and 1 mM EDTA. Stromal vascular fraction was then passed through 425 and 180 μm sieves (WS Tyler), and finally through 40 μm filter (BD Falcon). The remaining stromal vascular fraction was stained for flow cytometry. Flow cytometry antibodies: CD45 (2D1), CD20 (L27), CD3e (5KY), CD27 (M-T271), CD43 (84-3C1) were purchased from eBioscience and BD Bioscience. Cells were run on a CyAN ADP (Beckman Coulter) or sorted on an Influx Cell Sorter (Benton-Dickenson). Data were analyzed with FlowJo software (Tree Star inc). All gates were determined using fluorescence minus one (FMO) controls.

Enzyme-Linked Immunospot (ELISPOT) Assay

Single cell suspensions of aorta, PVAT, spleen and BM were prepared as described above in the flow cytometry section. ELISPOT was performed as previously described (Rosenfeld et al., 2015; Srikakulapu et al., 2016). Sterile MultiScreen IP-Plates (Millipore, MSIPS4510) were used for the assay according to manufacturer's protocol. Wells were coated with unlabeled goat anti-mouse IgM antibody (10 μg/ml; Southern Biotech) or malondialdehyde-modified low density lipoprotein (MDA-LDL) (10 μg/ml) and incubated overnight at 4°C. The following day, antibody solution was decanted, membrane was washed with PBS and then blocked with RPMI 1640+10% FCS for 2 h at 37°C. A suspension of 1×10^6 cells / ml was prepared in ice cold culture media for spleen and BM from which 250,000 cells were plated for each of the sample as starting concentration and then were serially diluted in subsequent wells. For aorta and PVAT samples, total sample resuspended in 250 μl culture media and were used as starting concentration from which serial dilutions in subsequent wells were prepared. The plate was incubated overnight at 37°C in a cell culture incubator (5% CO_2). Cells were decanted, washed (PBS+0.01% tween-20) and incubated with biotin-labeled goat anti-mouse IgM antibody (1:500 dilution; Southern Biotech) for 2 h in a cell culture incubator. After washing, cells were incubated for 30 min at room temperature in streptavidin alkaline phosphatase (Abcam). Again following washing BCIP/NBT (Gene Tex Inc.) was added and incubated until spots became visible. Each spot on the membrane indicated an antibody secreting cell. Wells were imaged under a dissecting microscope (Zeiss) then spots were counted manually.

Enface Staining

Aortas were isolated as mentioned above in the flow cytometry section. Aortas were opened longitudinally, fixed in 4% formaldehyde, pinned, and stained with Sudan IV (Sigma). Aortas were imaged with a Nikon D70 DSLR camera.

Histology

Oil red O and Hematoxylin staining was performed as published before (Rosenfeld et al., 2015). Briefly, OCT blocks were prepared for aorta samples with PVAT and without PVAT, sectioned (5 μm) and stored at −80°C. At the time of staining, sections were fixed with 4% formalin for 5 min, 60% isopropanol for 5 min and then stained with Oilred O (O0625, Sigma) for 10 min. After staining, sections were washed briefly in tap water and stained with hematoxylin for 4 min. After washing, sections were mounted with aqueous Vecta mount (H-5501, Vector). Hematoxylin and eosin staining was performed in human coronary artery sections. First, slides were de-paraffinized and hydrated through two changes of xylene, 100, 95% ethanol, and one change of 70% ethanol by incubating slides for 5 min in each change. Slides were rinsed with two changes of distilled tap water and stained with Hematoxylin for 5 min. After rinsing, bluing was performed in Ammonia water. After rinsing, slides were incubated in 70% ethanol and stained with Eosin for 10 min. Slides were dehydrated through three changes of 100% ethanol, followed by two changes of Xylene, 5 min each. Slides were mounted with aqueous clear mounting media. Images were taken using Olympus Hi-Mag microscope.

Multiplex Immuno Histo Chemistry (IHC)

The Opal Multiplex Manual IHC Kit (PerkinElemer, Waltham, MA) was used to perform IHC staining. Tonsil and normal lymph node specimens were used as positive and negative staining controls. Single stained slides were also generated for use in spectral unmixing. Staining was performed according to the manufacturer's protocol; however, slides were allowed to cool for 30 min at room temperature post microwaving in Antigen Retrieval (AR) buffer. To facilitate continuation of staining, slides were stored overnight in AR buffer at 4°C. Staining sequence and antibodies: AR9—CD8 (dilution 1:500, Dako, Santa Clara, CA)—Opal540, AR6—CD20 (1:1000, Dako)—Opal520, AR6—PNAD (1:1000, BD Biosciences, Franklin Lakes, NJ)—Opal620 and AR6—DAPI for nuclear staining. Slides were mounted used Prolong diamond antifade (Life Technologies, Carlsbad, CA). Pictures were taken with Vectra microscope (PerkinElemer).

Statistics

Student's *t*-test was used for analyzing data with normal distribution and equal variance. For data sets with unequal variance, *t*-test with Welch's correction was used. Repeated measures one way ANOVA with Bonferroni's multiple comparison post-test was used to compare multiple groups. Results are displayed containing all replicated experiments, and values shown are mean ± SEM. Data were analyzed using Prism 5 (GraphPad Software, Inc).

RESULTS

PVAT Is the Predominant Source of Aortic-Associated B Lymphocytes

To determine the predominant location of aortic-associated B cells in atherosclerosis-prone mice at homeostasis, flow cytometry was performed in young ApoE$^{-/-}$ mice (8 weeks old) fed normal Chow diet. Aorta, from the arch to the iliac bifurcation was carefully dissected to retain the adventitia excluding PVAT. Oil-red O/ hematoxylin staining of aorta cross sections confirmed that the dissected aorta retained the adventitia but no PVAT (**Figure 1A**). Flow cytometry revealed greater numbers of CD19^{+} B cells, CD5^{+} T cells and double negative cells (DN: CD19^{-} CD5^{-}) in the PVAT compared to the aorta (**Figure 1B**). Lymphocytes (B and T) made up a greater percentage of the total leukocytes (CD45^{+}) in the PVAT compared to the aorta. In contrast, DN cells made up a greater percentage of CD45^{+} cells in the aorta compared to the PVAT, although PVAT still contained large numbers of DN cells (**Figure 1B**). Next, to determine the effect of WD and atherosclerosis development on B and T cells in aorta and PVAT, 8 week old ApoE$^{-/-}$ mice were fed 12 weeks of WD and flow cytometry for B and T cells was performed. Sudan IV staining for atherosclerosis lesions in 8 and 20 weeks old mice confirmed atherosclerosis development in the ApoE$^{-/-}$ mice fed 12 weeks of WD but not in 8 week old Chow fed ApoE$^{-/-}$ mice (**Figure 1C**). The percentage of CD45^{+} cells that are B and T cells was significantly higher in the PVAT than in the aorta in both Chow fed and 12 weeks WD fed mice (**Figure 1D**).

B Cells Reside in Human Coronary Artery PVAT

To determine if human PVAT contains FALCs, coronary arteries from human hearts explanted at the time of heart transplantation were sectioned and stained with eosin and hematoxylin. Microscopic examination of these sections revealed that in addition to scattered lymphocytes throughout the PVAT, the PVAT also contained FALCs in the PVAT close to the diseased coronary artery (**Figure 2A**). Next, we performed multiplex IHC to determine what type of cells and structures are located in these FALCs. The majority of the immune cells in human FALCs were CD20^{+} B cells (**Figure 2B**). These FALCs also harbored few numbers of CD8^{+} T cells (**Figure 2B**), FoxP3^{+} regulatory T cells and proliferating Ki67^{+} cells (data not shown). In addition, FALCs in human coronary PVAT contained structures of PNAD^{+} high endothelial venules (HEV) (**Figure 2B**), which are important for lymphocyte recruitment into lymphoid tissues (Girard and Springer, 1995).

To quantify immune cell subtypes in human coronary artery PVAT, a large segment of PVAT from the coronary arteries of human hearts explanted at the time of heart transplantation was harvested and analyzed by flow cytometry. Blood was analyzed as a comparator. Total CD20^{+} B cells, CD3^{+} T cells and DN (CD20^{-} CD3^{-}) non B and T cells were gated from total CD45^{+} live cells (**Figure 3A**). Results demonstrated that PVAT near coronary arteries contain B cells, T cells, and DN cells

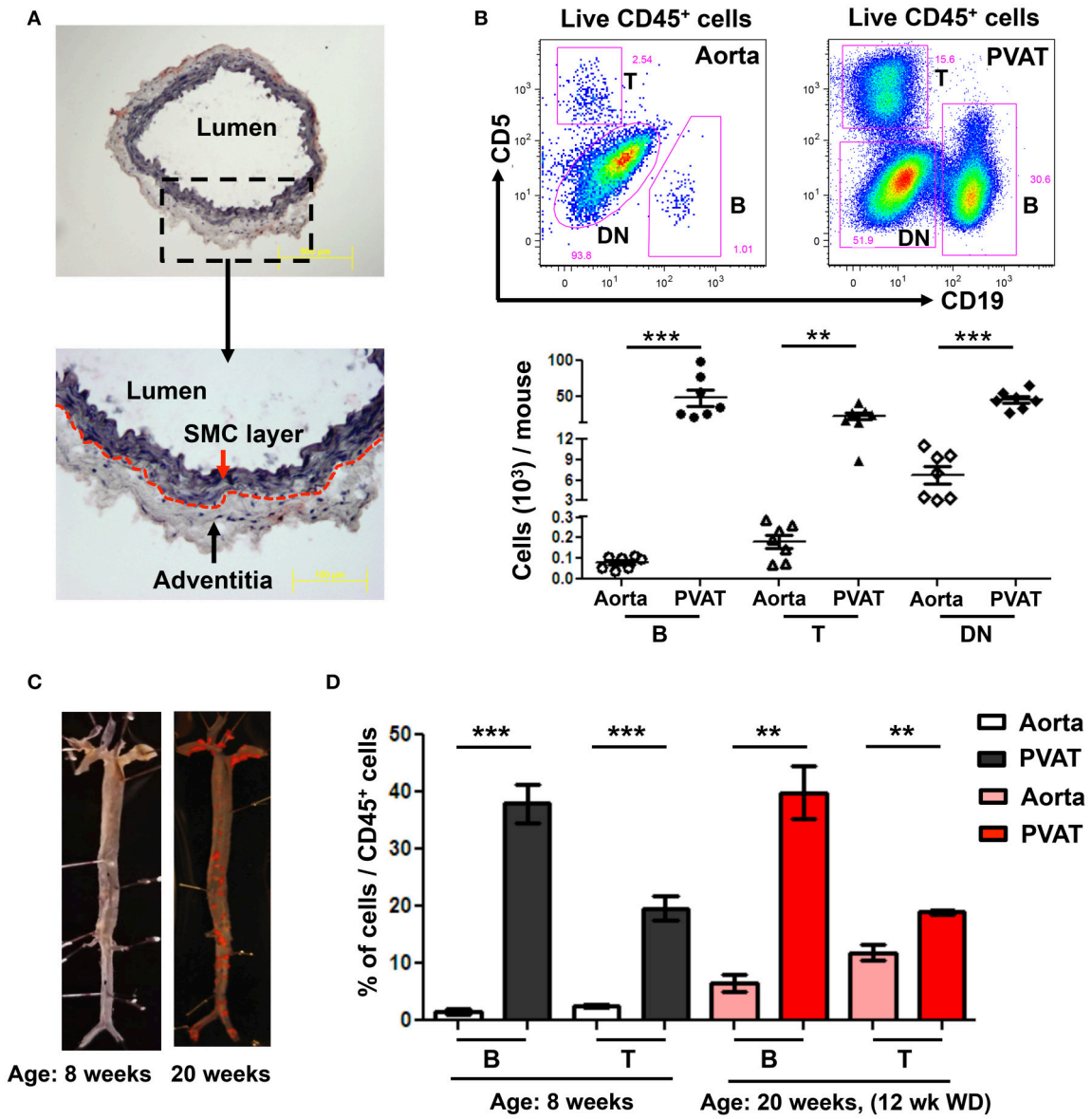

FIGURE 1 | High numbers of B and T cells are harbored in perivascular adipose tissue (PVAT). **(A)** Aorta (without PVAT) of young ApoE$^{-/-}$ mice was carefully dissected, stained with OilRedO and Hematoxylin. Dotted line represents the border between smooth muscle cell (SMC) and adventitial layers. **(B)** CD19^{+} B cells, CD5^{+} T cells and CD5 and CD19 double negative (DN) non T and B cells were gated from total live CD45^{+} cells and these B, T and DN subsets were quantified in aorta and PVAT of 8–10 weeks old ApoE$^{-/-}$ mice fed normal Chow diet by flow cytometry. **(C)** Representative Sudan IV staining of aortas collected from Chow-fed ApoE$^{-/-}$ mice at 8 weeks and 20 weeks (maintained on Western diet (WD) for the last 12 weeks) of age. **(D)** Quantification of the percent of leukocytes (CD45^{+}) in the aorta and PVAT of these 8 weeks ($n = 7$) and 20 weeks ($n = 3$) old ApoE$^{-/-}$ mice that were CD19^{+} B cells and CD5^{+} T cells. Results are mean ± SEM, unpaired student t-test was performed (**$p < 0.01$, ***$p < 0.001$).

(**Figures 3B–D**). This finding is not due to blood contamination as the percentage of T cells is actually lower and the percentage of DN cells is higher in the WB (**Figures 3C,D**). Quantification of lymphocyte numbers (B and T cells) per gram of fat revealed equivalent numbers in PVAT from LAD and RCA (**Figures 3E,F**). In contrast to murine aortic PVAT that was dissected down to the region directly abutting the adventitia (**Figures 1B,D**), the majority of the lymphocytes in the human PVAT removed without care to include the peri-adventitial area where FALC are present were T cells (**Figures 3C,F**). B cells were also present and of these nearly 7–8% were B-1 cells (**Figure 3G**).

B-1 Cells Are Enriched in PVAT and Secrete IgM Locally

We returned to our murine model where we are able to carefully dissect all the PVAT down to the adventitial interface (**Figure 1A**) to further subset the B cells in the aorta and PVAT and to determine if IgM can be locally produced. Aorta and

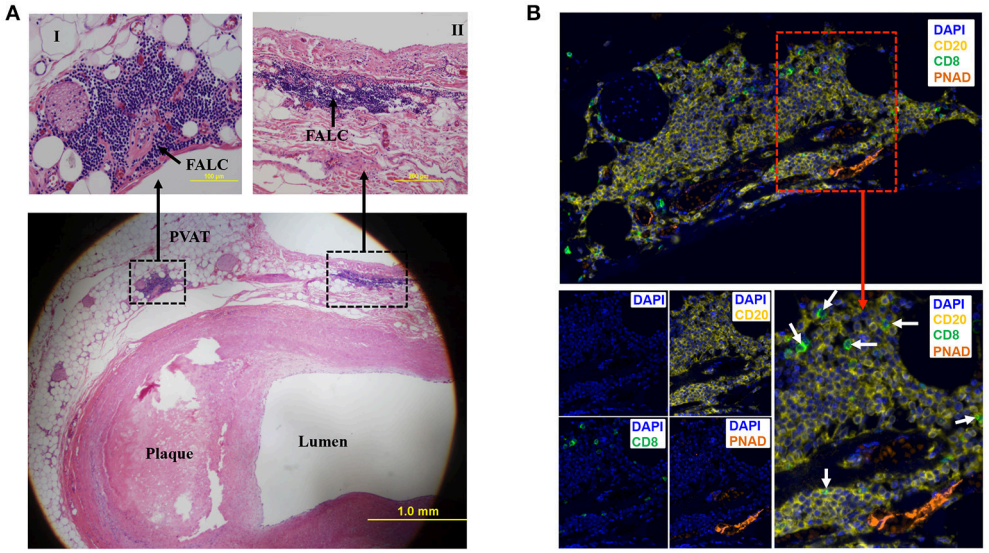

FIGURE 2 | Fat associated lymphoid clusters (FALCs) in human coronary artery PVAT. **(A)** Sections of diseased human coronary artery including PVAT ($n = 1$) were stained with hematoxylin and eosin. FALCs were identified in the PVAT adjacent to coronary artery. High magnification of FALCs (I and II) regions are indicated in dotted box. **(B)** Consecutive sections of hematoxylin stained slides were used for multiplex IHC staining ($n = 1$). $CD20^+$ B cells, $CD8^+$ T cells and $PNAD^+$ high endothelial venules were observed in FALC. $CD8^+$ T cells were marked with white arrows (merged lower left picture). DAPI stains for nuclear DNA.

PVAT were carefully separated and flow cytometry to identify B cell subtypes was performed. B-1 ($CD19^+$ $B220^{lo\text{-}mid}$) and B-2 ($CD19^+$ $B220^{hi}$) cells were confirmed based on surface expression of IgD and CD43 (**Figure 4A**). Significantly greater numbers of both B-1 and B-2 cells were present in PVAT compared to the aorta (**Figure 4B**). Notably, while B-2 cells are the predominant B cell subtype in the spleen and bone marrow (Srikakulapu and McNamara, 2017), there was a >10-fold higher B-1/B-2 ratio in PVAT compared to these lymphoid organs (**Figure 4C**). In mice, B-1 cells are divided into B-1a and B-1b based on surface expression of CD5 (**Figure 4D**). Flow cytometry revealed small numbers of B-1a and B-1b cells in the aorta. In contrast, significantly higher numbers of both subsets were present in the PVAT (**Figure 4D**). To determine whether these B cells are capable of antibody production in aorta and PVAT, ELISPOT experiments were performed. Very low numbers of IgM secreting cells were in aorta. In contrast, there were abundant IgM secreting cells in PVAT (**Figure 4E**).

B Cell Specific Id3 Deficiency Increases B-1b Cell Numbers and MDA-LDL Specific IgM Production in PVAT

Next, to determine the effect of B cell specific Id3 deficiency on B cells in PVAT, B cell subsets in PVAT of young (8–10 weeks) $ApoE^{-/-}Id3^{WT}$ and $ApoE^{-/-}Id3^{BKO}$ mice were quantified by flow cytometry. There was no difference in total B cell and B-2 cell numbers. However, there was a trending increase in number of B-1 cells as well as B-1/B-2 ratio in the PVAT of $ApoE^{-/-}Id3^{BKO}$ mice compared to $ApoE^{-/-}Id3^{WT}$ control mice (**Figures 5A–C**). Notably, while B-1a cell numbers trended to be lower, B-1b cells were significantly greater in PVAT of $ApoE^{-/-}Id3^{BKO}$ mice compared to $ApoE^{-/-}Id3^{WT}$ control group mice (**Figure 5D**). ELISPOT data demonstrated increased numbers of IgM secreting cells in the PVAT of $ApoE^{-/-}Id3^{BKO}$ compared to $ApoE^{-/-}Id3^{WT}$ mice (**Figure 5E**). To determine how much of this IgM recognized specific OSE, ELISPOT for MDA-LDL-specific IgM was performed in spleen, BM and PVAT of $ApoE^{-/-}Id3^{WT}$ and $ApoE^{-/-}Id3^{BKO}$ mice. Interestingly, there was a significantly higher percentage of MDA-LDL-specific IgM observed in the PVAT but not in spleen and BM of $ApoE^{-/-}Id3^{BKO}$ mice compared to $ApoE^{-/-}Id3^{WT}$ control mice (**Figure 5F**), suggesting that local MDA-LDL from the aorta or PVAT in the context of greater B-1b cell numbers may lead to enhanced production of MDA-LDL specific IgM.

DISCUSSION

PVAT inflammation promotes atherosclerosis in the underlying vessel through "outside-in" signaling (Brown et al., 2014; Omar et al., 2014; Konaniah et al., 2017). Adipocyte-derived MCP-1 (Manka et al., 2014) and low-density lipoprotein receptor-related protein-1 (Konaniah et al., 2017) are two of the factors that have been implicated in promoting PVAT inflammation. However, immune cell composition of the PVAT at homeostasis and in response to atherosclerosis and molecular mechanisms that regulate the proportion of pro- and anti-inflammatory immune cell subsets are poorly understood. Here, we provide the first evidence that the immune cell composition of the PVAT of young (8–10 weeks), Chow fed $ApoE^{-/-}$ mice is distinct from that of the aorta, with PVAT harboring higher numbers of leukocytes, notably B and T lymphocytes. In contrast, aorta primarily contains $CD45^+$ non B and T

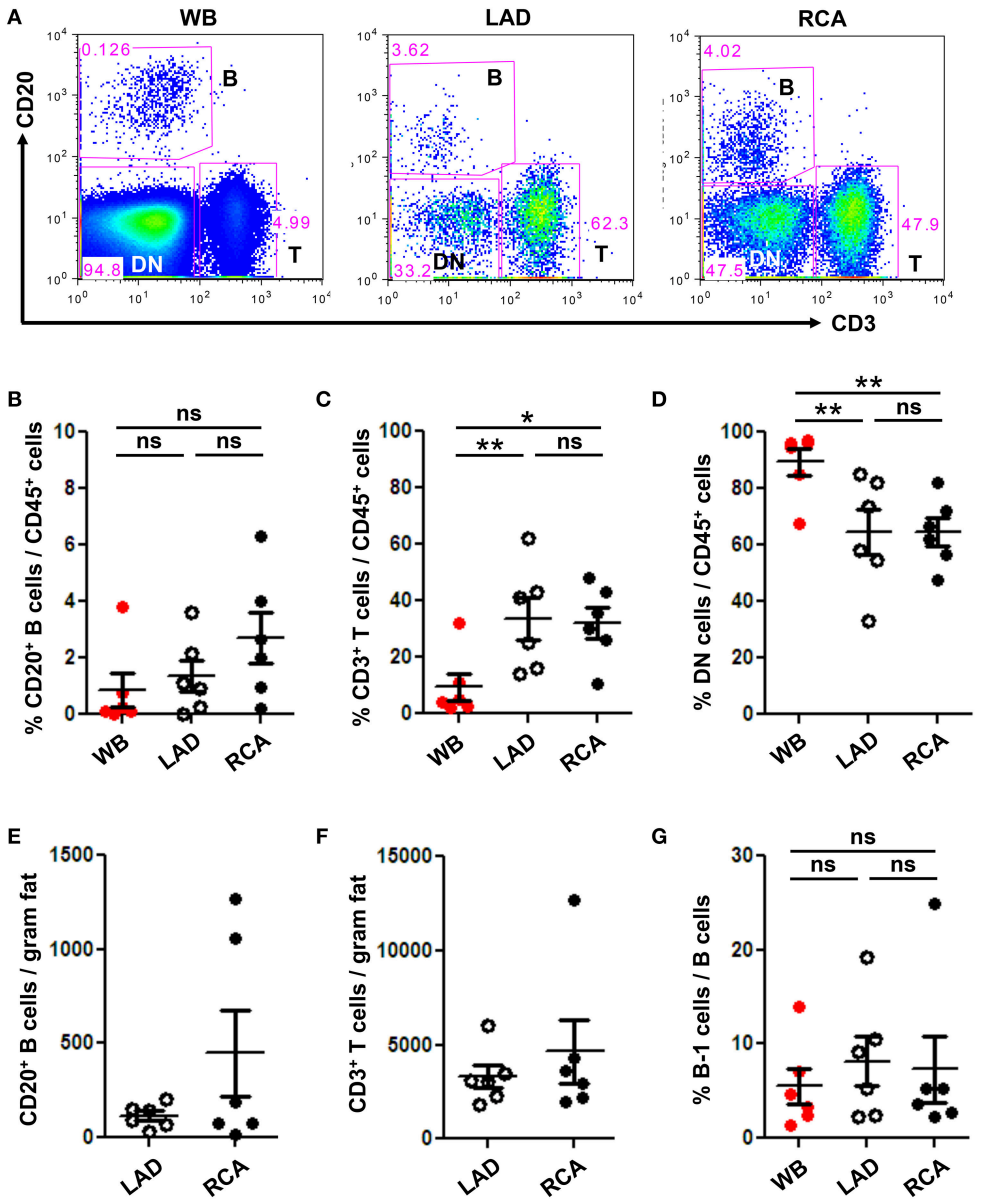

FIGURE 3 | B and T cells reside in human coronary artery PVAT. Coronary artery PVAT from human hearts ($n = 6$) explanted at the time of heart transplantation was analyzed by flow cytometry. **(A)** Gating strategy of B cells ($CD20^+$), T cells ($CD3^+$), and DN ($CD45^+$ non B and T cells) in whole blood (WB), PVAT near LAD, and RCA for flow cytometry. Percentages of **(B)** B cells, **(C)** T cells, and **(D)** DN cells from total $CD45^+$ cells were quantified in PVAT from the LAD and RCA, and WB as a comparator. Total number of **(E)** B cells and **(F)** T cells per gram adipose tissue was quantified. **(G)** Quantification of the percentage of B cells that were B-1 ($CD20^+$ $CD27^+$ $CD43^+$). Results are mean ± SEM, unpaired student *t*-test was performed. Repeated measures one way ANOVA with Bonferroni's multiple comparison post-test was used to compare multiple groups (*$P < 0.05$, **$P < 0.01$).

cells at steady state. Previous studies have demonstrated that macrophages are abundant in the $CD45^+$ non B and T cell compartment in the aorta of Chow fed $ApoE^{-/-}$ mice (Galkina et al., 2006). Recent studies report that resident macrophages ($CD11b^+F4/80^+CD115^+Lyve\text{-}1^+$) in the aorta are derived from yolk sac and fetal liver during development and these resident macrophages have self-renewal capacity and maintain tissue homeostasis in steady state. In response to inflammatory signals, inflammatory macrophages ($CD11b^+F4/80^+CD115^-Lyve\text{-}1^-$) from BM, are recruited into the aorta (Ensan et al., 2016). Consistent with this, WD fed $ApoE^{-/-}$ mice have a marked increase in activated macrophages in the aorta (Galkina et al., 2006). There is also an increase in B and T cells in the aorta of WD fed mice (Galkina et al., 2006). However, the predominance of lymphocytes in the PVAT compared to aorta persisted after WD (**Figure 1D**), suggesting that PVAT lymphocytes play key roles in both tissue homeostasis and in regulating inflammation due to lipid deposition in the artery

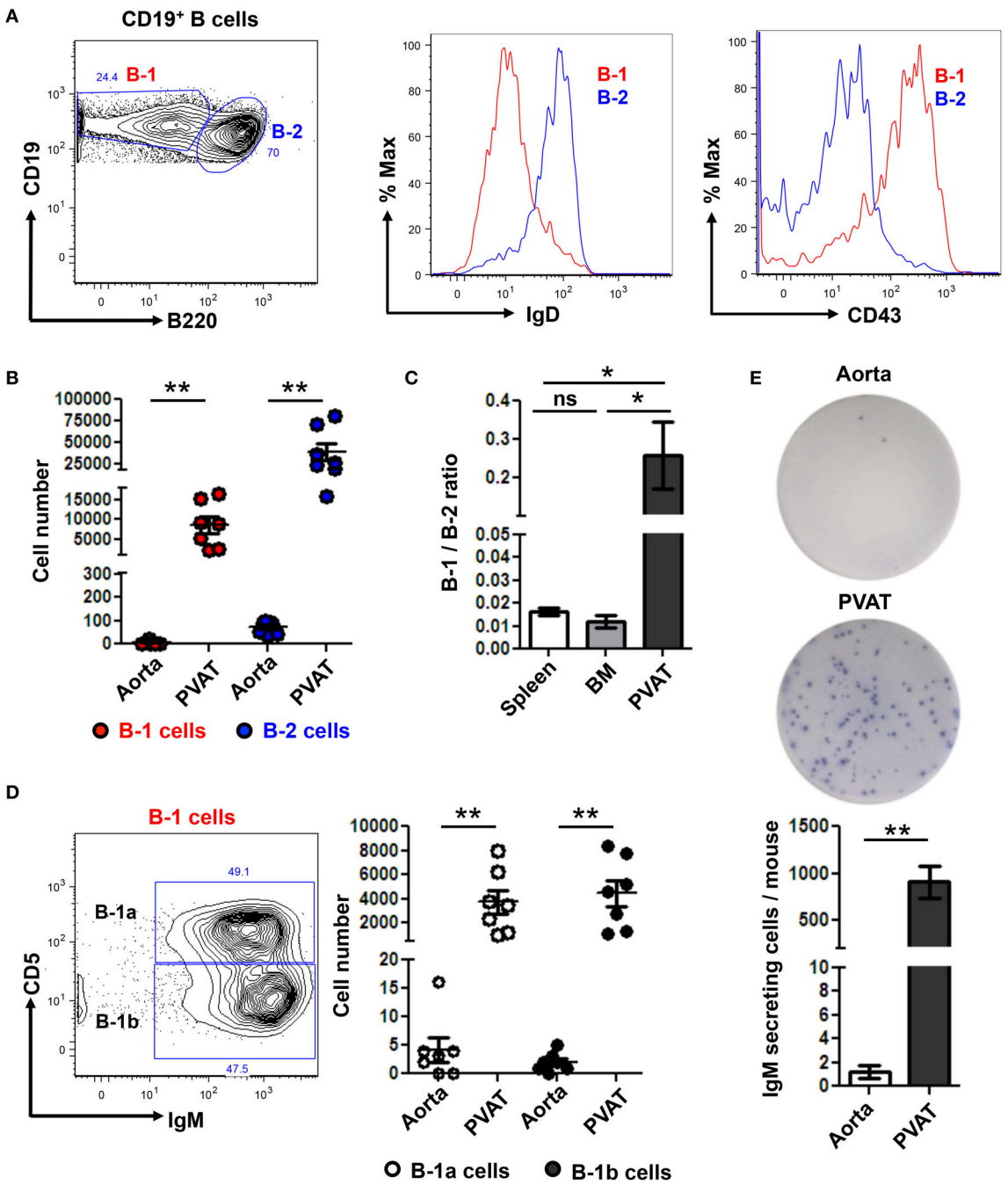

FIGURE 4 | IgM secreting B-1 cells reside in PVAT. **(A)** Gating strategy of B-1 ($CD19^+$, $B220^{lo\text{-}mid}$) and B2 ($CD19^+$, $B220^{hi}$) cells. B-1 (IgD^- $CD43^+$) and B-2 (IgD^+ $CD43^-$) cells were further confirmed based on surface expression of IgD and CD43. **(B)** Quantification of total numbers of B-1 and B-2 cells in the aorta and PVAT. **(C)** Comparative ratio of B-1 to B-2 cells in spleen, bone marrow (BM) and PVAT. **(D)** B-1a and B-1b cells were gated from total B-1 cells and absolute numbers were quantified in aorta and PVAT of young $ApoE^{-/-}$ mice. **(E)** IgM antibody production was measured by ELISPOT in aorta and PVAT of Chow diet fed young $ApoE^{-/-}$ mice ($n = 7$) (representative plate and quantitation). Results are mean ± SEM, unpaired student *t*-test was performed. Repeated measures one way ANOVA with Bonferroni's multiple comparison post-test was used to compare multiple groups (*$p < 0.05$, **$p < 0.01$).

wall. Whether lymphocytes in the aorta are recruited from the PVAT and whether lesion immune cell accumulation is regulated by lymphocytes in the PVAT remain important unanswered questions.

Notably, in contrast to the aorta, B cells outnumber T cells in PVAT of $ApoE^{-/-}$ mice. As such, defining B cell subsets in the PVAT may provide important insights into PVAT regulation of inflammation. B cells have been implicated in regulating visceral

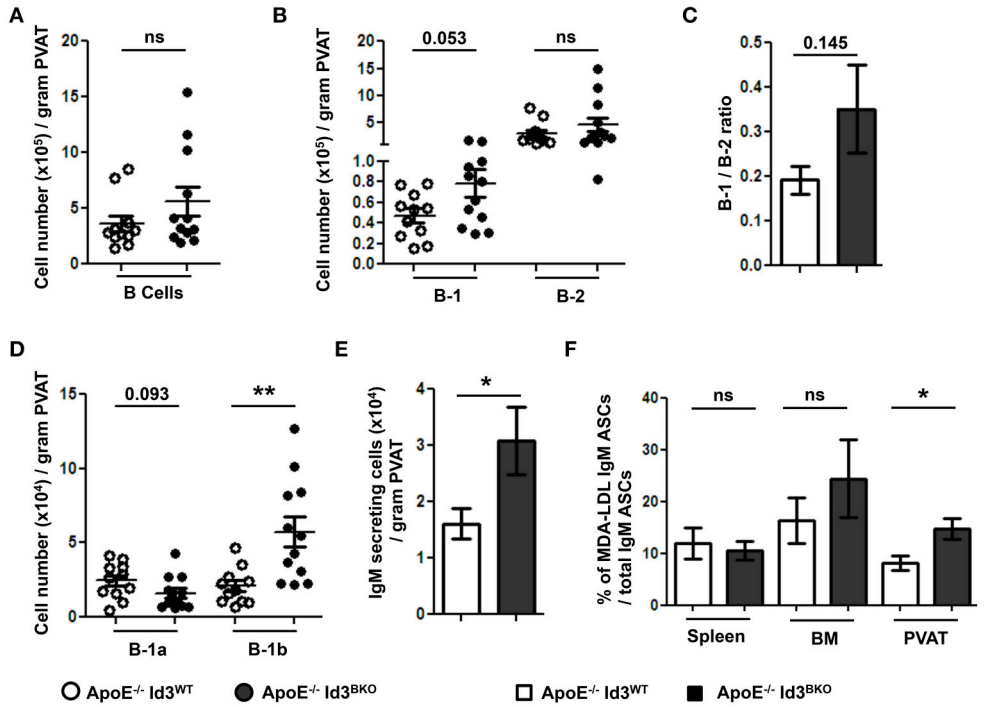

FIGURE 5 | B-1b cells and IgM secreting B cells are increased in the PVAT of mice with B cell specific deletion of Id3 ($ApoE^{-/-}Id3^{BKO}$). Flow cytometry quantification in the PVAT of 8 weeks old $ApoE^{-/-}Id3^{WT}$ ($n = 11$) and $ApoE^{-/-}Id3^{BKO}$ ($n = 12$) mice for **(A)** total $CD19^{+}$ B cells, **(B)** B-1 and B-2 cells, **(C)** B-1/B-2 ratio, **(D)** B-1a and B-1b cells, and **(E)** ELISPOT for total IgM secreting cells. **(F)** Percentage of malondialdehyde modified low density lipoprotein (MDA-LDL) specific IgM secreting cells in spleen, BM and PVAT of $ApoE^{-/-}Id3^{WT}$ ($n = 5$) and $ApoE^{-/-}Id3^{BKO}$ ($n = 4$–5) mice as measured by ELISPOT. Results are mean ± SEM, unpaired student *t*-test was performed (*$p < 0.05$, **$p < 0.01$).

adipose tissue inflammation and its metabolic consequences. B-2 cells worsen insulin sensitivity through their production of IgG (Winer et al., 2011) while B-1 derived natural IgM and regulatory B cell (B_{regs})-derived anti-inflammatory cytokine interleukin −10 (IL-10), attenuate adipose tissue inflammation, glucose intolerance, and improve metabolic syndrome in diet induced obese mice and humans (Nishimura et al., 2013; Harmon et al., 2016). Yet, B cell subset composition of PVAT is relatively unknown. In the present study, we provide the first evidence that, in contrast to other sites that harbor significant B cell accumulation (spleen and BM), the PVAT contains a significantly higher B-1/B-2 ratio suggesting that B cells in PVAT may have anti-inflammatory effects. Of these B-1 cells, there are equal numbers of B-1a and B-1b cells in the PVAT. Both of these B-1 subtypes have been shown to produce atheroprotective IgM and attenuate atherosclerosis in mice (Kyaw et al., 2011; Rosenfeld et al., 2015). Consistent with prior studies that B-1 cells are the predominant source of IgM (Corte-Real et al., 2009; Holodick et al., 2010; Choi et al., 2012), equivalent numbers of cultured B-1 cells from spleen, BM (sites considered to be the main source of B-1 cell-derived IgM) and PVAT produced substantially more IgM than B-2 cells from these same tissues (data not shown).

Previous studies have demonstrated that PVAT differs between species and anatomic location. In rodents, the thoracic aorta is predominantly surrounded by brown adipose tissue, whereas the abdominal aorta is surrounded by a mixture of white and brown adipose tissue (Brown et al., 2014). The expression of genes encoding inflammatory cytokines and infiltrated immune cell markers are greater in PVAT near abdominal aorta than thoracic aorta of rats (Padilla et al., 2013). In addition, our group has reported that radiolabeled splenic B cells, which are predominantly B-2 cells, adoptively transferred to B cell deficient mice were preferentially recruited into the aortic arch and abdominal aortic region. However, no/very low numbers of B cells were recruited into the thoracic aorta region (Doran et al., 2012). Altogether, these reports suggest that PVAT at different parts of the aorta have different immune cell compositions. Future studies are needed to provide more insights into aortic region-specific differences in immune cell composition of PVAT and its impact on region-specific aortic vascular diseases.

There may also be important differences between coronary and aortic PVAT as the adipocytes in these regions are thought to derive from unique embryologic origins and may differ metabolically (Aldiss et al., 2017). This is important as inflammation of the PVAT around coronary arteries has been linked to coronary artery disease pathophysiology. In humans, PVAT thickness around coronary arteries has been associated with coronary artery calcification, cardiovascular risk factors (de Vos et al., 2008), the degree of plaque burden (Iacobellis and Willens, 2009), and stenosis (Verhagen et al., 2012). The number of macrophages in PVAT has been related to the size and characteristics of the atherosclerotic plaque such as, lipid core,

calcification, collagen, and smooth muscle cell content, and to the degree of plaque infiltration by macrophages and lymphocytes (Konishi et al., 2010; Verhagen et al., 2012). In addition, the PVAT near coronary arteries and epicardial adipose tissue has been reported to show high levels of inflammatory cytokines (Mazurek et al., 2003; Chatterjee et al., 2009) and infiltration of leukocytes (Konishi et al., 2010), particularly macrophages and T lymphocytes (Mazurek et al., 2003; Hirata et al., 2011). As such, strategies to modify PVAT inflammation may impact on underlying CVD. This underscores the importance of characterizing human coronary artery PVAT. Our findings demonstrated that, in contrast to our murine aortic findings, T cells outnumbered B cells in the human coronary PVAT analyzed by flow cytometry. Whether this was due to differences in coronary vs. aortic PVAT or murine vs. human PVAT was difficult for us to resolve directly as murine coronary PVAT yields insufficient cells for analysis by flow cytometry and we were unable to take aortic samples from our live subjects donating their explanted hearts at the time of heart transplantation for our human coronary PVAT analysis. Our IHC staining of the human coronary PVAT may provide one explanation to resolve this discrepancy. Consistent with our murine aorta flow cytometry, the predominant lymphocyte that aggregates in FALCs in close proximity to the coronary artery are B cells. It is notable that the PVAT used for the human flow cytometry was not as closely associated with the artery as the FALC. As such, while flow cytometry confirmed that B cells including B-1 were present in human PVAT, future studies utilizing flow cytometry will be needed to analyze the immune composition of human PVAT in close proximity compared to more distant to the coronary artery to help resolve this issue. In addition, further studies to understand site-specific effects of B-1 cells on PVAT inflammation are needed.

We had previously shown that B-1 cell-derived IgM inhibited inflammatory cytokine production by M1 macrophages in visceral adipose tissue and promoted insulin sensitivity in mice (Harmon et al., 2016). Furthermore, B-1 cells and IgM to oxidation-specific epitopes (OSE) on LDL were found in human omental adipose tissue and there was a correlation between omental production and plasma levels of IgM to OSE. Moreover, levels of IgM to OSE inversely correlated with plasma levels of the inflammatory cytokine MCP-1, suggesting that homeostatic immune mechanisms in adipose tissue may dampen both local and systemic inflammatory responses (Harmon et al., 2016). As plasma levels of IgM to OSE are inversely associated with coronary artery disease in humans (Tsimikas et al., 2007, 2012), further studies are needed to determine if PVAT B-1 cell production of IgM to OSE can reduce PVAT inflammation and the atherosclerosis lesion underlying it.

Earlier study from our lab demonstrated that C57BL6 mice with B cell specific Id3 deficiency had greater visceral adipose tissue B-1b cells and IgM production and less adipose tissue inflammation compared to WT littermate controls (Harmon et al., 2016). Here, we demonstrate for the first time that Id3 also regulates the number of B-1b cells in the PVAT. Consistent with the higher number of B-1b cells in ApoE$^{-/-}$Id3^{BKO} compared to control group mice, we demonstrate that ApoE$^{-/-}$Id3^{BKO} mice have significantly greater amounts of IgM in the PVAT. Notably, not only was the amount of total IgM higher, the percentage of IgM that was specific for MDA-LDL was greater in the PVAT of ApoE$^{-/-}$Id3^{BKO} mice compared to littermate controls. Previous studies have demonstrated that circulatory IgM but not IgG to MDA-LDL negatively correlates with angiographically determined coronary artery disease and CV events in humans (Tsimikas et al., 2007, 2012) suggesting a protective role of IgM to MDA-LDL in atherosclerosis. The fact that MDA-LDL specific IgM was greater in PVAT of ApoE$^{-/-}$Id3^{BKO} mice, but not in other major IgM producing sites such as, BM and spleen, raises the interesting possibility that the IgM responses in PVAT may be stimulated by local sources of OSE. While the source of modified LDL in atherosclerotic lesions had been thought to come from the circulation, Uchida et al, recently provided data to support PVAT as a source of OxLDL in human coronary lesions (Uchida et al., 2016). Additional studies are needed to determine if PVAT may be an important source of inflammation stimulating OSE.

Understanding immune modulation of PVAT in mice may provide novel strategies to limit atherosclerosis development in humans. However, direct evaluation of PVAT surrounding human coronary arteries is important for determining if these murine findings may be relevant to human disease. Recent studies have shed light on the role of FALCs in adipose tissue. FALCs develop in both steady state and inflammatory condition (Benezech et al., 2015). It has been shown that, B cells in FALCs secrete IgM and attenuate local inflammation (Jackson-Jones et al., 2016). Recent studies have demonstrated that innate lymphoid cell type-2 derived IL-13 and IL-5 cytokines in PVAT are important to maintain atheroprotective IgM producing B-1 cells in PVAT and attenuate diet induced atherosclerosis (Perry et al., 2013; Newland et al., 2017). However, it is not known whether B and T cells are present in specialized structures like FALCs in the young murine PVAT or whether they are scattered in the entire tissue. The present study demonstrates that PVAT adjacent to diseased coronary artery in humans contains FALCs. Similar to FALCs in mice (Benezech et al., 2015; Newland et al., 2017), FALCs in human PVAT harbors abundant B cells.

In summary, our results provide novel evidence that atheroprotective B-1 cells accumulate in PVAT and secrete natural IgM, particularly MDA-LDL specific IgM. Based on our murine findings that B-1b cells in the adipose tissue regulate M-1 macrophage inflammation (Harmon et al., 2016), we hypothesize that B-1 cells in the PVAT can modulate local inflammation and potentially atherosclerosis development. Further studies are needed to test this novel hypothesis. These studies will be important to do given findings that B-1 cells reside in human PVAT and B cell-rich FALC are closely associated with coronary arteries. These findings may lead to novel strategies targeting PVAT to limit atherosclerosis development.

AUTHOR CONTRIBUTIONS

PS: designed and performed the experiments, acquired and analyzed the data, prepared figures, and wrote the manuscript. AU, SR, MM, CM, AH, and IM performed the experiments.

GA, ML, and AT: provided human samples. CAM: designed the experiments and wrote the manuscript.

FUNDING

Funding for this work was provided by National Heart, Lung, and Blood Institute Grants R01-HL-136098, P01-HL-055798, and R01-HL-107490 (to CAM). We also gratefully acknowledge Jamie Morton and Mimi's Run for raising additional needed funds to support this work.

ACKNOWLEDGMENTS

We thank Dr. Sotirios Tsimikas (University of California, San Diego) for providing MDA-LDL reagent, Jim Garmey from the McNamara laboratory (University of Virginia) for his organizational assistance, Frances Gilbert (University of Virginia) for her organization of our human data and Claude Chew from the University of Virginia flow cytometry core for his excellent technical assistance.

REFERENCES

Aldiss, P., Davies, G., Woods, R., Budge, H., Sacks, H. S., and Symonds, M. E. (2017). 'Browning' the cardiac and peri-vascular adipose tissues to modulate cardiovascular risk. *Int. J. Cardiol.* 228, 265–274. doi: 10.1016/j.ijcard.2016.11.074

Amano, S. U., Cohen, J. L., Vangala, P., Tencerova, M., Nicoloro, S. M., Yawe, J. C., et al. (2014). Local proliferation of macrophages contributes to obesity-associated adipose tissue inflammation. *Cell. Metab.* 19, 162–171. doi: 10.1016/j.cmet.2013.11.017

Bai, Y., and Sun, Q. (2015). Macrophage recruitment in obese adipose tissue. *Obes. Rev.* 16, 127–136. doi: 10.1111/obr.12242

Benezech, C., Luu, N. T., Walker, J. A., Kruglov, A. A., Loo, Y., Nakamura, K., et al. (2015). Inflammation-induced formation of fat-associated lymphoid clusters. *Nat. Immunol.* 16, 819–828. doi: 10.1038/ni.3215

Binder, C. J., Papac-Milicevic, N., and Witztum, J. L. (2016). Innate sensing of oxidation-specific epitopes in health and disease. *Nat. Rev. Immunol.* 16, 485–497. doi: 10.1038/nri.2016.63

Brown, N. K., Zhou, Z., Zhang, J., Zeng, R., Wu, J., Eitzman, D. T., et al. (2014). Perivascular adipose tissue in vascular function and disease: a review of current research and animal models. *Arterioscler. Thromb. Vasc. Biol.* 34, 1621–1630. doi: 10.1161/ATVBAHA.114.303029

Chan, C. T., Moore, J. P., Budzyn, K., Guida, E., Diep, H., Vinh, A., et al. (2012). Reversal of vascular macrophage accumulation and hypertension by a CCR2 antagonist in deoxycorticosterone/salt-treated mice. *Hypertension* 60, 1207–1212. doi: 10.1161/HYPERTENSIONAHA.112.201251

Chang, M. K., Binder, C. J., Miller, Y. I., Subbanagounder, G., Silverman, G. J., Berliner, J. A., et al. (2004). Apoptotic cells with oxidation-specific epitopes are immunogenic and proinflammatory. *J. Exp. Med.* 200, 1359–1370. doi: 10.1084/jem.20031763

Chatterjee, T. K., Stoll, L. L., Denning, G. M., Harrelson, A., Blomkalns, A. L., Idelman, G., et al. (2009). Proinflammatory phenotype of perivascular adipocytes: influence of high-fat feeding. *Circ. Res.* 104, 541–549. doi: 10.1161/CIRCRESAHA.108.182998

Choi, Y. S., Dieter, J. A., Rothaeusler, K., Luo, Z., and Baumgarth, N. (2012). B-1 cells in the bone marrow are a significant source of natural IgM. *Eur. J. Immunol.* 42, 120–129. doi: 10.1002/eji.201141890

Chou, M. Y., Hartvigsen, K., Hansen, L. F., Fogelstrand, L., Shaw, P. X., Boullier, A., et al. (2008). Oxidation-specific epitopes are important targets of innate immunity. *J. Intern. Med.* 263, 479–488. doi: 10.1111/j.1365-2796.2008.01968.x

Corte-Real, J., Rodo, J., Almeida, P., Garcia, J., Coutinho, A., Demengeot, J., et al. (2009). Irf4 is a positional and functional candidate gene for the control of serum IgM levels in the mouse. *Genes Immun.* 10, 93–99. doi: 10.1038/gene.2008.73

de Vos, A. M., Prokop, M., Roos, C. J., Meijs, M. F., van der Schouw, Y. T., Rutten, A., et al. (2008). Peri-coronary epicardial adipose tissue is related to cardiovascular risk factors and coronary artery calcification in post-menopausal women. *Eur. Heart J.* 29, 777–783. doi: 10.1093/eurheartj/ehm564

Doran, A. C., Lipinski, M. J., Oldham, S. N., Garmey, J. C., Campbell, K. A., Skaflen, M. D., et al. (2012). B-cell aortic homing and atheroprotection depend on Id3. *Circ. Res.* 110, e1–e12. doi: 10.1161/CIRCRESAHA.111.256438

Ensan, S., Li, A., Besla, R., Degousee, N., Cosme, J., Roufaiel, M., et al. (2016). Self-renewing resident arterial macrophages arise from embryonic CX3CR^{1+} precursors and circulating monocytes immediately after birth. *Nat. Immunol.* 17, 159–168. doi: 10.1038/ni.3343

Fuster, J. J., Ouchi, N., Gokce, N., and Walsh, K. (2016). Obesity-induced changes in adipose tissue microenvironment and their impact on cardiovascular disease. *Circ. Res.* 118, 1786–1807. doi: 10.1161/CIRCRESAHA.115.306885

Galkina, E., Kadl, A., Sanders, J., Varughese, D., Sarembock, I. J., and Ley, K. (2006). Lymphocyte recruitment into the aortic wall before and during development of atherosclerosis is partially L-selectin dependent. *J. Exp. Med.* 203, 1273–1282. doi: 10.1084/jem.20052205

Girard, J. P., and Springer, T. A. (1995). High endothelial venules (HEVs): specialized endothelium for lymphocyte migration. *Immunol. Today* 16, 449–457. doi: 10.1016/0167-5699(95)80023-9

Gustafson, B. (2010). Adipose tissue, inflammation and atherosclerosis. *J. Atheroscler. Thromb.* 17, 332–341. doi: 10.5551/jat.3939

Guzik, T. J., Hoch, N. E., Brown, K. A., McCann, L. A., Rahman, A., Dikalov, S., et al. (2007). Role of the T cell in the genesis of angiotensin II induced hypertension and vascular dysfunction. *J. Exp. Med.* 204, 2449–2460. doi: 10.1084/jem.20070657

Hansson, G. K., and Hermansson, A. (2011). The immune system in atherosclerosis. *Nat. Immunol.* 12, 204–212. doi: 10.1038/ni.2001

Harmon, D. B., Srikakulapu, P., Kaplan, J. L., Oldham, S. N., McSkimming, C., Garmey, J. C., et al. (2016). Protective role for B-1b B cells and IgM in obesity-associated inflammation, glucose intolerance, and insulin resistance. *Arterioscler. Thromb. Vasc. Biol.* 36, 682–691. doi: 10.1161/ATVBAHA.116.307166

Henrichot, E., Juge-Aubry, C. E., Pernin, A., Pache, J. C., Velebit, V., Dayer, J. M., et al. (2005). Production of chemokines by perivascular adipose tissue: a role in the pathogenesis of atherosclerosis? *Arterioscler. Thromb. Vasc. Biol.* 25, 2594–2599. doi: 10.1161/01.ATV.0000188508.40052.35

Hirata, Y., Kurobe, H., Akaike, M., Chikugo, F., Hori, T., Bando, Y., et al. (2011). Enhanced inflammation in epicardial fat in patients with coronary artery disease. *Int. Heart J.* 52, 139–142. doi: 10.1536/ihj.52.139

Holodick, N. E., Tumang, J. R., and Rothstein, T. L. (2010). Immunoglobulin secretion by B1 cells: differential intensity and IRF4-dependence of spontaneous IgM secretion by peritoneal and splenic B1 cells. *Eur. J. Immunol.* 40, 3007–3016. doi: 10.1002/eji.201040545

Iacobellis, G., and Willens, H. J. (2009). Echocardiographic epicardial fat: a review of research and clinical applications. *J. Am. Soc. Echocardiogr.* 22, 1311–1319. doi: 10.1016/j.echo.2009.10.013

Jackson-Jones, L. H., Duncan, S. M., Magalhaes, M. S., Campbell, S. M., Maizels, R. M., McSorley, H. J., et al. (2016). Fat-associated lymphoid clusters control local IgM secretion during pleural infection and lung inflammation. *Nat. Commun.* 7:12651. doi: 10.1038/ncomms12651

Kaplan, J. L., Marshall, M. A. C., McSkimming, C., Harmon, D. B., Garmey, J. C., Oldham, S. N., et al. (2015). Adipocyte progenitor cells initiate monocyte chemoattractant protein-1-mediated macrophage accumulation in visceral adipose tissue. *Mol. Metab.* 4, 779–794. doi: 10.1016/j.molmet.2015.07.010

Konaniah, E. S., Kuhel, D. G., Basford, J. E., Weintraub, N. L., and Hui, D. Y. (2017). Deficiency of LRP1 in mature adipocytes promotes diet-induced inflammation and atherosclerosis-brief report. *Arterioscler. Thromb. Vasc. Biol.* 37, 1046–1049. doi: 10.1161/ATVBAHA.117.309414

Konishi, M., Sugiyama, S., Sato, Y., Oshima, S., Sugamura, K., Nozaki, T., et al. (2010). Pericardial fat inflammation correlates with coronary artery disease. *Atherosclerosis* 213, 649–655. doi: 10.1016/j.atherosclerosis.2010.10.007

Kyaw, T., Tay, C., Krishnamurthi, S., Kanellakis, P., Agrotis, A., Tipping, P., et al. (2011). B1a B lymphocytes are atheroprotective by secreting natural IgM that increases IgM deposits and reduces necrotic cores in atherosclerotic lesions. *Circ. Res.* 109, 830–840. doi: 10.1161/CIRCRESAHA.111.248542

Manka, D., Chatterjee, T. K., Stoll, L. L., Basford, J. E., Konaniah, E. S., Srinivasan, R., et al. (2014). Transplanted perivascular adipose tissue accelerates injury-induced neointimal hyperplasia: role of monocyte chemoattractant protein-1. *Arterioscler. Thromb. Vasc. Biol.* 34, 1723–1730. doi: 10.1161/ATVBAHA.114.303983

Mazurek, T., Zhang, L., Zalewski, A., Mannion, J. D., Diehl, J. T., Arafat, H., et al. (2003). Human epicardial adipose tissue is a source of inflammatory mediators. *Circulation* 108, 2460–2466. doi: 10.1161/01.CIR.0000099542.57313.C5

Mikolajczyk, T. P., Nosalski, R., Szczepaniak, P., Budzyn, K., Osmenda, G., Skiba, D., et al. (2016). Role of chemokine RANTES in the regulation of perivascular inflammation, T-cell accumulation, and vascular dysfunction in hypertension. *FASEB J.* 30, 1987–1999. doi: 10.1096/fj.201500088R

Miller, Y. I., Choi, S. H., Wiesner, P., Fang, L., Harkewicz, R., Hartvigsen, K., et al. (2011). Oxidation-specific epitopes are danger-associated molecular patterns recognized by pattern recognition receptors of innate immunity. *Circ. Res.* 108, 235–248. doi: 10.1161/CIRCRESAHA.110.223875

Moore, J. P., Vinh, A., Tuck, K. L., Sakkal, S., Krishnan, S. M., Chan, C. T., et al. (2015). M2 macrophage accumulation in the aortic wall during angiotensin II infusion in mice is associated with fibrosis, elastin loss, and elevated blood pressure. *Am. J. Physiol. Heart Circ. Physiol.* 309, H906–H917. doi: 10.1152/ajpheart.00821.2014

Moro, K., Yamada, T., Tanabe, M., Takeuchi, T., Ikawa, T., Kawamoto, H., et al. (2010). Innate production of T(H)2 cytokines by adipose tissue-associated c-Kit$^{(+)}$Sca-1$^{(+)}$ lymphoid cells. *Nature* 463, 540–544. doi: 10.1038/nature08636

Newland, S. A., Mohanta, S., Clement, M., Taleb, S., Walker, J. A., Nus, M., et al. (2017). Type-2 innate lymphoid cells control the development of atherosclerosis in mice. *Nat. Commun.* 8:15781. doi: 10.1038/ncomms15781

Nishimura, S., Manabe, I., Takaki, S., Nagasaki, M., Otsu, M., Yamashita, H., et al. (2013). Adipose natural regulatory B cells negatively control adipose tissue inflammation. *Cell. Metab.* 18, 759–766. doi: 10.1016/j.cmet.2013.09.017

Nosalski, R., and Guzik, T. J. (2017). Perivascular adipose tissue inflammation in vascular disease. *Br. J. Pharmacol.* doi: 10.1111/bph.13705. [Epub ahead of print].

Omar, A., Chatterjee, T. K., Tang, Y., Hui, D. Y., and Weintraub, N. L. (2014). Proinflammatory phenotype of perivascular adipocytes. *Arterioscler. Thromb. Vasc. Biol.* 34, 1631–1636. doi: 10.1161/ATVBAHA.114.303030

Padilla, J., Jenkins, N. T., Vieira-Potter, V. J., and Laughlin, M. H. (2013). Divergent phenotype of rat thoracic and abdominal perivascular adipose tissues. *Am. J. Physiol. Regul. Integr. Comp. Physiol.* 304, R543–R552. doi: 10.1152/ajpregu.00567.2012

Perry, H. M., Oldham, S. N., Fahl, S. P., Que, X., Gonen, A., Harmon, D. B., et al. (2013). Helix-loop-helix factor inhibitor of differentiation 3 regulates interleukin-5 expression and B-1a B cell proliferation. *Arterioscler. Thromb. Vasc. Biol.* 33, 2771–2779. doi: 10.1161/ATVBAHA.113.302571

Rajsheker, S., Manka, D., Blomkalns, A. L., Chatterjee, T. K., Stoll, L. L., and Weintraub, N. L. (2010). Crosstalk between perivascular adipose tissue and blood vessels. *Curr. Opin. Pharmacol.* 10, 191–196. doi: 10.1016/j.coph.2009.11.005

Rosenfeld, S. M., Perry, H. M., Gonen, A., Prohaska, T. A., Srikakulapu, P., Grewal, S., et al. (2015). B-1b cells secrete atheroprotective IgM and attenuate atherosclerosis. *Circ. Res.* 117, e28–e39. doi: 10.1161/CIRCRESAHA.117.306044

Srikakulapu, P., and McNamara, C. A. (2017). B cells and atherosclerosis. *Am. J. Physiol. Heart Circ. Physiol.* 312, H1060–H1067. doi: 10.1152/ajpheart.00859.2016

Srikakulapu, P., Hu, D., Yin, C., Mohanta, S. K., Bontha, S. V., Peng, L., et al. (2016). Artery tertiary lymphoid organs control multilayered territorialized atherosclerosis B-cell responses in aged ApoE-/- mice. *Arterioscler. Thromb. Vasc. Biol.* 36, 1174–1185. doi: 10.1161/ATVBAHA.115.306983

Tsiantoulas, D., Perkmann, T., Afonyushkin, T., Mangold, A., Prohaska, T. A., Papac-Milicevic, N., et al. (2015). Circulating microparticles carry oxidation-specific epitopes and are recognized by natural IgM antibodies. *J. Lipid Res.* 56, 440–448. doi: 10.1194/jlr.P054569

Tsimikas, S., Brilakis, E. S., Lennon, R. J., Miller, E. R., Witztum, J. L., McConnell, J. P., et al. (2007). Relationship of IgG and IgM autoantibodies to oxidized low density lipoprotein with coronary artery disease and cardiovascular events. *J. Lipid Res.* 48, 425–433. doi: 10.1194/jlr.M600361-JLR200

Tsimikas, S., Willeit, P., Willeit, J., Santer, P., Mayr, M., Xu, Q., et al. (2012). Oxidation-specific biomarkers, prospective 15-year cardiovascular and stroke outcomes, and net reclassification of cardiovascular events. *J. Am. Coll. Cardiol.* 60, 2218–2229. doi: 10.1016/j.jacc.2012.08.979

Uchida, Y., Uchida, Y., Shimoyama, E., Hiruta, N., Kishimoto, T., and Watanabe, S. (2016). Pericoronary adipose tissue as storage and supply site for oxidized low-density lipoprotein in human coronary plaques. *PLoS ONE* 11:e0150862. doi: 10.1371/journal.pone.0150862

Verhagen, S. N., Vink, A., van der Graaf, Y., and Visseren, F. L. (2012). Coronary perivascular adipose tissue characteristics are related to atherosclerotic plaque size and composition. A post-mortem study. *Atherosclerosis* 225, 99–104. doi: 10.1016/j.atherosclerosis.2012.08.031

Wensveen, F. M., Jelencic, V., Valentic, S., Sestan, M., Wensveen, T. T., Theurich, S., et al. (2015). NK cells link obesity-induced adipose stress to inflammation and insulin resistance. *Nat. Immunol.* 16, 376–385. doi: 10.1038/ni.3120

Wigren, M., Nilsson, J., and Kolbus, D. (2012). Lymphocytes in atherosclerosis. *Clin. Chim. Acta* 413, 1562–1568. doi: 10.1016/j.cca.2012.04.031

Winer, D. A., Winer, S., Shen, L., Wadia, P. P., Yantha, J., Paltser, G., et al. (2011). B cells promote insulin resistance through modulation of T cells and production of pathogenic IgG antibodies. *Nat. Med.* 17, 610–617. doi: 10.1038/nm.2353

Zimmerlin, L., Donnenberg, V. S., and Donnenberg, A. D. (2011). Rare event detection and analysis in flow cytometry: bone marrow mesenchymal stem cells, breast cancer stem/progenitor cells in malignant effusions, and pericytes in disaggregated adipose tissue. *Methods Mol. Biol.* 699, 251–273. doi: 10.1007/978-1-61737-950-5_12

Conflict of Interest Statement: The authors declare that the research was conducted in the absence of any commercial or financial relationships that could be construed as a potential conflict of interest.

Advantages of publishing in Frontiers

OPEN ACCESS
Articles are free to read for greatest visibility and readership

FAST PUBLICATION
Around 90 days from submission to decision

HIGH QUALITY PEER-REVIEW
Rigorous, collaborative, and constructive peer-review

TRANSPARENT PEER-REVIEW
Editors and reviewers acknowledged by name on published articles

Frontiers
Avenue du Tribunal-Fédéral 34
1005 Lausanne | Switzerland

Visit us: www.frontiersin.org
Contact us: info@frontiersin.org | +41 21 510 17 00

REPRODUCIBILITY OF RESEARCH
Support open data and methods to enhance research reproducibility

DIGITAL PUBLISHING
Articles designed for optimal readership across devices

FOLLOW US
@frontiersin

IMPACT METRICS
Advanced article metrics track visibility across digital media

EXTENSIVE PROMOTION
Marketing and promotion of impactful research

LOOP RESEARCH NETWORK
Our network increases your article's readership